

NASA
Reference Publication 1212

AVSCOM
Technical Report 88-C-035

Theory of Gearing

Faydor L. Litvin

*The University of Illinois at Chicago
Department of Mechanical Engineering
Chicago, Illinois*

NASA
National Aeronautics and
Space Administration

**Scientific and Technical
Information Division**



US ARMY
AVIATION
SYSTEMS COMMAND
AVIATION R&T ACTIVITY

RECEDING PAGE BLANK NOT FILMED

BASE  INTENTIONALLY BLANK

Library of Congress Cataloging-in-Publication Data

Litvin, Faydor L.

Theory of gearing.

(NASA reference publication; 1212) (AVSCOM
technical report; 88-C-035)

Bibliography: pp. 465-466

Includes index.

1. Gearing. I. Title. II. Series. III. Series:
AVSCOM technical report; 88-C-035.
TJ184.L53 1989 621.8'33 89-600204

For sale by the Superintendent of Documents
U.S. Government Printing Office, Washington, DC 20402

IV

Foreword

The United States is a world leader in aviation and space technology. The role of the National Aeronautics and Space Administration is to provide leadership through advances in science and technology for both aeronautics and space.

The NASA Lewis Research Center has maintained a strong research program in aeronautics, beginning in 1942. During the period from the late 1940's to the late 1960's, the helicopter came into wide use in the military and civil arenas. In 1970, the United States Army and NASA began a joint effort at Lewis which focused on helicopter propulsion technology. A significant portion of that program is devoted to advanced transmission technology. The advanced transmission technology program at the Lewis Research Center is augmented through the use of contracts and grants with U.S. industry and universities. Working at the University of Illinois at Chicago, under NASA/Army sponsorship, Dr. Faydor L. Litvin has developed many new and important ideas for the mathematical formulation and theoretical understanding of spur, helical, and spiral bevel gears—gears that are of very great importance to the transfer of power from engine to rotor blades in modern helicopters.

Dr. Faydor L. Litvin has significantly contributed to the goals of the NASA/Army transmission program by his accomplishments in the science of gearing and his authorship of this book. His work has provided a mathematical basis which improves our understanding of bevel gear geometry and the manufacturing procedure. His work has provided solutions to reduce gear noise and to enable a smoother transfer of power in helicopters. In summary, he has directly contributed to advance the state of the art in helicopter power transmission technology, and has made a significant contribution to NASA's research projects and to the public good.

This book explains the most general problems of the theory of gearing, but it represents only a part of Dr. Litvin's accomplishments. His research contributions have improved (1) almost all types of gearing including spur, helical, hypoid, bevel, worm, and noncircular gears; (2) tools for gear manufacture; and (3) computer programs for simulation of meshing and contact. His theorems, methods for gear synthesis, and methods for gear generation represent a very significant contribution to the science of gearing. His influence has spread throughout the world via his many lectures, publications, and approximately 60 doctoral students who have settled in Europe, Asia, and North America. Because of his career achievements, I believe Dr. Litvin is a true leader in the development of the theory of gearing.

It is my pleasure to recommend this book to all who desire a deeper knowledge of the theory of gearing.

John J. Coy
NASA Lewis Research Center

Preface

This edition is the first English version of the author's monograph on the theory of gearing. The first and second editions of this work were published in Russian in 1962 and 1968. Both of those editions were translated into Chinese by Dr. Go-Kai, one of the author's former doctoral students, to whom he is very thankful for his devoted work. The second edition was translated also into Hungarian by Dr. Zeno Therplan and Dr. Jozsef Drobni, who accomplished an excellent work.

This English version is substantially different from the previous editions. The author has paid particular attention to the basic mathematical problems of the theory of gearing, such as the necessary and sufficient conditions of envelope existence, relations between principal curvatures and directions for surfaces of mating gears, singularities of surfaces accompanied by undercutting in the process of generation, the phenomena of envelope of lines of contact, the principles for generation of conjugate surfaces, and others. Special attention has been paid to the algorithms for computer aided simulation of meshing and tooth contact. !!

This edition has been complemented with the results of research recently performed by the author and his doctoral students. The book is supplied with sample problems and problems proposed for the reader to solve that the author believes will be helpful for the study of the book.

The manuscript of this book has been used as a textbook for two courses (Theory of Gearing and Advanced Theory of Gearing) that have been taught by the author for graduate and undergraduate mechanical engineering students at The University of Illinois at Chicago.

The author would like to express his deep gratitude to the National Aeronautics and Space Administration and to the United States Army who have, by numerous grants, sponsored the work that went into the preparation and publication of this book and a significant portion of his research efforts since coming to the United States of America. In particular, the author is grateful to Mr. Erwin V. Zaretsky, Mr. Gilbert J. Weden, and Mr. Dennis P. Townsend for their encouragement and support of the publication of this work. The progress of the work was continuously overseen by Dr. John J. Coy, who also provided sound advice and counsel throughout the project. A thorough technical review was conducted by Mr. Robert F. Handschuh, which resulted in helpful corrections and a fine index. The author also thanks Mr. Steven B. Brunn for his editorial suggestions and help in the preparation of the manuscript for publication.

Faydor L. Litvin
*The University of Illinois
at Chicago*

Dedicated to my Parents

Contents

| | | |
|------------------|---|-----|
| Chapter 1 | Coordinate Transformation | |
| 1.1 | Introduction to Coordinate Transformation | 1 |
| 1.2 | Systems of Coordinates With a Common Origin | 1 |
| 1.3 | Coordinate Systems With Noncoincident Origins and Noncollinear Axes | 7 |
| 1.4 | Generation of Curves and Surfaces in Matrix Representation | 14 |
| Chapter 2 | Transformation of Motion | |
| 2.1 | Parallel Axes of Rotation | 20 |
| 2.2 | Intersected Axes of Rotation | 29 |
| 2.3 | Crossed Axes of Rotation: Relative Velocity | 32 |
| 2.4 | Crossed Axes of Rotation: Screw Axis of Relative Motion | 36 |
| 2.5 | Crossed Axes of Rotation: Hyperboloid Surfaces of Revolution | 40 |
| Chapter 3 | Plane Curves | |
| 3.1 | Planar Curves: Definitions and Representations | 42 |
| 3.2 | Tangent and Normal to a Plane Curve | 50 |
| 3.3 | Curvature of Plane Curves | 56 |
| Chapter 4 | Conjugate Shapes | |
| 4.1 | Generation of a Locus of Planar Curves | 63 |
| 4.2 | Envelope of a Locus of Plane Curves: Parametric Representation | 68 |
| 4.3 | Envelope of a Locus of Plane Curves: Representation in Implicit Form | 74 |
| 4.4 | Envelope of a Plane Curve Locus: Kinematic Method of Determination | 79 |
| 4.5 | Conjugate Shapes: Working Equations for Their Determination | 83 |
| Chapter 5 | Plane Gearing Analysis | |
| 5.1 | Equations of Tooth Shape Tangency | 87 |
| 5.2 | Analysis of Meshing | 89 |
| 5.3 | Computation Process | 90 |
| Chapter 6 | Basic Kinematic Relations of Plane Gearings and Their Application | |
| 6.1 | Basic Kinematic Relations | 93 |
| 6.2 | Conjugate Shapes: Relations Between Curvatures | 97 |
| 6.3 | Relations Between Centrode and Shape Curvatures | 112 |
| 6.4 | Theorem of Direction of Line of Action in the Neighborhood of the Instantaneous Center of Rotation | 119 |
| 6.5 | Conditions of Tooth Nonundercutting | 120 |

| | | |
|-------------------|--|-----|
| Chapter 7 | Generation of Conjugate Shapes | |
| 7.1 | Methods of Tooth Cutting | 128 |
| 7.2 | Principles of Generation of Conjugate Shapes | 130 |
| 7.3 | The Camus Theorem | 132 |
| 7.4 | Evolutes of Conjugate Shapes | 134 |
| Chapter 8 | Surfaces | |
| 8.1 | Surfaces: Definitions and Representations | 146 |
| 8.2 | Curvilinear Coordinates | 149 |
| 8.3 | Tangent Plane and Normal Vector to a Surface | 150 |
| 8.4 | Examples of Surfaces | 154 |
| Chapter 9 | Conjugated Surfaces | |
| 9.1 | Introduction to Problem of Conjugated Surfaces | 166 |
| 9.2 | Family of Given Surfaces | 167 |
| 9.3 | Envelope of a Family of Surfaces: Representation in Parametric Form | 168 |
| 9.4 | Envelope of a Locus of Surfaces: Representation in Implicit Form | 180 |
| 9.5 | Theorem of Singular Points of Generated Surface Σ_2 | 187 |
| 9.6 | Envelope of a Family of Surfaces: Kinematic Method of Determination | 193 |
| 9.7 | Envelope of Contact Lines on the Generating Surface Σ_1 | 196 |
| 9.8 | Conjugate Surfaces: Working Equations | 200 |
| Chapter 10 | Curvatures of a Surface | |
| 10.1 | First and Second Fundamental Forms | 215 |
| 10.2 | Surface Normal Section: Osculating Plane | 221 |
| 10.3 | Curvature of a Spatial Curve | 222 |
| 10.4 | The Meusnier Theorem | 225 |
| 10.5 | Normal Curvature | 228 |
| 10.6 | Principal Directions and Curvatures, Indicatrix of Dupin, and Working Equations | 232 |
| 10.7 | Geodesic Curvature | 237 |
| Chapter 11 | Spatial Gearing Analysis | |
| 11.1 | Tangency of Gear-Tooth Surfaces | 241 |
| 11.2 | Analysis of Meshing of Spatial Gearings | 243 |
| 11.3 | Process of Computation | 244 |
| Chapter 12 | Basic Kinematic Relations of Spatial Gearing | |
| 12.1 | Relations of Contact Point Velocity and Surface Unit Normal Velocity | 253 |
| 12.2 | Relations of Contact Point Acceleration and Surface Unit Normal Acceleration | 257 |
| Chapter 13 | Relations Between Curvatures of Mating Surfaces | |
| 13.1 | Relations Between Principal Curvatures and Directions for Mating Surfaces ... | 260 |
| 13.2 | Contact Point Path as a Local Geodetic Curve | 275 |
| 13.3 | Relative Normal Curvature | 286 |
| 13.4 | Contact Ellipse | 288 |

| | |
|--|-----|
| Chapter 14 Pitch Surfaces | |
| 14.1 Introduction | 296 |
| 14.2 Operating Pitch Surfaces: Transformation of Rotation Between Crossed Axes | 297 |
| 14.3 Helical Gears with Crossed Axes and Worm-Gear Drives: Operating Pitch Surfaces | 298 |
| 14.4 Hypoid Gears: Operating Pitch Surfaces | 304 |
| 14.5 Limiting Contact Normal | 313 |
| Chapter 15 Axes of Meshing | |
| 15.1 Crossed Axes of Gear Rotation: Axes of Meshing | 319 |
| 15.2 Milling of Worms by Peripheral Milling Cutters: Axes of Meshing | 324 |
| 15.3 Application of the Theory of Axes of Meshing: Generation of Worm With Concave-Convex Surface | 327 |
| 15.4 Knots of Meshing | 331 |
| Chapter 16 Methods for Generation of Conjugate Gear-Tooth Surfaces | |
| 16.1 Introduction to Gear Generation | 336 |
| 16.2 Generation Method 1 | 337 |
| 16.3 Generation Method 2 | 337 |
| 16.4 Generation Method 3 | 341 |
| 16.5 Generation Method 4 | 344 |
| Chapter 17 Synthesis of Spiral Bevel Gears | |
| 17.1 Introduction to Gear Geometry | 350 |
| 17.2 Introduction to Synthesis | 354 |
| 17.3 Generating Surfaces and Coordinate Systems | 355 |
| 17.4 Generating Tool Surfaces | 357 |
| 17.5 Equations of Meshing by Cutting | 358 |
| 17.6 Local Synthesis: Conditions of Tangency | 362 |
| 17.7 Basic Machine-Tool Settings | 369 |
| 17.8 Local Synthesis: Determination of Corrections of Machine-Tool Settings | 371 |
| 17.9 Bearing Contact at the Main Contact Point | 377 |
| 17.10 Contact Ellipse | 384 |
| 17.11 Tooth-Contact Analysis | 385 |
| Chapter 18 Kinematic Precision of Gear Trains | |
| 18.1 Introduction | 390 |
| 18.2 Theory and Exact Solution Method for Kinematic Precision | 391 |
| 18.3 Application of Theory to Helical Gears with Circular Arc Teeth: Sensitivity to the Change of Center Distance | 395 |
| 18.4 Approximate Method of Calculation of Gear Drive Kinematic Errors | 405 |
| 18.5 Application of Theory to Eccentricity of Involute Spur Gears | 409 |
| 18.6 Application of Theory to Eccentricity of Spiral Bevel Gears | 412 |
| 18.7 Backlash of Spur Gears | 415 |
| 18.8 Application of Theory to Transformation of Rotation With a Varied Ratio by Eccentric Gears | 419 |
| 18.9 Measurement of Rotation Angles With Eccentric Disks | 419 |

| | |
|--|------------|
| Chapter 19 Force Transmission | |
| 19.1 Force Transmission of Gears With Crossed Axes | 425 |
| 19.2 Force Transmission for Spiral Bevel Gears | 432 |
| Appendix A Matrices: Properties and Operations | |
| A.1 Introduction | 435 |
| A.2 Equality of Matrices | 437 |
| A.3 Addition and Subtraction of Matrices | 438 |
| A.4 Multiplication of Matrices | 438 |
| A.5 Transpose Matrix | 440 |
| A.6 Inverse Matrix | 442 |
| A.7 Matrix Differentiation | 445 |
| A.8 Matrix Representation of Vector Formulas | 445 |
| Appendix B Theorem of Implicit Function System Existence | 449 |
| Appendix C Linear Vector Function. Principal Curvatures and Directions of Surface | |
| C.1 Linear Vector Function | 451 |
| C.2 Characteristic Roots and Vectors | 456 |
| C.3 Surface Principal Directions and Curvatures | 459 |
| References | 465 |
| Index | 467 |

Chapter 1

Coordinate Transformation

1.1 Introduction to Coordinate Transformation

Consider a set of Cartesian systems $S_1 (x_1, y_1, z_1)$, $S_2 (x_2, y_2, z_2)$, . . . , $S_n (x_n, y_n, z_n)$. Point M is specified in these systems by coordinates $M (x_1, y_1, z_1)$, $M (x_2, y_2, z_2)$, . . . , $M (x_n, y_n, z_n)$.

Coordinate transformation is a set of relations which associate point coordinates of one system with the point coordinates of other systems. For instance, through coordinate transformation we may relate the given set (x_1, y_1, z_1) with (x_k, y_k, z_k) , ($k=2, 3, \dots, n$). It will be shown below that the relations between sets of coordinates depend on the location of the origins of the considered systems and on the orientation of their respective axes.

Coordinate transformation is a powerful technique of engineering mechanics. It may be used to study the motion of rigid bodies and their kinematical and dynamic characteristics, which are associated with different coordinate systems. In the theory of gearing, coordinate transformation will be applied in the following ways:

(1) For determining the equations of (a) the path traced out by a point of a moving body, (b) the surface traced out by a line rigidly connected to a moving body, and (c) the locus of surfaces generated by a surface rigidly connected to the moving body.

(2) For expressing equations of a given surface (line) in several different coordinate systems which belong to the same rigid body.

Coordinate transformation will be considered for systems with (1) common origin and noncoincident coordinate axes and (2) noncoincident origins and noncollinear coordinate axes. Coordinate transformation is studied in matrix presentation. Properties of matrices and matrix operations are summarized in appendix A.

1.2 Systems of Coordinates With a Common Origin

Consider a rigid body which is free to rotate about a fixed axis. We set up two coordinate systems as follows: $S_f (x_f, y_f, z_f)$, which is rigidly connected to the frame—the fixed coordinate system, and $S_g (x_g, y_g, z_g)$, which is rigidly connected to the body—the moving coordinate system (fig. 1.2.1). Systems S_f and S_g are located such that they share a common origin and their axes x_f and x_g coincide

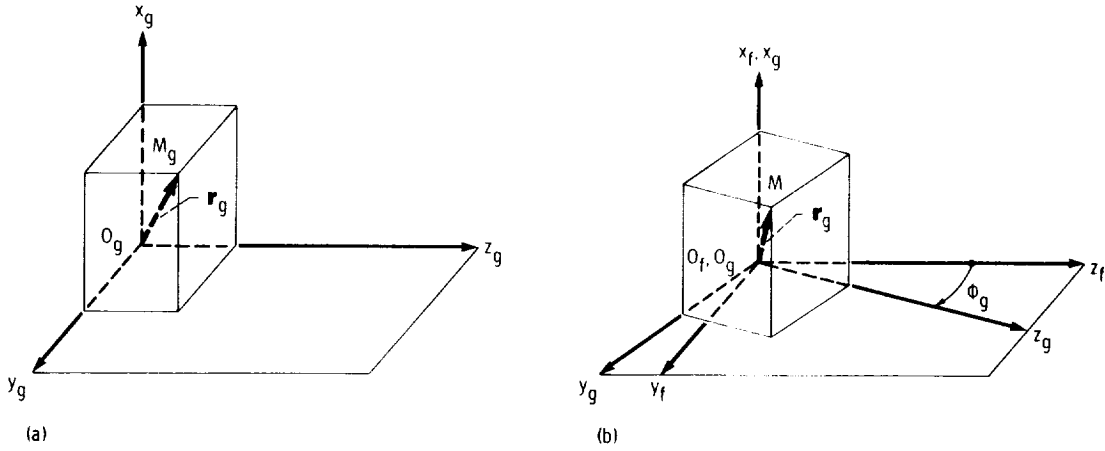


Figure 1.2.1.

with the axis of rotation. To identify a point M in the rigid body, we use the position vector¹ (fig. 1.2.1(a)) $\mathbf{r}_g = \overline{O_g M}$, which may be expressed as a 3×1 matrix

$$[\mathbf{r}_g] = \begin{bmatrix} x_g \\ y_g \\ z_g \end{bmatrix} \quad (1.2.1)$$

Assume that the body is rotated by an angle ϕ_g (fig. 1.2.1(b)). Point M is still specified by its original coordinates in system S_g , but must now be identified by new coordinates in system S_f . The new coordinates are given by the matrix

$$[\mathbf{r}_f(\phi_g)] = \begin{bmatrix} x_f(\phi_g) \\ y_f(\phi_g) \\ z_f(\phi_g) \end{bmatrix} \quad (1.2.2)$$

where ϕ_g is the angle formed by axes z_f and z_g (or by axes y_f and y_g).

To express coordinates (x_f, y_f, z_f) in terms of (x_g, y_g, z_g) and the angular parameter ϕ_g , let us represent the two position vectors \mathbf{r}_g and \mathbf{r}_f in terms of the unit vectors and Cartesian components of their respective coordinate systems

$$\mathbf{r}_g = x_g \mathbf{i}_g + y_g \mathbf{j}_g + z_g \mathbf{k}_g \quad (1.2.3)$$

$$\mathbf{r}_f = x_f \mathbf{i}_f + y_f \mathbf{j}_f + z_f \mathbf{k}_f \quad (1.2.4)$$

Since \mathbf{r}_g and \mathbf{r}_f locate the same point, they are equal (i.e., $\mathbf{r}_g = \mathbf{r}_f$), and by using equations (1.2.3) and (1.2.4), we obtain

$$x_f \mathbf{i}_f + y_f \mathbf{j}_f + z_f \mathbf{k}_f = x_g \mathbf{i}_g + y_g \mathbf{j}_g + z_g \mathbf{k}_g \quad (1.2.5)$$

¹Henceforth, a quantity denoted in the form \overline{AB} has the meaning of a vector which spans the line segment AB and points from A to B . Further, AB denotes the magnitude of vector \overline{AB} .

We now multiply each side of equation (1.2.5) successively by unit vectors \mathbf{i}_f , \mathbf{j}_f , and \mathbf{k}_f and obtain the following three expressions:

$$x_f(\mathbf{i}_f \cdot \mathbf{i}_f) + y_f(\mathbf{i}_f \cdot \mathbf{j}_f) + z_f(\mathbf{i}_f \cdot \mathbf{k}_f) = x_g(\mathbf{i}_f \cdot \mathbf{i}_g) + y_g(\mathbf{i}_f \cdot \mathbf{j}_g) + z_g(\mathbf{i}_f \cdot \mathbf{k}_g) \quad (1.2.6)$$

$$x_f(\mathbf{j}_f \cdot \mathbf{i}_f) + y_f(\mathbf{j}_f \cdot \mathbf{j}_f) + z_f(\mathbf{j}_f \cdot \mathbf{k}_f) = x_g(\mathbf{j}_f \cdot \mathbf{i}_g) + y_g(\mathbf{j}_f \cdot \mathbf{j}_g) + z_g(\mathbf{j}_f \cdot \mathbf{k}_g) \quad (1.2.7)$$

$$x_f(\mathbf{k}_f \cdot \mathbf{i}_f) + y_f(\mathbf{k}_f \cdot \mathbf{j}_f) + z_f(\mathbf{k}_f \cdot \mathbf{k}_f) = x_g(\mathbf{k}_f \cdot \mathbf{i}_g) + y_g(\mathbf{k}_f \cdot \mathbf{j}_g) + z_g(\mathbf{k}_f \cdot \mathbf{k}_g) \quad (1.2.8)$$

Since unit vectors \mathbf{i}_f , \mathbf{j}_f , and \mathbf{k}_f are mutually perpendicular, we may write

$$\mathbf{i}_f \cdot \mathbf{i}_f = 1 \quad \mathbf{i}_f \cdot \mathbf{j}_f = 0 \quad \mathbf{i}_f \cdot \mathbf{k}_f = 0 \text{ etc.} \quad (1.2.9)$$

Equations (1.2.6) to (1.2.9) now yield three linear equations

$$x_f = x_g(\mathbf{i}_f \cdot \mathbf{i}_g) + y_g(\mathbf{i}_f \cdot \mathbf{j}_g) + z_g(\mathbf{i}_f \cdot \mathbf{k}_g) \quad (1.2.10)$$

$$y_f = x_g(\mathbf{j}_f \cdot \mathbf{i}_g) + y_g(\mathbf{j}_f \cdot \mathbf{j}_g) + z_g(\mathbf{j}_f \cdot \mathbf{k}_g) \quad (1.2.11)$$

$$z_f = x_g(\mathbf{k}_f \cdot \mathbf{i}_g) + y_g(\mathbf{k}_f \cdot \mathbf{j}_g) + z_g(\mathbf{k}_f \cdot \mathbf{k}_g) \quad (1.2.12)$$

which may be represented in matrix form as

$$\begin{bmatrix} x_f \\ y_f \\ z_f \end{bmatrix} = \begin{bmatrix} \mathbf{i}_f \cdot \mathbf{i}_g & \mathbf{i}_f \cdot \mathbf{j}_g & \mathbf{i}_f \cdot \mathbf{k}_g \\ \mathbf{j}_f \cdot \mathbf{i}_g & \mathbf{j}_f \cdot \mathbf{j}_g & \mathbf{j}_f \cdot \mathbf{k}_g \\ \mathbf{k}_f \cdot \mathbf{i}_g & \mathbf{k}_f \cdot \mathbf{j}_g & \mathbf{k}_f \cdot \mathbf{k}_g \end{bmatrix} \begin{bmatrix} x_g \\ y_g \\ z_g \end{bmatrix} \quad (1.2.13)$$

It may be verified from figure 1.2.1(b) that the 3×3 matrix in equation (1.2.13) is given by

$$\begin{bmatrix} 1 & 0 & 0 \\ 0 & \cos \phi_g & \sin \phi_g \\ 0 & -\sin \phi_g & \cos \phi_g \end{bmatrix} \quad (1.2.14)$$

and thus matrix equation (1.2.13) becomes

$$\begin{bmatrix} x_f \\ y_f \\ z_f \end{bmatrix} = \begin{bmatrix} 1 & 0 & 0 \\ 0 & \cos \phi_g & \sin \phi_g \\ 0 & -\sin \phi_g & \cos \phi_g \end{bmatrix} \begin{bmatrix} x_g \\ y_g \\ z_g \end{bmatrix} \quad (1.2.15)$$

or in a shortened form

$$[r_f] = [L_{fg}][r_g] \quad (1.2.16)$$

Matrix

$$[L_{fg}] = \begin{bmatrix} a_{11} & a_{12} & a_{13} \\ a_{21} & a_{22} & a_{23} \\ a_{31} & a_{32} & a_{33} \end{bmatrix} \quad (1.2.17)$$

uniquely describes the transformation of coordinates to the new coordinate system S_f from the old coordinate system S_g . The subscripts fg in L_{fg} indicate the order of such a transformation (i.e., to f from g , the new coordinate system being denoted by the left-hand subscript).

It is noted that each element of matrix $[L_{fg}]$ is the scalar product of two unit vectors which belong to systems S_f and S_g . For instance, element a_{21} may be represented as

$$a_{21} = \mathbf{j}_f \cdot \mathbf{i}_g = j_f i_g \cos(\mathbf{j}_f, \mathbf{i}_g) = \cos(\mathbf{j}_f, \mathbf{i}_g)$$

where $\cos(\mathbf{j}_f, \mathbf{i}_g)$ is the cosine of the angle formed by new axis number 2 (axis y_f) and old axis number 1 (axis x_g). This quantity is known as the direction cosine of unit vectors \mathbf{j}_f and \mathbf{i}_g . To generalize this, we say that the elements of $[L_{fg}]$ are of the form $a_{k\ell}$ ($k = 1, 2, 3; \ell = 1, 2, 3$), where $a_{k\ell}$ is the direction cosine of the new unit vector k and old unit vector ℓ ; unit vectors \mathbf{i}, \mathbf{j} , and \mathbf{k} correspond to the numbers 1, 2, and 3, respectively. Consequently,

$$a_{23} = \mathbf{j}_f \cdot \mathbf{k}_g = \cos(\mathbf{j}_f, \mathbf{k}_g) \quad \text{and} \quad a_{31} = \mathbf{k}_f \cdot \mathbf{i}_g = \cos(\mathbf{k}_f, \mathbf{i}_g)$$

With all of the results derived above, matrix equation (1.2.13) may now be expressed in the general form

$$\begin{bmatrix} x_f \\ y_f \\ z_f \end{bmatrix} = \begin{bmatrix} a_{11} & a_{12} & a_{13} \\ a_{21} & a_{22} & a_{23} \\ a_{31} & a_{32} & a_{33} \end{bmatrix} \begin{bmatrix} x_g \\ y_g \\ z_g \end{bmatrix} \quad (1.2.18)$$

This matrix equation represents a system of three linear equations which relates the set of new coordinates (x_f, y_f, z_f) with the set of old coordinates (x_g, y_g, z_g) and direction cosines $a_{k\ell}$ ($k = 1, 2, 3; \ell = 1, 2, 3$) of the transformation matrix $[L_{fg}]$.

The matrix method of coordinate transformation works equally well between rigidly connected systems and between systems which move relative to one another. If we deal with two rigidly connected systems, all elements of $[L_{fg}]$ are constant and point M in one system is seen as the same point in the other system, although point M is specified with different sets of coordinates in each system. If, however, one coordinate system moves relative to the other, some elements of $[L_{fg}]$ vary in the process of motion, and point M of the moving system traces out a path in the fixed system. Referring to figure 1.2.1(b), the angle ϕ_g changes in the process of motion and thus elements of matrix equation (1.2.2) will vary with ϕ_g . Accordingly, point M of system S_g traces out a curve in system S_f whose coordinates are a function of ϕ_g and are, in fact, coordinates of a circle. It will be shown in section 1.4 that the matrix method of coordinate transformation is a valuable tool for deriving the equations of curves and surfaces.

Once it is known how to transform coordinates from system S_g to system S_f , it is useful to develop the reverse operation, coordinate transformation from S_f to S_g , which may be represented as follows:

$$[r_g] = [L_{gf}][r_f] \quad (1.2.19)$$

Matrix $[L_{gf}]$, the operator of the reverse transformation, is, in fact, the inverse of matrix $[L_{fg}]$. It may be proven that the determinant of a general transformation matrix $[L_{fg}]$ is equal to unity and therefore its inverse will always exist. It may also be shown that transformation matrix $[L_{fg}]$ is an orthogonal matrix; that is, its transpose and inverse are identical

$$[L_{gf}] = [L_{fg}]^T = [L_{fg}]^{-1} \quad (1.2.20)$$

For instance, referring to figure 1.2.1(b), matrix $[L_{gf}]$ may be obtained as the transpose of matrix (1.2.14); thus

$$[L_{gf}] = [L_{fg}]^T = \begin{bmatrix} 1 & 0 & 0 \\ 0 & \cos \phi_g & -\sin \phi_g \\ 0 & \sin \phi_g & \cos \phi_g \end{bmatrix} \quad (1.2.21)$$

Since $[L_{gf}]$ is the inverse of matrix $[L_{fg}]$, we may write that

$$[L_{gf}][L_{fg}] = [L_{fg}][L_{gf}] = [I] \quad (1.2.22)$$

where $[I]$ is the 3×3 unit (identity) matrix. Similarly, by equations (1.2.20) and (1.2.22) we get

$$[L_{fg}]^T[L_{fg}] = [L_{fg}][L_{fg}]^T = [I] \quad (1.2.23)$$

Still further, it must be pointed out that while a general transformation matrix

$$[L_{fg}] = \begin{bmatrix} a_{11} & a_{12} & a_{13} \\ a_{21} & a_{22} & a_{23} \\ a_{31} & a_{32} & a_{33} \end{bmatrix} = \begin{bmatrix} \mathbf{i}_f \bullet \mathbf{i}_g & \mathbf{i}_f \bullet \mathbf{j}_g & \mathbf{i}_f \bullet \mathbf{k}_g \\ \mathbf{j}_f \bullet \mathbf{i}_g & \mathbf{j}_f \bullet \mathbf{j}_g & \mathbf{j}_f \bullet \mathbf{k}_g \\ \mathbf{k}_f \bullet \mathbf{i}_g & \mathbf{k}_f \bullet \mathbf{j}_g & \mathbf{k}_f \bullet \mathbf{k}_g \end{bmatrix} \quad (1.2.24)$$

consists of nine elements, only three of them are independent. This results from the fact that the nine elements of $[L_{fg}]$ are related by six orthogonality conditions, which are as follows:

$$a_{11}^2 + a_{12}^2 + a_{13}^2 = 1 \quad a_{21}^2 + a_{22}^2 + a_{23}^2 = 1 \quad a_{31}^2 + a_{32}^2 + a_{33}^2 = 1 \quad (1.2.25)$$

$$a_{11}a_{21} + a_{12}a_{22} + a_{13}a_{23} = 0 \quad a_{11}a_{31} + a_{12}a_{32} + a_{13}a_{33} = 0 \quad a_{21}a_{31} + a_{22}a_{32} + a_{23}a_{33} = 0 \quad (1.2.26)$$

Equations (1.2.25) demonstrate that each unit vector of the new system has unit length, while equations (1.2.26) ensure that the three new axes are mutually perpendicular.

To perform successive coordinate transformations, we need only follow the product rule of matrix algebra. For instance, the following matrix equation

$$[r_n] = [L_{n(n-1)}][L_{(n-1)(n-2)}] \cdot \cdot \cdot [L_{32}][L_{21}][r_1] \quad (1.2.27)$$

represents the successive transformation of point coordinates, specified in system S_1 , to S_2 , to S_3 , . . . , to S_n .

Example problem 1.2.1 By using the method of successive coordinate transformation described above, derive the transformation matrix $[L_{1g}]$ for systems S_1 , S_p , S_f , and S_g shown in figure 1.2.2. Write the three equations which relate (x_g, y_g, z_g) with (x_1, y_1, z_1) . Find the inverse matrix $[L_{g1}]$.

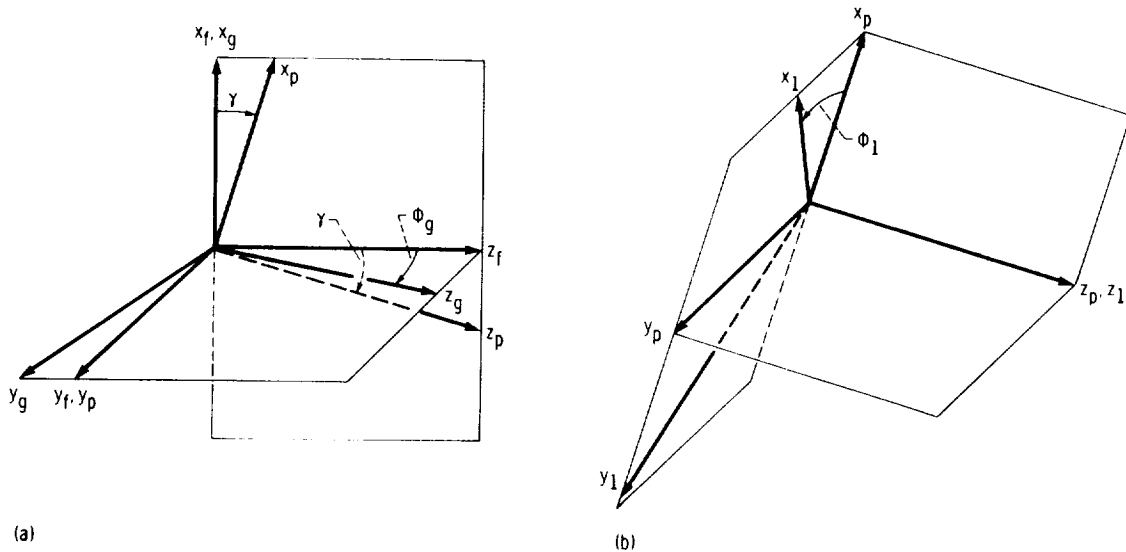


Figure 1.2.2.

Solution. Transformation matrices are as follows:

$$[L_{fg}] = \begin{bmatrix} 1 & 0 & 0 \\ 0 & \cos \phi_g & \sin \phi_g \\ 0 & -\sin \phi_g & \cos \phi_g \end{bmatrix} \quad [L_{pf}] = \begin{bmatrix} \cos \gamma & 0 & \sin \gamma \\ 0 & 1 & 0 \\ -\sin \gamma & 0 & \cos \gamma \end{bmatrix}$$

$$[L_{1p}] = \begin{bmatrix} \cos \phi_1 & \sin \phi_1 & 0 \\ -\sin \phi_1 & \cos \phi_1 & 0 \\ 0 & 0 & 1 \end{bmatrix} \quad [r_g] = \begin{bmatrix} x_g \\ y_g \\ z_g \end{bmatrix} \quad r_f = \begin{bmatrix} x_f \\ y_f \\ z_f \end{bmatrix}$$

Matrix multiplication yields

$$[L_{1p}][L_{pg}][L_{fg}] = [L_{1g}] = \begin{bmatrix} b_{11} & b_{12} & b_{13} \\ b_{21} & b_{22} & b_{23} \\ b_{31} & b_{32} & b_{33} \end{bmatrix}$$

$$= \begin{bmatrix} \cos \gamma \cos \phi_1 & -\sin \gamma \cos \phi_1 \sin \phi_g & \sin \gamma \cos \phi_1 \cos \phi_g \\ & +\sin \phi_1 \cos \phi_g & +\sin \phi_1 \sin \phi_g \\ -\cos \gamma \sin \phi_1 & \sin \gamma \sin \phi_1 \sin \phi_g & -\sin \gamma \sin \phi_1 \cos \phi_g \\ & +\cos \phi_1 \cos \phi_g & +\cos \phi_1 \sin \phi_g \\ -\sin \gamma & -\cos \gamma \sin \phi_g & \cos \gamma \cos \phi_g \end{bmatrix}$$

Coordinates (x_1, y_1, z_1) and (x_g, y_g, z_g) are related by equations

$$x_1 = b_{11}x_g + b_{12}y_g + b_{13}z_g \quad y_1 = b_{21}x_g + b_{22}y_g + b_{23}z_g \quad z_1 = b_{31}x_g + b_{32}y_g + b_{33}z_g$$

The inverse matrix $[L_{g1}]$ may be determined as the transpose of the matrix $[L_{1g}]$

$$[L_{g1}] = [L_{1g}]^T = \begin{bmatrix} b_{11} & b_{21} & b_{31} \\ b_{12} & b_{22} & b_{32} \\ b_{13} & b_{23} & b_{33} \end{bmatrix}$$

1.3 Coordinate Systems With Noncoincident Origins and Noncollinear Axes

Consider a rigid body which moves in space. System S_m is rigidly connected to the moving body and S_n is a fixed coordinate system (fig. 1.3.1). Point M of the body is specified by the position vector $\overline{O_m M} = \mathbf{r}_m(x_m, y_m, z_m)$ and its instantaneous position in space S_n is determined by the position vector $\mathbf{r}_n(x_n, y_n, z_n)$. Position vector $\mathbf{r}_n^{(O)}$ indicates the initial position of point $M, M^{(O)}$, when systems S_m and S_n coincide.

Point M of the moving body traces out a path in space S_n , whose instantaneous point is represented by the position vector \mathbf{r}_n . Components of \mathbf{r}_n are given by the following functions:

$$x_n(x_m, y_m, z_m, \phi) \quad y_n(x_m, y_m, z_m, \phi) \quad z_n(x_m, y_m, z_m, \phi) \quad (1.3.1)$$

where ϕ is the variable parameter of motion. These functions (1.3.1) may be derived through the technique of coordinate transformation.

The position vector \mathbf{r}_n may be represented as

$$\mathbf{r}_n = \overline{O_n O_m} + \overline{O_m M} = \overline{O_n O_m} + \mathbf{r}_m \quad (1.3.2)$$

Equation (1.3.2) yields

$$x_n \mathbf{i}_n + y_n \mathbf{j}_n + z_n \mathbf{k}_n = x_n^{(O_m)} \mathbf{i}_n + y_n^{(O_m)} \mathbf{j}_n + z_n^{(O_m)} \mathbf{k}_n + x_m \mathbf{i}_m + y_m \mathbf{j}_m + z_m \mathbf{k}_m \quad (1.3.3)$$

Here $x_n^{(O_m)}$, $y_n^{(O_m)}$, $z_n^{(O_m)}$ determine the position of origin O_m in system S_n ; \mathbf{i}_n , \mathbf{j}_n , \mathbf{k}_n , and \mathbf{i}_m , \mathbf{j}_m , \mathbf{k}_m are the unit vectors of systems S_n and S_m respectively.

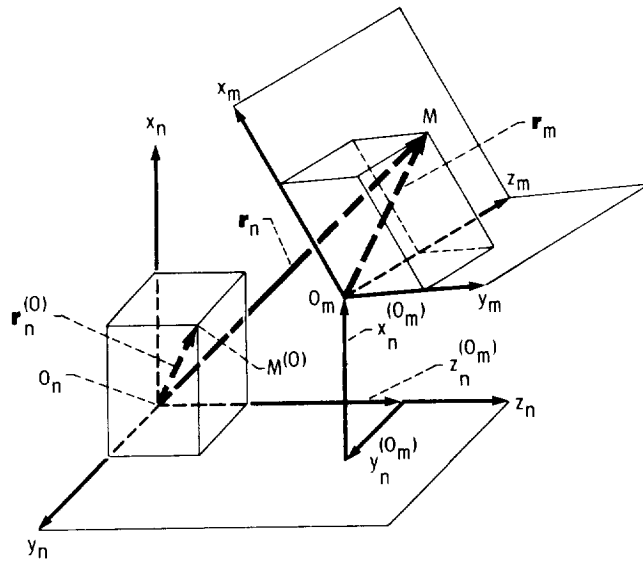


Figure 1.3.1.

We now multiply each side of equation (1.3.3) successively by unit vectors \mathbf{i}_n , \mathbf{j}_n , and \mathbf{k}_n . Taking into account that

$$\mathbf{i}_n \cdot \mathbf{i}_n = \mathbf{j}_n \cdot \mathbf{j}_n = \mathbf{k}_n \cdot \mathbf{k}_n = 1 \quad \text{and} \quad \mathbf{i}_n \cdot \mathbf{j}_n = \mathbf{i}_n \cdot \mathbf{k}_n = \mathbf{j}_n \cdot \mathbf{k}_n = 0$$

we obtain three linear equations

$$\begin{aligned} x_n &= x_m(\mathbf{i}_n \cdot \mathbf{i}_m) + y_m(\mathbf{i}_n \cdot \mathbf{j}_m) + z_m(\mathbf{i}_n \cdot \mathbf{k}_m) + x_n^{(O_m)} \\ y_n &= x_m(\mathbf{j}_n \cdot \mathbf{i}_m) + y_m(\mathbf{j}_n \cdot \mathbf{j}_m) + z_m(\mathbf{j}_n \cdot \mathbf{k}_m) + y_n^{(O_m)} \\ z_n &= x_m(\mathbf{k}_n \cdot \mathbf{i}_m) + y_m(\mathbf{k}_n \cdot \mathbf{j}_m) + z_m(\mathbf{k}_n \cdot \mathbf{k}_m) + z_n^{(O_m)} \end{aligned} \quad (1.3.4)$$

which may be represented in matrix form as follows:

$$\begin{bmatrix} x_n \\ y_n \\ z_n \end{bmatrix} = \begin{bmatrix} a_{11} & a_{12} & a_{13} \\ a_{21} & a_{22} & a_{23} \\ a_{31} & a_{32} & a_{33} \end{bmatrix} \begin{bmatrix} x_m \\ y_m \\ z_m \end{bmatrix} + \begin{bmatrix} a_{14} \\ a_{24} \\ a_{34} \end{bmatrix} \quad (1.3.5)$$

As noted in section 1.2, a general element $a_{k\ell}$ ($k = 1, 2, 3$; $\ell = 1, 2, 3$) is the direction cosine of new unit vector k and old unit vector ℓ ; unit vectors \mathbf{i} , \mathbf{j} , \mathbf{k} correspond to the numbers 1, 2, and 3, respectively. Elements a_{14} , a_{24} , and a_{34} represent the new coordinates $x_n^{(O_m)}$, $y_n^{(O_m)}$, and $z_n^{(O_m)}$ of the old origin O_m ; that is, the location of the old origin in the new coordinate system.

Coordinate transformation (eq. (1.3.5)) requires mixed matrix operations where both multiplication and addition of matrices must be used. Matrix representation of coordinate transformation will need only multiplication of matrices if position vectors are determined by homogeneous coordinates. These coordinate transformations were applied to spatial linkages by Denavit and Hartenberg (1955) and to spatial gears by Litvin (1955). Homogeneous coordinates of a point in three-dimensional space are determined by four numbers (x', y', z', t') which are not equal to zero simultaneously and of which only three are independent. Assuming $t' \neq 0$, regular coordinates and homogeneous coordinates are related as follows:

$$x = \frac{x'}{t'} \quad y = \frac{y'}{t'} \quad z = \frac{z'}{t'} \quad (1.3.6)$$

With $t' = 1$, a point may be specified by homogeneous coordinates such as $(x, y, z, t = 1)$, and thus linear equations (1.3.4) may be represented as

$$\begin{aligned} x_n &= a_{11}x_m + a_{12}y_m + a_{13}z_m + a_{14}t_m \\ y_n &= a_{21}x_m + a_{22}y_m + a_{23}z_m + a_{24}t_m \\ z_n &= a_{31}x_m + a_{32}y_m + a_{33}z_m + a_{34}t_m \\ t_n &= t_m = 1 \end{aligned} \quad (1.3.7)$$

The matrix representation of equation system (1.3.7) is

$$\begin{bmatrix} x_n \\ y_n \\ z_n \\ t_n = 1 \end{bmatrix} = \begin{bmatrix} a_{11} & a_{12} & a_{13} & a_{14} \\ a_{21} & a_{22} & a_{23} & a_{24} \\ a_{31} & a_{32} & a_{33} & a_{34} \\ 0 & 0 & 0 & 1 \end{bmatrix} \begin{bmatrix} x_m \\ y_m \\ z_m \\ t_m = 1 \end{bmatrix} \quad (1.3.8)$$

or in shortened form

$$[r_n] = [M_{nm}][r_m] \quad (1.3.9)$$

Unlike transformation (1.3.5), coordinate transformation (1.3.8) needs only one type of operation – multiplication of matrices.

Let us now develop the inverse coordinate transformation, from system S_n to system S_m , which may be expressed by the following linear equations:

$$\begin{aligned} x_m &= b_{11}x_n + b_{12}y_n + b_{13}z_n + b_{14}t_n \\ y_m &= b_{21}x_n + b_{22}y_n + b_{23}z_n + b_{24}t_n \\ z_m &= b_{31}x_n + b_{32}y_n + b_{33}z_n + b_{34}t_n \\ t_m &= t_n = 1 \end{aligned} \quad (1.3.10)$$

The matrix representation of equation (1.3.10) is

$$\begin{bmatrix} x_m \\ y_m \\ z_m \\ t_m = 1 \end{bmatrix} = \begin{bmatrix} b_{11} & b_{12} & b_{13} & b_{14} \\ b_{21} & b_{22} & b_{23} & b_{24} \\ b_{31} & b_{32} & b_{33} & b_{34} \\ 0 & 0 & 0 & 1 \end{bmatrix} \begin{bmatrix} x_n \\ y_n \\ z_n \\ t_n = 1 \end{bmatrix} \quad (1.3.11)$$

or

$$[r_n] = [M_{nm}][r_n] \quad (1.3.12)$$

The inverse coordinate transformation exists indeed, if the system of linear equations (1.3.7) has a unique solution for unknowns x_m, y_m, z_m, t_m (in terms of x_n, y_n, z_n, t_n and elements $a_{k\ell}$ ($k = 1, 2, 3; \ell = 1, 2, 3, 4$)). For this the determinant of the coefficient matrix must differ from zero; that is,

$$\det M_{nm} = \begin{vmatrix} a_{11} & a_{12} & a_{13} & a_{14} \\ a_{21} & a_{22} & a_{23} & a_{24} \\ a_{31} & a_{32} & a_{33} & a_{34} \\ 0 & 0 & 0 & 1 \end{vmatrix} = \begin{vmatrix} a_{11} & a_{12} & a_{13} \\ a_{21} & a_{22} & a_{23} \\ a_{31} & a_{32} & a_{33} \end{vmatrix} \neq 0 \quad (1.3.13)$$

If inequality (1.3.13) is observed, new coordinates (x_m, y_m, z_m, t_m) may be expressed in terms of x_n, y_n, z_n, t_n and elements $b_{k\ell}$ of the matrix $[M_{mn}]$ (eq. (1.3.11)). Therefore, inequality (1.3.13) is the requirement for existence of an inverse matrix.

Let us now express elements $b_{k\ell}$ of matrix $[M_{mn}]$ in terms of elements $a_{k\ell}$ of given matrix $[M_{nm}]$. The product of the given matrix and its inverse yields

$$[M_{nm}][M_{mn}] = [M_{mn}][M_{nm}] = [I] \quad (1.3.14)$$

where $[I]$ is the 4×4 unitary matrix. It results from equation (1.3.14) that

$$[M_{mn}] = \begin{bmatrix} a_{11} & a_{21} & a_{31} & b_{14} \\ a_{12} & a_{22} & a_{32} & b_{24} \\ a_{13} & a_{23} & a_{33} & b_{34} \\ 0 & 0 & 0 & 1 \end{bmatrix} \quad (1.3.15)$$

where

$$\begin{aligned} b_{14} &= -(a_{11}a_{14} + a_{21}a_{24} + a_{31}a_{34}) \\ b_{24} &= -(a_{12}a_{14} + a_{22}a_{24} + a_{32}a_{34}) \\ b_{34} &= -(a_{13}a_{14} + a_{23}a_{24} + a_{33}a_{34}) \end{aligned} \quad (1.3.16)$$

and $a_{k\ell}$ are elements of matrix

$$[M_{nm}] = \begin{bmatrix} a_{11} & a_{12} & a_{13} & a_{14} \\ a_{21} & a_{22} & a_{23} & a_{24} \\ a_{31} & a_{32} & a_{33} & a_{34} \\ 0 & 0 & 0 & 1 \end{bmatrix} \quad (1.3.17)$$

Equations (1.3.15) and (1.3.16) may be derived in a rigorous manner as follows:

Step 1.—Set up the 3×3 submatrix $[L_{nm}]$ from $[M_{nm}]$ and determine its transpose $[L_{nm}]^T$, which is equal to the submatrix $[L_{mn}]$, where

$$[L_{mn}] = \begin{bmatrix} b_{11} & b_{12} & b_{13} \\ b_{21} & b_{22} & b_{23} \\ b_{31} & b_{32} & b_{33} \end{bmatrix} = [L_{nm}]^T = \begin{bmatrix} a_{11} & a_{12} & a_{13} \\ a_{21} & a_{22} & a_{23} \\ a_{31} & a_{32} & a_{33} \end{bmatrix}^T = \begin{bmatrix} a_{11} & a_{21} & a_{31} \\ a_{12} & a_{22} & a_{32} \\ a_{13} & a_{23} & a_{33} \end{bmatrix} \quad (1.3.18)$$

Matrix equations (1.3.18) determine nine elements $b_{k\ell}$ in terms of elements $a_{k\ell}$ ($k = 1, 2, 3$; $\ell = 1, 2, 3$).

Step 2.—To express elements b_{14} , b_{24} , and b_{34} in terms of elements $a_{k\ell}$, multiply elements of corresponding columns of known $[M_{nm}]$, add the products, and change the sign of the final result as it is shown in the following expressions:

$$b_{14} = - (a_{11}a_{14} + a_{21}a_{24} + a_{31}a_{34}) \rightarrow \begin{bmatrix} a_{11} & a_{12} & a_{13} & a_{14} \\ a_{21} & a_{22} & a_{23} & a_{24} \\ a_{31} & a_{32} & a_{33} & a_{34} \\ 0 & 0 & 0 & 1 \end{bmatrix}$$

$$b_{24} = - (a_{12}a_{14} + a_{22}a_{24} + a_{32}a_{34}) \rightarrow \begin{bmatrix} a_{11} & a_{12} & a_{13} & a_{14} \\ a_{21} & a_{22} & a_{23} & a_{24} \\ a_{31} & a_{32} & a_{33} & a_{34} \\ 0 & 0 & 0 & 1 \end{bmatrix}$$

$$b_{34} = - (a_{13}a_{14} + a_{23}a_{24} + a_{33}a_{34}) \rightarrow \begin{bmatrix} a_{11} & a_{12} & a_{13} & a_{14} \\ a_{21} & a_{22} & a_{23} & a_{24} \\ a_{31} & a_{32} & a_{33} & a_{34} \\ 0 & 0 & 0 & 1 \end{bmatrix}$$

As noted in section 1.2, the matrix method of coordinate transformation works equally well between rigidly connected coordinate systems and between systems which move relative to one another. If systems S_m and S_n are rigidly connected, all elements of matrices $[M_{nm}]$ (and thus $[M_{mn}]$) are constant. Consequently, point M in one system is seen as the same point in the other system, although M is specified with different coordinates in each system. If, however, one coordinate system moves relative to the other, some elements of $[M_{nm}]$ vary in the process of motion, and point M of the moving system traces out a path in the fixed system.

To perform successive coordinate transformation, we need only follow the product rule of matrix algebra. For instance, the matrix equation

$$[r_p] = [M_{p(p-1)}][M_{(p-1)(p-2)}] \dots [M_{32}][M_{21}][r_1] \quad (1.3.19)$$

represents successive coordinate transformation from system S_1 to S_2 , from S_2 to S_3 , . . . , to S_p .

To perform a transformation of vector components, we need only apply 3×3 submatrices $[L]$, which may be obtained by eliminating the last row and last column of the corresponding matrix $[M]$. This results from the fact that vector components (projections on coordinate axes) do not depend on the location of origin of the coordinate system.

The transformation of vector components of vector \mathbf{A} from system S_m to S_n is represented by the matrix equation

$$[A_n] = [L_{nm}][A_m] \quad (1.3.20)$$

where

$$[A_n] = \begin{bmatrix} A_{xn} \\ A_{yn} \\ A_{zn} \end{bmatrix} \quad [L_{nm}] = \begin{bmatrix} a_{11} & a_{12} & a_{13} \\ a_{21} & a_{22} & a_{23} \\ a_{31} & a_{32} & a_{33} \end{bmatrix} \quad [A_m] = \begin{bmatrix} A_{xm} \\ A_{ym} \\ A_{zm} \end{bmatrix} \quad (1.3.21)$$

Example problem 1.3.1 Gears 1 and 2 rotate about axes z_f and z_p (fig. 1.3.2), which form a crossing angle γ and shortest axes distance C . Consider coordinate systems S_1 , S_2 , and S_f , which are rigidly connected to gear 1, gear 2, and the frame, respectively. The auxiliary system S_p is also rigidly connected to the frame.

By using the method of successive coordinate transformations described above, determine the transformation matrix $[M_{21}]$ for systems S_1 , S_f , S_p , and S_2 , which are shown in figures 1.3.2 and 1.3.3. Obtain the three equations which relate (x_2, y_2, z_2) with (x_1, y_1, z_1) . Find the inverse matrix $[M_{12}]$.

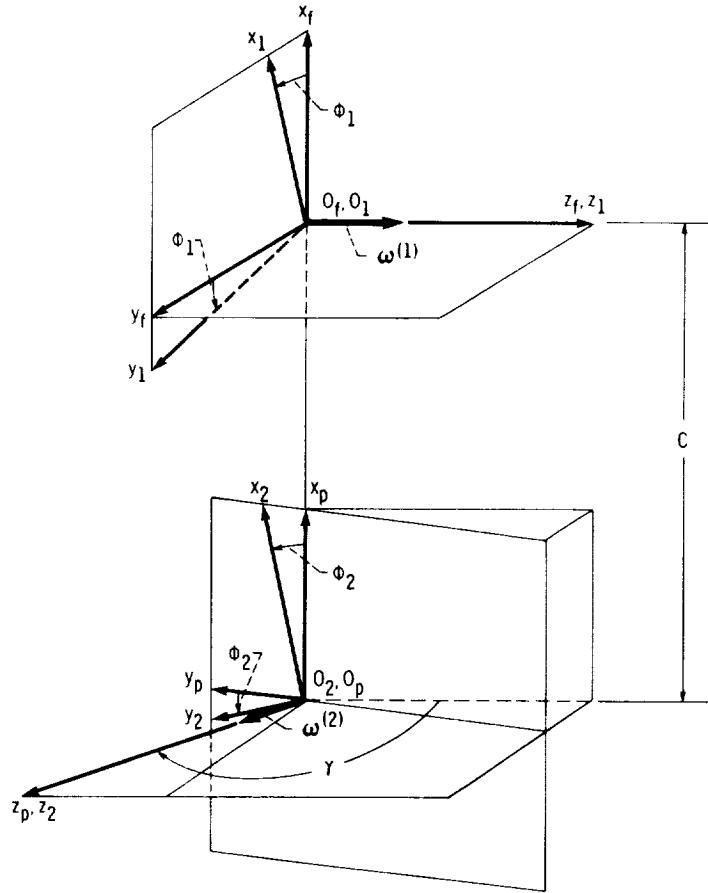


Figure 1.3.2.

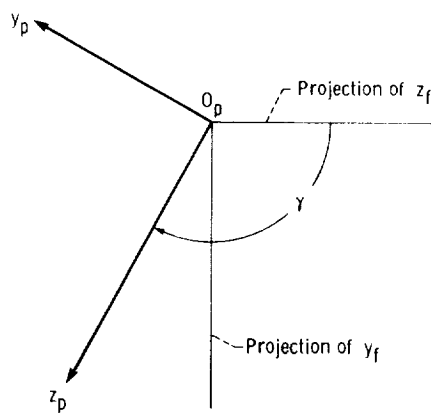


Figure 1.3.3.

Solution. The transformation matrices are as follows:

$$[M_{f1}] = \begin{bmatrix} \cos \phi_1 & -\sin \phi_1 & 0 & 0 \\ \sin \phi_1 & \cos \phi_1 & 0 & 0 \\ 0 & 0 & 1 & 0 \\ 0 & 0 & 0 & 1 \end{bmatrix} \quad (1.3.22)$$

$$[M_{pf}] = \begin{bmatrix} 1 & 0 & 0 & C \\ 0 & \cos \gamma & -\sin \gamma & 0 \\ 0 & \sin \gamma & \cos \gamma & 0 \\ 0 & 0 & 0 & 1 \end{bmatrix} \quad (1.3.23)$$

$$[M_{2p}] = \begin{bmatrix} \cos \phi_2 & \sin \phi_2 & 0 & 0 \\ -\sin \phi_2 & \cos \phi_2 & 0 & 0 \\ 0 & 0 & 1 & 0 \\ 0 & 0 & 0 & 1 \end{bmatrix} \quad (1.3.24)$$

The matrix product is thus

$$[M_{21}] = [M_{2p}][M_{pf}][M_{f1}]$$

$$= \begin{bmatrix} \cos \phi_1 \cos \phi_2 & -\sin \phi_1 \cos \phi_2 & -\sin \gamma \sin \phi_2 & C \cos \phi_2 \\ + \cos \gamma \sin \phi_1 \sin \phi_2 & + \cos \gamma \cos \phi_1 \sin \phi_2 & & \\ -\cos \phi_1 \sin \phi_2 & \sin \phi_1 \sin \phi_2 & -\sin \gamma \cos \phi_2 & -C \sin \phi_2 \\ + \cos \gamma \sin \phi_1 \cos \phi_2 & + \cos \gamma \cos \phi_1 \cos \phi_2 & & \\ \sin \gamma \sin \phi_1 & \sin \gamma \cos \phi_1 & \cos \gamma & 0 \\ 0 & 0 & 0 & 1 \end{bmatrix} \quad (1.3.25)$$

Coordinates (x_2, y_2, z_2) and (x_1, y_1, z_1) are related by the equations

$$\begin{aligned} x_2 &= x_1(\cos \phi_1 \cos \phi_2 + \cos \gamma \sin \phi_1 \sin \phi_2) \\ &\quad + y_1(-\sin \phi_1 \cos \phi_2 + \cos \gamma \cos \phi_1 \sin \phi_2) \\ &\quad - z_1 \sin \gamma \sin \phi_2 + C \cos \phi_2 \\ y_2 &= x_1(-\cos \phi_1 \sin \phi_2 + \cos \gamma \sin \phi_1 \cos \phi_2) \\ &\quad + y_1(\sin \phi_1 \sin \phi_2 + \cos \gamma \cos \phi_1 \cos \phi_2) \\ &\quad - z_1 \sin \gamma \cos \phi_2 - C \sin \phi_2 \\ z_2 &= x_1 \sin \gamma \sin \phi_1 + y_1 \sin \gamma \cos \phi_1 + z_1 \cos \gamma \end{aligned} \quad (1.3.26)$$

$$t_2 = t_1 = 1$$

The inverse matrix $[M_{12}]$ is given by

$$[M_{12}] = \begin{bmatrix} \cos \phi_1 \cos \phi_2 & -\cos \phi_1 \sin \phi_2 & \sin \gamma \sin \phi_1 & -C \cos \phi_1 \\ +\cos \gamma \sin \phi_1 \sin \phi_2 & +\cos \gamma \sin \phi_1 \cos \phi_2 & & \\ -\sin \phi_1 \cos \phi_2 & \sin \phi_1 \sin \phi_2 & \sin \gamma \cos \phi_1 & C \sin \phi_1 \\ +\cos \gamma \cos \phi_1 \sin \phi_2 & +\cos \gamma \cos \phi_1 \cos \phi_2 & & \\ -\sin \gamma \sin \phi_2 & -\sin \gamma \cos \phi_2 & \cos \gamma & 0 \\ 0 & 0 & 0 & 1 \end{bmatrix} \quad (1.3.27)$$

Coordinates (x_1, y_1, z_1) are expressed in terms of (x_2, y_2, z_2) by the following equations:

$$\begin{aligned} x_1 &= x_2(\cos \phi_1 \cos \phi_2 + \cos \gamma \sin \phi_1 \sin \phi_2) \\ &\quad + y_2(-\cos \phi_1 \sin \phi_2 + \cos \gamma \sin \phi_1 \cos \phi_2) \\ &\quad + z_2 \sin \gamma \sin \phi_1 - C \cos \phi_1 \\ y_1 &= x_2(-\sin \phi_1 \cos \phi_2 + \cos \gamma \cos \phi_1 \sin \phi_2) \\ &\quad + y_2(\sin \phi_1 \sin \phi_2 + \cos \gamma \cos \phi_1 \cos \phi_2) \\ &\quad + z_2 \sin \gamma \cos \phi_1 + C \sin \phi_1 \\ z_1 &= -x_2 \sin \gamma \sin \phi_2 - y_2 \sin \gamma \cos \phi_2 + z_2 \cos \gamma \end{aligned} \quad (1.3.28)$$

$$t_1 = t_2 = 1$$

1.4 Generation of Curves and Surfaces in Matrix Representation

In some cases, curves (surfaces) applied in engineering mechanics may be determined as a locus of points (lines) generated by a point (line) of a moving body. Equations of such curves or surfaces may be derived by following the rules of coordinate transformation.

Figure 1.4.1(a) shows an extended epicycloid. This curve is generated by point M , which is connected to the plane of circle A (of radius ρ) as it rolls over circle I (of radius r). Points M_0 and M represent two positions of the generating point; A and I are the movable and fixed centres.

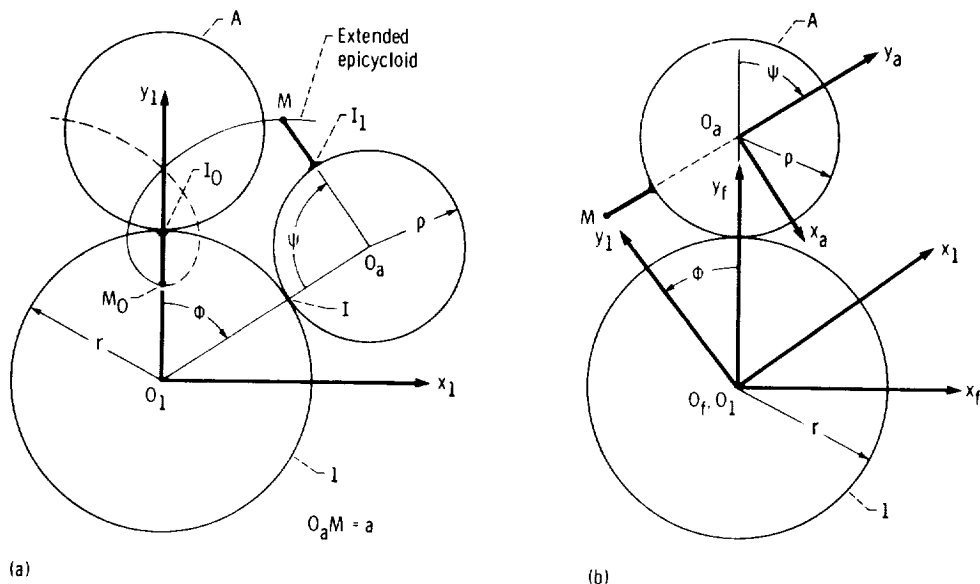


Figure 1.4.1.

The same extended epicycloid may be generated in coordinate system S_1 if both centrodes move (fig. 1.4.1(b)) and their angles of rotation ψ and θ are related; thus

$$\frac{\psi}{\theta} = \frac{r}{\rho}$$

We set up coordinate systems $S_a(x_a, y_a, z_a)$ and $S_1(x_1, y_1, z_1)$ rigidly connected to the rolling circles A and 1 and the fixed coordinate system $S_f(x_f, y_f, z_f)$.

Equations of the generated curve may be derived with the matrix equation

$$[r_1] = [M_{1a}][r_a] = [M_{1f}][M_{fa}][r_a] \quad (1.4.1)$$

where column matrices $[r_a]$ and $[r_1]$ represent the coordinates of the generating point and the generated curve, respectively; matrices $[M_{fa}]$ and $[M_{1f}]$ describe coordinate transformation from S_a to S_f and from S_f to S_1 . Here

$$[r_a] = \begin{bmatrix} 0 \\ -a \\ 1 \end{bmatrix} \quad [r_1] = \begin{bmatrix} x_1 \\ y_1 \\ 1 \end{bmatrix} \quad [M_{1f}] = \begin{bmatrix} \cos \phi & \sin \phi & 0 \\ -\sin \phi & \cos \phi & 0 \\ 0 & 0 & 1 \end{bmatrix}$$

$$[M_{fa}] = \begin{bmatrix} \cos \psi & \sin \psi & 0 \\ -\sin \psi & \cos \psi & r + \rho \\ 0 & 0 & 1 \end{bmatrix} \quad [M_{1a}] = \begin{bmatrix} \cos(\phi + \psi) & \sin(\phi + \psi) & (r + \rho) \sin \phi \\ -\sin(\phi + \psi) & \cos(\phi + \psi) & (r + \rho) \cos \phi \\ 0 & 0 & 1 \end{bmatrix} \quad (1.4.2)$$

where $a = O_aM$ (fig. 1.4.1 (b)). Matrix equation (1.4.1) and expressions (1.4.2) yield

$$x_1 = (r + \rho) \sin \phi - a \sin(\phi + \psi) \quad y_1 = (r + \rho) \cos \phi - a \cos(\phi + \psi) \quad (1.4.3)$$

Because of rolling we have that

$$\rho \psi = r \phi \quad (1.4.4)$$

and

$$\psi = \frac{r}{\rho} \phi \quad (1.4.5)$$

Equations (1.4.3) and (1.4.5) represent the extended epicycloid with functions

$$x_1(\phi) \quad y_1(\phi) \quad \phi_1 < \phi < \phi_2 \quad (1.4.6)$$

The alternative way of determining these functions is based on the vector equation (fig. 1.4.1(a))

$$\overline{O_1M} = \overline{O_1O_a} + \overline{O_aM} \quad (1.4.7)$$

Multiplying both sides of this vector equation successively by unit vectors \mathbf{i}_1 and \mathbf{j}_1 of coordinate axes x_1 and y_1 , we get

$$x_1 = \overline{O_1M} \cdot \mathbf{i}_1 = \overline{O_1O_a} \cdot \mathbf{i}_1 + \overline{O_aM} \cdot \mathbf{i}_1 = (r + \rho) \sin \phi - a \sin (\phi + \psi)$$

$$y_1 = \overline{O_1M} \cdot \mathbf{j}_1 = \overline{O_1O_a} \cdot \mathbf{j}_1 + \overline{O_aM} \cdot \mathbf{j}_1 = (r + \rho) \cos \phi - a \cos (\phi + \psi)$$

These equations concur with equations (1.4.3).

Generally, we are able to use two alternative methods to generate plane curves. However, the great advantage of the matrix method of curve and surface generation becomes more obvious for the case of surface generation. In the following example, a plane curve L generates, in screw motion, a surface called a helicoid (fig. 1.4.2(a)), which may be represented as a locus of lines L . The angle of rotation ψ and the axial displacement s are related by the equation

$$s = p\psi \quad (1.4.8)$$

Here p is the parameter of screw motion—the pitch of the screw—and is given by

$$p = \frac{h}{2\pi} \quad (1.4.9)$$

where h is the axial displacement corresponding to one complete revolution.

Assume that the plane curve L is given in coordinate system $S_a(x_a, y_a)$ (fig. 1.4.2(b)) by equations

$$x_a = x_a(\theta) \quad y_a = y_a(\theta) \quad z_a = 0 \quad \theta_1 \leq \theta \leq \theta_2 \quad (1.4.10)$$

where parameter θ is the independent variable. The generated surface is determined in the coordinate system S_1 with the matrix equation

$$[r_1] = [M_{1a}][r_a] \quad (1.4.11)$$

where

$$[r_1] = \begin{bmatrix} x_1 \\ y_1 \\ z_1 \\ 1 \end{bmatrix} \quad [M_{1a}] = \begin{bmatrix} \cos \psi & -\sin \psi & 0 & 0 \\ \sin \psi & \cos \psi & 0 & 0 \\ 0 & 0 & 1 & p\psi \\ 0 & 0 & 0 & 1 \end{bmatrix} \quad [r_a] = \begin{bmatrix} x_a(\theta) \\ y_a(\theta) \\ 0 \\ 1 \end{bmatrix} \quad (1.4.12)$$

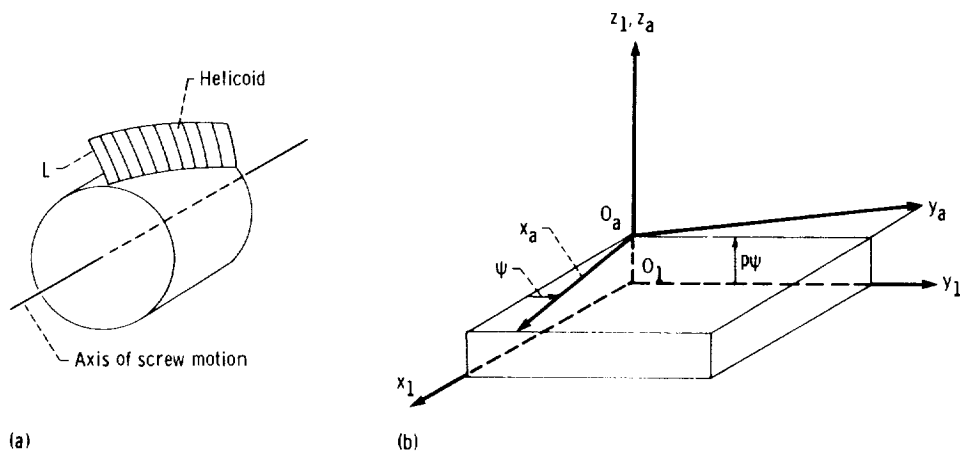


Figure 1.4.2.

Matrix equations (1.4.11) and (1.4.12) yield

$$x_1 = x_a(\theta) \cos \psi - y_a(\theta) \sin \psi \quad y_1 = x_a(\theta) \sin \psi + y_a(\theta) \cos \psi \quad z_1 = p\psi \quad (1.4.13)$$

where $\theta_1 \leq \theta \leq \theta_2$ and $\psi_1 \leq \psi \leq \psi_2$. Equations (1.4.13) represent the generated helicoid with surface coordinates θ and ψ . By surface coordinates it is meant that a point on the surface is uniquely specified by the given values of θ and ψ .

Problem 1.4.1 A surface of revolution is generated by rotation of a plane curve about the fixed axis z_1 . Figure 1.4.3 shows the axial section of the surface. The generating curve (fig. 1.4.4(a)) is represented in coordinate system $S_a(x_a, y_a, z_a)$ by equations

$$x_a = x_a(\theta) \quad y_a = 0 \quad z_a = z_a(\theta) \quad (1.4.14)$$

The angle of rotation ψ (fig. 1.4.4(b)) lies within the interval $0 \leq \psi \leq 2\pi$. Using the matrix method of surface generation, determine the equations of the generated surface.

Answer.

$$x_1 = x_a(\theta) \cos \psi \quad y_1 = x_a(\theta) \sin \psi \quad z_1 = z_a(\theta) \quad (1.4.15)$$

where $\theta_1 \leq \theta \leq \theta_2$ and $0 \leq \psi \leq 2\pi$.

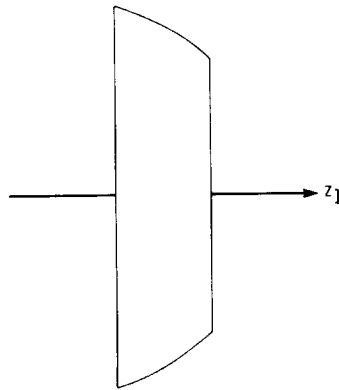


Figure 1.4.3.

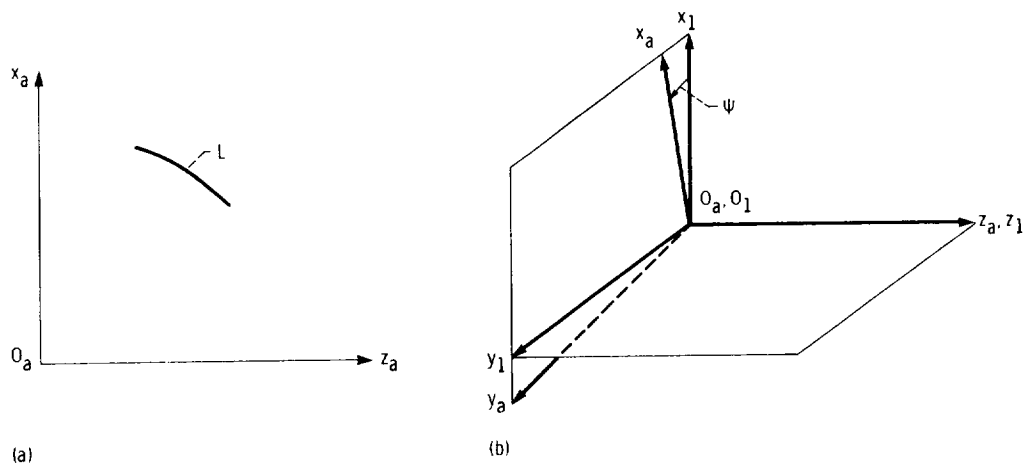


Figure 1.4.4.

Problem 1.4.2 With the conditions of problem 1.4.1, determine the equations of the surface generated by a segment of a circle with center C (fig. 1.4.5).

Answer.

$$x_1 = (a \cos \theta + C_x) \cos \psi \quad y_1 = (a \cos \theta + C_x) \sin \psi \quad z_1 = a \sin \theta + C_z \quad (1.4.16)$$

where

$$\theta_1 \leq \theta \leq \theta_2 \quad 0 \leq \psi \leq 2\pi \quad C_x < 0 \quad C_z < 0$$

Problem 1.4.3 With the conditions of problem 1.4.2, determine the equations for the conical surface generated by a segment of a straight line which forms an angle $180^\circ - \alpha$ with axis x_a (fig. 1.4.6). Coordinates x_a, z_a of a point M of the straight line are represented as functions of parameter θ .

Answer.

$$x_1 = (d - \theta \cos \alpha) \cos \psi \quad y_1 = (d - \theta \cos \alpha) \sin \psi \quad z_1 = \theta \sin \alpha \quad (1.4.17)$$

Problem 1.4.4 A spherical surface may be represented as a particular case of the surface represented by equations (1.4.16). Determine equations of a spherical surface which is centered at O_a (fig. 1.4.5).

Answer.

$$x_1 = a \cos \theta \cos \psi \quad y_1 = a \cos \theta \sin \psi \quad z_1 = a \sin \theta \quad (1.4.18)$$

where $0 \leq \theta \leq 2\pi$ and $0 \leq \psi \leq 2\pi$.

Problem 1.4.5 A screw surface is generated by a straight-lined edge AO_a of a blade (fig. 1.4.7(a)). While the blank of the screw rotates with angular velocity ω , the blade translates with velocity v in the direction of axis z_f . The velocities v and ω are related with the equation

$$v = p\omega = \frac{h}{2\pi} \omega \quad (1.4.19)$$

where p is the pitch of the screw and h is the lead of the thread (h is the axial displacement of the blade corresponding to one complete revolution of the thread).

The straight line $O_a A$ forms an angle α with axis x_a , and coordinates x_a, y_a are represented by functions $x_a(u), z_a(u)$. Determine the equations of the generated screw by using the matrix method of surface generation. The coordinate systems used are shown in figure 1.4.7(b).

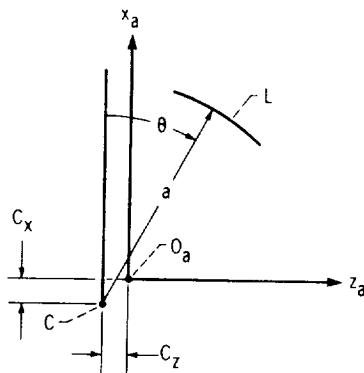


Figure 1.4.5.

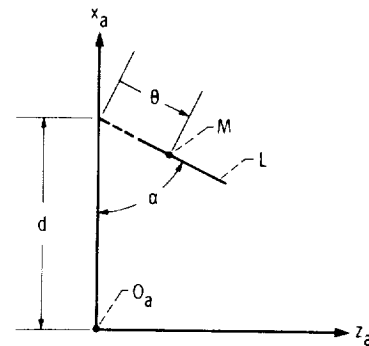


Figure 1.4.6.

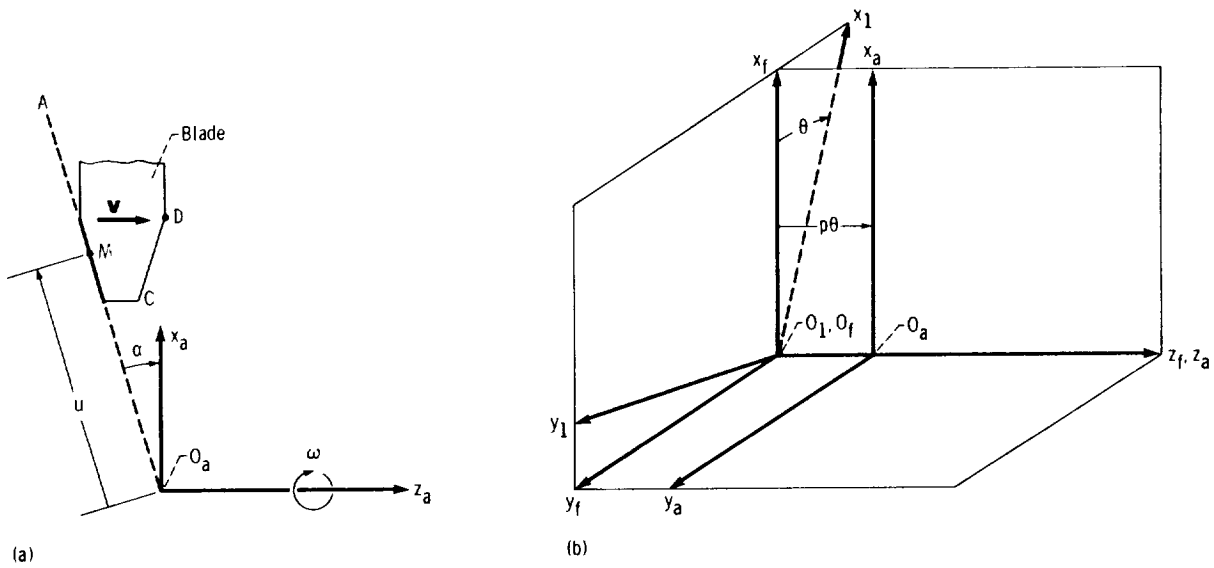


Figure 1.4.7.

Answer.

$$x_1 = u \cos \alpha \cos \theta \quad y_1 = u \cos \alpha \sin \theta \quad z_1 = -u \sin \alpha + p\theta \quad (1.4.20)$$

where $u_1 \leq u \leq u_2$ and $0 \leq \theta \leq 2\pi$.

Problem 1.4.6 With the main conditions of problem 1.4.5, assume that a left-handed screw surface is generated instead of a right-handed screw surface. Derive new equations from equation (1.4.20) for this surface.

Answer. Only the coordinate z_1 is changed; thus $z_1 = -u \sin \alpha - p\theta$.

Problem 1.4.7 With the main conditions of problem 1.4.5, assume that edge CD (fig. 1.4.7(a)) of the blade generates the screw surface belonging to the other side of the thread space. Derive equations of this surface from equation (1.4.20).

Answer. Change the sign before $\sin \alpha$, which yields the change of z_1 only; thus $z_1 = u \sin \alpha + p\theta$.

Chapter 2

Transformation of Motion

2.1 Parallel Axes of Rotation

Consider that two planar links 1 and 2 rotate in opposite directions about their respective centers O_1 and O_2 with angular velocities $\omega^{(1)}$ and $\omega^{(2)}$ (fig. 2.1.1). In the most general case, the ratio of angular velocities changes in the process of motion and may be represented by the function

$$m_{12} = \frac{\omega^{(1)}}{\omega^{(2)}} = f(\phi_1) \quad f(\phi_1) \in C^1 \quad a < \phi_1 < b \quad (2.1.1)$$

where ϕ_1 is the angle of rotation of link 1.

The instantaneous center of rotation, denoted I , is the point in the plane of motion at which the relative linear velocity of the links $\mathbf{v}_{I1/12}$ (or $\mathbf{v}_{I2/11}$) is equal to zero. The relative velocity may be represented as

$$\mathbf{v}_{I1/12} = \mathbf{v}_{I1} - \mathbf{v}_{I2} \quad (2.1.2)$$

or as

$$\mathbf{v}_{I2/11} = \mathbf{v}_{I2} - \mathbf{v}_{I1} \quad (2.1.3)$$

Here

$$\mathbf{v}_{I1} = \boldsymbol{\omega}^{(1)} \times \overline{O_1 I} \quad \text{and} \quad \mathbf{v}_{I2} = \boldsymbol{\omega}^{(2)} \times \overline{O_2 I} \quad (2.1.4)$$

are the linear velocities of links 1 and 2, respectively, at their common point I , and $\overline{O_1 I}$ and $\overline{O_2 I}$ are position vectors drawn from points O_1 and O_2 to point I , respectively.

Equations (2.1.2) and (2.1.3) show that the relative velocity $\mathbf{v}_{I1/12}$ (or $\mathbf{v}_{I2/11}$) is zero if

$$\mathbf{v}_{I1} = \mathbf{v}_{I2} \quad (2.1.5)$$

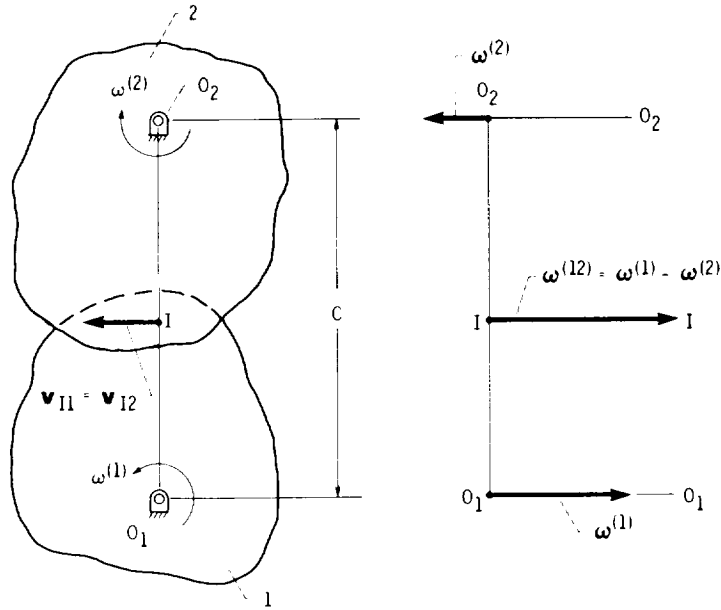


Figure 2.1.1.

Consequently, the instantaneous center of rotation is the point at which linear velocities v_{I1} and v_{I2} have the same direction and magnitude. For velocities v_{I1} and v_{I2} to have the same direction, the instantaneous center of rotation I must be located on the straight line drawn through centers O_1 and O_2 . For the magnitudes of v_{I1} and v_{I2} to be equal (i.e., $|v_{I1}| = |v_{I2}|$), point I must be located such that

$$\frac{O_1 I}{O_2 I} = \frac{\omega^{(2)}}{\omega^{(1)}} \quad (2.1.6)$$

The location of the instantaneous center of rotation on line $O_1 O_2$ is determined by the following equations:

$$\frac{O_2 I}{O_1 I} = \frac{\omega^{(1)}}{\omega^{(2)}} = m_{12}(\phi_1) \quad O_2 I + O_1 I = C \quad (2.1.7)$$

where C is the distance between centers O_1 and O_2 , henceforth known as the center distance (fig. 2.1.1). It may be easily verified that if the ratio m_{12} is not constant the instantaneous center of rotation I moves along line $O_1 O_2$ as the links rotate. It follows that point I is fixed in space if m_{12} is constant.

Figure 2.1.1 shows links 1 and 2 being rotated in opposite directions, whereby the instantaneous center of rotation I lies between centers O_1 and O_2 . If links 1 and 2 rotate in the same direction, point I is located outside line segment $O_1 O_2$ (fig. 2.1.2). For this case, assuming that $\omega^{(1)} > \omega^{(2)}$, we get

$$O_2 I - O_1 I = C \quad (2.1.8)$$

Considering the motion of links in a three-dimensional space, we may say that the relative motion of links 1 and 2 is rotation about the instantaneous axis of rotation $I-I$ (figs. 2.1.1 and 2.1.2). Axis $I-I$ passes through point I and is parallel to the link axes of rotation. The relative angular velocity of link 1 with respect to link 2 is given by

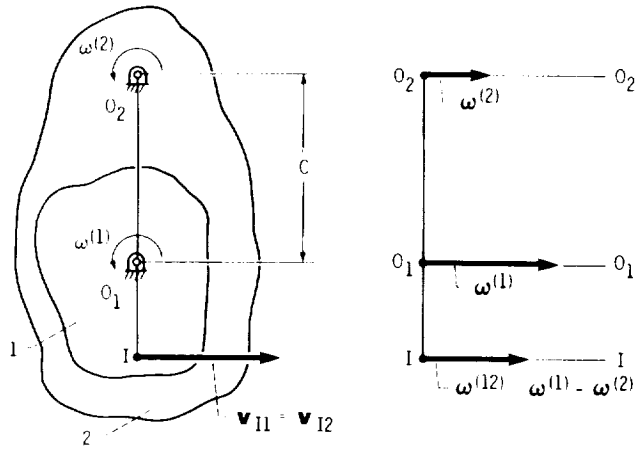


Figure 2.1.2.

$$\omega^{(12)} = \omega^{(1)} - \omega^{(2)} \quad (2.1.9)$$

A particular case of motion transformation is shown in figure 2.1.3. Here link 2 translates with linear velocity $\mathbf{v}^{(2)}$, while link 1 rotates about point O_1 with angular velocity $\omega^{(1)}$. Vector equation $\mathbf{v}_{I1} = \mathbf{v}_{I2}$ yields that (1) the instantaneous center of rotation I is located on a straight line O_1n , which is drawn through point O_1 perpendicular to vector $\mathbf{v}^{(2)}$ and (2) the distance O_1I is determined by the equation

$$O_1I = \frac{v^{(2)}}{\omega^{(1)}} = f(\phi_1) \quad f(\phi_1) \in C^1 \quad a \leq \phi_1 \leq b \quad (2.1.10)$$

In this case, the motion of link 1 relative to link 2 is rotation about axis $I-I$ with angular velocity

$$\omega^{(12)} = \omega^{(1)}$$

In the process of link motions, the instantaneous center of rotation (which is a point in the plane of motion) traces out a path on each link. The locus of instantaneous centers of rotation in a coordinate system rigidly connected to a movable link is known as the link centrode. Link centrodes roll over each other without sliding because the relative velocity $\mathbf{v}_{I1/I2}$ at their point of contact (point I) is equal to zero by definition.

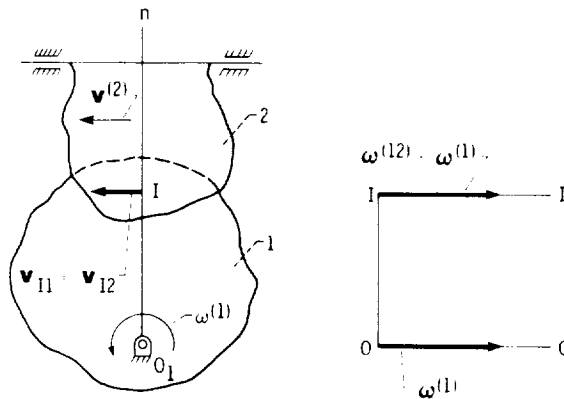


Figure 2.1.3.

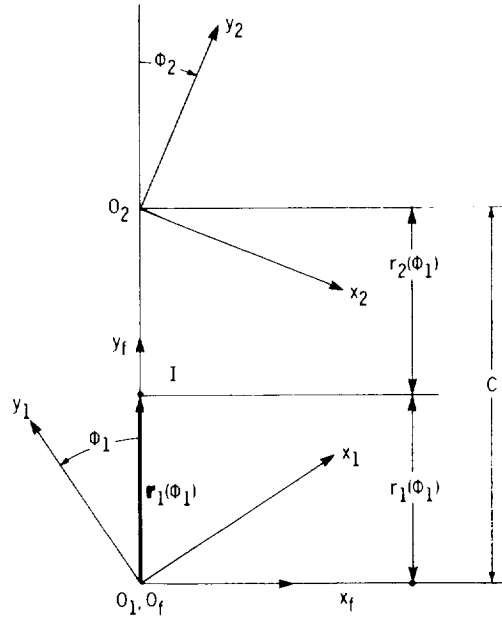


Figure 2.1.4.

Figure 2.1.4 shows three coordinate systems, $S_1(x_1, y_1)$, $S_2(x_2, y_2)$, and $S_f(x_f, y_f)$, which are rigidly connected to links 1 and 2 and the frame, respectively. Links 1 and 2 rotate in opposite directions.

Let us denote the lengths O_1I and O_2I by $r_1(\phi_1)$ and $r_2(\phi_1)$. The centroid of link 1 (i.e., the locus of points I in coordinate system $S_1(x_1, y_1)$) is determined by the following matrix equation (fig. 2.1.4):

$$[r_1] = [M_{1f}][r_f]$$

or by

$$\begin{bmatrix} x_1 \\ y_1 \\ 1 \end{bmatrix} = \begin{bmatrix} \cos \phi_1 & \sin \phi_1 & 0 \\ -\sin \phi_1 & \cos \phi_1 & 0 \\ 0 & 0 & 1 \end{bmatrix} \begin{bmatrix} 0 \\ r_1(\phi_1) \\ 1 \end{bmatrix} \quad (2.1.11)$$

This yields

$$x_1 = r_1(\phi_1) \sin \phi_1 \quad y_1 = r_1(\phi_1) \cos \phi_1 \quad (2.1.12)$$

Equations (2.1.12) represent the centroid of link 1 as a polar vector function $r_1(\phi_1)$ with a variable magnitude. Here ϕ_1 is the angle formed by vector $r_1(\phi_1)$ and axis y_1 .

On the basis of equations (2.1.7), the magnitude $|r_1| = O_1I$ may be determined with the following equation:

$$r_1 = \frac{O_2I}{m_{12}} = \frac{C - r_1}{m_{12}}$$

This yields

$$r_1 = \frac{C}{m_{12} + 1}$$

where

$$m_{12}(\phi_1) = \frac{\omega^{(1)}}{\omega^{(2)}} \quad m_{12}(\phi_1) \in C^1 \quad a \leq \phi_1 \leq b$$

Equations of gear centres may also be represented in polar form. Choosing axis y_1 as the polar axis (fig. 2.1.5(a)), we get

$$r_1 = \frac{C}{m_{12}(\phi_1) + 1} \quad \theta_1 = \phi_1 \quad m_{12}(\phi_1) \in C^1 \quad a \leq \phi_1 \leq b \quad (2.1.13)$$

The polar angle θ_1 , formed by vector \mathbf{r}_1 and the polar axis, is equal to the angle of rotation of gear 1 but is measured in the direction opposite that of gear 1 rotation.

The centre of gear 2 is the locus of instantaneous centers of rotation I in the coordinate system $S_2(x_2, y_2)$ (fig. 2.1.4). Equations of this centre are given by the matrix equation

$$[r_2] = [M_{2f}][r_f]$$

or by

$$\begin{bmatrix} x_2 \\ y_2 \\ 1 \end{bmatrix} = \begin{bmatrix} \cos \phi_2 & -\sin \phi_2 & C \sin \phi_2 \\ \sin \phi_2 & \cos \phi_2 & -C \cos \phi_2 \\ 0 & 0 & 1 \end{bmatrix} \begin{bmatrix} 0 \\ r_1(\phi_1) \\ 1 \end{bmatrix} \quad (2.1.14)$$

This yields

$$x_2 = [C - r_1(\phi_1)] \sin \phi_2 \quad y_2 = -[C - r_1(\phi_1)] \cos \phi_2 \quad (2.1.15)$$

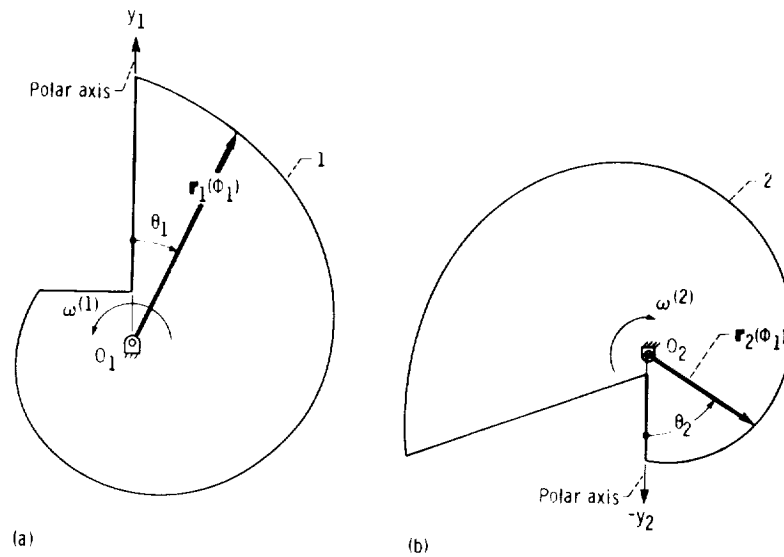


Figure 2.1.5.

Vector O_2I and the negative y_2 axis form the angle ϕ_2 (fig. 2.1.4).

Angles of gear rotation ϕ_2 and ϕ_1 are related by the following equation

$$\phi_2 = \int_0^{\phi_1} \frac{d\phi_1}{m_{12}(\phi_1)} \quad (2.1.16)$$

which results from the expression of the ratio function

$$m_{12}(\phi_1) = \frac{\omega^{(1)}}{\omega^{(2)}} = \frac{\frac{d\phi_1}{dt}}{\frac{d\phi_2}{dt}} = \frac{d\phi_1}{d\phi_2} \quad (2.1.17)$$

Equation (2.1.17) yields

$$d\phi_2 = \frac{d\phi_1}{m_{12}(\phi_1)} \quad \phi_2 = \int_0^{\phi_1} \frac{d\phi_1}{m_{12}(\phi_1)}$$

Centrode 2 may also be represented in polar form. Choosing the negative y_2 axis as the polar axis, we get

$$r_2 = O_2I = C - r_1(\phi_1) = C - \frac{C}{m_{12}(\phi_1) + 1} = C \frac{m_{12}(\phi_1)}{m_{12}(\phi_1) + 1}$$

The polar angle θ_2 (fig. 2.1.5(b)) is equal to the angle ϕ_2 but is measured in the direction opposite that of gear 2 rotation. Thus, the polar representation of the gear 2 centrode in terms of ϕ_1 is

$$r_2 = C \frac{m_{12}(\phi_1)}{m_{12}(\phi_1) + 1} \quad m_{12}(\phi_1) \in C^1 \quad a \leq \phi_1 \leq b \quad \theta_2 = \phi_2 = \int_0^{\phi_1} \frac{d\phi_1}{m_{12}(\phi_1)} \quad (2.1.18)$$

Centroides 1 and 2, which are in rolling contact, are shown in figure 2.1.6. Here it is assumed that the maximum angle of gear rotation is less than 360° and the centroides are open curves. If m_{12} is not equal to a constant, the link centroides correspond to those of noncircular gears. If m_{12} is equal to a constant, the centroides correspond to those of circular gears and are known as pitch circles. Since centroides roll over each other without sliding, the centrode arcs \widehat{MM}_1 and \widehat{MM}_2 , corresponding to the related angles θ_1 and θ_2 , have equal lengths. Also, the sum of centrode radii is constant, that is,

$$r_1(\theta_1) + r_2(\theta_2) = C \quad (2.1.19)$$

If we assume that links 1 and 2 rotate in the same direction (fig. 2.1.2) and that $\omega^{(1)} > \omega^{(2)}$, we get

$$m_{12}(\phi_1) = \frac{\omega^{(1)}}{\omega^{(2)}} = \frac{O_2I}{O_1I} = \frac{C + r_1}{r_1} \quad (2.1.20)$$

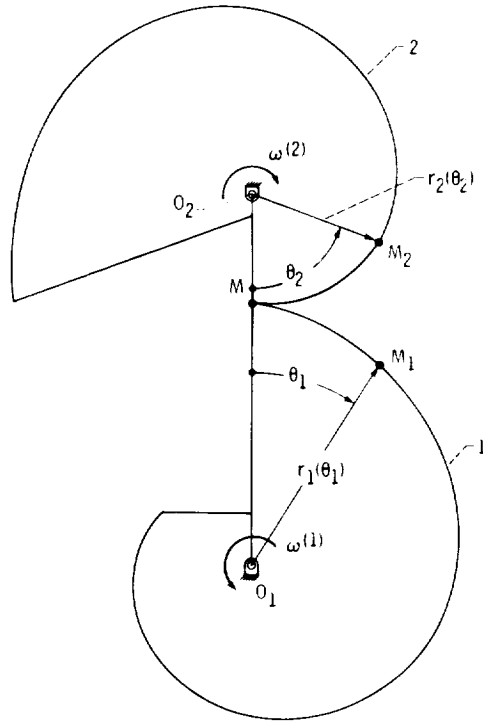


Figure 2.1.6.

Centroides 1 and 2 are represented by the following equations:

$$r_1 = \frac{C}{m_{12}(\phi_1) - 1} \quad \theta_1 = \phi_1 \quad m_{12}(\phi_1) \in C^1 \quad a \leq \phi_1 \leq b \quad (2.1.21)$$

$$r_2 = C \frac{m_{12}(\phi_1)}{m_{12}(\phi_1) - 1} \quad \theta_2 = \phi_2 = \int_0^{\phi_1} \frac{d\phi_1}{m_{12}(\phi_1)} \quad m_{12}(\phi_1) \in C^1 \quad a \leq \phi_1 \leq b \quad (2.1.22)$$

Let us now determine the link centroides which correspond to the transformation of motion shown in figure 2.1.3. Coordinate systems S_1 , S_2 , and S_f (fig. 2.1.7) are rigidly connected to links 1 and 2 and the frame, respectively. Let us denote the distance $O_f I$ as follows:

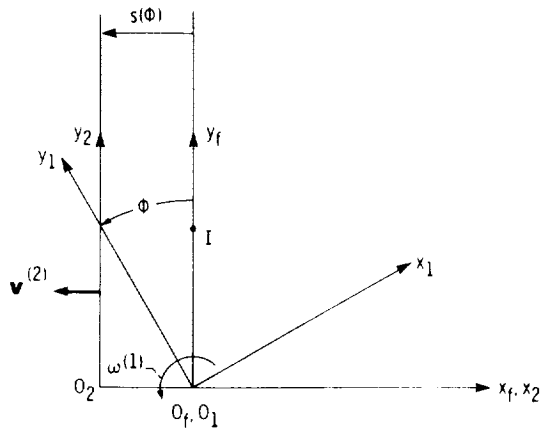


Figure 2.1.7.

$$O_1I = \frac{v^{(2)}}{\omega^{(1)}} = \psi(\phi) \quad (2.1.23)$$

(See eq. (2.1.10).)

The location of the instantaneous center of rotation I is represented in coordinate system S_f by the matrix

$$[r_f] = \begin{bmatrix} 0 \\ \psi(\phi) \\ 1 \end{bmatrix} \quad (2.1.24)$$

Link centrodes may be determined with the following matrix equations:

$$[r_1] = [M_{1f}][r_f] \quad (2.1.25)$$

$$[r_2] = [M_{2f}][r_f] \quad (2.1.26)$$

These yield

$$x_1 = \psi(\phi) \sin \phi \quad y_1 = \psi(\phi) \cos \phi \quad (2.1.27)$$

and

$$x_2 = s(\phi) \quad y_2 = \psi(\phi) \quad (2.1.28)$$

where $\psi(\phi) \in C^1$ and $a \leq \phi \leq b$.

Here $s(\phi)$ represents the displacement of the translating link (link 2) relative to the frame. This displacement function may be expressed as follows:

$$s(\phi) = \int_0^\phi \psi(\phi) d\phi \quad (2.1.29)$$

which results from the relation

$$\psi(\phi) = \frac{v^{(2)}}{\omega^{(1)}} = \frac{\frac{ds}{dt}}{\frac{d\phi}{dt}} = \frac{ds}{d\phi} \quad (2.1.30)$$

The centrode of link 1 may be represented in polar form with axis y_1 as its polar axis. The equation of this centrode is

$$r_1(\theta) = \psi(\phi) \quad \theta = \phi \quad (2.1.31)$$

where θ is the polar angle measured from axis y_1 in the direction opposite that of gear 1 rotation.

Figure 2.1.8 shows the centrodes of a noncircular gear (1) and its corresponding rack (2). These centrodes are known, respectively, as the pitch curve and the pitch line. If function $\psi(\phi)$ has a

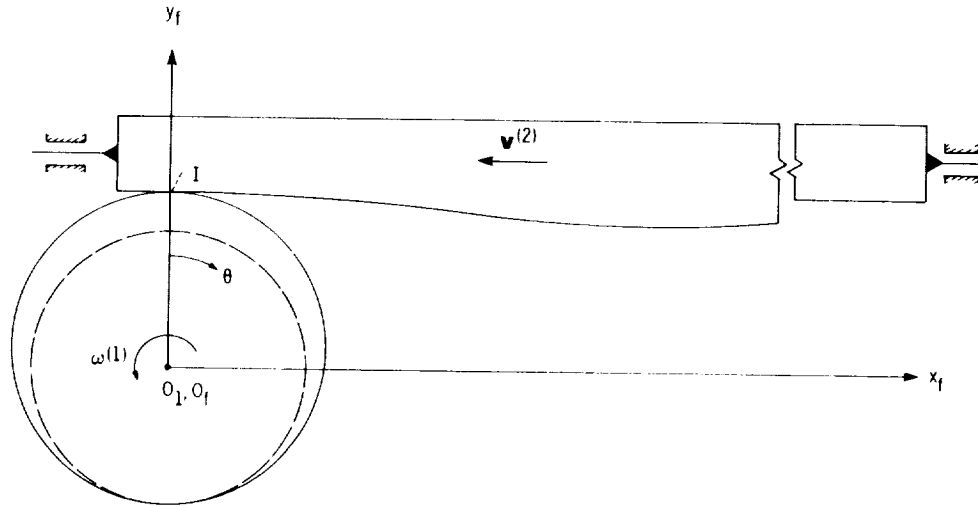


Figure 2.1.8.

constant value for all ϕ (as with a spur gear and its rack), centrode 1 is a circle (called the pitch circle), and centrode 2 is a straight line (called the pitch line).

Problem 2.1.1 Given the following:

- (1) The relationship of the gear rotation angles

$$\phi_2 = \frac{\phi_1}{a_2 + a_3\phi_1} \quad 0 \leq \phi_1 \leq \phi_{1,\max}$$

- (2) $\phi_{2,\max} = \phi_{1,\max}$

- (3) The magnitudes of the ratio function $m_{12}(\phi_1)$ at $\phi_1 = 0$ and $\phi_1 = \phi_{1,\max}$

- (4) The center distance C

- (5) The gears rotate in opposite directions.

Derive gear centrode equations (2.1.12) and (2.1.15), and calculate them by assuming $\phi_{1,\max} = \phi_{2,\max} = 5\pi/3$, $m_{12}(0) = 1/2.5$, and $m_{12}(\phi_{1,\max}) = 2.5$.

Hint: The key to this solution is the ratio function

$$m_{12}(\phi_1) = \frac{(a_2 + a_3\phi_1)^2}{a_2}$$

Coefficients a_2 and a_3 are related as follows:

$$m_{12}(0) = a_2 \quad \phi_{1,\max} = \frac{1 - a_2}{a_3}$$

Problem 2.1.2 Given the function

$$s(\phi) = a\phi + b \sin \phi \quad 0 \leq \phi \leq 2\pi$$

which relates the rack translation s and the gear angle of rotation ϕ ; (1) derive equations for the rack and gear centrodes, and compute them by assuming $a=2$ in. and $b=0.2$ in. and (2) find the coefficient b for which the centrodes are a straight line and a circle.

Hint: The key for solution is the function

$$\psi(\phi) = a + b \cos \phi$$

When $b = 0$, the gear centrode is a circle of radius a , and the rack centrode is a straight line tangent to this circle.

2.2 Intersected Axes of Rotation

Consider two rigid bodies 1 and 2 which rotate about axes Oa and Ob with angular velocities $\omega^{(1)}$ and $\omega^{(2)}$, respectively. Axes Oa and Ob are intersected and form the angle γ (fig. 2.2.1).

To determine the relative motion of the bodies at one instant, let us fix one of them, for instance body 1, and consider the motion of body 2. In order to fix body 1 and not change the relative motion of the two bodies, we rotate each body about axis Oa with the angular velocity $(-\omega^{(1)})$. Body 2 takes part in the following two rotations: (1) about axis Oa with angular velocity $(-\omega^{(1)})$ and (2) about axis Ob with angular velocity $\omega^{(2)}$. The resultant angular velocity represents the relative angular velocity of body 2 with respect to body 1. Thus,

$$\omega^{(21)} = \omega^{(2)} + (-\omega^{(1)}) = \omega^{(2)} - \omega^{(1)} \quad (2.2.1)$$

It is easily verified that this instantaneous relative motion is simply the rotation of body 2 about axis OI with angular velocity $\omega^{(21)}$ (fig. 2.2.1). Similarly, we may consider the instantaneous relative motion of body 1 with respect to body 2. In this case, body 2 is fixed while body 1 rotates about the same axis OI with angular velocity

$$\omega^{(12)} = \omega^{(1)} - \omega^{(2)} = -\omega^{(21)}$$

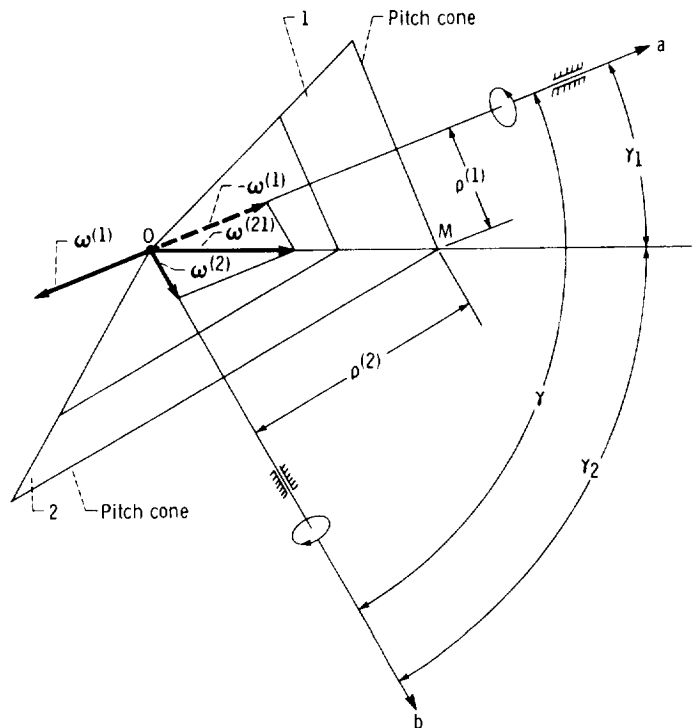


Figure 2.2.1.

Axis OI is known as the instantaneous axis of relative rotation. This axis forms angles γ_1 and γ_2 with axes of rotation Oa and Ob , respectively. These angles may be expressed in terms of the angular velocity ratio m_{12} and the angle γ (fig. 2.2.1) as follows:

$$\frac{\sin \gamma_2}{\sin \gamma_1} = \frac{\omega^{(1)}}{\omega^{(2)}} = m_{12} \quad \gamma_1 + \gamma_2 = \gamma \quad (2.2.2)$$

Expanding equations (2.2.2) yields

$$\frac{\sin (\gamma - \gamma_1)}{\sin \gamma_1} = \frac{\sin \gamma \cos \gamma_1 - \cos \gamma \sin \gamma_1}{\sin \gamma_1} = m_{12}$$

and

$$\cot \gamma_1 = \frac{m_{12} + \cos \gamma}{\sin \gamma} \quad \left(m_{12} = \frac{\omega^{(1)}}{\omega^{(2)}} \right) \quad (2.2.3)$$

Similarly, we may derive expressions for γ_2

$$\cot \gamma_2 = \frac{m_{21} + \cos \gamma}{\sin \gamma} = \frac{1 + m_{12} \cos \gamma}{m_{12} \sin \gamma} \quad (2.2.4)$$

where

$$m_{21} = \frac{\omega^{(2)}}{\omega^{(1)}} = \frac{1}{m_{12}}$$

The location of the instantaneous axis of rotation may also be determined as the locus of points M at which the linear velocity vectors of both bodies, $\mathbf{v}^{(1)}$ and $\mathbf{v}^{(2)}$, are equal. Thus,

$$\boldsymbol{\omega}^{(1)} \times \mathbf{r}^{(1)} = \boldsymbol{\omega}^{(2)} \times \mathbf{r}^{(2)} \quad (2.2.5)$$

Here $\mathbf{r}^{(i)}$ ($i = 1, 2$) is the position vector drawn to point M from an arbitrary point on the axis of rotation of body i ($i = 1, 2$). Since the point from which vector $\mathbf{r}^{(i)}$ is drawn may be chosen arbitrarily, so long as it lies on the axis of rotation i , let us choose (fig. 2.2.1)

$$\mathbf{r}^{(i)} = \boldsymbol{\rho}^{(i)}$$

Here $\boldsymbol{\rho}^{(i)}$ is the position vector drawn perpendicular to the axis of rotation of body i .

It results from equation (2.2.5) that vectors $\mathbf{v}^{(1)}$ and $\mathbf{v}^{(2)}$ are perpendicular to the plane Π drawn through axes Oa and Ob . Consequently, the instantaneous axis of relative rotation OI belongs to plane Π . Due to the equation

$$|\boldsymbol{\omega}^{(1)} \times \boldsymbol{\rho}^{(1)}| = |\boldsymbol{\omega}^{(2)} \times \boldsymbol{\rho}^{(2)}|$$

we get $\omega^{(1)}\rho^{(1)} = \omega^{(2)}\rho^{(2)}$.

This yields the relation

$$m_{12} = \frac{\omega^{(1)}}{\omega^{(2)}} = \frac{\rho^{(2)}}{\rho^{(1)}} = \frac{OM \sin \gamma_2}{OM \sin \gamma_1} = \frac{\sin \gamma_2}{\sin \gamma_1}$$

which coincides with equation (2.2.2).

The location of the instantaneous axis of rotation OI does not change in the process of body motion if rotation axes Oa and Ob form a constant angle γ and the angular velocity ratio is constant. As bodies 1 and 2 rotate about their respective axes, they roll (without sliding) over each other about an imaginary line of tangency, axis OI . Thus we may determine certain surfaces in bodies 1 and 2 which roll over each other. Extending the concept of centrodes to three-dimensional space, the locus of instantaneous axes of rotation in a coordinate system rigidly connected to a movable body is known as the body axode. The rolling surfaces described previously are, in fact, the axodes of links 1 and 2. For instance, if links 1 and 2 rotate with a constant angular velocity ratio m_{12} and if $\gamma = \text{constant}$, then the corresponding body axodes are cones with vertex angles of $2\gamma_1$ and $2\gamma_2$, respectively. Here γ_1 and γ_2 are related by equation (2.2.2).

The equations for body axodes may be determined using the matrix representation of coordinate transformation. Figure 2.2.2 shows fixed coordinate systems $S_f(x_f, y_f, z_f)$ and $S_a(x_a, y_a, z_a)$, which are rigidly connected to the frame, and coordinate system $S_1(x_1, y_1, z_1)$, which is rigidly connected to rotating body 1. Axis z_f is the instantaneous axis of rotation, which is expressed by the matrix

$$[r_f] = \begin{bmatrix} 0 \\ 0 \\ u \end{bmatrix} \quad (2.2.6)$$

where $u = |\overline{OM}|$; parameter u specifies the location of a point M on axis z_f .

The locus of instantaneous axes of rotation in coordinate system S_1 is represented by the matrix equation

$$[r_1] = [L_{1f}][r_f] = [L_{1a}][L_{af}][r_f]$$

$$= \begin{bmatrix} \cos \phi_1 & -\sin \phi_1 & 0 \\ \sin \phi_1 & \cos \phi_1 & 0 \\ 0 & 0 & 1 \end{bmatrix} \begin{bmatrix} \cos \gamma_1 & 0 & -\sin \gamma_1 \\ 0 & 1 & 0 \\ \sin \gamma_1 & 0 & \cos \gamma_1 \end{bmatrix} \begin{bmatrix} 0 \\ 0 \\ u \end{bmatrix} \quad (2.2.7)$$

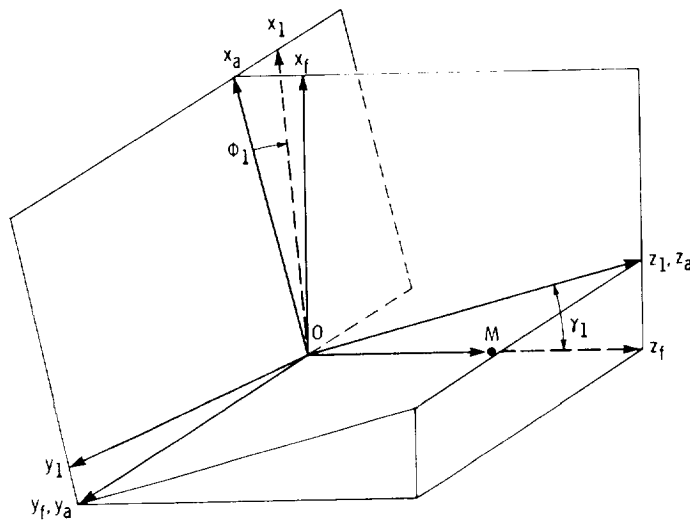


Figure 2.2.2.

This yields

$$x_1 = -u \cos \phi_1 \sin \gamma_1 \quad y_1 = -u \sin \phi_1 \sin \gamma_1 \quad z_1 = u \cos \gamma_1 \quad (2.2.8)$$

Equations (2.2.8) represent a cone with axis of symmetry z_1 and vertex angle $2\gamma_1$ (fig. 2.2.3); $u = OM$ and ϕ_1 are surface coordinates which determine the location of a point M on the cone surface. Similar coordinate transformations yield that the locus of the instantaneous axes of rotation z_2 in coordinate system $S_2(x_2, y_2, z_2)$ represents a cone with apex angle $2\gamma_2$. (System $S_2(x_2, y_2, z_2)$ is rigidly connected to moving body 2.) The cones with apex angles $2\gamma_1$ and $2\gamma_2$ are known as the pitch cones of links 1 and 2, respectively.

Problem 2.2.1 Consider the transformation of motion between intersected axes by which the surface of pitch cone 2 becomes a plane. Determine γ and m_{21} .

Hint: Apply equations (2.2.4) and (2.2.2).

Answer.

$$\gamma = 90^\circ + \gamma_1 \quad m_{21} = \sin \gamma_1$$

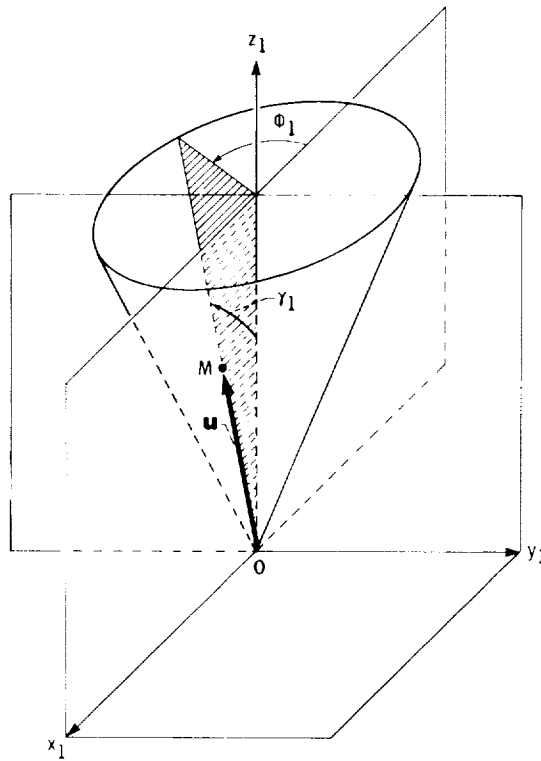


Figure 2.2.3.

2.3 Crossed Axes of Rotation: Relative Velocity

Consider two bodies 1 and 2 which rotate about crossed axes with angular velocities $\omega^{(1)}$ and $\omega^{(2)}$, respectively (fig. 2.3.1). The axes form an angle γ , and the shortest distance between them is $O_1O_2 = C$. Suppose M is a point which is common to both rotating bodies. The velocity $\mathbf{v}^{(1)}$ of point M of body 1 is

$$\mathbf{v}^{(1)} = \omega^{(1)} \times \mathbf{r}^{(1)} \quad (2.3.1)$$

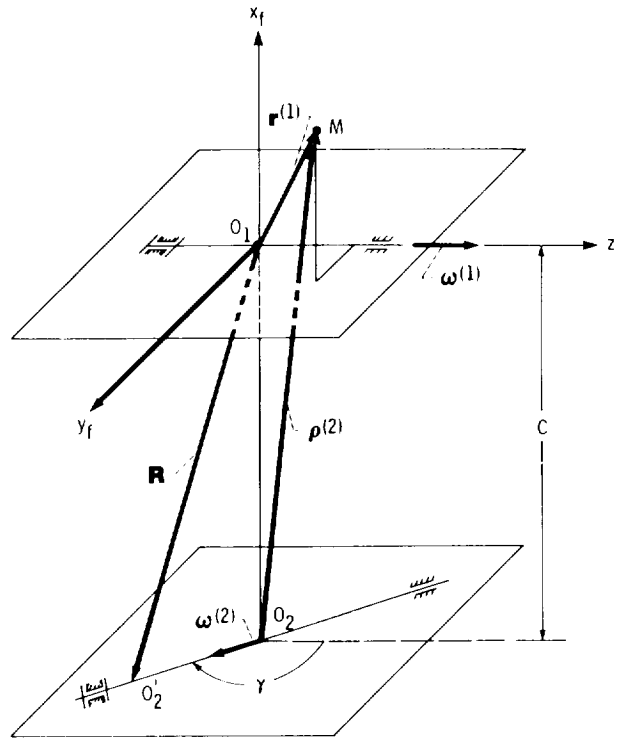


Figure 2.3.1.

where $\mathbf{r}^{(1)}$ is a position vector drawn to point M from an arbitrary point on the line of action of $\boldsymbol{\omega}^{(1)}$ (e.g., point O_1) (fig. 2.3.1). Similarly, we have

$$\mathbf{v}^{(2)} = \boldsymbol{\omega}^{(2)} \times \boldsymbol{\rho}^{(2)} \quad (2.3.2)$$

where $\boldsymbol{\rho}^{(2)}$ is a position vector drawn to point M from an arbitrary point on the line of action of $\boldsymbol{\omega}^{(2)}$ (e.g., point O_2) (fig. 2.3.1). The relative velocity $\mathbf{v}^{(12)}$ is

$$\mathbf{v}^{(12)} = \mathbf{v}^{(1)} - \mathbf{v}^{(2)} = (\boldsymbol{\omega}^{(1)} \times \mathbf{r}^{(1)}) - (\boldsymbol{\omega}^{(2)} \times \boldsymbol{\rho}^{(2)}) \quad (2.3.3)$$

Accordingly,

$$\mathbf{v}^{(21)} = \mathbf{v}^{(2)} - \mathbf{v}^{(1)} = (\boldsymbol{\omega}^{(2)} \times \boldsymbol{\rho}^{(2)}) - (\boldsymbol{\omega}^{(1)} \times \mathbf{r}^{(1)}) = -\mathbf{v}^{(12)}$$

Relative velocity $\mathbf{v}^{(12)}$ is defined in physical terms as the velocity of point M of body 1 as seen by an observer at point M of body 2. Similarly, $\mathbf{v}^{(21)}$ is the velocity of a point on body 2 as seen by an observer on body 1.

We may develop useful expressions for relative velocities $\mathbf{v}^{(12)}$ and $\mathbf{v}^{(21)}$ by replacing the sliding vector $\boldsymbol{\omega}^{(2)}$ to point O_1 . It is known from theoretical mechanics that the sliding vector $\boldsymbol{\omega}^{(2)}$ may be replaced by an equal vector $\boldsymbol{\omega}^{(2)}$ which passes through point O_1 and a moment

$$\mathbf{m} = \mathbf{R} \times \boldsymbol{\omega}^{(2)} \quad (2.3.4)$$

where \mathbf{R} is a position vector drawn from point O_1 to any point on the line of action of $\boldsymbol{\omega}^{(2)}$. For instance, we may choose $\mathbf{R} = \overline{O_1 O_2}$. Note that the moment \mathbf{m} has the units and physical meaning of linear velocity. By replacing $\boldsymbol{\omega}^{(2)}$ which passes through point O_2 with an equal vector passing through point O_1 and moment \mathbf{m} , we may represent the velocity $\mathbf{v}^{(2)}$ as

$$\mathbf{v}^{(2)} = \left(\boldsymbol{\omega}^{(2)} \times \mathbf{r}^{(1)} \right) + \left(\mathbf{R} \times \boldsymbol{\omega}^{(2)} \right) \quad (2.3.5)$$

It is easy to see (fig. 2.3.1) that equation (2.3.5) may be transformed into equation (2.3.2) as follows:

$$\mathbf{v}^{(2)} = \boldsymbol{\omega}^{(2)} \times \left(\mathbf{r}^{(1)} - \mathbf{R} \right) = \boldsymbol{\omega}^{(2)} \times \left(\mathbf{r}^{(1)} - \overline{O_1 O_2} \right) + \boldsymbol{\omega}^{(2)} \times \left(-\overline{O_2 O_2'} \right) = \boldsymbol{\omega}^{(2)} \times \boldsymbol{\rho}^{(2)} \quad (2.3.6)$$

Note that $\overline{O_1 O_2} + \boldsymbol{\rho}^{(2)} = \mathbf{r}^{(1)}$, and that the cross product $\boldsymbol{\omega}^{(2)} \times (-\overline{O_2 O_2'}) = 0$. (Here vectors $\overline{O_2 O_2'}$ and $\boldsymbol{\omega}^{(2)}$ are collinear.) With expressions (2.3.1) and (2.3.5), the relative velocity $\mathbf{v}^{(12)}$ may be represented as

$$\mathbf{v}^{(12)} = \left(\boldsymbol{\omega}^{(12)} \times \mathbf{r}^{(1)} \right) - \left(\mathbf{R} \times \boldsymbol{\omega}^{(2)} \right) \quad (2.3.7)$$

where $\boldsymbol{\omega}^{(12)} = \boldsymbol{\omega}^{(1)} - \boldsymbol{\omega}^{(2)}$. Also

$$\mathbf{v}^{(21)} = \left(\boldsymbol{\omega}^{(21)} \times \mathbf{r}^{(1)} \right) + \left(\mathbf{R} \times \boldsymbol{\omega}^{(2)} \right) \quad (2.3.8)$$

where $\boldsymbol{\omega}^{(21)} = \boldsymbol{\omega}^{(2)} - \boldsymbol{\omega}^{(1)}$.

Let us represent the relative velocity vector (1) in coordinate system S_f , which is rigidly connected to the frame and (2) in coordinate system S_1 , which is rigidly connected to body 1 (fig. 2.3.1). Taking into account that

$$\boldsymbol{\omega}^{(12)} = \omega^{(1)} \mathbf{k}_f - \left(\omega^{(2)} \sin \gamma \mathbf{j}_f + \omega^{(2)} \cos \gamma \mathbf{k}_f \right) \quad (2.3.9)$$

$$\mathbf{r}^{(1)} = x_f \mathbf{i}_f + y_f \mathbf{j}_f + z_f \mathbf{k}_f \quad (2.3.10)$$

$$\mathbf{R} = -C \mathbf{i}_f \quad (2.3.11)$$

(\mathbf{i}_f , \mathbf{j}_f , and \mathbf{k}_f are unit vectors of coordinate axes of system S_f), we get

$$\begin{aligned} \mathbf{v}_f^{(12)} &= \begin{bmatrix} \mathbf{i}_f & \mathbf{j}_f & \mathbf{k}_f \\ 0 & -\omega^{(2)} \sin \gamma & \omega^{(1)} - \omega^{(2)} \cos \gamma \\ x_f & y_f & z_f \end{bmatrix} - \begin{bmatrix} \mathbf{i}_f & \mathbf{j}_f & \mathbf{k}_f \\ -C & 0 & 0 \\ 0 & \omega^{(2)} \sin \gamma & \omega^{(2)} \cos \gamma \end{bmatrix} \\ &= \begin{bmatrix} -y_f(\omega^{(1)} - \omega^{(2)} \cos \gamma) - z_f \omega^{(2)} \sin \gamma \\ x_f(\omega^{(1)} - \omega^{(2)} \cos \gamma) - C \omega^{(2)} \cos \gamma \\ (x_f + C) \omega^{(2)} \sin \gamma \end{bmatrix} \end{aligned} \quad (2.3.12)$$

The relative velocity may be expressed in terms of components of coordinate system S_1 with the matrix equation

$$\left[v_1^{(12)} \right] = \left[L_{1f} \right] \left[v_f^{(12)} \right] \quad (2.3.13)$$

From figure 1.3.2, we have

$$[L_{1f}] = \begin{bmatrix} \cos \phi_1 & \sin \phi_1 & 0 \\ -\sin \phi_1 & \cos \phi_1 & 0 \\ 0 & 0 & 1 \end{bmatrix} \quad (2.3.14)$$

Expressions (2.3.12) to (2.3.14) yield

$$\begin{bmatrix} v_1^{(12)} \end{bmatrix} = \begin{bmatrix} (-y_f \cos \phi_1 + x_f \sin \phi_1)(\omega^{(1)} - \omega^{(2)} \cos \gamma) - z_f \omega^{(2)} \sin \gamma \cos \phi_1 - C \omega^{(2)} \cos \gamma \sin \phi_1 \\ (y_f \sin \phi_1 + x_f \cos \phi_1)(\omega^{(1)} - \omega^{(2)} \cos \gamma) + z_f \omega^{(2)} \sin \gamma \sin \phi_1 - C \omega^{(2)} \cos \gamma \cos \phi_1 \\ (x_f + C) \omega^{(2)} \sin \gamma \end{bmatrix} \quad (2.3.15)$$

The coordinate transformation from S_1 to S_f is

$$\begin{bmatrix} x_f \\ y_f \\ z_f \end{bmatrix} = \begin{bmatrix} \cos \phi_1 & -\sin \phi_1 & 0 \\ \sin \phi_1 & \cos \phi_1 & 0 \\ 0 & 0 & 1 \end{bmatrix} \begin{bmatrix} x_1 \\ y_1 \\ z_1 \end{bmatrix} \quad (2.3.16)$$

and thus

$$x_f = x_1 \cos \phi_1 - y_1 \sin \phi_1 \quad y_f = x_1 \sin \phi_1 + y_1 \cos \phi_1 \quad z_f = z_1 \quad (2.3.17)$$

Equations (2.3.15) and (2.3.17) yield

$$\begin{bmatrix} v_1^{(12)} \end{bmatrix} = \begin{bmatrix} -y_1 (\omega^{(1)} - \omega^{(2)} \cos \gamma) - z_1 \omega^{(2)} \sin \gamma \cos \phi_1 - C \omega^{(2)} \cos \gamma \sin \phi_1 \\ x_1 (\omega^{(1)} - \omega^{(2)} \cos \gamma) + z_1 \omega^{(2)} \sin \gamma \sin \phi_1 - C \omega^{(2)} \cos \gamma \cos \phi_1 \\ (x_1 \cos \phi_1 - y_1 \sin \phi_1 + C) \omega^{(2)} \sin \gamma \end{bmatrix} \quad (2.3.18)$$

Although equations (2.3.17) and (2.3.18) were derived for gearings with crossed axes, they may be applied for gear mechanisms with parallel and intersecting axes also. In the case of parallel axes of rotation with opposite directions of rotation, we set $\gamma = \pi$. In the case of intersecting axes of rotation with opposite directions of rotation, we set $C = 0$ and change the sign of $\omega^{(2)}$. We emphasize that both axes of rotation are now located in the plane $x_f = 0$ (fig. 2.3.2).

Problem 2.3.1 Consider rotation transformed between gears which rotate in the same direction on parallel axes. (1) Change equations (2.3.12) for relative velocity $v_f^{(12)}$ to make them applicable to this case. (2) Prove that the relative velocity is zero for points which belong to the instantaneous axis of rotation.

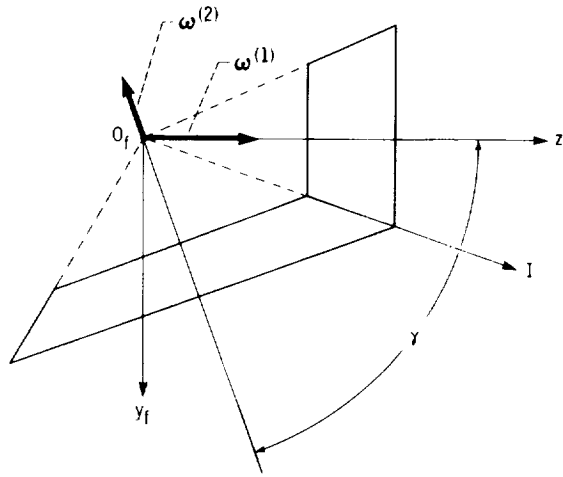


Figure 2.3.2.

Answer. Set $\gamma = 180^\circ$ and change the sign of $\omega^{(2)}$, or set $\gamma = 0$. The relative velocity $\mathbf{v}_f^{(12)}$ is zero for points where

$$x_f = C \frac{\omega^{(2)}}{\omega^{(1)} - \omega^{(2)}} \quad \text{and} \quad y_f = 0$$

These points belong to the instantaneous axis of rotation.

Problem 2.3.2 Consider the rotation between intersecting axes (fig. 2.3.2). (1) Change equations (2.3.12) to make them applicable to this case. (2) Prove that the relative velocity $\mathbf{v}_f^{(12)}$ is zero for points on the instantaneous axis of rotation.

Answer. Set $C = 0$, and change the sign for $\omega^{(2)}$. Vector $\mathbf{v}^{(12)}$ is zero for points

$$x_f = 0 \quad \text{and} \quad \frac{y_f}{z_f} = \tan \gamma_1$$

which belong to the instantaneous axis of rotation.

2.4 Crossed Axes of Rotation: Screw Axis of Relative Motion

Consider again the rotation of two bodies about their crossed axes with angular velocities $\omega^{(1)}$ and $\omega^{(2)}$ (fig. 2.4.1). The relative motion of body 1 with respect to body 2 may be represented as a motion with two components, (1) rotation about axis z_2 with angular velocity $(-\omega^{(2)})$ and (2) rotation about axis z_1 with angular velocity $\omega^{(1)}$. The resultant motion may be represented as a screw motion about some axis $s-s$ (fig. 2.4.1). The screw motion of a body is a general case of spatial motion which is represented as a rotation about and a translation along a single axis called the screw axis.

Let us replace vectors $\omega^{(1)}$ and $(-\omega^{(2)})$ to a point B which is located on the shortest distance between the axes of $\omega^{(1)}$ and $\omega^{(2)}$ (line segment O_1O_2). Vector $\omega^{(1)}$, which passes through point O_1 , is substituted by an equal vector $\omega^{(1)}$, which passes through point B , and the moment

$$\mathbf{m}_1 = \overline{BO}_1 \times \omega^{(1)} = -\overline{O_1B} \times \omega^{(1)} \quad (2.4.1)$$

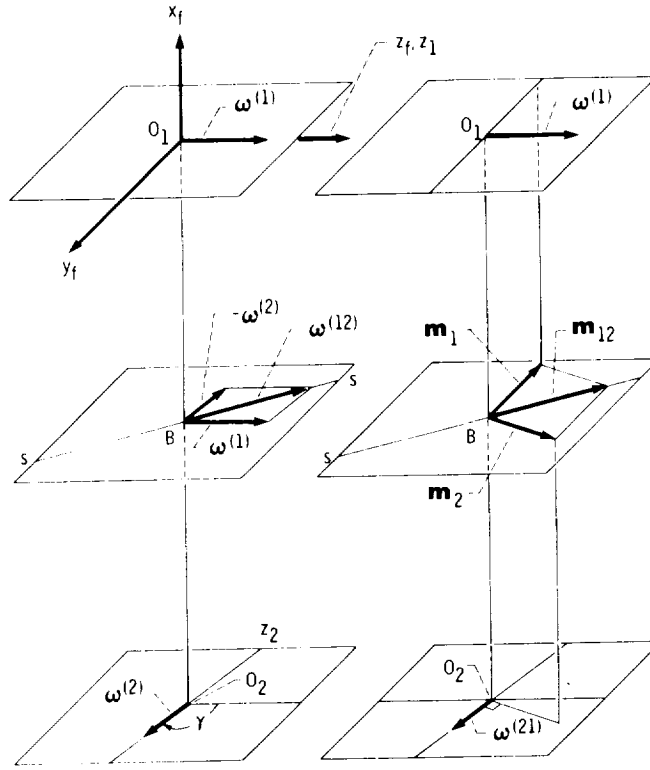


Figure 2.4.1.

Similarly, vector $-\omega^{(2)}$, which passes through point O_2 , is substituted by an equal vector $-\omega^{(2)}$, which passes through point B , and the moment

$$\mathbf{m}_2 = \overline{BO_2} \times (-\omega^{(2)}) = (\overline{O_1O_2} - \overline{O_1B}) \times (-\omega^{(2)}) \quad (2.4.2)$$

Consequently, vectors $\omega^{(1)}$ and $-\omega^{(2)}$, which pass through points O_1 and O_2 , respectively, are substituted by the vector

$$\omega^{(12)} = \omega^{(1)} + (-\omega^{(2)}) = \omega^{(1)} - \omega^{(2)} \quad (2.4.3)$$

and the moment

$$\mathbf{m} = \mathbf{m}_1 + \mathbf{m}_2 = (-\overline{O_1B} \times \omega^{(1)}) + (\overline{O_1O_2} - \overline{O_1B}) \times (-\omega^{(2)}) \quad (2.4.4)$$

Notice that both the magnitude and direction of moment \mathbf{m} depend on the location of point B , whereas the vector $\omega^{(12)}$ does not depend on this location.

Summarizing, we may say that the resultant motion of body 1 with respect to body 2 is the rotation with angular velocity $\omega^{(12)}$ about an axis which passes through point B and a translation with the linear velocity represented by equation (2.4.4).

Choosing a certain location of point B , we may represent the resultant relative motion as a screw motion; that is, rotation with angular velocity $\omega^{(12)}$ about axis s - s and sliding along this axis with velocity \mathbf{m} . This occurs if, by a certain location of point B , vector \mathbf{m} is collinear to vector $\omega^{(12)}$. The location of point B may be determined from the equation

$$\omega^{(12)} \times \mathbf{m} = 0 \quad (2.4.5)$$

We set up the coordinate system $S_f(x_f, y_f, z_f)$ rigidly connected to the frame and represent vector $\omega^{(12)}$ as

$$\boldsymbol{\omega}^{(12)} = -\omega^{(2)} \sin \gamma \mathbf{j}_f + (\omega^{(1)} - \omega^{(2)} \cos \gamma) \mathbf{k}_f \quad (2.4.6)$$

The moment \mathbf{m} is represented as follows:

$$\begin{aligned} \mathbf{m} &= \begin{vmatrix} \mathbf{i}_f & \mathbf{j}_f & \mathbf{k}_f \\ -x_f & 0 & 0 \\ 0 & 0 & \omega^{(1)} \end{vmatrix} + \begin{vmatrix} \mathbf{i}_f & \mathbf{j}_f & \mathbf{k}_f \\ -(C+x_f) & 0 & 0 \\ 0 & -\omega^{(2)} \sin \gamma & -\omega^{(2)} \cos \gamma \end{vmatrix} \\ &= \left[-C\omega^{(2)} \cos \gamma + x_f(\omega^{(1)} - \omega^{(2)} \cos \gamma) \right] \mathbf{j}_f + (C+x_f)\omega^{(2)} \sin \gamma \mathbf{k}_f \end{aligned} \quad (2.4.7)$$

where x_f determines the location of point B on axis x_f . Due to the collinearity of $\boldsymbol{\omega}^{(12)}$ and \mathbf{m} , we get

$$\frac{\omega^{(2)} \sin \gamma}{C\omega^{(2)} \cos \gamma - x_f(\omega^{(1)} - \omega^{(2)} \cos \gamma)} = \frac{\omega^{(1)} - \omega^{(2)} \cos \gamma}{(C+x_f)\omega^{(2)} \sin \gamma} \quad (2.4.8)$$

Equation (2.4.8) yields

$$x_f = -C \frac{m_{21}(m_{21} - \cos \gamma)}{1 - 2m_{21} \cos \gamma + m_{21}^2} \quad (2.4.9)$$

where

$$m_{21} = \frac{\omega^{(2)}}{\omega^{(1)}}$$

The line of action of the instantaneous axis of screw motion coincides with the line of action of $\boldsymbol{\omega}^{(12)}$. Consequently, the axis of screw motion s - s is located in a plane which is perpendicular to axis x_f and determined by coordinate x_f . The direction of the axis of screw motion in this plane is determined by the ratio

$$\frac{y_f}{z_f} = \frac{\omega_{y_f}^{(12)}}{\omega_{z_f}^{(12)}} = \frac{m_{21} \sin \gamma}{1 - m_{21} \cos \gamma} \quad (2.4.10)$$

The collinear vectors of rotation about and translation along the screw axis, $\boldsymbol{\omega}^{(12)}$ and \mathbf{m} , may be related as follows:

$$\mathbf{m} = p\boldsymbol{\omega}^{(12)} \quad (2.4.11)$$

Here p is the so-called screw parameter. If the screw parameter is positive (negative), vectors \mathbf{m} and $\boldsymbol{\omega}^{(12)}$ point in the same (opposite) direction and the screw is said to be right- (left-) handed.

Equation (2.4.11) yields

$$p = \frac{m_{y_f}}{\omega_{y_f}^{(12)}} = \frac{m_{z_f}}{\omega_{z_f}^{(12)}} = C \frac{m_{21} \sin \gamma}{1 - 2m_{21} \cos \gamma + m_{21}^2} \quad (2.4.12)$$

Equations (2.4.9), (2.4.10), and (2.4.12) determine the location and direction of the screw axis of relative motion and the screw parameter of motion. If body 2 rotates in a direction opposite

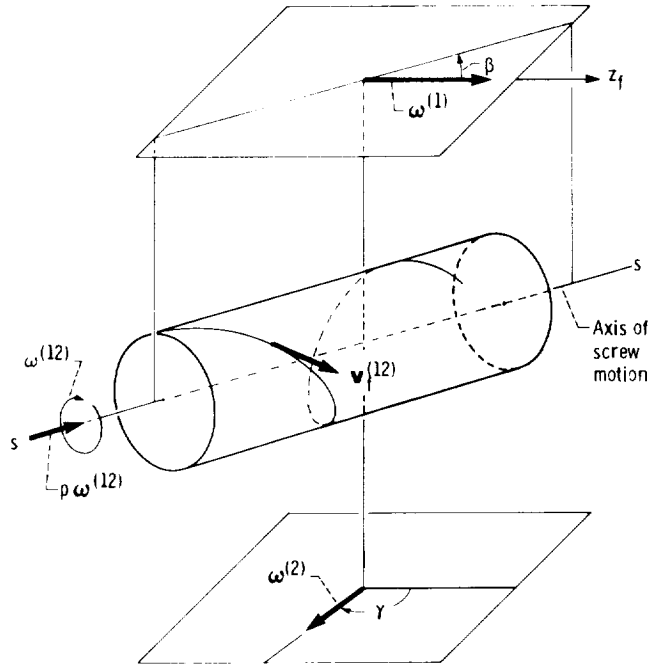


Figure 2.4.2.

the one shown in figure 2.4.1, the sign of m_{21} must be changed in equations (2.4.9), (2.4.10), and (2.4.12).

It must be emphasized that the screw axis of relative motion is fixed in space only if the ratio m_{12} is constant. Knowing that the relative motion between two gears may be represented as a screw motion, we can develop a corresponding vector field for the vectors of relative linear velocity $\mathbf{v}_j^{(12)}$. This vector field may be represented as a locus of an infinitely large number of coaxial cylinders whose axes coincide with the axis of screw motion (fig. 2.4.2). At any point of a cylinder a helix is traced out by the screw motion. The vector of relative velocity $\mathbf{v}_j^{(12)}$ is always tangent to this helix. We recall that vector $\mathbf{v}_j^{(12)}$ may also be determined analytically by equation (2.3.12).

Problem 2.4.1 Considering equations (2.4.9), (2.4.10), and (2.4.12) (1) prove that the instantaneous axis of screw motion becomes an instantaneous axis of rotation for parallel axes of rotation and (2) find the location of this axis.

Answer. For the case when the direction of $\omega^{(2)}$ is opposite to the direction of $\omega^{(1)}$, take $\gamma = 180^\circ$. Then

$$p = 0 \quad x_f = -C \frac{m_{21}}{1 + m_{21}} \quad \omega_{yf} = 0$$

The instantaneous axis of rotation is parallel to axis z_f .

If the directions of $\omega^{(2)}$ and $\omega^{(1)}$ coincide, take $\gamma = 0$. Then

$$p = 0 \quad x_f = -C \frac{m_{21}(m_{21} - 1)}{1 - 2m_{21} + m_{21}^2} \quad \omega_{yf} = 0$$

The instantaneous axis of rotation is parallel to axis z_f .

Problem 2.4.2 Using the conditions of problem 2.4.1, consider the case of intersecting axes of rotation.

Answer. By using equations (2.4.9), (2.4.10), (2.4.12), and (2.2.3) and by setting $C = 0$ and changing the sign of m_{21} , we get

$$p = 0 \quad x_f = 0 \quad \frac{y_f}{z_f} = \frac{m_{21} \sin \gamma}{1 + m_{21} \cos \gamma} = \tan \gamma_1$$

2.5 Crossed Axes of Rotation: Hyperboloid Surfaces of Revolution

Consider again the case of motion transformation between two crossed axes of rotation (sections (2.3) and (2.4)). As bodies 1 and 2 rotate, the instantaneous axis of screw motion generates in each body a hyperboloid surface of revolution (fig. 2.5.1). The two hyperboloids are in tangency along a straight line, the screw axis of motion. Considering that the equations of the instantaneous screw axis are known, let us develop the equations of these two hyperboloids.

According to equations (2.4.9) and (2.4.10), the axis of screw motion may be represented by the following equations:

$$x_f = -C \frac{m_{21}(m_{21} - \cos \gamma)}{1 - 2m_{21} \cos \gamma + m_{21}^2} \quad y_f = -u \sin \beta \quad z_f = u \cos \beta \quad (2.5.1)$$

Here β is the angle made by the instantaneous axis of rotation and axis z_f (fig. 2.4.2), which is determined by

$$\tan \beta = \frac{m_{21} \sin \gamma}{1 - m_{21} \cos \gamma} \quad 0 \leq \beta \leq \pi \quad (2.5.2)$$

The matrix representation of the hyperboloids generated in bodies 1 and 2 is

$$[r_1] = [M_{1f}][R_f] \quad (2.5.3)$$

$$[r_2] = [M_{2f}][R_f] \quad (2.5.4)$$

Elements x_f , y_f , and z_f of column matrix $[R_f]$ are represented by equations (2.5.1). From figure 1.3.2 and expressions (1.3.22) to (1.3.24), matrices $[M_{1f}]$ and $[M_{2f}]$ are represented as follows:

$$[M_{1f}] = \begin{bmatrix} \cos \phi_1 & \sin \phi_1 & 0 & 0 \\ -\sin \phi_1 & \cos \phi_1 & 0 & 0 \\ 0 & 0 & 1 & 0 \\ 0 & 0 & 0 & 1 \end{bmatrix} \quad (2.5.5)$$

$$[M_{2f}] = \begin{bmatrix} \cos \phi_2 & \cos \gamma \sin \phi_2 & -\sin \gamma \sin \phi_2 & C \cos \phi_2 \\ -\sin \phi_2 & \cos \gamma \cos \phi_2 & -\sin \gamma \cos \phi_2 & -C \sin \phi_2 \\ 0 & \sin \gamma & \cos \gamma & 0 \\ 0 & 0 & 0 & 1 \end{bmatrix} \quad (2.5.6)$$

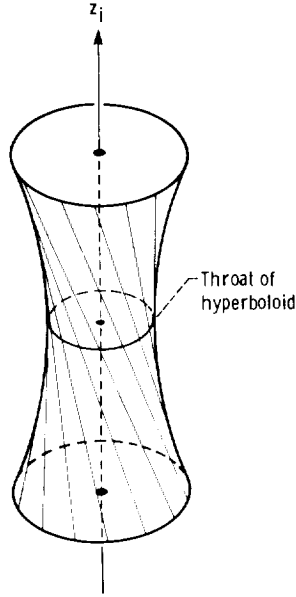


Figure 2.5.1.

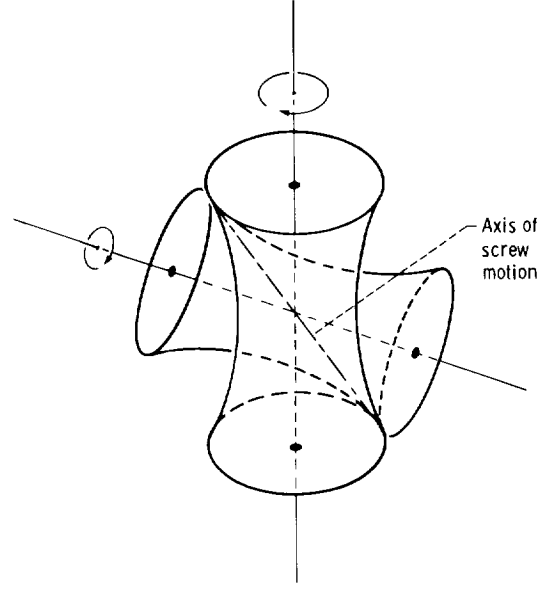


Figure 2.5.2.

Expressions (2.5.1) and (2.5.3) to (2.5.6) yield the following equations for the hyperboloid surfaces of revolution:

$$x_1 = -r_0 \cos \phi_1 - u \sin \beta \sin \phi_1 \quad y_1 = r_0 \sin \phi_1 - u \sin \beta \cos \phi_1 \quad z_1 = u \cos \beta \quad (2.5.7)$$

$$x_2 = (C - r_0) \cos \phi_2 - u \sin (\beta + \gamma) \sin \phi_2 \quad (2.5.8)$$

$$y_2 = -(C - r_0) \sin \phi_2 - u \sin (\beta + \gamma) \cos \phi_2 \quad z_2 = u \cos (\beta + \gamma)$$

Here $r_0 = -x_p$, and u and $\phi_i (i = 1, 2)$ are surface coordinates.

The axial section of a hyperboloid cut by a plane drawn through axis z_i (for instance, a plane determined by $y_i = 0 (i = 1, 2)$) represents a hyperbola. The equations of the hyperbola corresponding to hyperboloid 1 are thus

$$\frac{x_1^2}{r_0^2} - \frac{z_1^2}{r_0^2 \cot^2 \beta} = 1 \quad (2.5.9)$$

where $z_1 = 0$. We find that $x_1 = \pm r_0$ and r_0 is the radius at the throat of the hyperboloid. Similarly, we find that an axial section of hyperboloid 2 is also a hyperbola, and the radius of the throat is equal to $C - r_0$.

Figure 2.5.2 shows two contacting hyperboloids of revolution. The line of tangency of the two hyperboloids is the instantaneous axis of screw motion. The relative motion of the two hyperboloids is rolling with sliding about and along the instantaneous axis of screw motion.

Chapter 3

Planar Curves

3.1 Planar Curves: Definitions and Representations

The concept of a plane curve is usually based on intuition, but it must be based on strict definitions proposed in the field of differential geometry. (See the books by Zalgaller, 1975 and Goetz, 1970.) We begin with the mapping (transformation) of a set X of elements $x (x \in X)$ into a set Y of elements $y (y \in Y)$. The symbol \in denotes that the element belongs to the set. Mapping may be illustrated schematically, as shown in figure 3.1.1. Choosing an element x_i , we determine the unique element y_i which corresponds to x_i . The mathematical essence of mapping set X into set Y is a set of rules which associate an element $y \in Y$ with an element $x \in X$.

A curve may be represented in parametric form or by an explicit or implicit function which associates the coordinates of curve points. A plane curve in parametric representation is defined as the continuous transformation of an open interval $a < \theta < b$ (here θ is the parameter) into two-dimensional space. This transformation may be represented as follows:

$$\mathbf{r}(\theta) \in C^0 \quad \theta \in G \tag{3.1.1}$$

Here

$$\mathbf{r}(\theta) = x(\theta)\mathbf{i} + y(\theta)\mathbf{j} \tag{3.1.2}$$

where \mathbf{i} and \mathbf{j} are unit vectors of given coordinate axes. The symbol C^0 denotes that $x(\theta)$ and $y(\theta)$ are continuous functions and G denotes the open interval (a, b) . The mapping (3.1.1) may be illustrated schematically as shown in figure 3.1.2. A unique point M_i of the curve corresponds to a given value of the parameter θ_i .

The concept of a simple curve is based on mapping with a one-to-one correspondence between parameter θ_i and point M_i of the curve. A unique point M_i of the curve corresponds to the given parameter θ_i , and a unique parameter θ_i corresponds to the given curve point M_i . The mapping illustrated in figure 3.1.3 does not represent a simple curve because two different parameters θ_1 and θ_2 correspond to the same point M of the curve.

Consider the curve shown in figure 3.1.4, which is generated by point C of figure $ABCD$ as

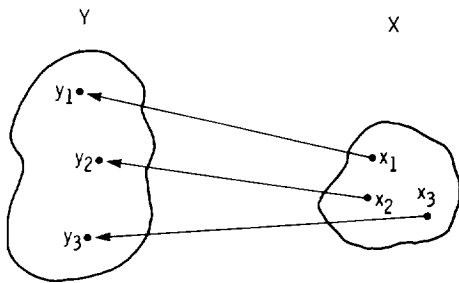


Figure 3.1.1.

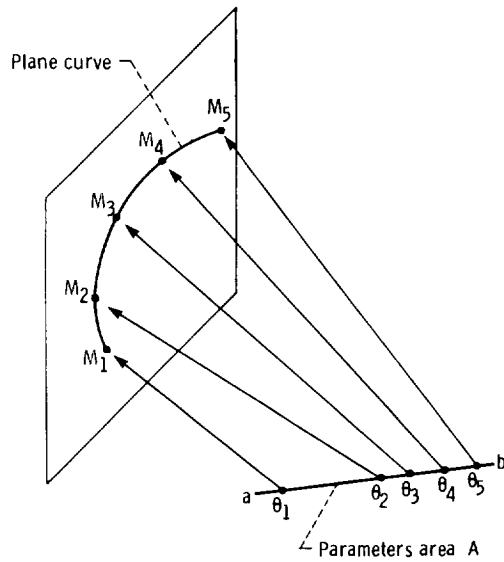


Figure 3.1.2.

its segment DB rolls without sliding over the circle of radius r_b . This curve, known as an extended involute, is an example of a nonsimple curve because its point M corresponds to two different parameters θ_1 and θ_2 ; that is, $\overline{OM} = \mathbf{r}(\theta_1) = \mathbf{r}(\theta_2)$.

Sometimes transformation (3.1.1) may determine a simple curve if the interval (a, b) is sufficiently limited. In the above case, the extended involute curve becomes a simple curve if, by limiting θ , only one branch of the curve, for instance CMN , is generated.

A parametric curve is said to be a regular curve if

$$\mathbf{r}(\theta) \in C^1 \quad \mathbf{r}_\theta \neq 0 \quad \theta \in G \quad (3.1.3)$$

where

$$\mathbf{r}_\theta = \frac{d\mathbf{r}}{d\theta}$$

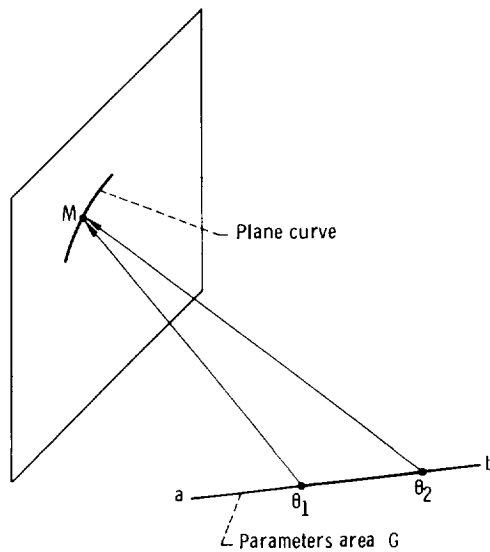
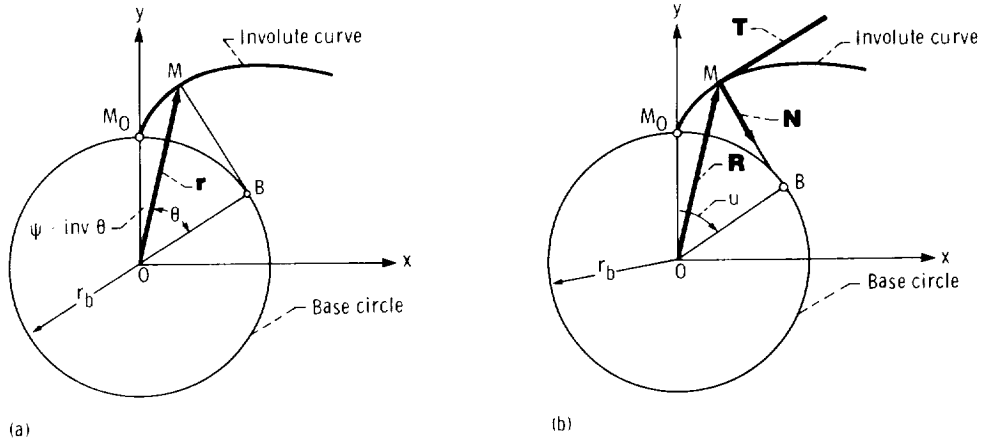


Figure 3.1.3.



(a) Representation 1.
(b) Representation 2.

Figure 3.1.5.

$$\theta(u) \in C^1 \quad \theta_u \neq 0 \quad \mathbf{r}(\theta(u)) = \mathbf{R}(u) \quad (3.1.9)$$

Example 3.1.1 Consider the following two parametric representations of an involute curve:

Representation 1.—In figure 3.1.5(a)

$$\mathbf{r}(\theta) = \frac{r_b}{\cos \theta} [\sin(\text{inv } \theta)\mathbf{i} + \cos(\text{inv } \theta)\mathbf{j}] \quad \text{inv } \theta = \tan \theta - \theta \quad -\frac{\pi}{2} < \theta < \frac{\pi}{2} \quad (3.1.10)$$

Equation (3.1.10) may be derived as follows:

$$\begin{aligned} OM &= \frac{r_b}{\cos \theta} & x &= OM \sin \psi & y &= OM \cos \psi \\ \widehat{M_O B} &= r_b(\psi + \theta) & MB &= r_b \tan \theta & \widehat{M_O B} &= MB & \psi &= \tan \theta - \theta = \text{inv } \theta \end{aligned}$$

Representation 2.—In figure 3.1.5(b)

$$\mathbf{R}(u) = r_b[\sin u - u \cos u]\mathbf{i} + (\cos u + u \sin u)\mathbf{j} \quad -\infty < u < \infty \quad (3.1.11)$$

To develop this equation, we use the following relations:

$$\begin{aligned} \overline{OM} &= \overline{OB} + \overline{BM} & x &= (\overline{OB} \cdot \mathbf{i}) + (\overline{BM} \cdot \mathbf{i}) \\ y &= (\overline{OB} \cdot \mathbf{j}) + (\overline{MB} \cdot \mathbf{j}) & MB &= \widehat{M_O B} = r_b u \end{aligned}$$

Parametric representation (3.1.11) may be derived from equation (3.1.10) by changing the parameter θ for parameter u by using a continuous, strongly monotonic function

$$\theta(u) = \arctan u \quad -\infty < u < \infty \quad (3.1.12)$$

Substituting θ by $\arctan u$ in equation (3.1.10), we get that equation (3.1.6) is indeed observed. Relation (3.1.12) may be verified by the drawings of figure 3.1.5, which yield

$$MB = r_b \tan \theta \quad (\text{fig. 3.1.5(a)})$$

$$MB = \widehat{MOB} = r_b u \quad (\text{fig. 3.1.5(b)})$$

Another representation of a curve is based on application of the implicit function. An equation

$$\phi(x,y) = 0 \quad (x,y) \in G \quad (3.1.13)$$

does not necessarily represent a plane curve. Rather, it merely represents a set of points in the (x,y) plane. Some of these points may be isolated, and some may form a curve. Equation (3.1.13) can represent a curve if, in addition to equation (3.1.13), the following requirements are observed:

$$\phi(x,y) \in C^1 \quad |\phi_x| + |\phi_y| \neq 0 \quad (3.1.14)$$

Here

$$\phi_x = \frac{\partial \phi}{\partial x} \quad \text{and} \quad \phi_y = \frac{\partial \phi}{\partial y}$$

The requirement

$$|\phi_x| + |\phi_y| \neq 0 \quad (3.1.15)$$

means that at least one partial derivative differs from zero at every point on the curve (x_0, y_0) . Requirements (3.1.14) result from the Theorem of Implicit Function System Existence. (See appendix B.) Regarding equation (3.1.13), this theorem states the following: If equation (3.1.13) is satisfied at the point

$$P = (x_0, y_0) \quad (3.1.16)$$

and at least one partial derivative, for instance ϕ_y , differs from zero at this point, then equation (3.1.13) may be solved in the neighborhood of P by a function

$$y(x) \in C^1 \quad x_0 - \delta < x < x_0 + \delta \quad y_0 - h < y < y_0 + h \quad (3.1.17)$$

which represents a simple and regular curve in the neighborhood of P . Here δ and h are small positive numbers which limit the neighborhood of point P .

Remark: If the other partial derivative ϕ_x differs from zero at point P , the set of points (3.1.13) represents a simple and regular curve in the neighborhood of P as follows:

$$x(y) \in C^1 \quad x_0 - \delta < x < x_0 + \delta \quad y_0 - h < h < y < y_0 + h \quad (3.1.18)$$

Example problem 3.1.2 A set of points which belong to the circle of radius r is represented by the equation

$$\phi(x,y) = x^2 + y^2 - r^2 = 0 \quad -r \leq x \leq r \quad -r \leq y \leq r \quad (3.1.19)$$

Determine (1) whether mapping (3.1.19) is a simple curve and if it is not, (2) the additional requirements necessary for equation (3.1.19) to represent a simple curve.

Solution. Mapping (3.1.19) is not a simple curve because elements x and y are not in one-to-one correspondence. By a given element x we get

$$y = \pm \sqrt{r^2 - x^2} \quad (3.1.20)$$

that is, two elements of Y

$$y_1 = \sqrt{r^2 - x^2} \quad \text{and} \quad y_2 = -\sqrt{r^2 - x^2} \quad (3.1.21)$$

correspond to one element of X . Similarly, by a given element y we get

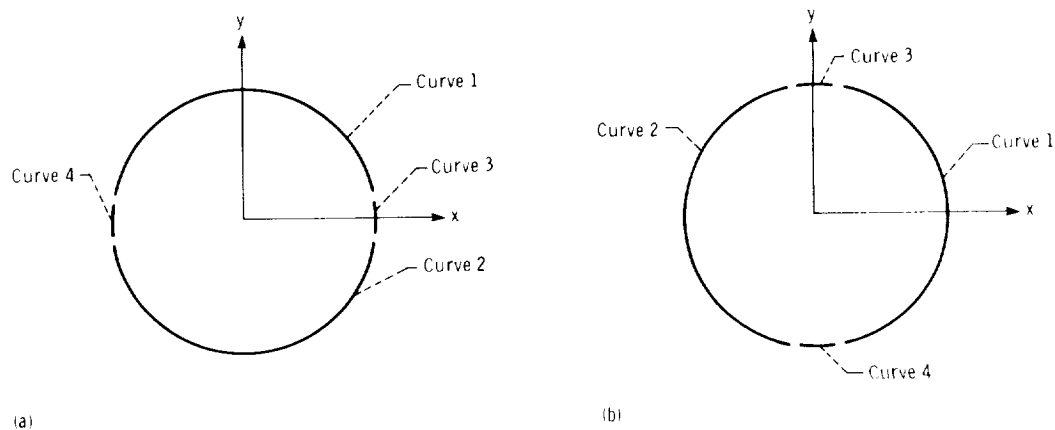
$$x = \pm \sqrt{r^2 - y^2} \quad (3.1.22)$$

that is, two elements of X correspond to one given element of Y . The set of points (3.1.19) may be represented by four simple, regular curves on the basis of the inequality

$$|\phi_x| + |\phi_y| \neq 0 \quad (3.1.23)$$

where $\phi_x = 2x$ and $\phi_y = 2y$.

Version 1.—In figure 3.1.6(a), the four curves are as follows:



(a) Version 1.
(b) Version 2.

Figure 3.1.6.

Curve 1 ($\phi_y \neq 0$)

$$y = \sqrt{r^2 - x^2} \quad -r < x < r \quad (3.1.24)$$

Curve 2 ($\phi_y \neq 0$)

$$y = -\sqrt{r^2 - x^2} \quad -r < x < r \quad (3.1.25)$$

Curve 3 ($\phi_x \neq 0$)

$$x = \sqrt{r^2 - y^2} \quad -\delta < y < \delta \quad (3.1.26)$$

Curve 4 ($\phi_x \neq 0$)

$$x = -\sqrt{r^2 - y^2} \quad -\delta < y < \delta \quad (3.1.27)$$

where δ is a small positive number.

Version 2.—In figure 3.1.6(b), the four curves are as follows:

Curve 1 ($\phi_x \neq 0$)

$$x = \sqrt{r^2 - y^2} \quad -r < y < r \quad (3.1.28)$$

Curve 2 ($\phi_x \neq 0$)

$$x = -\sqrt{r^2 - y^2} \quad -r < y < r \quad (3.1.29)$$

Curve 3 ($\phi_y \neq 0$)

$$y = \sqrt{r^2 - x^2} \quad -\delta < x < \delta \quad (3.1.30)$$

Curve 4 ($\phi_y \neq 0$)

$$y = -\sqrt{r^2 - x^2} \quad -\delta < x < \delta \quad (3.1.31)$$

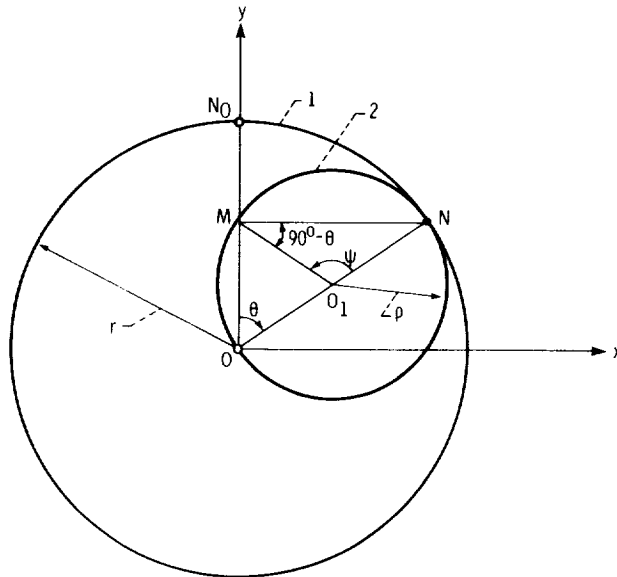


Figure 3.1.7.

Problem 3.1.1 Suppose that circle 2 of radius ρ rolls without slipping inside circle 1 of radius r (fig. 3.1.7). In the process of motion, point M of circle 2 traces out a hypocycloid. By $\rho = r/2$, the hypocycloid becomes a straight line which coincides with the y -axis and may be represented as

$$y = r \cos \theta \quad 0 < \theta < 2\pi \quad (3.1.32)$$

Equation (3.1.32) may be derived from the following relations (fig. 3.1.7):

(1) Due to pure rolling,

$$r\theta = \rho\psi \quad \widehat{N_0N} = \widehat{NM} \quad (3.1.33)$$

Equation (3.1.33) yields that

$$\psi = \frac{r}{\rho}\theta = 2\theta \quad (3.1.34)$$

(2) Considering triangle O_1MN , we get

$$\widehat{O_1MN} = \frac{180^\circ - \psi}{2} = 90^\circ - \theta \quad \widehat{MOO_1} = \theta \quad \widehat{OMN} = 90^\circ \quad OM = r \cos \theta \quad (3.1.35)$$

Determine if mapping (3.1.32) represents a simple curve.

Answer. Mapping (3.1.32) does not represent a simple curve because y and θ are not in one-to-one correspondence.

Problem 3.1.2 With the conditions of problem (3.1.1), limit the interval for θ in mapping (3.1.32) so that it represents a simple curve.

Answer. Mapping (3.1.32) represents a simple curve if θ is limited to the range $0 < \theta < \pi$.

Problem 3.1.3 The path traced out by point M (fig. 3.1.7) may be represented as

$$y = u \quad -r < u < r \quad (3.1.36)$$

where $u = r \cos \theta$ and $0 < \theta < 2\pi$. Are parametric representations (3.1.32) and (3.1.36) equivalent?

Answer. The parametric representations above are not equivalent because the function $u(\theta)$ is not strongly monotonic on the interval $0 < \theta < 2\pi$.

Problem 3.1.4 Using the conditions of problem (3.1.3), limit the interval for θ to make the parametric representations equivalent.

Answer. The interval for θ is $0 < \theta < \pi$.

Problem 3.1.5 The equation

$$f(x,y) = \frac{x^2}{a^2} + \frac{y^2}{b^2} - 1 = 0 \quad -a < x < a \quad -b < y < b \quad (3.1.37)$$

represents a set of points which form an ellipse. Does mapping (3.1.37) represent a simple curve or several simple curves?

Answer. Considering x as a regular parameter, we get

$$y = \pm b \sqrt{1 - \frac{x^2}{a^2}} \quad -a < x < a \quad (3.1.38)$$

Considering y as a regular parameter, we get

$$x = \pm a \sqrt{1 - \frac{y^2}{b^2}} \quad -b < y < b \quad (3.1.39)$$

Mappings (3.1.38) and (3.1.39) represent a two-to-one correspondence. Therefore, the set of points (3.1.37) does not form a simple curve.

The set of points (3.1.37) represents four simple and regular curves of two versions if

$$\left| \frac{\partial f}{\partial x} \right| + \left| \frac{\partial f}{\partial y} \right| \neq 0 \quad \delta_1 < x < \delta_2 \quad \gamma_1 < y < \gamma_2$$

(See example problem (3.1.2).)

Problem 3.1.6 The parametric representation of an ellipse is

$$x = a \cos \theta \quad y = b \sin \theta \quad 0 < \theta < 2\pi \quad (3.1.40)$$

Does mapping (3.1.40) represent a simple curve?

Answer. Mapping (3.1.40) represents a simple curve because point (x, y) and parameter θ are in one-to-one correspondence.

3.2 Tangent and Normal to a Plane Curve

The concept of a tangent line to a plane curve is based on the so-called limiting positions of rays (Zalgaller, 1975).

Consider a set of rays which are drawn through a curve point M and its neighboring curve points M_i ($i=1, 2, \dots, n$). As points M_i approach point M , all rays come to some limiting position. In the case shown in figure 3.2.1(a), there are two limiting rays with coinciding lines of action. These two rays form the tangent to the curve at point M .

Point M is known as a regular point of the curve. Only one limiting ray exists at the curve point M shown in figures 3.2.1(b) and (c); only a half tangent exists at these points. Point M , shown in figures 3.2.1(b) and (c), is known as a point of regression—a so-called singular point of the curve. The definition of regular and singular points of a curve are as follows:

Parametric Representation

A point of a curve

$$\mathbf{r}(\theta) \in C^1 \quad \theta \in G \quad (3.2.1)$$

at which $\mathbf{r}'_\theta \neq 0$ is called a regular point. Points such that the derivative \mathbf{r}'_θ does not exist or $\mathbf{r}'_\theta = 0$ are called singular points.

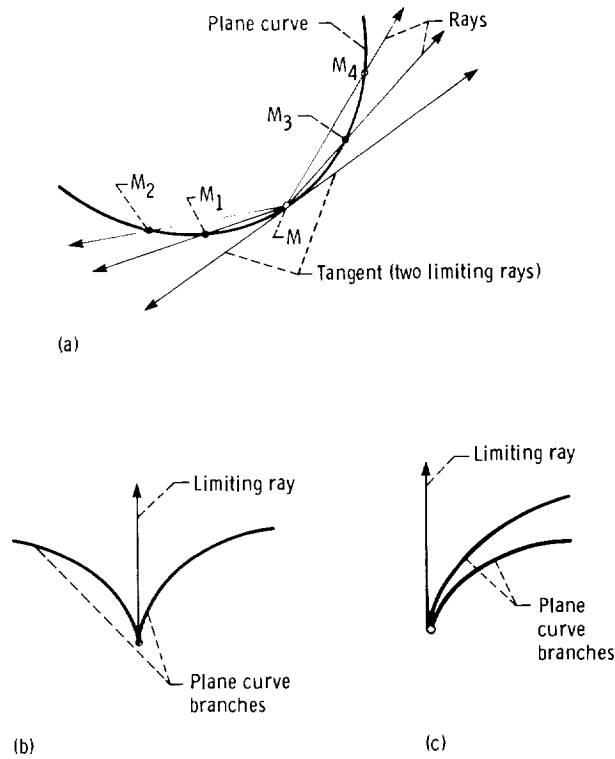


Figure 3.2.1.

Implicit Function Representation

Considering a set of points represented by the equation

$$\phi(x,y) = 0 \quad \phi \in C^1 \quad (x,y) \in G \quad (3.2.2)$$

we say that regular points are points where the partial derivatives of function $\phi(x,y)$ satisfy the following inequality:

$$|\phi_x| + |\phi_y| \neq 0 \quad (3.2.3)$$

Singular points of the set (3.2.2) are such that $\phi_x = 0$ and $\phi_y = 0$ simultaneously. A curve has a unique tangent at a regular point.

The tangent to the parametric curve at a point M is represented by vector

$$\mathbf{T} = \mathbf{r}_\theta = x_\theta \mathbf{i} + y_\theta \mathbf{j} \quad (3.2.4)$$

drawn through point M . The positive direction of the tangent corresponds to the direction of increasing θ .

Suppose that a curve is given in implicit form as

$$\phi(x,y) = 0 \quad \phi \in C^1 \quad (x,y) \in G \quad |\phi_x| + |\phi_y| \neq 0 \quad (3.2.5)$$

The tangent vector

$$\mathbf{T} = T_x \mathbf{i} + T_y \mathbf{j} \quad (3.2.6)$$

is determined with the equation

$$T_x \phi_x + T_y \phi_y = 0 \quad (3.2.7)$$

Equation (3.2.7) may be derived as follows:

(1) Due to the tangency of vector \mathbf{T} and the plane curve

$$\frac{dx}{dy} = \frac{T_x}{T_y} \quad (3.2.8)$$

(2) Differentiation of equation (3.2.5) gives

$$\phi_x dx + \phi_y dy = 0 \quad (3.2.9)$$

Equations (3.2.8) and (3.2.9) yield equation (3.2.7).

Figure 3.2.2(a) shows the tangent of a plane curve at its point M ; D is a point of the tangent. The position vector

$$\overline{OD} = X\mathbf{i} + Y\mathbf{j} \quad (3.2.10)$$

may be determined as follows:

$$\overline{OD} = \overline{OM} + \overline{MD} = x\mathbf{i} + y\mathbf{j} + \lambda_T(T_x\mathbf{i} + T_y\mathbf{j}) \quad (3.2.11)$$

where

$$\overline{MD} = \lambda_T \mathbf{T}$$

Here $\lambda_T \neq 0$ is a scalar factor to equate vector \mathbf{T} with \overline{MD} . Equations (3.2.10) and (3.2.11) yield

$$X = x + \lambda_T T_x \quad Y = y + \lambda_T T_y \quad (3.2.12)$$

or

$$\frac{X - x}{T_x} - \frac{Y - y}{T_y} = 0 \quad (3.2.13)$$

where (x, y) are the coordinates of point M . For a curve represented in parametric form, we get

$$\frac{X - x(\theta)}{x_\theta} - \frac{Y - y(\theta)}{y_\theta} = 0 \quad x_\theta = \frac{d\theta}{dx} \quad y_\theta = \frac{dy}{d\theta} \quad (3.2.14)$$

For a curve represented by an implicit function (eq. (3.2.5)), we get

$$(X - x)\phi_x + (Y - y)\phi_y = 0 \quad (3.2.15)$$

The unit tangent vector $\boldsymbol{\tau}$ may be represented as

$$\boldsymbol{\tau} = \frac{\mathbf{T}}{|\mathbf{T}|} = \frac{\mathbf{T}}{\sqrt{T_x^2 + T_y^2}} = \frac{1}{\sqrt{T_x^2 + T_y^2}} (T_x\mathbf{i} + T_y\mathbf{j}) \quad (3.2.16)$$

At the point of regression a curve has a half tangent (one limiting ray only, figures 3.2.1(b) and (c)). Limiting our discussion to parametric curves, we say (Rashevsky, 1956) (1) a point of regression exists if $\mathbf{r}_\theta = 0$ and $\mathbf{r}_{\theta\theta} \neq 0$ and (2) the direction of the tangent is determined by vector $\mathbf{r}_{\theta\theta}$.

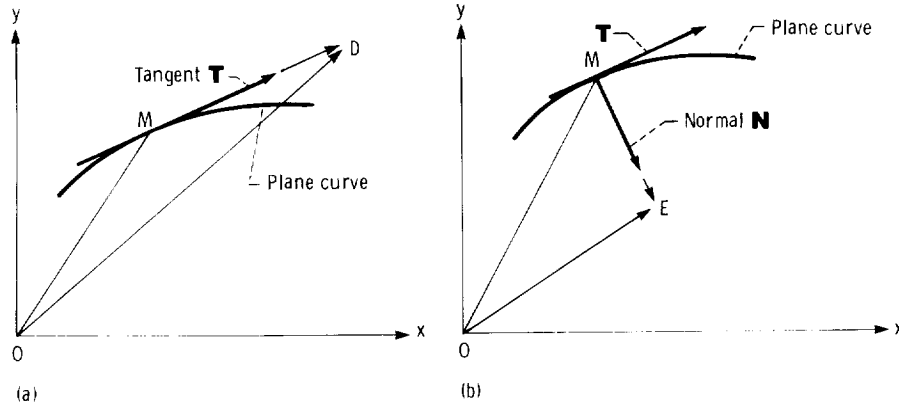


Figure 3.2.2.

Example 3.2.1 An involute curve $\mathbf{R}(u)$, represented by equations (3.1.11), is considered. These equations yield

$$\mathbf{R}_u = r_b(u \sin u \mathbf{i} + u \cos u \mathbf{j}) \quad \mathbf{R}_{uu} = r_b[(\sin u + u \cos u)\mathbf{i} + (\cos u - u \sin u)\mathbf{j}] \quad (3.2.17)$$

At $u \neq 0$, $\mathbf{R}_u \neq 0$, and such points are regular. At the point corresponding to $u = 0$, we have

$$\mathbf{R}_u(O) = 0 \quad \mathbf{R}_{uu}(O) = r_b \mathbf{j} \quad (3.2.18)$$

This point (point M_O , fig. (3.1.5)) is singular ($\mathbf{R}_u = 0$) and is a point of regression ($\mathbf{R}_{uu} \neq 0$). The half tangent determined by \mathbf{R}_{uu} is directed along the positive y -axis.

The normal to a plane curve is perpendicular to its tangent and may be represented by

$$\mathbf{N} = \mathbf{T} \times \mathbf{k} \quad \text{or} \quad \mathbf{N} = \mathbf{k} \times \mathbf{T}$$

Here \mathbf{k} is the unit vector of the z -axis.

The direction of the normal depends on the order of factors in the cross product. Henceforth, we will use the equation

$$\mathbf{N} = \mathbf{T} \times \mathbf{k} = \begin{vmatrix} \mathbf{i} & \mathbf{j} & \mathbf{k} \\ T_x & T_y & 0 \\ 0 & 0 & 1 \end{vmatrix} = \begin{vmatrix} T_y \\ -T_x \\ 0 \end{vmatrix} \quad (3.2.19)$$

The unit normal is determined by

$$\mathbf{n} = \frac{\mathbf{N}}{|\mathbf{N}|} = \frac{1}{\sqrt{T_x^2 + T_y^2}} (T_y \mathbf{i} - T_x \mathbf{j}) \quad (3.2.20)$$

Now consider a point E of the normal (fig. 3.2.2(b)). The position vector \overline{OE} is represented by

$$\overline{OE} = \overline{OM} + \overline{ME} \quad \overline{ME} = \lambda_N \mathbf{N} \quad \lambda_N \neq 0 \quad (3.2.21)$$

Here λ_N is a scalar factor to equate vector \mathbf{T} with \overline{MD} .

$$\overline{OE} = X\mathbf{i} + Y\mathbf{j} \quad \overline{OM} = x\mathbf{i} + y\mathbf{j} \quad \overline{ME} = \lambda_N N_x \mathbf{i} + \lambda_N N_y \mathbf{j} \quad (3.2.22)$$

Equations (3.2.21) and (3.2.22) yield $X = x + \lambda_N N_x$, $Y = y + \lambda_N N_y$, and

$$\frac{X - x}{N_x} - \frac{Y - y}{N_y} = 0 \quad (3.2.23)$$

For a curve represented in parametric form by equation (3.2.1) and in implicit form by equation (3.2.2) we get, respectively,

$$\frac{X - x(\theta)}{y_\theta} + \frac{Y - y(\theta)}{x_\theta} = 0 \quad (3.2.24)$$

$$\frac{X - x}{\phi_x} - \frac{Y - y}{\phi_y} = 0 \quad (3.2.25)$$

Some curves which are applied as gear tooth shapes are generated by the rolling of circle 2 of radius ρ over circle 1 of radius r . These circles can be in internal or external tangency. In particular, a straight line may be applied instead of circle 2. The curve is generated by a point which is rigidly connected to circle (straight line) 2, which rolls over circle 1.

Figure 3.2.3 shows a plane curve (an extended epicycloid) which is traced out by point M ; M is rigidly connected to circle 2. At every instant the relative motion of circle 2 with respect to circle 1 may be represented as rotation about the instantaneous center I with the angular velocity

$$\omega^{(21)} = \omega^{(2)} + \omega^{(1)}$$

where

$$\omega^{(2)} = \frac{d\psi}{dt} \quad \omega^{(1)} = \frac{d\theta}{dt}$$

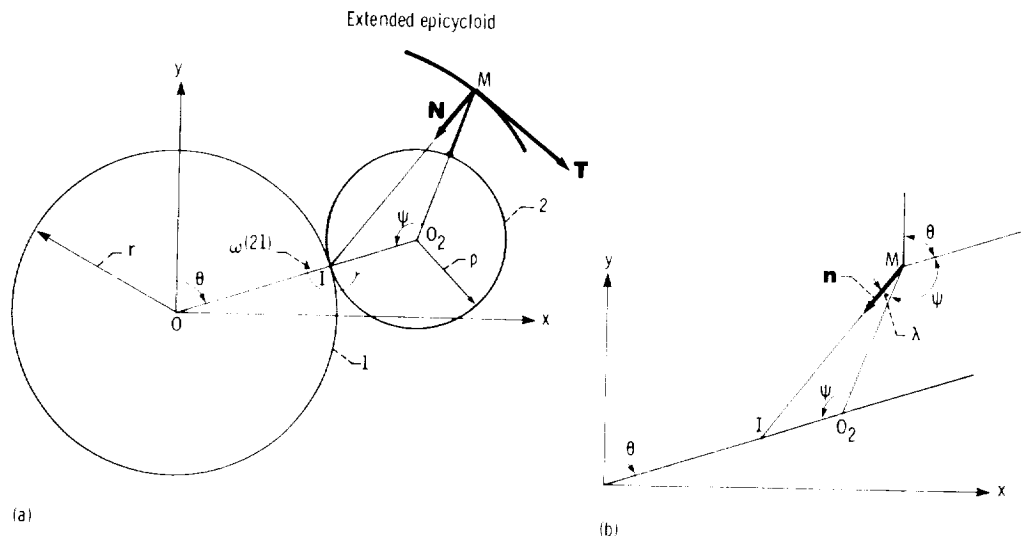


Figure 3.2.3.

We may easily determine the tangent \mathbf{T} and the normal \mathbf{N} to the curve at point M by using the following considerations:

(1) While circle 2 rotates about I through an angle $d\phi$, point M moves along the tangent \mathbf{T} to the curve. Thus \mathbf{T} is perpendicular to MI .

(2) The direction of the normal \mathbf{N} at point M coincides with MI and is directed from M to I according to the cross product

$$\mathbf{N} = \mathbf{T} \times \mathbf{k}$$

Problem 3.2.1 Derive the equations, tangent, normal, and unit normal of the extended epicycloid (fig. 3.2.3(a)). Investigate the existence of singular points.

Answer. Equations of the extended epicycloid are

$$x = (r + \rho) \sin \theta - a \sin (\theta + \psi) \quad y = (r + \rho) \cos \theta - a \cos (\theta + \psi) \quad (3.2.26)$$

where

$$a = O_2M \quad \psi = \frac{r}{\rho} \theta$$

The tangent is represented as

$$T_x = x_\theta = (r + \rho)[\cos \theta - m \cos (\theta + \psi)] \quad T_y = y_\theta = -(r + \rho)[\sin \theta - m \sin (\theta + \psi)] \quad (3.2.27)$$

where

$$m = \frac{a}{\rho}$$

An extended epicycloid has no singular points. If, however, $m = 1$, whereby the generated curve is an ordinary epicycloid, singular points occur at positions where $\theta = 2\pi n (\rho/r)$ ($n = 0, 1, 2, \dots$).

The normal is

$$N_x = y_\theta = -(r + \rho)[\sin \theta - m \sin (\theta + \psi)] \quad N_y = -x_\theta = -(r + \rho)[\cos \theta - m \cos (\theta + \psi)] \quad (3.2.28)$$

The unit normal is

$$n_x = -\frac{\sin \theta - m \sin (\theta + \psi)}{\sqrt{1 - 2m \cos \psi + m^2}} \quad n_y = -\frac{\cos \theta - m \cos (\theta + \psi)}{\sqrt{1 - 2m \cos \psi + m^2}} \quad (3.2.29)$$

Simple equations for the unit normal vector \mathbf{n} may be derived considering that \mathbf{n} is directed along vector \overline{MI} (fig. 3.2.3(b)). Thus,

$$n_x = \sin (\theta + \psi + \lambda) \quad n_y = \cos (\theta + \psi + \lambda) \quad (3.2.30)$$

Here

$$\tan \lambda = \frac{\sin \psi}{m - \cos \psi} \quad 0 \leq \psi \leq 2\pi \quad (3.2.31)$$

where

$$m = \frac{a}{\rho}$$

To get equation (3.2.31), consider the triangle IMO_2 (fig. 3.2.3(b)).

3.3 Curvature of Plane Curves

A parametric curve is represented by

$$\mathbf{r}(\theta) \in C^2 \quad \theta \in G \quad (3.3.1)$$

Consider two neighboring points M and N of the curve which correspond to θ and $\theta + \Delta\theta$, respectively (fig. 3.3.1(a)). The length of the arc between points M and N is Δs , and $\Delta\alpha$ is the angle between the tangent vectors at M and N .

The limit of the ratio $\Delta\alpha/\Delta s$ as point N approaches point M is known as the curvature (denoted as κ) of the curve at point M . We may also consider the limit of the inverse ratio $\Delta s/\Delta\alpha$, which is known as the radius of curvature (denoted as ρ_c) of the curve at point M . Here ρ_c is the radius of the limiting circle which is drawn through point M and two neighboring points N_1 and N_2 as they approach point M (fig. 3.3.1(b)). The center of this circle is called the center of curvature.

The so-called Frenet's trihedron is formed by three unit vectors—the unit tangent vector $\boldsymbol{\tau}$, the principal normal vector \mathbf{n} , and the binormal vector \mathbf{b} (fig. 3.3.2). The principal normal vector \mathbf{n} lies in plane Π in which the plane curve is located. The binormal vector \mathbf{b} lies in plane H , which is perpendicular to plane Π . These three unit vectors form a right-handed trihedron.

Consider two trihedrons, $(\boldsymbol{\tau}, \mathbf{n}, \mathbf{b})$ and $(\boldsymbol{\tau}', \mathbf{n}', \mathbf{b}')$, which are located at neighboring points M and N of the curve. The motion of trihedron $(\boldsymbol{\tau}, \mathbf{n}, \mathbf{b})$ which is to be coincided with trihedron

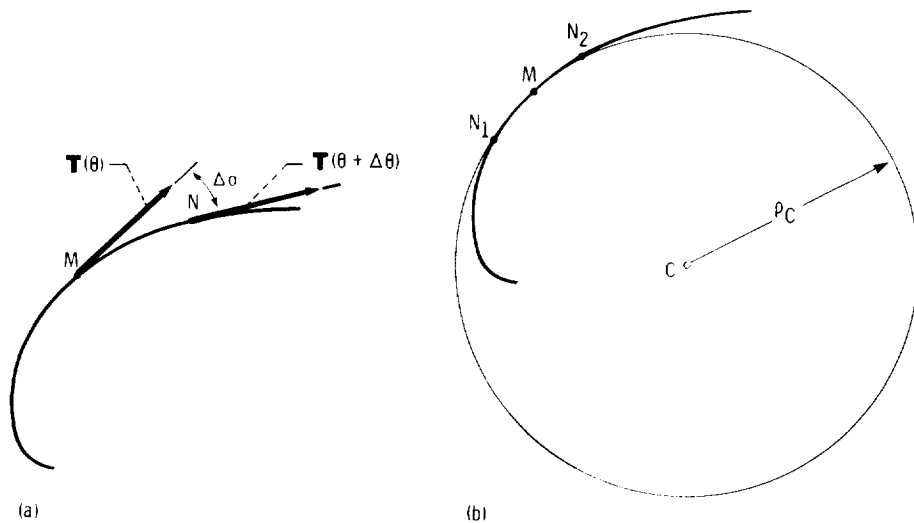


Figure 3.3.1.

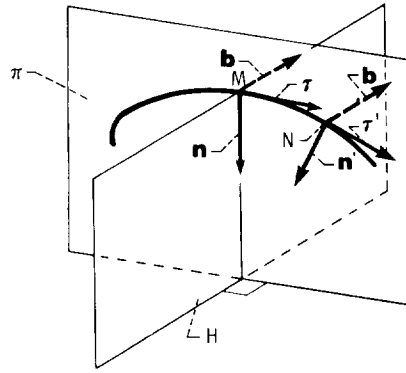


Figure 3.3.2.

$(\tau', \mathbf{n}', \mathbf{b})$ may be represented as a motion of two components. These components are (1) translation along the curve from M to N (unit vectors $\tau, \mathbf{n}, \mathbf{b}$ of the trihedron keep their original directions) and (2) rotation about \mathbf{b} (trihedron $\tau, \mathbf{n}, \mathbf{b}$ coincides with trihedron $\tau', \mathbf{n}', \mathbf{b}$).

The velocity in translational motion is

$$\mathbf{v} = \mathbf{r}_\theta \frac{d\theta}{dt} \quad (3.3.2)$$

$$|\mathbf{v}| = \frac{ds}{dt} \quad (3.3.3)$$

Here t is time and $\theta(t)$ is a strongly monotonic function (a linear function in the simplest case).

The angular velocity is

$$\boldsymbol{\omega} = \omega \mathbf{b} \quad (3.3.4)$$

and

$$|\boldsymbol{\omega}| = \frac{d\alpha}{dt} \quad (3.3.5)$$

where $d\alpha$ is the angle between the tangents at points M and N .

The directions of vectors τ and \mathbf{n} do not change by translation, but they do change by rotation. The linear velocity of the tip of the unit vector \mathbf{n} is

$$\dot{\mathbf{n}} = \boldsymbol{\omega} \times \mathbf{n} = \begin{vmatrix} \tau & \mathbf{n} & \mathbf{b} \\ 0 & 0 & \omega \\ 0 & 1 & 0 \end{vmatrix} = -\omega \tau \quad (3.3.6)$$

Considering the function $\mathbf{n}(\theta)$, we get

$$\dot{\mathbf{n}} = \mathbf{n}_\theta \frac{d\theta}{dt} \quad (3.3.7)$$

where $\mathbf{n}_\theta = d\mathbf{n}/d\theta$.

Equations (3.3.6) and (3.3.7) yield

$$\mathbf{n}_\theta \frac{d\theta}{dt} = -\omega \boldsymbol{\tau} = -\frac{d\alpha}{dt} \boldsymbol{\tau} \quad (3.3.8)$$

The unit tangent vector $\boldsymbol{\tau}$ may be expressed as

$$\boldsymbol{\tau} = \frac{\mathbf{v}}{|\mathbf{v}|} = \frac{\mathbf{r}_\theta \frac{d\theta}{dt}}{\frac{ds}{dt}} \quad (3.3.9)$$

It results from equations (3.3.8) and (3.3.9) that

$$\mathbf{n}_\theta = -\frac{\frac{d\alpha}{dt} \mathbf{r}_\theta}{\frac{ds}{dt}} \quad (3.3.10)$$

According to the definition of curvature, we have

$$\kappa = \frac{d\alpha}{ds} = \frac{\frac{d\alpha}{dt}}{\frac{ds}{dt}} \quad (3.3.11)$$

Equations (3.3.10) and (3.3.11) yield

$$\mathbf{n}_\theta = -\kappa \mathbf{r}_\theta \quad (3.3.12)$$

If we consider equation (3.3.12) and the projections of \mathbf{n}_θ and \mathbf{r}_θ on two orthogonal axes (x, y) , we get

$$\kappa = -\frac{n_{\theta x}}{x_\theta} = -\frac{n_{\theta y}}{y_\theta} \quad (3.3.13)$$

where $\mathbf{n}_\theta = n_{\theta x} \mathbf{i} + n_{\theta y} \mathbf{j}$ and $\mathbf{r}_\theta = x_\theta \mathbf{i} + y_\theta \mathbf{j}$. The sense of the curvature depends on the location of the center of curvature C on the normal. The center C is located on the positive normal if $\kappa > 0$.

Another equation for curvature may be derived by considering the linear velocity $\dot{\boldsymbol{\tau}}$ of the tip of unit vector $\boldsymbol{\tau}$.

$$\dot{\boldsymbol{\tau}} = \boldsymbol{\omega} \times \boldsymbol{\tau} = \begin{vmatrix} \boldsymbol{\tau} & \mathbf{n} & \mathbf{b} \\ 0 & 0 & \omega \\ 1 & 0 & 0 \end{vmatrix} = \omega \mathbf{n} \quad (3.3.14)$$

Considering function $\tau(\theta)$, we get that

$$\dot{\mathbf{r}} = \tau_\theta \frac{d\theta}{dt} \quad (3.3.15)$$

where $\tau_\theta = d\tau/d\theta$.

Equations (3.3.14) and (3.3.15) yield

$$\tau_\theta \frac{d\theta}{dt} = \omega \mathbf{n} = \frac{d\alpha}{dt} \mathbf{n} \quad (3.3.16)$$

It results from the equation

$$|\mathbf{r}_\theta| \frac{d\theta}{dt} = \frac{ds}{dt}$$

that

$$\frac{d\theta}{dt} = \frac{\frac{ds}{dt}}{|\mathbf{r}_\theta|} \quad (3.3.17)$$

Substituting $d\theta/dt$ in equation (3.3.16) and considering equation (3.3.17), we get

$$\frac{\tau_\theta}{|\mathbf{r}_\theta|} = \frac{\frac{d\alpha}{dt}}{\frac{ds}{dt}} \mathbf{n} = \kappa \mathbf{n} \quad (3.3.18)$$

which yields

$$\kappa = \frac{\tau_{\theta x}}{|\mathbf{r}_\theta| n_x} = \frac{\tau_{\theta y}}{|\mathbf{r}_\theta| n_y} \quad (3.3.19)$$

where $\tau_\theta = \tau_{\theta x} \mathbf{i} + \tau_{\theta y} \mathbf{j}$. Equations (3.3.13) and (3.3.19) may be applied to determine the curvature of a curve given in parametric representation.

A kinematic representation of curvature equations may be developed as follows. Instead of equation (3.3.12), we may apply

$$\mathbf{n}_\theta \frac{d\theta}{dt} = -\kappa \mathbf{r}_\theta \frac{d\theta}{dt}$$

or

$$\dot{\mathbf{n}}_r = -\kappa \mathbf{v}_r \quad (3.3.20)$$

The subscript r denotes that the velocity in relative motion with respect to the curve is considered (the velocity of a point which moves along the curve). Equation (3.3.20) yields

$$\kappa = -\frac{\dot{\mathbf{n}}_r \cdot \mathbf{v}_r}{\mathbf{v}_r \cdot \mathbf{v}_r} \quad (3.3.21)$$

A second kinematic representation of curvature is based on the equation

$$\mathbf{n} \cdot \mathbf{v}_r = 0 \quad (3.3.22)$$

which results from the collinearity of vectors \mathbf{v}_r and $\boldsymbol{\tau}$. Differentiation of equation (3.3.22) gives

$$(\dot{\mathbf{n}}_r \cdot \mathbf{v}_r) + (\mathbf{n} \cdot \mathbf{a}_r) = 0$$

or

$$\dot{\mathbf{n}}_r \cdot \mathbf{v}_r = -\mathbf{n} \cdot \mathbf{a}_r \quad (3.3.23)$$

where $\mathbf{a}_r = \dot{\mathbf{v}}_r$ is the acceleration of the point which moves along the curve. Equations (3.3.21) and (3.3.23) yield

$$\kappa = \frac{\mathbf{a}_r \cdot \mathbf{n}}{\mathbf{v}_r \cdot \mathbf{v}_r} \quad (3.3.24)$$

To simplify the expression for the acceleration \mathbf{a}_r , we may assume that $\theta(t)$ is a linear function and $d\theta/dt$ is constant. By $d\theta/dt$ not being constant, a tangential component $\mathbf{a}_r^{(t)}$ of the acceleration occurs but it does not change the result of the scalar product in equation (3.3.24) because

$$\mathbf{a}_r^{(t)} \cdot \mathbf{n} = 0$$

The acceleration \mathbf{a}_r , where $d\theta/dt$ is constant, may be derived as follows:

$$\mathbf{v}_r = \mathbf{r}_\theta \frac{d\theta}{dt}$$

and

$$\mathbf{a}_r = \dot{\mathbf{v}}_r = \mathbf{r}_{\theta\theta} \left(\frac{d\theta}{dt} \right)^2 = (x_{\theta\theta} \mathbf{i} + y_{\theta\theta} \mathbf{j}) \left(\frac{d\theta}{dt} \right)^2 \quad (3.3.25)$$

Let us now derive the equations of curvature for a curve given by a function in explicit form

$$y(x) \in C^2 \quad x_1 < x < x_2 \quad (3.3.26)$$

or in implicit form

$$F(x,y) = 0 \quad F \in C^2 \quad |F_x| + |F_y| \neq 0 \quad (3.3.27)$$

The curvature is represented by

$$\kappa = \frac{d\alpha}{ds} \quad (3.3.28)$$

For the curve given by equation (3.3.26), we have

$$\tan \alpha = \frac{dy}{dx} = y_x \quad (3.3.29)$$

$$ds = \sqrt{dx^2 + dy^2} = \sqrt{1 + y_x^2} dx \quad (3.3.30)$$

Differentiating equation (3.3.29) we get

$$\frac{1}{\cos^2 \alpha} d\alpha = \frac{d^2y}{dx^2} dx = y_{xx} dx$$

and

$$d\alpha = \cos^2 \alpha y_{xx} dx = \frac{1}{1 + \tan^2 \alpha} y_{xx} dx = \frac{y_{xx}}{(1 + y_x^2)} dx \quad (3.3.31)$$

Equations (3.3.28), (3.3.30), and (3.3.31) yield

$$\kappa = \frac{y_{xx}}{(1 + y_x^2)^{3/2}} \quad (3.3.32)$$

For the curve represented by equation (3.3.27), we get $F_x dx + F_y dy = 0$. Assuming that $F_y \neq 0$, we get

$$\frac{dy}{dx} = -\frac{F_x}{F_y} \quad (3.3.33)$$

$$\frac{d^2y}{dx^2} = \frac{2F_x F_y F_{xy} - F_x^2 F_{yy} - F_{xx} F_y^2}{F_y^3} \quad (3.3.34)$$

and

$$\kappa = \frac{2F_x F_y F_{xy} - F_x^2 F_{yy} - F_{xx} F_y^2}{(F_x^2 + F_y^2)^{3/2}} \quad (3.3.35)$$

Differentiating equation (3.3.33), we consider that

$$F_x = F_x(x,y) \quad F_y = F_y(x,y)$$

and

$$\frac{\partial}{\partial x} (F_x) = F_{xx} + F_{xy} \frac{dy}{dx} = F_{xx} - F_{xy} \frac{F_x}{F_y} \quad \frac{\partial}{\partial x} (F_y) = F_{yx} + F_{yy} \frac{dy}{dx} = F_{yx} - F_{yy} \frac{F_x}{F_y}$$

Problem 3.3.1 Given an involute curve represented by equation (3.1.11). Develop the equation of curvature by using equations (3.3.13) and (3.3.19). Be sure that the results match.

Answer.

$$\kappa = \frac{1}{r_b u}$$

Problem 3.3.2 With the conditions of problem (3.2.1), find the curvature of an extended epicycloid and ordinary epicycloid using the unit normal equations (3.2.30), and curvature equations (3.3.13).

Answer.

$$\kappa = - \frac{\cos(\theta + \psi + \lambda) \left[1 + \frac{r}{\rho} + \frac{r(m \cos \psi - 1) \cos^2 \lambda}{\rho(m - \cos \psi)^2} \right]}{(r + \rho)[\cos \theta - m \cos(\theta + \psi)]}$$

where

$$m = \frac{a}{\rho} \quad \tan \lambda = \frac{\sin \psi}{m - \cos \psi}$$

For an ordinary epicycloid, $m = 1$, $\lambda = 90^\circ - \psi/2$, and

$$\kappa = \frac{2\rho + r}{4\rho(r + \rho) \sin \frac{\psi}{2}}$$

Chapter 4

Conjugate Shapes

4.1 Generation of a Locus of Planar Curves

Consider a gear train of gears 1 and 2 which transforms rotational motion between parallel axes with the given function

$$\phi_2(\phi_1) \in C^1 \quad a < \phi_1 < b \quad (4.1.1)$$

Here ϕ_1 and ϕ_2 are the angles of gear rotation. We set up the following coordinate systems: $S_1(x_1, y_1)$ and $S_2(x_2, y_2)$, rigidly connected to gears 1 and 2, respectively, and $S_f(x_f, y_f)$, rigidly connected to the frame (fig. 4.1.1(a)). We assume here that the shape of gear tooth 1 is a simple regular curve Σ_1 which is given in parametric representation in coordinate system S_1 as follows (fig. 4.1.1(b)):

$$\mathbf{r}_1(\theta) \in C^1 \quad \frac{d\mathbf{r}_1}{d\theta} \neq 0 \quad \theta \in G \quad (4.1.2)$$

The problem to be solved is to determine the shape of the tooth of gear 2 (Σ_2) which will provide conjugate action when in mesh with gear tooth 1. Gears are said to have conjugate tooth shapes if they transform motion by a prescribed function (eq. (4.1.1)). To solve this problem we must find (1) the locus of planar curves Σ_ϕ generated by the given curve Σ_1 in coordinate system S_2 and (2) the envelope Σ_2 of the locus of planar curves Σ_ϕ (the shape of gear tooth 2). The determination of the envelope Σ_2 is considered in section 4.2.

Although we shall limit our discussion to the case with $\phi_2(\phi_1)$ as a linear function, the following results may be extended to the case where $\phi_2(\phi_1)$ is a nonlinear function and the angular velocity ratio is

$$m_{21} = \frac{d}{d\phi_1}(\phi_2(\phi_1)) \neq \text{constant}$$

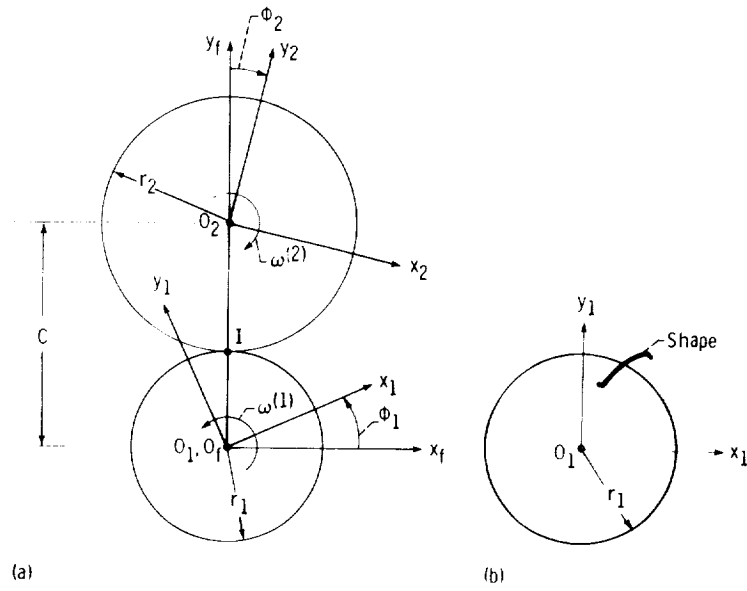


Figure 4.1.1.

The matrix representation of the locus of planar curves Σ_ϕ may be represented by the equations

$$\mathbf{r}_1(\theta) = x_1(\theta)\mathbf{i}_1 + y_1(\theta)\mathbf{j}_1 \quad \mathbf{r}_1(\theta) \in C^1 \quad (4.1.3)$$

$$\left| \frac{dx_1}{d\theta} \right| + \left| \frac{dy_1}{d\theta} \right| \neq 0 \quad \theta \in G$$

$$[\mathbf{r}_2] = [M_{21}] [\mathbf{r}_1] \quad (4.1.4)$$

Here

$$[\mathbf{r}_1(\theta)] = \begin{bmatrix} x_1(\theta) \\ y_1(\theta) \\ 1 \end{bmatrix}$$

is the matrix of coordinates of the given shape Σ_1 and $[M_{21}]$ is the matrix which represents the coordinate transformation from system S_1 to S_2 . Elements of this matrix depend on angles of rotation ϕ_1 and ϕ_2 . Taking into account that ϕ_2 and ϕ_1 are related by the function (4.1.1), we can say that elements of matrix $[M_{21}]$ may be expressed solely in terms of ϕ_1 . The locus of planar curves Σ_ϕ may be represented as follows:

$$\mathbf{r}_2(\theta, \phi_1) \in C^1 \quad \frac{\partial \mathbf{r}_2}{\partial \theta} \neq 0 \quad \theta \in G \quad a < \phi_1 < b \quad (4.1.5)$$

For the case shown in figure 4.1.1(a), we have

$$\phi_2 = m_{21}\phi_1 \quad m_{21} = \frac{\omega_2}{\omega_1} = \frac{r_1}{r_2} = \text{constant}$$

where r_1 and r_2 are centrode radii and the matrix $[M_{21}]$ is

$$\begin{aligned} [M_{21}] &= [M_{2f}][M_{f1}] = \begin{bmatrix} \cos \phi_2 & -\sin \phi_2 & C \sin \phi_2 \\ \sin \phi_2 & \cos \phi_2 & -C \cos \phi_2 \\ 0 & 0 & 1 \end{bmatrix} \begin{bmatrix} \cos \phi_1 & -\sin \phi_1 & 0 \\ \sin \phi_1 & \cos \phi_1 & 0 \\ 0 & 0 & 1 \end{bmatrix} \\ &= \begin{bmatrix} \cos (\phi_1 + \phi_2) & -\sin (\phi_1 + \phi_2) & C \sin \phi_2 \\ \sin (\phi_1 + \phi_2) & \cos (\phi_1 + \phi_2) & -C \cos \phi_2 \\ 0 & 0 & 1 \end{bmatrix} \end{aligned} \quad (4.1.6)$$

Expressions (4.1.4), (4.1.6), and (4.1.2) yield

$$\begin{aligned} x_2(\theta, \phi) &= x_1(\theta) \cos (\phi_1 + \phi_2) - y_1(\theta) \sin (\phi_1 + \phi_2) + C \sin \phi_2 \\ y_2(\theta, \phi) &= x_1(\theta) \sin (\phi_1 + \phi_2) + y_1(\theta) \cos (\phi_1 + \phi_2) - C \cos \phi_2 \end{aligned} \quad (4.1.7)$$

$$\left| \frac{\partial x_1}{\partial \theta} \right| + \left| \frac{\partial y_1}{\partial \theta} \right| \neq 0 \quad \theta \in G \quad a < \phi < b$$

Here $\phi \equiv \phi_1$, and ϕ_2 is determined by the given function $\phi_2(\phi_1)$. Equations (4.1.7) represent the locus of regular curves (gear 1 shapes) which is generated in coordinate system S_2 .

By a fixed value of ϕ_1 , equations (4.1.7) represent a single curve of the locus whose location in coordinate system S_2 depends on the value of ϕ_1 . The partial derivative

$$\frac{\partial \mathbf{r}_2}{\partial \theta} = \frac{\partial x_2}{\partial \theta} \mathbf{i}_2 + \frac{\partial y_2}{\partial \theta} \mathbf{j}_2 \quad (4.1.8)$$

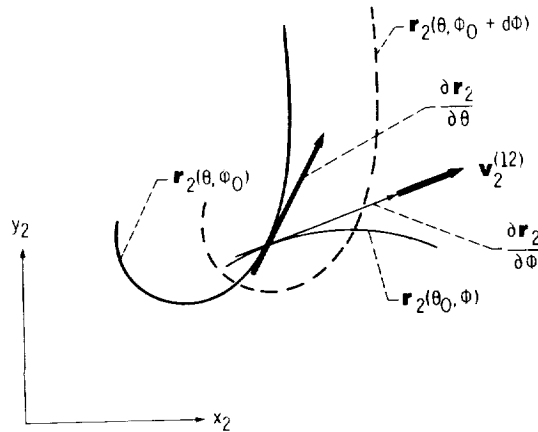


Figure 4.1.2.

is the tangent vector at any point of this curve (fig. 4.1.2). Here \mathbf{i}_2 and \mathbf{j}_2 are unit vectors of the coordinate axes of system S_2 . By a fixed value of θ , equations (4.1.7) represent the path which is traced out in coordinate system S_2 by a single point of curve Σ_1 (fig. 4.1.2). Here ϕ is the parameter of motion of the generated path. Different paths are traced out by different points on curve Σ_1 . The location of these points on curve Σ_1 depends on the chosen parameter θ . The partial derivative

$$\frac{\partial \mathbf{r}_2}{\partial \phi} = \frac{\partial x_2}{\partial \phi} \mathbf{i}_2 + \frac{\partial y_2}{\partial \phi} \mathbf{j}_2 \quad (4.1.9)$$

represents the tangent to the path which is generated by a point on curve Σ_1 as it moves relative to system S_2 (fig. 4.1.2). Considering the time derivative equivalent of equation (4.1.9), we get that

$$\mathbf{v}_2^{(12)} = \frac{\partial \mathbf{r}_2}{\partial \phi} \frac{d\phi}{dt} = \frac{\partial x_2}{\partial \phi} \frac{d\phi}{dt} \mathbf{i}_2 + \frac{\partial y_2}{\partial \phi} \frac{d\phi}{dt} \mathbf{j}_2 \quad (4.1.10)$$

where $\mathbf{v}_2^{(12)}$ is the velocity of a point of curve Σ_1 in its motion relative to coordinate system S_2 (represented in system S_2).

Consider a case where the given shape is represented in coordinate system $S_1(x_1, y_1)$ by an implicit function as follows:

$$F(x_1, y_1) = 0 \quad (x_1, y_1) \in A \quad F \in C^1 \quad |F_{x_1}| + |F_{y_1}| \neq 0 \quad (4.1.11)$$

We may derive the locus of planar curves generated in coordinate system S_2 through the equations

$$x_1 = g_1(x_2, y_2, \phi) \quad y_1 = g_2(x_2, y_2, \phi) \quad (4.1.12)$$

which expresses the coordinate transformation from coordinate system S_2 to S_1 . The matrix representation of equations (4.1.12) is

$$[r_1] = [M_{12}][r_2] \quad (4.1.13)$$

Here $[M_{12}]$ is the inverse of matrix $[M_{21}]$. Equations (4.1.11) and (4.1.12) yield

$$H(x_2, y_2, \phi) = F(x_1(x_2, y_2, \phi), y_1(x_2, y_2, \phi)) = 0 \quad (4.1.14)$$

$$(x_2, y_2) \in E \quad H \in C^1 \quad |H_{x_2}| + |H_{y_2}| \neq 0$$

Equations (4.1.14) represent the locus of plane curves generated in coordinate system S_2 .

Problem 4.1.1 Consider the coordinate systems shown in figure 4.1.3(a). The shape of the rack tooth is represented in coordinate system S_2 (fig. 4.1.3(b)) by the equations

$$x_2 = u \sin \psi_c \quad y_2 = u \cos \psi_c \quad -u_1 < u < u_2 \quad O_2M = u \quad (4.1.15)$$

The displacement s of the rack and the angle of gear rotation ϕ are related by

$$\frac{s}{\phi} = r \quad (r \text{ is constant})$$

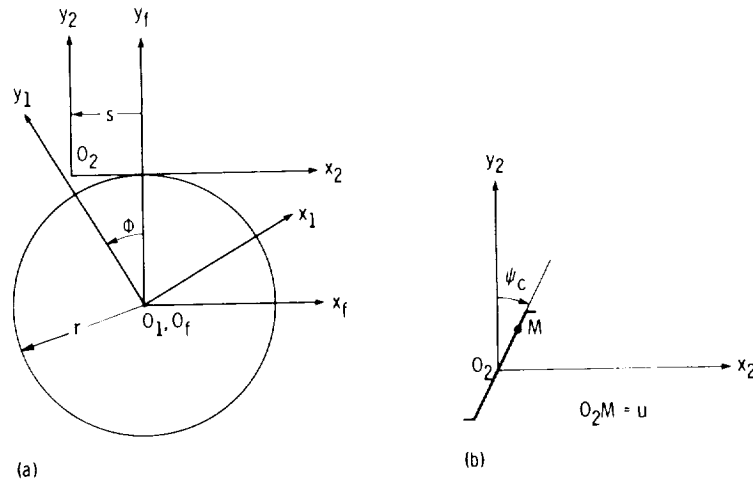


Figure 4.1.3.

Find equations of the locus of shapes which is generated in coordinate system S_1 . The shape is represented by equation (4.1.15).

Answer.

$$\left. \begin{aligned} x_1 &= u \sin(\psi_c + \phi) + r(\sin \phi - \phi \cos \phi) \\ y_1 &= u \cos(\psi_c + \phi) + r(\cos \phi + \phi \sin \phi) \end{aligned} \right\} \quad (4.1.16)$$

where $-u < u < u_2$ and $a < \phi < b$.

Problem 4.1.2 Consider the locus of curves represented by equations (4.1.7). Assume that $\phi_2(\phi_1)$ is a linear function given as

$$\phi_2 = m_{21}\phi_1 \quad m_{21} = \frac{\omega_2}{\omega_1} = \frac{r_1}{r_2}$$

Determine a general expression for the relative velocity $\mathbf{v}_2^{(12)}$. Prove that $\mathbf{v}_2^{(12)}$ is equal to zero at the pitch point I —the point of tangency of centrodes (fig. 4.1.1(a)).

Answer.

$$\begin{aligned} \mathbf{v}_2^{(12)} &= \left[-x_1 \sin(\phi_1 + \phi_2)(\omega_1 + \omega_2) - y_1 \cos(\phi_1 + \phi_2)(\omega_1 + \omega_2) + C\omega_2 \cos \phi_2 \right] \mathbf{i}_2 \\ &\quad + \left[x_1 \cos(\phi_1 + \phi_2)(\omega_1 + \omega_2) - y_1 \sin(\phi_1 + \phi_2)(\omega_1 + \omega_2) + C\omega_2 \sin \phi_2 \right] \mathbf{j}_2 \end{aligned} \quad (4.1.17)$$

To prove that $\mathbf{v}_2^{(12)} = 0$ at the pitch point I , substitute x_1 and y_1 by (fig. 4.1.1(a))

$$x_1 = r_1 \sin \phi_1 \quad y_1 = r_1 \cos \phi_1$$

and take into account that $C = r_1 + r_2$ and $\omega_1 r_1 = \omega_2 r_2$.

4.2 Envelope of a Locus of Planar Curves: Parametric Representation

Equations (4.1.5) and (4.1.7) represent a locus of regular planar curves. Simplifying our notation, we may represent the locus of curves in a coordinate system $S(x,y)$ as follows:

$$\mathbf{r}(\theta, \phi) \in C^1 \quad \mathbf{r}_\theta \neq 0 \quad \theta \in G \quad a < \phi < b \quad (4.2.1)$$

Here

$$\mathbf{r}(\theta, \phi) = x(\theta, \phi)\mathbf{i} + y(\theta, \phi)\mathbf{j} \quad (4.2.2)$$

where \mathbf{i} and \mathbf{j} denote the unit vectors of coordinate axes x and y .

With the fixed parameter of motion ϕ_0 , the function $\mathbf{r}(\theta, \phi_0)$ represents the position vector of a curve point which corresponds to the parameter θ . Parameter of motion ϕ_0 determines the location of the curve in the coordinate system $S(x,y)$. Henceforth, we assume that the curve locus (eq. (4.2.1)) is generated by the motion of a nonchanging curve. However, in the most general case, vector function (4.2.1) may represent a locus of planar curves which changes in the process of motion. Vector functions $\mathbf{r}(\theta, \phi_0^{(1)})$ and $\mathbf{r}(\theta, \phi_0^{(2)})$ represent two such curves which differ not only by their locations but also by their shapes. All the results found in this chapter hold true for both cases above.

Figure 4.2.1 shows a locus of planar curves 1, 2, 3, 4, etc. The envelope of a locus of planar curves is the simple, regular planar curve which is in tangency with every curve of the locus. This geometric concept of an envelope must be based on strict definitions proposed in the field of differential geometry by Zalgaller (1975), Favard (1957), and other authors. These definitions state the necessary and sufficient conditions for the existence of a *piece* of the envelope in the neighborhood of a point (θ_0, ϕ_0) .

The necessary conditions of envelope existence determine points on the locus of curves in the neighborhood of point (θ_0, ϕ_0) at which the curves can be in tangency with the piece of the envelope if the envelope exists. The sufficient conditions of envelope existence determine the requirements by which, if observed, the piece of the envelope really exists as a *simple, regular curve*. Although in most applications in the Theory of Gearing we may limit our investigation to necessary conditions only, cases do arise where both the necessary and sufficient conditions must be used to guarantee the existence of a piece of an envelope at point (θ_0, ϕ_0) .

A piece of the envelope of a locus of planar curves (4.2.1) is a regular curve

$$\mathbf{R}(\phi) \in C^1 \quad \mathbf{R}_\phi \neq 0 \quad \phi \in (a,b) \quad (4.2.3)$$

such that it is in tangency with at least one of the curves of the locus at any value of ϕ . The correspondence between parameters θ and ϕ is set up by the equation

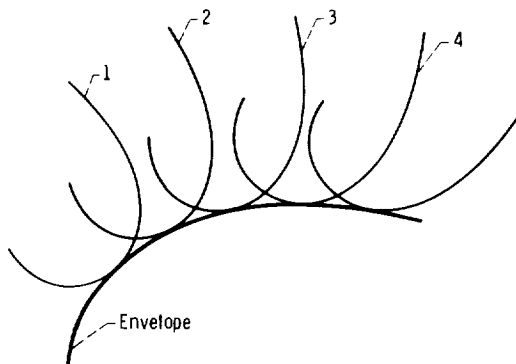


Figure 4.2.1.

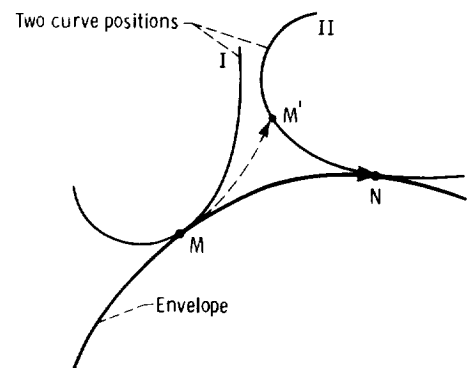


Figure 4.2.2.

$$f(\theta, \phi) = 0 \quad f_\theta \neq 0 \quad (4.2.4)$$

The whole complex of envelope pieces which are determined separately in the neighborhood of individual points $(\theta_0^{(1)}, \phi_0^{(1)})$, $(\theta_0^{(2)}, \phi_0^{(2)})$, . . . represents the envelope in totality.

Theorem The necessary condition of envelope existence is established by the following theorem. Assume that the locus of curves (eq. (4.2.1)) has an envelope (eq. (4.2.3)) in the neighborhood of point (θ_0, ϕ_0) . This point corresponds to the point of tangency between curve $\mathbf{r}(\theta, \phi_0)$ of the locus and the envelope $\mathbf{R}(\phi)$. Then the point (θ_0, ϕ_0) (parameters of value θ_0, ϕ_0) must satisfy the equation

$$f(\theta, \phi) = [\mathbf{k} \mathbf{r}_\theta \mathbf{r}_\phi] = 0 \quad (4.2.5)$$

Here \mathbf{k} is the unit vector of the z -axis which is perpendicular to the planar curves (eq. (4.2.1)).

The aim of this theorem is to develop a relation between parameters (θ, ϕ) in equations (4.2.1) by which a curve of the locus may be in tangency with the envelope. By choosing a point on the planar curve (choosing the parameter θ_0), we can find the corresponding parameter ϕ_0 by using equation (4.2.5). The position vector $\mathbf{r}(\theta_0, \phi_0)$ determines the point of tangency of the curve $\mathbf{r}(\theta, \phi_0)$ with the envelope $\mathbf{R}(\phi)$. (Here, ϕ_0 is fixed.)

Proof: Suppose that I and II are two infinitesimally close positions of the same curve, and M and N are their points of tangency with the envelope (fig. 4.2.2). By taking into account that function (4.2.3) represents the envelope, the displacement of the point of tangency \widehat{MN} along the envelope may be determined as

$$d\mathbf{R} = \mathbf{R}_\phi d\phi \quad (4.2.6)$$

where

$$\mathbf{R}_\phi = \frac{d}{d\phi}(\mathbf{R}(\phi))$$

As the planar curve comes to position II, a different point (point N) comes into tangency with the envelope. The old point of tangency on the curve (point M) moves to point M' . The arc $\widehat{MM'}$ is the displacement of the curve point M with the curve (the parameter of motion ϕ changes while the parameter θ is fixed). The arc $\widehat{M'N}$ is the displacement of the point of tangency along the curve (the parameter θ changes while the parameter ϕ is fixed). The resulting displacement \widehat{MN} may be represented as

$$\widehat{MN} = \widehat{MM'} + \widehat{M'N} \quad (4.2.7)$$

By using the function $\mathbf{r}(\theta, \phi)$, we represent the resulting displacement by

$$d\mathbf{r} = \mathbf{r}_\phi d\phi + \mathbf{r}_\theta d\theta \quad (4.2.8)$$

where $\mathbf{r}_\phi d\phi = \widehat{MM'}$ and $\mathbf{r}_\theta d\theta = \widehat{M'N}$.

Due to the continuity of tangency of the locus curves with the envelope, we have

$$\mathbf{R}_\phi d\phi = \mathbf{r}_\phi d\phi + \mathbf{r}_\theta d\theta \quad (4.2.9)$$

Vector \mathbf{R}_ϕ represents the tangent vector to the envelope and vector \mathbf{r}_θ represents the tangent vector to the curve of the locus. By definition of an envelope, vectors \mathbf{R}_ϕ and \mathbf{r}_θ must be collinear at the point of tangency. Since we consider a locus of regular curves only, we have $\mathbf{r}_\theta \neq 0$. Thus,

equation (4.2.9) may be observed if and only if \mathbf{r}_θ is collinear to \mathbf{r}_ϕ and \mathbf{R}_ϕ . The collinearity of these three vectors yields that

$$\mathbf{r}_\theta \times \mathbf{r}_\phi = \mathbf{0} \quad (4.2.10)$$

which may be also represented as

$$\frac{D(x,y)}{D(\theta,\phi)} = \begin{vmatrix} x_\theta & y_\theta \\ x_\phi & y_\phi \end{vmatrix} = f(\theta,\phi) = 0 \quad (4.2.11)$$

On the basis of equation (4.2.10), another form of the relation between θ and ϕ may be developed. The normal \mathbf{N} to a planar curve may be represented as

$$\mathbf{N} = \mathbf{r}_\theta \times \mathbf{k}$$

where \mathbf{k} is the unit vector of the axis which is perpendicular to the plane of the planar curve. Since \mathbf{N} is perpendicular to the tangent vector \mathbf{r}_θ , and because \mathbf{r}_ϕ and \mathbf{r}_θ are collinear, we get

$$\mathbf{N} \cdot \mathbf{r}_\theta = \mathbf{N} \cdot \mathbf{r}_\phi = 0$$

This yields

$$[\mathbf{r}_\theta \ \mathbf{k} \ \mathbf{r}_\phi] = 0$$

or (since the scalar triple product is equal to zero)

$$[\mathbf{k} \ \mathbf{r}_\theta \ \mathbf{r}_\phi] = f(\theta,\phi) = 0 \quad (4.2.12)$$

The sufficient conditions of envelope existence is given by the following theorem.

Theorem Consider a locus of planar curves given as

$$\mathbf{r}(\theta,\phi) \in C^2 \quad \mathbf{r}_\theta \neq 0 \quad \theta \in G \quad a < \phi < b \quad (4.2.13)$$

If at a point (θ_0, ϕ_0) the following requirements are observed

$$f(\theta,\phi) = [\mathbf{k} \ \mathbf{r}_\theta \ \mathbf{r}_\phi] = 0 \quad (4.2.14)$$

$$f_\theta \neq 0 \quad (4.2.15)$$

$$\mathbf{T} = \mathbf{r}_\phi f_\theta - \mathbf{r}_\theta f_\phi \neq 0 \quad (4.2.16)$$

then the envelope exists in the neighborhood of that point and is a regular curve.

Proof: Due to the requirement (4.2.15), the equation (4.2.12) possesses a unique solution as

$$\theta(\phi) \in C^1 \quad (4.2.17)$$

(See app. B.) With function (4.2.17), the vector function $\mathbf{r}(\theta,\phi)$ may be represented as

$$\mathbf{r}(\theta(\phi),\phi) = \mathbf{R}(\phi) \quad (4.2.18)$$

The tangent vector to the curve (eq. (4.2.18)) is

$$\mathbf{R}_\phi = \mathbf{r}_\theta \theta_\phi + \mathbf{r}_\phi \quad (4.2.19)$$

Differentiation of the identity

$$f(\theta(\phi), \phi) = 0$$

yields

$$f_\theta \theta_\phi + f_\phi = 0$$

and thus

$$\theta_\phi = -\frac{f_\phi}{f_\theta} \quad (f_\theta \neq 0) \quad (4.2.20)$$

Substituting θ_ϕ into equation (4.2.19) and considering expression (4.2.20), we get

$$\mathbf{R}_\phi = -\mathbf{r}_\theta \frac{f_\phi}{f_\theta} + \mathbf{r}_\phi = \mathbf{T} \quad (4.2.21)$$

Due to equation (4.2.14), vectors \mathbf{r}_θ and \mathbf{r}_ϕ are collinear. Vectors \mathbf{R}_ϕ and \mathbf{r}_θ are collinear due to equation (4.2.19). Thus, the curve $\mathbf{R}(\phi)$ is in tangency with the curve $\mathbf{r}(\theta, \phi_0)$. Due to inequality (4.2.16), $\mathbf{R}(\phi)$ represents a *regular* curve. This curve is the envelope and may be represented by

$$\mathbf{r}(\theta, \phi) \quad f(\theta, \phi) = [\mathbf{k} \mathbf{r}_\theta \mathbf{r}_\phi] = 0 \quad (4.2.22)$$

Example problem 4.2.1 Consider the locus of straight lines represented by the equations shown in (4.1.16), which are repeated here for convenience (the subscript 1 has temporarily been dropped)

$$\left. \begin{aligned} x(u, \phi) &= u \sin(\psi_c + \phi) + r(\sin \phi - \phi \cos \phi) \\ y(u, \phi) &= u \cos(\psi_c + \phi) + r(\cos \phi + \phi \sin \phi) \end{aligned} \right\} \quad (4.2.23)$$

where $-u_1 < u < u_2$ and $a < \phi < b$. Determine the necessary and sufficient conditions of envelope existence.

Solution. The necessary condition of envelope existence (eq. (4.2.12)) is

$$f(u, \phi) = [\mathbf{k} \mathbf{r}_u \mathbf{r}_\phi] = 0$$

which yields

$$\begin{aligned} f(u, \phi) &= \begin{vmatrix} x_u & y_u \\ x_\phi & y_\phi \end{vmatrix} = \begin{vmatrix} \sin(\psi_c + \phi) & \cos(\psi_c + \phi) \\ u \cos(\psi_c + \phi) + r\phi \sin \phi & -u \sin(\psi_c + \phi) + r\phi \cos \phi \end{vmatrix} \\ &= -u + r\phi \sin \psi_c = 0 \end{aligned} \quad (4.2.24)$$

The first of the sufficient conditions of envelope existence, inequality (4.2.15), is observed because

$$f_u = -1 \neq 0$$

The tangent \mathbf{T} to the envelope is (use equations (4.2.16) and (4.2.24))

$$\begin{aligned} \mathbf{T} &= \mathbf{r}_\phi f_u - \mathbf{r}_u f_\phi = (x_\phi f_u - x_u f_\phi)\mathbf{i} + (y_\phi f_u - y_u f_\phi)\mathbf{j} \\ &= -r \left\{ \phi [\sin \psi_c \cos (\psi_c + \phi) + \sin \phi] + \sin \psi_c \sin (\psi_c + \phi) \right\} \mathbf{i} \\ &\quad + r \left\{ \phi [\sin \psi_c \sin (\psi_c + \phi) - \cos \phi] - \sin \psi_c \cos (\psi_c + \phi) \right\} \mathbf{j} \end{aligned} \quad (4.2.25)$$

Equations (4.2.25) yield that $T_x = 0$ and $T_y = 0$ by

$$\phi = -\tan \psi_c \quad (4.2.26)$$

The value of u , which corresponds to the value of ϕ , is (see equation (4.2.24))

$$u = -r \tan \psi_c \sin \psi_c \quad (4.2.27)$$

Consequently, a piece of the envelope does not exist in the neighborhood of the point with the values of u and ϕ above. At all other points the envelope exists and may be represented by equations (4.2.23) and (4.2.24). These equations, after eliminating parameter u , yield

$$\left. \begin{aligned} x &= r \sin \phi - r\phi \cos \psi_c \cos (\phi + \psi_c) \\ y &= r \cos \phi + r\phi \cos \psi_c \sin (\phi + \psi_c) \end{aligned} \right\} \quad (4.2.28)$$

To prove that the envelope is an involute curve, let us apply a new coordinate system $S_e(x_e, y_e)$ whose axis x_e forms a constant angle $q = \text{inv}(\psi_c) = \tan \psi_c - \psi_c$ with the x_1 axis of coordinate system $S_1(x_1, y_1)$ (fig. 4.2.3).

The matrix representation of coordinate transformation is

$$[r_e] = [M_{e1}][r_1] \quad (4.2.29)$$

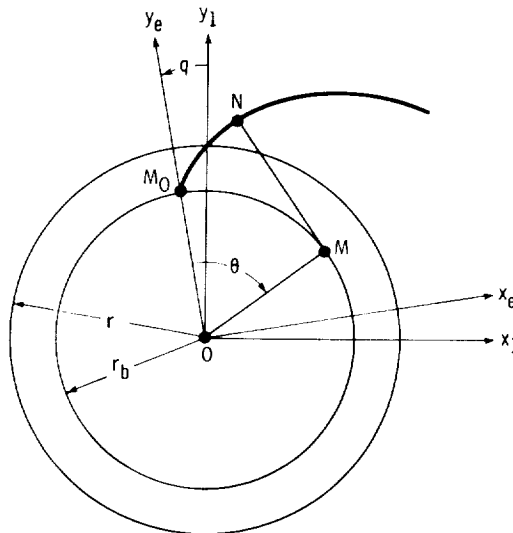


Figure 4.2.3.

Here

$$[r_1] = \begin{bmatrix} x \\ y \\ 1 \end{bmatrix} \text{ and } [M_{e1}] = \begin{bmatrix} \cos q & \sin q & 0 \\ -\sin q & \cos q & 0 \\ 0 & 0 & 1 \end{bmatrix} \quad (4.2.30)$$

where x and y are represented by equations (4.2.28). Equations (4.2.28) to (4.2.30) yield

$$\left. \begin{aligned} x_e &= r \sin(\phi + q) - r\phi \cos \psi_c \cos(\phi + \psi_c + q) \\ y_e &= r \cos(\phi + q) + r\phi \cos \psi_c \sin(\phi + \psi_c + q) \end{aligned} \right\} \quad (4.2.31(a))$$

Using substitutions

$$\phi + \psi_c + q = \phi + \psi_c + \text{inv}(\psi_c) = \phi + \tan \psi_c = \theta$$

and $\phi = \theta - \tan \psi_c$ and $\phi + q = \theta - \psi_c$, we get

$$\left. \begin{aligned} x_e &= r_b \sin \theta - r_b \theta \cos \theta \\ y_e &= r_b \cos \theta + r_b \theta \sin \theta \end{aligned} \right\} \quad (4.2.31(b))$$

where $r_b = r \cos \psi_c$. Equations (4.2.31(b)) represent an involute curve which corresponds to the base circle of radius r_b (fig. 4.2.3).

Problem 4.2.1 Consider a gear mechanism formed by gear 1 and rack 2 (fig. 4.1.3(a)). Coordinate systems S_1 , S_2 , and S_f are rigidly connected with gear 1, rack 2, and the frame, respectively. The shape of the gear tooth is an involute curve represented by the equations

$$x_1 = r_b \sin \theta - r_b \theta \cos \theta \quad y_1 = r_b \cos \theta + r_b \theta \sin \theta \quad (4.2.32)$$

where $0 < \theta < \theta_1$.

The translation of rack 2 and the rotation of gear 1 are related by the equation

$$s = r\phi = \frac{r_b}{\cos \psi_c} \phi \quad (4.2.33)$$

Derive equations of the locus of involute curves generated in coordinate system S_2 , and find necessary and sufficient conditions for the existence of the envelope. Develop equations of the envelope.

Answer. The locus of involute curves generated in coordinate system $S_2(x_2, y_2)$ is represented by the following equations (the subscript 2 in x_2 and y_2 is omitted for simplification)

$$\left. \begin{aligned} x &= x_1 \cos \phi - y_1 \sin \phi + r\phi = r_b \sin(\theta - \phi) - r_b \theta \cos(\theta - \phi) + r\phi \\ y &= x_1 \sin \phi + y_1 \cos \phi - r = r_b \cos(\theta - \phi) + r_b \theta \sin(\theta - \phi) - r \end{aligned} \right\} \quad (4.2.34)$$

where $0 < \theta < \theta_1$ and $a < \phi_1 < b$. The necessary condition of envelope existence, equation (4.2.14), is as follows:

$$f(\theta, \phi) = \cos \psi_c - \cos (\theta - \phi) = 0 \quad (\theta \neq 0) \quad (4.2.35)$$

Thus, $\theta - \phi = \psi_c$. Inequality (4.2.15)

$$f_\theta = \sin (\theta - \phi) \neq 0 \quad (4.2.36)$$

is observed, if $\psi_c \neq 0$. (See eq. (4.2.35).)

The tangent vector \mathbf{T} (see expression (4.2.16) is given by

$$\left. \begin{aligned} T_x &= x_\alpha f_\theta - x_\theta f_\phi = r_b \sin^2 \psi_c \tan \psi_c \neq 0 \\ T_y &= y_\alpha f_\theta - y_\theta f_\phi = r_b \sin^2 \psi_c \neq 0 \end{aligned} \right\} \quad (4.2.37)$$

Since inequality (4.2.16) is observed, the envelope exists and may be represented by equations (4.2.34) and (4.2.35), which yield

$$\left. \begin{aligned} x &= r_b \operatorname{inv} \psi_c \cos \psi_c + r_b \phi \sin \psi_c \tan \psi_c \\ y &= -r_b \operatorname{inv} \psi_c \sin \psi_c + r_b \phi \sin \psi_c \end{aligned} \right\} \quad (4.2.38)$$

where ϕ is the shape parameter and $\operatorname{inv} \psi_c = \tan \psi_c - \psi_c$. Equations (4.2.38) represent a straight line which forms an angle of ψ_c with the y_2 -axis. This straight line is the shape of the rack tooth which is conjugate to the involute curve (the shape of the gear tooth).

Problem 4.2.2 Given the conditions of problem 4.2.1, consider the case when $r = r_b$ and $\psi_c = 0$. Prove that the envelope does not exist as a regular curve. What kind of rack tooth shape do equations (4.2.38) now represent?

Answer. The envelope does not exist as a regular curve because none of the inequalities (eq. (4.2.37)) are observed. Equations (4.2.38) represent the rack tooth "shape" which is, in fact, a single point ($x = 0, y = 0$). This point generates an involute curve if the rack is the tool and the gear is to be cut (fig. 4.2.4).

4.3 Envelope of a Locus of Planar Curves: Representation in Implicit Form

Consider the equation

$$F(x, y, \phi) = 0 \quad (x, y) \in G \quad a < \phi < b \quad (4.3.1)$$

The equation

$$F(x, y, \phi_0) = 0 \quad (4.3.2)$$

(ϕ_0 is fixed) represents a simple regular curve in the neighborhood of the point (x_0, y_0) if at this point the following requirements are observed:

$$F(x, y, \phi_0) \in C^1 \quad |F_x| + |F_y| \neq 0 \quad (4.3.3)$$

If the requirements of equation (4.3.3) are observed for different values of ϕ_0 , then equation (4.3.1) represents a locus of locally simple regular curves (in the neighborhood of the point (x_0, y_0, ϕ_0)). The envelope of this locus is defined as follows: A piece of the envelope of a locus of curves is such a regular curve represented by

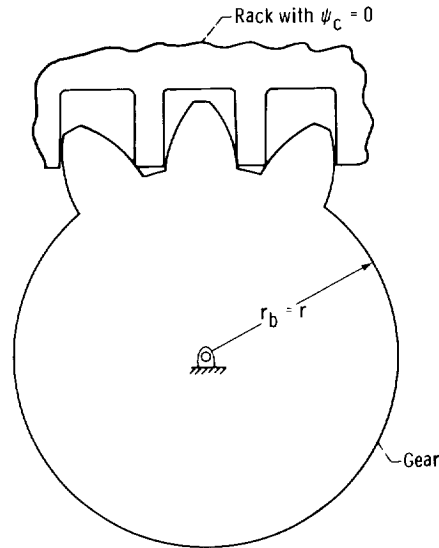


Figure 4.2.4.

$$\mathbf{R}(\phi) = x(\phi)\mathbf{i} + y(\phi)\mathbf{j} \quad \mathbf{R}(\phi) \in C^1 \quad \mathbf{R}_\phi = \frac{d}{d\phi}(\mathbf{R}(\phi)) \neq \mathbf{0}$$

$$(x, y) \in G \quad a < \phi < b \quad (4.3.4)$$

which is in tangency with curves $F(x, y, \phi_0)$ for every value of ϕ_0 .

Theorem The necessary condition for existence of the envelope is given by the following theorem. Assume that at the point (x_0, y_0, ϕ_0) equation (4.3.1) and requirements (4.3.3) are observed. If the envelope indeed exists in the neighborhood of the point (x_0, y_0, ϕ_0) , this point belongs to the set

$$F_\phi(x, y, \phi) = 0 \quad (4.3.5)$$

where

$$F_\phi = \frac{\partial}{\partial \phi}(F(x, y, \phi))$$

Proof: Assume that just the partial derivative F_y differs from zero at the point (x_0, y_0, ϕ_0) . Then, as is stated by the Theorem of Implicit Function Existence (app. B), equation (4.3.1) (by observing requirements (4.3.3)) may be solved as a function

$$y(x, \phi) \in C^1 \quad (4.3.6)$$

in the neighborhood of the point (x_0, y_0, ϕ_0) . With function (4.3.6), equation (4.3.1) becomes an identity

$$F(x, y(x, \phi), \phi) \equiv 0 \quad (4.3.7)$$

and its differentiation yields

$$F_x + F_y y_x = 0 \quad (4.3.8)$$

$$F_\phi + F_y y_\phi = 0 \quad (4.3.9)$$

Consequently,

$$y_x = -\frac{F_x}{F_y} \quad (F_y \neq 0) \quad (4.3.10)$$

$$y_\phi = -\frac{F_\phi}{F_y} \quad (F_y \neq 0) \quad (4.3.11)$$

Function $y(x, \phi_0)$ (ϕ_0 is the fixed value of ϕ) represents a single curve of the locus in the coordinate system $S(x, y)$. Here x and y are coordinates of the curve point whose position vector may be represented as

$$\mathbf{r}(x, y(x, \phi_0)) = \{x\mathbf{i} + y(x, \phi_0)\mathbf{j}\} \in C^1 \quad (x, y) \in G \quad (4.3.12)$$

If we allow the value of ϕ to vary from $\phi = \phi_0$, we get the following vector equation:

$$\mathbf{r}(x, y(x, \phi)) = \{x\mathbf{i} + y(x, \phi)\mathbf{j}\} \in C^1 \quad (x, y) \in G \quad a < \phi < b \quad (4.3.13)$$

Let us now differentiate equations (4.3.12) and (4.3.13) and get

$$\delta \mathbf{r} = \delta x (\mathbf{i} + y_x \mathbf{j}) \quad (4.3.14)$$

$$d\mathbf{r} = dx \mathbf{i} + (y_x dx + y_\phi d\phi) \mathbf{j} \quad (4.3.15)$$

Since ϕ_0 is fixed in equation (4.3.12), vector $\delta \mathbf{r}$ represents the infinitesimal displacement of a point along the curve. Further, since ϕ is a variable parameter in equation (4.3.13), vector $d\mathbf{r}$ represents the infinitesimal displacement of a point both along and with the curve. (See fig. 4.2.2.) For a piece of the envelope of locus (4.3.13) to exist in the neighborhood of the point (x_0, y_0) and for the envelope to be in continuous tangency with the locus, vectors $\delta \mathbf{r}$ and $d\mathbf{r}$ must be collinear. Due to this collinearity we may write

$$\frac{dx}{\delta x} = \frac{y_x dx + y_\phi d\phi}{y_x \delta x} = \lambda \quad (4.3.16)$$

where $\lambda \neq 0$. It is easily seen from this equation that

$$y_\phi d\phi = 0 \quad (4.3.17)$$

Equations (4.3.17) and (4.3.11) yield

$$-\frac{F_\phi}{F_y} d\phi = 0 \quad (F_y \neq 0) \quad (4.3.18)$$

It is clear that $d\phi \neq 0$ because the changing values of ϕ correspond to different points on the envelope. Consequently, equation (4.3.18) may be observed if and only if the partial derivative $F_\phi = 0$.

Sufficient Conditions of Envelope Existence

Theorem Consider a locus of curves

$$F(x, y, \phi) = 0 \quad F \in C^2 \quad (x, y) \in G \quad a < \phi < b \quad (4.3.19)$$

Assume that at the point (x_0, y_0, ϕ_0) the following requirements are observed:

$$F(x_0, y_0, \phi_0) = 0 \quad |F_x| + |F_y| \neq 0 \quad F_\phi = 0 \quad F_{\phi\phi} \neq 0$$

$$\Delta = \frac{D(F, F_\phi)}{D(x, y)} = \begin{vmatrix} F_x & F_y \\ F_{\phi x} & F_{\phi y} \end{vmatrix} \neq 0 \quad (4.3.20)$$

where

$$F_{\phi x} = \frac{\partial}{\partial x} [F_\phi(x, y, \phi)] \quad F_{\phi y} = \frac{\partial}{\partial y} [F_\phi(x, y, \phi)] \quad F_\phi = \frac{\partial}{\partial \phi} [F(x, y, \phi)]$$

A piece of the envelope indeed exists in the neighborhood of the point (x_0, y_0, ϕ_0) , and it is a simple, regular curve which may be represented by the following equations:

$$F(x, y, \phi) = 0 \quad F_\phi(x, y, \phi) = 0 \quad (4.3.21)$$

Proof: Assume that at the point (x_0, y_0, ϕ_0) , the equations

$$F(x, y, \phi) = 0 \quad F_\phi(x, y, \phi) = 0 \quad F \in C^2 \quad F_\phi \in C^1$$

are observed, and the inequality

$$\Delta = \frac{D(F, F_\phi)}{D(x, y)} \neq 0$$

is also observed. Due to this inequality, equations $F = 0$ and $F_\phi = 0$ may be solved as functions

$$\{x(\phi), y(\phi)\} \in C^1 \quad (4.3.22)$$

in the neighborhood of the point (x_0, y_0, ϕ_0) . These functions represent a curve

$$\mathbf{R}(\phi) = x(\phi)\mathbf{i} + y(\phi)\mathbf{j} \quad \{x(\phi), y(\phi)\} \in C^1 \quad (4.3.23)$$

which exists in the neighborhood of point (x_0, y_0, ϕ_0) .

Let us now prove that the envelope is in tangency with single curves of the locus in the neighborhood of the point (x_0, y_0, ϕ_0) and that it is a regular curve. Considering functions (4.3.22) and equation (4.3.1) we get the following two identities:

$$F(x(\phi), y(\phi), \phi) \equiv 0 \quad F \in C^2 \quad (4.3.24)$$

$$F_\phi(x(\phi), y(\phi), \phi) \equiv 0 \quad F_\phi \in C^1 \quad (4.3.25)$$

Differentiation of identity (4.3.24) with respect to ϕ yields

$$\frac{\partial}{\partial \phi} \left[F(x(\phi), y(\phi), \phi) \right] = F_x x_\phi + F_y y_\phi + F_\phi = 0$$

where

$$x_\phi = \frac{dx}{d\phi} \quad y_\phi = \frac{dy}{d\phi}$$

Taking into account that $F_\phi = 0$ (eq. (4.3.20)), we get

$$F_x x_\phi + F_y y_\phi = 0 \quad (4.3.26)$$

Similarly, differentiation of identity (4.3.25) yields

$$F_{\phi x} x_\phi + F_{\phi y} y_\phi + F_{\phi\phi} = 0 \quad (4.3.27)$$

Equations (4.3.26) and (4.3.27) represent a system of two linear equations in unknowns x_ϕ and y_ϕ . The solution of these two equations for x_ϕ and y_ϕ is as follows:

$$x_\phi = \frac{\begin{vmatrix} 0 & F_y \\ -F_{\phi\phi} & F_{\phi y} \end{vmatrix}}{\begin{vmatrix} F_x & F_y \\ F_{\phi x} & F_{\phi y} \end{vmatrix}} = \frac{F_{\phi\phi} F_y}{\Delta} \quad (4.3.28)$$

$$y_\phi = \frac{\begin{vmatrix} F_x & 0 \\ F_{\phi x} & -F_{\phi\phi} \end{vmatrix}}{\begin{vmatrix} F_x & F_y \\ F_{\phi x} & F_{\phi y} \end{vmatrix}} = -\frac{F_{\phi\phi} F_x}{\Delta} \quad (4.3.29)$$

It results from equations (4.3.28) and (4.3.29) that

$$|x_\phi| + |y_\phi| \neq 0 \quad (4.3.30)$$

because $F_{\phi\phi} \neq 0$, $\Delta \neq 0$, and $|F_x| + |F_y| \neq 0$. (See eq. (4.3.20).) Consequently, the curve (eq. (4.3.23)) is a regular curve.

It is easy to prove that equation (4.3.26) represents the tangency of the envelope with the curves of the locus in the neighborhood of the point (x_0, y_0, ϕ_0) . These curves are indeed in tangency if their tangent vectors are collinear.

The tangent vector to the envelope given by

$$\mathbf{R}(\phi) = x(\phi)\mathbf{i} + y(\phi)\mathbf{j}$$

is represented by

$$\mathbf{t} = x_\phi \mathbf{i} + y_\phi \mathbf{j} \quad (4.3.31)$$

A curve of the locus is represented by the equation

$$F(x, y, \phi_0) = 0 \quad |F_x| + |F_y| \neq 0 \quad (4.3.32)$$

Recalling equation (3.2.9), we may express projections of the tangent $\boldsymbol{\tau}$ to this curve as follows:

$$\frac{\tau_y}{\tau_x} = -\frac{F_x}{F_y} \quad (4.3.33)$$

If vectors \mathbf{t} and $\boldsymbol{\tau}$ are collinear, their projections are related by

$$\frac{t_y}{t_x} = \frac{\tau_y}{\tau_x} \quad (4.3.34)$$

Equations (4.3.34), (4.3.31), and (4.3.33) yield

$$\frac{y_\phi}{x_\phi} = -\frac{F_x}{F_y} \quad (4.3.35)$$

Relation (4.3.35) results directly from equation (4.3.26), and the envelope is indeed in tangency with the locus curves. Since the curve represented by equation (4.3.23) is a regular curve and since it is in tangency with the curves of the locus in the neighborhood of the point (x_0, y_0, ϕ_0) , it is indeed a piece of the envelope.

4.4 Envelope of Planar Curve Locus: Kinematic Method of Determination

The necessary conditions of envelope existence may be interpreted kinematically. This interpretation simplifies the synthesis of planar gearings. The necessary condition for envelope existence is given by equation (4.2.12) which is

$$f(\theta, \phi) = \mathbf{N} \cdot \mathbf{r}_\phi = [\mathbf{r}_\theta \ \mathbf{k} \ \mathbf{r}_\phi] = 0 \quad (4.4.1)$$

This equation expresses the requirement that at points of tangency of the curves of the locus (1) with their envelope (2), the normal \mathbf{N} to the curve of the locus is perpendicular to vector \mathbf{r}_ϕ . As noted in section 4.2, vector \mathbf{r}_ϕ represents the linear velocity of a point M of curve (1) with respect to point M of the envelope (2); here M is the point of tangency of curves 1 and 2. Taking this into account, we may represent equation (4.4.1) as follows:

$$\mathbf{N} \cdot \mathbf{v}^{(12)} = f(\theta, \phi) = 0 \quad (4.4.2)$$

or as

$$\mathbf{N} \cdot \mathbf{v}^{(21)} = f(\theta, \phi) = 0 \quad (4.4.3)$$

where $\mathbf{v}^{(21)} = -\mathbf{v}^{(12)}$.

The scalar product (4.4.2) or (4.4.3) is an invariant property—it does not depend on the coordinate system in which it is applied. Usually we apply three coordinate systems; S_1 and S_2 , rigidly connected to gears 1 and 2, respectively, and S_f , rigidly connected to the frame. Vectors of the scalar product (4.4.2) or (4.4.3) may be represented in any of these three systems.

Equations (4.4.2) and (4.4.3) are known in the Theory of Gearing as equations of meshing. The most simple method for determination of this equation is based on the kinematic properties of planar motion.

We begin with determination of the relative velocity $\mathbf{v}^{(12)}$ for the situation shown in figure 4.1.1. Gears 1 and 2 rotate about axes z_1 and z_2 (they are not shown in figure 4.1.1) with angular velocities

$$\boldsymbol{\omega}^{(1)} = \omega^{(1)} \mathbf{k}_1 \quad (4.4.4)$$

$$\boldsymbol{\omega}^{(2)} = -\omega^{(2)} \mathbf{k}_2 \quad (4.4.5)$$

where \mathbf{k}_1 and \mathbf{k}_2 are unit vectors of axes z_1 and z_2 .

Suppose that vector $\mathbf{v}^{(12)}$ is to be expressed in terms of components of coordinate system S_1 (fig. 4.1.1). The sliding vector $\boldsymbol{\omega}^{(2)}$ does not pass through the origin O_1 of coordinate system S_1 ; therefore we replace it with an equal vector which passes through point O_1 and a moment

$$\mathbf{m} = \overline{O_1O_2} \times \boldsymbol{\omega}^{(2)} \quad (4.4.6)$$

Then the linear velocity of a point of gear 2 may be represented as follows:

$$\mathbf{v}^{(2)} = \left(\boldsymbol{\omega}^{(2)} \times \mathbf{r}_1 \right) + \left(\overline{O_1O_2} \times \boldsymbol{\omega}^{(2)} \right) \quad (4.4.7)$$

Here \mathbf{r}_1 is a position vector drawn from the origin O_1 to a point on gear 2.

The velocity of a point on gear 1 may be determined as

$$\mathbf{v}^{(1)} = \boldsymbol{\omega}^{(1)} \times \mathbf{r}_1 \quad (4.4.8)$$

The relative velocity $\mathbf{v}^{(12)}$ may be represented by the following equation:

$$\begin{aligned} \mathbf{v}_1^{(12)} &= \mathbf{v}_1^{(1)} - \mathbf{v}_1^{(2)} = \left(\left(\boldsymbol{\omega}_1^{(1)} - \boldsymbol{\omega}_1^{(2)} \right) \times \mathbf{r}_1 \right) - \left(\overline{O_1O_2} \times \boldsymbol{\omega}_1^{(2)} \right) \\ &= \left(\boldsymbol{\omega}_1^{(12)} \times \mathbf{r}_1 \right) - \left(\overline{O_1O_2} \times \boldsymbol{\omega}_1^{(2)} \right) \\ &= \begin{vmatrix} \mathbf{i}_1 & \mathbf{j}_1 & \mathbf{k}_1 \\ 0 & 0 & \omega_1^{(1)} + \omega_1^{(2)} \\ x_1 & y_1 & 0 \end{vmatrix} - \begin{vmatrix} \mathbf{i}_1 & \mathbf{j}_1 & \mathbf{k}_1 \\ C \sin \phi_1 & C \cos \phi_1 & 0 \\ 0 & 0 & -\omega_1^{(2)} \end{vmatrix} \\ &= - \left[\left(\omega^{(1)} + \omega^{(2)} \right) y_1 - \omega_1^{(2)} C \cos \phi_1 \right] \mathbf{i}_1 \\ &\quad + \left[\left(\omega^{(1)} + \omega^{(2)} \right) x_1 - \omega_1^{(2)} C \sin \phi_1 \right] \mathbf{j}_1 \end{aligned} \quad (4.4.9)$$

The subscript 1 in equation (4.4.9) denotes that vectors are expressed in terms of components of coordinate system $S_1(x_1, y_1)$.

Assuming that the shape of the gear 1 tooth is represented in parametric form by equation (4.1.3), we express the normal vector \mathbf{N} as

$$\mathbf{N}_1 = \frac{\partial y_1}{\partial \theta} \mathbf{i}_1 - \frac{\partial x_1}{\partial \theta} \mathbf{j}_1 \quad (4.4.10)$$

Now, the equation of meshing may be represented as

$$\frac{\partial y_1}{\partial \theta} v_{x_1}^{(12)} - \frac{\partial x_1}{\partial \theta} v_{y_1}^{(12)} = f(\theta, \phi) = 0 \quad (4.4.11)$$

Here v_{x_1} and v_{y_1} are components of the vector $\mathbf{v}_1^{(12)}$ represented by equation (4.4.9).

Similar results may be obtained if the scalar product is expressed in terms of components of coordinate system S_f . Hence, the matrix of the normal \mathbf{N}_f is (fig. 4.1.1)

$$\begin{aligned} [N_f] &= [L_f][N_1] = \begin{bmatrix} \cos \phi_1 & -\sin \phi_1 \\ \sin \phi_1 & \cos \phi_1 \end{bmatrix} \begin{bmatrix} \frac{\partial y_1}{\partial \theta} \\ -\frac{\partial x_1}{\partial \theta} \end{bmatrix} \\ &= \begin{bmatrix} \frac{\partial y_1}{\partial \theta} \cos \phi_1 + \frac{\partial x_1}{\partial \theta} \sin \phi_1 \\ \frac{\partial y_1}{\partial \theta} \sin \phi_1 - \frac{\partial x_1}{\partial \theta} \cos \phi_1 \end{bmatrix} \end{aligned} \quad (4.4.12)$$

The relative velocity $\mathbf{v}_f^{(12)}$ is represented by

$$\begin{aligned} \mathbf{v}_f^{(12)} &= (\boldsymbol{\omega}_f^{(12)} \times \mathbf{r}_f) - (\overline{O_1 O_2} \times \boldsymbol{\omega}_f^{(2)}) \\ &= \begin{bmatrix} \mathbf{i}_f & \mathbf{j}_f & \mathbf{k}_f \\ 0 & 0 & \omega_f^{(1)} + \omega_f^{(2)} \\ x_f & y_f & z_f \end{bmatrix} - \begin{bmatrix} \mathbf{i}_f & \mathbf{j}_f & \mathbf{k}_f \\ 0 & C & 0 \\ 0 & 0 & -\omega^{(2)} \end{bmatrix} \\ &= - \left[(\omega^{(1)} + \omega^{(2)}) y_f - \omega_f^{(2)} C \right] \mathbf{i}_f + (\omega_f^{(1)} + \omega_f^{(2)}) x_f \mathbf{j}_f \end{aligned} \quad (4.4.13)$$

Coordinates x_f and y_f may be expressed in terms of x_1 and y_1 with the matrix equation

$$[r_f] = [M_f][r_1]$$

or

$$\begin{bmatrix} x_f \\ y_f \\ 1 \end{bmatrix} = \begin{bmatrix} \cos \phi_1 & -\sin \phi_1 & 0 \\ \sin \phi_1 & \cos \phi_1 & 0 \\ 0 & 0 & 1 \end{bmatrix} \begin{bmatrix} x_1 \\ y_1 \\ 1 \end{bmatrix}$$

This yields

$$x_f = x_1 \cos \phi_1 - y_1 \sin \phi_1 \quad y_f = x_1 \sin \phi_1 + y_1 \cos \phi_1 \quad (4.4.14)$$

Using the results from equations (4.4.12) to (4.4.14), we may determine the equation of meshing by

$$f(\theta, \phi) = \mathbf{N}_f \cdot \mathbf{v}_f^{(12)} = 0 \quad (4.4.15)$$

Another kinematic representation of the equation of meshing is based on the following General Theorem of Plane Gearing.

General Theorem of Plane Gearing Conjugate tooth shapes must be such that their common normal at point of tangency intersects the line of rotation centers O_1O_2 (fig. 4.4.1) and divides it into two segments, O_1I and O_2I , which are related as follows:

$$\frac{O_2I}{O_1I} = \frac{\omega_1}{\omega_2} = m_{12} \quad (O_1I + O_2I = C) \quad (4.4.16)$$

Here m_{12} may be a prescribed function such as $m_{12}(\phi_1)$ or a constant.

Proof: Consider that gears 1 and 2 rotate about centers O_1 and O_2 (fig. 4.4.1), respectively, and that the given instantaneous angular velocity ratio is m_{12} . Thus, the location of the instantaneous center of rotation is determined by equation (4.4.16), and the relative motion of gear 1 with respect to gear 2 is rotation about point I (with angular velocity $\omega^{(12)} = \omega^{(1)} + \omega^{(2)}$ if the gears rotate in opposite directions).

Suppose that the shape Σ_1 of gear tooth 1 is given and it is necessary to determine the shape Σ_2 of gear 2. We know that at the point of tangency of shapes Σ_1 and Σ_2 , point M , equation (4.4.2)

$$\mathbf{N} \cdot \mathbf{v}^{(12)} = 0$$

must be observed.

The relative velocity $\mathbf{v}^{(12)}$ is given by

$$\mathbf{v}^{(12)} = \boldsymbol{\omega}^{(12)} \times \overline{IM} \quad (4.4.17)$$

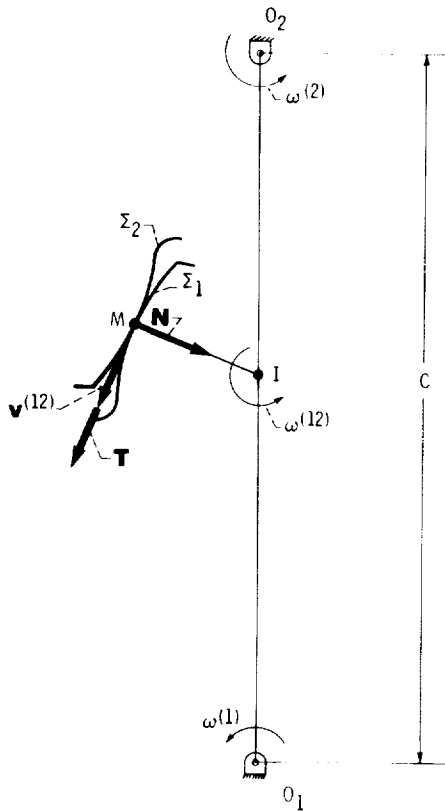


Figure 4.4.1.

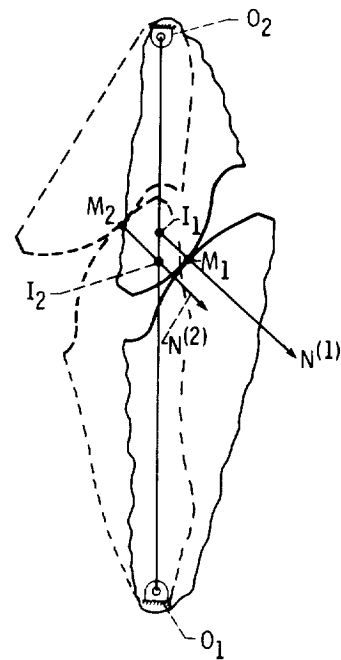


Figure 4.4.2.

and is directed along \mathbf{T} , the common tangent vector of the shapes. The normal \mathbf{N} is perpendicular to the tangent \mathbf{T} . Consequently, the normal drawn at the point of the shape tangency M must pass through the instantaneous center of rotation I .

If shapes Σ_1 and Σ_2 are chosen arbitrarily, they cannot transform rotational motion with the prescribed angular velocity ratio m_{12} . Suppose that m_{12} must be a constant but the shapes of the gear teeth are not conjugate. Figure 4.4.2 shows such shapes in two positions. The normals $\mathbf{N}^{(1)}$ and $\mathbf{N}^{(2)}$ at points of tangency M_1 and M_2 intersect the center distance at two different points (I_1, I_2). This is the sign that the motion is transformed with a nonconstant angular velocity ratio.

4.5 Conjugate Shapes: Working Equations for Their Determination

The key to the problem of conjugated shapes lies in determining the equation of meshing

$$f(\theta, \phi) = 0 \quad (4.5.1)$$

As stated earlier, this equation relates the parameter θ of the given shape Σ_1 with the parameter ϕ of the locus generation (curve Σ_1 motion).

To find a conjugate shape with the classical methods of differential geometry, the following procedure must be applied:

- (1) The locus of shapes Σ_1 , represented by the vector function

$$\mathbf{r}_2(\theta, \phi) \in C^1 \quad (4.5.2)$$

must be determined. This locus is generated in coordinate system S_2 , which is rigidly connected to gear 2.

- (2) The equation of meshing (4.5.1) given by

$$\frac{\partial \mathbf{r}_2}{\partial \theta} \times \frac{\partial \mathbf{r}_2}{\partial \phi} = \mathbf{0} \quad (4.5.3)$$

must be determined.

Although the above method is, of course, workable, the following procedure substantially simplifies the determination of conjugate shapes. To determine the equation of meshing (eq. (4.5.1)), it is not necessary to develop vector function (4.5.2), determine its partial derivatives, and then derive equation (4.5.3). Representing the given shape Σ_1 by

$$\mathbf{r}_1(\theta) \in C^1 \quad \frac{d\mathbf{r}_1}{d\theta} \neq 0 \quad \theta \in G \quad (4.5.4)$$

we just require that the normal $\mathbf{N}_1(\theta)$ passes through the instantaneous center of rotation I . The shape Σ_1 , represented by equation (4.5.4), is a simple, regular curve.

To find the conjugate shape Σ_2 , it is necessary to determine the following: (1) the relation between the location of contact points on shape Σ_1 and the angle of gear 1 rotation ϕ_1 and (2) the shape of gear 2 tooth Σ_2 as the locus of contact points in coordinate system S_2 (rigidly connected to gear 2). In addition, we may determine the line of action as the locus of contact points in the fixed coordinate system S_f .

We shall limit our discussion to the case of a constant angular velocity ratio m_{12} . However, the equations given below may be easily applied to the case of $m_{12}(\phi_1) \neq \text{constant}$.

Location of Pitch Point

Coordinates of the pitch point I (the instantaneous center of rotation and the point of tangency of gear centrodes) are represented in coordinate systems S_f and S_1 as follows:

$$X_f = 0 \quad Y_f = OI = \frac{C}{1 + m_{12}} = r_1 \quad (4.5.5)$$

$$X_1 = r_1 \sin \phi_1 \quad Y_1 = r_1 \cos \phi_1 \quad (4.5.6)$$

The normal to shape Σ_1 is

$$\mathbf{N}_1 = \frac{\partial \mathbf{r}_1}{\partial \theta} \times \mathbf{k}_1 = \frac{\partial y_1}{\partial \theta} \mathbf{i}_1 - \frac{\partial x_1}{\partial \theta} \mathbf{j}_1 \quad (4.5.7)$$

where \mathbf{i}_1 , \mathbf{j}_1 , and \mathbf{k}_1 are unit vectors of the axes of coordinate system $S_1(x_1, y_1, z_1)$.

Equation of Meshing

The normal \mathbf{N}_1 to shape Σ_1 must pass through the pitch point I . Thus,

$$\frac{X_1(\phi_1) - x_1(\theta)}{N_{x1}(\theta)} - \frac{Y_1(\phi_1) - y_1(\theta)}{N_{y1}(\theta)} = f(\theta, \phi_1) = 0 \quad (4.5.8)$$

Equations (4.5.6), (4.5.7), and (4.5.8) yield

$$\frac{r_1 \sin \phi_1 - x_1(\theta)}{\frac{\partial y_1}{\partial \theta}} + \frac{r_1 \cos \phi_1 - y_1(\theta)}{\frac{\partial x_1}{\partial \theta}} = f(\theta, \phi_1) = 0 \quad (4.5.9)$$

This equation relates the location of the contact point on Σ_1 (parameter θ) with the angle of gear rotation ϕ_1 .

The equation of meshing may also be derived by using the equation of the normal represented in coordinate system S_f

$$\frac{X_f - x_f}{N_{xf}} - \frac{Y_f - y_f}{N_{yf}} = f(\theta, \phi_1) = 0 \quad (4.5.10)$$

Here $X_f = 0$, $Y_f = r_1$, and (x_f, y_f) , and (N_{xf}, N_{yf}) are represented by the following matrix equations:

$$[r_f] = [M_f][r_1] \quad [N_f] = [L_f][N_1] \quad (4.5.11)$$

where (fig. 4.5.1)

$$[M_f] = \begin{bmatrix} \cos \phi_1 & -\sin \phi_1 & 0 \\ \sin \phi_1 & \cos \phi_1 & 0 \\ 0 & 0 & 1 \end{bmatrix} \quad [L_f] = \begin{bmatrix} \cos \phi_1 & -\sin \phi_1 \\ \sin \phi_1 & \cos \phi_1 \end{bmatrix}$$

Line of Action

The line of action is determined by the following equations:

$$[r_f] = [M_f][r_1] \quad f(\theta, \phi_1) = 0 \quad (4.5.13)$$

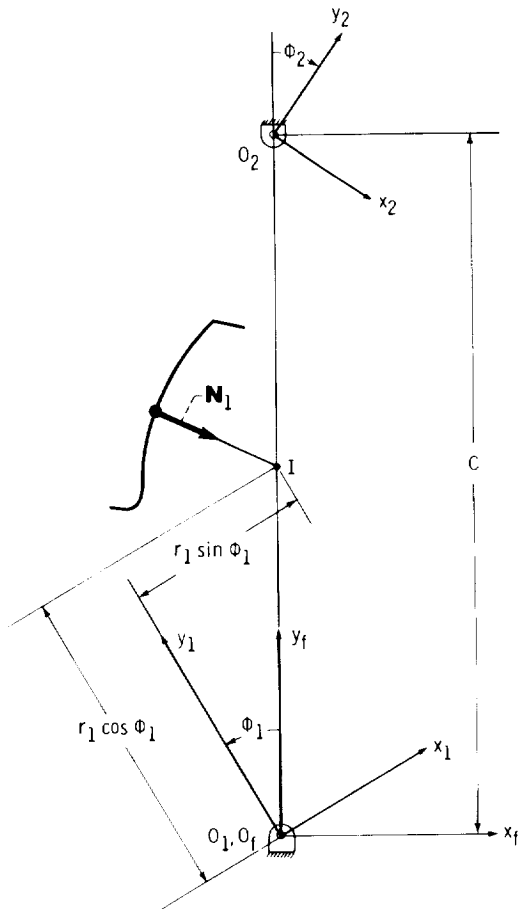
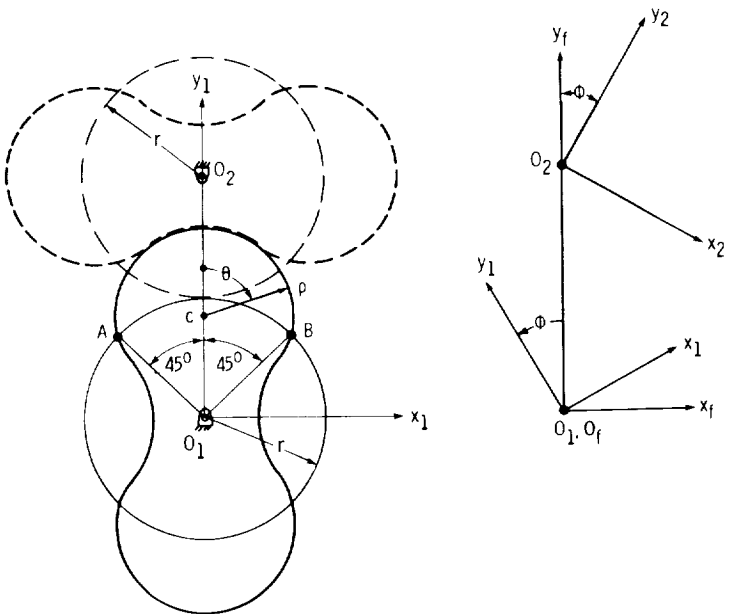


Figure 4.5.1.



(a)

(b)

Figure 4.5.2.

Shape Σ_2 is determined as follows:

$$[r_2] = [M_{21}][r_1] = [M_{2f}][M_{f1}][r_1] \quad f(\theta, \phi_1) = 0 \quad (4.5.13)$$

Problem 4.5.1 Consider the Root's blower which consists of two, two-lobed gears (fig. 4.5.2(a)). The shape Σ_1 is a circular arc of radius ρ centered at point C . The angle AO_1B , corresponding to the tooth addendum, is equal to 90° , and parameters $a = O_1C$, ρ , and r are related through the following equation:

$$r^2 + a^2 - 2ar \cos 45^\circ = \rho^2$$

The shape Σ_1 is represented by the equations

$$x_1 = \rho \sin \theta \quad y_1 = \rho \cos \theta + a \quad -45^\circ < \theta < 45^\circ \quad (4.5.14)$$

Determine (1) the equation of meshing, (2) the line of action, and (3) equations of the shape Σ_2 , which is conjugate to Σ_1 . Apply coordinate systems shown in figure 4.5.2(b).

Answer. The equation of meshing is

$$f(\theta, \phi_1) = r \sin(\theta - \phi) - a \sin \theta = 0 \quad (4.5.15)$$

The line of action is represented by

$$x_f = \rho \sin(\theta - \phi) - a \sin \phi \quad y_f = \rho \cos(\theta - \phi) + a \cos \phi \quad r \sin(\theta - \phi) - a \sin \theta = 0 \quad (4.5.16)$$

The equations of shape Σ_2 are

$$\left. \begin{aligned} x_2 &= \rho \sin(\theta - 2\phi) - a \sin 2\phi + 2r \sin \phi \\ y_2 &= \rho \cos(\theta - 2\phi) + a \cos 2\phi - 2r \cos \phi \\ r \sin(\theta - \phi) - a \sin \theta &= 0 \end{aligned} \right\} \quad (4.5.17)$$

Here $\phi_1 = \phi_2 = \phi$ is the angle of rotation of gear 1 and $r_1 = r_2 = r$ is the centrod radius.

Chapter 5

Plane Gearing Analysis

The essence of the problem of plane gearing analysis may be stated as follows: The tooth shapes of the meshing gears are defined, and the distance between centers of gear rotation is given. We wish to determine (1) the law of motion—the relation between angles of gear rotation and (2) the line of action of the gear teeth.

There are two typical cases when gearing analysis is applied: (1) to determine the kinematical errors in a gear mechanism which are induced by errors of manufacturing and assembly and (2) for the optimal synthesis of gears (especially for synthesis of spatial gearings). The optimal synthesis of gearings is usually an iterative computational procedure which requires intermediate analysis between iterations. Such analysis provides information on the achieved results and is the basis for the next iteration.

The method of analysis discussed in this chapter was first proposed by F.L. Litvin (1968). This method may be applied not only for gears but for most direct-contact mechanisms (such as cam mechanisms).

5.1 Equations of Tooth Shape Tangency

Consider again coordinate systems S_1 , S_2 , and S_f rigidly connected to gears 1 and 2, and the frame, respectively. Tooth shapes Σ_1 and Σ_2 (of gears 1 and 2) and their respective unit normals are represented by the following equations:

$$\mathbf{r}_1 = \mathbf{r}_1(\theta_1) \quad \mathbf{r}_1(\theta_1) \in C^2 \quad \frac{\partial \mathbf{r}_1}{\partial \theta_1} \neq 0 \quad \theta_1 \in G_1 \quad (5.1.1)$$

$$\mathbf{n}_1 = \mathbf{n}_1(\theta_1) \quad (5.1.2)$$

$$\mathbf{r}_2 = \mathbf{r}_2(\theta_2) \quad \mathbf{r}_2(\theta_2) \in C^2 \quad \frac{\partial \mathbf{r}_2}{\partial \theta_2} \neq 0 \quad \theta_2 \in G_2 \quad (5.1.3)$$

$$\mathbf{n}_2 = \mathbf{n}_2(\theta_2) \quad (5.1.4)$$

(See ch. 3, secs. 1 and 2.) The transformation of the point coordinates and unit normal projections from moving systems S_1 and S_2 to fixed system S_f is given by

$$\begin{bmatrix} r_f^{(1)} \end{bmatrix} = \begin{bmatrix} M_{f1} \end{bmatrix} \begin{bmatrix} r_1 \end{bmatrix} \quad (5.1.5)$$

$$\begin{bmatrix} n_f^{(1)} \end{bmatrix} = \begin{bmatrix} L_{f1} \end{bmatrix} \begin{bmatrix} n_1 \end{bmatrix} \quad (5.1.6)$$

$$\begin{bmatrix} r_f^{(2)} \end{bmatrix} = \begin{bmatrix} M_{f2} \end{bmatrix} \begin{bmatrix} r_2 \end{bmatrix} \quad (5.1.7)$$

$$\begin{bmatrix} n_f^{(2)} \end{bmatrix} = \begin{bmatrix} L_{f2} \end{bmatrix} \begin{bmatrix} n_2 \end{bmatrix} \quad (5.1.8)$$

Henceforth, superscripts (1) and (2) will refer to tooth shapes Σ_1 and Σ_2 , whereas subscripts will denote the coordinate system in which the shapes are represented. Equations (5.1.1) to (5.1.8) represent the locus of shapes $\Sigma_{1\phi}$ and $\Sigma_{2\phi}$ and their corresponding unit normals in coordinate system S_f . From these equations we get

$$\mathbf{r}_f^{(1)} = \mathbf{r}_f^{(1)}(\theta_1, \phi_1) \quad \phi_1 \in E_1 \quad (5.1.9)$$

$$\mathbf{n}_f^{(1)} = \mathbf{n}_f^{(1)}(\theta_1, \phi_1) \quad (5.1.10)$$

$$\mathbf{r}_f^{(2)} = \mathbf{r}_f^{(2)}(\theta_2, \phi_2) \quad \phi_2 \in E_2 \quad (5.1.11)$$

$$\mathbf{n}_f^{(2)} = \mathbf{n}_f^{(2)}(\theta_2, \phi_2) \quad (5.1.12)$$

In order to be in tangency, shapes Σ_1 and Σ_2 must coincide at some point where their unit normals are collinear. Hence,

$$\mathbf{r}_f^{(1)}(\theta_1, \phi_1) = \mathbf{r}_f^{(2)}(\theta_2, \phi_2) \quad (5.1.13)$$

$$\mathbf{n}_f^{(1)}(\theta_1, \phi_1) = \mathbf{n}_f^{(2)}(\theta_2, \phi_2) \quad (5.1.14)$$

Notice that equation (5.1.13) expresses only that shapes Σ_1 and Σ_2 share a common point in space. However, this point can be either a point of tangency or a point of intersection of the two curves. Only when both equations (5.1.13) and (5.1.14) are satisfied a point common to curves θ_1 and θ_2 is indeed a point of tangency.

In place of equation (5.1.14), the equation

$$\mathbf{N}_f^{(1)}(\theta_1, \phi_1) = \lambda \mathbf{N}_f^{(2)}(\theta_2, \phi_2) \quad (5.1.15)$$

may be used to express the collinearity of normal vectors. It will be seen, however, that equation (5.1.14) is the basis for important kinematic relations in plane gearings (see ch. 6) and, thus, is preferred. It is important to note that the directions of unit normals $\mathbf{n}_f^{(1)}$ and $\mathbf{n}_f^{(2)}$ may either coincide or be opposite each other and still insure the tangency of shapes Σ_1 and Σ_2 . If the latter case is considered, equation (5.1.14) may still be observed by changing the order of the factors in one of the cross products which define the normal vectors. For example

$$\mathbf{N}_1 = \frac{\partial \mathbf{r}_1}{\partial \theta_1} \times \mathbf{k}_1 \quad \mathbf{n}_1 = \frac{\mathbf{N}_1}{|\mathbf{N}_1|} \quad \mathbf{N}_2 = \mathbf{k}_2 \times \frac{\partial \mathbf{r}_2}{\partial \theta_2} \quad \mathbf{n}_2 = \frac{\mathbf{N}_2}{|\mathbf{N}_2|} \quad (5.1.16)$$

5.2 Analysis of Meshing

Equations (5.1.13) and (5.1.14) may be rewritten as

$$\mathbf{r}_f^{(1)}(\theta_1, \phi_1) - \mathbf{r}_f^{(2)}(\theta_2, \phi_2) = 0 \quad (5.2.1)$$

$$\mathbf{n}_f^{(1)}(\theta_1, \phi_1) - \mathbf{n}_f^{(2)}(\theta_2, \phi_2) = 0 \quad (5.2.2)$$

By projecting the above position vectors and unit normal vectors on a set of coordinate axes, we obtain a system of four scalar equations, only three of which are independent. Since $\mathbf{n}_f^{(1)}$ and $\mathbf{n}_f^{(2)}$ are unit vectors, we have one ‘‘built-in’’ relation

$$|\mathbf{n}_f^{(1)}| = |\mathbf{n}_f^{(2)}| = 1 \quad (5.2.3)$$

Consequently, if one component of the unit normal vectors is equal, for instance, if

$$n_{f_x}^{(1)} = n_{f_x}^{(2)} \quad (5.2.4)$$

is observed, then the other projections are also equal

$$n_{f_y}^{(1)} = n_{f_y}^{(2)} \quad (5.2.5)$$

Equations (5.2.1) to (5.2.3) yield the following three equations in four unknowns:

$$f_1(\theta_1, \phi_1, \theta_2, \phi_2) = 0 \quad f_2(\theta_1, \phi_1, \theta_2, \phi_2) = 0 \quad f_3(\theta_1, \phi_1, \theta_2, \phi_2) = 0 \quad (5.2.6)$$

where

$$\{f_1, f_2, f_3\} \in C^1$$

The analysis of plane gearing may be completed if equations (5.2.6) can provide three functions of one variable parameter, such as

$$\{\theta_1(\phi_1), \theta_2(\phi_1), \phi_2(\phi_1)\} \in C^1 \quad (5.2.7)$$

According to the Theorem of Implicit Function System Existence (see app. B), functions (5.2.7) exist (at least) in the neighborhood of a point

$$P^\circ = (\theta_1^\circ, \phi_1^\circ, \theta_2^\circ, \phi_2^\circ) \quad (5.2.8)$$

if

- (1) $\{f_1, f_2, f_3\} \in C^1$
- (2) Equations (5.2.6) are satisfied at point P°
- (3) The following Jacobian differs from zero

$$\frac{D(f_1, f_2, f_3)}{D(\theta_1, \theta_2, \phi_2)} = \begin{vmatrix} \frac{\partial f_1}{\partial \theta_1} & \frac{\partial f_1}{\partial \theta_2} & \frac{\partial f_1}{\partial \phi_2} \\ \frac{\partial f_2}{\partial \theta_1} & \frac{\partial f_2}{\partial \theta_2} & \frac{\partial f_2}{\partial \phi_2} \\ \frac{\partial f_3}{\partial \theta_1} & \frac{\partial f_3}{\partial \theta_2} & \frac{\partial f_3}{\partial \phi_2} \end{vmatrix} \quad (5.2.9)$$

Functions (5.2.7) provide complete information about the meshing of gears with profiles Σ_1 and Σ_2 : (1) function $\phi_2(\phi_1)$ represents the relation between angles of gear rotation – the law of motion and (2) functions $\theta_1(\phi_1)$ and $\theta_2(\phi_1)$ define the points on shapes Σ_1 and Σ_2 , which are in tangency for a given value of gear 1 rotation.

The line of action of contacting profiles Σ_1 and Σ_2 is given by the functions

$$\mathbf{r}_f^{(1)}(\theta_1, \phi_1) \quad \theta_1(\phi_1) \quad (5.2.10)$$

or by

$$\mathbf{r}_f^{(2)}(\theta_2, \phi_2) \quad \theta_2(\phi_1) \quad \phi_2(\phi_1) \quad (5.2.11)$$

In some cases a variable parameter other than ϕ_1 , for instance θ_1 , may be chosen when solving equations (5.2.6). In this case, the solution of these equations is given by the functions

$$\{\phi_1(\theta_1), \theta_2(\theta_1), \phi_2(\theta_1)\} \in C^1 \quad (5.2.12)$$

and the following Jacobian must differ from zero:

$$\frac{D(f_1, f_2, f_3)}{D(\phi_1, \theta_2, \phi_2)} \neq 0 \quad (5.2.13)$$

As mentioned earlier, the method of analysis proposed here may be applied not only for gear drives but, in fact, for most types of direct-contact mechanisms. For instance, application to a cam mechanism with a flat-faced follower is considered in problem 5.3.1.

5.3 Computation Process

In general, the determination of functions (5.2.7) or (5.2.12) requires an iterative numerical procedure and the aid of a computer. To start iterations, one point (eq. (5.2.8)), a set of parameters $(\theta_1^\circ, \phi_1^\circ, \theta_2^\circ, \phi_2^\circ)$ with which the system of equations (5.2.6) is satisfied, must be known. The aim of the next step is to determine a new point which satisfies equations (5.2.6)

$$P^{(1)} = (\theta_1^{(1)}, \phi_1^{(1)}, \theta_2^{(1)}, \phi_2^{(1)}) \quad (5.3.1)$$

The iterative process of computation may be based on the following procedure:

- (1) Pick a subsystem of two equations from the system of three equations(5.2.6).
- (2) Assume that this subsystem is

$$f_2(\theta_1, \phi_1, \theta_2, \phi_2) = 0 \quad f_3(\theta_1, \phi_1, \theta_2, \phi_2) = 0 \quad (5.3.2)$$

Consider $\phi_1 = \phi_1^{(1)}$ as given, and choose $\theta_1 = \theta_1^{(1)}$. Thus, the system of equations (5.3.2) may be solved for θ_2 and ϕ_2 . Let the solution be $\theta_2^{(1)}, \phi_2^{(1)}$.

- (3) The new set of parameters (point (5.3.1)) is determined indeed if the remaining equation

$$f_1(\theta_1, \phi_1, \theta_2, \phi_2) = 0 \quad (5.3.3)$$

is satisfied by the set $(\theta_1^{(1)}, \phi_1^{(1)}, \theta_2^{(1)}, \phi_2^{(1)})$. If equation (5.3.3) is not satisfied, then a new value for $\theta_1^{(1)}$ must be chosen, and equation (5.3.2) must be solved and checked with equation (5.3.3), etc.

The above iterative process is based on dividing the system of three equations (5.2.6) into two subsystems, two equations (eqs. (5.3.2)) and one equation (eq. (5.3.3)), and their separate solutions.

Equations (5.3.2) and (5.3.3) are nonlinear algebraic equations, and we must apply a standard computer program for their solution, for instance, a program which is based on the Newton algorithm (Korn, 1968).

Problem 5.3.1 Consider a cam mechanism with a flat-faced follower. The cam profile is a circle of radius ρ centered at point C (fig. 5.3.1) whose center of rotation is O_f . The follower contacts the cam at points on its straight line, which coincides with axis x_2 .

Set up coordinate systems $S_1(x_1, y_1)$ and $S_2(x_2, y_2)$, rigidly connected to links 1 and 2, and the fixed coordinate system $S_f(x_f, y_f)$. Represent conjugate shapes of the cam and the follower as follows:

- (1) The shape of the cam

$$x_1 = \rho \cos \theta_1 \quad y_1 = a + \rho \sin \theta_1 \quad (5.3.4)$$

where $a = O_f C$ and

- (2) The shape of the follower is given by

$$x_2 = \theta_2 \quad y = 0 \quad (5.3.5)$$

The parameter θ_2 is negative for points which belong to the negative x_2 axis.

Apply the method presented in this chapter and determine the following functions:

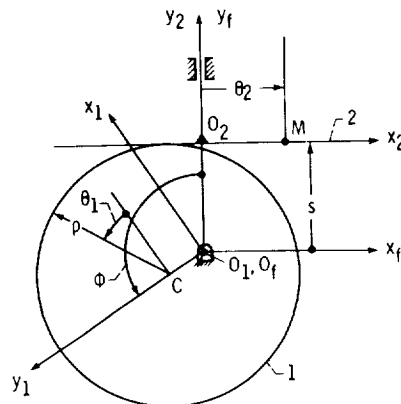


Figure 5.3.1.

- (1) $s(\phi)$, where $0 \leq \phi \leq 2\pi$, which represents the relation between parameters of motion s and ϕ
- (2) $\theta_1(\phi)$ and $\theta_2(\phi)$, which represent the relations between shape parameters and the parameter of motion ϕ
- (3) $x_f(\phi)$ and $y_f(\phi)$, which represent the line of action

Directions for the solution are as follows:

Step 1.—Determine unit normals for the conjugate shapes in coordinate systems S_1 and S_2 so they have coinciding directions.

Step 2.—Represent conjugate shapes and their unit normals in the coordinate system S_f .

Step 3.—Develop the equations of tangency of the two conjugate shapes which are analogous to equations (5.1.13) and (5.1.14), and obtain the desired functions.

Answer.

$$s = a \cos \phi + \rho \quad (\text{The cam mechanism performs harmonic motion.})$$

$$\theta_1 = \frac{\pi}{2} - \phi \quad \theta_2 = -a \sin \phi \quad x_f = -a \sin \phi \quad y_f = \rho + a \cos \phi$$

Chapter 6

Basic Kinematic Relations of Plane Gearings and Their Application

6.1 Basic Kinematic Relations

Consider two gears which are in mesh. As explained in chapter 5.1, for shapes Σ_1 and Σ_2 (of gears 1 and 2, respectively) to be in continuous tangency, the position vectors and unit normals of each gear must be equal at the instantaneous point of contact of gear shapes at every moment. These requirements are represented by equations (5.1.13) and (5.1.14). Since these equations are to be observed continuously at any instantaneous point of contact, we may differentiate them. This yields

$$\dot{\mathbf{r}}^{(1)}(\theta_1, \phi_1) = \dot{\mathbf{r}}^{(2)}(\theta_2, \phi_2) \quad (6.1.1)$$

and

$$\dot{\mathbf{n}}^{(1)}(\theta_1, \phi_1) = \dot{\mathbf{n}}^{(2)}(\theta_2, \phi_2) \quad (6.1.2)$$

Here $\dot{\mathbf{r}}^{(i)}$ ($i = 1, 2$) is the velocity of the contact point in absolute motion (motion relative to the frame); $\dot{\mathbf{n}}^{(i)}$ is the linear velocity of the tip of the unit normal vector in absolute motion. Equations (6.1.1) and (6.1.2) may be expressed as follows:

$$\mathbf{v}_{abs} = \dot{\mathbf{r}}^{(1)}(\theta_1, \phi_1) = \frac{\partial \mathbf{r}^{(1)}}{\partial \phi_1} \frac{d\phi_1}{dt} + \frac{\partial \mathbf{r}^{(1)}}{\partial \theta_1} \frac{d\theta_1}{dt} = \dot{\mathbf{r}}^{(2)}(\theta_2, \phi_2) = \frac{\partial \mathbf{r}^{(2)}}{\partial \phi_2} \frac{d\phi_2}{dt} + \frac{\partial \mathbf{r}^{(2)}}{\partial \theta_2} \frac{d\theta_2}{dt} \quad (6.1.3)$$

$$\dot{\mathbf{n}}_{abs} = \dot{\mathbf{n}}^{(1)}(\theta_1, \phi_1) = \frac{\partial \mathbf{n}^{(1)}}{\partial \phi_1} \frac{d\phi_1}{dt} + \frac{\partial \mathbf{n}^{(1)}}{\partial \theta_1} \frac{d\theta_1}{dt} = \dot{\mathbf{n}}^{(2)}(\theta_2, \phi_2) = \frac{\partial \mathbf{n}^{(2)}}{\partial \phi_2} \frac{d\phi_2}{dt} + \frac{\partial \mathbf{n}^{(2)}}{\partial \theta_2} \frac{d\theta_2}{dt} \quad (6.1.4)$$

Here t represents time.

Imagine that trihedrons $\boldsymbol{\tau}^{(i)}$, $\mathbf{n}^{(i)}$, and $\mathbf{b}^{(i)}$ (see ch. 3.3) are connected to shape Σ_i at shape contact point M_i ($i = 1, 2$) (fig. 6.1.1). Equation (6.1.1) indicates that the common origin of each

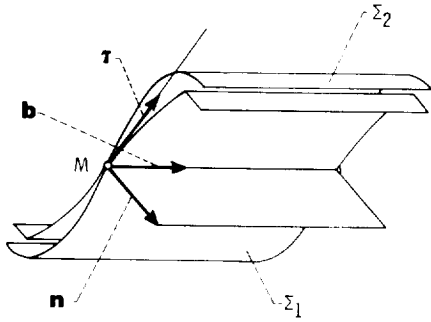


Figure 6.1.1.

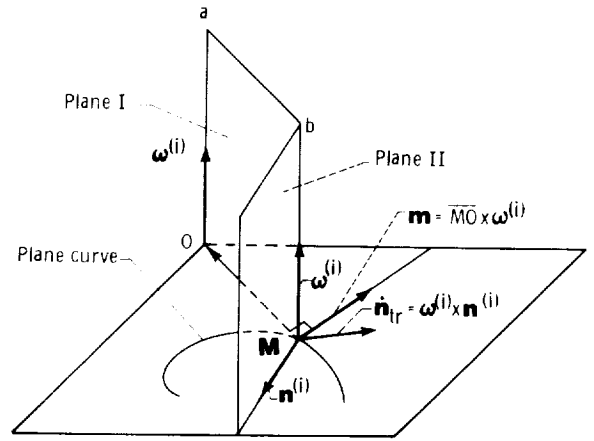


Figure 6.1.2.

trihedron moves with the same velocity, while equation (6.1.2) expresses that the tips of unit vectors $\mathbf{n}^{(1)}$ and $\mathbf{n}^{(2)}$ move with the same velocity. Similarly, the tips of unit vectors $\boldsymbol{\tau}^{(1)}$ and $\boldsymbol{\tau}^{(2)}$ move with equal velocities. Thus

$$\dot{\boldsymbol{\tau}}^{(1)} = \dot{\boldsymbol{\tau}}^{(2)} \quad (6.1.5)$$

Since we are dealing with planar curves, the unit vectors $\mathbf{b}^{(1)}$ and $\mathbf{b}^{(2)}$ keep their original directions, so

$$\dot{\mathbf{b}}^{(1)} = \dot{\mathbf{b}}^{(2)} = \mathbf{0} \quad (6.1.6)$$

Let us derive kinematic relations based on equations (6.1.1), (6.1.2), and (6.1.5). As the contact point moves through space during tooth meshing, so does each trihedron. The absolute motion of each trihedron may be represented as a motion of two components: (1) transfer motion—together with the shape (with coordinate system S_i) and (2) relative motion—relative to the shape (to coordinate system S_j). Equations (6.1.3) may be represented as

$$\mathbf{v}_{abs} = \mathbf{v}_{tr}^{(1)} + \mathbf{v}_r^{(1)} = \mathbf{v}_{tr}^{(2)} + \mathbf{v}_r^{(2)} \quad (6.1.7)$$

where

$$\mathbf{v}_{tr}^{(i)} = \frac{\partial \mathbf{r}^{(i)}}{\partial \phi_i} \frac{d\phi_i}{dt} \quad \mathbf{v}_r^{(i)} = \frac{\partial \mathbf{r}^{(i)}}{\partial \theta_i} \frac{d\theta_i}{dt} \quad (i = 1, 2)$$

Similarly,

$$\dot{\mathbf{n}}_{abs} = \dot{\mathbf{n}}_{tr}^{(1)} + \dot{\mathbf{n}}_r^{(1)} = \dot{\mathbf{n}}_{tr}^{(2)} + \dot{\mathbf{n}}_r^{(2)} \quad (6.1.8)$$

where

$$\dot{\mathbf{n}}_{tr}^{(i)} = \frac{\partial \mathbf{n}^{(i)}}{\partial \phi_i} \frac{d\phi_i}{dt}$$

and

$$\dot{\mathbf{n}}_r^{(i)} = \frac{\partial \mathbf{n}^{(i)}}{\partial \theta_i} \frac{d\theta_i}{dt}$$

The transfer velocity of a contact point may also be represented by the following equations:

$$\mathbf{v}_{ir}^{(1)} = \boldsymbol{\omega}^{(1)} \times \mathbf{r}^{(1)} \quad (6.1.9)$$

$$\mathbf{v}_{ir}^{(2)} = \left(\boldsymbol{\omega}^{(2)} \times \mathbf{r}^{(1)} \right) + \overline{O_f O_2} \times \boldsymbol{\omega}^{(2)} \quad (6.1.10)$$

(See ch. 2.3.) Here $\mathbf{r}^{(1)}$ is the position vector drawn from the origin O_f of coordinate system S_f to the point of contact. It is assumed that the line of action of $\boldsymbol{\omega}^{(1)}$ passes through origin O_f , and the line of action of $\boldsymbol{\omega}^{(2)}$ (which is parallel to $\boldsymbol{\omega}^{(1)}$) does not pass through O_f . The sliding vector $\boldsymbol{\omega}^{(2)}$, which passes through point O_2 (fig. 2.1.4), is substituted (1) by an equal vector $\boldsymbol{\omega}^{(2)}$, whose line of action passes through the point O_f and (2) by a moment $\overline{O_f O_2} \times \boldsymbol{\omega}^{(2)}$, which expresses a linear velocity.

Let us prove that the transfer velocity of the tip of the unit normal may be represented as follows:

$$\dot{\mathbf{n}}_{ir}^{(i)} = \boldsymbol{\omega}^{(i)} \times \mathbf{n}^{(i)} \quad (6.1.11)$$

Consider a planar curve (fig. 6.1.2) with a unit normal $\mathbf{n}^{(i)}$ at its point M . The curve rotates about axis Oa with angular velocity $\boldsymbol{\omega}^{(i)}$. Let us substitute the sliding vector $\boldsymbol{\omega}^{(i)}$ by an equal vector $\boldsymbol{\omega}^{(i)}$, whose line of action is Mb , and a moment $\mathbf{m} = \overline{MO} \times \boldsymbol{\omega}^{(i)}$. (See ch. 2.3.)

Then, point M , with the unit normal $\mathbf{n}^{(i)}$, takes part in two motions: (1) translation with linear velocity \mathbf{m} (it is perpendicular to plane I in figure 6.1.2) and (2) rotation about axis Mb with angular velocity $\boldsymbol{\omega}^{(i)}$. Vector $\mathbf{n}^{(i)}$ keeps its original direction in translational motion—its direction is changed only by rotation. Thus, the change of the direction of the unit normal depends on the angle of rotation only, and the velocity of the tip of the unit vector in rotational motion may be represented by equation (6.1.11).

Let us now transform equations (6.1.7) and (6.1.8). Equations (6.1.7), (6.1.9), and (6.1.10) yield

$$\begin{aligned} \mathbf{v}_r^{(2)} &= \mathbf{v}_r^{(1)} + \mathbf{v}_{ir}^{(1)} - \mathbf{v}_{ir}^{(2)} = \mathbf{v}_r^{(1)} + \mathbf{v}^{(12)} \\ &= \left(\mathbf{v}_r^{(1)} + \left(\boldsymbol{\omega}^{(12)} \times \mathbf{r}^{(1)} \right) \right) - \left(\overline{O_f O_2} \times \boldsymbol{\omega}^{(2)} \right) \end{aligned} \quad (6.1.12)$$

Here $\boldsymbol{\omega}^{(12)} = \boldsymbol{\omega}^{(1)} - \boldsymbol{\omega}^{(2)}$ and $\mathbf{v}^{(12)} = \mathbf{v}_{ir}^{(1)} - \mathbf{v}_{ir}^{(2)}$ is the velocity of point M_1 of shape Σ_1 with respect to point M_2 of shape Σ_2 , while points M_1 and M_2 coincide at a common point M —the point of tangency of shapes Σ_1 and Σ_2 . Similarly, equations (6.1.8) and (6.1.11) yield

$$\dot{\mathbf{n}}_r^{(2)} = \dot{\mathbf{n}}_r^{(1)} + \left(\dot{\mathbf{n}}_{ir}^{(1)} - \dot{\mathbf{n}}_{ir}^{(2)} \right) = \dot{\mathbf{n}}_r^{(1)} + \left(\boldsymbol{\omega}^{(12)} \times \mathbf{n} \right) \quad (6.1.13)$$

where $\boldsymbol{\omega}^{(12)} = \boldsymbol{\omega}^{(1)} - \boldsymbol{\omega}^{(2)}$. Similarly, we obtain

$$\dot{\boldsymbol{\tau}}_r^{(2)} = \dot{\boldsymbol{\tau}}_r^{(1)} + \left(\boldsymbol{\omega}^{(12)} \times \boldsymbol{\tau} \right) \quad (6.1.14)$$

We call equations (6.1.12), (6.1.13), and (6.1.14) the basic kinematic relations of plane gearing. These relations were first proposed by F.L. Litvin (1968). On the basis of these equations, important relations in the theory of gearing may be developed, such as relations between curvatures of conjugated shapes, conditions of tooth nonundercutting, and kinematic error analysis of gear trains. (See sec. 6.2 and 6.3.) Analogous relations may be established for spatial gearings too. (See ch. 12.)

Example 6.1.1 Consider the cam mechanism shown in figure 5.3.1. Figure 6.1.3 shows links of this mechanism in two neighboring positions, denoted by I and II. The fixed coordinate system is S_f . The cam shape is a circle centered at C ; $C^{(I)}$ and $C^{(II)}$ are two positions of this center corresponding to the initial position of the cam and its position after it rotates through an angle ϕ . The center of cam rotation is point O . Contact points of the cam and follower at their two positions are $M_f^{(I)}$ and $M_f^{(II)}$, respectively.

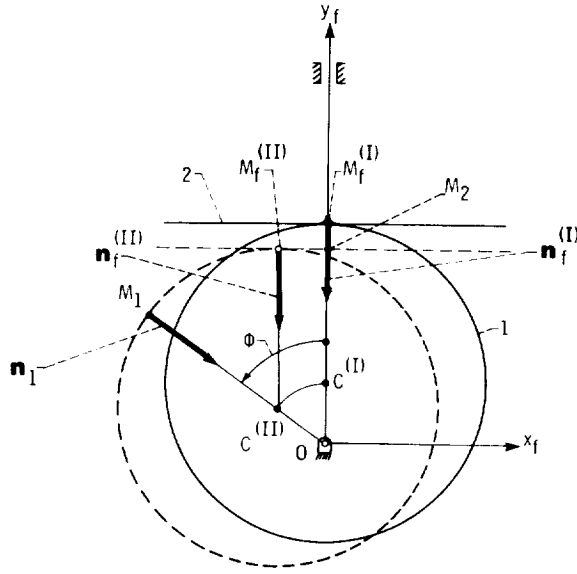


Figure 6.1.3.

Kinematic relations (6.1.12) and (6.1.13) may be illustrated in the following manner. (In this example displacements are considered instead of velocities.) The displacement of the contact point in absolute motion is

$$\widehat{\Delta s}_{abs} = \widehat{M_f^{(I)} M_f^{(II)}}$$

Denoting the cam as link 1 and the follower as link 2, we may represent $\widehat{\Delta s}_{abs}$ as follows:

$$\widehat{\Delta s}_{abs} = \widehat{\Delta s}_{ir}^{(1)} + \widehat{\Delta s}_r^{(1)} = \widehat{\Delta s}_{ir}^{(2)} + \widehat{\Delta s}_r^{(2)}$$

Here the transfer displacement of point M_1 with the cam is

$$\widehat{\Delta s}_{ir}^{(1)} = \widehat{M_f^{(I)} M_1}$$

The relative displacement of point M_1 along the cam shape is

$$\widehat{\Delta s}_r^{(1)} = \widehat{M_1 M_f^{(II)}}$$

The transfer displacement of point M_2 with the follower is

$$\overline{\Delta s}_{ir}^{(2)} = \overline{M_f^{(I)} M_2}$$

The relative displacement of point M_2 along the follower shape is

$$\overline{\Delta s}_r^{(2)} = \overline{M_2 M_f^{(II)}}$$

The change of the unit normal in absolute motion may be represented as

$$\Delta \mathbf{n}_{abs} = \mathbf{n}_f^{(II)} - \mathbf{n}_f^{(I)}$$

In this particular case $\Delta \mathbf{n}_{abs}$ is equal to zero. The displacement $\Delta \mathbf{n}_{abs}$ may also be represented as follows:

$$\Delta \mathbf{n}_{obs} = \Delta \mathbf{n}_{tr}^{(1)} + \Delta \mathbf{n}_r^{(1)} = \Delta \mathbf{n}_{tr}^{(2)} + \Delta \mathbf{n}_r^{(2)}$$

Here

$$\Delta \mathbf{n}_{tr}^{(1)} = \mathbf{n}_1 - \mathbf{n}_f^{(1)}$$

is the direction change for the unit normal of the cam shape by transfer motion (with the cam). The direction change

$$\Delta \mathbf{n}_r^{(1)} = \mathbf{n}_f^{(II)} - \mathbf{n}_1$$

is for the unit normal of the cam shape in relative motion while the contact point moves along the cam, and $\Delta \mathbf{n}_{tr}^{(2)}$ and $\Delta \mathbf{n}_r^{(2)}$ are the direction changes for the unit normal of the follower in the transfer and relative motions, respectively. In the particular case considered, $\Delta \mathbf{n}_{tr}^{(2)}$ and $\Delta \mathbf{n}_r^{(2)}$ are equal to zero.

6.2 Conjugate Shapes: Relations Between Curvatures

The determination of the curvature of an envelope of planar curves is a difficult problem taking into account that the envelope is usually represented by complicated equations, even if the equations of the locus of curves are simple. Thus, it is an attractive prospect to find the curvature of an envelope without having its equations (i.e., having only the equations of the curve of the locus). Such a method, based on relations between curvatures of conjugate shapes, was first proposed by F.L. Litvin (1968, 1969).

Consider the following conditions:

(1) Three coordinate systems S_1 , S_2 , and S_f are established. Coordinate systems S_1 and S_2 are rigidly connected to the driving and driven gears 1 and 2; coordinate system S_f is rigidly connected to the frame.

(2) The shape Σ_1 is represented by

$$\mathbf{r}_1(\theta_1) \in C^2 \quad \theta_1 \in G \quad \frac{d\mathbf{r}_1}{d\theta_1} \neq 0 \quad (6.2.1)$$

(3) The angles of gear rotation ϕ_1 and ϕ_2 are related by the function

$$\phi_2(\phi_1) \in C^2 \quad a < \phi_1 < b \quad (6.2.2)$$

(4) The equation of meshing is determined and represented by the equation (ch. 4.5)

$$\mathbf{n}_f^{(1)} \cdot \mathbf{v}_f^{(12)} = \mathbf{n}_f^{(1)} \cdot \left[\left(\boldsymbol{\omega}_f^{(12)} \times \mathbf{r}_f^{(1)} \right) - \left(\overline{O_1 O_2} \times \boldsymbol{\omega}_f^{(2)} \right) \right] = f(\theta_1, \phi_1) = 0 \quad (6.2.3)$$

(5) The curvature of the shape Σ_1 is represented by the equation

$$\kappa_1 \mathbf{v}_r^{(1)} = -\dot{\mathbf{n}}_r^{(1)} \quad (6.2.4)$$

(See ch. 3.3.) The problem is to determine the curvature of the shape Σ_2 .

The solution to this problem is based on the following equations:

$$\kappa_2 \mathbf{v}_r^{(2)} = -\dot{\mathbf{n}}_r^{(2)} \quad (6.2.5)$$

$$\mathbf{v}_r^{(2)} = \mathbf{v}_r^{(1)} + \mathbf{v}^{(12)} \quad (6.2.6)$$

$$\dot{\mathbf{n}}_r^{(2)} = \dot{\mathbf{n}}_r^{(1)} + \left(\boldsymbol{\omega}^{(12)} \times \mathbf{n}^{(1)} \right) \quad (6.2.7)$$

$$\frac{d}{dt} (\mathbf{n} \cdot \mathbf{v}^{(12)}) = 0 \quad (6.2.8)$$

Equation (6.2.8) is simply the equation of meshing differentiated with respect to time. The subscript f in equation (6.2.8) is dropped for simplification.

Let us transform equation (6.2.8) as follows:

$$\frac{d}{dt} (\mathbf{n} \cdot \mathbf{v}^{(12)}) = \left(\dot{\mathbf{n}}^{(1)} \cdot \mathbf{v}^{(12)} \right) + \left(\mathbf{n} \cdot \frac{d}{dt} (\mathbf{v}^{(12)}) \right) = 0 \quad (6.2.9)$$

Here

$$\dot{\mathbf{n}}^{(1)} = \dot{\mathbf{n}}_r^{(1)} + \dot{\mathbf{n}}_r^{(1)} = \left(\boldsymbol{\omega}^{(1)} \times \mathbf{n}^{(1)} \right) + \dot{\mathbf{n}}_r^{(1)} \quad (6.2.10)$$

We represent the derivative $\frac{d}{dt} (\mathbf{v}^{(12)})$ by

$$\frac{d}{dt} (\mathbf{v}^{(12)}) = \frac{d}{dt} \left\{ \left[\left(\boldsymbol{\omega}^{(1)} - \boldsymbol{\omega}^{(2)} \right) \times \mathbf{r}^{(1)} \right] - (\mathbf{C} \times \boldsymbol{\omega}^{(2)}) \right\} \quad (6.2.11)$$

where $\mathbf{C} = \overline{\mathbf{O}_1 \mathbf{O}_2}$. Not losing generality in our solution, we assume that gear 1 rotates counterclockwise with constant angular velocity $\boldsymbol{\omega}^{(1)}$. The angular velocity of gear 2 is

$$\boldsymbol{\omega}^{(2)} = \mp \omega^{(2)} \mathbf{k} = \mp \frac{\omega^{(1)}}{m_{12}(\phi_1)} \mathbf{k} \quad (6.2.12)$$

where

$$m_{12}(\phi_1) = \frac{d\phi_1}{d\phi_2} = \frac{1}{\frac{d}{d\phi_1} (\phi_2(\phi_1))}$$

The time derivative $\dot{\boldsymbol{\omega}}_2$ is

$$\begin{aligned} \dot{\boldsymbol{\omega}}^{(2)} &= \mp \frac{d}{d\phi_1} \left(\frac{\omega^{(1)}}{m_{12}(\phi_1)} \right) \frac{d\phi_1}{dt} \mathbf{k} = \pm \frac{m'_{12}(\omega^{(1)})^2}{(m_{12})^2} \mathbf{k} \\ &= \pm \frac{m'_{12} \omega^{(1)} \omega^{(2)}}{m_{12}} \mathbf{k} = - \frac{m'_{12} \omega^{(1)}}{m_{12}} \boldsymbol{\omega}^{(2)} \end{aligned} \quad (6.2.13)$$

Here the upper sign of \pm or \mp corresponds to gear rotations in opposite directions, $m'_{12} = \frac{d}{d\phi_1} (m_{12}(\phi_1))$, and \mathbf{k} is the unit vector of axis z_f .

Now let us transform equation (6.2.11)

$$\begin{aligned} \frac{d}{dt}(\mathbf{v}^{(12)}) &= -(\dot{\boldsymbol{\omega}}^{(2)} \times \mathbf{r}^{(1)}) + (\boldsymbol{\omega}^{(12)} \times \dot{\mathbf{r}}^{(1)}) - (\mathbf{C} \times \dot{\boldsymbol{\omega}}^{(2)}) \\ &= (-\dot{\boldsymbol{\omega}}^{(2)} \times \mathbf{r}^{(1)}) + (\boldsymbol{\omega}^{(12)} \times (\mathbf{v}_{ir}^{(1)} + \mathbf{v}_r^{(1)})) - (\mathbf{C} \times \dot{\boldsymbol{\omega}}^{(2)}) \end{aligned} \quad (6.2.14)$$

Note that expression $\dot{\mathbf{r}}^{(1)} = \mathbf{v}_{abs}^{(1)} = \mathbf{v}_{ir}^{(1)} \mathbf{v}_r^{(1)}$. Substituting $\dot{\boldsymbol{\omega}}^{(2)}$ from (6.2.13), we get

$$\begin{aligned} \frac{d}{dt}(\mathbf{v}^{(12)}) &= \frac{m'_{12}}{m_{12}} \boldsymbol{\omega}^{(1)} \left((\boldsymbol{\omega}^{(2)} \times \mathbf{r}^{(1)}) + (\mathbf{C} \times \boldsymbol{\omega}^{(2)}) \right) \\ &\quad + (\boldsymbol{\omega}^{(12)} \times \mathbf{v}_r^{(1)}) + (\boldsymbol{\omega}^{(12)} \times \mathbf{v}_{ir}^{(1)}) \\ &= \frac{m'_{12}}{m_{12}} \boldsymbol{\omega}^{(1)} \mathbf{v}_r^{(2)} + (\boldsymbol{\omega}^{(12)} \times \mathbf{v}_r^{(1)}) + (\boldsymbol{\omega}^{(12)} \times \mathbf{v}_{ir}^{(1)}) \end{aligned} \quad (6.2.15)$$

Equations (6.2.9), (6.2.10), and (6.2.15) yield

$$\begin{aligned} \frac{d}{dt}(\mathbf{n}^{(1)} \cdot \mathbf{v}^{(12)}) &= \dot{\mathbf{n}}_r^{(1)} \cdot \mathbf{v}^{(12)} + [\boldsymbol{\omega}^{(1)} \mathbf{n}^{(1)} \mathbf{v}^{(12)}] + [\mathbf{n}^{(1)} \boldsymbol{\omega}^{(12)} \mathbf{v}_r^{(1)}] \\ &\quad + [\mathbf{n}^{(1)} \boldsymbol{\omega}^{(12)} \mathbf{v}_{ir}^{(1)}] + \frac{m'_{12}}{m_{12}} \boldsymbol{\omega}^{(1)} (\mathbf{n}^{(1)} \cdot \mathbf{v}_r^{(2)}) = 0 \end{aligned} \quad (6.2.16)$$

We may transform equation (6.2.16) further by taking into account the following relations:

$$[\boldsymbol{\omega}^{(1)} \mathbf{n}^{(1)} \mathbf{v}^{(12)}] = -[\mathbf{n}^{(1)} \boldsymbol{\omega}^{(1)} \mathbf{v}_r^{(1)}] + [\mathbf{n}^{(1)} \boldsymbol{\omega}^{(1)} \mathbf{v}_{ir}^{(1)}] \quad (6.2.17)$$

$$[\mathbf{n}^{(1)} \boldsymbol{\omega}^{(12)} \mathbf{v}_{ir}^{(1)}] = [\mathbf{n}^{(1)} \boldsymbol{\omega}^{(1)} \mathbf{v}_r^{(1)}] - [\mathbf{n}^{(1)} \boldsymbol{\omega}^{(2)} \mathbf{v}_{ir}^{(1)}] \quad (6.2.18)$$

Equations (6.2.17) and (6.2.18) yield

$$\begin{aligned} [\boldsymbol{\omega}^{(1)} \mathbf{n}^{(1)} \mathbf{v}^{(12)}] + [\mathbf{n}^{(1)} \boldsymbol{\omega}^{(12)} \mathbf{v}_{ir}^{(1)}] &= [\mathbf{n}^{(1)} \boldsymbol{\omega}^{(1)} \mathbf{v}_{ir}^{(1)}] \\ -[\mathbf{n}^{(1)} \boldsymbol{\omega}^{(2)} \mathbf{v}_{ir}^{(1)}] &= \mathbf{n}^{(1)} \cdot \left[(\boldsymbol{\omega}^{(1)} \times \mathbf{v}_r^{(2)}) - (\boldsymbol{\omega}^{(2)} \times \mathbf{v}_{ir}^{(1)}) \right] \end{aligned} \quad (6.2.19)$$

Further transformation of equation (6.2.19) may be done by noting that

$$\begin{aligned}
\boldsymbol{\omega}^{(1)} \times \mathbf{v}_{ir}^{(2)} &= \left(\boldsymbol{\omega}^{(1)} \times (\boldsymbol{\omega}^{(2)} \times \mathbf{r}^{(1)}) \right) + \left(\boldsymbol{\omega}^{(1)} \times (\mathbf{C} \times \boldsymbol{\omega}^{(2)}) \right) \\
&= \boldsymbol{\omega}^{(2)}(\boldsymbol{\omega}^{(1)} \cdot \mathbf{r}^{(1)}) - \mathbf{r}^{(1)}(\boldsymbol{\omega}^{(1)} \cdot \boldsymbol{\omega}^{(2)}) + \mathbf{C}(\boldsymbol{\omega}^{(1)} \cdot \boldsymbol{\omega}^{(2)}) - \boldsymbol{\omega}^{(2)}(\boldsymbol{\omega}^{(1)} \cdot \mathbf{C}) \\
&= (\mathbf{C} - \mathbf{r}^{(1)})(\boldsymbol{\omega}^{(1)} \cdot \boldsymbol{\omega}^{(2)})
\end{aligned} \tag{6.2.20}$$

Here $\boldsymbol{\omega}^{(1)} \cdot \mathbf{r}^{(1)} = 0$ and $\boldsymbol{\omega}^{(1)} \cdot \mathbf{C} = 0$ because of the perpendicularity of vectors in these scalar products. Similarly,

$$\begin{aligned}
\boldsymbol{\omega}^{(2)} \times \mathbf{v}_{ir}^{(1)} &= \boldsymbol{\omega}^{(2)} \times (\boldsymbol{\omega}^{(1)} \times \mathbf{r}^{(1)}) = \boldsymbol{\omega}^{(1)}(\boldsymbol{\omega}^{(2)} \cdot \mathbf{r}^{(1)}) - \mathbf{r}^{(1)}(\boldsymbol{\omega}^{(1)} \cdot \boldsymbol{\omega}^{(2)}) \\
&= -\mathbf{r}^{(1)}(\boldsymbol{\omega}^{(1)} \cdot \boldsymbol{\omega}^{(2)})
\end{aligned} \tag{6.2.21}$$

Equations (6.2.19) to (6.2.21) yield

$$\mathbf{n}^{(1)} \cdot \left[\left(\boldsymbol{\omega}^{(1)} \times \mathbf{v}_{ir}^{(2)} \right) - \left(\boldsymbol{\omega}^{(2)} \times \mathbf{v}_{ir}^{(1)} \right) \right] = (\mathbf{n}^{(1)} \cdot \mathbf{C})(\boldsymbol{\omega}^{(1)} \cdot \boldsymbol{\omega}^{(2)}) \tag{6.2.22}$$

The final expression of equation (6.2.16) is as follows:

$$\begin{aligned}
\frac{d}{dt} \left(\mathbf{n}^{(1)} \cdot \mathbf{v}^{(12)} \right) &= \dot{\mathbf{n}}_r^{(1)} \cdot \mathbf{v}^{(12)} + \left[\mathbf{n}^{(1)} \boldsymbol{\omega}^{(12)} \mathbf{v}_r^{(1)} \right] \\
&+ (\mathbf{n}^{(1)} \cdot \mathbf{C})(\boldsymbol{\omega}^{(1)} \cdot \boldsymbol{\omega}^{(2)}) + \frac{m_{12}'}{m_{12}} \boldsymbol{\omega}^{(1)} (\mathbf{n}^{(1)} \cdot \mathbf{v}_{ir}^{(2)}) = 0
\end{aligned} \tag{6.2.23}$$

To get the direct relation between curvatures of conjugate shapes κ_1 and κ_2 , we apply a system of equations (6.2.23) and (6.2.4) to (6.2.7). We may transform this system of equations and obtain a system of three equations to two unknowns, $v_r^{(1)}$ and $v_r^{(2)}$. For these transformations we represent that

$$v_r^{(1)} = \mathbf{v}_r^{(1)} \cdot \mathbf{i}_t \quad v_r^{(2)} = \mathbf{v}_r^{(2)} \cdot \mathbf{i}_t \quad v^{(12)} = \mathbf{v}^{(12)} \cdot \mathbf{i}_t \tag{6.2.24}$$

Here \mathbf{i}_t is the unit vector of the common tangent to the conjugate shapes, vectors $\mathbf{v}_r^{(2)}$ and $\mathbf{v}^{(12)}$ are collinear at the point of shape tangency, and $v_r^{(1)}$, $v_r^{(2)}$, and $v^{(12)}$ must be considered as algebraic quantities (they may be positive or negative). Next we substitute vector $\dot{\mathbf{n}}_r^{(1)}$ by using equation (6.2.4). Equations (6.2.23) and (6.2.4) yield

$$-\kappa_1 v_r^{(1)} (\mathbf{v}^{(12)} \cdot \mathbf{i}_t) + v_r^{(1)} \left[\mathbf{i}_t \mathbf{n}^{(1)} \boldsymbol{\omega}^{(12)} \right] = -(\mathbf{n}^{(1)} \cdot \mathbf{C})(\boldsymbol{\omega}^{(1)} \cdot \boldsymbol{\omega}^{(2)}) - \frac{m_{12}'}{m_{12}} \boldsymbol{\omega}^{(1)} (\mathbf{n}^{(1)} \cdot \mathbf{v}_{ir}^{(2)})$$

We may represent the unit normal vectors as

$$\mathbf{n}^{(1)} = \mathbf{i}_r \times \mathbf{k} \quad (6.2.25)$$

which yields the triple product

$$\begin{aligned} \left[\mathbf{i}_r \mathbf{n}^{(1)} \boldsymbol{\omega}^{(12)} \right] &= -\mathbf{i}_r \cdot \left[\boldsymbol{\omega}^{(12)} \times (\mathbf{i}_r \times \mathbf{k}) \right] = -\mathbf{i}_r \cdot \left[\mathbf{i}_r (\boldsymbol{\omega}^{(12)} \cdot \mathbf{k}) - \mathbf{k} (\boldsymbol{\omega}^{(12)} \cdot \mathbf{i}_r) \right] \\ &= -\boldsymbol{\omega}^{(12)} \cdot \mathbf{k} \end{aligned} \quad (6.2.26)$$

Here \mathbf{k} is the unit vector of axis z , and

$$\boldsymbol{\omega}^{(12)} \cdot \mathbf{i}_r = 0$$

due to the perpendicularity of these vectors.

Equations (6.2.24) to (6.2.26) give

$$\left[\kappa_1 (\mathbf{v}^{(12)} \cdot \mathbf{i}_r) + (\boldsymbol{\omega}^{(12)} \cdot \mathbf{k}) \right] v_r^{(1)} = b_1 \quad (6.2.27)$$

where

$$b_1 = (\mathbf{n}^{(1)} \cdot \mathbf{C})(\boldsymbol{\omega}^{(1)} \cdot \boldsymbol{\omega}^{(2)}) + \frac{m_{12}}{m_{12}} \boldsymbol{\omega}^{(1)} (\mathbf{n}^{(1)} \cdot \mathbf{v}_{rr}^{(2)})$$

Equation (6.2.6) yields

$$-v_r^{(1)} + v_r^{(2)} = \mathbf{v}^{(12)} \cdot \mathbf{i}_r \quad (6.2.28)$$

Equations (6.2.7), (6.2.4), (6.2.5), and (6.2.26) yield

$$\kappa_1 v_r^{(1)} - \kappa_2 v_r^{(2)} = \boldsymbol{\omega}^{(12)} \cdot \mathbf{k} \quad (6.2.29)$$

Equations (6.2.27) to (6.2.29) represent a system of three linear equations in two unknowns as follows:

$$a_{i1} x_1 + a_{i2} x_2 = b_i \quad (i = 1, 2, 3) \quad (6.2.30)$$

where

$$\begin{aligned}
a_{11} &= \kappa_1(\mathbf{v}^{(12)} \cdot \mathbf{i}_t) + (\boldsymbol{\omega}^{(12)} \cdot \mathbf{k}) & a_{12} &= 0 \\
b_1 &= (\mathbf{n}^{(1)} \cdot \mathbf{C})(\boldsymbol{\omega}^{(1)} \cdot \boldsymbol{\omega}^{(2)}) + \frac{m_{12}'}{m_{12}} \omega^{(1)} (\mathbf{n}^{(1)} \cdot \mathbf{v}_{tr}^{(2)}) \\
a_{21} &= -1 & a_{22} &= 1 & b_2 &= \mathbf{v}^{(12)} \cdot \mathbf{i}_t \\
a_{31} &= \kappa_1 & a_{32} &= -\kappa_2 & b_3 &= \boldsymbol{\omega}^{(12)} \cdot \mathbf{k} \\
x_1 &= v_r^{(1)} & x_2 &= v_r^{(2)}
\end{aligned}$$

It is known from linear algebra that the system of equations (6.2.30) possesses a unique solution if and only if the system matrix

$$\begin{bmatrix} a_{11} & a_{12} \\ a_{21} & a_{22} \\ a_{31} & a_{32} \end{bmatrix}$$

and the augmented matrix

$$\begin{bmatrix} a_{11} & a_{12} & b_1 \\ a_{21} & a_{22} & b_2 \\ a_{31} & a_{32} & b_3 \end{bmatrix}$$

are of the same rank. This results in the requirement that

$$\begin{vmatrix} a_{11} & a_{12} & b_1 \\ a_{21} & a_{22} & b_2 \\ a_{31} & a_{32} & b_3 \end{vmatrix} = \begin{vmatrix} a_{11} & 0 & b_1 \\ -1 & 1 & b_2 \\ \kappa_1 & -\kappa_2 & b_3 \end{vmatrix} = 0 \quad (6.2.31)$$

Substituting coefficients of the determinant (6.2.31) with the above expressions, we get

$$\kappa_2 = \frac{\kappa_1 [b_1 - (\mathbf{v}^{(12)} \cdot \mathbf{i}_t)(\boldsymbol{\omega}^{(12)} \cdot \mathbf{k})] - (\boldsymbol{\omega}^{(12)})^2}{\kappa_1 (v_r^{(12)})^2 + (\boldsymbol{\omega}^{(12)} \cdot \mathbf{k})(\mathbf{v}^{(12)} \cdot \mathbf{i}_t) + b_1} \quad (6.2.32)$$

The expression for the coefficient b_1 was presented above. Equation (6.2.32) is the basic equation which relates the curvatures of tooth shapes in planar gearings.

Consider a particular case when shapes Σ_1 and Σ_2 are in contact at the pitch point. At this point $\mathbf{v}^{(12)}=0$, and the curvature of shape Σ_2 is

$$\kappa_2 = \kappa_1 - \frac{(\boldsymbol{\omega}^{(12)})^2}{b_1} \quad (6.2.33)$$

Transformation of Translation into Rotation and Rotation into Translation

Consider that a rack cutter 1 generates a gear 2. The shape Σ_1 is given, and it is necessary to determine relations between the curvatures of shapes Σ_1 and Σ_2 . We set up three coordinate systems S_1 , S_2 , and S_r , as shown in figure 6.2.1(a). It is assumed that

$$\frac{v}{\omega} = r = \text{constant}$$

Here v is the velocity of the rack translation, ω is the angular velocity of gear rotation, and r is the radius of the gear centre. The relation between curvatures of shapes Σ_1 and Σ_2 is based on equations (6.2.4) to (6.2.7) and (6.2.16). But for the considered case, new equations must be developed instead of equations (6.2.7) and (6.2.16) due to new conditions of motion transformation. Taking into account that translation is transformed into rotation, we have

$$\omega^{(1)} = 0 \quad \omega^{(2)} = \omega \quad \omega^{(12)} = \omega^{(1)} - \omega^{(2)} = -\omega$$

The equations which we apply instead of equations (6.2.7) and (6.2.16) are represented by

$$\dot{\mathbf{n}}_r^{(2)} = \dot{\mathbf{n}}_r^{(1)} - (\boldsymbol{\omega} \times \mathbf{n}^{(1)}) \quad (6.2.34)$$

$$\dot{\mathbf{n}}_r^{(1)} \cdot \mathbf{v}^{(12)} - [\mathbf{n}^{(1)} \boldsymbol{\omega} \mathbf{v}_r^{(1)}] - [\mathbf{n}^{(1)} \boldsymbol{\omega} \mathbf{v}_{rr}^{(1)}] = 0 \quad (6.2.35)$$

Developing equation (6.2.35), we assume that $\mathbf{v}_{rr}^{(1)} = \text{constant}$ and $\boldsymbol{\omega} = \text{constant}$. The triple product $[\mathbf{n}^{(1)} \boldsymbol{\omega} \mathbf{v}_{rr}^{(1)}]$ may be represented as

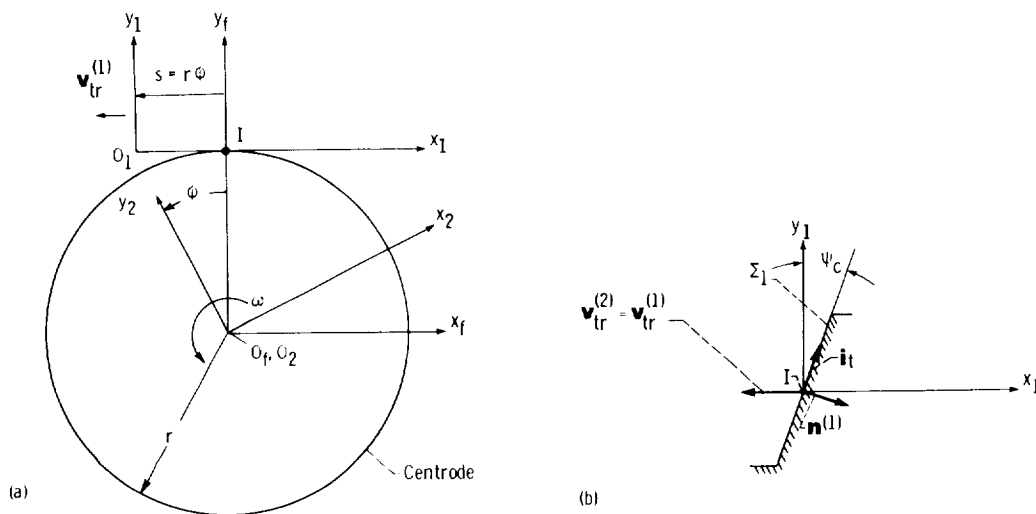


Figure 6.2.1.

$$\begin{aligned} \left[\mathbf{n}^{(1)} \boldsymbol{\omega} \mathbf{v}_{tr}^{(1)} \right] &= (\mathbf{i}_t \times \mathbf{k}) \cdot (\boldsymbol{\omega} \times \mathbf{v}_{tr}^{(1)}) \\ &= \begin{vmatrix} (\mathbf{i}_t \cdot \boldsymbol{\omega}) & (\mathbf{i}_t \cdot \mathbf{v}_{tr}^{(1)}) \\ (\mathbf{k} \cdot \boldsymbol{\omega}) & (\mathbf{k} \cdot \mathbf{v}_{tr}^{(1)}) \end{vmatrix} = -(\mathbf{i}_t \cdot \mathbf{v}_{tr}^{(1)})(\boldsymbol{\omega} \cdot \mathbf{k}) \end{aligned} \quad (6.2.36)$$

because $\mathbf{i}_t \cdot \boldsymbol{\omega} = 0$, $\mathbf{k} \cdot \mathbf{v}_{tr}^{(1)} = 0$ due to the perpendicularity of vectors. Thus,

$$\dot{\mathbf{n}}_r^{(1)} \cdot \mathbf{v}^{(12)} - \left[\mathbf{n}^{(1)} \boldsymbol{\omega} \mathbf{v}_r^{(1)} \right] = -(\mathbf{i}_t \cdot \mathbf{v}_{tr}^{(1)}) \cdot (\mathbf{k} \cdot \boldsymbol{\omega}) \quad (6.2.37)$$

Equations (6.2.4) to (6.2.6), (6.2.34), and (6.2.37) yield a system of three linear equations in two unknowns

$$a_{i1}x_1 + a_{i2}x_2 = b_i \quad (i = 1,2,3) \quad (6.2.38)$$

Here

$$x_1 = v_r^{(1)} \quad x_2 = v_r^{(2)}$$

$$a_{11} = \kappa_1(\mathbf{v}^{(12)} \cdot \mathbf{i}_t) - (\boldsymbol{\omega} \cdot \mathbf{k}) \quad a_{12} = 0 \quad b_1 = (\mathbf{v}_{tr}^{(1)} \cdot \mathbf{i}_t)(\boldsymbol{\omega} \cdot \mathbf{k})$$

$$a_{21} = -1 \quad a_{22} = 1 \quad b_2 = (\mathbf{v}^{(12)} \cdot \mathbf{i}_t)$$

$$a_{31} = \kappa_1 \quad a_{32} = -\kappa_2 \quad b_3 = -(\boldsymbol{\omega} \cdot \mathbf{k})$$

Discussions similar to those above regarding the system of linear equations (6.2.30) result in

$$\begin{vmatrix} a_{11} & 0 & b_1 \\ -1 & 1 & b_2 \\ \kappa_1 & -\kappa_2 & b_3 \end{vmatrix} = 0$$

This yields

$$\kappa_2 = \frac{\kappa_1 b_1 - a_{11} b_3}{a_{11} b_2 + b_1} = \frac{\kappa_1 [(\boldsymbol{\omega} \cdot \mathbf{k})(\mathbf{v}_{tr}^{(1)} + \mathbf{v}^{(12)}) \cdot \mathbf{i}_t] - \omega^2}{\kappa_1 (v^{(12)})^2 + (\boldsymbol{\omega} \cdot \mathbf{k})(\mathbf{v}_{tr}^{(2)} \cdot \mathbf{i}_t)} \quad (6.2.39)$$

Consider a case when the contact point coincides with the pitch point I (fig. 6.2.1(a)). Then $\mathbf{v}^{(12)} = 0$,

$$\mathbf{v}_{tr}^{(1)} = \mathbf{v}_{tr}^{(2)}$$

and equation (6.2.39) yields

$$\kappa_2 = \kappa_1 - \frac{\omega^2}{(\boldsymbol{\omega} \cdot \mathbf{k})(\mathbf{v}_{ir}^{(2)} \cdot \mathbf{i}_t)} \quad (6.2.40)$$

If the rack cutter is applied for cutting involute gears, its shape Σ_1 is a straight line (fig. 6.2.1(b)) and its curvature is $\kappa_1 = 0$. Equation (6.2.40) yields (fig. 6.2.1(b))

$$\kappa_2 = - \frac{\omega^2}{(\boldsymbol{\omega} \cdot \mathbf{k})(\mathbf{v}_{ir}^{(2)} \cdot \mathbf{i}_t)} = \frac{1}{r \sin \psi_c} \quad (6.2.41)$$

The positive sign of the curvature κ_2 means that the curvature center is located on the positive unit normal

$$\mathbf{n}^{(1)} = \mathbf{i}_t \times \mathbf{k}$$

A more complicated case dealing with the curvature of generated shape Σ_2 is discussed in example problem 6.2.3.

Example problem 6.2.1 Consider that the shape of gear 1 is an involute curve corresponding to the base circle of radius r_{b1} . The centrode of gear 1 is the circle of radius r_1 . The ratio of these radii is

$$\frac{r_{b1}}{r_1} = \cos \psi_c$$

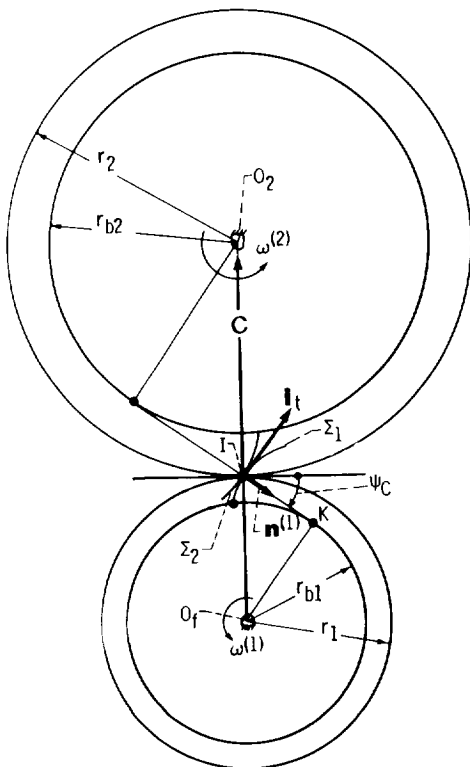


Figure 6.2.2.

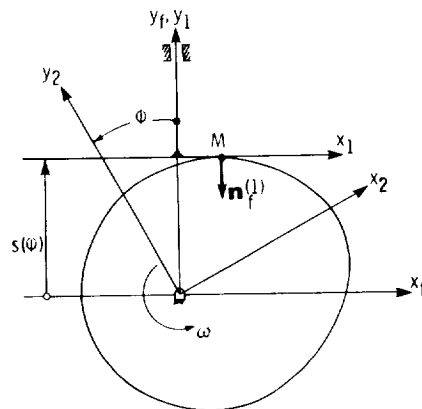


Figure 6.2.3.

Here we shall consider the case whereby the contact point coincides with the pitch point I (fig. 6.2.2). The angular velocity ratio m_{12} is constant and is represented as

$$m_{12} = \frac{\omega^{(1)}}{\omega^{(2)}} = \frac{r_2}{r_1} \quad (6.2.42)$$

where r_1 and r_2 are gear centrode radii. Determine the curvature of gear shape Σ_2 at the contact point assuming that the curvature κ_1 of the shape Σ_1 is given.

Solution. At the pitch point I the velocity of sliding vector $\mathbf{v}^{(12)} = 0$ and shape curvatures are related by equation (6.2.33).

Since the constant angular velocity ratio the derivative $m'_{12} = 0$, and

$$b_1 = (\mathbf{n}^{(1)} \cdot \mathbf{C}) (\boldsymbol{\omega}^{(1)} \cdot \boldsymbol{\omega}^{(2)})$$

Vectors $\mathbf{n}^{(1)}$ and \mathbf{C} form the angle $90^\circ + \psi_c$. Gears rotate in opposite directions, and

$$\boldsymbol{\omega}^{(1)} \cdot \boldsymbol{\omega}^{(2)} = -\omega^{(1)}\omega^{(2)} \quad \boldsymbol{\omega}^{(12)} = \boldsymbol{\omega}^{(1)} - \boldsymbol{\omega}^{(2)} \quad |\boldsymbol{\omega}^{(12)}| = \omega^{(1)} + \omega^{(2)}$$

At point I the curvature radius of shape Σ_1 is IK and the curvature is

$$\kappa_1 = \frac{1}{r_1 \sin \psi_c}$$

The curvature $\kappa_1 > 0$ because the center of curvature κ_1 is located on the positive normal.

The coefficient b_1 may be expressed as follows:

$$b_1 = (\mathbf{n}^{(1)} \cdot \mathbf{C})(\boldsymbol{\omega}^{(1)} \cdot \boldsymbol{\omega}^{(2)}) = \omega^{(1)}\omega^{(2)}(r_1 + r_2) \sin \psi_c$$

Then, we get

$$\frac{(\omega^{(12)})^2}{b_1} = \frac{(\omega^{(1)} + \omega^{(2)})^2}{\omega^{(1)}\omega^{(2)}(r_1 + r_2) \sin \psi_c} = \frac{r_1 + r_2}{r_1 r_2 \sin \psi_c}$$

and (see eq. (6.2.23))

$$\kappa_2 = \frac{1}{r_1 \sin \psi_c} - \frac{r_1 + r_2}{r_1 r_2 \sin \psi_c} = -\frac{1}{r_2 \sin \psi_c} \quad (6.2.43)$$

The negative sign for curvature κ_2 means that the curvature center of shape Σ_2 is located on the negative normal.

Equation (6.2.43) may be obtained by using more simple methods; however, the application of general equations (6.2.32) and (6.2.33) illustrates the power of those equations even for this particular case.

Example Problem 6.2.2 Consider a cam mechanism with a flat-faced follower (fig. 6.2.3). We set up coordinate systems S_1 , S_2 , and S_f rigidly connected to the follower, cam, and frame, respectively. Given are the displacement function

$$s(\phi) \in C^2 \quad 0 < \phi < 2\pi \quad (6.2.44)$$

and the shape Σ_1 represented by the equations

$$x_1 = \theta_1 \quad y_1 = 0 \quad (6.2.45)$$

where $a < \theta_1 < b$.

Determine (1) the equations of the cam shape Σ_2 , (2) the line of action, and (3) the curvature $\kappa_2(\phi)$ of the cam.

Equation of Meshing.—We represent shape Σ_1 in the coordinate system S_f by

$$\mathbf{r}_f^{(1)} = \theta_1 \mathbf{i}_f + s(\phi) \mathbf{j}_f \quad (6.2.46)$$

The normal to the shape Σ_1 is

$$\mathbf{N}_f^{(1)} = \frac{\partial \mathbf{r}_f^{(1)}}{\partial \theta} \times \mathbf{k} = -\mathbf{j}_f \quad (6.2.47)$$

The sliding velocity is represented by

$$\begin{aligned} \mathbf{v}^{(12)} &= \mathbf{v}_{ir}^{(1)} - \mathbf{v}_{ir}^{(2)} = \frac{ds}{dt} - \boldsymbol{\omega} \times \mathbf{r}_f^{(1)} = \frac{ds}{d\phi} \omega \mathbf{j}_f - \begin{vmatrix} \mathbf{i}_f & \mathbf{j}_f & \mathbf{k}_f \\ 0 & 0 & \omega \\ x_f^{(1)} & y_f^{(1)} & 0 \end{vmatrix} \\ &= \omega \left[s(\phi) \mathbf{i}_f + \left(\frac{ds}{d\phi} - \theta_1 \right) \mathbf{j}_f \right] \end{aligned} \quad (6.2.48)$$

The equation of meshing may be determined by

$$\mathbf{N}_f^{(1)} \cdot \mathbf{v}^{(12)} = f(\theta_1, \phi) = -\omega \left(\frac{ds}{d\phi} - \theta_1 \right) = 0 \quad (6.2.49)$$

Equation (6.2.49) yields that

$$f(\theta_1, \phi) = \theta_1 - \frac{ds}{d\phi} = 0 \quad (6.2.50)$$

This equation determines the location of the contact point M (fig. 6.2.3) as a function of the parameter ϕ .

Equations of shape Σ_2 .—Shape Σ_2 is determined as follows:

$$[r_2] = [M_{21}][r_1] = [M_{2f}][r_f^{(1)}] \quad f(\theta_1, \phi) = 0 \quad (6.2.51)$$

Here

$$[M_{21}] = [M_{2f}][M_{f1}] = \begin{bmatrix} \cos \phi & \sin \phi & s(\phi) \sin \phi \\ -\sin \phi & \cos \phi & s(\phi) \cos \phi \\ 0 & 0 & 1 \end{bmatrix}$$

Equations (6.2.51), (6.2.50), and (6.2.45) yield

$$x_2 = \theta_1 \cos \phi + s(\phi) \sin \phi \quad y_2 = -\theta_1 \sin \phi + s(\phi) \cos \phi \quad \theta_1 - \frac{ds}{d\phi} = 0 \quad (6.2.52)$$

Substituting θ_1 by $\frac{ds}{d\phi}$ in x_2 and y_2 , we get the following equations of shape Σ_2 :

$$x_2 = s(\phi) \sin \phi + \frac{ds}{d\phi} \cos \phi \quad y_2 = s(\phi) \cos \phi - \frac{ds}{d\phi} \sin \phi \quad (6.2.53)$$

Line of Action.—We represent the line of action by the expressions

$$\mathbf{r}_f(\theta_1, \phi) \quad f(\theta_1, \phi) = 0 \quad (6.2.54)$$

which yield

$$\mathbf{r}_f = \frac{ds}{d\phi} \mathbf{i}_f + s(\phi) \mathbf{j}_f \quad (6.2.55)$$

Cam Curvature.—To determine the cam curvature, we apply equations (6.2.4) to (6.2.7) which yield

$$-\kappa_2(\mathbf{v}_r^{(1)} + \mathbf{v}^{(12)}) = -\kappa_1 \mathbf{v}_r^{(1)} + (\boldsymbol{\omega}^{(12)} \times \mathbf{n}^{(1)})$$

For the considered case $\kappa_1 = 0$ (shape Σ_1 is a straight line), $\boldsymbol{\omega}^{(12)} = \boldsymbol{\omega}$, and we get

$$\kappa_2(\mathbf{v}_r^{(1)} + \mathbf{v}^{(12)}) = \boldsymbol{\omega} \times \mathbf{n}^{(1)} \quad (6.2.56)$$

Equation (6.2.46) yields

$$\mathbf{v}_r^{(1)} = \frac{\partial \mathbf{r}_r^{(1)}}{\partial \theta_1} \frac{d\theta_1}{dt} = \frac{d\theta_1}{dt} \mathbf{i}_f \quad (6.2.57)$$

Differentiation of equation (6.2.50) gives

$$\frac{d\theta_1}{dt} = \frac{d^2 s}{d\phi^2} \boldsymbol{\omega} \quad (6.2.58)$$

Then

$$\mathbf{v}_r^{(1)} = \omega \frac{d^2s}{d\phi^2} \mathbf{i}_f \quad (6.2.59)$$

Equations (6.2.48) and (6.2.50) yield

$$\mathbf{v}^{(12)} = \omega s(\phi) \mathbf{i}_f \quad (6.2.60)$$

Equations (6.2.56) to (6.2.60) yield that

$$\kappa_2 \omega \left[\frac{d^2s}{d\phi^2} + s(\phi) \right] \mathbf{i}_f = \begin{vmatrix} \mathbf{i}_f & \mathbf{j}_f & \mathbf{k}_f \\ 0 & 0 & \omega \\ 0 & -1 & 0 \end{vmatrix} = \omega \mathbf{i}_f$$

and

$$\kappa_2 = \frac{1}{\frac{d^2s}{d\phi^2} + s(\phi)} \quad (6.2.61)$$

Cam shape Σ_2 must be a convex curve with the curvature center located on the positive unit normal $\mathbf{n}_f^{(1)}$ (fig. 6.2.3). The curvature κ_2 is positive if the following inequality is observed:

$$s(\phi) + \frac{d^2s}{d\phi^2} > 0 \quad (6.2.62)$$

Example 6.2.3 Figure 6.2.4(a) shows a rack cutter tooth which generates spur involute gears. The straight-lined edge of the rack cutter generates the involute curve, and the arc of the circle of radius ρ , centered at point C_1 (fig. 6.2.4(a) and (b)), generates the fillet of the gear. The displacement of the rack cutter s and the angle of gear rotation ϕ are related by

$$s = r \phi \quad (6.2.63)$$

where r is the radius of the gear pitch circle.

Develop equations of the gear fillet and its curvature. Apply the coordinate systems shown in figure 6.2.1(a).

Equations of shape Σ_1 .—The position vector of an current point M of shape Σ_1 (fig. 6.2.4(a)) is

$$\mathbf{r}_1(\theta_1) = \overline{O_1M} = \overline{O_1C_1} + \overline{C_1M} \quad (6.2.64)$$

Projecting this vector equation on the x_1 - and y_1 -axes (fig. 6.2.4(a) and (b)), we get the following equations for shape Σ_1 :

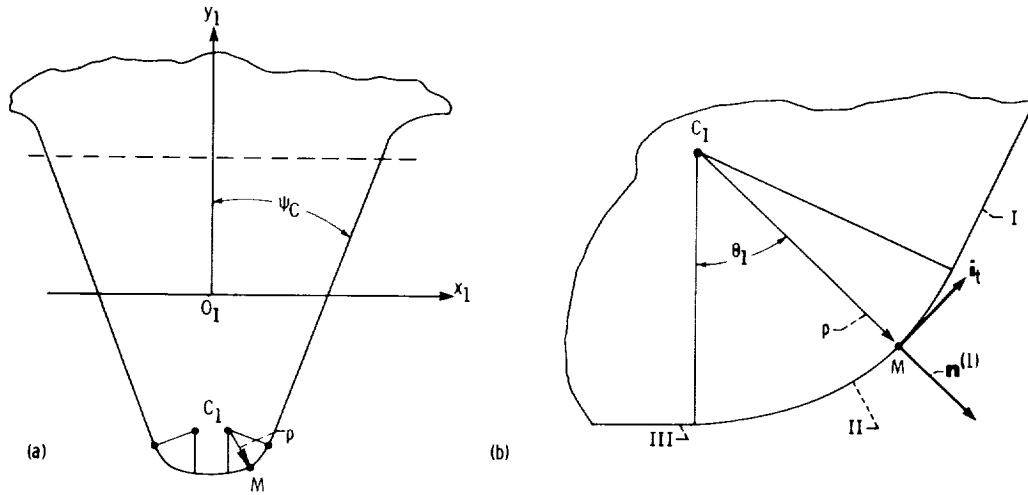


Figure 6.2.4.

$$x_1 = a + \rho \sin \theta_1 \quad y_1 = b - \rho \cos \theta_1 \quad (6.2.65)$$

where

$$\{x_1(\theta), y_1(\theta)\} \in C^1 \quad 0 < \theta < 90^\circ - \psi_c$$

Here $a = x_1^{(C_1)}$ and $b = y_1^{(C_1)}$ are coordinates of point C_1 .

Shape Σ_1 is a simple and regular curve. The unit normal \mathbf{n}_1 to shape Σ_1 is

$$\mathbf{n}_1 = \frac{\frac{\partial \mathbf{r}_1}{\partial \theta_1} \times \mathbf{k}_1}{\left| \frac{\partial \mathbf{r}_1}{\partial \theta_1} \times \mathbf{k}_1 \right|} = \sin \theta_1 \mathbf{i}_1 - \cos \theta_1 \mathbf{j}_1 \quad (6.2.66)$$

Equation of meshing.—We apply the equation of meshing which expresses that the unit normal at the contact point passes through the instantaneous center of rotation (pitch point) I (see ch. 4.5)

$$\frac{X_1(\phi) - x_1(\theta_1)}{n_{x_1}(\theta_1)} - \frac{Y_1(\phi) - y_1(\theta_1)}{n_{y_1}(\theta_1)} = f(\theta_1, \phi) = 0 \quad (6.2.67)$$

Here (fig. 6.2.1(a))

$$X_1(\phi) = r\phi \quad Y_1 = 0 \quad (6.2.68)$$

Equations (6.2.65) to (6.2.68) yield

$$f(\theta_1, \phi) = r\phi - a - b \tan \theta_1 = 0 \quad (6.2.69)$$

Equations of shape Σ_2 .—Shape Σ_2 is represented by the following equations:

$$[r_2] = [M_{21}][r_1] \quad f(\theta_1, \phi) = 0 \quad (6.2.70)$$

Here (fig. 6.2.1(a))

$$[M_{21}] = [M_{2f}][M_{f1}] = \begin{bmatrix} \cos \phi & \sin \phi & -r\phi \cos \phi + r \sin \phi \\ -\sin \phi & \cos \phi & r\phi \sin \phi + r \cos \phi \\ 0 & 0 & 1 \end{bmatrix}$$

Equations (6.2.65), (6.2.29), and (6.2.70) yield

$$\begin{aligned} x_2 &= a \cos \phi + b \sin \phi - \rho \sin(\phi - \theta_1) - r\phi \cos \phi + r \sin \phi \\ y_2 &= -a \sin \phi + b \cos \phi - \rho \cos(\phi - \theta_1) - r\phi \sin \phi + r \cos \phi \\ r\phi - a - b \tan \theta_1 &= 0 \end{aligned} \quad (6.2.71)$$

Line of Action.—We represent the line of action by the equations

$$[r_f] = [M_{f1}][r_1] \quad f(\theta_1, \phi) = 0$$

which yield

$$\mathbf{r}_f = (a + \rho \sin \theta_1 - r\phi)\mathbf{i}_f + (b - \rho \cos \theta_1 + r)\mathbf{j}_f \quad r\phi - a - b \tan \theta_1 = 0 \quad (6.2.72)$$

Curvature of shape Σ_2 .—To determine the curvature κ_2 we apply equation (6.2.39).
Here

$$\kappa_1 = -\frac{1}{\rho} \quad \mathbf{i}_t = \frac{\frac{\partial \mathbf{r}_f}{\partial \theta_1}}{\left| \frac{\partial \mathbf{r}_f}{\partial \theta_1} \right|} = \cos \theta_1 \mathbf{i}_f + \sin \theta_1 \mathbf{j}_f$$

$\boldsymbol{\omega} \cdot \mathbf{k} = \omega$ (assume that the gear rotates counterclockwise)

$$\mathbf{v}_{tr}^{(1)} = -r\omega\mathbf{i}_f$$

$$\mathbf{v}^{(12)} = \mathbf{v}_{tr}^{(1)} - \mathbf{v}_{tr}^{(2)} = -r\omega\mathbf{i}_f - (\boldsymbol{\omega} \times \mathbf{r}_f)$$

$$= -r\omega\mathbf{i}_f - \begin{vmatrix} \mathbf{i}_f & \mathbf{j}_f & \mathbf{k}_f \\ 0 & 0 & \omega \\ x_f & y_f & 0 \end{vmatrix}$$

$$= \omega[(b - \rho \cos \theta_1)\mathbf{i}_f + (b \tan \theta_1 - \rho \sin \theta_1)\mathbf{j}_f]$$

$$(v^{(12)})^2 = \omega^2 \left(\frac{b}{\cos \theta_1} - \rho \right)^2$$

Deriving the equation for $v^{(12)}$, we eliminated $r\phi$ by using equation of meshing (6.2.69). Thus we have (see eq. (6.2.39))

$$\kappa_2(\theta_1) = -\frac{r \cos^3 \theta_1 - b \cos \theta_1}{b^2 + \rho(r \cos^3 \theta_1 - b \cos \theta_1)} \quad 0 < \theta_1 < 90^\circ - \psi_c \quad (b \text{ is negative}) \quad (6.2.73)$$

The negative sign of κ_2 indicates that the center of curvature of the generated fillet is located on the negative direction of the normal (fig. 6.2.4(b)). Consequently, the rack cutter and the gear fillet are in internal tangency by cutting.

The rack cutter shape Σ_1 , shown in figure 6.2.4(b), generates shape Σ_2 which contains three curves. These curves are (1) the involute curve, generated by the straight line I, (2) the fillet, generated by the arc of circle II, and (3) a circle which belongs to the dedendum, generated by the straight line III. The curvature at the point of tangency of the involute curve and the fillet corresponds to the parameter $\theta_1 = 90^\circ - \psi_c$. The curvature of the fillet at the point of its tangency with the dedendum circle corresponds to $\theta_1 = 0$.

6.3. Relations Between Centrode and Shape Curvatures

The well-known Euler-Savary equation relates the curvatures of two centrodes and the conjugate shapes with which they are provided. The theory presented in this chapter allows us to develop equations which may be considered as a modified form of the Euler-Savary equation.

Figure 6.3.1 shows two centrodes, 1 and 2, which are in tangency at point I , the instantaneous center of rotation. In general, the centrodes are noncircular curves. The shapes with which centrodes 1 and 2 are provided are denoted by Σ_1 and Σ_2 , respectively. Shapes Σ_1 and Σ_2 are in tangency at point M . Further, we denote \mathbf{i}_c as the unit vector of the tangent to the centrodes, $\mathbf{n}_c = \mathbf{i}_c \times \mathbf{k}$ as the common unit normal of the centrodes, \mathbf{i}_s as the unit vector of the tangent to the shapes, and \mathbf{n}_s as the common unit normal of the shapes. We developed equation (6.2.33) which relates the curvatures of two shapes which are in tangency at the instantaneous center of rotation. Considering the centrodes as conjugated shapes, we may apply this equation to relate centrode curvatures. With modified notation we get

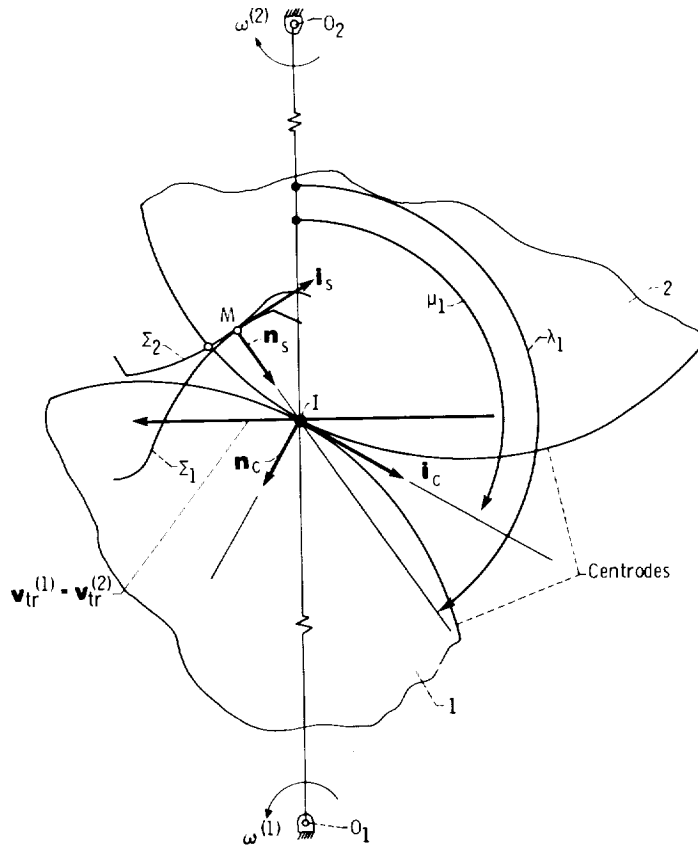


Figure 6.3.1.

$$q_2 = q_1 - \frac{(\omega^{(12)})^2}{b_c} \quad (6.3.1)$$

Here q_1 and q_2 are centrode curvatures, $\omega^{(12)} = \omega^{(1)} - \omega^{(2)}$ is the relative angular velocity of centrodes 1 and 2

$$b_c = (\mathbf{n}_c \cdot \mathbf{C})(\omega^{(1)} \cdot \omega^{(2)}) + \frac{m'_{12}}{m_{12}} \omega^{(1)} (\mathbf{n}_c \cdot \mathbf{v}_{tr}^{(2)}) \quad (6.3.2)$$

(See coefficient b_1 of equation (6.2.30).)

A similar equation may be developed for shapes Σ'_1 and Σ'_2 which are in tangency at point I instead of point M (fig. 6.3.2). Shapes Σ_i and Σ'_i are equidistant curves ($i = 1, 2$). Curvatures of shapes Σ'_1 and Σ'_2 are related by

$$\kappa'_2 = \kappa'_1 - \frac{(\omega^{(12)})^2}{b_s} \quad (6.3.3)$$

Here

$$b_s = (\mathbf{n}_s \cdot \mathbf{C})(\omega^{(1)} \cdot \omega^{(2)}) + \frac{m'_{12}}{m_{12}} \omega^{(1)} (\mathbf{n}_s \cdot \mathbf{v}_{tr}^{(2)}) \quad (6.3.4)$$

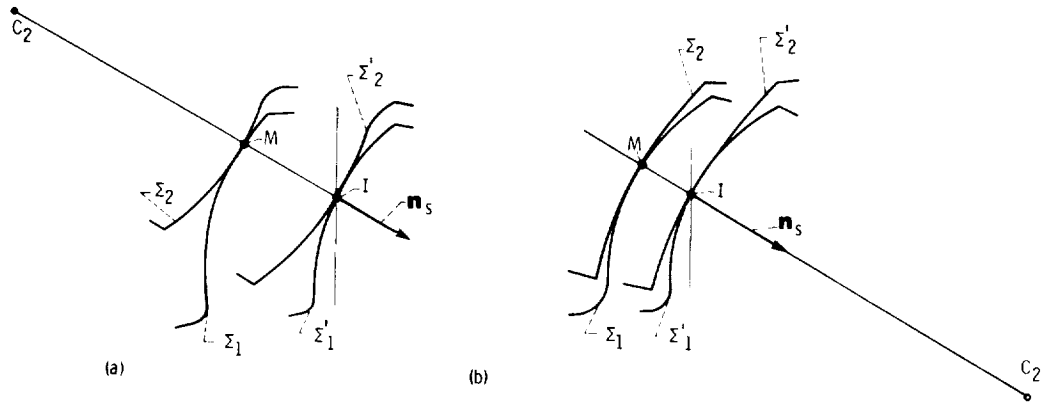


Figure 6.3.2.

At point I we have

$$\mathbf{v}_{tr}^{(2)} = \mathbf{v}_{tr}^{(1)}$$

because the point of centrod tangency I is the instantaneous center of rotation (fig. 6.3.1). By knowing the curvature κ'_2 of shape Σ'_2 at point I , it is easy to find the curvature κ_2 of shape Σ_2 at the point M (fig. 6.3.2) by applying the following equation:

$$\frac{1}{\kappa_2} = \frac{1}{\kappa'_2} \mp |\overline{IM}| \quad (6.3.5)$$

where κ_2 and κ'_2 are the curvatures of shapes Σ_2 and Σ'_2 respectively. Signs of κ_2 and κ'_2 are positive if the curvature centers are located on the positive direction of unit normal \mathbf{n}_s . The upper sign corresponds to the case where the direction of vector \overline{IM} coincides with the direction of the unit normal \mathbf{n}_s .

Figures 6.3.2(a) and (b) show two pairs of equidistant shapes Σ_1 and Σ_2 and Σ'_1 and Σ'_2 for cases of both external and internal tangency. Shapes Σ_1 and Σ_2 contact each other at point M . The contact point of shapes Σ'_1 and Σ'_2 is point I . Point C_2 is the center of curvature of shapes Σ_2 and Σ'_2 .

Equation (6.3.5) is derived by using the following suggestions. For the case shown in figure 6.3.2(a) we have

$$\overline{MC_2} = \overline{IC_2} - \overline{IM}$$

The curvature of shapes Σ_2 and Σ'_2 is negative because center C_2 is located on the negative direction of normal \mathbf{n}_s , and the relation above may be represented by

$$-\frac{1}{\kappa_2} = -\frac{1}{\kappa'_2} + |\overline{IM}| \quad (6.3.6)$$

Similarly, we may get, for the case shown in figure 6.3.2(b), the equation

$$\overline{MC_2} = \overline{IC_2} - \overline{IM}$$

which may be represented as

$$\frac{1}{\kappa_2} = \frac{1}{\kappa'_2} + |\overline{IM}| \quad (6.3.7)$$

Equations (6.3.6) and (6.3.7) may be substituted by one equation (eq. (6.3.5)) with the mentioned rule of signs for the segment $|\overline{IM}|$.

Summarizing the above discussion, we may state the following: Given (1) the curvatures of one centrode and one shape and (2) the location of the contact point and parameters of motion of the gears. Then curvatures of the second centrode and the second shape may be determined separately by using equations (6.3.1), (6.3.3), and (6.3.5).

System of equations (6.3.1) and (6.3.3) may be substituted by one equation which is similar to the equation of Euler-Savary

$$(q_1 - q_2)b_c - (\kappa_1' - \kappa_2')b_s = 0 \quad (6.3.8)$$

The system of two equations (6.3.1) and (6.3.3) has a certain advantage over equation (6.3.8) for the reason that one equation (eq. (6.3.8)) relates four algebraic quantities q_1 , q_2 , κ_1' , and κ_2' . Consequently, we may determine only one of these quantities, considering the other three as given. Having two equations (eqs. (6.3.1) and (6.3.3)), we may determine two of four quantities q_1 , q_2 , κ_1' , and κ_2' .

Let us express coefficient b_c and b_s in terms of μ_1 and λ_1 shown in figure 6.3.1.

Henceforth, we shall consider both cases of transformation of rotation when the driving and driven gears rotate in opposite directions and in the same direction. We assume that gear 1 rotates counterclockwise, and in both cases $|\omega^{(1)}| > |\omega^{(2)}|$. We begin with transformation of some auxiliary expressions. By taking into account that $\mathbf{v}_I^{(1)} = \mathbf{v}_I^{(2)}$ at point I , we have

$$\omega^{(1)} \times \overline{O_1I} = (\omega^{(2)} \times \overline{O_1I}) + (\overline{O_1O_2} \times \omega^{(2)}) = (\omega^{(2)} \times \overline{O_1I}) + (\mathbf{C} \times \omega^{(2)}) \quad (6.3.9)$$

Using the vector products

$$\omega^{(1)} \times (\omega^{(1)} \times \overline{O_1I}) = (\omega^{(1)} \times (\omega^{(2)} \times \overline{O_1I})) + (\omega^{(1)} \times (\mathbf{C} \times \omega^{(2)}))$$

we get

$$-\overline{O_1I}(\omega^{(1)})^2 = -\overline{O_1I}(\omega^{(1)} \cdot \omega^{(2)}) + \mathbf{C}(\omega^{(1)} \cdot \omega^{(2)}) \quad (6.3.10)$$

Vector $\omega^{(2)}$ may be expressed as

$$\omega^{(2)} = \mp \frac{\omega^{(1)}}{m_{12}(\phi_1)} \quad (6.3.11)$$

where $m_{12}(\phi_1) = \omega^{(1)}/\omega^{(2)}$ is the angular velocity ratio. The upper sign in equation (6.3.11) (and in all succeeding equations in this discussion) corresponds to the case where gears 1 and 2 rotate in opposite directions.

Equations (6.3.10) and (6.3.11) yield

$$\overline{O_1I} = \mathbf{r} = \frac{\mathbf{C}}{1 \pm m_{12}(\phi_1)} \quad (6.3.12)$$

We must recall that the gear which rotates with the higher speed is denoted by 1, and $m_{12} > 1$. Consequently, vectors $\mathbf{r}_1 = \overline{O_1I}$ and $\mathbf{C} = \overline{O_1O_2}$ are directed in opposite directions if gears 1 and 2 rotate in the same direction.

The absolute magnitude of \mathbf{r}_1 is

$$r_1 = |\mathbf{r}_1| = \frac{C}{m_{12}(\phi_1) \pm 1} \quad (6.3.13)$$

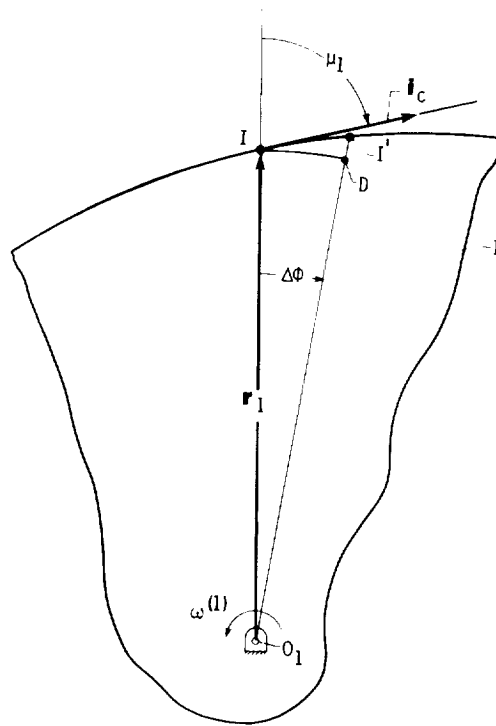


Figure 6.3.3.

The unit tangent vector of centrodes \mathbf{i}_c and vector $\overline{O_1 I} = \mathbf{r}_1$ form the angle μ_1 (fig. 6.3.3). Point I is the instantaneous center of rotation for the shown position of the centrode. The neighboring point I' becomes the instantaneous center of rotation after gear 1 rotates through the angle $\Delta\phi_1$. It results from the drawings of figure 6.3.3 that

$$\tan \mu_1 = \lim_{\Delta\phi \rightarrow 0} \left(\frac{ID}{I'D} \right) = \lim_{\Delta\phi \rightarrow 0} \left(\frac{r_1 \Delta\phi_1}{\Delta r_1} \right) = \frac{r_1}{\frac{dr_1}{d\phi_1}} \quad (6.3.14)$$

The differentiation of equation (6.3.13) gives that

$$\frac{dr_1}{d\phi_1} = - \frac{Cm'_{12}}{(m_{12} \pm 1)^2} \quad (6.3.15)$$

where

$$m'_{12} = \frac{d}{d\phi_1} (m_{12}(\phi_1))$$

Equations (6.3.13) to (6.3.15) yield

$$\tan \mu_1 = - \frac{m_{12} \pm 1}{m'_{12}} \quad (6.3.16)$$

Substituting \mathbf{n}_c (fig. 6.3.1) by

$$\mathbf{n}_c = \mathbf{i}_c \times \mathbf{k}$$

and $\mathbf{v}_{ir}^{(2)} = \mathbf{v}_{ir}^{(1)}$ by

$$\mathbf{v}_{ir}^{(1)} = \boldsymbol{\omega}^{(1)} \times \overline{O_1I} = \boldsymbol{\omega}^{(1)} \times \mathbf{r}^{(1)}$$

we get

$$\mathbf{n}_c \cdot \mathbf{v}_{ir}^{(2)} = (\mathbf{i}_c \times \mathbf{k}) \cdot (\boldsymbol{\omega}^{(1)} \times \mathbf{r}_1) = -(\mathbf{k} \cdot \boldsymbol{\omega}^{(1)})(\mathbf{i}_c \cdot \mathbf{r}_1) = -\omega^{(1)} r_1 \cos \mu_1 \quad (6.3.17)$$

Substituting vector \mathbf{C} by vector \mathbf{r}_1 with aid of equation (6.3.12) and by taking into account that vectors \mathbf{n}_c and \mathbf{r}_1 make an angle $(\mu_1 + 90^\circ)$ (fig. 6.3.1), we get

$$(\mathbf{n}_c \cdot \mathbf{C}) = (\mathbf{n}_c \cdot \mathbf{r}_1)(1 \pm m_{12}) = -r_1 \sin \mu_1 (1 \pm m_{12}) \quad (6.3.18)$$

The magnitude of $\omega^{(12)}$ may be expressed by

$$\omega^{(12)} = \omega^{(1)} \pm \omega^{(2)} = \omega^{(1)} \frac{m_{12} \pm 1}{m_{12}} \quad (6.3.19)$$

Equations (6.3.1), (6.3.2), (6.3.11), (6.3.13), and (6.3.16) to (6.3.19) yield

$$q_1 - q_2 = \frac{(m_{12}(\phi_1) \pm 1)^2 \sin \mu_1}{C m_{12}(\phi_1)} \quad (6.3.20)$$

Similarly, we get for the coefficient b_s

$$(\mathbf{n}_s \cdot \mathbf{C}) = (\mathbf{n}_s \cdot \mathbf{r}_1)(1 \pm m_{12}) = r_1 \cos \lambda_1 (1 \pm m_{12}) \quad (6.3.21)$$

$$\boldsymbol{\omega}^{(1)} \cdot \boldsymbol{\omega}^{(2)} = \mp \frac{(\omega^{(1)})^2}{m_{12}} \quad (6.3.22)$$

$$\mathbf{n}_s \cdot \mathbf{v}_{ir}^{(2)} = \mathbf{n}_s \cdot \mathbf{v}_{ir}^{(1)} = -\omega^{(1)} r_1 \sin \lambda_1 \quad (6.3.23)$$

$$m'_{12} = -\frac{m_{12} \pm 1}{\tan \mu_1} \quad (6.3.24)$$

Equations (6.3.3), (6.3.4), (6.3.13), (6.3.19), and (6.3.21) to (6.3.24) yield

$$\kappa'_1 - \kappa'_2 = \frac{(m_{12}(\phi_1) \pm 1)^2 \sin \mu_1}{C m_{12}(\phi_1) \sin(\lambda_1 - \mu_1)} \quad (6.3.25)$$

We consider equations (6.3.20) and (6.3.25) as an equivalent to the Euler-Savary equation.

Considering these equations together, we get one equation

$$(\kappa'_1 - \kappa'_2) \sin(\lambda_1 - \mu_1) + q_2 - q_1 = 0 \quad (6.3.26)$$

Example problem 6.3.1 Rotation is transformed between parallel axes with the same direction of angular velocities $\boldsymbol{\omega}^{(1)}$ and $\boldsymbol{\omega}^{(2)}$ (fig. 6.3.4). Given are (1) the angular velocity ratio m_{12} (m_{12}

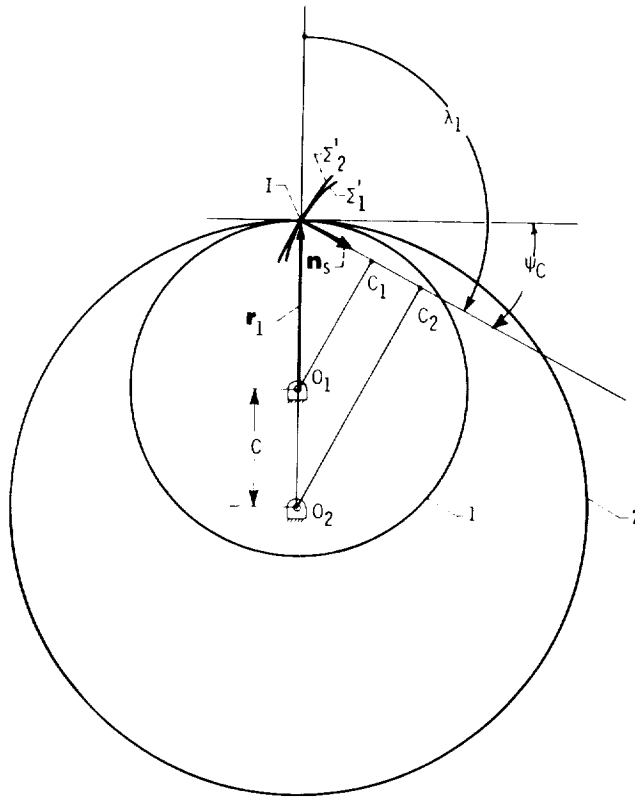


Figure 6.3.4.

is constant), (2) the center distance C , and (3) the curvature κ_1' of shape Σ_1' . Shapes Σ_1' and Σ_2' contact each other at the instantaneous center of rotation I , and the unit normal to the shape, \mathbf{n}_s , and vector \mathbf{r}_1 form the angle $\lambda_1 = 90^\circ + \psi_c$. Determine (1) the centrod curvature, q_2 and (2) the curvature κ_2 of shape Σ_2 .

Solution. Centrode 1 is represented by equation (6.3.13)

$$r_1 = \frac{C}{m_{12} - 1}$$

The centrode 1 curvature is

$$q_1 = \frac{1}{r_1} = \frac{m_{12} - 1}{C}$$

The curvature q_1 is positive because the curvature center is located on the positive direction of normal \mathbf{n}_c which is directed from I to O_1 , (fig. 6.3.4). The centrode 2 curvature is represented by equation (6.3.20) which yields

$$q_2 = q_1 - \frac{(m_{12} - 1)^2 \sin \mu_1}{C m_{12}} = \frac{m_{12} - 1}{C m_{12}}$$

($\mu_1 = 90^\circ$ when $m_{12} = \text{constant}$). The curvature of shape Σ_2 is determined by equation (6.3.25) which yields

$$\kappa_2' = \kappa_1' - \frac{(m_{12} - 1)^2}{C m_{12} \sin \psi_c}$$

By

$$\kappa_1' = \frac{1}{r_1 \sin \psi_c} = \frac{m_{12} - 1}{C \sin \psi_c}$$

we get

$$\kappa_2' = \frac{m_{12} - 1}{C m_{12} \sin \psi_c}$$

Results obtained for this example correspond to the case of involute gears which are in internal tangency (fig. 6.3.4). Centers of curvature of centrodes 1 and 2 are points O_1 and O_2 . Centers of curvatures of shapes Σ_1' and Σ_2' are points C_1 and C_2 .

6.4 Theorem of Direction of Line of Action in the Neighborhood of the Instantaneous Center of Rotation

Theorem Consider that shapes Σ_1 and Σ_2 , being in mesh at the instantaneous center of rotation I , transform rotation and the derivative $m_{12}'(\phi_1) = d/d\phi_1 (m_{12}(\phi_1)) = 0$ where $m_{12}(\phi_1)$ is the function of angular velocity ratio, and ϕ_1 is the angle of gear 1 rotation. Then, in the neighborhood of point I , the tangent to the line of action coincides with the common normal to shapes Σ_1 and Σ_2 .

Proof: The equation of meshing is

$$\mathbf{n}^{(1)} \cdot \mathbf{v}^{(12)} = 0 \quad (6.4.1)$$

where $\mathbf{n}^{(1)}$ is the unit normal to shapes Σ_1 and Σ_2 , and $\mathbf{v}^{(12)}$ is the sliding velocity represented by

$$\mathbf{v}^{(12)} = \left((\boldsymbol{\omega}^{(1)} - \boldsymbol{\omega}^{(2)}) \times \mathbf{r}^{(1)} \right) - \left(\mathbf{C} \times \boldsymbol{\omega}^{(2)} \right) \quad (6.4.2)$$

Here $\mathbf{r}^{(1)}$ is the position vector of the contact point and $\mathbf{C} = \overline{O_1 O_2}$ is the distance between centers of rotation.

The differentiation of equation (6.4.1) yields

$$\dot{\mathbf{n}}^{(1)} \cdot \mathbf{v}^{(12)} + \mathbf{n}^{(1)} \cdot [\boldsymbol{\omega}^{(1)} - \boldsymbol{\omega}^{(2)}] \times \dot{\mathbf{r}}^{(1)} = 0 \quad (6.4.3)$$

It was assumed by differentiation that $\boldsymbol{\omega}^{(1)} = \text{constant}$ and $\boldsymbol{\omega}^{(2)} = \text{constant}$.

Taking into account that the sliding velocity $\mathbf{v}^{(12)} = \mathbf{0}$ at the instantaneous center of rotation, we get

$$[\mathbf{n} \boldsymbol{\omega}^{(12)} \dot{\mathbf{r}}^{(1)}] = 0 \quad (\boldsymbol{\omega}^{(12)} = \boldsymbol{\omega}^{(1)} - \boldsymbol{\omega}^{(2)}) \quad (6.4.4)$$

Vectors \mathbf{n} and $\dot{\mathbf{r}}^{(1)}$ belong to the plane of motion, and vector $\boldsymbol{\omega}^{(12)}$ is perpendicular to this plane; thus, it is perpendicular to vectors \mathbf{n} and $\dot{\mathbf{r}}^{(1)}$. Since the triple product (6.4.4) is equal to zero,

all three vectors, $\omega^{(12)}$, \mathbf{n} and $\dot{\mathbf{r}}^{(1)}$, must belong to the same plane P . This becomes possible only if \mathbf{n} and $\dot{\mathbf{r}}^{(1)}$ are collinear and plane P is drawn through $\omega^{(12)}$ and \mathbf{n} (or through $\omega^{(12)}$ and $\dot{\mathbf{r}}^{(1)}$). Vector $\dot{\mathbf{r}}^{(1)}$ may be interpreted kinematically as the velocity of the contact point in absolute motion (see sec. 6.1) and is directed along the tangent to the line of action. (The line of action is the locus of contact points in the fixed coordinate system.) Because of the collinearity of vectors \mathbf{n} and $\dot{\mathbf{r}}^{(1)}$ in the neighborhood of the instantaneous center of rotation, we may state as follows: The common normal to the shapes, which are in mesh at the instantaneous center I of rotation, coincides with the tangent to the line of action at point I .

It is easy to verify that this theorem may be applied for the widespread planar gearings, whose shapes are involute curves and cycloidal curves. Regarding involute gears the line of action is at the same time the common normal to the contacting shapes. Regarding cycloidal gears (gears whose conjugated pair shapes are an epicycloid and hypocycloid), the tangent to the line of action coincides with the common normal to the shapes only at the pitch point.

6.5 Conditions of Tooth Nonundercutting

During cutting, gear generation is based on the simulation of the mesh of the gear to be cut with a tool—a rack cutter, shaper, or hob. (See ch. 7.1.)

Consider that Σ_1 is the shape of a tool tooth which must generate the shape of gear tooth Σ_2 . We set up coordinate systems S_1 , S_2 , and S_f , rigidly connected to the tool, the generated gear, and the frame, respectively. Considering the relative motion of Σ_1 with respect to coordinate system S_2 , we may find the locus of shapes Σ_1 in coordinate system S_2 and then determine the envelope of this locus, the generated shape Σ_2 . (See ch. 4.) At certain tool settings gear teeth may be undercut. Figure 6.5.1 shows teeth of involute gears generated by a rack cutter. In the first case (fig. 6.5.1(a)) teeth are not undercut, but in the second case (fig. 6.5.1(b)) they are undercut. Mathematically, the problem of tooth nonundercutting is the problem of how to avoid the appearance of singular points on the generated shape Σ_2 . At such points the tangent vector to Σ_2 is $\mathbf{T} = 0$.

Consider that the locus of tool shape Σ_1 is represented in coordinate system S_2 by the vector function

$$\mathbf{r}(\theta, \phi) \in C^1 \quad (\theta, \phi) \in G \quad (6.5.1)$$

Here θ is the parameter of tool shape Σ_1 and ϕ is the parameter of relative motion. By definite conditions (see ch. 4) there exists a function

$$\theta(\phi) \in C^1 \quad (6.5.2)$$

and

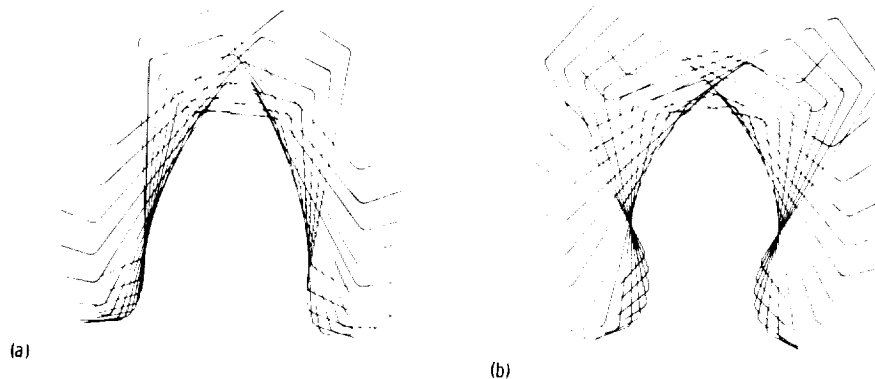


Figure 6.5.1.

$$\mathbf{r}(\phi, \theta(\phi)) = \mathbf{R}(\phi) \quad (6.5.3)$$

represents the generated shape Σ_2 , the envelope of locus of tool shapes Σ_1 . At a regular point of Σ_2 , shapes Σ_1 and Σ_2 are in tangency, and the tangent vector to shape Σ_2 is $\mathbf{T} \neq 0$. At such a point the following vector equation is observed:

$$\mathbf{R}_\phi \frac{d\phi}{dt} = \mathbf{r}_\theta \frac{d\theta}{dt} + \mathbf{r}_\phi \frac{d\phi}{dt}$$

Vectors of equation (6.5.3) represent the velocities of the contact point in the following displacements: (1) along the shape Σ_2 ($\mathbf{R}_\phi d\phi/dt$), (2) along the shape Σ_1 ($\mathbf{r}_\theta d\theta/dt$), and (3) in the relative motion with respect to Σ_2 ($\mathbf{r}_\phi d\phi/dt$). Vector $\mathbf{R}_\phi d\phi/dt$ is collinear to the tangent vector \mathbf{T} . Vector equation (6.5.3) may be represented as

$$\mathbf{v}_r^{(2)} = \mathbf{v}_r^{(1)} + \mathbf{v}^{(12)} \quad (6.5.4)$$

which was represented earlier by equation (6.1.12). At a singular point of shape Σ_2 its tangent \mathbf{T} does not exist, and the necessary condition of existence of singular points of shape Σ_2 may be represented as

$$\mathbf{v}_r^{(1)} + \mathbf{v}^{(12)} = 0 \quad (6.5.5)$$

The advantage of equation (6.5.5) is that we may investigate the existence of singular points on shape Σ_2 by using only the equations of shape Σ_1 and its relative motion with respect to shape Σ_2 . It is not necessary to use the more complicated equations of shape Σ_2 for this purpose.

To avoid the appearance of singular points on the generated shape Σ_2 , it is sufficient to limit the settings of tool shape Σ_1 by cutting. Mathematically, this means that we must limit the area E of θ_1 , considering that the shape Σ_1 is given by

$$\mathbf{r}_1(\theta_1) \in C^1 \quad \theta_1 \in E \quad (6.5.6)$$

Let us explain how this may be done. Vector equation (6.5.5) may be expressed in terms of components in coordinate systems S_1 as follows:

$$\frac{dx_1}{d\theta_1} \frac{d\theta_1}{dt} = -v_{x_1}^{(12)} \quad \frac{dy_1}{d\theta_1} \frac{d\theta_1}{dt} = -v_{y_1}^{(12)} \quad (6.5.7)$$

Differentiation of the equation of meshing

$$f(\theta_1, \phi_1) = 0 \quad (6.5.8)$$

gives

$$\frac{\partial f}{\partial \theta_1} \frac{d\theta_1}{dt} = - \frac{\partial f}{\partial \phi_1} \frac{d\phi_1}{dt} \quad (6.5.9)$$

We consider the system of equations (6.5.7) and (6.5.9) as a system of three linear equations in one unknown.

$$a_{1,i} \zeta = b_i \quad (i = 1, 2, 3) \quad (6.5.10)$$

Here

$$a_{11} = \frac{dx_1}{d\theta_1} \quad a_{12} = \frac{dy_1}{d\theta_1} \quad a_{13} = \frac{\partial f}{\partial \theta_1}$$

$$b_1 = -v_{x_1}^{(12)} \quad b_2 = -v_{y_1}^{(12)} \quad b_3 = -\frac{\partial f}{\partial \phi_1} \frac{d\phi_1}{dt} \quad \zeta = \frac{d\theta_1}{dt}$$

Coefficients a_{11} and a_{12} are such that

$$|a_{11}| + |a_{12}| \neq 0$$

because we assume that shape Σ_1 does not have singular points.

It is known from linear algebra that the system of equations (6.5.10) has a unique solution for ζ_1 if the rank of matrix

$$\begin{bmatrix} a_{11} & b_1 \\ a_{12} & b_2 \\ a_{13} & b_3 \end{bmatrix} \quad (6.5.11)$$

is $r = 1$. This requirement may be observed if all three determinants of the second order which correspond to matrix (6.5.11) are equal to zero. It is easy to verify that the first determinant of the above three is equal to zero

$$\begin{vmatrix} a_{11} & b_1 \\ a_{12} & b_2 \end{vmatrix} = \begin{vmatrix} \frac{dx_1}{d\theta_1} & -v_{x_1}^{(12)} \\ \frac{dy_1}{d\theta_1} & -v_{y_1}^{(12)} \end{vmatrix} = 0 \quad (6.5.12)$$

To prove this, let us consider the equation of meshing which may be represented by

$$\mathbf{N}_1 \cdot \mathbf{v}^{(12)} = \left(\frac{d\mathbf{r}_1}{d\theta_1} \times \mathbf{k}_1 \right) \cdot \mathbf{v}^{(12)} = 0 \quad (6.5.13)$$

Here \mathbf{N}_1 is the vector of the normal to shape Σ_1 , and \mathbf{k}_1 is the unit vector of the z_1 -axis.

Equation (6.5.13) yields that

$$\begin{aligned}
\left[\frac{d\mathbf{r}_1}{d\theta_1} \mathbf{k}_1 \mathbf{v}^{(12)} \right] &= \begin{vmatrix} \frac{dx_1}{d\theta_1} & \frac{dy_1}{d\theta_1} & 0 \\ 0 & 0 & 1 \\ v_{x_1}^{(12)} & v_{y_1}^{(12)} & 0 \end{vmatrix} \\
&= \begin{vmatrix} \frac{dx_1}{d\theta_1} & \frac{dy_1}{d\theta_1} \\ v_{x_1}^{(12)} & v_{y_1}^{(12)} \end{vmatrix} = 0
\end{aligned} \tag{6.5.14}$$

This equation coincides with equation (6.5.12). To observe the requirement that the rank $r = 1$, both remaining determinants of the second order must be equal to zero

$$\begin{vmatrix} a_{11} & b_1 \\ a_{13} & b_3 \end{vmatrix} = \begin{vmatrix} \frac{dx_1}{d\theta_1} & -v_{x_1}^{(12)} \\ \frac{\partial f}{\partial \theta_1} & -\frac{\partial f}{\partial \phi_1} \frac{d\phi_1}{dt} \end{vmatrix} = 0 \tag{6.5.15}$$

$$\begin{vmatrix} a_{12} & b_2 \\ a_{13} & b_3 \end{vmatrix} = \begin{vmatrix} \frac{dy_1}{d\theta_1} & -v_{y_1}^{(12)} \\ \frac{\partial f}{\partial \theta_1} & -\frac{\partial f}{\partial \phi_1} \frac{d\phi_1}{dt} \end{vmatrix} = 0 \tag{6.5.16}$$

Taking into account that equation (6.5.5) provides that

$$\frac{\frac{dx_1}{d\theta_1}}{\frac{dy_1}{d\theta_1}} = \frac{v_{x_1}^{(12)}}{v_{y_1}^{(12)}}$$

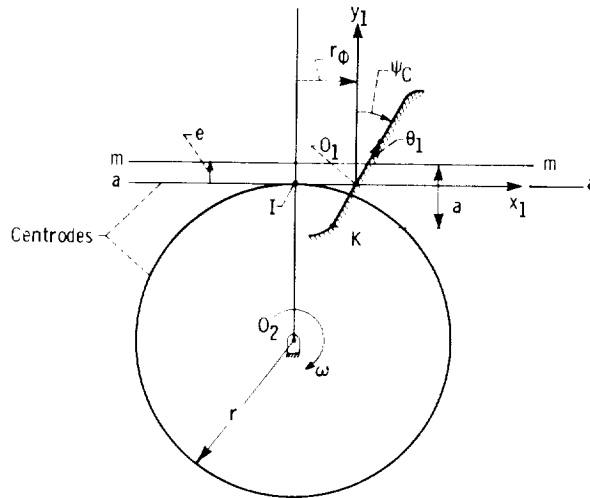


Figure 6.5.2.

it is sufficient to observe only one of two equations, (6.5.16) or (6.5.15). Each of these equations yields the relation

$$F(\theta_1, \phi_1) = 0 \quad (6.5.17)$$

Equations (6.5.17) and (6.5.8) determine the limiting value of θ_1 which corresponds to the singular point of the generated shape Σ_2 . To avoid undercutting of shape Σ_2 , it is sufficient to exclude from meshing the limiting value of θ_1 of shape Σ_1 . This may be done by limiting the setting of tool shape Σ_1 .

Example problem 6.5.1 Consider that a rack cutter, whose shape Σ_1 is a straight line (fig. 6.5.2), generates a gear with shape Σ_2 . Determine the conditions of tooth nonundercutting.

Equations of shape Σ_1 .—Shape Σ_1 is represented in coordinate system S_1 by

$$\mathbf{r}_1(\theta_1) = \theta_1 \sin \psi_c \mathbf{i}_1 + \theta_1 \cos \psi_c \mathbf{j}_1 \quad (6.5.18)$$

Its normal is

$$\mathbf{N}_1 = \frac{d\mathbf{r}_1}{d\theta_1} \times \mathbf{k}_1 = \cos \psi_c \mathbf{i}_1 - \sin \psi_c \mathbf{j}_1 \quad (6.5.19)$$

Relative velocity $\mathbf{v}_1^{(12)}$.—The velocity of the rack cutter is

$$\mathbf{v}_1^{(1)} = \omega r \mathbf{i}_1 \quad (6.5.20)$$

where ω is the angular velocity of the gear, and r is the radius of its centrode which coincides with the pitch circle.

The linear velocity of the gear contact point is

$$\mathbf{v}_1^{(2)} = (\boldsymbol{\omega} \times \mathbf{r}_1) + (\mathbf{R}_1 \times \boldsymbol{\omega}) \quad (6.5.21)$$

Here \mathbf{r}_1 is the position vector drawn from the origin O_1 of coordinate system S_1 to a point of shape Σ_1 and \mathbf{R}_1 is the position vector drawn from point O_1 to an arbitrary point of the line of action of vector $\boldsymbol{\omega}$, for instance, to point O_2 . The position vector \mathbf{R}_1 is represented by

$$\mathbf{R}_1 = \overline{O_1 O_2} = -r\phi \mathbf{i}_1 - r\mathbf{j}_1$$

Equation (6.5.21) yields

$$\begin{aligned} \mathbf{v}_1^{(2)} &= (\boldsymbol{\omega} \times \mathbf{r}_1) + (\overline{O_1 O_2} \times \boldsymbol{\omega}) \\ &= \begin{bmatrix} \mathbf{i}_1 & \mathbf{j}_1 & \mathbf{k}_1 \\ 0 & 0 & -\omega \\ \theta_1 \sin \psi_c & \theta_1 \cos \psi_c & 0 \end{bmatrix} + \begin{bmatrix} \mathbf{i}_1 & \mathbf{j}_1 & \mathbf{k}_1 \\ -r\phi & -r & 0 \\ 0 & 0 & -\omega \end{bmatrix} \\ &= \omega[(\theta_1 \cos \psi_c + r)\mathbf{i}_1 - (\theta_1 \sin \psi_c + r\phi)\mathbf{j}_1] \end{aligned} \quad (6.5.22)$$

The relative linear velocity is

$$\mathbf{v}_1^{(12)} = \mathbf{v}_1^{(1)} - \mathbf{v}_1^{(2)} = \omega[-\theta_1 \cos \psi_c \mathbf{i}_1 + (\theta_1 \sin \psi_c + r\phi)\mathbf{j}_1] \quad (6.5.23)$$

Equation of meshing.—Using the equation of meshing

$$\mathbf{N}_1 \cdot \mathbf{v}_1^{(12)} = 0$$

we get

$$f(\theta_1, \phi_1) = \theta_1 + r\phi \sin \psi_c = 0 \quad (6.5.24)$$

Equation (6.5.24) can also be derived by applying the equation (see ch. 4.5)

$$\frac{X_1 - x_1(\theta_1)}{N_{x_1}} = \frac{Y_1 - y_1(\theta_1)}{N_{y_1}} \quad (6.5.25)$$

Here

$$X_1 = -r\phi$$

$$Y_1 = 0$$

are coordinates of the instantaneous center of rotation I ; $x_1(\theta_1)$ and $y_1(\theta_1)$ are coordinates of a point of shape Σ_1 , which is represented by equation (6.5.18); and N_{x_1} and N_{y_1} are projections of the normal represented by equation (6.5.19).

Limiting point of the rack cutter.—Using equation (6.5.15), we get

$$\begin{vmatrix} \frac{dx_1}{d\theta_1} & -v_{x_1}^{(12)} \\ \frac{\partial f}{\partial \theta_1} & -\frac{\partial f}{\partial \phi} \frac{d\phi}{dt} \end{vmatrix} = \begin{vmatrix} \sin \psi_c & \omega \theta_1 \cos \psi_c \\ 1 & -\omega r \sin \psi_c \end{vmatrix} = -\omega(r \sin^2 \psi_c + \theta_1 \cos \psi_c) = 0 \quad (6.5.26)$$

Equation (6.5.26) yields that the limiting value of parameter θ_1 is

$$\theta_1 = -r \tan \psi_c \sin \psi_c \quad (6.5.27)$$

The negative sign of θ_1 means that θ_1 must be measured in the direction opposite to the direction shown in figure 6.5.2. Point K of the rack cutter (fig. 6.5.2) will not undercut the gear shape Σ_2 if the following inequality is observed:

$$|\overline{O_1K}| < r \tan \psi_c \sin \psi_c \quad (6.5.28)$$

The middle line of the rack cutter mm is located at a distance e from the centrode of the rack cutter aa ; we denote the change of rack cutter setting by e .

According to the drawings of figure 6.5.2, we get

$$|\overline{O_1K}| = \frac{a - e}{\cos \psi_c} \quad (6.5.29)$$

Equations (6.5.29) and (6.5.28) yield

$$a - e < r \sin^2 \psi_c = \frac{N}{2p} \sin^2 \psi_c \quad (6.5.30)$$

Here N represents the number of teeth on the generated gear, P is the diametral pitch, and a is the standardized parameter of the rack cutter. Equation (6.5.30) determines the parameter of rack cutter setting e which corresponds to gear tooth nonundercutting.

$$e \geq a - \frac{N}{2p} \sin^2 \psi_c \quad (6.5.31)$$

Problem 6.5.1 The shape Σ_1 of a rack cutter is an arc of a circle (fig. 6.5.3) represented by equations

$$\mathbf{r}_1(\theta_1) = (a + \rho \cos \theta_1)\mathbf{i}_1 + (b + \rho \sin \theta_1)\mathbf{j}_1 \quad (6.5.32)$$

Here a and b are coordinates of point K , the center of the circular arc. (Depending on location of point K , parameters a and b can be given as positive or negative.) Shape Σ_1 generates gear tooth shape Σ_2 . Determine the limiting point of shape Σ_1 to avoid undercutting of shape Σ_2 .

Directions are as follows: (1) develop the equation of meshing, (2) determine the relative velocity $\mathbf{v}_1^{(12)}$, and (3) apply equation (6.5.15) or (6.5.16) with the equation of meshing.

Answer.

$$\sin^3 \theta_1 - \frac{b}{r} \sin \theta_1 - \frac{b^2}{\rho r} = 0$$

Problem 6.5.2 A shaft is to be generated by a shaper (or by rolling with a master). The shaft shape Σ_1 is represented by equation (fig. 6.5.4)

$$r_1(\theta_1) = h\mathbf{i}_1 + \theta_1\mathbf{j}_1 \quad \theta_{1,\min} < \theta_1 < \theta_{1,\max} \quad (6.5.33)$$

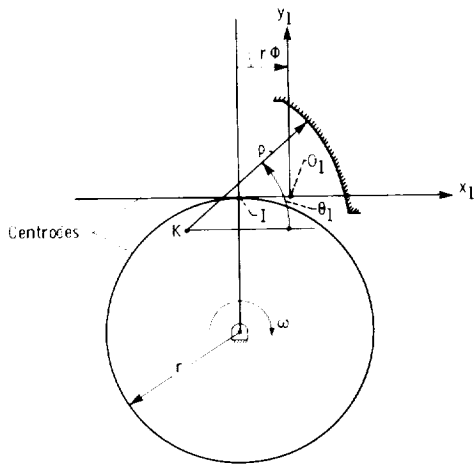


Figure 6.5.3.

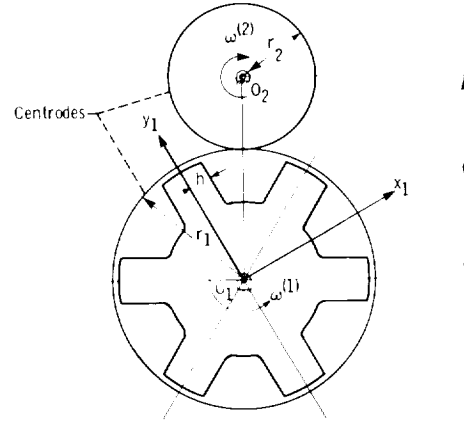


Figure 6.5.4.

The angular velocity ratio by cutting is

$$m_{21} = \frac{\omega^{(2)}}{\omega^{(1)}} = \frac{r_1}{r_2} = \frac{N_1}{N_2} \quad (6.5.34)$$

where r_1 and r_2 are centrode radii and N_1 and N_2 are numbers of teeth on the shaft and tool, respectively.

The undercutting of the tool shape by the given shaft shape (the interference of these shapes) does not occur if the tool shape is a regular curve (it has no singular points).

Develop an equation which relates the limiting value of θ_1 , the radius of the shaft centrode r_1 , and the angular velocity ratio m_{21} .

Directions are as follows: (1) develop the equation of meshing, (2) find the expression of relative velocity $v_1^{(12)}$, and (3) use equation (6.5.16). (Do not use equation (6.5.15). In this case it will yield an identity.)

Answer.

$$r_1^2 - \theta_1^2 - \left(\frac{1 + m_{21}}{2 + m_{21}} \right)^2 h^2 = 0 \quad (6.5.35)$$

Consider m_{21} as given. To avoid undercutting, observe the following inequality:

$$r_1^2 \geq \theta_{1,\max}^2 + \left(\frac{1 + m_{21}}{2 + m_{21}} \right)^2 h^2 \quad (6.5.36)$$

where $(\theta_{1,\max}^2 + h^2)^{1/2}$ is the radius of the shaft addendum circle.

Chapter 7

Generation of Conjugate Shapes

Shape Σ_2 , which must be conjugated with a given shape Σ_1 , is determined as the envelope of the locus of curves Σ_1 . (See ch. 4.) In this chapter we discuss the kinematic principles of tooth generation by which conjugate shapes may be generated automatically in the process of cutting. These principles may be realized by the application of an auxiliary shape Σ_3 , which is in mesh with conjugate shapes Σ_1 and Σ_2 which are to be generated.

7.1 Methods of Tooth Cutting

In general, tooth shapes are generated with a rack cutter, with a hob, and with a shaper. The mesh of the tool with the generated gear during cutting simulates the mesh of a rack with a spur gear (as with a rack cutter or a hob) or the mesh of two spur gears (as with a shaper).

The principle of tooth generation with a rack cutter is shown in figure 7.1.1. The gear to be cut translates with velocity v and rotates about gear center O with angular velocity ω . The velocity $|v|$ and angular velocity ω are related by the equation

$$\frac{v}{\omega} = r \quad (7.1.1)$$

where r is the radius of the gear pitch circle. The pitch circle of the gear and straight line aa of the rack cutter are centrodes during cutting, and point I , the point of tangency of the centrodes, is the instantaneous center of rotation.

During tooth generation, the rack cutter reciprocates parallel to the gear's axis of rotation. The gear tooth shape Σ_2 is generated as the envelope of the locus of rack cutter shapes Σ_1 , which is formed in relative motion (fig. 7.1.2). The hob simulates a worm (usually a worm with a single thread, fig. 7.1.3(a)). The thread is slotted in the axial direction to form a series of cutting blades. The axial section of the worm may be considered to be a rack. The rotation of the hob simulates the translation of the imaginary rack. During cutting the hob and the gear to be generated rotate about their respective axes (fig. 7.1.3), while the hob gradually translates parallel to the gear axis. This is the feed motion of the hob.

The angles of rotation of a single-threaded hob ϕ_h and of the gear ϕ_g are related by

$$\frac{\phi_h}{\phi_g} = N_g \quad (7.1.2)$$

where N_g is the number of teeth on the generated gear.

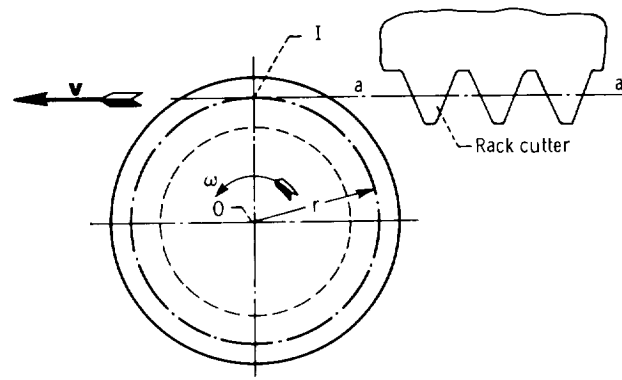


Figure 7.1.1.

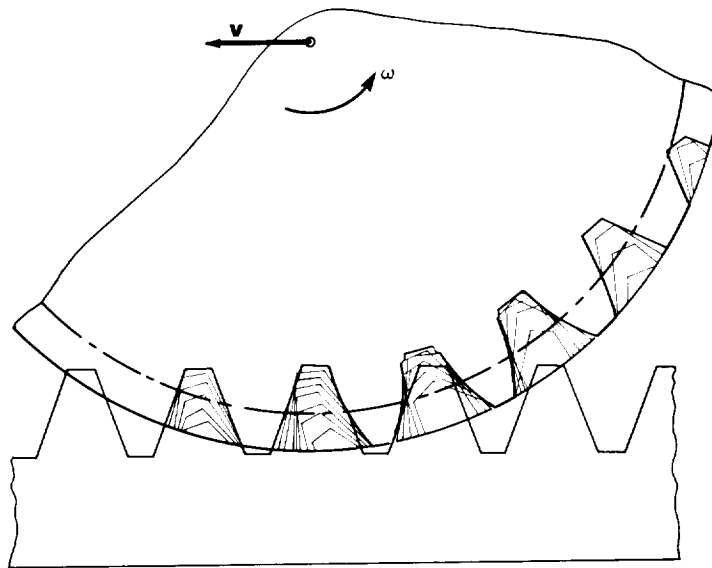


Figure 7.1.2.

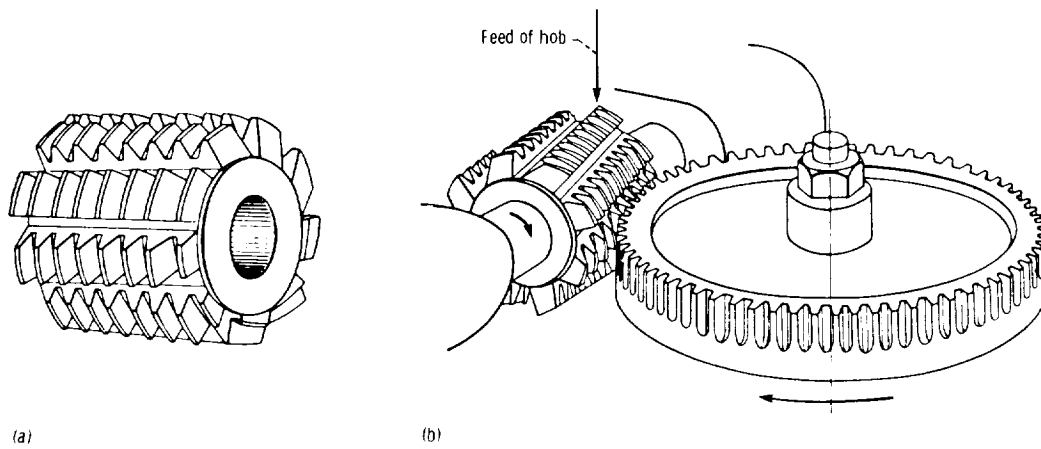


Figure 7.1.3.

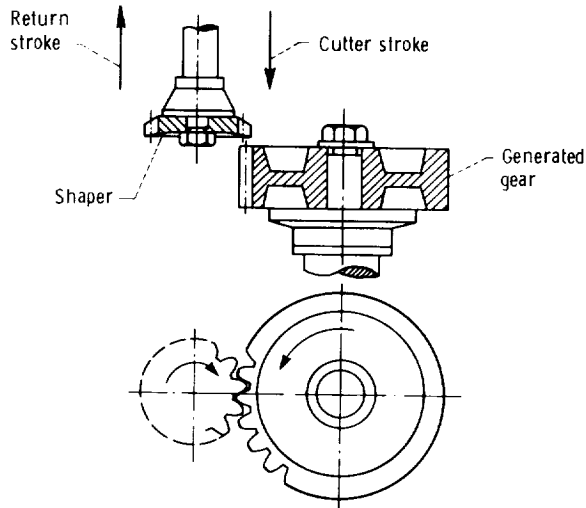


Figure 7.1.4.

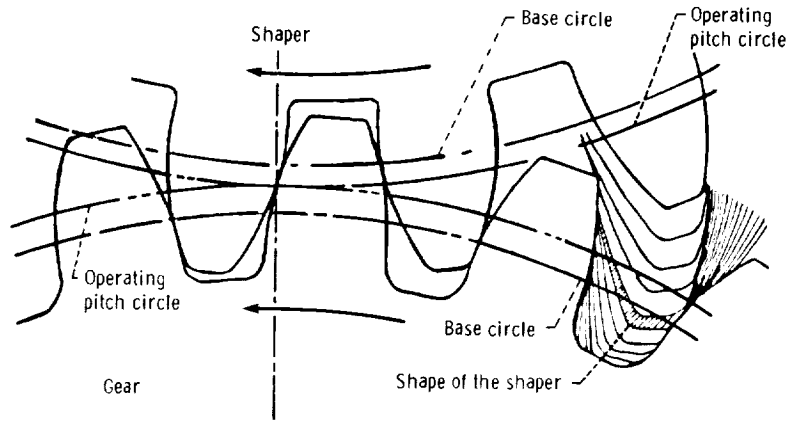


Figure 7.1.5.

Tooth generation by a shaper simulates the mesh of two gears, one of which is the shaper (fig. 7.1.4). The shape Σ_2 of the gear teeth is generated as the envelope of the locus of shaper shapes Σ_1 , which is formed in relative motion (fig. 7.1.5).

7.2 Principles of Generation of Conjugate Shapes

Consider that the centrodes of a pair of gears are determined (fig. 7.2.1). These centrodes may be provided with conjugate shapes Σ_1 and Σ_2 if the following principle of generation is applied: A tool (a rack cutter or shaper) with a shape Σ_3 is put in mesh with gears 1 and 2 which are to be generated, and the relative motion of the tool with respect to gears 1 and 2 is such that the tool has the same centrode while in mesh with each other.

The three centrodes (two gear centrodes and one tool centrode) are in continuous tangency, and the point of their tangency I is the instantaneous center of rotation. According to the General Theorem of Plane Gearing (see ch. 4.4), shapes Σ_1 , Σ_2 , and Σ_3 are conjugate because their common normal at the point of shape tangency passes through their common instantaneous center of rotation I .

The tool shape Σ_3 is an imaginary curve which generates conjugate shapes Σ_1 and Σ_2 . In practice, however, we must apply two separate rack cutters (fig. 7.2.2), which may be considered as a mold and its corresponding cast. One of these rack cutters generates gear 1 and the other generates gear 2.

The above principle may also be applied to generate gears 1 and 2 by a shaper (fig. 7.2.3). The shaper centrode is the same for both cases of meshing: the meshing of gear 1 with the shaper and

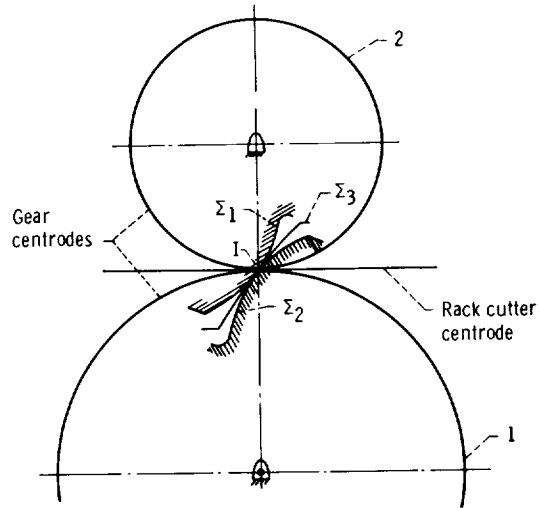


Figure 7.2.1.

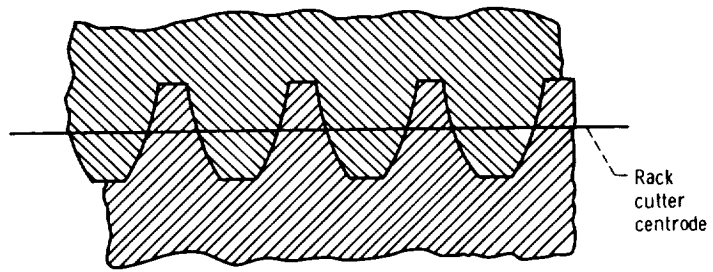


Figure 7.2.2.

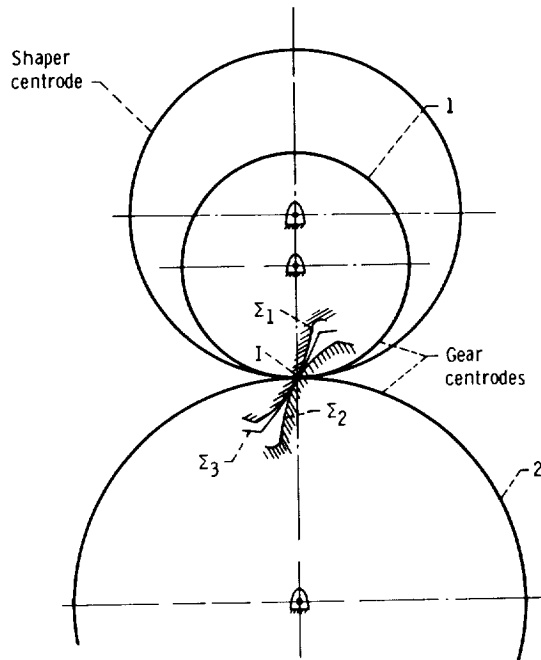


Figure 7.2.3.

the meshing of gear 2 with the shaper. Similarly, we must apply two shapers; one to generate gear 1 (the shaper and gear 1 are in internal tangency) and the other to generate gear 2 (the shaper and gear 2 are in external tangency).

It is assumed here that gears 1 and 2 transform motion with a constant angular velocity ratio, and thus the gear centrodes are circles (figs. 7.2.1 and 7.2.3). However, the principles given above may also be applied to generate gears with noncircular centrodes.

There is one important case where we may generate two gears with conjugate shapes by using only one rack cutter (shaper). This is possible for involute gears. The generation of gears with only one rack cutter allows us to interchange the gears freely.

7.3 The Camus Theorem

Consider that gear centrodes are given. An auxiliary centrode a (fig. 7.3.1) is in tangency with centrodes 1 and 2, and I is their common instantaneous center of rotation. An arbitrarily chosen point M is rigidly connected to centrode a . Point M traces out in relative motion (with respect to centrodes 1 and 2) the curves Σ_1 and Σ_2 , respectively.

Camus' theorem states that curves Σ_1 and Σ_2 may be chosen as conjugated shapes for teeth of gears 1 and 2, respectively.

To prove this theorem, let us consider an instantaneous position of centrodes 1, 2, and a . Supposing that centrode 1 is fixed and centrode a rolls over centrode 1, we say that the motion of centrode a relative to centrode 1 is rotation about point I . Assume that centrode a rotates about point I through a small angle. Then point M of centrode 3 traces out in this motion a small piece of curve Σ_1 (point M moves along Σ_1). Line MI is the normal to Σ_1 at point M . Similarly, by rotation of centrode a about I with respect to centrode 2, point M traces out a small piece of shape Σ_2 (M moves along shape Σ_2). Line MI is also the normal to shape Σ_2 at point M .

Thus, shapes Σ_1 and Σ_2 have a common point M , are in tangency at M , and their common normal MI passes through point I , the instantaneous center of rotation of centrodes 1 and 2. According to the General Theorem of Plane Gearing (see ch. 4.4), the generated shapes Σ_1 and Σ_2 are conjugate shapes.

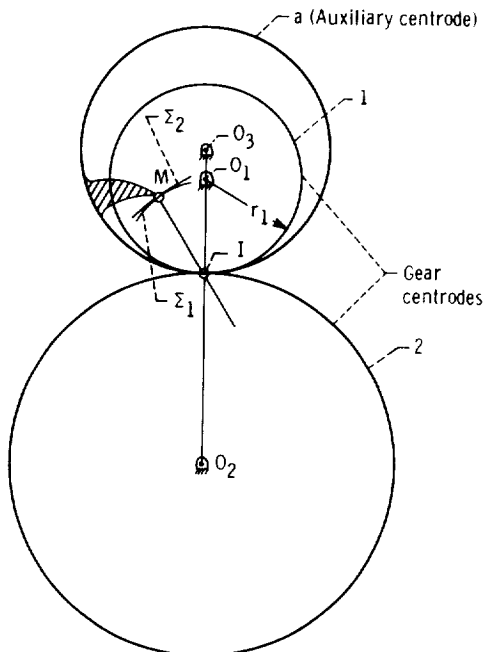


Figure 7.3.1.

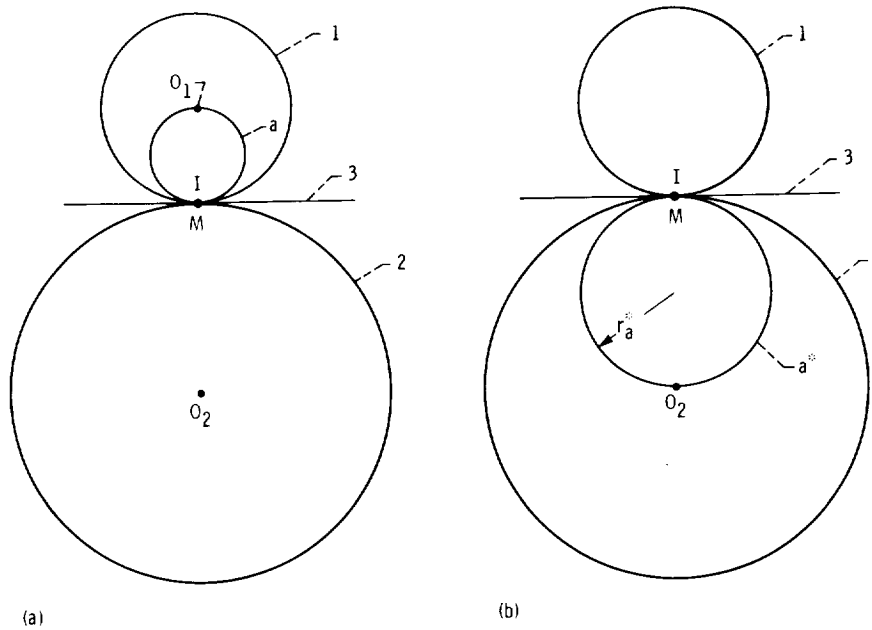


Figure 7.3.2.

By applying the Camus theorem, we may determine the shape of a rack cutter which generates gears 1 and 2. Consider a particular case where $r_a = r_1/2$, and the generating point M is located on centre a . The quantities r_a and r_1 are radii of centres a and 1. The rack cutter centre 3 is a straight line which is the tangent to centres 1, 2, and a at point I (fig. 7.3.2(a)). Let us suppose that point M coincides with I at the initial position of generation.

In coordinate systems S_1 , S_2 , and S_3 (rigidly connected to centres 1, 2, and 3) point M traces out a hypocycloid Σ_1 , epicycloid Σ_2 , and cycloid Σ_3 , respectively. With $r_a = r_1/2$, hypocycloid Σ_1 becomes a straight line directed from I to O_1 . The generated cycloid forms the addendum shape Σ_3 of the rack cutter (fig. 7.3.3). In a similar manner, the dedendum shape of the rack cutter Σ_3^* (fig. 7.3.3) and corresponding shapes Σ_1^* and Σ_2^* may be generated by rolling of centre a^* over centres 3, 1, and 2 (fig. 7.3.2(b)). With $r_a^* = r_2/2$, the generated hypocycloid Σ_2^* becomes a straight line IO_2 , directed from I to O_2 .

As mentioned earlier, the generation of conjugate shapes of gears 1 and 2, is accomplished by the application of two rack cutters (fig. 7.2.2) which supplement each other like a mold and cast. Shapes of these rack cutters are shown in figure 7.3.3. One of the rack cutters generates gear 1 and the other generates gear 2.

To generate cycloidal gears, the rack cutters may be designed by using more general considerations than assumed in this section. For instance, the generating point M may be chosen outside of the auxiliary centres.

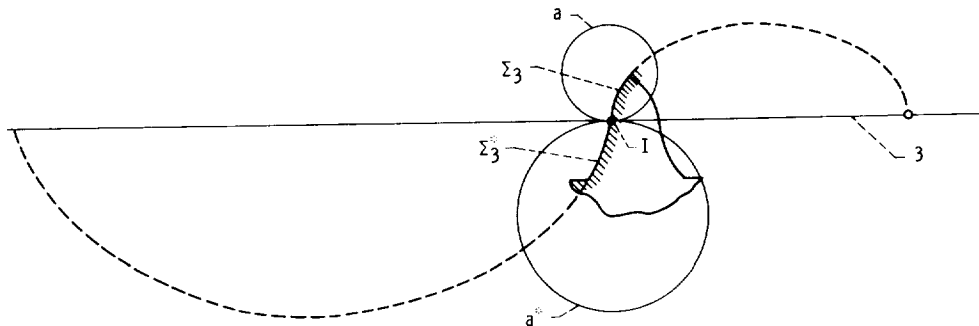


Figure 7.3.3.

7.4 Evolutes of Conjugate Shapes

Relations Between Directions of Shape Normals

Consider centrodes 1 and 2 with shapes Σ_1 and Σ_2 which are to be in mesh (fig. 7.4.1). We denote the corresponding (contacting) points of the centrodes and shapes as $I_1^{(i)}, I_2^{(i)}, I_3^{(i)}, \dots$ and $M_1^{(i)}, M_2^{(i)}, M_3^{(i)}, \dots$ ($i = 1, 2$), respectively. Due to pure rolling, the lengths of corresponding centrode arcs are equal, that is,

$$\begin{aligned} \overbrace{I_1^{(1)} I_2^{(1)}} &= \overbrace{I_1^{(2)} I_2^{(2)}} \\ \overbrace{I_2^{(1)} I_3^{(1)}} &= \overbrace{I_2^{(2)} I_3^{(2)}} \end{aligned} \quad (7.4.1)$$

The unit tangents to the centrodes and unit normals to the shapes are denoted by $\tau^{(i)}$ and $\mathbf{n}^{(i)}$, respectively. Gear rotation causes the corresponding points of centrodes $I^{(i)}$ to coincide with each other, forming the instantaneous center of rotation. The corresponding unit tangents to the centrodes, $\tau^{(1)}$ and $\tau^{(2)}$, will also coincide, making a common tangent to the centrodes at their point of tangency. At the same time, the corresponding points $M^{(1)}$ and $M^{(2)}$ and unit normals $\mathbf{n}^{(1)}$ and $\mathbf{n}^{(2)}$ of shapes Σ_1 and Σ_2 must also coincide. This is possible only if the unit normals of conjugate shapes are related by the following relations

$$\tau^{(1)} \cdot \mathbf{n}^{(1)} = \tau^{(2)} \cdot \mathbf{n}^{(2)} \quad (7.4.2)$$

$$\overline{I^{(1)} M^{(1)}} = \overline{I^{(2)} M^{(2)}} \quad (7.4.3)$$

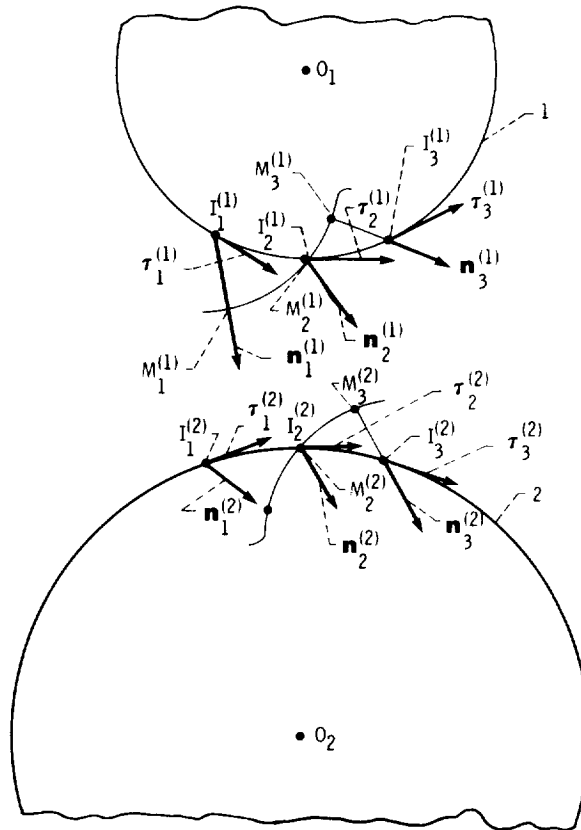


Figure 7.4.1.

Equation (7.4.2) expresses that the corresponding unit normals of conjugate shapes form equal angles with the coinciding unit tangents of the centrodes. Equation (7.4.3) expresses that corresponding segments of shape normals (measured from centrode point I to shape point M along the shape normal) must be equal. Methods of generation of conjugate shapes must satisfy requirements (7.4.2) and (7.4.3).

The orientation of the shape unit normals with respect to the centrodes depends on the methods of generation. Let us consider some typical examples. By generation of noncircular gears (fig. 7.4.2), the centrode of the rack cutter is a straight line which rolls over the centrode of the noncircular gear. The shapes of the rack cutter are straight lines which form an angle of $2\psi_c$. The tangent to the gear centrode τ and the normal to the left-sided shapes \mathbf{n}_l form the angle ψ_c ; accordingly, τ and the normal to the right-sided shapes \mathbf{n}_r form the angle $\pi - \psi_c$.

Consider figure 7.4.2. Position vector \mathbf{r} is drawn from the center of gear rotation to the point of tangency of the gear and rack centrodes, μ is the angle formed by \mathbf{r} and the centrode tangent τ , and λ is the angle formed by \mathbf{r} and the shape normal \mathbf{n} . The orientation of shape normals \mathbf{n} is represented by the following equations:

(1) Left-sided shapes.

$$\lambda_l = \mu + \psi_c \quad (7.4.4)$$

(2) Right-sided shapes.

$$\lambda_r = \pi + \mu - \psi_c \quad (7.4.5)$$

The angle λ is measured in the same direction as μ . When a circular gear is generated (fig. 7.4.3), the angle μ is 90° and λ_l and λ_r are constant angles represented as

$$\lambda_l = \frac{\pi}{2} + \psi_c \quad (7.4.6)$$

$$\lambda_r = \frac{3\pi}{2} - \psi_c \quad (7.4.7)$$

A noncircular gear may be generated by a rack cutter whose centrode is in tangency with the gear centrode at points on line On (fig. 7.4.4). This line is drawn from the gear center of rotation O perpendicular to the direction of rack cutter displacement s . (See section 2.1.) Here the orientation of shape normals is also represented by equations (7.4.6) and (7.4.7).

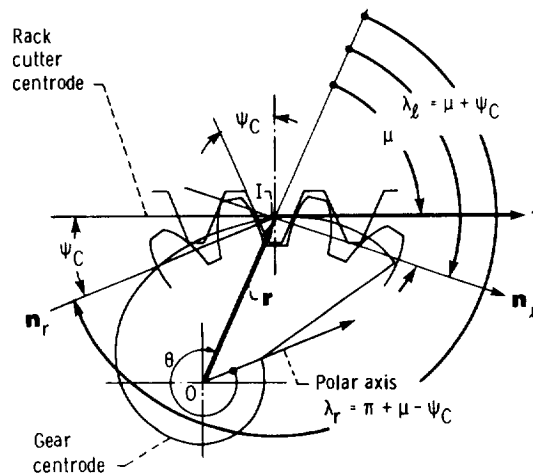


Figure 7.4.2.

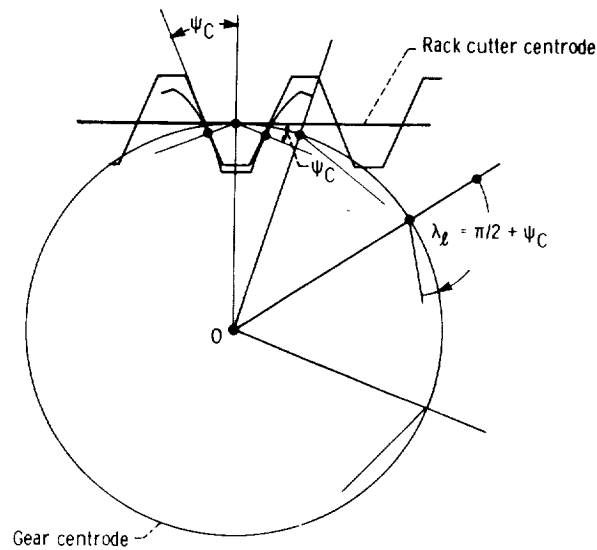


Figure 7.4.3.

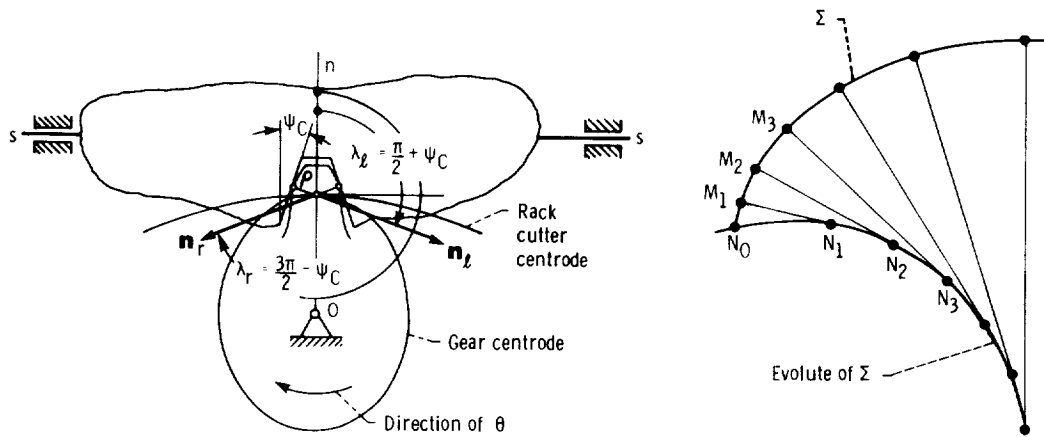


Figure 7.4.4.

Figure 7.4.5.

Shape Evolutes

Let a curve Σ be given (fig. 7.4.5) with $M_i N_i$ as a locus of radii of curvature of this curve. The locus of curvature centers $N_i (i = 0, 1, 2, \dots)$ is called the evolute of Σ . The evolute of the given curve Σ may be determined as the envelope of the locus of normals to the curve Σ .

Consider that a gear centrede is given by the equation

$$\mathbf{r}(\theta) = r(\theta) \sin \theta \mathbf{i} + r(\theta) \cos \theta \mathbf{j} \quad (7.4.8)$$

where $r(\theta)$ represents the magnitude of the position vector as a function of the polar angle θ (fig. 7.4.6(a)). The orientation of shape normals is represented by the function $\lambda(\theta) \in C^1$, where λ is the angle made by vectors \mathbf{r} and \mathbf{n} .

The locus of normals \mathbf{n} may be represented by the equations

$$\mathbf{r}_e = \mathbf{r} + \ell = [r(\theta) \sin \theta + \ell \sin(\theta + \lambda)] \mathbf{i} + [r(\theta) \cos \theta + \ell \cos(\theta + \lambda)] \mathbf{j} \quad (7.4.9)$$

Here ℓ is the parameter which represents the location of a point N on the normal (fig. 7.4.6). Equation (7.4.9) represents a locus of straight lines IN . The envelope of the locus of straight lines IN represents

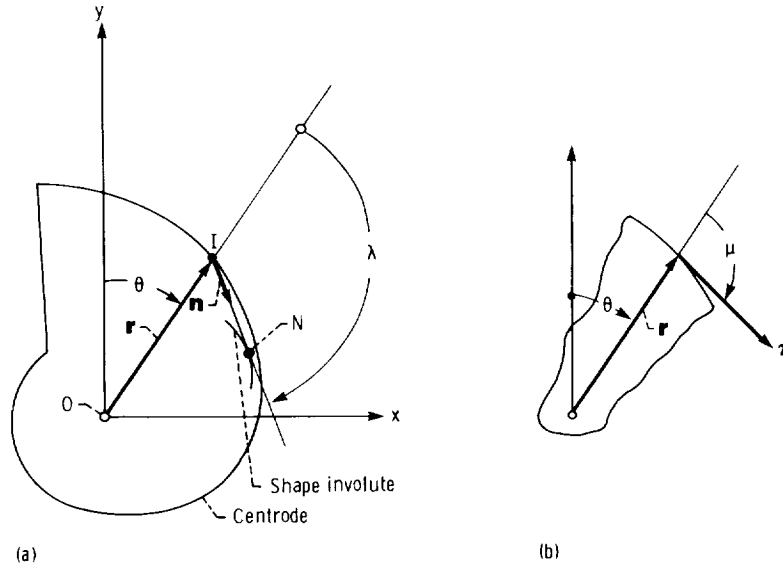


Figure 7.4.6.

the evolute of the shape whose normal orientation is given by function $\lambda(\theta) \in C^1$.

The displacement of a point of the normal may be determined by

$$d\mathbf{r}_e = dx_e \mathbf{i} + dy_e \mathbf{j} \quad (7.4.10)$$

Here

$$dx_e = r \cos \theta d\theta + dr \sin \theta + \ell \cos (\theta + \lambda)(d\theta + d\lambda) + d\ell \sin (\theta + \lambda) \quad (7.4.11)$$

$$dy_e = -r \sin \theta d\theta + dr \cos \theta - \ell \sin (\theta + \lambda)(d\theta + d\lambda) + d\ell \cos (\theta + \lambda) \quad (7.4.12)$$

At the point of tangency of the normal IN and the envelope (point N , fig. 7.4.6) the displacement of the normal point $d\mathbf{r}_e$ must be collinear to the envelope tangent τ . Taking into account that the envelope tangent coincides with the normal IN , we may state that $d\mathbf{r}_e$ must be collinear to the normal IN . Thus,

$$\frac{dx_e}{dy_e} = \frac{n_x}{n_y} = \frac{\sin (\theta + \lambda)}{\cos (\theta + \lambda)} \quad (7.4.13)$$

Equations (7.4.11) to (7.4.13) yield

$$r \cos \lambda - \frac{dr}{d\theta} \sin \lambda + \ell \left(1 + \frac{d\lambda}{d\theta} \right) = 0 \quad (7.4.14)$$

The position vector \mathbf{r} and the tangent τ to the centrode form the angle μ determined by (fig. 7.4.6(b))

$$\tan \mu = \frac{r}{\frac{dr}{d\theta}} \quad (7.4.15)$$

Substituting $\frac{dr}{d\theta}$ with $r \cot \mu$, we get

$$\ell = \frac{r \sin (\lambda - \mu)}{\sin \mu \left(1 + \frac{d\lambda}{d\theta} \right)} \quad (7.4.16)$$

Equation (7.4.16) represents the function $\ell(\theta)$, where ℓ is the radius of curvature of the shape at the point where it intersects the centrode. Equations (7.4.9) and (7.4.16) considered together represent the shape evolute.

Equation (7.4.16) may be expressed in terms of centrode curvature. The radius of curvature ρ of a curve is represented by

$$\rho = \frac{ds}{d\alpha} \quad (7.4.17)$$

Here $ds = I I^*$ is the infinitesimal arc length between two neighboring points I and I^* on the centrode (fig. 7.4.7), and $d\alpha$ is the infinitesimal angle between the unit tangent vectors τ and τ^* drawn at points I and I^* .

The tangent τ forms the angle $\mu + \theta$ with the polar axis, and

$$d\alpha = d\theta + d\mu \quad (7.4.18)$$

The arc length is

$$ds = \sqrt{(IE)^2 + (EI^*)^2} = \sqrt{(rd\theta)^2 + (dr)^2} = d\theta \sqrt{r^2 + \left(\frac{dr}{d\theta} \right)^2} \quad (7.4.19)$$

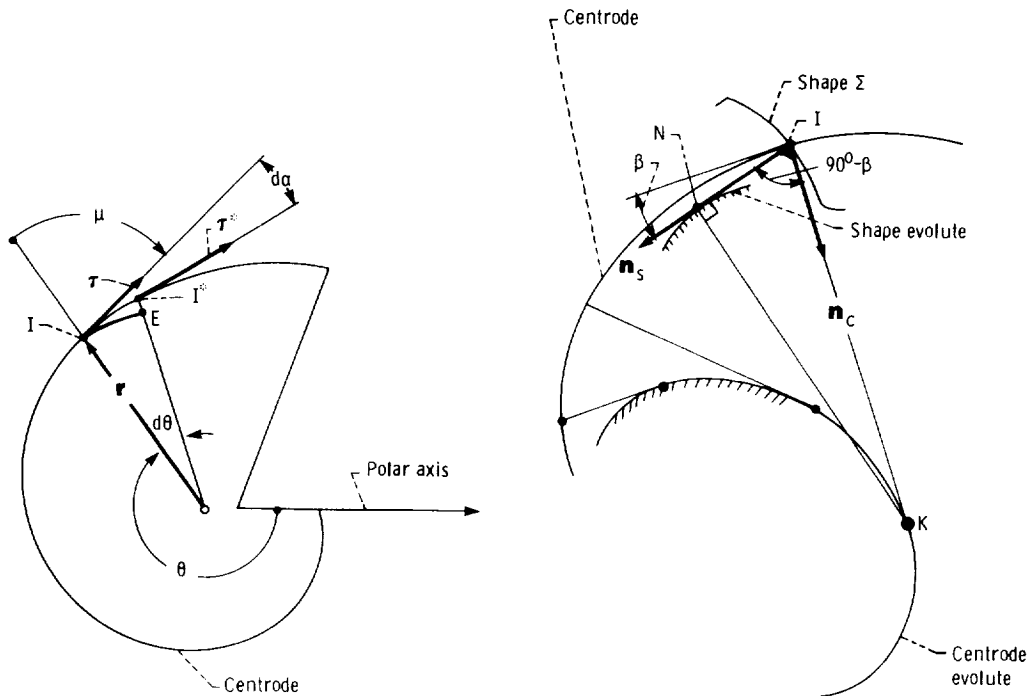


Figure 7.4.7.

Figure 7.4.8.

centrode normal \mathbf{n}_c make a constant angle of $90^\circ - \beta$. It is necessary to determine point N of tangency of the shape normal with the shape evolute. Let us prove that point N , the point of tangency of the shape normal \mathbf{n}_s and the shape evolute, is the point of intersection of \mathbf{n}_s and line KN . Line KN is drawn from point K and is perpendicular to \mathbf{n}_s .

This statement is based on the following suggestions:

(1) Point K is the instantaneous center of rotation of straight line IK which rolls over the centrode evolute.

(2) The velocity of any point N rigidly connected to IK is perpendicular to the radius of rotation KN .

(3) If point N is the point of tangency of the shape normal \mathbf{n}_s and the shape evolute, then the velocity of such a point, \mathbf{v}_N , must be directed along the tangent to the shape evolute. This requirement is observed if line KN is perpendicular to line IN .

It is verifiable that

$$IN = IK \sin \beta$$

Taking into account that the centrode radius of curvature $IK = \rho$, $IN = \ell$, and $\beta = \lambda - \mu$, we get equation (7.4.24).

Example problem 7.4.1 The centrode is a circle of radius r is given by the following equations (fig. 7.4.9):

$$x = r \sin \theta \quad y = r \cos \theta \quad (7.4.25)$$

The orientation of shape normals is represented by equations (7.4.6) and (7.4.7). Determine the evolute for left-sided and right-sided shapes.

Solution.

Step 1.—Determine ℓ for the left-sided and right-sided shapes by using equations (7.4.6), (7.4.7), (7.4.15), (7.4.16), and (7.4.25).

$$\ell_l = \ell_r = \frac{r \sin(\lambda - \mu)}{\sin \mu \left(1 + \frac{d\lambda}{d\theta}\right)} = r \sin \psi_c \quad (7.4.26)$$

Step 2.—Determine the evolute of shapes Σ_l and Σ_r (fig. 7.4.9) by using equations (7.4.9), (7.4.6), (7.4.7), and (7.4.26).

(a) Left-sided shapes Σ_l

$$x_e = r \cos \psi_c \sin(\theta + \psi_c) \quad y_e = r \cos \psi_c \cos(\theta + \psi_c) \quad (7.4.27)$$

(b) Right-sided shapes Σ_r

$$x_e = r \cos \psi_c \sin(\theta - \psi_c) \quad y_e = r \cos \psi_c \cos(\theta - \psi_c) \quad (7.4.28)$$

The evolute of shapes Σ_l and Σ_r is the circle of radius $\rho = r \cos \psi_c$ centered at the same point O as the centrode.

Example problem 7.4.2 Consider that the displacement s of the rack cutter and the rotation angle ϕ of the gear are related by the function

$$s = \frac{N}{2P} \phi + a \sin \phi \quad (7.4.29)$$

Here N is the gear tooth number and P is the diametral pitch. Usually $a = 0$ and function (7.4.29) is linear. The additional term $a \sin \phi$ is induced by kinematical errors in the gearing which relates the motions of the tool (rack cutter or hob) and the generated gear.

By applying methods presented in chapter 2, we may find that the gear centrode is represented by the equations

$$x = r \sin \theta = \left(\frac{N}{2P} + a \cos \theta \right) \sin \theta \quad y = r \cos \theta = \left(\frac{N}{2P} + a \cos \theta \right) \cos \theta \quad (7.4.30)$$

Here $r = ds/d\phi$ and $\phi = \theta$. (See ch. 2.1.) The orientation of shape normals is given by equations (7.4.6) and (7.4.7). Determine the equations of the evolutes of the gear tooth shapes.

Solution.

Step 1.—Determine ℓ for left-sided and right-sided shapes by using equations (7.4.6), (7.4.7), (7.4.15), (7.4.16), and (7.4.30).

$$\tan \mu = \frac{r}{\frac{dr}{d\theta}} = - \frac{\frac{N}{2P} + a \cos \theta}{a \sin \theta} \quad (7.4.31)$$

(a) Left-sided shapes

$$\begin{aligned} \ell_t &= r \frac{\sin(\lambda - \mu)}{\sin \mu \left(1 + \frac{d\lambda}{d\theta} \right)} = r \frac{\sin \lambda}{\tan \mu} - r \cos \lambda = \frac{dr}{d\theta} \sin \lambda - r \cos \lambda \\ &= -a \sin \theta \sin \lambda - r \cos \lambda = \left(\frac{N}{2P} + a \cos \theta \right) \sin \psi_c - a \sin \theta \cos \psi_c \end{aligned} \quad (7.4.32)$$

(b) Right-sided shapes

$$\ell_r = \left(\frac{N}{2P} + a \cos \theta \right) \sin \psi_c + a \sin \theta \cos \psi_c \quad (7.4.33)$$

Step 2.—Determine the evolutes of shapes by using equations (7.4.9), (7.4.6), (7.4.7), (7.4.32), and (7.4.33).

(a) Left-sided shapes

$$\begin{aligned} x_e &= r \sin \theta + \ell_t \sin(\theta + \lambda) \\ &= r \sin \theta + (r \sin \psi_c - a \sin \theta \cos \psi_c) \sin \left(\frac{\pi}{2} + \psi_c + \theta \right) \\ &= \frac{N}{2P} \cos \psi_c \sin(\theta + \psi_c) + a \cos \psi_c \sin \psi_c \end{aligned} \quad (7.4.34)$$

$$y_e = r \cos \theta + \ell_t \cos(\theta + \lambda) = \frac{N}{2P} \cos \psi_c \cos(\theta + \psi_c) + a \cos^2 \psi_c \quad (7.4.35)$$

Equations (7.4.34) and (7.4.35) represent a circle of radius

$$\rho_l = \frac{N}{2P} \cos \psi_c$$

centered at point O_l (fig. 7.4.10(a)). Vector $\overline{OO_l}$ and the y_e -axis make an angle ψ_c measured clockwise from the y_e -axis and $|\overline{OO_l}| = a \cos \psi_c$. The evolute of left-sided shapes may be represented in coordinate system S_l by the following matrix equation:

$$[r_l] = [M_{le}][r_e] \quad (7.4.36)$$

Here

$$[r_l] = \begin{bmatrix} x_l \\ y_l \\ 1 \end{bmatrix} \quad [M_{le}] = \begin{bmatrix} \cos \psi_c & -\sin \psi_c & 0 \\ \sin \psi_c & \cos \psi_c & -a \cos \psi_c \\ 0 & 0 & 1 \end{bmatrix} \quad [r_e] = \begin{bmatrix} x_e \\ y_e \\ 1 \end{bmatrix} \quad (7.4.37)$$

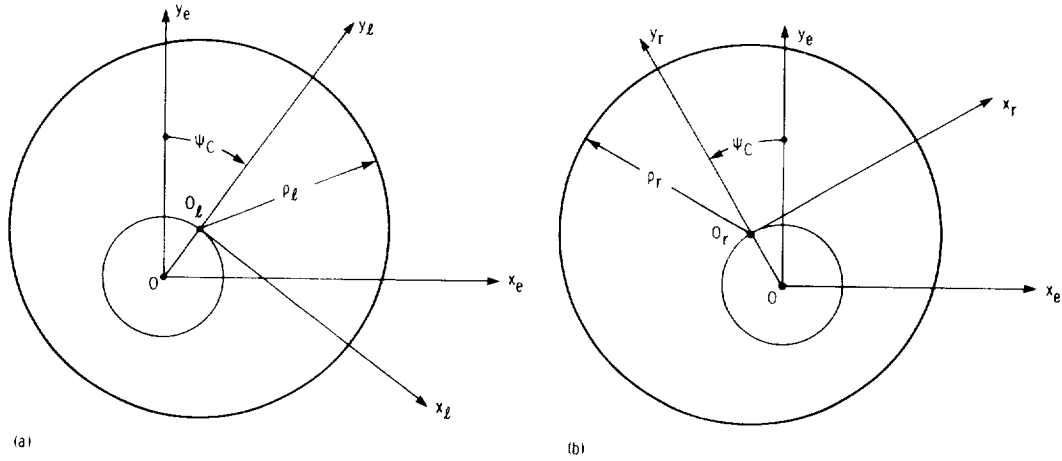


Figure 7.4.10.

Coordinates (x_e, y_e) are given by equations (7.4.34) and (7.4.35). Equations (7.4.34) to (7.4.37) yield

$$x_l = \frac{N}{2P} \cos \psi_c \sin \theta \quad y_l = \frac{N}{2P} \cos \psi_c \cos \theta \quad (7.4.38)$$

(b) Right-sided shapes

$$\begin{aligned} x_e &= r \sin \theta + \ell \sin (\theta + \lambda) \\ &= r \sin \theta + (r \sin \psi_c + a \sin \theta \cos \psi_c) \sin \left(\theta + \frac{3\pi}{2} - \psi_c \right) \\ &= \frac{N}{2P} \cos \psi_c \sin (\theta - \psi_c) - a \cos \psi_c \sin \psi_c \end{aligned} \quad (7.4.39)$$

$$y_e = r \cos \theta + l_r \sin (\theta + \lambda) = \frac{N}{2P} \cos \psi_c \cos (\theta - \psi_c) + a \cos^2 \psi_c \quad (7.4.40)$$

To represent evolute equations in coordinate system S_r (fig. 7.4.10(b)), we use the following matrix equation:

$$[r_r] = [M_{re}][r_e] \quad (7.4.41)$$

where

$$[M_{re}] = \begin{bmatrix} \cos \psi_c & \sin \psi_c & 0 \\ -\sin \psi_c & \cos \psi_c & -a \cos \psi_c \\ 0 & 0 & 1 \end{bmatrix} \quad (7.4.42)$$

Equations (7.4.31) to (7.4.34) yield

$$x_r = \frac{N}{2P} \cos \psi_c \sin \theta \quad y_r = \frac{N}{2P} \cos \psi_c \cos \theta \quad (7.4.43)$$

Equations (7.4.43) represent the evolute of right-sided shapes as a circle of radius $\rho_r = \frac{N}{2P} \cos \psi_c$ centered at point O_r .

Summarizing our results we may state the following:

- (1) The generation of spur gears by a rack cutter (a hob) with the function of displacements $s(r)$ represented as the sum of a linear function and harmonic function of the first order (see eq. (7.4.29)) results in the existence of two different evolutes for the left-sided and right-sided shapes of teeth of the generated gear.
- (2) The evolutes are circles whose centers are offset from the center of gear rotation (fig. 7.4.11). This location of evolutes is equivalent to an error of eccentricity for the tooth shapes.
- (3) Although gear teeth have different tooth thicknesses (fig. 7.4.11), these eccentricity errors cannot be discovered by measuring the distance between a rack tooth and the center of rotation of the gear.

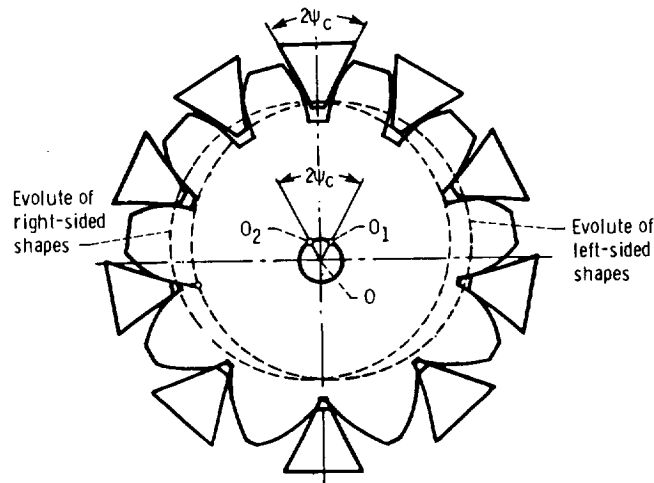


Figure 7.4.11.

Problem 7.4.1 Consider that the gear centrode is an ellipse (fig. 7.4.12). Usually the center of gear rotation is one of the ellipse foci, but we locate the origin of the applied coordinate system at the symmetry center O and represent the centrode equations by

$$x = a \sin \theta \quad y = b \cos \theta \quad (7.4.44)$$

The unit tangent τ to the ellipse forms an angle γ with the y -axis and is represented by the following equations (see ch. 3.2)

$$\tau_x = \sin \gamma = \frac{a \cos \theta}{(a^2 \cos^2 \theta + b^2 \sin^2 \theta)^{1/2}} \quad (7.4.45)$$

$$\tau_y = \cos \gamma = -\frac{b \sin \theta}{(a^2 \cos^2 \theta + b^2 \sin^2 \theta)^{1/2}} \quad (7.4.46)$$

The unit normal to the ellipse \mathbf{n} is (see ch. 3.2)

$$n_x = \tau_y \quad n_y = -\tau_x \quad (7.4.47)$$

The radius of curvature of the ellipse $\rho = MK$ is (see ch. 3.3)

$$\rho = -\frac{dx}{dn_x} = -\frac{dy}{dn_y} = \frac{(a^2 \cos^2 \theta + b^2 \sin^2 \theta)^{3/2}}{ab} \quad (7.4.48)$$

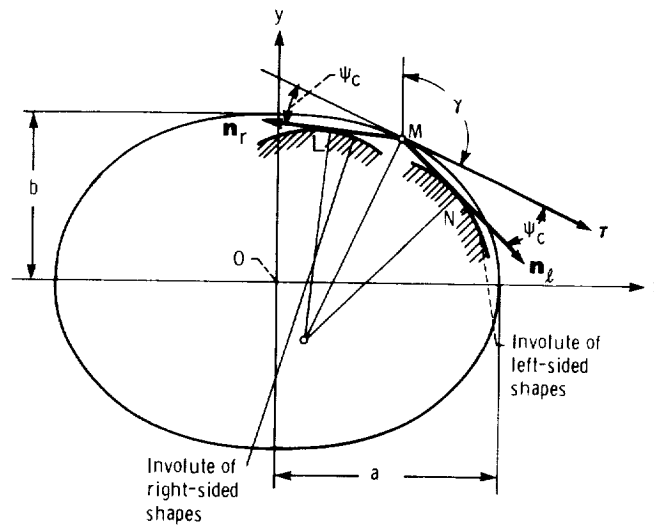


Figure 7.4.12.

Normals \mathbf{n}_l to the left-sided shapes make the angle $(\gamma + \psi_c)$ with the y -axis. Normals to the right-sided shapes make the angle $(\gamma + \pi - \psi_c)$ with the y -axis. Determine equations of shape evolutes by using equations (7.4.9) and (7.4.24).

Answer.

$$x_e = a \sin \theta \pm \frac{a^2 \cos^2 \theta + b^2 \sin^2 \theta}{ab} \sin \psi_c (a \cos \theta \cos \psi_c \mp b \sin \theta \sin \psi_c)$$

$$y_e = b \cos \theta - \frac{a^2 \cos^2 \theta + b^2 \sin^2 \theta}{ab} \sin \psi_c (a \cos \theta \sin \psi_c \pm b \sin \theta \cos \psi_c)$$

The upper sign corresponds to the evolute of left-sided shapes.

Chapter 8

Surfaces

8.1 Surfaces: Definitions and Representations

Like the concept of a plane curve used in the Theory of Plane Gearing, we need the concept of a surface based on strict definitions proposed in the field of differential geometry. (See the books by Zalgaller 1975, Lipshutz 1969, Goetz 1970, and other authors.)

A parametric representation of a surface Σ is a continuous mapping of an open rectangle G , given in the plane P of parameters (u, θ) , onto a three-dimensional space R^3 such that

$$\mathbf{r}(u, \theta) \in C^0 \quad a < u < b \quad c < \theta < d \quad (8.1.1)$$

Here \mathbf{r} is the position vector which determines the point surface (fig. 8.1.1). The vector function $\mathbf{r}(u, \theta)$ may be represented by

$$\mathbf{r}(u, \theta) = f(u, \theta)\mathbf{i} + g(u, \theta)\mathbf{j} + s(u, \theta)\mathbf{k} \quad (8.1.2)$$

where \mathbf{i} , \mathbf{j} , and \mathbf{k} are unit vectors of the coordinate axes.

Expression (8.1.1) sets the correspondence between points of plane P and surface Σ such that only a single point $\mathbf{r}(u, \theta)$ corresponds to the given point (u, θ) . One-to-one correspondence is not guaranteed; it may happen that the given point $\mathbf{r}(u, \theta)$ corresponds to more than one point of the plane P . For instance, the mapping

$$\mathbf{r} = r_b[(\sin \theta - \theta \cos \theta)\mathbf{i} + (\cos \theta + \theta \sin \theta)\mathbf{j}] + u\mathbf{k} \quad (8.1.3)$$

where $-\infty < \theta < \infty$ and $a < u < b$ represents a cylindrical involute surface of two branches, I and II (fig. 8.1.2). Lines of self intersection L of this surface belong to the plane $x = 0$ and may be determined by equation (8.1.3) and the equation

$$\theta - \tan \theta = 0 \quad (8.1.4)$$

Consequently, any point M of the surface line L is determined by a single value of u and two different values of θ : θ_1 and θ_2 (θ_1 and θ_2 have the same absolute value but they are of opposite signs).

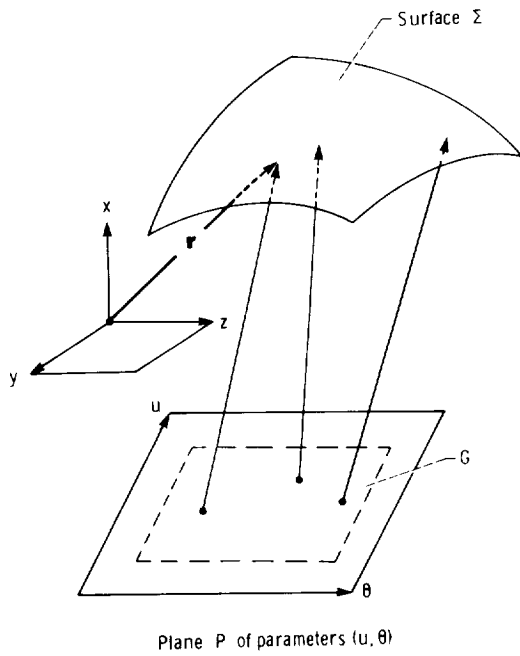


Figure 8.1.1.

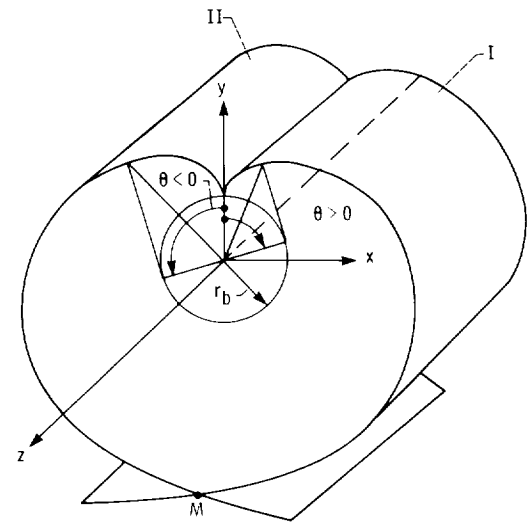


Figure 8.1.2.

A simple surface is a continuous mapping (8.1.1) with a one-to-one correspondence between points of plane P (of parameters (u, θ)) and points of the three-dimensional space R^3 . In some cases the mapping (8.1.1) may represent a simple surface just by the limitation $(u, \theta) \in G$. For instance, if we limit parameter θ by

$$0 < \theta < \infty \quad (\text{or } -\infty < \theta < 0)$$

mapping (8.1.3) will generate a simple surface; only one branch of the pair I and II (fig. 8.1.2) is formed. If mapping (8.1.1) is continuous and of one-to-one correspondence in the neighborhood of the set of parameters $(x_0, y_0, z_0, u_0, \theta_0)$, we say that it represents a locally simple surface.

A surface in parametric representation is called regular if the requirements

$$\mathbf{r}(u, \theta) \in C^1 \quad \mathbf{r}_u \times \mathbf{r}_\theta \neq 0 \quad a < u < b \quad c < \theta < d \quad (8.1.5)$$

are observed throughout the mapping from the plane of parameters (u, θ) onto the three-dimensional space. Here

$$\mathbf{r}_u = \frac{\partial \mathbf{r}}{\partial u} \quad \mathbf{r}_\theta = \frac{\partial \mathbf{r}}{\partial \theta}$$

A regular surface has a tangent plane at all its points. (See sec. 8.3.)

Theorem A surface is regular locally if requirements given in equation (8.1.5) are observed in the neighborhood of a point $M(x_0, y_0, z_0, u_0, \theta_0)$. It may be proven that such a surface is a simple one in the neighborhood of point M .

Proof: The inequality

$$\mathbf{r}_u \times \mathbf{r}_\theta \neq 0 \quad (8.1.6)$$

may be represented by

$$\begin{vmatrix} \mathbf{i} & \mathbf{j} & \mathbf{k} \\ x_u & y_u & z_u \\ x_\theta & y_\theta & z_\theta \end{vmatrix} = \begin{vmatrix} y_u & z_u \\ y_\theta & z_\theta \end{vmatrix} \mathbf{i} + \begin{vmatrix} z_u & x_u \\ z_\theta & x_\theta \end{vmatrix} \mathbf{j} + \begin{vmatrix} x_u & y_u \\ x_\theta & y_\theta \end{vmatrix} \mathbf{k} \neq 0 \quad (8.1.7)$$

The inequality (8.1.7) is observed if at least one of the three determinants of the second order is not equal to zero. Taking into account the designations applied in equation (8.1.2), we say that inequality (8.1.7) is observed if at least one of the following determinants is not equal to zero:

$$\begin{vmatrix} g_u & s_u \\ g_\theta & s_\theta \end{vmatrix} \quad \begin{vmatrix} s_u & f_u \\ s_\theta & f_\theta \end{vmatrix} \quad \begin{vmatrix} f_u & g_u \\ f_\theta & g_\theta \end{vmatrix} \quad (8.1.8)$$

Let us suppose that just the determinant

$$\begin{vmatrix} f_u & g_u \\ f_\theta & g_\theta \end{vmatrix} \quad (8.1.9)$$

is not equal to zero. Consider a system of three equations

$$\begin{aligned} F_1(u, \theta, x, y, z) &= f(u, \theta) - x = 0 & F_2(u, \theta, x, y, z) &= g(u, \theta) - y = 0 \\ F_3(u, \theta, x, y, z) &= s(u, \theta) - z = 0 \end{aligned} \quad (8.1.10)$$

which are satisfied at the point

$$M(u_0, \theta_0, x_0, y_0, z_0) \quad (8.1.11)$$

According to the Theorem of Implicit Function System Existence (app. B), equations (8.1.10) may be solved in the neighborhood of point (8.1.11) by the functions

$$\{u(x, y), \theta(x, y), z(x, y)\} \in C^1 \quad (8.1.12)$$

if the Jacobian

$$\frac{D(F_1, F_2, F_3)}{D(u, \theta, z)} = \begin{vmatrix} f_u & g_u & s_u \\ f_\theta & g_\theta & s_\theta \\ 0 & 0 & -1 \end{vmatrix} \neq 0 \quad (8.1.13)$$

The inequality (8.1.13) is equivalent to the inequality (8.1.9); therefore, if inequality (8.1.9) is observed, functions (8.1.12) indeed exist. Consequently, a definite point (u, θ) on the plane of parameters (u, θ) is determined if the point (x, y, z) in the three-dimensional space R^3 is given. Thus, the mapping (8.1.5) is of one-to-one correspondence in the neighborhood of point M , and this mapping represents a simple curve.

The existence of function

$$z(x, y) \in C^1 \quad (8.1.14)$$

shows that a regular surface may be represented in the neighborhood of M by this function.

For certain reasons, other parameters— ϕ and ψ —are to be applied for the surface parametric representation. Two parametric representations

$$\mathbf{r}(u, \theta) \in C^1 \quad (u, \theta) \in G$$

and

$$\mathbf{R}(\phi, \psi) \in C^1 \quad (\phi, \psi) \in Q$$

represent the same regular surface if the following requirements are observed:

$$\mathbf{R}(\phi, \psi) = \mathbf{r}[u(\phi, \psi), \theta(\phi, \psi)] \quad \{u(\phi, \psi), \theta(\phi, \psi)\} \in C^1$$

$$\frac{D(u, \theta)}{D(\phi, \psi)} = \begin{vmatrix} \frac{\partial u}{\partial \phi} & \frac{\partial u}{\partial \psi} \\ \frac{\partial \theta}{\partial \phi} & \frac{\partial \theta}{\partial \psi} \end{vmatrix} \neq 0 \quad (8.1.15)$$

There is another form of surface representation known as the implicit equation of the surface. Equation

$$F(x, y, z) = 0 \quad (8.1.16)$$

generally represents a set of points in three-dimensional space. To represent a surface, equation (8.1.16) must be supplemented with additional requirements as follows:

$$F \in C^1 \quad |F_x| + |F_y| + |F_z| \neq 0 \quad (8.1.17)$$

Equation (8.1.16), with requirements (8.1.17), represents a locally simple and regular surface in the neighborhood of point

$$M_0(x_0, y_0, z_0) \quad (8.1.18)$$

This statement may be proven with the Theorem of Implicit Function System Existence. Assume that inequality (8.1.16) is observed because $F_z \neq 0$. Then equation (8.1.16) may be solved in the neighborhood of point (8.1.18) by the function

$$z(x, y) \in C^1$$

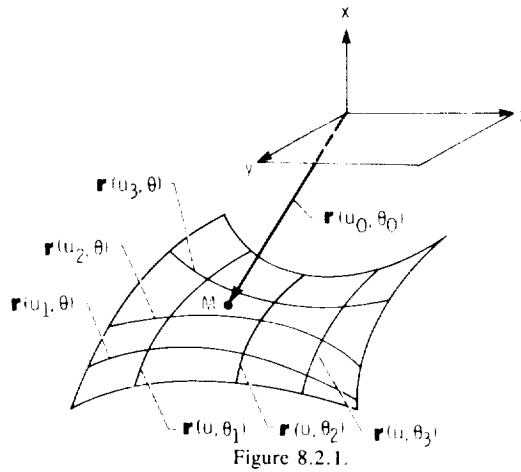
This function represents a simple and regular surface.

8.2. Curvilinear Coordinates

Considering the parametric representation

$$\mathbf{r}(u, \theta) = x(u, \theta)\mathbf{i} + y(u, \theta)\mathbf{j} + z(u, \theta)\mathbf{k} \quad \mathbf{r}(u, \theta) \in C^0 \quad (8.2.1)$$

where $a < u < b$ and $c < \theta < d$, we say that with given values of (u_0, θ_0) , the position vector $\mathbf{r}(u_0, \theta_0)$ determines the surface point M (fig. 8.2.1). Thus, parameters (u, θ) are called curvilinear coordinates (Gaussian coordinates) on the surface.



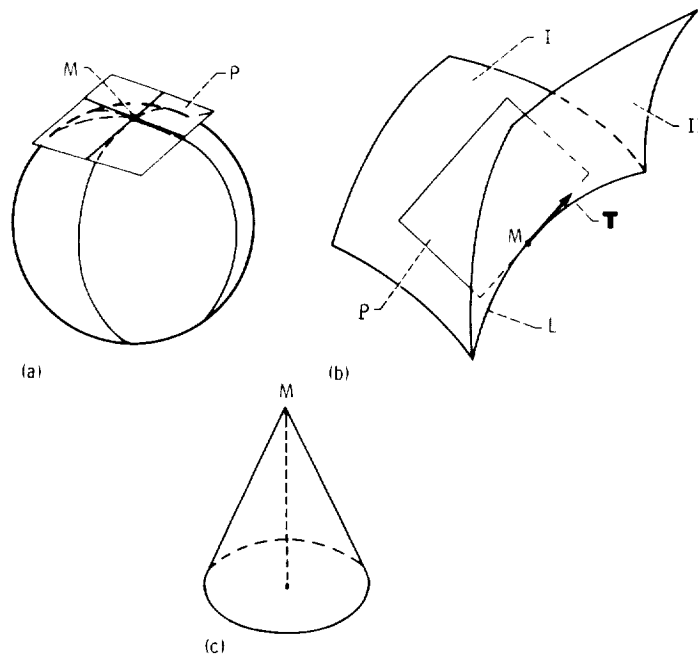
Fixing the value of one parameter (assume $u = u_0$) and varying the other parameter θ , we may determine, by $\mathbf{r}(u_0, \theta)$, the coordinate line of θ (the θ line) on the surface (fig. 8.2.1). Similarly, by setting $\theta = \theta_0$, we may determine, by $\mathbf{r}(u, \theta_0)$, the u -line on the surface. Thus, the surface is covered with u -lines and θ -lines, as shown in figure 8.2.1.

8.3 Tangent Plane and Normal Vector to a Surface

Consider a surface-fixed point M_0 , determined by $\mathbf{r}(u_0, \theta_0)$, and a neighboring point M

$$\mathbf{r}(u, \theta) = \mathbf{r}(u_0 + \Delta u, \theta_0 + \Delta\theta)$$

of a varied location. Draw a ray A from point M_0 to point M . The direction of this ray depends on the ratio $\Delta u / \Delta\theta$. The position of the ray when point M approaches M_0 (when (u, θ) approaches (u_0, θ_0)) is called the limiting position. With M approaching M_0 , we may find a set of limiting rays



by changing the ratio $\Delta u/\Delta\theta$. We say that a surface has a tangent plane at M_0 if the set of limiting rays fills in a plane.

Figure 8.3.1 shows three types of sets of limiting rays. In the first case, the set of limiting rays fills in a plane P (fig. 8.3.1(a)). In the second case, two surface branches I and II are connected by the so-called edge of regression, labeled L . The set of limiting rays corresponding to point M of the line L fills in only a half-plane which is limited by the tangent T drawn to L at point M (fig. 8.3.1(b)). In the third case, point M is the cone apex (fig. 8.3.1(c)), and the set of limiting rays fills in the cone surface; the tangent plane does not exist.

A surface point at which the tangent plane exists is called a regular point. A surface point at which the tangent plane does not exist is called a singular point. There are different types of surface singular points. A surface may have one singular point (fig. 8.3.1(c)) or several separated singular points. Also, singular points may form a line (the edge of regression) that connects two branches of a surface (fig. 8.3.1(b)).

The tangent plane P to a surface (if such a plane exists) is determined by the pair of vectors \mathbf{r}_u and \mathbf{r}_θ , which are tangents to the u -line and θ -line, respectively (fig. 8.3.2). The tangent plane P at the surface point $\mathbf{r}(u_0, \theta_0)$ is represented by the equation

$$[\mathbf{A}\mathbf{r}_u\mathbf{r}_\theta] = 0 \quad (8.3.1)$$

where

$$\mathbf{A} = \mathbf{R} - \mathbf{r}(u_0, \theta_0) = \overline{MM^*}$$

Position vector $\mathbf{r}(u_0, \theta_0)$ represents the surface given point M (fig. 8.3.2). Position vector \mathbf{R} , which is drawn from the same origin O as $\mathbf{r}(u, \theta)$, represents an arbitrary point M^* of the tangent plane P . Equation (8.3.1) yields that vector \mathbf{A} belongs to the plane P drawn through vectors $\mathbf{r}_u(u_0, \theta_0)$ and $\mathbf{r}_\theta(u_0, \theta_0)$.

The normal vector \mathbf{N} , at a regular point of the surface, is perpendicular to the tangent plane P . Thus, \mathbf{N} is perpendicular to vectors \mathbf{r}_u and \mathbf{r}_θ (fig. 8.3.2) and we get

$$\mathbf{N} = \mathbf{r}_u \times \mathbf{r}_\theta \quad (8.3.2)$$

The surface normal may be expressed in terms of projections on coordinate axes by

$$\mathbf{N} = \begin{vmatrix} \mathbf{i} & \mathbf{j} & \mathbf{k} \\ x_u & y_u & z_u \\ x_\theta & y_\theta & z_\theta \end{vmatrix} = \begin{vmatrix} y_u & z_u \\ y_\theta & z_\theta \end{vmatrix} \mathbf{i} + \begin{vmatrix} z_u & x_u \\ z_\theta & x_\theta \end{vmatrix} \mathbf{j} + \begin{vmatrix} x_u & y_u \\ x_\theta & y_\theta \end{vmatrix} \mathbf{k} \quad (8.3.3)$$

The unit normal is represented by

$$\mathbf{n} = \frac{\mathbf{N}}{|\mathbf{N}|} = \frac{N_x}{|\mathbf{N}|} \mathbf{i} + \frac{N_y}{|\mathbf{N}|} \mathbf{j} + \frac{N_z}{|\mathbf{N}|} \mathbf{k} \quad (8.3.4)$$

where $|\mathbf{N}| = (N_x^2 + N_y^2 + N_z^2)^{1/2}$.

The direction of the surface normal \mathbf{N} and unit normal \mathbf{n} , with respect to the surface, depends on the order of the factors of the cross product (eq. (8.3.2)). By changing the order of the factors, we may change the direction of the normal to the opposite direction.

We call a surface point $\mathbf{r}(u_0, \theta_0)$ a singular point if at this point

$$\mathbf{r}_u \times \mathbf{r}_\theta = 0 \quad (8.3.5)$$

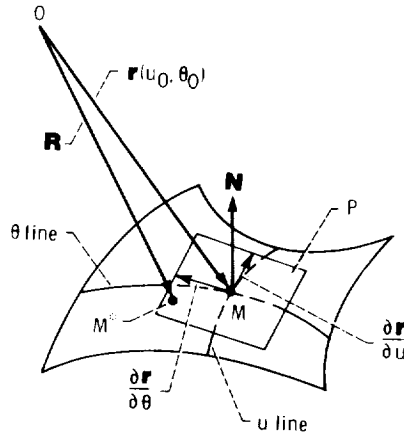


Figure 8.3.2.

Vector equation (8.3.5) gives rise to the following four cases:

- (1) $\mathbf{r}_u = 0$ and $\mathbf{r}_\theta \neq 0$
- (2) $\mathbf{r}_u \neq 0$ and $\mathbf{r}_\theta = 0$
- (3) $\mathbf{r}_u = 0$ and $\mathbf{r}_\theta = 0$
- (4) $\mathbf{r}_u \neq 0$ and $\mathbf{r}_\theta \neq 0$, but $\mathbf{r}_u = \lambda \mathbf{r}_\theta (\lambda \neq 0)$ and the tangent vectors to coordinate lines are collinear.

As a rule, in this book we apply surfaces given in the parametric form. However, we consider surfaces represented by the implicit equation (eq. (8.1.16)) with requirements (8.1.17). If these requirements are observed, the surface points are regular. Considering a set of points given by the equation

$$F(x, y, z) = 0 \quad F \in C^1 \quad (8.3.6)$$

we say a surface point is singular if

$$F_x = F_y = F_z = 0 \quad (8.3.7)$$

Equation (8.3.6) may represent a set of points of which only a part belong to a surface. Therefore, equations (8.3.6) and (8.3.7) represent all singular points of the set (including singular points of a surface if this surface indeed exists).

Consider a regular point (x_0, y_0, z_0) of a surface represented by equation (8.1.16) and expressions (8.1.17). Let us develop the equation of the tangent plane drawn at point (x_0, y_0, z_0) .

Suppose a line L is given in the three-dimensional space by

$$\begin{aligned} \mathbf{R}(\psi) &= x(\psi)\mathbf{i} + y(\psi)\mathbf{j} + z(\psi)\mathbf{k} \quad \{x(\psi), y(\psi), z(\psi)\} \in C^1 \\ |x_\psi| + |y_\psi| + |z_\psi| &\neq 0 \quad \psi_1 < \psi < \psi_2 \end{aligned} \quad (8.3.8)$$

Line L belongs to the surface

$$F(x, y, z) = 0 \quad F \in C^1 \quad |F_x| + |F_y| + |F_z| \neq 0 \quad (8.3.9)$$

if the identity

$$F(x(\psi), y(\psi), z(\psi)) = 0 \quad (8.3.10)$$

is observed by any value of ψ .

The differentiation of equation (8.3.10) with respect to ψ yields

$$F_x x_\psi + F_y y_\psi + F_z z_\psi = 0 \quad (8.3.11)$$

Here

$$\mathbf{R}_\psi = x_\psi \mathbf{i} + y_\psi \mathbf{j} + z_\psi \mathbf{k} \quad (8.3.12)$$

is the tangent vector to the line L , and

$$\nabla \mathbf{F} = F_x \mathbf{i} + F_y \mathbf{j} + F_z \mathbf{k} \quad (8.3.13)$$

is the so-called gradient of the function $F(x,y,z)$. Equation (8.3.11) yields

$$\nabla \mathbf{F} \cdot \mathbf{R}_\psi = 0 \quad (8.3.14)$$

That is, the gradient $\nabla \mathbf{F}$ and the tangent vector \mathbf{R}_ψ are perpendicular to each other.

Equation (8.3.14) is observed for all lines L which belong to the surface (8.3.9) and pass through the point (x_0, y_0, z_0) . The tangent vectors \mathbf{R}_ψ are all located in the same plane P , which is tangent to the surface at surface point (x_0, y_0, z_0) . The gradient vector $\nabla \mathbf{F}$ is perpendicular to all tangent vectors \mathbf{R}_ψ . Thus, $\nabla \mathbf{F}(x_0, y_0, z_0)$ is the normal vector to the surface at surface point (x_0, y_0, z_0) .

The tangent plane P drawn at point (x_0, y_0, z_0) is represented by the equation

$$F_x(x_0, y_0, z_0) (X - x_0) + F_y(x_0, y_0, z_0) (Y - y_0) + F_z(x_0, y_0, z_0) (Z - z_0) = 0 \quad (8.3.15)$$

where X , Y , and Z are coordinates of a point in the plane P (point M^* in fig. 8.3.2), and x_0 , y_0 , and z_0 are coordinates of the surface point M .

The surface normal \mathbf{N} at the point (x_0, y_0, z_0) is

$$\mathbf{N} = F_x(x_0, y_0, z_0) \mathbf{i} + F_y(x_0, y_0, z_0) \mathbf{j} + F_z(x_0, y_0, z_0) \mathbf{k} \quad (8.3.16)$$

The unit normal \mathbf{n} is

$$\mathbf{n} = \frac{F_x \mathbf{i} + F_y \mathbf{j} + F_z \mathbf{k}}{m} \quad (8.3.17)$$

where $m = (F_x^2 + F_y^2 + F_z^2)^{1/2}$.

Generally, the direction of the surface unit normal is a function of both curvilinear coordinates of the surface. An exception to this rule is a developable ruled surface. A ruled surface may be

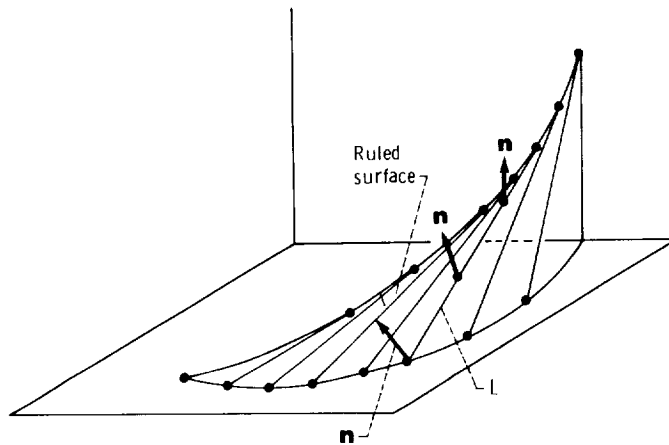


Figure 8.3.3.

generated by a certain motion of a straight line. Thus, a ruled surface may be considered as a family of straight lines. We say that a straight line may be drawn through any point of a ruled surface such that it lies entirely on the surface.

Considering surface unit normals distributed at points of the straight line L , we usually find that the direction of the surface unit normal changes while the surface point moves along L (fig. 8.3.3). However, there are known developable ruled surfaces for which the direction of the normal is the same for all points of surface straight line. Such surfaces may be developed on a plane. Typical examples of ruled, developable surfaces are the cone surface, cylindrical surface, and involute screw surface. (See sec. 8.4.)

8.4 Examples of Surfaces

In this section, we will consider some types of surfaces which are widespread in the field of spatial gear mechanisms.

Surface of Revolution

This surface (fig. 8.4.1) may be generated by rotation of a planar curve L about the z -axis; curve L is located in a plane drawn through the z -axis. Consider that the planar curve L , which generates the surface of revolution, is represented in the auxiliary coordinate system S_a (fig. 8.4.2(a)) by the equations

$$x_a = f(\theta) \quad y_a = 0 \quad z_a = g(\theta) \quad (8.4.1)$$

The auxiliary coordinate system rotates about the z -axis and the coordinate transformation from $S_a(x_a, y_a, z_a)$ to $S(x, y, z)$ (fig. 8.4.2(b)) is represented by the matrix equation

$$\begin{bmatrix} x \\ y \\ z \\ 1 \end{bmatrix} = \begin{bmatrix} \cos \psi & -\sin \psi & 0 & 0 \\ \sin \psi & \cos \psi & 0 & 0 \\ 0 & 0 & 1 & 0 \\ 0 & 0 & 0 & 1 \end{bmatrix} \begin{bmatrix} x_a \\ y_a \\ z_a \\ 1 \end{bmatrix} \quad (8.4.2)$$

Equations (8.4.1) and (8.4.2) yield

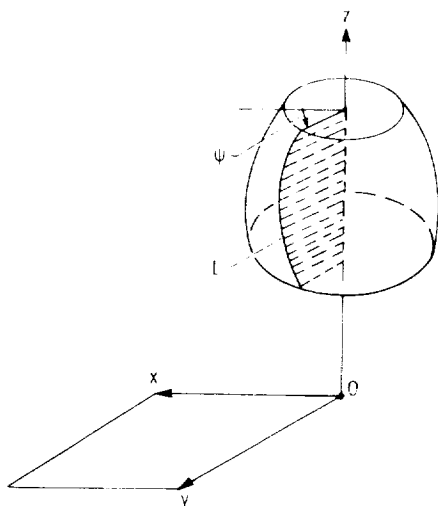


Figure 8.4.1.

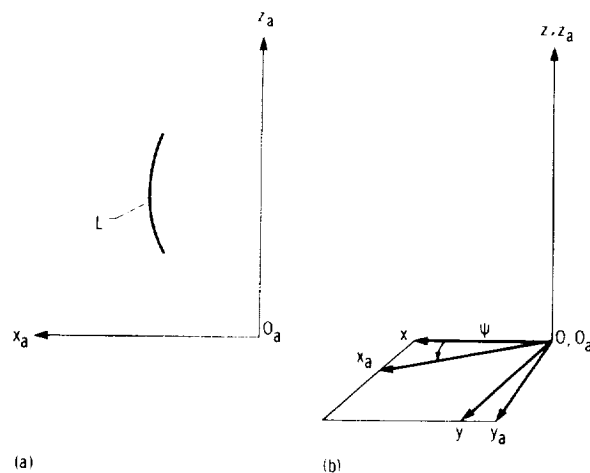


Figure 8.4.2.

$$x = f(\theta) \cos \psi \quad y = f(\theta) \sin \psi \quad z = g(\theta) \quad (8.4.3)$$

where $\theta_1 < \theta < \theta_2$ and $0 \leq \psi \leq 2\pi$.

Problem 8.4.1 Given the surface of revolution represented by equations (8.4.3). Determine (1) equations of the θ -lines and ψ -lines and explain their geometric essence and (2) equations of the surface normal \mathbf{N} and the surface unit normal \mathbf{n} .

Answer. (1) The θ -line is represented by the equations

$$x = f(\theta) \cos \psi_0 \quad y = f(\theta) \sin \psi_0 \quad z = g(\theta) \quad (8.4.4)$$

where $\psi_0 = \text{constant}$ and is located in the plane which passes through the z -axis and makes an angle $\psi = \psi_0$ with the x -axis (fig. 8.4.1). The ψ -line is represented by the equations

$$x = f(\theta_0) \cos \psi \quad y = f(\theta_0) \sin \psi \quad z = g(\theta_0) \quad (8.4.5)$$

Equations (8.4.5) represent a circle of radius

$$\rho = (x^2 + y^2)^{1/2} = f(\theta_0)$$

which is located in the plane $z = g(\theta_0)$ and centered on the z -axis.

(2) With the cross product $\mathbf{r}_\theta \times \mathbf{r}_\psi$, the surface normal may be represented as follows:

$$N_x = -f(\theta)g'(\theta) \cos \psi \quad N_y = -f(\theta)g'(\theta) \sin \psi \quad N_z = f(\theta)f'(\theta) \quad (8.4.6)$$

The unit normal is (provided $f(\theta) \neq 0$)

$$n_x = -\frac{g'(\theta) \cos \psi}{A} \quad n_y = -\frac{g'(\theta) \sin \psi}{A} \quad n_z = \frac{f'(\theta)}{A} \quad (8.4.7)$$

where

$$A^2 = [f'(\theta)]^2 + [g'(\theta)]^2 \quad f'(\theta) = \frac{d}{d\theta} (f(\theta)) \quad g'(\theta) = \frac{d}{d\theta} (g(\theta))$$

Spherical Surface

This surface (fig. 8.4.3) is a particular case of the surface of revolution. The generating planar curve L is a circle of radius ρ centered at the origin O of the coordinate system $S(x, y, z)$. The spherical surface is generated by the circle in rotational motion about the z -axis; L_I and L_{II} are two positions of the generating circle, and ψ is the angle of rotation about the z -axis.

Consider again an auxiliary coordinate system S_a , rigidly connected to the generating circle (fig. 8.4.4). The generating circle is represented in the coordinate system S_a by the equations

$$x_a = \rho \cos \theta \quad y_a = 0 \quad z_a = \rho \sin \theta \quad (8.4.8)$$

Using the matrix equation (8.4.2) and equation (8.4.8), we represent the equations of the spherical surface as follows:

$$x = \rho \cos \theta \cos \psi \quad y = \rho \cos \theta \sin \psi \quad z = \rho \sin \theta \quad (8.4.9)$$

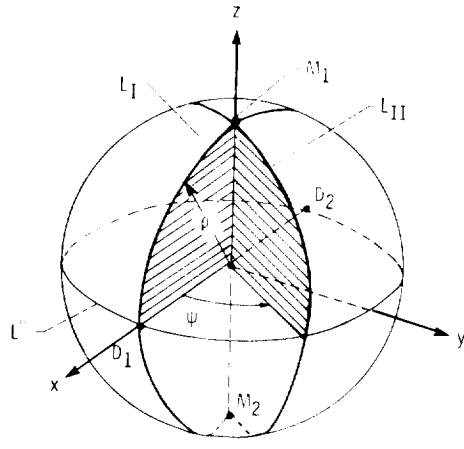


Figure 8.4.3.

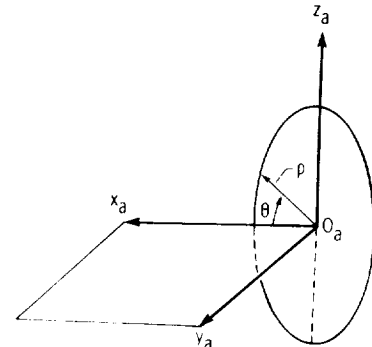


Figure 8.4.4.

where $0 < \theta < 2\pi$ and $0 < \psi < 2\pi$. The surface normal vector $\mathbf{N} = \mathbf{r}_\theta \times \mathbf{r}_\psi$ is given by

$$N_x = -\rho^2 \cos^2 \theta \cos \psi \quad N_y = -\rho^2 \cos^2 \theta \sin \psi \quad N_z = -\rho^2 \cos \theta \sin \theta \quad (8.4.10)$$

The normal \mathbf{N} is equal to zero at $\cos \theta = 0$. Thus, points M_1 and M_2 (fig. 8.4.3) are singular.

We must differentiate between singular and pseudosingular points of a surface. Pseudosingular points appear only as a result of the chosen parametric representation, and they become regular by the changing of parameters of representation.

To prove this, let us consider that the spherical surface is generated by the circle L^* in rotational motion about the x -axis (fig. 8.4.3). The circle L^* is represented in the coordinate system S_a (fig. 8.4.5(a)) by equations

$$x_a = \rho \cos u \quad y_a = \rho \sin u \quad z_a = 0 \quad (8.4.11)$$

The coordinate transformation in transition from S_a to S (fig. 8.4.5(b)) is represented by the matrix equation

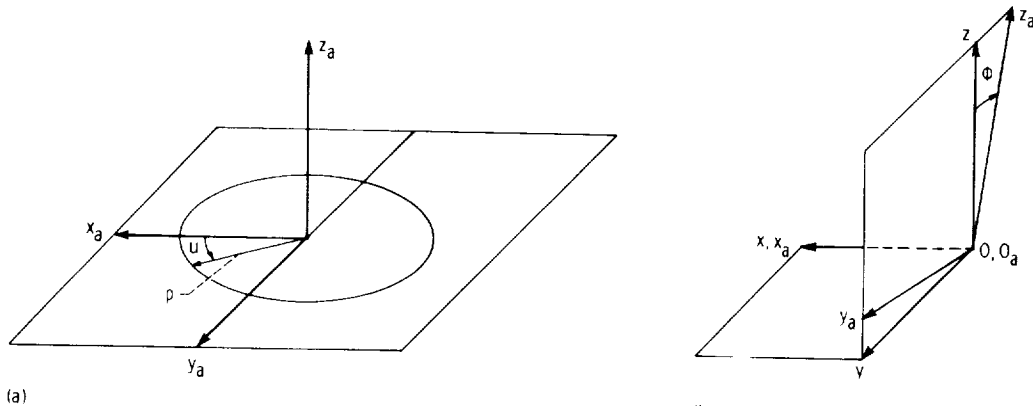


Figure 8.4.5.

$$\begin{bmatrix} x \\ y \\ z \\ 1 \end{bmatrix} = \begin{bmatrix} 1 & 0 & 0 & 0 \\ 0 & \cos \phi & -\sin \phi & 0 \\ 0 & \sin \phi & \cos \phi & 0 \\ 0 & 0 & 0 & 1 \end{bmatrix} \begin{bmatrix} x_a \\ y_a \\ z_a \\ 1 \end{bmatrix} \quad (8.4.12)$$

Equations (8.4.11) and (8.4.12) yield

$$x = \rho \cos u \quad y = \rho \sin u \cos \phi \quad z = \rho \sin u \sin \phi \quad (8.4.13)$$

The surface normal \mathbf{N}^* is given by

$$\mathbf{N}^* = \mathbf{r}_u \times \mathbf{r}_\phi = \rho^2 \sin u (\cos u \mathbf{i} + \sin u \cos \phi \mathbf{j} + \sin u \sin \phi \mathbf{k}) \quad (8.4.14)$$

Surface points D_1 and D_2 (fig. 8.4.3), which correspond to $\sin u = 0$, are singular because at these points $\mathbf{N}^* = 0$. All other surface points, including points M_1 and M_2 (fig. 8.4.3), are regular. We may see that the singularity of surface points M_1 and M_2 , which results from the parametric representation (eq. (8.4.9)), disappears when the new parametric representation (eq. (8.4.13)) is employed. But, at the same time, the singularity of surface points D_1 and D_2 occurs.

Actually, a spherical surface does not have singular points; that is, the normal to the surface has a definite direction at all surface points. This direction at pseudosingular points like M_1 and M_2 and D_1 and D_2 may be determined by using a new parametric representation.

Considering the parametric representation (eq. (8.4.13)) and the equation of the surface normal (eq. (8.4.14)), we find that the surface unit normal is (provided $\sin u \neq 0$)

$$\mathbf{n}^* = \frac{\mathbf{N}^*}{|\mathbf{N}^*|} = \cos u \mathbf{i} + \sin u \cos \phi \mathbf{j} + \sin u \sin \phi \mathbf{k} \quad (8.4.15)$$

Cone Surface

This surface may be generated by a straight line L in rotation about an axis with which line L forms an angle ψ_c (the x -axis in fig. 8.4.6). Curvilinear coordinates of the cone surface are θ and $u = |AM|$, where A is the cone apex. Equations of the cone surface are

$$x = \rho \cot \psi_c - u \cos \psi_c \quad y = u \sin \psi_c \sin \theta \quad z = u \sin \psi_c \cos \theta \quad (8.4.16)$$

where $0 \leq u \leq u_1$ and $0 \leq \theta \leq 2\pi$.

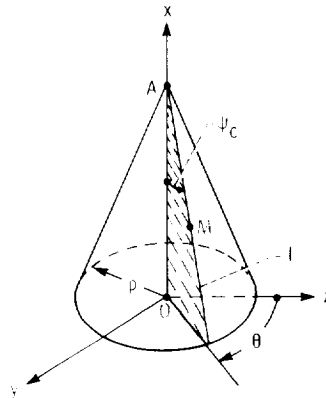


Figure 8.4.6.

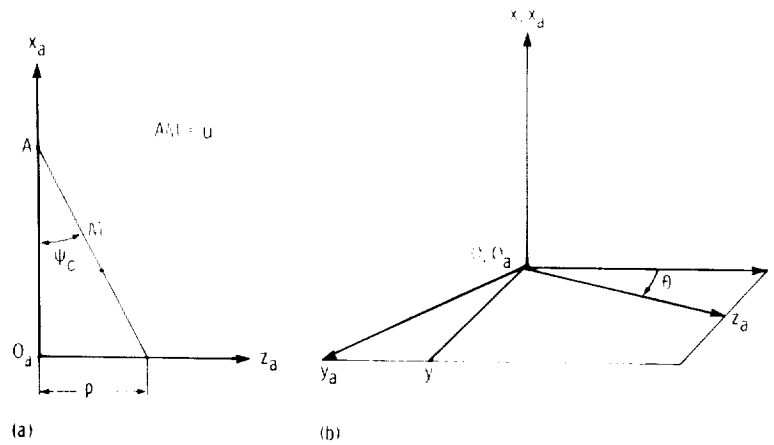


Figure 8.4.7.

Equations (8.4.16) may also be derived using the following considerations:

(1) The generating straight line L is represented in the auxiliary coordinate system S_a (fig. 8.4.7(a)) by the equations

$$x_a = \rho \cot \psi_c - u \cos \psi_c \quad y_a = 0 \quad z_a = u \sin \psi_c \quad (8.4.17)$$

(2) The coordinate transformation in transition from S_a to S (fig. 8.4.7(b)) is

$$\begin{bmatrix} x \\ y \\ z \\ 1 \end{bmatrix} = \begin{bmatrix} 1 & 0 & 0 & 0 \\ 0 & \cos \theta & \sin \theta & 0 \\ 0 & -\sin \theta & \cos \theta & 0 \\ 0 & 0 & 0 & 1 \end{bmatrix} \begin{bmatrix} x_a \\ y_a \\ z_a \\ 1 \end{bmatrix} \quad (8.4.18)$$

Equations (8.4.17) and (8.4.18) yield equations (8.4.16).

A cone surface is an example of a developable ruled surface. The cone normal and its unit normal may be represented by

$$\mathbf{N} = \mathbf{r}_\theta \times \mathbf{r}_u = u \sin \psi_c (\sin \psi_c \mathbf{i} + \cos \psi_c \sin \theta \mathbf{j} + \cos \psi_c \cos \theta \mathbf{k}) \quad (8.4.19)$$

$$\mathbf{n} = \frac{\mathbf{N}}{|\mathbf{N}|} = \sin \psi_c \mathbf{i} + \cos \psi_c \sin \theta \mathbf{j} + \cos \psi_c \cos \theta \mathbf{k} \quad (\text{by } u \sin \psi_c \neq 0) \quad (8.4.20)$$

Equation (8.4.20) yields that the surface unit normal \mathbf{n} is a function of only one curvilinear coordinate, θ . Consequently, the surface unit normals are the same for all points of the straight line L (fig. 8.4.6).

The cone apex, which corresponds to $u = 0$, is a singular surface point. This results from equations (8.4.19), where $\mathbf{N} = 0$ when $u = 0$.

Helicoid

A helicoid is a surface which is generated by a line in a screw motion. The generating line may be a curve or a straight line. Helicoids are widespread in the field of gears. Surfaces of helical gears and cylindrical worms of worm-gear drives are helicoids.

General equations of a helicoid.—Consider a screw motion of a planar curve L such that the axis of screw motion is perpendicular to the plane of L . In this motion, curve L generates a helicoid. Let us represent curve L in an auxiliary coordinate system S_a (fig. 8.4.8(a)) by equations

$$x_a = r_a(\theta) \cos \theta \quad y_a = r_a(\theta) \sin \theta \quad z_a = 0 \quad (8.4.21)$$

where $r_a = \overline{O_a M}$ and $\theta_1 < \theta < \theta_2$. The axis of the screw motion is the z -axis (fig. 8.4.8(b)), and the screw parameter is h . The screw parameter h represents the displacement along the z -axis, which corresponds to the rotation about z through an angle of one radian. The sign of h is positive for a right-hand screw motion.

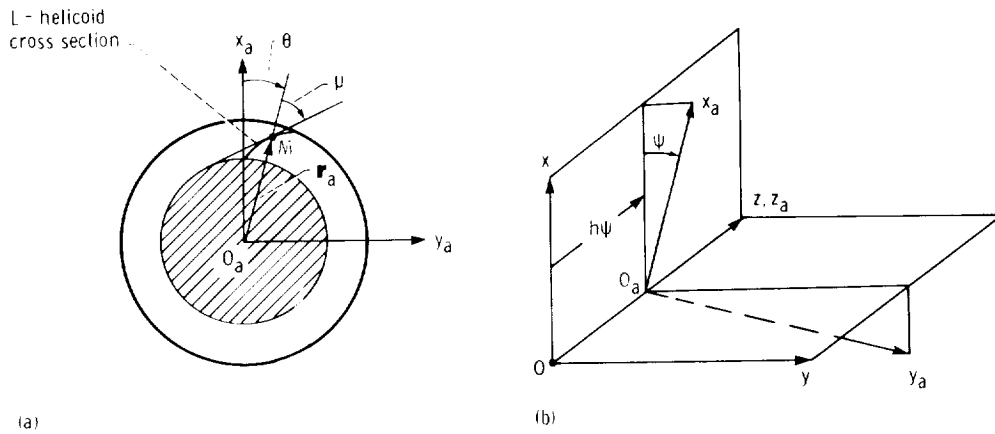


Figure 8.4.8.

Coordinate transformation in transition from S_a to S is represented by the matrix equation

$$\begin{bmatrix} x \\ y \\ z \\ 1 \end{bmatrix} = \begin{bmatrix} \cos \psi & -\sin \psi & 0 & 0 \\ \sin \psi & \cos \psi & 0 & 0 \\ 0 & 0 & 1 & h\psi \\ 0 & 0 & 0 & 1 \end{bmatrix} \begin{bmatrix} x_a \\ y_a \\ z_a \\ 1 \end{bmatrix} \quad (8.4.22)$$

Equations (8.4.21) and (8.4.22) yield

$$x = r_a(\theta) \cos(\theta + \psi) \quad y = r_a(\theta) \sin(\theta + \psi) \quad z_a = h\psi \quad (8.4.23)$$

where $\theta_1 < \theta < \theta_2$ and $0 < \psi < 2\pi$.

The helicoid normal is

$$\mathbf{N} = \frac{\partial \mathbf{r}}{\partial \theta} \times \frac{\partial \mathbf{r}}{\partial \psi} = \frac{r_a(\theta)}{\sin \mu} [h \sin(\theta + \psi + \mu) \mathbf{i} - h \cos(\theta + \psi + \mu) \mathbf{j} + r_a(\theta) \cos \mu \mathbf{k}] \quad (8.4.24)$$

$$\text{where } \mu = \arctan \left(\frac{r_a(\theta)}{\frac{dr_a}{d\theta}} \right)$$

The helicoid unit normal is (provided $r_a(\theta) \neq 0$)

$$\mathbf{n} = \frac{\mathbf{N}}{|\mathbf{N}|} = \frac{1}{\sqrt{h^2 + r_a^2 \cos^2 \mu}} [h \sin(\theta + \psi + \mu)\mathbf{i} - h \cos(\theta + \psi + \mu)\mathbf{j} + r_a \cos \mu \mathbf{k}] \quad (8.4.25)$$

Helicoid with ruled surface.—A helicoid with a ruled surface is generated by a screw motion of a straight line L . The axis of screw motion and the generating line may form a crossed angle or they may intersect each other.

Given (a) two coordinate systems S_a and S_b rigidly connected to the generating line L (fig. 8.4.9(a)) and (b) a coordinate system S in which the helicoid is represented (figs. 8.4.9(b) and (c)). The coordinate system S_a performs a screw motion with respect to S , and z is the axis of the screw motion. Each point of the coordinate system S_a generates in the screw motion a helix on a cylinder. Point M generates a helix on the cylinder of radius $O_aM = \rho$, and MT is the tangent to the helix at point M (figs. 8.4.9(a) and (b)). We consider two lines MT and MN rigidly connected with each other. Line MN is the generating line which, while performing a screw motion, generates the helicoid.

We may derive the helicoid equations by using the rules of coordinate transformation. Consider that the generating line is represented in the coordinate system S_b by equations

$$x_b = 0 \quad y_b = u \cos \delta \quad z_b = -u \sin \delta \quad (8.4.26)$$

where $u = MN$. The coordinate transformation from S_b to S is represented by the matrix equation

$$[r_0] = [M_{0a}][M_{ab}][r_b]$$

$$\begin{bmatrix} x \\ y \\ z \\ 1 \end{bmatrix} = \begin{bmatrix} \cos \theta & -\sin \theta & 0 & 0 \\ \sin \theta & \cos \theta & 0 & 0 \\ 0 & 0 & 1 & h\theta \\ 0 & 0 & 0 & 1 \end{bmatrix} \begin{bmatrix} 1 & 0 & 0 & \rho \\ 0 & 1 & 0 & 0 \\ 0 & 0 & 1 & 0 \\ 0 & 0 & 0 & 1 \end{bmatrix} \begin{bmatrix} x_b \\ y_b \\ z_b \\ 1 \end{bmatrix} \quad (8.4.27)$$

Equations (8.4.26) and (8.4.27) represent the equations of the helicoid surface as follows:

$$\mathbf{r} = (\rho \cos \theta - u \cos \delta \sin \theta)\mathbf{i} + (\rho \sin \theta + u \cos \delta \cos \theta)\mathbf{j} + (h\theta - u \sin \delta)\mathbf{k} \quad (8.4.28)$$

Vector equation (8.4.28) represents a ruled surface. The u -line (surface parameter θ is considered fixed) represents a straight line and the θ -line represents a helix. Vector equation (8.4.23) is a general

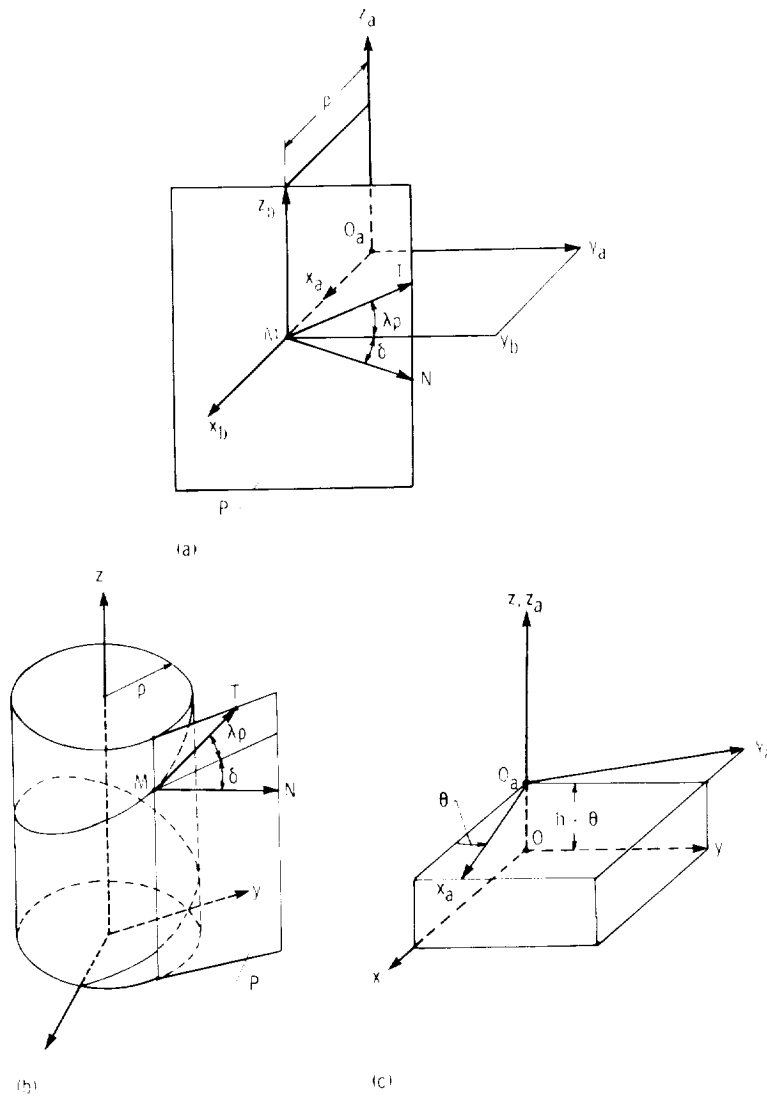


Figure 8.4.9.

equation of a helicoid. In a particular case, equation (8.4.23) may represent a helicoid with a ruled surface if the generating plane curve L is given as a cross section of a helicoid with a ruled surface.

The normal to the helicoid with the ruled surface (eq. (8.4.28)) is

$$\mathbf{N} = \frac{\partial \mathbf{r}}{\partial u} \times \frac{\partial \mathbf{r}}{\partial \theta} = [(h \cos \delta + \rho \sin \delta) \cos \theta - u \cos \delta \sin \delta \sin \theta] \mathbf{i} + [h \cos \delta + \rho \sin \delta) \sin \theta + u \cos \delta \sin \delta \cos \theta] \mathbf{j} + u \cos^2 \delta \mathbf{k} \quad (8.4.29)$$

The unit normal is

$$\mathbf{n} = \frac{\mathbf{N}}{|\mathbf{N}|} = \frac{\mathbf{N}}{m} \quad (8.4.30)$$

where

$$m^2 = (h \cos \delta + \rho \sin \delta)^2 + u^2 \cos^2 \delta \quad (8.4.31)$$

There are two particular but important cases of helicoids with ruled surfaces. In the first case, the generating line L coincides with the tangent \mathbf{T} to the helix on the cylinder surface C . The straight line L generates a helicoid, an involute screw surface. We may obtain equations of such a surface from equations (8.4.28) by setting $\delta = -\lambda_\rho$ (fig. 8.4.9(a)). This yields

$$\mathbf{r} = (\rho \cos \theta - u \cos \lambda_\rho \sin \theta)\mathbf{i} + (\rho \sin \theta + u \cos \lambda_\rho \cos \theta)\mathbf{j} + (h\theta + u \sin \lambda_\rho)\mathbf{k} \quad (8.4.32)$$

Equations of the normal \mathbf{N} and unit normal \mathbf{n} to this surface may be derived from equations (8.4.29) and (8.4.30) to (8.4.31), respectively, making $\delta = -\lambda_\rho$ where $\tan \lambda_\rho = h/\rho$. We then obtain

$$h \cos \delta + \rho \sin \delta = h \cos \lambda_\rho - \rho \sin \lambda_\rho = 0 \quad (8.4.33)$$

$$\begin{aligned} m^2 &= (h \cos \delta + \rho \sin \delta)^2 + u^2 \cos^2 \delta \\ &= u^2 \cos^2 \lambda_\rho \end{aligned} \quad (8.4.34)$$

and

$$\mathbf{N} = u \cos \lambda_\rho (\sin \lambda_\rho \sin \theta \mathbf{i} - \sin \lambda_\rho \cos \theta \mathbf{j} + \cos \lambda_\rho \mathbf{k}) \quad (8.4.35)$$

With $u \cos \lambda_\rho \neq 0$, all points of the screw involute surface are regular, and the equation of the unit normal at these points is

$$\mathbf{n} = \sin \lambda_\rho (\sin \theta \mathbf{i} - \cos \theta \mathbf{j}) + \cos \lambda_\rho \mathbf{k} \quad (8.4.36)$$

The direction of the unit normal \mathbf{n} does not depend on the surface parameter u . This means that the unit normal has the same direction for all points of the generating straight line L , and the involute screw surface is a ruled developable surface.

The second particular case of a helicoid with a ruled surface is the Archimedes screw surface. This surface is generated by a straight line which does not cross, but intersects the axis of screw motion. The Archimedes screw surface is applied not only for worms but for screws which are cut by straight-edged blades.

The equation of the Archimedes screw surface may be derived from equation (8.4.28) by setting $\rho = 0$. This yields

$$\mathbf{r} = u \cos \delta (-\sin \theta \mathbf{i} + \cos \theta \mathbf{j}) + (h\theta - u \sin \delta)\mathbf{k} \quad (8.4.37)$$

Equations of the normal \mathbf{N} may be derived from equation (8.4.29) by setting $\rho = 0$ and dividing all three normal projections by a common factor $\cos \delta$ (with the assumption that $\delta \neq 90^\circ$). This yields

$$\mathbf{N} = (h \cos \theta - u \sin \delta \sin \theta)\mathbf{i} + (h \sin \theta + u \sin \delta \cos \theta)\mathbf{j} + u \cos \delta \mathbf{k} \quad (8.4.38)$$

The unit normal \mathbf{n} is

$$\mathbf{n} = \frac{\mathbf{N}}{m} \quad (8.4.39)$$

where

$$m = (h^2 + u^2)^{1/2} \quad (8.4.40)$$

Relationship between helicoid coordinates and the surface normal projections.—This relationship proposed by Litvin (1968) may be represented as follows:

$$yN_x - xN_y - hN_z = 0 \quad (8.4.41)$$

or

$$yn_x - xn_y - hn_z = 0 \quad (8.4.42)$$

This statement may be proven by substituting in equations (8.4.41) and (8.4.42) helicoid coordinates and projections of the surface normal \mathbf{N} and the surface unit normal \mathbf{n} with the formerly derived expressions.

The kinematic interpretation of equations (8.4.41) and (8.4.42) is based on the following suggestions: Consider the screw motion of a helicoid. The screw parameter of this motion h is the same as the screw parameter of the helicoid. A fixed point of the helicoid traces out a helix, and the velocity vector in screw motion \mathbf{v} is a tangent to the helix. The helix belongs to the helicoid, and the velocity vector \mathbf{v} is a tangent to the helicoid. Consequently, the following equation must be observed:

$$\mathbf{n} \cdot \mathbf{v} = \mathbf{N} \cdot \mathbf{v} = 0 \quad (8.4.43)$$

The velocity vector in screw motion may be determined by the equation

$$\begin{aligned} \mathbf{v} &= (\boldsymbol{\omega} \times \mathbf{r}) + h\boldsymbol{\omega} \\ &= \begin{vmatrix} \mathbf{i} & \mathbf{j} & \mathbf{k} \\ 0 & 0 & \omega \\ x & y & x \end{vmatrix} + h\omega\mathbf{k} \\ &= \omega(-y\mathbf{i} + x\mathbf{j} + h\mathbf{k}) \end{aligned} \quad (8.4.44)$$

The surface normal and the surface unit normal are determined as

$$\mathbf{N} = N_x \mathbf{i} + N_y \mathbf{j} + N_z \mathbf{k} \quad \mathbf{n} = n_x \mathbf{i} + n_y \mathbf{j} + n_z \mathbf{k} \quad (8.4.45)$$

Equations (8.4.43), (8.4.44), and (8.4.45) yield relations (8.4.41) and (8.4.42).

Cross section of a helicoid.—The cross section of a helicoid is formed by cutting the surface with a plane perpendicular to the z -axis, the axis of screw motion. This section may be represented by the equations of the helicoid and the equation $z = c$, where c is a constant. To simplify transformations, we may set $z = 0$. The cross sections of a helicoid corresponding to $z = 0$ and $z = c$ represent the same plane curve in two positions. One cross section will coincide with the other after rotation about the z -axis through the angle

$$\psi = \frac{c}{h} \quad (8.4.46)$$

Let us determine the cross section of the helicoid (eq. (8.4.28)) cut by the plane $z = 0$. Using the relation

$$u = \frac{h}{\sin \delta} \theta \quad (8.4.47)$$

we get

$$x = \rho \cos \theta - \theta \sin \theta h \cot \delta \quad y = \rho \sin \theta + \theta \cos \theta h \cot \delta \quad z = 0 \quad (8.4.48)$$

In polar form the cross section may be represented as

$$r(\theta) = (x^2 + y^2)^{1/2} = \left[\rho^2 + (\theta h \cot \delta)^2 \right]^{1/2}$$

$$\tan q = \frac{y}{x} = \frac{\rho \tan \theta + \theta h \cot \delta}{\rho - \theta \tan \theta h \cot \delta} \quad (8.4.49)$$

Here q is the angle which is formed by the position vector $\mathbf{r}(\theta)$ and axis x . The cross section is an extended involute. The generation of such a curve is shown in figure 8.4.10.

Consider that a straight line S rolls over a circle of radius $OA = h \cot \delta$. Point B , whose location is determined by

$$AB = AO + OB = h \cot \delta + \rho$$

is rigidly connected to the straight line S (fig. 8.4.10). The instantaneous position of the rolling straight line S is IA^* , and B^* is a point of the extended involute which is traced out by point B considered above.

Chapter 9

Conjugated Surfaces

9.1 Introduction to Problem of Conjugated Surfaces

Consider a gear mechanism consisting of two gears which transforms rotation between crossed axes with the given ratio of angular velocities

$$m_{12} = \frac{\omega^{(1)}}{\omega^{(2)}} \quad (9.1.1)$$

We assume that the ratio m_{12} is constant. However, the methods to be discussed may be applied for a more general case where the angular velocity ratio is given by a function $m_{12}(\phi_1) \in C^1$ (ϕ_1 is the angle of rotation of gear 1).

We then assume that surface Σ_1 of the teeth of gear 1 is given. We must determine the surface Σ_2 of the teeth of gear 2 while observing the following conditions: (1) surface Σ_1 and Σ_2 must be in line contact (they contact each other along a line which moves over them in the process of meshing) and (2) teeth of gears 1 and 2, having surfaces Σ_1 and Σ_2 , must transform rotation with the prescribed angular velocity ratio m_{12} .

Surfaces of gear teeth where the required transformation of motion is observed are termed conjugate surfaces. In some cases (discussed below), conjugated surfaces may not be in line contact but in point contact.

In a mathematical sense, the determination of a conjugate surface is based on the theory of an envelope of a locus (family) of given surfaces. Assume that gear 2 is fixed and consider the relative motion of gear 1 with the given surface Σ_1 (with respect to the coordinate system S_2 rigidly connected to gear 2). By using a method of coordinate transformation, we may get a locus of given surfaces Σ_1 . The desired surface Σ_2 is to be determined as the envelope of the locus of surface Σ_1 , which is generated in the coordinate system S_2 .

We will discuss in sections of this chapter the following topics:

- (1) The generation of a locus of given surfaces
- (2) The determination of the envelope Σ_2 of the locus of surfaces (including a simplified method for this operation)
- (3) Properties of the generated surface Σ_2

9.2 Family of Given Surfaces

We set up three coordinate systems: $S_1(x_1, y_1, z_1)$ and $S_2(x_2, y_2, z_2)$, rigidly connected to gears 1 and 2, respectively, and $S_f(x_f, y_f, z_f)$, rigidly connected to the frame. We assume that gears 1 and 2 rotate about crossed axes and we designate their angles of rotation by ϕ_1 and ϕ_2 and their angular velocities by

$$\omega^{(1)} = \frac{d\phi_1}{dt} \quad \omega^{(2)} = \frac{d\phi_2}{dt}$$

Consider that the surface of teeth of gear 1 is regular and is given in parametric form as follows:

$$\mathbf{r}_1(u, \theta) = \{x_1(u, \theta), y_1(u, \theta), z_1(u, \theta)\} \in C^1 \quad \frac{\partial \mathbf{r}_1}{\partial u} \times \frac{\partial \mathbf{r}_1}{\partial \theta} \neq 0 \quad (u, \theta) \in G \quad (9.2.1)$$

A family Σ_ϕ of generating surface Σ_1 is generated in the coordinate system S_2 by the relative motion of Σ_1 with respect to S_2 . This family may be determined by equation (9.2.1) and the following matrix equation:

$$[r_2] = [M_{21}][r_1] = [M_{2f}][M_{f1}][r_1] \quad (9.2.2)$$

Here matrices $[M_{2f}]$ and $[M_{f1}]$ represent the coordinate transformation from S_f to S_2 and from S_1 to S_f , respectively. Equations (9.2.1) and (9.2.2) represent the family Σ_ϕ of surfaces Σ_1 as follows:

$$\mathbf{r}_2(u, \theta, \phi_1) \in C^1 \quad \frac{\partial \mathbf{r}_2}{\partial u} \times \frac{\partial \mathbf{r}_2}{\partial \theta} \neq 0 \quad (u, \theta) \in G \quad a < \phi_1 < b \quad (9.2.3)$$

The surface Σ_1 may be given by an implicit equation

$$F(x_1, y_1, z_1) = 0 \quad F \in C^1 \quad \left| \frac{\partial F}{\partial x_1} \right| + \left| \frac{\partial F}{\partial y_1} \right| + \left| \frac{\partial F}{\partial z_1} \right| \neq 0 \quad (9.2.4)$$

To derive equations of the locus of surfaces, it is necessary to substitute x_1 , y_1 , and z_1 into the equation $F(x_1, y_1, z_1) = 0$ by using the expressions

$$x_1 = x_1(x_2, y_2, z_2, \phi_1) \quad y_1 = y_1(x_2, y_2, z_2, \phi_1) \quad z_1 = z_1(x_2, y_2, z_2, \phi_1) \quad (9.2.5)$$

Equations (9.2.5) may be derived from the matrix equation

$$[r_1] = [M_{12}][r_2] \quad (9.2.6)$$

Here matrix $[M_{12}]$ is the inverse of matrix $[M_{21}]$.

Equations (9.2.4) and (9.2.5) represent the family Σ_ϕ of surface Σ_1 by

$$G(x_2, y_2, z_2, \phi) = F(x_1(x_2, y_2, z_2, \phi), y_1(x_2, y_2, z_2, \phi), z_1(x_2, y_2, z_2, \phi)) = 0 \quad (9.2.7)$$

$$G \in C^1 \quad \left| \frac{\partial G}{\partial x_2} \right| + \left| \frac{\partial G}{\partial y_2} \right| + \left| \frac{\partial G}{\partial z_2} \right| \neq 0$$

9.3 Envelope of a Family of Surfaces: Representation in Parametric Form

Consider a family (locus) Σ_ϕ of regular surfaces represented by

$$\begin{aligned} \mathbf{r}(u, \theta, \phi) \in C^1 \quad \mathbf{r}_u \times \mathbf{r}_\theta \neq 0 \quad (u, \theta) \in G \quad \{\alpha < u < \beta \text{ and } \gamma < \theta < \delta\} \\ a < \phi < b \end{aligned} \quad (9.3.1)$$

The function $\mathbf{r}(u, \theta, \phi)$, with a fixed value of ϕ , represents a regular surface of the family. To simplify notations, we drop the subscripts 2 for \mathbf{r}_2 , u_2 , and θ_2 and 1 for ϕ_1 .

We begin with the definition of an envelope. A piece of the envelope of a locus of surfaces (9.3.1) is a regular surface and may be represented as

$$\begin{aligned} \mathbf{r}(u, \theta(u, \phi), \phi) = \mathbf{R}(u, \phi) \in C^1 \quad \alpha_0 < u < \beta_0 \quad a_0 < \phi < b_0 \quad \mathbf{R}_u \times \mathbf{R}_\phi \neq 0 \\ \theta(u, \phi) \in C^1 \end{aligned} \quad (9.3.2)$$

or

$$\begin{aligned} \mathbf{r}(u(\theta, \phi), \theta, \phi) = \boldsymbol{\rho}(\theta, \phi) \in C^1 \quad \gamma_0 < \theta < \delta_0 \quad a_0 < \phi < b_0 \quad \boldsymbol{\rho}_\theta \times \boldsymbol{\rho}_\phi \neq 0 \\ u(\theta, \phi) \in C^1 \end{aligned} \quad (9.3.3)$$

if the piece of the envelope is in tangency with a single surface of the locus at any value of ϕ . The total complex of the envelope pieces (which are determined separately for intervals (α_0, β_0) and (a_0, b_0) , respectively, and for intervals (γ_0, δ_0) and (a_0, b_0) , respectively) represents the envelope in totality.

Henceforth, we will differentiate between the necessary and sufficient conditions of envelope piece existence. The necessary conditions determine the requirements by which, if observed, the piece of the envelope can be in tangency with the surface of the locus. The sufficient conditions determine the requirements by which, if observed, the piece of the envelope actually exists as a regular surface and is actually in tangency with the surface of the locus.

Theorem of Necessary Conditions of Envelope Existence Consider the family of surfaces (9.3.1) and assume that functions

$$\theta(u, \phi) \in C^1 \quad \text{or} \quad u(\theta, \phi) \in C^1 \quad (9.3.4)$$

and a corresponding envelope piece (9.3.2) or (9.3.3) exist. The point (u_0, θ_0, ϕ_0) corresponds to the point of tangency of the envelope piece with the locus (family) of surfaces. The theorem states that the point (u_0, θ_0, ϕ_0) must belong to the set determined by the equation

$$f(u, \theta, \phi) = [\mathbf{r}_u \ \mathbf{r}_\theta \ \mathbf{r}_\phi] = \frac{D(x, y, z)}{D(u, \theta, \phi)} = 0 \quad (9.3.5)$$

Proof: Suppose the function $\theta(u, \phi) \in C^1$ exists and surface (9.3.2), designated by E_1 , is considered. The tangent plane Π to surface E_1 may be determined by vectors

$$\mathbf{R}_u = \mathbf{r}_u + \mathbf{r}_\theta \theta_u \quad \mathbf{R}_\phi = \mathbf{r}_\phi + \mathbf{r}_\theta \theta_\phi \quad (9.3.6)$$

The tangent plane P to surface Σ_1 of the locus is determined by vectors $(\mathbf{r}_u, \mathbf{r}_\theta)$. If the envelope piece exists, surfaces E_1 and Σ_1 are in tangency and planes Π and P must coincide.

Equations (9.3.6) yield that vector \mathbf{R}_u belongs to plane P . Vector \mathbf{R}_ϕ can belong to plane P if the following condition is observed:

$$[\mathbf{R}_\phi \mathbf{r}_u \mathbf{r}_\theta] = 0 \quad (9.3.7)$$

Substituting \mathbf{R}_ϕ by its expression in equation (9.3.6), we get $[\mathbf{r}_u \mathbf{r}_\theta \mathbf{r}_\phi] = 0$ which may be represented by

$$\begin{vmatrix} x_u & x_\theta & x_\phi \\ y_u & y_\theta & y_\phi \\ z_u & z_\theta & z_\phi \end{vmatrix} = 0$$

Thus, the theorem is proven.

Similarly, the theorem may be proven for the case when the function $u(\theta, \phi) \in C^1$ is considered.

Theorem of Sufficient Conditions of Envelope Existence (Zalgaller, 1975) Consider the family of surfaces (9.3.1) represented by $\mathbf{r}(u, \theta, \phi) \in C^2$. If at the point $M(u_0, \theta_0, \phi_0)$ the following conditions are observed:

$$f(u, \theta, \phi) = [\mathbf{r}_u \mathbf{r}_\theta \mathbf{r}_\phi] = 0 \quad f \in C^1 \quad (9.3.8)$$

$$|f_u| + |f_\theta| \neq 0 \quad (9.3.9)$$

and

$$\mathbf{N} = (\mathbf{r}_\theta \times \mathbf{r}_\phi)f_u + (\mathbf{r}_\phi \times \mathbf{r}_u)f_\theta + (\mathbf{r}_u \times \mathbf{r}_\theta)f_\phi \neq 0 \quad (9.3.10)$$

then the envelope piece exists in the neighborhood of point M and may be represented by the vector function $\mathbf{r}(u, \theta, \phi)$, with the relationship between parameters given by equation (9.3.5).

Proof: Let the inequality (9.3.9) be observed with $f_\theta \neq 0$. Then equation (9.3.8) may be solved in the neighborhood of point M by the function $\theta(u, \phi) \in C^1$. (See app. B.) Considering the identity

$$f(u, \theta(u, \phi), \phi) = 0 \quad (9.3.11)$$

we get

$$f_u + f_\theta \theta_u = 0 \quad f_\phi + f_\theta \theta_\phi = 0 \quad (9.3.12)$$

These equations yield

$$\theta_u = -\frac{f_u}{f_\theta} \quad \theta_\phi = -\frac{f_\phi}{f_\theta} \quad (9.3.13)$$

From equations (9.3.13) and (9.3.6), we obtain

$$\mathbf{R}_u = \mathbf{r}_u - \frac{f_u}{f_\theta} \mathbf{r}_\theta \quad \mathbf{R}_\phi = \mathbf{r}_\phi - \frac{f_\phi}{f_\theta} \mathbf{r}_\theta \quad (9.3.14)$$

According to the definition, the envelope must be a regular surface and therefore the surface normal $\mathbf{N} \neq 0$. Thus,

$$\mathbf{N} = \mathbf{R}_\phi \times \mathbf{R}_u \neq 0 \quad (9.3.15)$$

Equations (9.3.14) and (9.3.15) yield the envelope normal

$$\mathbf{N} = (\mathbf{r}_\theta \times \mathbf{r}_\phi)f_u + (\mathbf{r}_\phi \times \mathbf{r}_u)f_\theta + (\mathbf{r}_u \times \mathbf{r}_\theta)f_\phi \neq 0$$

The theorem is proven.

Contact Lines

Each surface of the family contacts the envelope at every instance along a line which is called the characteristic or the contact line. The location of the instantaneous contact line on the contacting surface depends on the parameter of motion ϕ and is changed in the process of motion. In the coordinate system S_1 , which is rigidly connected to gear 1 with the given surface Σ_1 , the contact line is represented by the following equations:

$$\begin{aligned} \mathbf{r}_1 = \mathbf{r}_1(u, \theta) \in C^2 \quad (u, \theta) \in G \quad \{\alpha < u < \beta \text{ and } \gamma < \theta < \delta\} \\ a < \phi < b \quad f(u, \theta, \phi) = 0 \end{aligned} \quad (9.3.16)$$

Here ϕ has a fixed value ($\phi = \phi^{(1)}, \phi = \phi^{(2)}, \dots, \phi = \phi^{(n)}$).

Surface Σ_1 is covered by contact lines which will in turn come into tangency by the rotation of gear 1 (fig. 9.3.1). To determine an instantaneous point M of the contact line, the following procedure must be applied:

Step 1.—Fix the parameter of motion ϕ , for example $\phi = \phi^{(1)}$

Step 2.—Choose one of the surface parameters, for example θ , and determine u from the equation $f(u, \theta, \phi^{(1)}) = 0$

Step 3.—Determine coordinates of point M by applying the vector function $\mathbf{r}_1(u, \theta) = x_1(u, \theta)\mathbf{i}_1 + y_1(u, \theta)\mathbf{j}_1 + z_1(u, \theta)\mathbf{k}_1$

Step 4.—To determine another point M^* of the same contact line, keep the same magnitude $\phi = \phi^{(1)}$, change the surface parameter θ , and apply the procedure described previously

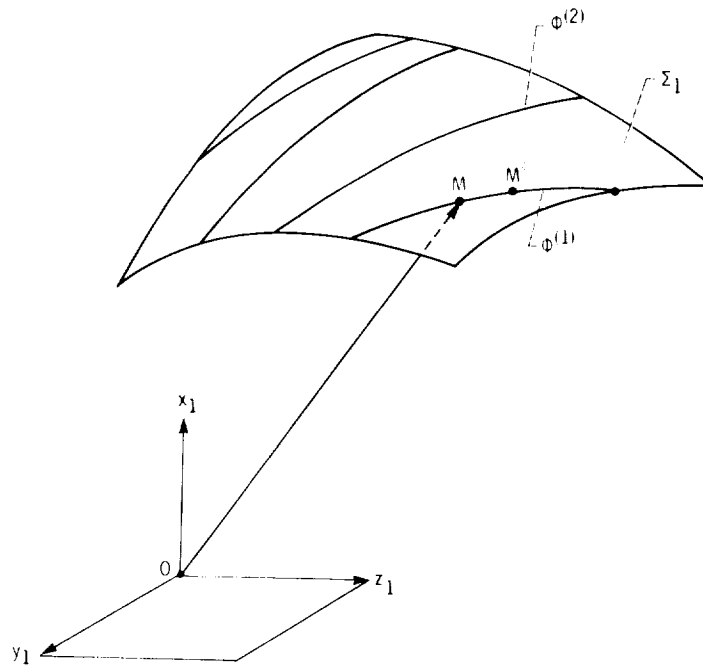


Figure 9.3.1.

The set of contact lines in the coordinate system S_f , rigidly connected to the frame, represents the surface of action Σ_f . This surface is determined by the following equations:

$$\begin{aligned} \mathbf{r}_f(u, \theta, \phi) \in C^2 \quad (u, \theta) \in G \quad \{ \alpha < u < \beta \text{ and } \gamma < \theta < \delta \} \\ a < \phi < b \quad f(u, \theta, \phi) = 0 \end{aligned} \quad (9.3.17)$$

The vector function $\mathbf{r}_f(u, \theta, \phi)$ may be determined by the matrix equation

$$[\mathbf{r}_f] = [M_{f1}][\mathbf{r}_1] \quad (9.3.18)$$

Here $[M_{f1}]$ is a 4×4 matrix which represents the coordinate transformation by transition from the coordinate system S_1 to S_f . The method to calculate the points of the contact lines on the surface of action is similar to the aforementioned procedure.

Contact lines on the envelope are represented by equations

$$\begin{aligned} \mathbf{r}_2(u, \theta, \phi) \in C^2 \quad (u, \theta) \in G \quad \{ \alpha < u < \beta \text{ and } \gamma < \theta < \delta \} \\ a < \phi < b \quad f(u, \theta, \phi) = 0 \end{aligned} \quad (9.3.19)$$

Here

$$[\mathbf{r}_2] = [M_{21}][\mathbf{r}_1] = [M_{2f}][M_{f1}][\mathbf{r}_1] \quad (9.3.20)$$

The 4×4 matrix $[M_{21}]$ represents the coordinate transformation by transition from the coordinate system S_1 to S_2 . The method to calculate the points of the contact lines is similar to the method given above.

Example 9.3.1 Consider that a gear mechanism transforms translation into rotation. Link 1 is a rack and link 2 is a gear. We set up three coordinate systems S_1 , S_2 , and S_f , rigidly connected to links 1 and 2, and to the frame, respectively (fig. 9.3.2(a)). While the rack translates a distance s the gear rotates about the z_f -axis through an angle ϕ .

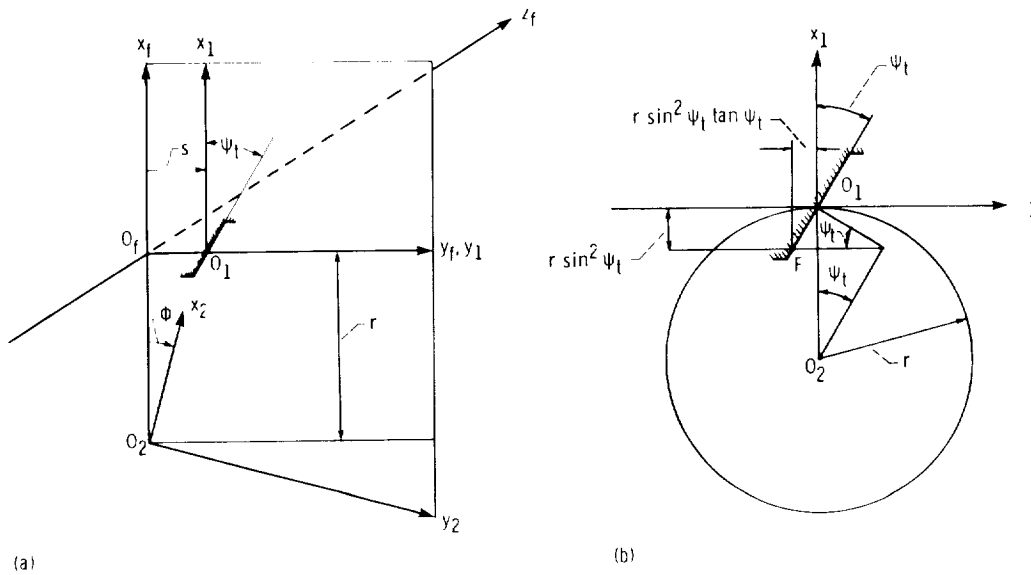


Figure 9.3.2.

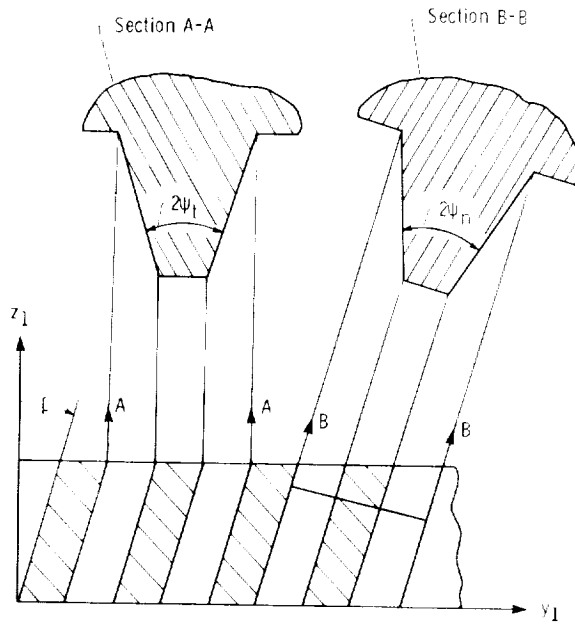


Figure 9.3.3.

Equations of rack surface Σ_1 .—Figure 9.3.3 shows sections of a rack tooth. Surface Σ_1 , which generates the surface Σ_2 of the gear tooth, is a plane. The section of Σ_1 cut by the plane $z_1 = 0$ is a straight line which forms an angle ψ_r with axis x_1 (fig. 9.3.4(a)). The section of generating surface Σ_1 cut by the plane $x_1 = 0$ is a straight line which forms an angle β with axis z_1 (fig. 9.3.4(a)).

To derive the equations of the generating surface Σ_1 , let us use an auxiliary coordinate system S_a (fig. 9.3.4(b)). Consider that a straight line L_1 is rigidly connected to the coordinate system S_a and that $\overline{O_a M}$ is the position vector of a point M of this line. The plane Σ_1 is generated in the coordinate system S_1 as a family of lines L_1 , while the coordinate system S_a translates with respect to S_1 . In this motion the axes of coordinate system S_a are parallel to the corresponding axes of coordinate system S_1 , and the origin O_a moves along the line L_2 . Homogeneous coordinates of point M (see app. A) are represented by the matrix

$$[r_a] = \begin{bmatrix} u \cos \psi_r \\ u \sin \psi_r \\ 0 \\ 1 \end{bmatrix} \quad (9.3.21)$$

where $u = |\overline{O_a M}|$.

Equations of the generating surface Σ_1 may be derived by the matrix equation

$$[r_1] = [M_{1a}][r_a] \quad (9.3.22)$$

Here $[M_{1a}]$ is the matrix of coordinate transformation by transition from S_a to S_1 (fig. 9.3.4(b)) represented as follows:

$$[M_{1a}] = \begin{bmatrix} 1 & 0 & 0 & 0 \\ 0 & 1 & 0 & \ell \sin \beta \\ 0 & 0 & 1 & \ell \cos \beta \\ 0 & 0 & 0 & 1 \end{bmatrix} \quad (9.3.23)$$

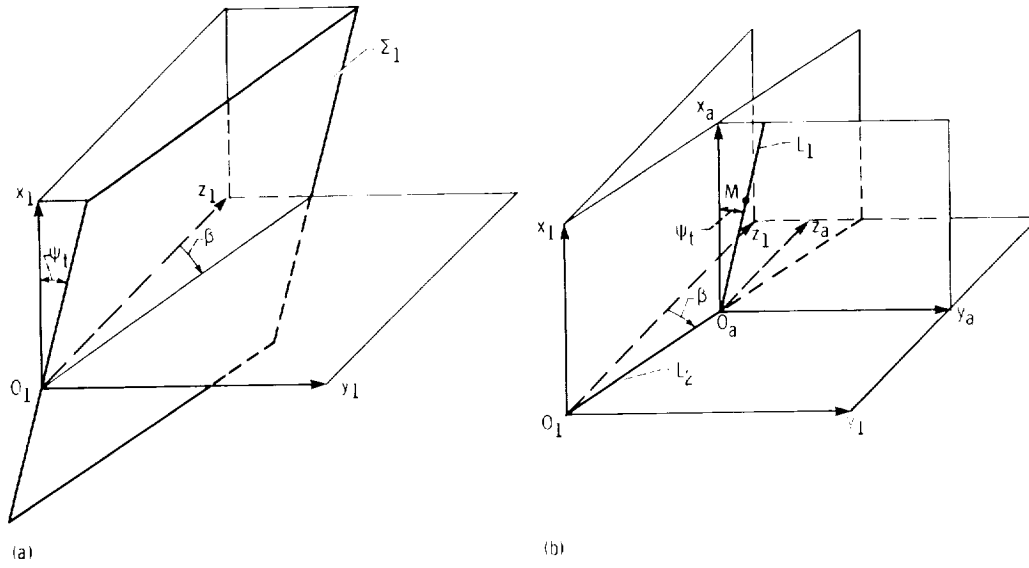


Figure 9.3.4.

where $\ell = |\overline{O_1 O_a}|$.

Equations (9.3.21) to (9.3.23) represent the generating plane Σ_1 in parametric form as follows:

$$x_1 = u \cos \psi_t \quad y_1 = u \sin \psi_t + \ell \sin \beta \quad z_1 = \ell \cos \beta \quad (9.3.24)$$

where $(u, \ell) \in E$. Here (u, ℓ) are the surface coordinates.

Consider the section of generating surface Σ_1 cut by a plane P , which is drawn through axis x_a perpendicular to the line L_2 (fig. 9.3.4(b)). This section may be represented by equations (9.3.24) and the equation

$$\frac{z_1}{y_1} = -\tan \beta \quad (9.3.25)$$

Equations (9.3.24) and (9.3.25) yield

$$x_1 = u \cos \psi_t \quad y_1 = u \sin \psi_t \cos^2 \beta \quad z_1 = -u \sin \psi_t \sin \beta \cos \beta \quad (9.3.26)$$

The unit vector of straight line (9.3.26) is

$$\tau_1 = \frac{1}{m} (\cos \psi_t \mathbf{i}_1 + \sin \psi_t \cos^2 \beta \mathbf{j}_1 - \sin \psi_t \sin \beta \cos \beta \mathbf{k}_1) \quad (9.3.27)$$

where $m^2 = \cos^2 \psi_t (1 + \tan^2 \psi_t \cos^2 \beta)$.

Applying the relation

$$\tan \psi_t \cos \beta = \tan \psi_n \quad (9.3.28)$$

we get $m = \cos \psi_t / \cos \psi_n$ and the unit vector τ_1 is

$$\tau_1 = \cos \psi_n \mathbf{i}_1 + \sin \psi_n \cos \beta \mathbf{j}_1 - \sin \psi_n \sin \beta \mathbf{k}_1 \quad (9.3.29)$$

The straight line (9.3.26) with the unit vector (9.3.29) represents the shape of a rack which is applied for spur gears.

The family of generating surfaces in the coordinate system S_2 .—This family may be represented by equations (9.3.24) and (9.3.20), where matrix $[M_{21}]$ (fig. 9.3.2(a)) is

$$[M_{21}] = [M_{2f}][M_{f1}] = \begin{bmatrix} \cos \phi & \sin \phi & 0 & r \cos \phi \\ -\sin \phi & \cos \phi & 0 & -r \sin \phi \\ 0 & 0 & 1 & 0 \\ 0 & 0 & 0 & 1 \end{bmatrix} \begin{bmatrix} 1 & 0 & 0 & 0 \\ 0 & 1 & 0 & s \\ 0 & 0 & 1 & 0 \\ 0 & 0 & 0 & 1 \end{bmatrix} \quad (9.3.30)$$

The translation s and the angle of rotation ϕ are related by

$$s = r\phi \quad (9.3.31)$$

where r is the radius of the gear 2 axoid. It is assumed that the z_f axis is the instantaneous axis of rotation in the relative motion of the rack and the gear. (See sec. 2.1.)

Equations (9.3.24), (9.3.20), (9.3.30), and (9.3.31) yield

$$\begin{aligned} x_2 &= u \cos(\phi - \psi_f) + \ell \sin \beta \sin \phi + r(\phi \sin \phi + \cos \phi) \\ y_2 &= -u \sin(\phi - \psi_f) + \ell \sin \beta \cos \phi + r(\phi \cos \phi - \sin \phi) \\ z_2 &= \ell \cos \beta \end{aligned} \quad (9.3.32)$$

where $(u, \ell) \in E$ and $a < \phi < b$.

Equation of meshing.—To get the equation of meshing, we must apply the equation

$$\left[\frac{\partial \mathbf{r}_2}{\partial u} \frac{\partial \mathbf{r}_2}{\partial \ell} \frac{\partial \mathbf{r}_2}{\partial \phi} \right] = 0 \quad (9.3.33)$$

which is similar to equation (9.3.5). From equations (9.3.32), we obtain

$$\begin{aligned} \frac{\partial \mathbf{r}_2}{\partial u} &= \cos(\phi - \psi_f) \mathbf{i}_2 - \sin(\phi - \psi_f) \mathbf{j}_2 & \frac{\partial \mathbf{r}_2}{\partial \ell} &= \sin \beta (\sin \phi \mathbf{i}_2 + \cos \phi \mathbf{j}_2) + \cos \beta \mathbf{k}_2 \\ \frac{\partial \mathbf{r}_2}{\partial \phi} &= [-u \sin(\phi - \psi_f) + \ell \sin \beta \cos \phi + r\phi \cos \phi] \mathbf{i}_2 \\ &+ [-u \cos(\phi - \psi_f) - \ell \sin \beta \sin \phi - r\phi \sin \phi] \mathbf{j}_2 \end{aligned} \quad (9.3.34)$$

Equations (9.3.33) and (9.3.34) yield the following equation of meshing:

$$f(u, \ell, \phi) = \cos \beta [\sin \psi_f (r\phi + \ell \sin \beta) + u] = 0 \quad (9.3.35)$$

Generated gear-tooth surface Σ_2 .—The tooth surface Σ_2 of the generated gear (gear 2) is represented by equations (9.3.32) and (9.3.35) as follows:

$$\mathbf{r}_2 = \mathbf{r}_2(u, \ell, \phi) \quad f(u, \ell, \phi) = 0 \quad (9.3.36)$$

This is a parametric representation of a surface with three parameters (u, ℓ, ϕ) . These three parameters are related by the equation of meshing.

Generally, it is hard (sometimes even impossible) to represent the generated surface by only two parameters. The discussed case is an exception, because the equation of meshing (9.3.35) contains all three parameters as linear parameters and it is easy to eliminate one of them from equations (9.3.32). For instance, knowing that $f_t \neq 0$ and according to the Theorem of Implicit Function System Existence (see app. B), we may solve the equation of meshing (9.3.35) in the neighborhood of point (u_0, ℓ_0, ϕ_0) by the function

$$\ell = - \left(\frac{u}{\sin \psi_t} + r\phi \right) \frac{1}{\sin \beta} \quad (9.3.37)$$

Equations (9.3.37) and (9.3.32) yield

$$\begin{aligned} x_2 &= -u \cot \psi_t \sin (\phi - \psi_t) + r \cos \phi & y_2 &= -u \cot \psi_t \cos (\phi - \psi_t) - r \sin \phi \\ z_2 &= - \left(\frac{u}{\sin \psi_t} + r\phi \right) \cot \beta \end{aligned} \quad (9.3.38)$$

It is easy to verify that surface (9.3.38) is a screw involute surface. Let us consider a cross section of the surface cut by the plane $z_2 = 0$. Equations (9.3.38) and the equation

$$u = -r\phi \sin \psi_t \quad (9.3.39)$$

represent the plane curve given by equations

$$\begin{aligned} x_2 &= -r\phi \cos \psi_t \sin (\psi_t - \phi) + r \cos \phi & y_2 &= r\phi \cos \psi_t \cos (\psi_t - \phi) - r \sin \phi \\ z_2 &= 0 \end{aligned} \quad (9.3.40)$$

These equations represent an involute curve with the base circle (fig. 9.3.5)

$$r_b = r \cos \psi_t \quad (9.3.41)$$

The geometric interpretation of equation (9.3.40) is as follows: Point I of the involute curve has coordinates $x_2 = r$ and $y_2 = 0$ and is generated when $\phi = 0$. Points up to I (i.e., point M)

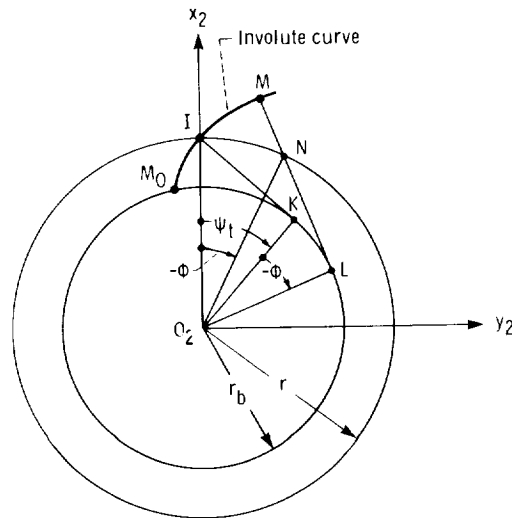


Figure 9.3.5.

correspond to positive values of the rack parameter u , and to negative values of ϕ . The position vector of point M is

$$\overline{O_2M} = \overline{O_2N} + \overline{NM} \quad (9.3.42)$$

Here $|\overline{O_2N}| = r$ and makes the angle $-\phi$ with the x_2 -axis. Vector \overline{NM} and the x_2 -axis form an angle of $90^\circ - (\psi_l - \phi)$.

According to the method of generation of involute curves

$$|\overline{NM}| = -r_b\phi = -r\phi \cos \psi_l \quad (\phi < 0) \quad (9.3.43)$$

We get equations (9.3.40) by applying equations (9.3.42) and (9.3.43) and the following equations:

$$x_2 = \overline{O_2M} \cdot i \quad y_2 = \overline{O_2M} \cdot j \quad (9.3.44)$$

Similarly, we may determine the cross section of surface (9.3.38) cut by the plane $z_2 = m$. This cross section also represents an involute curve. For the cross section $z_2 = 0$ to coincide with the cross section $z_2 = m$, we must translate the $z_2 = 0$ cross section along the z_2 -axis by an amount m and rotate about this axis by an angle ϕ^* where

$$\phi^* = \frac{m \tan \beta}{r}$$

Investigation of the generated surface Σ_2 .—Sufficient conditions of envelope existence guarantee that the generated surface is regular. The generated surface represented by

$$\mathbf{r}_2(u, l, \phi) \in C^2 \quad f(u, l, \phi) = 0 \quad f \in C^1$$

is regular if the following inequalities are observed (see inequalities (9.3.9) and (9.3.10)):

$$|f_u| + |f_l| \neq 0 \quad (9.3.45)$$

and

$$\mathbf{N} = (\mathbf{r}_l \times \mathbf{r}_\phi)f_u + (\mathbf{r}_\phi \times \mathbf{r}_u)f_l + (\mathbf{r}_u \times \mathbf{r}_l)f_\phi \neq 0 \quad (9.3.46)$$

In the case discussed above, the generated surface could be represented by two parameters instead of three. (See eqs. (9.3.38).) This simplifies the investigation of the generated surface to that of a regular surface. We say that surface (9.3.38) is regular if its normal

$$\mathbf{N} = \frac{\partial \mathbf{r}_2}{\partial u} \times \frac{\partial \mathbf{r}_2}{\partial \phi} \quad (9.3.47)$$

is not equal to zero.

Equations (9.3.38) and (9.3.47) yield

$$\begin{aligned} N_x &= \left(\frac{u \cot \psi_l}{\sin \psi_l} + r \right) \cot \beta \sin (\phi - \psi_l) & N_y &= \left(\frac{u \cot \psi_l}{\sin \psi_l} + r \right) \cot \beta \cos (\phi - \psi_l) \\ N_z &= - \left(\frac{u \cot \psi_l}{\sin \psi_l} + r \right) \cos \psi_l \end{aligned} \quad (9.3.48)$$

The normal $\mathbf{N} = 0$ for

$$\frac{u \cot \psi_t}{\sin \psi_t} + r = 0 \quad (9.3.49)$$

To avoid the appearance of singular points on the generated surface Σ_2 , it is sufficient to limit surface Σ_1 of the rack. The limiting line on the surface Σ_1 may be determined by the following equations (see eqs. (9.3.49), (9.3.37), and (9.3.24)):

$$u = -r \sin \psi_t \tan \psi_t \quad (9.3.50)$$

$$\ell = - \left(\frac{u}{\sin \psi_t} + r\phi \right) \frac{1}{\sin \beta} = \frac{r(\tan \psi_t - \phi)}{\sin \beta} \quad (9.3.51)$$

$$x_1 = -r \sin^2 \psi_t \quad y_1 = r \tan \psi_t \cos^2 \psi_t - r\phi \quad z_1 = r(\tan \psi_t - \phi) \cot \beta \quad (9.3.52)$$

Equations (9.3.52) determine the limiting line on the generating surface Σ_1 . This line may be found as the line of intersection of surface Σ_1 and the plane that is perpendicular to the x_1 -axis and is represented by the equation

$$x_1 = -r \sin^2 \psi_t \quad (9.3.53)$$

Figure 9.3.2(b) shows the cross section of Σ_1 which is formed by the cutting of Σ_1 by the plane $z_1 = 0$. Point F is the point of intersection of the limiting line of the rack cutter with the plane $z_1 = 0$. Equations (9.3.52) and $z_1 = 0$ yield $\phi = \tan \psi_t$ and the coordinates of the limiting point F are given by $x_1 = -r \sin^2 \psi_t$ and $y_1 = -r \sin^2 \psi_t \tan \psi_t$. Equation $\phi = \tan \psi_t$ determines the parameter of motion with which point F will come in tangency with the mating point of the gear.

To avoid undercutting, we have to increase the radius of the pitch circle r (by increasing the number of gear teeth) or set up appropriately the generating surface with respect to O_2 . The displacement of the rack cutter (a nonstandard machine setting of the rack cutter) is used for generation of nonstandard gears.

Surface of action.—The surface of action may be determined as the locus of contact lines represented in the fixed coordinate system S_f . The surface of action is represented by equations (9.3.24), (9.3.35), and the equation

$$[r_f] = [M_{f1}][r_1] \quad (9.3.54)$$

where (fig. 9.3.2(a))

$$[M_{f1}] = \begin{bmatrix} 1 & 0 & 0 & 0 \\ 0 & 1 & 0 & r\phi \\ 0 & 0 & 1 & 0 \\ 0 & 0 & 0 & 1 \end{bmatrix} \quad (9.3.55)$$

Using equations (9.3.24), (9.3.37), (9.3.54), and (9.3.55), we may express the surface of action by two parameters. These equations yield

$$x_f = u \cos \psi_t \quad y_f = -\frac{u \cos^2 \psi_t}{\sin \psi_t} \quad z_f = - \left(\frac{u}{\sin \psi_t} + r\phi \right) \cot \beta \quad (9.3.56)$$

Equations (9.3.56) represent the contact lines as a family of parallel straight lines. The unit vector of these straight lines is determined by

$$\boldsymbol{\tau} = \frac{\frac{\partial \mathbf{r}_f}{\partial u}}{\left| \frac{\partial \mathbf{r}_f}{\partial u} \right|} = \frac{1}{m} \left(\cos \psi_t \mathbf{i}_f - \frac{\cos^2 \psi_t}{\sin \psi_t} \mathbf{j}_f - \frac{\cot \beta}{\sin \psi_t} \mathbf{k}_f \right) \quad (9.3.57)$$

where

$$m^2 = \frac{\cos^2 \psi_t + \cot^2 \beta}{\sin^2 \psi_t}$$

It is easy to verify that the mentioned straight lines lie in a plane which passes through the z_f -axis and makes angles of $(90^\circ - \psi_t)$ and $(180^\circ - \psi_t)$ with the x_f - and y_f -axes, respectively. To prove this, we consider three vectors $\boldsymbol{\tau}$, \mathbf{k} , and \mathbf{a} , where

$$\mathbf{a} = \sin \psi_t \mathbf{i}_f - \cos \psi_t \mathbf{j}_f \quad (9.3.58)$$

Vector \mathbf{a} determines the orientation of the plane of action and \mathbf{k} is the unit vector of the z -axis. The triple product of $\boldsymbol{\tau}$, \mathbf{k} , and \mathbf{a} yields

$$[\boldsymbol{\tau} \mathbf{k} \mathbf{a}] = \begin{vmatrix} \cos \psi_t & -\frac{\cos^2 \psi_t}{\sin \psi_t} & -\frac{\cot \beta}{\sin \psi_t} \\ 0 & 0 & 1 \\ \sin \psi_t & -\cos \psi_t & 0 \end{vmatrix} = 0 \quad (9.3.59)$$

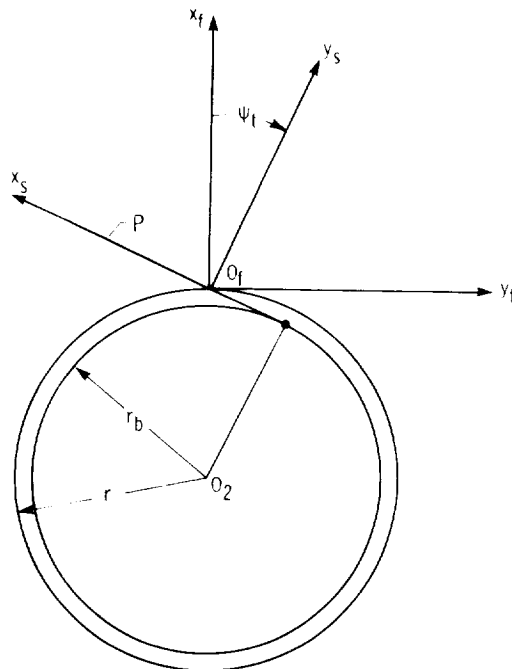


Figure 9.3.6.

Thus, the contact lines lie in the plane which is drawn through vectors \mathbf{k} and \mathbf{a} . This plane P passes through the z_f -axis and the x_s -axis (fig. 9.3.6).

Using a new coordinate system S_s (fig. 9.3.6), we may simplify the equations of contact lines. Using the matrix equation

$$[r_s] = [M_{sf}][r_f] \quad (9.3.60)$$

where

$$[M_{sf}] = \begin{bmatrix} \sin \psi_f & -\cos \psi_f & 0 & 0 \\ \cos \psi_f & \sin \psi_f & 0 & 0 \\ 0 & 0 & 1 & 0 \\ 0 & 0 & 0 & 1 \end{bmatrix} \quad (9.3.61)$$

we get the following equations of contact lines L_s on the surface of action:

$$x_s = u \cot \psi_f \quad y_s = 0 \quad z_s = -\left(\frac{u}{\sin \psi_f} + r\phi\right) \cot \beta \quad (9.3.62)$$

Contact lines L_s belong to the plane $y_s = 0$ and are parallel straight lines whose location in the plane depends on the parameter of motion ϕ (fig. 9.3.7). Contact lines L_2 , which are located on the generating surface Σ_2 , are also straight lines; but unlike contact lines L_s , the set of lines L_2 belong to the screw involute surface Σ_2 .

Particular case of a generating surface.—Consider that parameter ψ_f of the generating surface Σ_1 , represented by equations (9.3.24), is equal to zero. The generating surface Σ_1 is thus represented by the following equations:

$$x_1 = u \quad y_1 = \ell \sin \beta \quad z_1 = \ell \cos \beta \quad (9.3.63)$$

where $(u, \ell) \in E$. The equation of meshing (9.3.35) yields

$$u = 0 \quad (9.3.64)$$

The contact line on the generating surface Σ_1 is therefore represented by equations

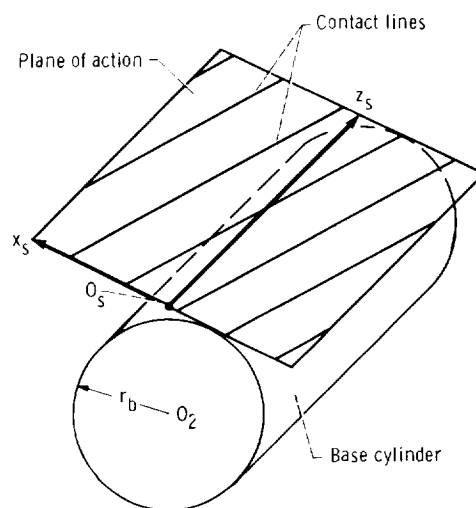


Figure 9.3.7.

$$x_1 = 0 \quad y_1 = \ell \sin \beta \quad z_1 = \ell \cos \beta \quad (9.3.65)$$

Unlike the general case discussed above, there is only one contact line on the generating surface Σ_1 which does not move over Σ_1 in the process of meshing.

Equations (9.3.64) and (9.3.32) yield the generated surface Σ_2 as

$$\begin{aligned} x_2 &= \ell \sin \beta \sin \phi + r(\phi \sin \phi + \cos \phi) & y_2 &= \ell \sin \beta \cos \phi + r(\phi \cos \phi - \sin \phi) \\ z_1 &= \ell \cos \beta \end{aligned} \quad (9.3.66)$$

This surface is a screw involute surface with the base cylinder $r_b = r$.

The surface normal is

$$\mathbf{N} = \frac{\partial \mathbf{r}_2}{\partial \ell} \times \frac{\partial \mathbf{r}_2}{\partial \phi} = (\ell \sin \beta + r\phi)(\cos \beta \sin \phi \mathbf{i}_2 + \cos \beta \cos \phi \mathbf{j}_2 - \sin \beta \mathbf{k}_2) \quad (9.3.67)$$

Singular points on surface Σ_2 exist for $\mathbf{N} = 0$, which yields the following relation between the surface parameters:

$$\ell \sin \beta + r\phi = 0 \quad (9.3.68)$$

Equations (9.3.66) and (9.3.68) yield that singular points of surface Σ_2 compose a helix which belongs to the base cylinder of radius r and is represented by the equations

$$x_2 = r \cos \phi \quad y_2 = -r \sin \phi \quad z_2 = -r\phi \cot \beta \quad (9.3.69)$$

Appearance of singular points on the surface Σ_2 may be avoided by the limitation of the range of motion parameter ϕ .

9.4 Envelope of a Locus of Surfaces: Representation in Implicit Form

Representation of surfaces in parametric form is preferable to the implicit representation because it allows more freedom for investigation. However, we will also discuss the implicit representation so as to completely describe all methods of investigation.

We set up the same coordinate systems S_1 , S_2 , and S_f used in section 9.2. Consider a locus (family) of simple and regular surfaces given by expressions similar to (9.2.7)

$$G(x, y, z, \phi) = 0 \quad G \in C^1 \quad \left| \frac{\partial G}{\partial x} \right| + \left| \frac{\partial G}{\partial y} \right| + \left| \frac{\partial G}{\partial z} \right| \neq 0 \quad (x, y, z) \in A \quad a < \phi < b \quad (9.4.1)$$

The subscript 2 was dropped to simplify the designations. Equations (9.4.1) represent, in coordinate system S_2 , a simple and regular surface Σ_1 for any fixed-motion parameter ϕ .

A piece of the envelope of a locus of simple and regular surfaces Σ_1 , represented in implicit form, is a regular surface determined by

$$\mathbf{R}(z, \phi) = \mathbf{r}(x(z(\phi)), y(z(\phi)), z) \in C^1 \quad \mathbf{R}_z \times \mathbf{R}_\phi \neq 0 \quad z_1 < z < z_2 \quad a < \phi < b \quad (9.4.2)$$

if for any value of ϕ_0 the surface $G(x, y, z, \phi_0)$ is in tangency with the envelope $\mathbf{R}(z, \phi)$.

Another parameter, x or y , may be chosen instead of z so that the envelope may be represented by the vector function $\mathbf{R}(x, \phi)$ or $\mathbf{R}(y, \phi)$, respectively, instead of the vector function $\mathbf{R}(z, \phi)$. The following discussion may be used for such a new case just by changing the designations of the coordinate axes.

Similar to the discussions of section 9.3, we will differentiate the necessary and sufficient conditions of existence of an envelope of a locus of surfaces given in the implicit form. Necessary conditions of existence state the ability of a generating surface to be in tangency with the envelope if the envelope exists. Sufficient conditions state the requirements which, if observed, insure the existence of the envelope, its tangency with the generating surface, and regularity of the envelope for any fixed value of motion parameter ϕ .

Theorem of Necessary Conditions of Envelope Existence Consider the family of surfaces Σ_1 given by equation (9.4.1) and assume that the envelope Σ_2 and surface Σ_1 are in tangency at the point $M(x_0, y_0, z_0, \phi_0)$. Then the point M belongs to the set of points determined by the equation

$$G_\phi(x, y, z, \phi) = 0 \quad (9.4.3)$$

where G_ϕ is the designation of $\partial G / \partial \phi$.

Proof: Consider that the inequality in expression (9.4.1) is observed at point M just because $G_z \neq 0$. According to the Theorem of Implicit Function System Existence (see app. B), the equation

$$G(x, y, z, \phi) = 0 \quad (9.4.4)$$

may be solved in the neighborhood of point M by the function

$$z(x, y, \phi) \in C^1 \quad (9.4.5)$$

Then the locus of surfaces (9.4.1) may be represented locally in parametric form as follows:

$$\mathbf{r}(x, y, z, \phi) = \mathbf{r}(x, y, z(x, y, \phi)) \in C^1 \quad (9.4.6)$$

Here (x, y) are the surface coordinates and ϕ is the motion parameter. The differentiation of equation (9.4.6) gives

$$\mathbf{r}_x = \{1, 0, z_x\} \quad \mathbf{r}_y = \{0, 1, z_y\} \quad \mathbf{r}_\phi = \{0, 0, z_\phi\} \quad (9.4.7)$$

Equations

$$G(x, y, z, \phi) = 0 \quad z - z(x, y, \phi) = 0 \quad (9.4.8)$$

yield

$$G_x dx + G_y dy + G_\phi d\phi = -G_z dz \quad z_x dx + z_y dy + z_\phi d\phi = dz \quad (9.4.9)$$

It results from equations (9.4.9) that

$$\frac{-\frac{G_x}{G_z}}{z_x} = \frac{-\frac{G_y}{G_z}}{z_y} = \frac{-\frac{G_\phi}{G_z}}{z_\phi} = 1 \quad (9.4.10)$$

Equations (9.4.7) and (9.4.10) yield that

$$\mathbf{r}_x = \left\{ 1, 0, -\frac{G_x}{G_z} \right\} \quad \mathbf{r}_y = \left\{ 0, 1, -\frac{G_y}{G_z} \right\} \quad \mathbf{r}_\phi = \left\{ 0, 0, -\frac{G_\phi}{G_z} \right\} \quad (9.4.11)$$

and

$$\begin{aligned} d\mathbf{r} &= \mathbf{r}_x dx + \mathbf{r}_y dy + \mathbf{r}_\phi d\phi \\ &= dx \left(\mathbf{i} - \frac{G_x}{G_z} \mathbf{k} \right) + dy \left(\mathbf{j} - \frac{G_y}{G_z} \mathbf{k} \right) - \frac{G_\phi}{G_z} d\phi \mathbf{k} \\ &= dx \mathbf{i} + dy \mathbf{j} - \frac{G_x dx + G_y dy + G_\phi d\phi}{G_z} \mathbf{k} \end{aligned} \quad (9.4.12)$$

Vector $d\mathbf{r}$ represents the infinitesimal displacement of a point in absolute motion as the sum of two components; (1) a component in transfer motion with the surface Σ_1 (this is the component $\mathbf{r}_\phi d\phi$), and (2) a component in relative motion over the surface Σ_1 (this is the component $\mathbf{r}_x dx + \mathbf{r}_y dy$). Vector $d\mathbf{r}$ belongs to a plane tangent to the envelope Σ_2 .

Let us now determine the vector $\delta\mathbf{r}$ of the displacement of a point over the surface Σ_1 . Fixing the parameter of motion ϕ and differentiating function (9.4.6), we get

$$\begin{aligned} \delta\mathbf{r} &= \mathbf{r}_x \delta x + \mathbf{r}_y \delta y \\ &= \delta x \mathbf{i} + \delta y \mathbf{j} - \frac{G_x \delta x + G_y \delta y}{G_z} \mathbf{k} \end{aligned} \quad (9.4.13)$$

Due to the continuous tangency of surfaces Σ_1 and Σ_2 in the neighborhood of their common point M , vectors $d\mathbf{r}$ and $\delta\mathbf{r}$ are collinear. Thus,

$$d\mathbf{r} = \lambda \delta\mathbf{r} \quad (\lambda \neq 0) \quad (9.4.14)$$

Equations (9.4.12) to (9.4.14) yield

$$\frac{dx}{\delta x} = \frac{dy}{\delta y} = \frac{G_x dx + G_y dy + G_\phi d\phi}{G_x \delta x + G_y \delta y} = \lambda \quad (9.4.15)$$

Equations (9.4.15) may be observed if, and only if, $G_\phi d\phi = 0$. It is easy to verify that $d\phi \neq 0$ because the envelope points correspond to the continuously changing values of parameter ϕ , and $G_\phi d\phi = 0$ because $G_\phi = 0$. The theorem is proven.

Theorem of Sufficient Conditions of Envelope Existence Consider a family of surfaces given by

$$G(x, y, z, \phi) = 0 \quad G \in C^2 \quad |G_x| + |G_y| + |G_z| \neq 0 \quad (x, y, z) \in A \quad a < \phi < b \quad (9.4.16)$$

If at a point $M(x_0, y_0, z_0, \phi)$ the following conditions are observed:

$$G(x_0, y_0, z_0, \phi_0) = 0 \quad G_\phi = 0 \quad G_{\phi\phi} \neq 0$$

$$\Delta = \left| \frac{D(G, G_\phi)}{D(x, y)} \right| + \left| \frac{D(G, G_\phi)}{D(x, z)} \right| + \left| \frac{D(G, G_\phi)}{D(y, z)} \right| \neq 0 \quad (9.4.17)$$

then an envelope piece exists in the neighborhood of point M and the envelope is a regular surface that may be represented by equations

$$G(x, y, z, \phi) = 0 \quad \text{and} \quad G_\phi(x, y, z, \phi) = 0 \quad (9.4.18)$$

Proof: Assume that equations

$$G(x, y, z, \phi) = 0 \quad G_\phi(x, y, z, \phi) = 0 \quad G \in C^2 \quad (9.4.19)$$

are satisfied at the point $M(x_0, y_0, z_0, \phi_0)$, and the sum of the determinants $\Delta \neq 0$ because the determinant

$$\frac{D(G, G_\phi)}{D(x, y)} \neq 0 \quad (9.4.20)$$

According to the Theorem of Implicit Function System Existence (see app. B), equation $G(x, y, z, \phi) = 0$ may then be solved in the neighborhood of point M by functions

$$x(z, \phi) \in C^1 \quad y(z, \phi) \in C^1 \quad (9.4.21)$$

and the envelope may be represented in parametric form as follows:

$$\mathbf{R}(z, \phi) = \mathbf{r}(x(z, \phi), y(z, \phi), z) \quad (9.4.22)$$

The plane which is tangent to surface (9.4.22) may be determined by the vectors

$$\mathbf{R}_z = \{x_z, y_z, 1\} \quad \mathbf{R}_\phi = \{x_\phi, y_\phi, 0\} \quad (9.4.23)$$

A point of surface (9.4.22) is regular if the surface normal

$$\mathbf{N}^* = \mathbf{R}_z \times \mathbf{R}_\phi \neq 0 \quad (9.4.24)$$

Equations (9.4.23) yield that the envelope is a regular surface if its normal

$$\mathbf{N}^* = -y_\phi \mathbf{i} + x_\phi \mathbf{j} + \begin{vmatrix} x_z & y_z \\ x_\phi & y_\phi \end{vmatrix} \mathbf{k} \neq 0 \quad (9.4.25)$$

The generating surface Σ_1 is a regular surface because (see expressions (9.4.1))

$$|G_x| + |G_y| + G_z \neq 0$$

The normal \mathbf{N} to the generating surface Σ_1 may be determined in the coordinate system S_2 by

$$\mathbf{N} = G_x \mathbf{i} + G_y \mathbf{j} + G_z \mathbf{k} \quad (9.4.26)$$

The generating surface Σ_1 and the envelope Σ_2 are in tangency if their normals differ from zero and are collinear; that is, if

$$\mathbf{N}^* = \lambda \mathbf{N} \quad (\mathbf{N}^* \neq 0, \mathbf{N} \neq 0, \lambda \neq 0) \quad (9.4.27)$$

or if

$$\frac{N_x^*}{N_x} = \frac{N_y^*}{N_y} = \frac{N_z^*}{N_z} = \lambda \quad |N_x^*| + |N_y^*| + |N_z^*| \neq 0 \quad |N_x| + |N_y| + |N_z| \neq 0 \quad \lambda \neq 0 \quad (9.4.28)$$

Let us determine conditions by which expressions (9.4.28) may be observed. We begin with the differentiation of equations

$$G(x(z, \phi), y(z, \phi), z, \phi) = 0 \quad (9.4.29)$$

$$G_\phi(x(z, \phi), y(z, \phi), z, \phi) = 0 \quad (9.4.30)$$

We get

$$\frac{\partial G}{\partial z} = G_x x_z + G_y y_z + G_z = 0 \quad (9.4.31)$$

$$\frac{\partial G}{\partial \phi} = G_x x_\phi + G_y y_\phi + G_\phi = G_x x_\phi + G_y y_\phi = 0 \quad (9.4.32)$$

because $G_\phi = 0$;

$$\frac{\partial}{\partial z}(G_\phi) = G_{\phi x} x_z + G_{\phi y} y_z + G_{\phi z} = 0 \quad (9.4.33)$$

$$\frac{\partial}{\partial \phi}(G_\phi) = G_{\phi x} x_\phi + G_{\phi y} y_\phi + G_{\phi \phi} = 0 \quad (9.4.34)$$

We may represent these equations as two subsystems of two equations in two unknowns. Equations (9.4.31) and (9.4.33) yield

$$x_z = \frac{\begin{vmatrix} G_y & G_z \\ G_{\phi y} & G_{\phi z} \end{vmatrix}}{\begin{vmatrix} G_x & G_y \\ G_{\phi x} & G_{\phi y} \end{vmatrix}} \quad y_z = \frac{\begin{vmatrix} G_z & G_x \\ G_{\phi z} & G_{\phi x} \end{vmatrix}}{\begin{vmatrix} G_x & G_y \\ G_{\phi x} & G_{\phi y} \end{vmatrix}} \quad (9.4.35)$$

Similarly, considering the subsystem of equations (9.4.32) and (9.4.34), we get

$$x_\phi = \frac{\begin{vmatrix} G_y & 0 \\ G_{\phi y} & G_{\phi \phi} \end{vmatrix}}{\begin{vmatrix} G_x & G_y \\ G_{\phi x} & G_{\phi y} \end{vmatrix}} \quad y_\phi = \frac{\begin{vmatrix} G_x & 0 \\ G_{\phi x} & -G_{\phi \phi} \end{vmatrix}}{\begin{vmatrix} G_x & G_y \\ G_{\phi x} & G_{\phi y} \end{vmatrix}} \quad (9.4.36)$$

Equations (9.4.36) yield that

$$|x_\phi| + |y_\phi| \neq 0 \quad (9.4.37)$$

if the following conditions are observed:

$$G_{\phi\phi} \neq 0 \quad (9.4.38)$$

$$|G_y| + |G_x| \neq 0 \quad (9.4.39)$$

and

$$\frac{D(G, G_\phi)}{D(x, y)} = \begin{vmatrix} G_x & G_y \\ G_{\phi x} & G_{\phi y} \end{vmatrix} \neq 0 \quad (9.4.40)$$

According to equations (9.4.25), the envelope normal \mathbf{N}^* differs from zero if inequality (9.4.37) is observed.

To prove the collinearity of surface normals \mathbf{N}^* and \mathbf{N} , we must prove that expressions (9.4.28) are observed. Using expressions (9.4.25), (9.4.26), and (9.4.28), we get

$$-\frac{y_\phi}{G_x} = \frac{x_\phi}{G_y} = \frac{x_z y_\phi - y_z x_\phi}{G_z} \quad (9.4.41)$$

Using expressions (9.4.35) and (9.4.36) for x_z and y_z and x_ϕ and y_ϕ , respectively, we find that equations (9.4.41) are indeed observed, surface normals \mathbf{N}^* and \mathbf{N} are collinear, and the envelope Σ_2 is in tangency with the generating surface Σ_1 .

Remark: It is easy to verify that tangent \mathbf{T} to the contact line of surfaces Σ_1 and Σ_2 is represented by vector \mathbf{R}_z . This statement is based on the following consideration: The envelope is represented by the vector function $\mathbf{R}(z, \phi)$. Fixing the parameter of motion ϕ , we get that the tangent \mathbf{T} is

$$\mathbf{T} = \mathbf{R}_z = x_z \mathbf{i} + y_z \mathbf{j} + \mathbf{k} \quad (9.4.42)$$

Here x_z and y_z are represented by equations (9.4.35).

Example 9.4.1 With the same conditions as those stated for example 9.3.1, let us consider that the generating surface Σ_1 is represented in implicit form by the equation

$$x_1 \tan \psi_t - y_1 + z_1 \tan \beta = 0 \quad (x_1, y_1, z_1) \in B \quad (9.4.43)$$

This equation may be derived on the basis of equations (9.3.24). Let us determine the envelope, surface of action, and contact lines.

Family of generating surfaces in the coordinate system S_2 .—The coordinate transformation from coordinate system S_2 to S_1 is represented by matrix $[M_{12}]$, which is the inverse of matrix $[M_{21}]$ represented by expressions (9.3.30). We get

$$[M_{12}] = \begin{bmatrix} \cos \phi & -\sin \phi & 0 & -r \\ \sin \phi & \cos \phi & 0 & -r\phi \\ 0 & 0 & 1 & 0 \\ 0 & 0 & 0 & 1 \end{bmatrix} \quad (9.4.44)$$

and

$$x_1 = x_2 \cos \phi - y_2 \sin \phi - r \quad y_1 = x_2 \sin \phi + y_2 \cos \phi - r\phi \quad z_1 = z_2 \quad (9.4.45)$$

Equations (9.4.45) and (9.4.43) yield

$$G(x_2, y_2, z_2, \phi) = -x_2 \sin(\phi - \psi_i) - y_2 \cos(\phi - \psi_i) + z_2 \cos \psi_i \tan \beta + r(\phi \cos \psi_i - \sin \psi_i) = 0 \quad (9.4.46)$$

where

$$(x_2, y_2, z_2) \in E$$

$$a < \phi < b$$

Equation (9.4.46) represents the family of generating surfaces.

Envelope equations.—The necessary condition of envelope existence yields

$$G_{\phi}(x_2, y_2, z_2, \phi) = -x_2 \cos(\phi - \psi_i) + y_2 \sin(\phi - \psi_i) + r \cos \psi_i = 0 \quad (9.4.47)$$

If sufficient conditions of envelope existence are observed (see expressions (9.4.16) and (9.4.17)), equations (9.4.46) and (9.4.47) represent the envelope (the generated surface Σ_2) as a regular surface. The envelope is a screw involute surface. To prove this, we may investigate cross sections of the envelope by setting $z_2 = \text{constant}$ in equation (9.4.46). (See example 9.3.1.)

Singular points of the generated surface.—Singular points occur on the generated surface if $G_{\phi\phi} = 0$, which yields

$$G_{\phi\phi} = x_2 \sin(\phi - \psi_i) + y_2 \cos(\phi - \psi_i) = 0 \quad (9.4.48)$$

With $G_{\phi\phi} = 0$, the generated surface normal \mathbf{N}^* cannot differ from zero.

Singular points on the generated surface are determined by equations (9.4.46) to (9.4.48) which yield

$$x_2 = r_b \cos(\phi - \psi_i) \quad y_2 = -r_b \sin(\phi - \psi_i) \quad z_2 = -r_b \tan \lambda_b (\phi - \tan \psi_i) \quad (9.4.49)$$

Here $r_b = r \cos \psi_i$ is the radius of the base cylinder, $r_b \tan \lambda_b = r \cot \beta$ is the screw parameter h , and λ_b is the lead angle on the base cylinder. Equations (9.4.49) represent a helix on the base cylinder.

Surface of action.—The surface of action is the locus of contact lines determined in the fixed coordinate system S_f (S_f is rigidly connected to the frame). The contact lines in coordinate system S_2 (contact lines on the envelope) are represented by equations (9.4.46) and (9.4.47). To develop equations of contact lines in coordinate system S_f , it is necessary: (1) to determine equations

$$x_2 = x_2(x_f, y_f, z_f, \phi) \quad y_2 = y_2(x_f, y_f, z_f, \phi) \quad z_2 = z_2(x_f, y_f, z_f, \phi) \quad (9.4.50)$$

which express the coordinate transformation from S_f to S_2 and (2) to substitute (x_2, y_2, z_2) into equations (9.4.46) and (9.4.47) using expressions (9.4.50).

Equations (9.4.50) may be derived from the matrix equation

$$[r_2] = [M_{2f}][r_f] \quad (9.4.51)$$

where (fig. 9.3.2)

$$[M_{2f}] = \begin{bmatrix} \cos \phi & \sin \phi & 0 & r \cos \phi \\ -\sin \phi & \cos \phi & 0 & -r \sin \phi \\ 0 & 0 & 1 & 0 \\ 0 & 0 & 0 & 1 \end{bmatrix} \quad (9.4.52)$$

Equations (9.4.51) and (9.4.52) yield

$$\begin{aligned} x_2 &= x_f \cos \phi + y_f \sin \phi + r \cos \phi & y_2 &= -x_f \sin \phi + y_f \cos \phi - r \sin \phi \\ z_2 &= z_f \end{aligned} \quad (9.4.53)$$

Using equations (9.4.46), (9.4.47), and (9.4.53), we get the following equations of coordinate lines in coordinate system S_f :

$$x_f \tan \psi_t - y_f + z_f \tan \beta + r\phi = 0 \quad (9.4.54)$$

$$x_f \cos \psi_t + y_f \sin \psi_t = 0 \quad (9.4.55)$$

By fixing the parameter of motion ϕ , equations (9.4.54) and (9.4.55) represent contact line L as a straight line. Line L is the line of intersection of two planes: (1) generating plane Σ_1 , which is represented by equation (9.4.54) and (2) plane P , which is represented by equation (9.4.55). Plane P passes through axis z_f and is tangent to the cylinder of radius $r_b = r \cos \psi_t$ (fig. 9.3.6). The surface of action is the plane $y_s = 0$. All contact lines represented in the coordinate system S_f belong to the plane $y_s = 0$ (figs. 9.3.6 and 9.3.7).

9.5 Theorem of Singular Points of Generated Surface Σ_2

Sufficient conditions of envelope existence given in equations (9.3.8) to (9.3.10), if observed, guarantee that the generated surface Σ_2 is the envelope of the locus (family) of regular surfaces and all points of the envelope are regular points.

We consider the case when one of the requirements above $N_2 \neq 0$ is not observed (N_2 is the surface Σ_2 normal) and singular points on the generated surface Σ_2 occur. The locus of these points may be the edge of regression, the line which connects two pieces of the generated surface (fig. 8.3.1(b)). Appearance of such a line means that the generated surface will be undercut by the generating surface Σ_1 (the tool surface). This is the reason why the existence of singular points of surface Σ_2 is to be investigated.

We may determine singular points of surface Σ_2 by setting $N_2 = 0$ in inequality (9.3.10). But this method requires complicated transformations and therefore a more simple and effective method (proposed by Litvin, 1968) is applied. The essence of this method is based on the following theorem.

Theorem Consider a family of surfaces in the coordinate systems S_2 given by

$$\mathbf{r}_2(u, \theta, \phi) \in C^2 \quad \frac{\partial \mathbf{r}_2}{\partial u} \times \frac{\partial \mathbf{r}_2}{\partial \theta} \neq 0 \quad (u, \theta) \in G \quad a < \phi < b \quad (9.5.1)$$

Point $M(u_0, \theta_0, \phi_0)$ is given in the space of parameters (u, θ, ϕ) and at this point the following requirements are observed:

$$f(u, \theta, \phi) = \left[\frac{\partial \mathbf{r}_2}{\partial u} \frac{\partial \mathbf{r}_2}{\partial \theta} \frac{\partial \mathbf{r}_2}{\partial \phi} \right] = 0 \quad f \in C^1 \quad (9.5.2)$$

$$|f_u| + |f_\theta| \neq 0 \quad (9.5.3)$$

$$\frac{\partial \mathbf{r}_2}{\partial u} \frac{du}{dt} + \frac{\partial \mathbf{r}_2}{\partial \theta} \frac{d\theta}{dt} + \frac{\partial \mathbf{r}_2}{\partial \phi} \frac{d\phi}{dt} = 0 \quad (9.5.4)$$

A piece of the generated surface Σ_2 passes through point $Q(x_2, y_2, z_2)$, which corresponds to point $M(u_0, \theta_0, \phi_0)$. This surface piece may be represented by

$$\mathbf{R}_2(u, \phi) = \mathbf{r}_2(u, \theta(u, \phi), \phi) \in C^1 \quad (9.5.5)$$

if $f_\theta \neq 0$, or by

$$\mathbf{R}^*(\theta, \phi) = \mathbf{r}_2(u(\theta, \phi), \theta, \phi) \in C^1 \quad (9.5.6)$$

if

$$f_u \neq 0$$

At point Q the normal \mathbf{N}_2 of the surface, given by vector function (9.5.5) or (9.5.6), is equal to zero and point Q is a singular point.

Proof: Consider that the inequality (9.5.3) is observed just because $f_\theta \neq 0$. Then equation (9.5.2) may be solved in the neighborhood of point M by the function (see app. B)

$$\theta(u, \phi) \in C^1 \quad (9.5.7)$$

As a result of expression (9.5.7), a piece of surface Σ_2 may be represented by equation (9.5.5). To prove that point Q of this surface is a singular point, let us consider the following system of four linear equations in three unknowns (du/dt , $d\theta/dt$, $d\phi/dt$):

$$a_{i1} \frac{du}{dt} + a_{i2} \frac{d\theta}{dt} + a_{i3} \frac{d\phi}{dt} = 0 \quad (i = 1, 2, 3, 4) \quad (9.5.8)$$

Here

$$\begin{aligned} a_{11} &= \frac{\partial x_2}{\partial u} & a_{12} &= \frac{\partial x_2}{\partial \theta} & a_{13} &= \frac{\partial x_2}{\partial \phi} \\ a_{21} &= \frac{\partial y_2}{\partial u} & a_{22} &= \frac{\partial y_2}{\partial \theta} & a_{23} &= \frac{\partial y_2}{\partial \phi} \\ a_{31} &= \frac{\partial z_2}{\partial u} & a_{32} &= \frac{\partial z_2}{\partial \theta} & a_{33} &= \frac{\partial z_2}{\partial \phi} \\ a_{41} &= f_u & a_{42} &= f_\theta & a_{43} &= f_\phi \end{aligned} \quad (9.5.9)$$

By a randomly chosen value of $d\phi/dt \neq 0$, the system of equations (9.5.8) has a unique solution for du/dt and $d\theta/dt$ if the rank of matrix

$$\begin{bmatrix} a_{11} & a_{12} & a_{13} \\ a_{21} & a_{22} & a_{23} \\ a_{31} & a_{32} & a_{33} \\ a_{41} & a_{42} & a_{43} \end{bmatrix}$$

is equal to two. Consequently, four determinants of the third order must be equal to zero.

$$\frac{D(x_2, y_2, z_2)}{D(u, \theta, \phi)} = \begin{vmatrix} \frac{\partial x_2}{\partial u} & \frac{\partial x_2}{\partial \theta} & \frac{\partial x_2}{\partial \phi} \\ \frac{\partial y_2}{\partial u} & \frac{\partial y_2}{\partial \theta} & \frac{\partial y_2}{\partial \phi} \\ \frac{\partial z_2}{\partial u} & \frac{\partial z_2}{\partial \theta} & \frac{\partial z_2}{\partial \phi} \end{vmatrix} = 0 \quad (9.5.11)$$

$$\frac{D(y_2, z_2, f)}{D(u, \theta, \phi)} = \frac{D(z_2, x_2, f)}{D(u, \theta, \phi)} = \frac{D(x_2, y_2, f)}{D(u, \theta, \phi)} = 0 \quad (9.5.12)$$

Equation (9.5.11) is the same as equation (9.5.2). Equations (9.5.12), if observed, yield that the surface normal $\mathbf{N}_2 = 0$. To prove this statement, let us transform the equation of the normal \mathbf{N}_2 . According to expression (9.3.10), we get

$$\mathbf{N}_2 = \left(\frac{\partial \mathbf{r}_2}{\partial \theta} \times \frac{\partial \mathbf{r}_2}{\partial \phi} \right) f_u + \left(\frac{\partial \mathbf{r}_2}{\partial \phi} \times \frac{\partial \mathbf{r}_2}{\partial u} \right) f_\theta + \left(\frac{\partial \mathbf{r}_2}{\partial u} \times \frac{\partial \mathbf{r}_2}{\partial \theta} \right) f_\phi \quad (9.5.13)$$

Equation (9.5.13) yields

$$N_{x_2} = \begin{vmatrix} \frac{\partial y_2}{\partial u} & \frac{\partial y_2}{\partial \theta} & \frac{\partial y_2}{\partial \phi} \\ \frac{\partial z_2}{\partial u} & \frac{\partial z_2}{\partial \theta} & \frac{\partial z_2}{\partial \phi} \\ f_u & f_\theta & f_\phi \end{vmatrix} = \frac{D(y_2, z_2, f)}{D(u, \theta, \phi)} \quad (9.5.14)$$

$$N_{y_2} = \begin{vmatrix} \frac{\partial z_2}{\partial u} & \frac{\partial z_2}{\partial \theta} & \frac{\partial z_2}{\partial \phi} \\ \frac{\partial x_2}{\partial u} & \frac{\partial x_2}{\partial \theta} & \frac{\partial x_2}{\partial \phi} \\ f_u & f_\theta & f_\phi \end{vmatrix} = \frac{D(z_2, x_2, f)}{D(u, \theta, \phi)} \quad (9.5.15)$$

$$N_{z_2} = \begin{vmatrix} \frac{\partial x_2}{\partial u} & \frac{\partial x_2}{\partial \theta} & \frac{\partial x_2}{\partial \phi} \\ \frac{\partial y_2}{\partial u} & \frac{\partial y_2}{\partial \theta} & \frac{\partial y_2}{\partial \phi} \\ f_u & f_\theta & f_\phi \end{vmatrix} = \frac{D(x_2, y_2, f)}{D(u, \theta, \phi)} \quad (9.5.16)$$

Equations (9.5.12) to (9.5.16) yield, if conditions (9.5.2) to (9.5.4) are observed, the normal $\mathbf{N}_2 = 0$ and singular points on the generated surface occur.

The kinematic interpretation of this theorem may simplify its applications to the problem of avoiding undercutting of the generated gear. Consider the generated surfaces Σ_2 , which is represented in the coordinate system S_2 as follows:

$$\mathbf{r}_2 = \mathbf{r}_2(u, \theta, \phi) \in C^1 \quad f(u, \theta, \phi) = 0 \quad (9.5.17)$$

Vector function $\mathbf{r}_2(u, \theta, \phi)$ represents, in coordinate system S_2 , the locus of generating surfaces Σ_1 ; $f(u, \theta, \phi) = 0$ is the equation of meshing.

Differentiating equations (9.5.17), we receive

$$\dot{\mathbf{r}}_2 = \frac{\partial \mathbf{r}_2}{\partial u} \frac{du}{dt} + \frac{\partial \mathbf{r}_2}{\partial \theta} \frac{d\theta}{dt} + \frac{\partial \mathbf{r}_2}{\partial \phi} \frac{d\phi}{dt} \quad \frac{\partial f}{\partial u} \frac{du}{dt} + \frac{\partial f}{\partial \theta} \frac{d\theta}{dt} + \frac{\partial f}{\partial \phi} \frac{d\phi}{dt} = 0 \quad (9.5.18)$$

Here $\dot{\mathbf{r}}_2 \equiv \mathbf{v}_r^{(2)}$ is the velocity of the contact point in its motion with respect to the coordinate system S_2 (over the generated surface Σ_2). The velocity vector $\mathbf{v}_r^{(2)}$ may be represented as a sum of two components (1) $\mathbf{v}_r^{(1)}$, the velocity of a point which moves over the surface Σ_1 and (2) $\mathbf{v}^{(12)}$ the velocity of sliding (the velocity of a point which is rigidly connected to the generating surface Σ_1 and moves with respect to Σ_2). Thus,

$$\mathbf{v}_r^{(2)} = \mathbf{v}_r^{(1)} + \mathbf{v}^{(12)} \quad (9.5.19)$$

where

$$\mathbf{v}_r^{(1)} = \frac{\partial \mathbf{r}_2}{\partial u} \frac{du}{dt} + \frac{\partial \mathbf{r}_2}{\partial \theta} \frac{d\theta}{dt} \quad (9.5.20)$$

$$\mathbf{v}^{(12)} = \frac{\partial \mathbf{r}_2}{\partial \phi} \frac{d\phi}{dt} \quad (9.5.21)$$

According to the theorem discussed, singular points on the generated surface Σ_2 occur if equation (9.5.4) is observed. Equations (9.5.4) and (9.5.18) to (9.5.21) yield that singular points of surface Σ_2 occur if the velocity of the contact point in its motion over Σ_2 is equal to zero; that is, if

$$\mathbf{v}_r^{(2)} = \mathbf{v}_r^{(1)} + \mathbf{v}^{(12)} = 0 \quad (9.5.22)$$

Equation (9.5.22) is invariant under the applied coordinate system. Particularly, we may express vectors of this equation in terms of components of coordinate system S_1 . Consequently, we may consider equations

$$\frac{\partial \mathbf{r}_1}{\partial u} \frac{du}{dt} + \frac{\partial \mathbf{r}_1}{\partial \theta} \frac{d\theta}{dt} + \mathbf{v}_1^{(12)} = 0 \quad (9.5.23)$$

$$f_u \frac{du}{dt} + f_\theta \frac{d\theta}{dt} + f_\phi \frac{d\phi}{dt} = 0 \quad (9.5.24)$$

Here $\mathbf{v}_1^{(12)}$ is the velocity of sliding expressed in terms of components of coordinate system S_1 .

Equations (9.5.23) and (9.5.24) yield a system of four linear equations in two unknowns, which is similar to the system in equation (9.5.8) and is represented by

$$a_{i1} \frac{du}{dt} + a_{i2} \frac{d\theta}{dt} = b_i \quad (9.5.25)$$

Here

$$\begin{aligned} a_{11} &= \frac{\partial x_1}{\partial u} & a_{12} &= \frac{\partial x_1}{\partial \theta} & b_1 &= -v_{x1}^{(12)} \\ a_{21} &= \frac{\partial y_1}{\partial u} & a_{22} &= \frac{\partial y_1}{\partial \theta} & b_2 &= -v_{y1}^{(12)} \\ a_{31} &= \frac{\partial z_1}{\partial u} & a_{32} &= \frac{\partial z_1}{\partial \theta} & b_3 &= -v_{z1}^{(12)} \\ a_{41} &= f_u & a_{42} &= f_\theta & b_4 &= -\frac{\partial f}{\partial \phi} \frac{d\phi}{dt} \end{aligned}$$

where $d\phi/dt \neq 0$ is an arbitrarily chosen value; for instance, $d\phi/dt = 1$ rad/sec. The sliding velocity must correspond to the chosen value $d\phi/dt$.

Similarly, for the discussions above, we say that this system has a unique solution for du/dt and $d\phi/dt$, if the matrix

$$\begin{bmatrix} a_{11} & a_{12} & b_1 \\ a_{21} & a_{22} & b_2 \\ a_{31} & a_{32} & b_3 \\ a_{41} & a_{42} & b_4 \end{bmatrix} \quad (9.5.26)$$

has rank $r = 2$. This yields

$$\begin{vmatrix} \frac{\partial x_1}{\partial u} & \frac{\partial x_1}{\partial \theta} & -v_{x1}^{(12)} \\ \frac{\partial y_1}{\partial u} & \frac{\partial y_1}{\partial \theta} & -v_{y1}^{(12)} \\ \frac{\partial z_1}{\partial u} & \frac{\partial z_1}{\partial \theta} & -v_{z1}^{(12)} \end{vmatrix} = \begin{bmatrix} \frac{\partial \mathbf{r}_1}{\partial u} & \frac{\partial \mathbf{r}_1}{\partial \theta} & \mathbf{v}_1^{(12)} \end{bmatrix} = 0 \quad (9.5.27)$$

$$\begin{vmatrix} \frac{\partial x_1}{\partial u} & \frac{\partial x_1}{\partial \theta} & -v_{x1}^{(12)} \\ \frac{\partial y_1}{\partial u} & \frac{\partial y_1}{\partial \theta} & -v_{y1}^{(12)} \\ f_u & f_\theta & -f_\phi \frac{d\phi}{dt} \end{vmatrix} = 0 \quad (9.5.28)$$

$$\begin{vmatrix} \frac{\partial x_1}{\partial u} & \frac{\partial x_1}{\partial \theta} & -v_{x_1}^{(12)} \\ \frac{\partial z_1}{\partial u} & \frac{\partial z_1}{\partial \theta} & -v_{z_1}^{(12)} \\ f_u & f_\theta & -f_\phi \frac{d\phi}{dt} \end{vmatrix} = 0 \quad (9.5.29)$$

$$\begin{vmatrix} \frac{\partial y_1}{\partial u} & \frac{\partial y_1}{\partial \theta} & -v_{y_1}^{(12)} \\ \frac{\partial z_1}{\partial u} & \frac{\partial z_1}{\partial \theta} & -v_{z_1}^{(12)} \\ f_u & f_\theta & -f_\phi \frac{d\phi}{dt} \end{vmatrix} = 0 \quad (9.5.30)$$

Equation (9.5.27) is similar to the equation

$$\left[\frac{\partial \mathbf{r}_2}{\partial u} \frac{\partial \mathbf{r}_2}{\partial \theta} \frac{\partial \mathbf{r}_2}{\partial \phi} \right] = \left[\frac{\partial \mathbf{r}_2}{\partial u} \frac{\partial \mathbf{r}_2}{\partial \theta} v_2^{(12)} \right] \left(\frac{d\phi}{dt} \right)^{-1} = 0 \quad (9.5.31)$$

Here

$$v_2^{(12)} = \frac{\partial \mathbf{r}_2}{\partial \phi} \frac{d\phi}{dt}$$

is the sliding velocity.

The triple vector product (9.5.31) does not depend on the chosen coordinate system. Therefore, the triple vector product (9.5.27) may be applied instead of (9.5.31). Triple vector products (9.5.27) or (9.5.31) yield the equation of meshing.

$$f(u, \theta, \phi) = 0 \quad (9.5.32)$$

Therefore, equation (9.5.27) is observed for all contact points of the conjugate surfaces Σ_1 and Σ_2 , including singular points of the generated surface Σ_2 .

Equations (9.5.28) to (9.5.30) are additional equations to be observed if contact points of surface Σ_2 are singular points. It is sufficient to apply only one of equations (9.5.28) to (9.5.30) if the surface Σ_1 normal

$$\mathbf{N}_1 = \frac{\partial \mathbf{r}_1}{\partial u} \times \frac{\partial \mathbf{r}_1}{\partial \theta}$$

is not perpendicular to any coordinate axis of system S_1 . Thus, any equation of the system (9.5.28) to (9.5.30) yields the relation

$$F(u, \theta, \phi) = 0 \quad (9.5.33)$$

There is a simple way to avoid undercutting of the generated surface Σ_2 (proposed by Litvin, 1968). Equations (9.5.32), (9.5.33), and the vector equation which represents the generating surface

Σ_1 determine the line L on surface Σ_1 as a locus of points which generate singular points on the surface Σ_2 . This line is represented by

$$\mathbf{r}_1(u, \theta) \in C^1 \quad f(u, \theta, \phi) = 0 \quad F(u, \theta, \phi) = 0 \quad (9.5.34)$$

To avoid undercutting of the generated surface Σ_2 , we must limit the generating surface Σ_1 or apply special machine and tool settings to exclude the limiting line L (see example (9.8.1)).

9.6 Envelope of a Family of Surfaces: Kinematic Method of Determination

The determination of the envelope of a locus of surfaces is based on necessary and sufficient conditions of envelope existence worked out in classical differential geometry. These methods are of course workable, but the solution may be substantially simplified if a kinematic method of envelope determination is applied.

The key to the problem of envelope existence lies in (1) determining the equation of meshing and (2) observing the requirements that the envelope is a regular surface. We will discuss both of these stages.

Equation of Meshing

Consider a family of surfaces given in parametric form by

$$\mathbf{r}_2(u, \theta, \phi) \in C^1 \quad \frac{\partial \mathbf{r}_2}{\partial u} \times \frac{\partial \mathbf{r}_2}{\partial \theta} \neq 0 \quad (u, \theta) \in G \quad a < \phi < b \quad (9.6.1)$$

We found in section 9.3 that the equation of meshing may be represented by

$$f(u, \theta, \phi) = \left[\frac{\partial \mathbf{r}_2}{\partial u} \frac{\partial \mathbf{r}_2}{\partial \theta} \frac{\partial \mathbf{r}_2}{\partial \phi} \right] = 0 \quad (9.6.2)$$

Equation (9.6.1), with the fixed parameter ϕ , represents a single surface Σ_1 of the locus. The cross product

$$\mathbf{N}_2 = \frac{\partial \mathbf{r}_2}{\partial u} \times \frac{\partial \mathbf{r}_2}{\partial \theta} \quad (9.6.3)$$

represents the normal to surface Σ_1 in components of coordinate system S_2 .

Vector $\partial \mathbf{r}_2 / \partial \phi$ represents the velocity $\mathbf{v}_2^{(12)}$ of a fixed point M_1 on the surface Σ_1 with respect to the point M_2 of the envelope Σ_2 . Points M_1 and M_2 coincide and form a common point M , the point of tangency of surface Σ_1 and Σ_2 . The subscript 2 in $\mathbf{v}_2^{(12)}$ means that the velocity vector is represented in terms of components of coordinate system S_2 .

The equation of meshing (9.6.2) may be represented as

$$f(u, \theta, \phi) = \mathbf{N}_2 \cdot \mathbf{v}_2^{(12)} = 0 \quad (9.6.4)$$

The equality of the scalar product (9.6.4) to zero is an invariable property under the applied coordinate system. Instead of equation (9.6.4), we may apply the equation

$$\mathbf{N}_1 \cdot \mathbf{v}_1^{(12)} = 0 \quad (9.6.5)$$

with vectors expressed in components of the coordinate system S_1 .

Considering that the generating surface is given by the vector function

$$\mathbf{r}_1(u, \theta) \in C^1 \quad \frac{\partial \mathbf{r}_1}{\partial u} \times \frac{\partial \mathbf{r}_1}{\partial \theta} \neq 0 \quad (u, \theta) \in G \quad (9.6.6)$$

we obtain that

$$\mathbf{N}_1 = \frac{\partial \mathbf{r}_1}{\partial u} \times \frac{\partial \mathbf{r}_1}{\partial \theta}$$

and the equation of meshing may be expressed by

$$f(u, \theta, \phi) = \left[\frac{\partial \mathbf{r}_1}{\partial u} \frac{\partial \mathbf{r}_1}{\partial \theta} \mathbf{v}_1^{(12)} \right] = 0 \quad (9.6.7)$$

The velocity in relative motion (the sliding velocity $\mathbf{v}_1^{(12)}$) may be determined kinematically. (See sec. 2.3.) The representation of the meshing equation by expression (9.6.5) simplifies the transformations substantially.

Equation (9.6.4) may also be represented in terms of components of the coordinate system S_f as follows:

$$f(u, \theta, \phi) = \mathbf{N}_f \cdot \mathbf{v}_f^{(12)} = \left[\frac{\partial \mathbf{r}_f}{\partial u} \frac{\partial \mathbf{r}_f}{\partial \theta} \mathbf{v}_f^{(12)} \right] = 0 \quad (9.6.8)$$

Here $\partial \mathbf{r}_f / \partial u$ and $\partial \mathbf{r}_f / \partial \theta$ are partial derivatives of the vector function

$$\mathbf{r}_f(u, \theta, \phi) \in C^1 \quad \frac{\partial \mathbf{r}_f}{\partial u} \times \frac{\partial \mathbf{r}_f}{\partial \theta} \neq 0 \quad (u, \theta) \in G \quad a < \phi < b \quad (9.6.9)$$

Vector function (9.6.9) represents the family of surfaces Σ_1 in the coordinate system S_f . It may be derived on the basis of matrix equation

$$[r_f] = [M_f][r_1] \quad (9.6.10)$$

Here

$$[r_1] = \begin{bmatrix} x_1(u, \theta) \\ y_1(u, \theta) \\ z_1(u, \theta) \\ 1 \end{bmatrix} \quad (9.6.11)$$

are homogeneous coordinates of a point of the generating surface Σ_1 represented by the vector function (9.5.6). In the modern theory of gearing, equations of meshing are applied in forms represented by expressions (9.6.7) or (9.6.8).

Remarks: (1) The resulting equation

$$f(u, \theta, \phi) = 0$$

does not depend on the order of factors in the triple products (9.6.7) or (9.6.8) and (2) the vector of relative velocity $\mathbf{v}^{(12)} = -\mathbf{v}^{(21)}$ may be applied instead of relative velocity $\mathbf{v}^{(12)}$.

General Theorem of Conjugate Surfaces

Equations (9.5.4), (9.5.5), and (9.5.8) may be interpreted geometrically as the General Theorem of Conjugated Surfaces: At points of tangency of the generating surface Σ_1 and the generated surface Σ_2 , the common normal \mathbf{N} to the surfaces is perpendicular to the relative velocity vectors $\mathbf{v}^{(12)}$ or $\mathbf{v}^{(21)}$.

There is a particular case when the input and output gears rotate about parallel or intersected axes and the relative motion represents rotation about an instantaneous axis. (See secs. 2.1 and 2.2.) The relative velocity is

$$\mathbf{v}^{(12)} = \boldsymbol{\omega}^{(12)} \times \boldsymbol{\rho} \quad (9.6.12)$$

Here $\boldsymbol{\omega}^{(12)}$ is the angular velocity of rotation about instantaneous axis $I-I$ (fig. 9.6.1) and is directed along that axis, and $\boldsymbol{\rho}$ is a position vector drawn from a point of axis $I-I$ to the point M of tangency of surfaces Σ_1 and Σ_2 .

The triple product may now be represented by

$$\mathbf{N} \cdot \mathbf{v}^{(12)} = \mathbf{N} \cdot (\boldsymbol{\omega}^{(12)} \times \boldsymbol{\rho}) = [\mathbf{N}\boldsymbol{\omega}^{(12)}\boldsymbol{\rho}] = 0 \quad (9.6.13)$$

Equation (9.6.12) yields that vectors \mathbf{N} , $\boldsymbol{\omega}^{(12)}$, and $\boldsymbol{\rho}$ must belong to the same plane drawn through the instantaneous axis $I-I$. Thus, the common normal to contacting surfaces Σ_1 and Σ_2 must intersect the axis $I-I$ of instantaneous rotation.

The discussion above may be summarized by the following theorem: Consider gears which transform rotation between parallel or intersected axes. The instantaneous contact line of gear surfaces must be such that the common surface normal at any point M of the contact line would pass through the instantaneous axis of rotation in relative motion.

Applying this theorem, we may develop the following equation to determine the equation of meshing:

$$\frac{X_1 - x_1}{N_{x1}} = \frac{Y_1 - y_1}{N_{y1}} = \frac{Z_1 - z_1}{N_{z1}} \quad (9.6.14)$$

Here X_1 , Y_1 , and Z_1 are coordinates of a point of the instantaneous axis of rotation; x_1 , y_1 , and z_1 are coordinates of a point of the generating surface Σ_1 ; and N_{x1} , N_{y1} , and N_{z1} are projections of the normal \mathbf{N}_1 to the generating surface Σ_1 . Equations (9.6.14) yield the equation of meshing.

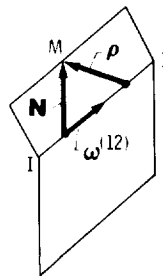


Figure 9.6.1.

Determination of Singular Points on the Generated Surface

The appearance of singular points on the generated surface Σ_2 means that this surface will be undercut by the generating surface Σ_1 in the process of meshing (generation). The existence of singular points on the generated surface Σ_2 may be determined by the equation $N_2 = 0$, where N_2 is the normal to the generated surface Σ_2 . This classical method needs a complicated transformation. A more effective and simple method is based on the theorem proposed by Litvin. (See sec. 9.5.) It follows from this theorem that singular points of surface Σ_2 are generated by such points of the generating surface Σ_1 at which the following equation is observed:

$$\mathbf{v}_{r_1}^{(1)} + \mathbf{v}_1^{(12)} = 0 \quad (9.6.15)$$

Here $\mathbf{v}_{r_1}^{(1)}$ is the velocity of the contact point in its relative motion over the generating surface Σ_1 and $\mathbf{v}_1^{(12)}$ is the sliding velocity. Both vectors of equation (9.6.15) are expressed in components of coordinate system S_1 rigidly connected to the generating surface Σ_1 .

9.7. Envelope of Contact Lines on the Generating Surface Σ_1

Usually, contact lines cover the entire working part of surface Σ_1 . There are cases (they are not so rare) when contact lines on the generating surface have their envelope and, therefore, these lines may cover only a part of the generating surface. Figure 9.7.1 shows a locus of contact lines L_ϕ on the generating surface Σ_1 . Line D is the envelope of these contact lines which divides surface Σ_1 into the following two parts: (1) part I, which is covered with contact lines (we include envelope D in part I) and (2) part II, which is free of contact lines. Line E is the edge of surface Σ_1 . The conditions of lubrication and heat transfer become unfavorable near envelope D . This is one of the reasons why the envelope D should be excluded from the meshing.

Consider generating surface Σ_1 represented by

$$\mathbf{r}_1(u, \theta) \in C^2 \quad \frac{\partial \mathbf{r}_1}{\partial u} \times \frac{\partial \mathbf{r}_1}{\partial \theta} \neq 0 \quad (u, \theta) \in G \quad (9.7.1)$$

Surface Σ_1 is covered with a locus of contact lines L_ϕ , whose location depends on the parameter of motion ϕ . Locus L_ϕ is represented by the vector equation (9.7.1) and equation

$$f(u, \theta, \phi) = \left[\frac{\partial \mathbf{r}_1}{\partial u} \frac{\partial \mathbf{r}_1}{\partial \theta} \mathbf{v}_1^{(12)} \right] = 0 \quad f \in C^1 \quad |f_u| + |f_\theta| \neq 0 \quad a < \phi < b \quad (9.7.2)$$

Here $\mathbf{v}_1^{(12)}$ is the velocity of sliding at the point of contact of surfaces Σ_1 and Σ_2 . The equation of meshing (9.7.2) relates surface Σ_1 parameters u and θ with the parameter of motion ϕ .

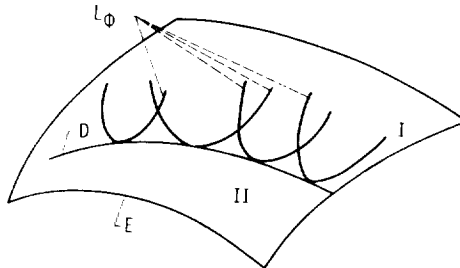


Figure 9.7.1.

We define a piece of envelope D as a regular curve

$$\mathbf{R}(\phi) \in C^1 \quad \mathbf{R}_\phi \neq 0 \quad (9.7.3)$$

on surface Σ_1 , which is in tangency with a single curve of the locus L_ϕ at each value of ϕ . We propose the following theorems of necessary and sufficient conditions of envelope D .

Theorem The necessary conditions of existence of an envelope of a locus of contact lines on the generating surface Σ_1 are described as follows: If the locus of contact lines L_ϕ has an envelope D and point (u_0, θ_0, ϕ_0) corresponds to the point of tangency of D with one of the contact lines L_ϕ , then this point (u_0, θ_0, ϕ_0) belongs to the set determined by the equation

$$f_\phi = q(u, \theta, \phi) = 0 \quad (9.7.4)$$

Proof: Consider vectors of displacement $\delta \mathbf{r}_1$ along the tangent \mathbf{T} to the contact line and $d\mathbf{r}_1$ whose direction differs from \mathbf{T} . The parameter of motion ϕ , which corresponds to the displacement along the contact line $\delta \mathbf{r}_1$, is fixed; however, ϕ must be considered as a variable for the displacement $d\mathbf{r}_1$. Vectors $\delta \mathbf{r}_1$ and $d\mathbf{r}_1$ are represented as follows:

$$\delta \mathbf{r}_1 = \frac{\partial \mathbf{r}_1}{\partial u} \delta u + \frac{\partial \mathbf{r}_1}{\partial \theta} \delta \theta \quad f_u \delta u + f_\theta \delta \theta = 0 \quad (9.7.5)$$

$$d\mathbf{r}_1 = \frac{\partial \mathbf{r}_1}{\partial u} du + \frac{\partial \mathbf{r}_1}{\partial \theta} d\theta \quad f_u du + f_\theta d\theta + f_\phi d\phi = 0 \quad (9.7.6)$$

If envelope D exists, displacement vectors $\delta \mathbf{r}_1$ and $d\mathbf{r}_1$ must be collinear at the point of tangency of the envelope D and a contact line. This yields the relation

$$\frac{\delta u}{du} = \frac{\delta \theta}{d\theta} \quad (9.7.7)$$

Equation (9.7.7) may be observed if, and only if,

$$f_\phi d\phi = 0 \quad (9.7.8)$$

Equation (9.7.8) may be observed only if $f_\phi = 0$, because continuously varying values of ϕ correspond to different points of envelope D .

Theorem The sufficient conditions of existence of an envelope of a locus of contact lines on the generating surface Σ_1 are described as follows: A locus L_ϕ of contact lines is represented by

$$\begin{aligned} \mathbf{r}_1(u, \theta) \in C^2 \quad \frac{\partial \mathbf{r}_1}{\partial u} \times \frac{\partial \mathbf{r}_1}{\partial \theta} \neq 0 \quad f(u, \theta, \phi) = \left[\frac{\partial \mathbf{r}_1}{\partial u} \frac{\partial \mathbf{r}_1}{\partial \theta} \mathbf{v}_1^{(12)} \right] = 0 \\ |f_u| + |f_\theta| \neq 0 \quad (u, \theta) \in G \quad a < \phi < b \end{aligned} \quad (9.7.9)$$

If at a point (u_0, θ_0, ϕ_0) the following conditions are observed:

$$f_\phi = q(u, \theta, \phi) = 0 \quad \frac{D(f, q)}{D(u, \theta)} \neq 0 \quad f_{\phi\phi} = q_\phi \neq 0 \quad (9.7.10)$$

then an envelope piece D is represented by

$$\mathbf{R}_1(\phi) = \mathbf{r}_1(u(\phi), \theta(\phi), \phi) \quad \mathbf{R}_1(\phi) \in C^1 \quad \frac{\partial \mathbf{R}_1}{\partial \phi} \neq 0 \quad (9.7.11)$$

Envelope piece D is a regular curve which is in tangency with a contact line of the locus L_ϕ at any value of ϕ . The envelope in question may be represented on surface Σ_1 by

$$\mathbf{r}_1(u, \theta) \in C^2 \quad f(u, \theta, \phi) = 0 \quad f_\phi = q(u, \theta, \phi) = 0 \quad (9.7.12)$$

Proof: Consider a system of equations

$$f(u, \theta, \phi) = 0 \quad f_\phi = q(u, \theta, \phi) = 0 \quad (9.7.13)$$

which are satisfied at the point (u_0, θ_0, ϕ_0) . Because of the inequality

$$\frac{D(f, q)}{D(u, \theta)} \neq 0$$

equations (9.7.13) may be solved by functions

$$\{u(\phi), \theta(\phi)\} \in C^1 \quad (9.7.14)$$

in the neighborhood of point (u_0, θ_0, ϕ_0) . With functions (9.7.14) we may represent a curve on surface Σ_1 by equations

$$\mathbf{R}_1(\phi) = \mathbf{r}_1(u(\phi), \theta(\phi)) \quad \mathbf{R}_1(\phi) \in C^1 \quad (9.7.15)$$

Let us now prove that the curve (9.7.15) is regular and that it is in tangency with a contact line at the point (u_0, θ_0, ϕ_0) . To prove this, we must observe the following conditions:

$$\frac{\partial \mathbf{R}_1}{\partial \phi} = \lambda \mathbf{T}_1 \quad (\lambda \neq 0) \quad \frac{\partial \mathbf{R}_1}{\partial \phi} \neq 0 \quad (9.7.16)$$

where \mathbf{T} is the tangent vector to the contact line. A contact line may be represented by equations

$$\mathbf{r}_1(u, \theta) \in C^2 \quad f(u, \theta, \phi_0) = 0 \quad (9.7.17)$$

where ϕ_0 has a fixed value.

A vector of displacement along the contact line $\delta \mathbf{r}_1$ is given by

$$\delta \mathbf{r}_1 = \frac{\partial \mathbf{r}_1}{\partial u} \delta u + \frac{\partial \mathbf{r}_1}{\partial \theta} \delta \theta \quad f_u \delta u + f_\theta \delta \theta = 0 \quad |f_u| + |f_\theta| \neq 0 \quad (9.7.18)$$

Assuming that the inequality

$$|f_u| + |f_\theta| \neq 0$$

is observed because $f_\phi \neq 0$, we obtain

$$\delta \mathbf{r}_1 = \left(\frac{\partial \mathbf{r}_1}{\partial u} f_\theta - \frac{\partial \mathbf{r}_1}{\partial \theta} f_u \right) \frac{\delta u}{f_\theta} \quad (9.7.19)$$

Equation (9.7.17) yields that for $f_\theta \neq 0$, the tangent \mathbf{T}_1 may be expressed as

$$\mathbf{T}_1 = \frac{\partial \mathbf{r}_1}{\partial u} f_\theta - \frac{\partial \mathbf{r}_1}{\partial \theta} f_u \quad \mathbf{T}_1 \neq 0 \quad (9.7.20)$$

The tangent \mathbf{T}_1 differs from zero because

$$\frac{\partial \mathbf{r}_1}{\partial u} \times \frac{\partial \mathbf{r}_1}{\partial \theta} \neq 0 \quad |f_u| + |f_\theta| \neq 0 \quad (9.7.21)$$

Let us now prove that equation (9.7.16) is indeed observed and that envelope D is in tangency with the corresponding contact line of the locus L_ϕ . After differentiation of equation (9.7.15), we get

$$\frac{\partial \mathbf{R}_1}{\partial \phi} = \frac{\partial \mathbf{r}_1}{\partial u} u_\phi + \frac{\partial \mathbf{r}_1}{\partial \theta} \theta_\phi \quad (9.7.22)$$

To determine the derivatives u_ϕ and θ_ϕ , let us differentiate equations

$$f(u(\phi), \theta(\phi), \phi) = 0 \quad q(u(\phi), \theta(\phi), \phi) = 0 \quad (9.7.23)$$

We get a system of two linear equations in two unknowns, u_ϕ and θ_ϕ

$$f_u u_\phi + f_\theta \theta_\phi = -f_\phi \quad q_u u_\phi + q_\theta \theta_\phi = -q_\phi \quad (9.7.24)$$

With

$$\Delta = \begin{vmatrix} f_u & f_\theta \\ q_u & q_\theta \end{vmatrix} = \frac{D(f, q)}{D(u, \theta)} \neq 0 \quad (9.7.25)$$

and taking into account that $f_\phi = 0$, we may get the following solutions for unknowns u_ϕ and θ_ϕ for points of the envelope:

$$u_\phi = \frac{f_\theta q_\phi}{\Delta} \quad \theta_\phi = -\frac{f_u q_\phi}{\Delta} \quad (9.7.26)$$

Equations (9.7.22) and (9.7.26) yield

$$\frac{\partial \mathbf{R}_1}{\partial \phi} = \left(\frac{\partial \mathbf{r}_1}{\partial u} f_\theta - \frac{\partial \mathbf{r}_1}{\partial \theta} f_u \right) \frac{q_\phi}{\Delta} \quad (9.7.27)$$

Equations (9.7.27) and (9.7.20) yield that the envelope tangent (9.7.27) is collinear with the

contact line tangent (9.7.20), the envelope tangent differs from zero since $q_\phi = f_{\phi\phi} \neq 0$, and the envelope is a regular curve. Due to the existence of functions (9.7.14), there is only one point (u, θ) which corresponds to the parameter of motion ϕ . Consequently, the contact line has only one point of tangency with the envelope D .

Representation of the Envelope on the Plane of Parameters (u, θ)

Contact lines L_ϕ on surface Σ_1 may be obtained by mapping a locus of plane curves represented on the plane (u, θ) by equations

$$f(u, \theta, \phi) = 0 \quad f(u, \theta, \phi) \in C^2 \quad |f_u| + |f_\theta| \neq 0 \quad (u, \theta) \in G \quad a < \phi < b \quad (9.7.28)$$

Here ϕ , if fixed, corresponds to a single contact line of the locus.

The locus of plane curves, represented in implicit form by equations (9.7.28), has an envelope, if the following requirements are observed (see sec. 4.3.):

$$f_\phi = q(u, \theta, \phi) = 0 \quad \frac{D(f, q)}{D(u, \theta)} \neq 0 \quad f_{\phi\phi} \neq 0 \quad (9.7.29)$$

Requirements (9.7.29) are sufficient for the existence of the envelope D of the locus of contact lines L_ϕ on the surface Σ_1 . Consequently, if the envelope D on surface Σ_1 exists, there is definitely an envelope of the locus of plane curves (9.7.28) on the plane of parameters (u, θ) . This result is important for applications. The graphical representation of the locus of contact lines L_ϕ , and their envelope D , on the generating surface Σ_1 needs complicated drawings. It is easier to represent images of L_ϕ and D on the plane of parameters (u, θ) . An example of the determination of envelope D is discussed in example problem 9.8.1.

9.8 Conjugate Surfaces: Working Equations

Initial Conditions

Given the generating surface Σ_1 by

$$\mathbf{r}_1(u, \theta) \in C^2 \quad \frac{\partial \mathbf{r}_1}{\partial u} \times \frac{\partial \mathbf{r}_1}{\partial \theta} \neq 0 \quad (u, \theta) \in G \quad (9.8.1)$$

The location of the rotation axes of gears 1 and 2 and the ratio of angular velocities are known. The parameter of motion ϕ belongs to the interval

$$a < \phi < b$$

We set up three coordinate systems S_1 , S_2 , and S_f rigidly connected to gears 1 and 2 and the frame, respectively. It is necessary to determine the generated surface Σ_2 , contact lines on surfaces Σ_1 and Σ_2 , surface of action, condition to avoid undercutting of surface Σ_2 , and the appearance of the envelope D of contact lines on the generating surface Σ_1 . The stages of investigation and solution are presented as follows.

Equations of meshing.—Generally this equation may be represented by

$$f(u, \theta, \phi) = \left[\frac{\partial \mathbf{r}_1}{\partial u} \frac{\partial \mathbf{r}_1}{\partial \theta} \mathbf{v}_1^{(12)} \right] = 0 \quad (9.8.2)$$

Here $v_1^{(12)}$ is the velocity of sliding determined kinematically. (See ch. 2.3.) After determination of equation (9.8.2) it is necessary to make sure that

$$|f_u| + |f_\theta| \neq 0 \quad (9.8.3)$$

If gears 1 and 2 transform motion between parallel or intersecting axes, the equation of meshing may be represented not only by equation (9.8.2), but by

$$\frac{X_1 - x_1(u, \theta)}{N_{x1}} = \frac{Y_1 - y_1(u, \theta)}{N_{y1}} = \frac{Z_1 - z_1(u, \theta)}{N_{z1}} \quad (9.8.4)$$

Here x_1 , y_1 , and z_1 are coordinates of a point on surface Σ_1 ; X_1 , Y_1 , and Z_1 are coordinates of a point of the instantaneous axis of rotation; and N_{x1} , N_{y1} , and N_{z1} are projections of surface normal \mathbf{N}_1 given by

$$\mathbf{N}_1 = \frac{\partial \mathbf{r}_1}{\partial u} \times \frac{\partial \mathbf{r}_1}{\partial \theta} \quad (9.8.5)$$

Contact lines on surface Σ_1 .—Contact lines on surface Σ_1 are represented by expressions (9.8.1) and (9.8.2) with fixed values of the parameter of motion ϕ .

Surface of action.—The surface of action is the locus of contact lines determined in the coordinate system S_f . This surface is represented by expression (9.8.1), equation (9.8.2), and matrix equation

$$[r_f] = [M_f][r_1] \quad (9.8.6)$$

Here matrix $[M_f]$ represents the coordinate transformation from coordinate system S_1 to S_f . Vector function (9.8.1) and equations (9.8.2) and (9.8.6) yield the following expressions for the surface of action:

$$\begin{aligned} r_f(u, \theta, \phi) \in C^2 \quad \frac{\partial r_f}{\partial u} \times \frac{\partial r_f}{\partial \theta} \neq 0 \quad f(u, \theta, \phi) = 0 \\ |f_u| + |f_\theta| \neq 0 \quad (u, \theta) \in G \quad a < \phi < b \end{aligned} \quad (9.8.7)$$

Generated surface.—The generated surface Σ_2 is the locus of contact lines determined in the coordinate systems S_2 . Surface Σ_2 is represented by vector equation (9.8.1), equation (9.8.2), and matrix equation

$$[r_2] = [M_2][r_1] \quad (9.8.8)$$

Matrix $[M_2]$ represents the coordinate transformation by transition from coordinate system S_1 to coordinate system S_2 . Vector function (9.8.1) and equations (9.8.2) and (9.8.8) yield the following expressions for the generated surface Σ_2 :

$$r_2(u, \theta, \phi) \in C^2 \quad f(u, \theta, \phi) = 0 \quad |f_u| + |f_\theta| \neq 0 \quad (u, \theta) \in G \quad a < \phi < b \quad (9.8.9)$$

Nonundercutting of the generated surface Σ_2 .—To avoid undercutting of the generated surface Σ_2 it is necessary to limit the dimensions and settings of the generating surface Σ_1 . The limiting line of surface Σ_1 is the locus of points of Σ_1 which generate singular points of the generated

surface Σ_2 . This line is determined by

$$\begin{aligned} \mathbf{r}_1(u, \theta) \in C^2 \quad \frac{\partial \mathbf{r}_1}{\partial u} \times \frac{\partial \mathbf{r}_1}{\partial \theta} \neq 0 \quad \left[\frac{\partial \mathbf{r}_1}{\partial u} \frac{\partial \mathbf{r}_1}{\partial \theta} \mathbf{v}^{(12)} \right] = f(u, \theta, \phi) = 0 \\ F(u, \theta, \phi) = 0 \quad |f_u| + |f_\theta| \neq 0 \quad (u, \theta) \in G \quad a < \phi < b \end{aligned} \quad (9.8.10)$$

The equation

$$F(u, \theta, \phi) = 0 \quad (9.8.11)$$

may be developed from equations

$$\begin{vmatrix} \frac{\partial x_1}{\partial u} & \frac{\partial x_1}{\partial \theta} & v_{x_1}^{(12)} \\ \frac{\partial y_1}{\partial u} & \frac{\partial y_1}{\partial \theta} & v_{y_1}^{(12)} \\ f_u & f_\theta & f_\phi \frac{d\phi}{dt} \end{vmatrix} = \begin{vmatrix} \frac{\partial x_1}{\partial u} & \frac{\partial x_1}{\partial \theta} & v_{x_1}^{(12)} \\ \frac{\partial z_1}{\partial u} & \frac{\partial z_1}{\partial \theta} & v_{z_1}^{(12)} \\ f_u & f_\theta & f_\phi \frac{d\phi}{dt} \end{vmatrix} = \begin{vmatrix} \frac{\partial y_1}{\partial u} & \frac{\partial y_1}{\partial \theta} & v_{y_1}^{(12)} \\ \frac{\partial z_1}{\partial u} & \frac{\partial z_1}{\partial \theta} & v_{z_1}^{(12)} \\ f_u & f_\theta & f_\phi \frac{d\phi}{dt} \end{vmatrix} = 0 \quad (9.8.12)$$

Usually it is sufficient to apply only one equality of the three equalities in equations (9.8.12) to get equation (9.8.11).

Investigation of existence of envelope of contact lines on the generating surface Σ_1 .—It is essential to investigate the existence of an envelope of contact lines considering the plane of parameters (u, θ) . The envelope in question is represented by equations

$$\begin{aligned} f(u, \theta, \phi) = 0 \quad f(u, \theta, \phi) \in C^2 \quad f_\phi = q(u, \theta, \phi) = 0 \quad |f_u| + |f_\theta| \neq 0 \\ \frac{D(f, q)}{D(u, \theta)} \neq 0 \quad f_{\phi\phi} \neq 0 \quad (u, \theta) \in G \quad a < \phi < b \end{aligned} \quad (9.8.13)$$

Example 9.8.1

Conjugate surfaces of a worm-gear drive are considered. Assuming that the surface of the worm is given, we must determine (1) the equation of meshing, (2) the surface of action, (3) the worm-gear surface, and (4) the equations of the envelope of contact lines on the worm surface. Conditions of nonundercutting of the worm-gear surface may be determined with the aid of a computer program. Because of the complexity of this program, it is not discussed in this example.

Solution

Worm thread surface.—Consider that the worm thread surface is an involute screw surface (fig. 9.8.1). Such a surface may be generated by a screw motion of the straight line ML . This line is the tangent to the helix on the base cylinder of radius r_b . (The helix in question is traced out on the base cylinder surface by point M , the point of tangency of the straight line ML with the cylinder.) The generating line ML forms the angle λ_b with the plane perpendicular to the z_1 -axis.

The position vector for point N of the screw involute surface is

$$\overline{O_1N} = \overline{O_1K} + \overline{KM} + \overline{MN} \quad (9.8.14)$$

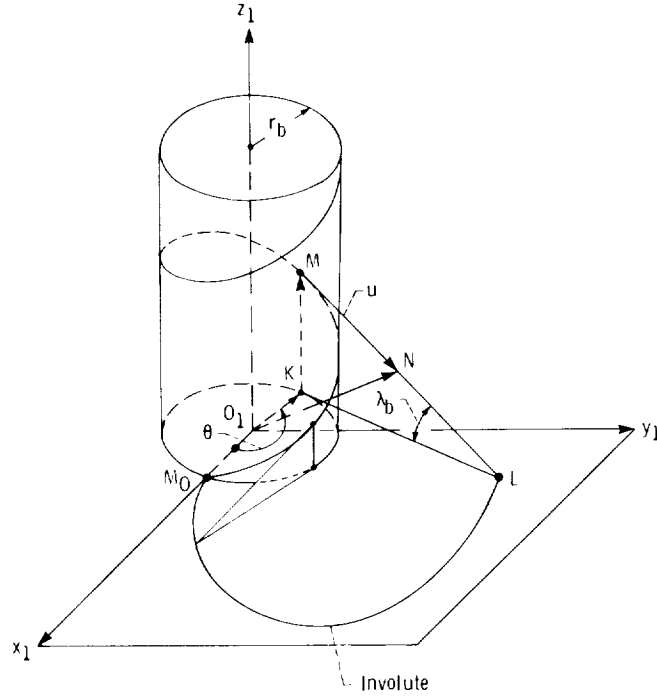


Figure 9.8.1.

Here $|\overline{MN}| = u$ is the segment of straight line \overline{ML} measured from the tangency point M to the point N , $|\overline{O_1K}|$ is the base cylinder radius r_b (vector $\overline{O_1K}$ makes the angle θ with the x_1 -axis), and $|\overline{KM}| = h\theta$ is the axial displacement in screw motion which corresponds to the rotation angle θ (h is the screw parameter). Projecting the vectors of equation (9.8.14) onto the coordinate axes, we get

$$\begin{aligned} x_1 &= r_b \cos \theta + u \cos \lambda_b \sin \theta & y_1 &= r_b \sin \theta - u \cos \lambda_b \cos \theta \\ z_1 &= h\theta - u \sin \lambda_b \end{aligned} \quad (9.8.15)$$

Equations (9.8.15) represent the involute screw surface with u and θ as surface coordinates. It is easy to verify that the cross section of the involute screw surface (cut by the plane $z_1 = \text{constant}$) is an involute curve with the base circle of radius r_b .

The normal \mathbf{N}_1 to surface (9.8.15) is

$$\begin{aligned} \mathbf{N}_1 &= \frac{\partial \mathbf{r}_1}{\partial u} \times \frac{\partial \mathbf{r}_1}{\partial \theta} \\ &= \begin{vmatrix} \mathbf{i}_1 & \mathbf{j}_1 & \mathbf{k}_1 \\ \cos \lambda_b \sin \theta & -\cos \lambda_b \cos \theta & -\sin \lambda_b \\ -r_b \sin \theta + u \cos \lambda_b \cos \theta & r_b \cos \theta + u \cos \lambda_b \sin \theta & h \end{vmatrix} \\ &= (-h \cos \lambda_b \cos \theta + r_b \sin \lambda_b \cos \theta + u \cos \lambda_b \sin \lambda_b \sin \theta) \mathbf{i}_1 \\ &\quad + (r_b \sin \lambda_b \sin \theta - u \cos \lambda_b \sin \lambda_b \cos \theta - h \cos \lambda_b \sin \theta) \mathbf{j}_1 \\ &\quad + u \cos^2 \lambda_b \mathbf{k}_1 \end{aligned} \quad (9.8.16)$$

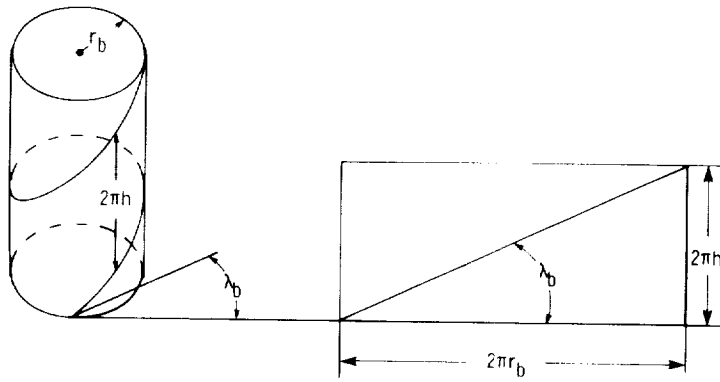


Figure 9.8.2.

Developing the cylinder surface (fig. 9.8.2) on a plane, we may represent the helix by a straight line and obtain

$$\tan \lambda_b = \frac{h}{r_b} \quad (9.8.17)$$

Equations (9.8.16) and (9.8.17) yield

$$\mathbf{N}_1 = u \cos \lambda_b (\sin \lambda_b \sin \theta \mathbf{i}_1 - \sin \lambda_b \cos \theta \mathbf{j}_1 + \cos \lambda_b \mathbf{k}_1) \quad (9.8.18)$$

With $u \neq 0$ the screw involute surface is a regular surface and the surface unit normal is

$$\mathbf{n}_1 = \sin \lambda_b \sin \theta \mathbf{i}_1 - \sin \lambda_b \cos \theta \mathbf{j}_1 + \cos \lambda_b \mathbf{k}_1 \quad (9.8.19)$$

Coordinate systems.—We set up coordinate systems S_1 , S_2 , and S_f rigidly connected with worm 1, gear 2, and the frame, respectively (fig. 9.8.3). An auxiliary coordinate system, also

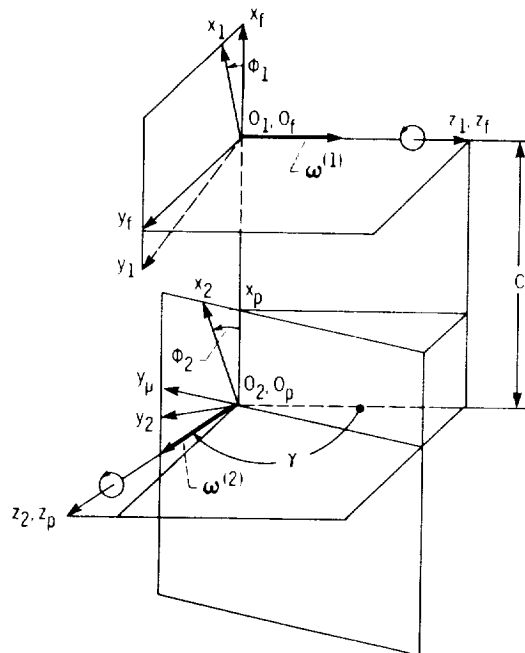


Figure 9.8.3.

rigidly connected to the frame, is designated by S_p . The worm and gear rotate about crossed axes which form an angle γ . Usually $\gamma = 90^\circ$, but we assume that $\gamma \neq 90^\circ$.

Coordinate transformation.—The coordinate transformation by transition from system S_1 to S_f is represented by the matrix equation

$$[r_f] = [M_{f1}][r_1] \quad (9.8.20)$$

Here

$$[M_{f1}] = \begin{bmatrix} \cos \phi_1 & -\sin \phi_1 & 0 & 0 \\ \sin \phi_1 & \cos \phi_1 & 0 & 0 \\ 0 & 0 & 1 & 0 \\ 0 & 0 & 0 & 1 \end{bmatrix}$$

Equations (9.8.18) to (9.8.20) yield

$$x_f = x_1 \cos \phi_1 - y_1 \sin \phi_1 \quad y_f = x_1 \sin \phi_1 + y_1 \cos \phi_1 \quad z_f = z_1 \quad (9.8.21)$$

Matrix equation

$$[r_2] = [M_{21}][r_1] = [M_{2p}][M_{pf}][M_{f1}][r_1] \quad (9.8.22)$$

represents the coordinate transformation from S_1 to S_2 . Here

$$[M_{pf}] = \begin{bmatrix} 1 & 0 & 0 & C \\ 0 & \cos \gamma & -\sin \gamma & 0 \\ 0 & \sin \gamma & \cos \gamma & 0 \\ 0 & 0 & 0 & 1 \end{bmatrix} \quad (9.8.23)$$

$$[M_{2p}] = \begin{bmatrix} \cos \phi_2 & \sin \phi_2 & 0 & 0 \\ -\sin \phi_2 & \cos \phi_2 & 0 & 0 \\ 0 & 0 & 1 & 0 \\ 0 & 0 & 0 & 1 \end{bmatrix} \quad (9.8.24)$$

Equations (9.8.22) to (9.8.24) yield

$$\begin{aligned} x_2 &= x_1(\cos \phi_1 \cos \phi_2 + \cos \gamma \sin \phi_1 \sin \phi_2) \\ &+ y_1(-\sin \phi_1 \cos \phi_2 + \cos \gamma \cos \phi_1 \sin \phi_2) \\ &- z_1 \sin \gamma \sin \phi_2 + C \cos \phi_2 \\ y_2 &= x_1(-\cos \phi_1 \sin \phi_2 + \cos \gamma \sin \phi_1 \cos \phi_2) \\ &+ y_1(\sin \phi_1 \sin \phi_2 + \cos \gamma \cos \phi_1 \cos \phi_2) \\ &- z_1 \sin \gamma \cos \phi_2 - C \sin \phi_2 \\ z_2 &= x_1 \sin \gamma \sin \phi_1 + y_1 \sin \gamma \cos \phi_1 + z_1 \cos \gamma \end{aligned} \quad (9.8.25)$$

Sliding velocity.—The sliding (relative) velocity $\mathbf{v}_f^{(12)}$ is

$$\mathbf{v}_f^{(12)} = \mathbf{v}_f^{(1)} - \mathbf{v}_f^{(2)} \quad (9.8.26)$$

Here $\mathbf{v}_f^{(1)}$ and $\mathbf{v}_f^{(2)}$ are velocities of the points of gears 1 and 2, respectively, which form their mutual contact point. The subscript f means that vectors are expressed in components of coordinate system S_f ; henceforth we will drop this subscript.

Gears 1 and 2 rotate about crossed axes z_f and z_p with angular velocities $\omega^{(1)}$ and $\omega^{(2)}$ (figs. 9.8.3 and 9.8.4). The velocity $\mathbf{v}^{(1)}$ may be represented by

$$\mathbf{v}^{(1)} = \omega^{(1)} \times \mathbf{r} \quad (9.8.27)$$

where \mathbf{r} is a position vector drawn from the origin O_f of the coordinate system S_f to the point of contact.

The sliding vector $\omega^{(2)}$ does not pass through the coordinate origin O_f . We substitute this vector by an equal vector $\omega^{(2)}$, which passes through O_f , and the moment (fig. 9.8.4)

$$\mathbf{m} = \mathbf{R} \times \omega^{(2)} \quad (9.8.28)$$

where \mathbf{R} is a vector drawn from point O_f to any point on the line of action z_p of vector $\omega^{(2)}$. We choose the vector $\mathbf{R} = \overline{O_f O_p}$.

The velocity $\mathbf{v}^{(2)}$ is

$$\mathbf{v}^{(2)} = (\omega^{(2)} \times \mathbf{r}) + (\mathbf{C} \times \omega^{(2)}) \quad (9.8.29)$$

Equations (9.8.26), (9.8.27), and (9.8.29) yield

$$\mathbf{v}^{(12)} = ((\omega^{(1)} - \omega^{(2)}) \times \mathbf{r}) - (\mathbf{C} \times \omega^{(2)}) = (\omega^{(12)} \times \mathbf{r}) - (\mathbf{C} \times \omega^{(2)}) \quad (9.8.30)$$

Here (fig. 9.8.4)

$$\omega^{(12)} = \omega^{(1)} - \omega^{(2)} \quad (9.8.31)$$

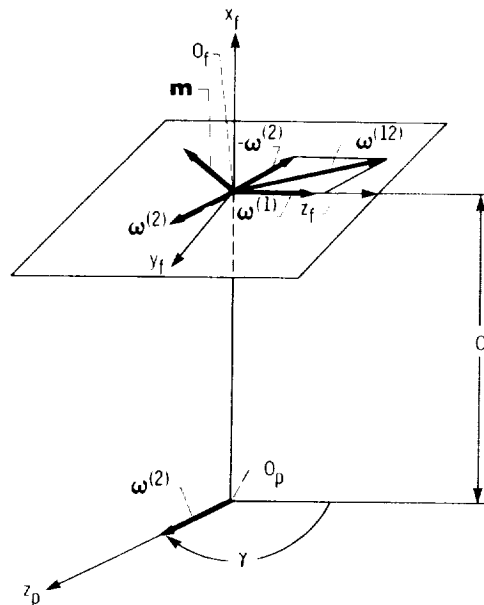


Figure 9.8.4.

**ORIGINAL PAGE IS
OF POOR QUALITY**

Taking into account that

$$\boldsymbol{\omega}^{(1)} = \omega^{(1)} \mathbf{k}_f \quad \boldsymbol{\omega}^{(2)} = \omega^{(2)} (\sin \gamma \mathbf{j}_f + \cos \gamma \mathbf{k}_f) \quad \mathbf{C} = -C \mathbf{i}_f \quad \mathbf{r} = x_f \mathbf{i}_f + y_f \mathbf{j}_f + z_f \mathbf{k}_f$$

we get

$$\begin{aligned} v_x^{(12)} &= [-y_f(1 - m_{21} \cos \gamma) - z_f m_{21} \sin \gamma] \omega^{(1)} \\ v_y^{(12)} &= [x_f(1 - m_{21} \cos \gamma) - C m_{21} \cos \gamma] \omega^{(1)} \\ v_z^{(12)} &= [(x_f + C) m_{21} \sin \gamma] \omega^{(1)} \end{aligned} \quad (9.8.32)$$

Here $m_{21} = \omega^{(2)}/\omega^{(1)}$.

The sliding vector $\mathbf{v}^{(12)}$ may be expressed in components of coordinate system S_1 by using the matrix equation

$$[v_i^{(12)}] = [L_{1f}] [v^{(12)}] \quad (9.8.33)$$

The 3×3 matrix $[L_{1f}]$ is represented by (fig. 9.8.3)

$$[L_{1f}] = \begin{bmatrix} \cos \phi_1 & \sin \phi_1 & 0 \\ -\sin \phi_1 & \cos \phi_1 & 0 \\ 0 & 0 & 1 \end{bmatrix} \quad (9.8.34)$$

Equations (9.8.21) and (9.8.32) to (9.8.34) yield

$$\begin{aligned} v_{x1}^{(12)} &= [-y_1(1 - m_{21} \cos \gamma) - z_1 m_{21} \sin \gamma \cos \phi_1 - C m_{21} \cos \gamma \sin \phi_1] \omega^{(1)} \\ v_{y1}^{(12)} &= [x_1(1 - m_{21} \cos \gamma) + z_1 m_{21} \sin \gamma \sin \phi_1 - C m_{21} \cos \gamma \cos \phi_1] \omega^{(1)} \\ v_{z1}^{(12)} &= [m_{21} \sin \gamma (x_1 \cos \phi_1 - y_1 \sin \phi_1 + C)] \omega^{(1)} \end{aligned} \quad (9.8.35)$$

Equation of meshing.—We apply the equation

$$\mathbf{N}_1 \cdot \mathbf{v}_1^{(12)} = 0 \quad (9.8.36)$$

where \mathbf{N}_1 is represented by equation (9.8.18) and $\mathbf{v}_1^{(12)}$ by equations (9.8.35). The involute screw surface is a helicoid and therefore we may use the relation (8.4.41), which may be represented as

$$y_1 N_{x1} - x_1 N_{y1} - h N_{z1} = 0 \quad (9.8.37)$$

Equations (9.8.15), (9.8.37), (9.8.18), and (9.8.36) yield the following equation of meshing:

$$\begin{aligned} f(u, \theta, \phi_1) &= (u - h\theta \sin \lambda_b) \sin (\theta + \phi_1) \sin \gamma \\ &+ \cos (\theta + \phi_1) (r_b \cos \lambda_b \sin \gamma + C \sin \lambda_b \cos \gamma) \\ &- [h(m_{12} - \cos \gamma) - C \sin \gamma] \cos \lambda_b = 0 \end{aligned} \quad (9.8.38)$$

where

$$m_{12} = \frac{1}{m_{21}} = \frac{\omega^{(1)}}{\omega^{(2)}}$$

Surface of action.—The surface of action is represented by equations

$$[r_2] = [M_{21}][r_1] \quad (9.8.20)$$

and

$$f(u, \theta, \phi_1) = 0 \quad (9.8.38)$$

Matrix equation (9.8.20) yields equations (9.8.21). Thus, the surface of action is represented by equations (9.8.15), (9.8.21), and (9.8.38).

Gear-tooth surface.—The gear-tooth surface is represented by equations

$$[r_2] = [M_{21}][r_1] \quad (9.8.22)$$

and

$$f(u, \theta, \phi_1) = 0 \quad (9.8.38)$$

Matrix equations (9.8.22) yields equations (9.8.25). Thus, the gear-tooth surface is represented by equations (9.8.15), (9.8.25), and (9.8.38).

Investigation of the existence of the envelope D of contact lines on the generating surface Σ_1 .—The envelope D is determined on the plane of parameters (u, θ) by equations (9.8.13). Equation

$$f_\phi(u, \theta, \phi_1) = 0$$

yields

$$\begin{aligned} & (u - h\theta \sin \lambda_b) \sin \gamma \cos(\theta + \phi_1) \\ & - [r_b \cos \lambda_b \sin \gamma + C \sin \lambda_b \cos \gamma] \sin(\theta + \phi_1) = 0 \end{aligned} \quad (9.8.39)$$

Considering equations (9.8.39) and (9.8.38), we get

$$\cos \nu = \frac{r_b \sin \gamma + C \tan \lambda_b \cos \gamma}{h(m_{12} - \cos \gamma) - C \sin \gamma} \quad (\nu = \theta + \phi_1) \quad (9.8.40)$$

$$\sin \nu = \frac{(u - h\theta \sin \lambda_b) \sin \gamma}{[h(m_{12} - \cos \gamma) - C \sin \gamma] \cos \lambda_b} \quad (9.8.41)$$

Due to the inequality

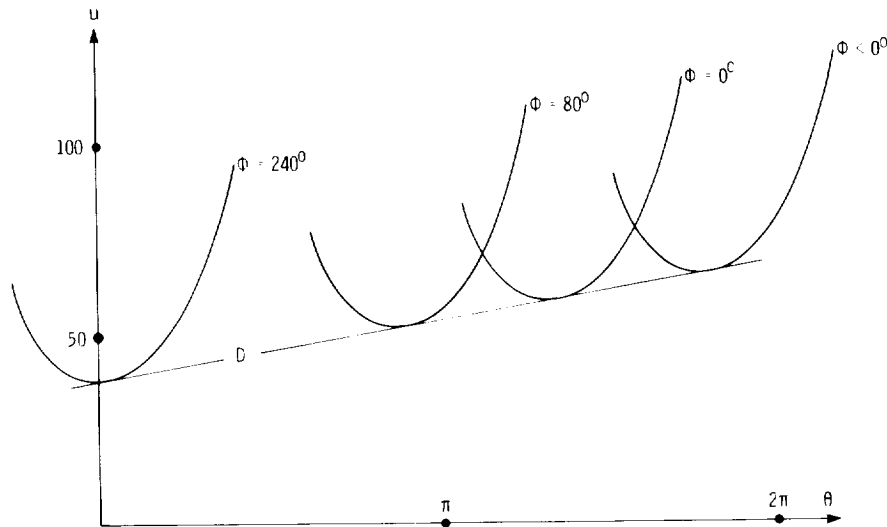
$$-1 \leq \cos(\theta + \phi) \leq 1$$

we get that equation (9.8.40) may exist (consequently the envelope D may appear) if, and only if,

$$|r_b \sin \gamma + C \tan \lambda_b \cos \gamma| \leq |h(m_{12} - \cos \gamma) - C \sin \gamma| \quad (9.8.42)$$

If inequality (9.8.42) and all inequalities of expression (9.8.13) are satisfied, the envelope D indeed exists. This envelope is a straight line in the plane of parameters (u, θ) and may be represented by the equation

$$(u - h\theta \sin \lambda_b) \sin \gamma - [h(m_{12} - \cos \gamma) - C \sin \gamma] \cos \lambda_b \sin \nu = 0 \quad (9.8.43)$$



where

$$\cos \nu = \frac{r_b \sin \gamma + C \tan \lambda_b \cos \gamma}{h(m_{12} - \cos \gamma) - C \sin \gamma}$$

(See eq. (9.8.40).)

Figure 9.8.5 shows the locus of contact lines given by equation (9.8.38) and their envelope D . (Envelope D is represented by equation (9.8.43).) The appearance of the envelope is inevitable for worm-gear drives with the crossing angle $\gamma = 90^\circ$. This envelope appearance is a disadvantage of such worm-gear drives.

With $\gamma = 90^\circ$, we represent the inequality (9.8.42) as

$$r_b \leq |m_{12}h - C| \quad (9.8.44)$$

It results from the geometry of involute worm-gear drives that

$$r_b = \frac{h}{\sqrt{\tan^2 \psi_c + \tan^2 \lambda_p}} = \frac{N_1}{2P_a \sqrt{\tan^2 \psi_c + \tan^2 \lambda_p}} \quad (9.8.45)$$

$$m_{12} = \frac{\omega^{(1)}}{\omega^{(2)}} = \frac{N_2}{N_1} \quad (9.8.46)$$

$$C = r_p + R_p = r_p + \frac{N_2}{2P_s} \quad (9.8.47)$$

Here r_p and R_p are the radii of pitch cylinders of the worm and of the worm gear, λ_p is the lead angle on the worm pitch cylinder, $P_a = N_1/2h$ is the axial pitch of the worm, $P_s = P_a$ is the worm-gear diametral pitch, N_1 and N_2 are numbers of worm and gear teeth, and ψ_c is the angle of the worm shape in its axial section.

We may avoid the appearance of envelope D by using definite crossing angles $\gamma \neq 90^\circ$. To get the range of angle γ with which the envelope D does not exist, we may find edges of this area making $\cos(\theta + \phi_1) = 1$ and $\cos(\theta + \phi_1) = -1$ in equation (9.8.40); this enables us to obtain

the limits of this range. We found that the area of γ is $125^\circ < \gamma < 155^\circ$ and $7^\circ < \gamma < 72^\circ$ for the worm-gear drive with parameters $C = 150$ mm, $h = 12$ mm, $r_b = 27.5$ mm, and $m_{12} = 25:3$. By applying a worm-gear drive with a crossing angle $\gamma \neq 90^\circ$, we may provide better conditions of lubrication due to the more favorable shape of contact lines. Figure 9.8.6 shows the contact lines determined for the worm-gear drive with the parameters listed above and crossing angle $\gamma = 130^\circ$.

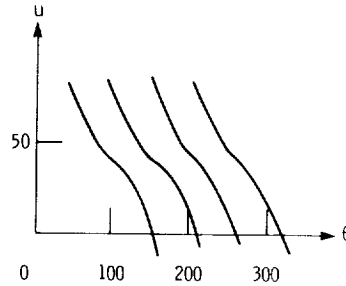


Figure 9.8.6.

Example 9.8.2

Consider that a rack, with the given surface Σ_1 , generates the gear tooth surface Σ_2 . We set up the coordinate systems S_1, S_2 , and S_f discussed in example 9.3.1 (fig. 9.3.2). Equations of the generating surface Σ_1 , according to equations (9.3.24), are

$$x_1 = u \cos \psi_t \quad y_1 = u \sin \psi_t + \ell \sin \beta \quad z_1 = \ell \cos \beta \quad (9.8.47)$$

where $(u, \ell) \in E$.

Determine the equations of (1) meshing, (2) surface of action, (3) generated surface, (4) conditions of nonundercutting of gear teeth, and (5) existence of an envelope of the contact line on the generating surface.

Solution

Equation of meshing.—The normal to the generating surface is

$$\mathbf{N}_1 = \frac{\partial \mathbf{r}_1}{\partial u} \times \frac{\partial \mathbf{r}_1}{\partial \ell} = \cos \beta \sin \psi_t \mathbf{i}_1 - \cos \beta \cos \psi_t \mathbf{j}_1 + \sin \beta \cos \psi_t \mathbf{k}_1 \quad (9.8.49)$$

We determine the sliding velocity by

$$\mathbf{v}_1^{(12)} = \mathbf{v}_1^{(1)} - \mathbf{v}_1^{(2)} \quad (9.8.50)$$

The velocity of the rack is (fig. 9.3.2(a))

$$\mathbf{v}_1^{(1)} = \frac{ds}{dt} \mathbf{j}_1 = \omega r \mathbf{j}_1 \quad (9.8.51)$$

The gear rotates about O_2 with the angular velocity

$$\boldsymbol{\omega}_2 = \omega \mathbf{k}_2 \quad (9.8.52)$$

The sliding vector (9.8.52) may be substituted by the equal vector

$$\boldsymbol{\omega} = \omega \mathbf{k}_1 \quad (9.8.53)$$

directed along the z_1 -axis and the moment

$$\mathbf{m} = \overline{O_1O_2} \times \boldsymbol{\omega} \quad (9.8.54)$$

where (fig. 9.3.2(a))

$$\overline{O_1O_2} = -r\mathbf{i}_1 - s\mathbf{j}_1 = -r(\mathbf{i}_1 + \phi\mathbf{j}_1) \quad (9.8.55)$$

Vector \mathbf{v}_2 of the gear velocity is

$$\mathbf{v}_1^{(2)} = (\boldsymbol{\omega} \times \mathbf{r}_1) + (\overline{O_1O_2} \times \boldsymbol{\omega}) \quad (9.8.56)$$

where

$$\mathbf{r}_1 = x_1\mathbf{i}_1 + y_1\mathbf{j}_1 + z_1\mathbf{k}_1 \quad (9.8.57)$$

Equations (9.8.48) and (9.8.50) to (9.8.57) yield

$$\mathbf{v}_1^{(12)} = \omega[(y_1 + r\phi)\mathbf{i}_1 - x_1\mathbf{j}_1] = \omega[(u \sin \psi_t + \ell \sin \beta + r\phi)\mathbf{i}_1 - u \cos \psi_t\mathbf{j}_1] \quad (9.8.58)$$

Using the equation

$$\mathbf{N}_1 \cdot \mathbf{v}_1^{(12)} = 0$$

we get

$$f(u, \ell, \phi) = \cos \beta [\sin \psi_t (r\phi + \ell \sin \beta) + u] = 0 \quad (9.8.59)$$

which is the same as equation (9.3.35). It is necessary to emphasize that we got the equation of meshing by a simpler method than the one applied in section 9.3.

Surface of action.—We use equation (9.8.59) and the matrix equation

$$[r_f] = [M_f][r_1] \quad (9.8.60)$$

where (fig. 9.3.2(a))

$$[M_f] = \begin{bmatrix} 1 & 0 & 0 & 0 \\ 0 & 1 & 0 & r\phi \\ 0 & 0 & 1 & 0 \\ 0 & 0 & 0 & 1 \end{bmatrix} \quad (9.8.61)$$

Equations (9.8.60), (9.8.61), (9.8.48), and (9.8.59) yield

$$\begin{aligned} x_f &= u \cos \psi_t & y_f &= u \sin \psi_t + \ell \sin \beta + r\phi & z_f &= \ell \cos \beta \\ \cos \beta [\sin \psi_t (r\phi + \ell \sin \beta) + u] &= 0 \end{aligned} \quad (9.8.62)$$

With $\beta \neq 90^\circ$, we represent the surface of action as follows:

$$x_f = u \cos \psi_t \quad y_f = -\frac{u \cos^2 \psi_t}{\sin \psi_t} \quad z_f = -\left(\frac{u}{\sin \psi_t} + r\phi\right) \cot \beta \quad (9.8.63)$$

which coincides with equations (9.3.56) of the surface of action determined in example 9.3.1. The surface of action is a plane shown in figure 9.3.7.

Generated surface.—We use equation (9.8.59) and the matrix equation

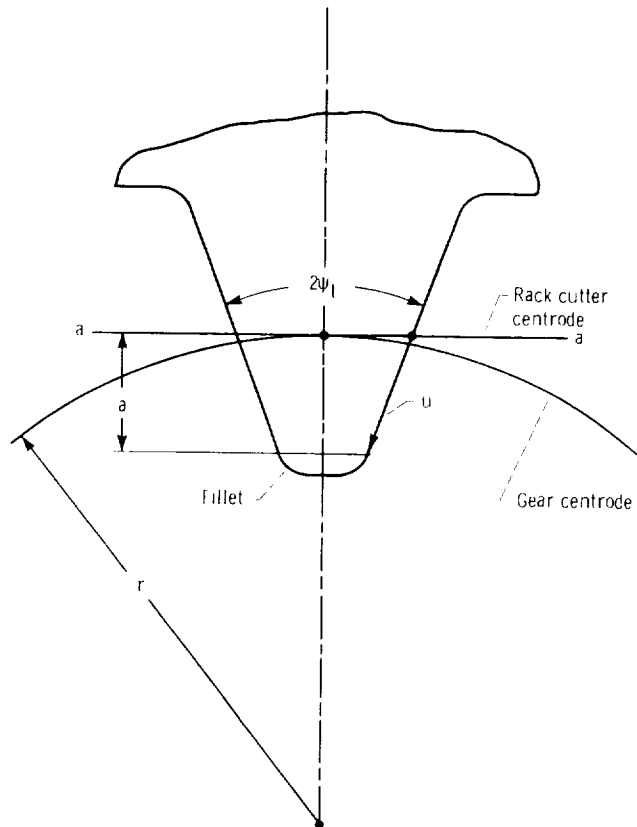
$$[r_2] = [M_{21}][r_1] = [M_{2f}][M_{f1}][r_1] \quad (9.8.64)$$

Here (fig. 9.3.2(a))

$$[M_{2f}] = \begin{bmatrix} \cos \phi & \sin \phi & 0 & r \cos \phi \\ -\sin \phi & \cos \phi & 0 & -r \sin \phi \\ 0 & 0 & 1 & 0 \\ 0 & 0 & 0 & 1 \end{bmatrix} \quad (9.8.65)$$

Equations (9.8.64), (9.8.65), (9.8.61), (9.8.48), and (9.8.59) yield

$$\begin{aligned} x_2 &= u \cos(\psi_t - \phi) + \ell \sin \beta \sin \phi + r(\phi \sin \phi + \cos \phi) \\ y_2 &= u \sin(\psi_t - \phi) + \ell \sin \beta \cos \phi + r(\phi \cos \phi - \sin \phi) \\ z_2 &= \ell \cos \beta \quad f(u, \theta, \phi) = \cos \beta [\sin \psi_t (r\phi + \ell \sin \beta) + u] = 0 \\ (u, \ell) &\in E \quad a < \phi < b \end{aligned} \quad (9.8.66)$$



Equations (9.8.66), which represent the generated surface Σ_2 , coincides with equations (9.3.32) and (9.3.35). Eliminating parameter ℓ (see example 9.3.1), we may represent the generated surface by

$$\begin{aligned} x_2 &= -u \cot \psi_t \sin(\phi - \psi_t) + r \cos \phi & y_2 &= -u \cot \psi_t \cos(\phi - \psi_t) - r \sin \phi \\ z_2 &= -\left(\frac{u}{\sin \psi_t} + r\phi\right) \cot \beta \end{aligned} \quad (9.8.67)$$

It was demonstrated previously (see example 9.3.1) that equations (9.8.67) represent an involute screw surface.

Conditions of nonundercutting of the tooth surface of gear 2.—We base the investigation on the effective method proposed in this section. Using equations (9.8.12), we get

$$\begin{vmatrix} \frac{\partial x_1}{\partial u} & \frac{\partial x_1}{\partial \ell} & v_{x_1}^{(12)} \\ \frac{\partial y_1}{\partial u} & \frac{\partial y_1}{\partial \ell} & v_{y_1}^{(12)} \\ f_u & f_\ell & f_\omega \end{vmatrix} = \begin{vmatrix} \cos \psi_t & 0 & u \sin \psi_t + \ell \sin \beta + r\phi \\ \sin \psi_t & \sin \beta & -u \cos \psi_t \\ 1 & \sin \beta \sin \psi_t & r \sin \psi_t \end{vmatrix} \omega = 0 \quad (9.8.68)$$

Equation (9.8.68) yields

$$F(u, \ell, \phi) = r\phi + \ell \sin \beta - r \tan \psi_t = 0 \quad (9.8.69)$$

Equations (9.8.69), (9.8.59), and (9.8.48) determine the line on surface Σ_1 by which Σ_1 must be limited to avoid undercutting of the generated surface Σ_2 . This line is represented by

$$u = -r \tan \psi_t \sin \psi_t \quad \ell = \frac{r(\tan \psi_t - \phi)}{\sin \beta}$$

$$x_1 = -r \sin^2 \psi_t \quad y_1 = -r \tan \psi_t \sin^2 \psi_t + r(\tan \psi_t - \phi) \quad z_1 = r(\tan \psi_t - \phi) \cot \beta \quad (9.8.70)$$

We derived equation (9.8.69) by using the first of three equations in equation set (9.8.12). We would get the same result by using the second or the third equation in equation set (9.8.12). Equation

$$x_1 = -r \sin^2 \psi_t \quad (9.8.71)$$

may be used to express conditions of nonundercutting in terms of the pressure angle of the rack cutter ψ_t and the number of teeth N of the generated gear.

Let us designate the limiting value of $|x_1|$ by a (fig. 9.8.7) where a is the height of the rack cutter measured from the rack cutter centrode aa to the fillet. Equation (9.8.71) yields that

$$a \leq r \sin^2 \psi_t = \frac{N}{2P_t} \sin^2 \psi_t$$

where N is the number of gear teeth and P_t is the diametral pitch measured in section AA (fig. 9.3.3).

According to equation (9.3.28)

$$\tan \psi_t = \frac{\tan \psi_n}{\cos \beta} = \frac{\tan \psi_c}{\cos \beta}$$

where $\psi_c = \psi_n$ is the shape angle of the rack cutter in section BB (fig. 9.3.3).

Investigation of existence of envelope of contact lines on the generating surface Σ_1 .—The necessary condition of envelope existence is represented by the equation

$$\frac{\partial}{\partial \phi} [f(u, \theta, \phi)] = f_\phi(u, \theta, \phi) = 0$$

Equation (9.8.59) yields that the envelope does not exist since $f_\phi \neq 0$. This result may be interpreted geometrically to mean that contact lines on the generating surface and on the surface of action are parallel straight lines (fig. 9.3.7) and therefore cannot have an envelope.

We used the simplified method of investigation (proposed by Litvin) in problems 9.8.1 and 9.8.2. Comparing this method with the ones used for solutions of problem 9.3.1 and 9.4.1, we may see its advantages.

Chapter 10

Curvatures of a Surface

10.1 First and Second Fundamental Forms

Definition of Forms

Consider a regular surface given by the vector function

$$\mathbf{r}(u, \theta) \in C^2 \quad \mathbf{r}_u \times \mathbf{r}_\theta \neq 0 \quad (u, \theta) \in A \quad (10.1.1)$$

The surface unit normal is represented by

$$\mathbf{n}(u, \theta) = \frac{\mathbf{r}_u \times \mathbf{r}_\theta}{|\mathbf{r}_u \times \mathbf{r}_\theta|} \quad (10.1.2)$$

The first fundamental form of a surface is defined as follows:

$$\begin{aligned} I = d\mathbf{r}^2 &= (\mathbf{r}_u du + \mathbf{r}_\theta d\theta)^2 = \mathbf{r}_u^2 du^2 + 2(\mathbf{r}_u \cdot \mathbf{r}_\theta) du d\theta + \mathbf{r}_\theta^2 d\theta^2 \\ &= E du^2 + 2F du d\theta + G d\theta^2 \end{aligned} \quad (10.1.3)$$

Here

$$d\mathbf{r} = \mathbf{r}_u du + \mathbf{r}_\theta d\theta \quad (10.1.4)$$

$$E = \mathbf{r}_u^2 \quad F = \mathbf{r}_u \cdot \mathbf{r}_\theta \quad G = \mathbf{r}_\theta^2 \quad (10.1.5)$$

The far right side of equation (10.1.3) is a quadratic form in differentials du and $d\theta$.

The second fundamental form of a surface is defined by

$$II = d^2\mathbf{r} \cdot \mathbf{n} = -d\mathbf{r} \cdot d\mathbf{n} \quad (10.1.6)$$

The equality of scalar products

$$d^2\mathbf{r} \cdot \mathbf{n} = -d\mathbf{r} \cdot d\mathbf{n} \quad (10.1.7)$$

results from the equation

$$d\mathbf{r} \cdot \mathbf{n} = 0 \quad (10.1.8)$$

after its differentiation.

Equation (10.1.8) is based on the following considerations: (1) vector $d\mathbf{r}$ represents an infinitesimal displacement over the surface from the given point M to the infinitesimally close point M^* and (2) vector $d\mathbf{r}$ is tangent to the surface at point M and therefore must be perpendicular to the surface unit normal \mathbf{n} at point M .

The differentiation of equation (10.1.8) gives

$$d(d\mathbf{r} \cdot \mathbf{n}) = (d^2\mathbf{r} \cdot \mathbf{n}) + (d\mathbf{r} \cdot d\mathbf{n}) = 0 \quad (10.1.9)$$

Thus,

$$d^2\mathbf{r} \cdot \mathbf{n} = -d\mathbf{r} \cdot d\mathbf{n}$$

and equality (10.1.7) is proven.

Let us develop the equation

$$\Pi = d^2\mathbf{r} \cdot \mathbf{n} \quad (10.1.10)$$

The differentiation of equation (10.1.4) yields

$$d^2\mathbf{r} = d(\mathbf{r}_u du + \mathbf{r}_\theta d\theta) = \mathbf{r}_{uu} du^2 + 2\mathbf{r}_{u\theta} du d\theta + \mathbf{r}_{\theta\theta} d\theta^2 + \mathbf{r}_u d^2u + \mathbf{r}_\theta d^2\theta$$

and

$$\begin{aligned} \Pi = d^2\mathbf{r} \cdot \mathbf{n} &= (\mathbf{r}_{uu} \cdot \mathbf{n}) du^2 + 2(\mathbf{r}_{u\theta} \cdot \mathbf{n}) du d\theta + (\mathbf{r}_{\theta\theta} \cdot \mathbf{n}) d\theta^2 + (\mathbf{r}_u \cdot \mathbf{n}) d^2u \\ &+ (\mathbf{r}_\theta \cdot \mathbf{n}) d^2\theta = L du^2 + 2M du d\theta + N d\theta^2 \quad (\mathbf{r}_u \cdot \mathbf{n} = 0 \quad \mathbf{r}_\theta \cdot \mathbf{n} = 0) \end{aligned} \quad (10.1.11)$$

where

$$L = \mathbf{r}_{uu} \cdot \mathbf{n} \quad M = \mathbf{r}_{u\theta} \cdot \mathbf{n} \quad N = \mathbf{r}_{\theta\theta} \cdot \mathbf{n}$$

The right side of equation (10.1.11) is a quadratic form in differentials du and $d\theta$.

We may get equation (10.1.11) by using the expression

$$\Pi = -d\mathbf{n} \cdot d\mathbf{r} \quad (10.1.12)$$

The differentiation of equation

$$\mathbf{n} = \mathbf{n}(u, \theta)$$

gives

$$d\mathbf{n} = \mathbf{n}_u du + \mathbf{n}_\theta d\theta \quad (10.1.13)$$

Equations (10.1.12), (10.1.13), and (10.1.4) yield

$$\Pi = - [(\mathbf{n}_u \cdot \mathbf{r}_u) du^2 + (\mathbf{n}_\theta \cdot \mathbf{r}_u + \mathbf{n}_u \cdot \mathbf{r}_\theta) du d\theta + (\mathbf{n}_\theta \cdot \mathbf{r}_\theta) d\theta^2] \quad (10.1.14)$$

We may transform the right side of equation (10.1.14) by taking into account that vectors \mathbf{r}_u and \mathbf{r}_θ are tangent to the surface and therefore

$$\mathbf{n} \cdot \mathbf{r}_u = 0 \quad \mathbf{n} \cdot \mathbf{r}_\theta = 0 \quad (10.1.15)$$

Equations (10.1.15) yield

$$\frac{\partial}{\partial u} (\mathbf{n} \cdot \mathbf{r}_u) = \mathbf{n}_u \cdot \mathbf{r}_u + \mathbf{n} \cdot \mathbf{r}_{uu} = 0 \quad (10.1.16)$$

$$\frac{\partial}{\partial \theta} (\mathbf{n} \cdot \mathbf{r}_u) = \mathbf{n}_\theta \cdot \mathbf{r}_u + \mathbf{n} \cdot \mathbf{r}_{u\theta} = 0 \quad (10.1.17)$$

$$\frac{\partial}{\partial u} (\mathbf{n} \cdot \mathbf{r}_\theta) = \mathbf{n}_u \cdot \mathbf{r}_\theta + \mathbf{n} \cdot \mathbf{r}_{u\theta} = 0 \quad (10.1.18)$$

$$\frac{\partial}{\partial \theta} (\mathbf{n} \cdot \mathbf{r}_\theta) = \mathbf{n}_\theta \cdot \mathbf{r}_\theta + \mathbf{n} \cdot \mathbf{r}_{\theta\theta} = 0 \quad (10.1.19)$$

Equations (10.1.14) and (10.1.15) to (10.1.19) yield expression (10.1.11).

Interpretations of Fundamental Forms

Consider a line L (fig. 10.1.1) given on surface (10.1.1) as follows:

$$\begin{aligned} \mathbf{r}(u(t), \theta(t)) \in C \quad \mathbf{r}_u \times \mathbf{r}_\theta \neq 0 \quad \{u(t), \theta(t)\} \in C^1 \\ |u_t| + |\theta_t| \neq 0 \quad (u, \theta) \in A \quad t_1 < t < t_2 \end{aligned} \quad (10.1.20)$$

where t is the curve parameter.

A point is displaced along the line L from position M to M^* and vector $d\mathbf{r} = \overline{MM^*}$ is the infinitesimal displacement of this point. With members of the first order only, we get

$$d\mathbf{r} = \mathbf{r}_u du + \mathbf{r}_\theta d\theta = \mathbf{r}_u u_t dt + \mathbf{r}_\theta \theta_t dt \quad (10.1.21)$$

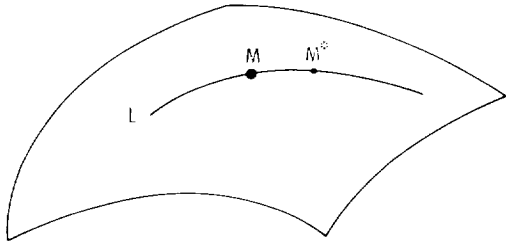


Figure 10.1.1.

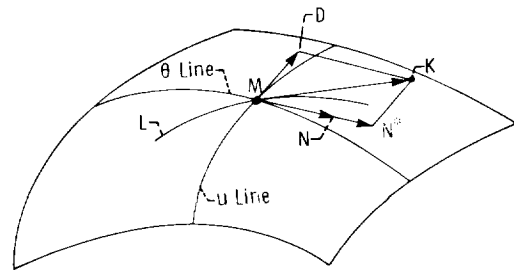


Figure 10.1.2.

Here

$$du = u_t dt = \frac{du}{dt} dt \quad d\theta = \theta_t dt = \frac{d\theta}{dt} dt \quad (10.1.22)$$

where \mathbf{r}_u and \mathbf{r}_θ are the tangents to the coordinate lines (the u -line and the θ -line, fig. 10.1.2) on the surface; the derivatives \mathbf{r}_u , and \mathbf{r}_θ , u_t , and θ_t are taken at the point M ; and the displacement vector $d\mathbf{r}$ lies in the tangent plane to the surface because vectors \mathbf{r}_u and \mathbf{r}_θ belong to this plane.

The point displacement $d\mathbf{r}$ (provided $du \neq 0$) may be represented by

$$d\mathbf{r} = du \left(\mathbf{r}_u + \mathbf{r}_\theta \frac{d\theta}{du} \right) \quad (10.1.23)$$

Here (fig. 10.1.2)

$$\mathbf{r}_u = \overline{MD} \quad \mathbf{r}_\theta = \overline{MN} \quad \mathbf{r}_\theta \frac{d\theta}{du} = \overline{MN^*} \quad \mathbf{r}_u + \mathbf{r}_\theta \frac{d\theta}{du} = \overline{MK} \quad (10.1.24)$$

Vectors $d\mathbf{r}$ and \overline{MK} are collinear. It results from equation (10.1.23) that the direction of the point displacement over the surface depends only on the ratio

$$\frac{d\theta}{du} = \frac{\theta_t}{u_t} \quad (10.1.25)$$

The point displacement is an arc of length

$$ds = |d\mathbf{r}| \quad (10.1.26)$$

and the first fundamental form I represents the squared length of this arc

$$ds^2 = d\mathbf{r}^2 = I \quad (10.1.27)$$

The first fundamental form is always positive and may be used for the determination of the length ds^2 for different curves which pass through the same point. If the curve parameter t is the time, it is seen that

$$\left(\frac{ds}{dt} \right)^2 = \mathbf{v}_r^2 = \frac{I}{dt^2} \quad (10.1.28)$$

where \mathbf{v}_r is the relative velocity, the velocity of the point in its motion over the surface. Vectors \mathbf{v}_r and $d\mathbf{r}$ are of the same direction, and their direction depends on the ratio (10.1.25).

Now, let us prove that the second fundamental form represents the deviation of the curve point M^* from the tangent plane T (fig. 10.1.3). Vector $\boldsymbol{\tau}$ is the unit tangent vector to the curve L . The perpendicular to the tangent plane T , drawn from point M^* , intersects T at point B . Vector

$$\overline{BM^*} = \ell \mathbf{n} \quad (10.1.29)$$

represents the deviation of point M^* from the tangent plane. Here ℓ is a signed value, and ℓ is positive if the direction of vector $\overline{BM^*}$ coincides with the direction of the surface unit normal \mathbf{n} .

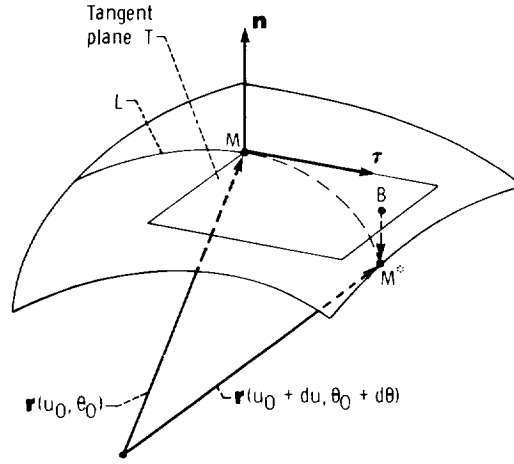


Figure 10.1.3.

There are two options for the determination of the direction of \mathbf{n} , and they are represented by

$$\mathbf{n} = \frac{\mathbf{r}_u \times \mathbf{r}_\theta}{|\mathbf{r}_u \times \mathbf{r}_\theta|} \quad \text{or} \quad \mathbf{n}^* = \frac{\mathbf{r}_\theta \times \mathbf{r}_u}{|\mathbf{r}_\theta \times \mathbf{r}_u|} \quad (10.1.30)$$

The unit normals \mathbf{n} and \mathbf{n}^* have opposite directions.

The relation between the signed deviation ℓ and the second fundamental form II is based on the following considerations:

- (1) We designate the position vectors of points M and M^* of the surface by $\mathbf{r}(u_0, \theta_0)$ and $\mathbf{r}(u_0 + du, \theta_0 + d\theta)$, respectively.
- (2) Taking into account that

$$\mathbf{r}(u_0, \theta_0) + \overline{MM^*} = \mathbf{r}(u_0 + du, \theta_0 + d\theta) \quad (10.1.31)$$

we get

$$\overline{MM^*} = \mathbf{r}(u_0 + du, \theta_0 + d\theta) - \mathbf{r}(u_0, \theta_0) \quad (10.1.32)$$

- (3) The deviation ℓ of point M^* from the tangent plane is

$$\ell = \overline{MM^*} \cdot \mathbf{n} \quad (10.1.33)$$

Equations (10.1.32) and (10.1.33) yield

$$\ell = [\mathbf{r}(u_0 + du, \theta_0 + d\theta) - \mathbf{r}(u_0, \theta_0)] \cdot \mathbf{n} \quad (10.1.34)$$

- (4) We apply Taylor's formula to the difference

$$\Delta \mathbf{r} = \mathbf{r}(u_0 + du, \theta_0 + d\theta) - \mathbf{r}(u_0, \theta_0) = \overline{MM^*} \quad (10.1.35)$$

and limit the series expansion to the members of second order only. Thus,

$$\Delta \mathbf{r} = (\mathbf{r}_u du + \mathbf{r}_\theta d\theta) + \frac{1}{2}(\mathbf{r}_{uu} du^2 + 2\mathbf{r}_{u\theta} du d\theta + \mathbf{r}_{\theta\theta} d\theta^2) \quad (10.1.36)$$

The derivatives of the function $\mathbf{r}(u, \theta)$ are taken at u_0, θ_0 .

(5) The derivatives \mathbf{r}_u and \mathbf{r}_θ lie in the tangent plane and

$$\mathbf{r}_u \cdot \mathbf{n} = \mathbf{r}_\theta \cdot \mathbf{n} = 0 \quad (10.1.37)$$

(6) Equations (10.1.33) to (10.1.37) yield

$$\ell = \frac{1}{2} [(\mathbf{r}_{uu} \cdot \mathbf{n})du^2 + (2\mathbf{r}_{u\theta} \cdot \mathbf{n})du d\theta + (\mathbf{r}_{\theta\theta} \cdot \mathbf{n})d\theta^2] = \frac{\Pi}{2} \quad (10.1.38)$$

Thus, the second fundamental form of the surface is equal to the doubled value of the deviation ℓ . Another representation of the second fundamental form is based on the relative acceleration \mathbf{a}_r , the acceleration of a point in its motion along the curve L .

Considering that the curve L is given by equation (10.1.20) and the curve parameter t is the time, we get

$$\frac{d\mathbf{r}}{dt} = \mathbf{v}_r = \mathbf{r}_u \frac{du}{dt} + \mathbf{r}_\theta \frac{d\theta}{dt} \quad (10.1.39)$$

$$\frac{d^2\mathbf{r}}{dt^2} = \mathbf{a}_r = \mathbf{r}_{uu} \left(\frac{du}{dt}\right)^2 + 2\mathbf{r}_{u\theta} \frac{du}{dt} \frac{d\theta}{dt} + \mathbf{r}_{\theta\theta} \left(\frac{d\theta}{dt}\right)^2 + \mathbf{r}_u \frac{d^2u}{dt^2} + \mathbf{r}_\theta \frac{d^2\theta}{dt^2} \quad (10.1.40)$$

Taking into account that

$$\mathbf{r}_u \cdot \mathbf{n} = 0 \quad \mathbf{r}_\theta \cdot \mathbf{n} = 0$$

we get

$$\mathbf{a}_r \cdot \mathbf{n} = \frac{\Pi}{dt^2} \quad (10.1.41)$$

Equation (10.1.41) expresses the second form in terms of \mathbf{a}_r , \mathbf{n} , and dt^2 .

Example problem 10.1 The surface of a cone (fig. 10.1.4) is represented by the equations

$$\mathbf{r}(u, \theta) = u \cos \psi_c \mathbf{i} + u \sin \psi_c \sin \theta \mathbf{j} + u \sin \psi_c \cos \theta \mathbf{k}$$

where

$$\mathbf{r}(u, \theta) \in C^k \quad k > 2 \quad 0 < u < u^* \quad 0 < \theta < 2\pi \quad (10.1.42)$$

and (u, θ) are the surface coordinates ($u = OM$).

Determine the first and second fundamental forms.

Solution. The surface unit normal (provided $u \sin \psi_c \neq 0$) is

$$\mathbf{n} = \frac{\mathbf{r}_u \times \mathbf{r}_\theta}{|\mathbf{r}_u \times \mathbf{r}_\theta|} = -\sin \psi_c \mathbf{i} + \cos \psi_c \sin \theta \mathbf{j} + \cos \psi_c \cos \theta \mathbf{k} \quad (10.1.43)$$

The first and second fundamental forms are, respectively:

$$I = du^2 + u^2 \sin^2 \psi_c d\theta^2 \quad (10.1.44)$$

$$II = -u \sin \psi_c \cos \psi_c d\theta^2 \quad (\text{provided } u \sin \psi_c \neq 0) \quad (10.1.45)$$

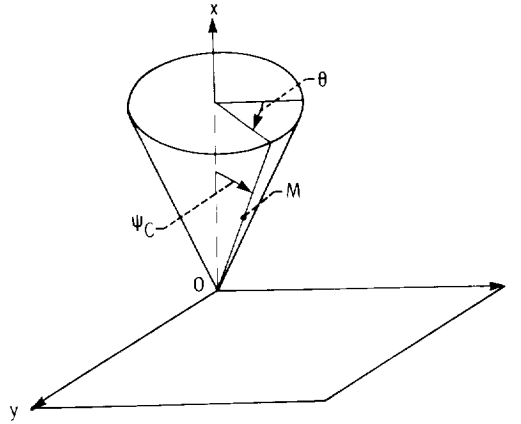


Figure 10.1.4.

10.2 Surface Normal Section: Osculating Plane

Consider, on the given surface, various curves which pass through a common point M and have the same unit tangent τ at M (fig. 10.2.1). One of these curves (designated by L_0) represents the normal section of the surface formed by cutting the surface with plane Π . This plane is drawn through the unit tangent vector τ and the surface unit normal \mathbf{n} (fig. 10.2.1). Curve L_0 is a plane curve—all points of L_0 belong to the plane Π . Other curves, designated by L , are spatial curves. But we can find such a plane P (fig. 10.2.2), that an infinitesimally small piece of a spatial curve L may be located on P . This plane is called the osculating plane. Consider three infinitesimally close points, M_1 , M , and M_2 , of the curve L (fig. 10.2.2). The osculating plane is the limiting position of a plane which is drawn through three infinitesimally close points M_1 , M , and M_2 that approach point M . The osculating plane for the curve L at its point M may be determined as the plane which is drawn through the unit tangent vector τ (or the relative velocity \mathbf{v}_r) and the acceleration vector \mathbf{a}_r (represented by equation (10.1.40)).

Let a point move along the curve L which is represented by equation (10.1.20). The total acceleration \mathbf{a}_r in this motion may be represented as the sum of two components: the normal acceleration \mathbf{a}_r^n and the tangential acceleration \mathbf{a}_r^t . These components are determined as follows:

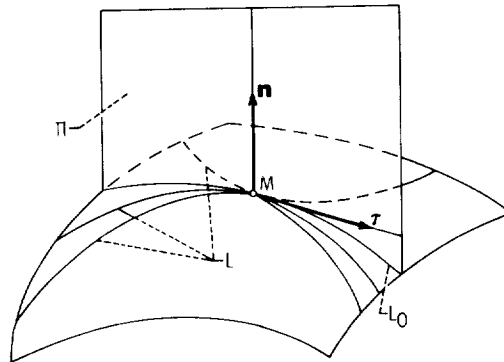


Figure 10.2.1.

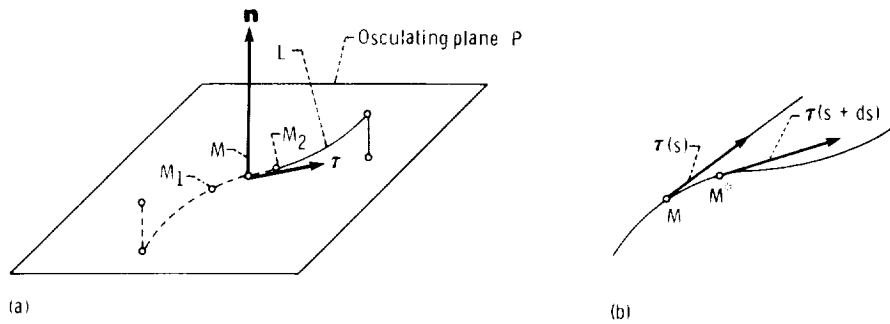


Figure 10.2.2.

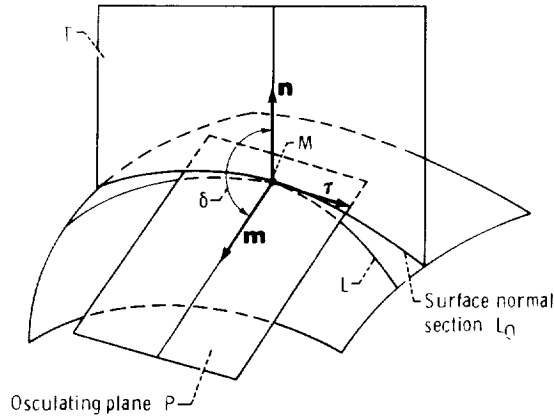


Figure 10.2.3.

$$\mathbf{a}_r^m = \mathbf{r}_{uu} \left(\frac{du}{dt} \right)^2 + 2\mathbf{r}_{u\theta} \frac{du}{dt} \frac{d\theta}{dt} + \mathbf{r}_{\theta\theta} \left(\frac{d\theta}{dt} \right)^2 \quad (10.2.1)$$

$$\mathbf{a}_r^t = \mathbf{r}_u \frac{d^2u}{dt^2} + \mathbf{r}_\theta \frac{d^2\theta}{dt^2} \quad (10.2.2)$$

(See eq. (10.1.40).)

Vector \mathbf{a}_r^t is collinear with the tangent vector $\boldsymbol{\tau}$. The direction of vector \mathbf{a}_r^m defines the direction of the so-called main normal \mathbf{m} to curve L (fig. 10.2.3) which belongs to the osculating plane. Thus, the osculating plane may be determined by vectors $\boldsymbol{\tau}$ and \mathbf{a}_r^m . The osculating plane and the surface unit normal \mathbf{n} form the angle δ (fig. 10.2.3) determined by

$$\cos \delta = \frac{\mathbf{a}_r^m \cdot \mathbf{n}}{|\mathbf{a}_r^m|} \quad (10.2.3)$$

10.3. Curvature of a Spatial Curve

Consider a regular spatial curve (fig. 10.3.1(a)) represented by the equations

$$\mathbf{r}(s) \in C^2 \quad \mathbf{r}_s \neq 0 \quad s_1 < s < s_2 \quad (10.3.1)$$

where s is the length of the arc of the curve. M and M^* are the infinitesimally close points of

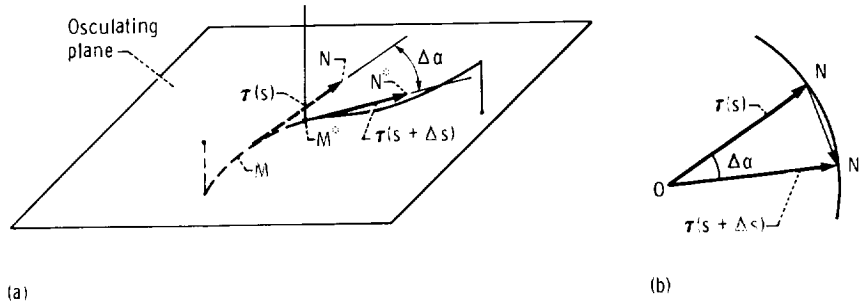


Figure 10.3.1.

the curve and $\tau(s)$ and $\tau(s + \Delta s)$ are the unit tangent vectors at points M and M^* , respectively. The curvature κ of the curve at point M is given by

$$\kappa = \lim_{M \rightarrow M^*} \left| \frac{\Delta \alpha}{\Delta s} \right| \quad (10.3.2)$$

where $\Delta \alpha$ is the angle formed by the unit tangents $\tau(s)$ and $\tau(s + \Delta s)$ (fig. 10.3.1(a)).

We may transform equation (10.3.2) by using the following relations:

(1) The derivative \mathbf{r}_s represents the unit tangent vector $\tau(s)$; that is,

$$\mathbf{r}_s(s) = \tau(s) \quad (|\tau(s)| = 1) \quad (10.3.3)$$

(2) The derivative $\tau_s(s)$ of the unit vector $\tau(s)$ is perpendicular to $\tau(s)$; that is,

$$\tau_s(s) \cdot \tau(s) = 0 \quad (10.3.4)$$

(3) The ratio $\left| \frac{d\alpha}{ds} \right|$ is equal to the absolute value of the derivative $|\tau_s|$; that is

$$\left| \frac{d\alpha}{ds} \right| = |\tau_s| \quad (10.3.5)$$

Let us prove equations (10.3.3) to (10.3.5)

(1) The elementary arc of the curve is

$$ds = |d\mathbf{r}| = |\mathbf{r}_s ds| = |\mathbf{r}_s| ds \quad (10.3.6)$$

where \mathbf{r}_s is the tangent to the curve.

Equation (10.3.6) yields

$$|\mathbf{r}_s| = 1 \quad \mathbf{r}_s = \tau \quad (10.3.7)$$

where τ is the unit tangent vector. Equation (10.3.3) is proven.

(2) Taking into account that

$$\tau(s) \cdot \tau(s) = \tau^2(s) = 1 \quad (10.3.8)$$

we get

$$\frac{d}{ds}(\tau^2(s)) = 2\tau(s) \cdot \tau_s(s) = 0 \quad (10.3.9)$$

Thus, vectors τ_s and τ are perpendicular. Equation (10.3.4) is proven.

(3) To prove equation (10.3.5), we consider the unit vectors $\tau(s)$ and $\tau(s + \Delta s)$ which form the angle $\Delta\alpha$; points N and N^* —the ends of the above vectors—belong to the circle of radius equal to 1; the circle is centered at 0 (fig. 10.3.1(b)). With the radius of the circle equal to 1, we get

$$|\widehat{NN^*}| = |\tau| |\Delta\alpha| = |\Delta\alpha| \quad (10.3.10)$$

Then,

$$|\widehat{NN^*}| = |\tau(s + \Delta s) - \tau(s)| \quad (10.3.11)$$

We represent the ratio $\left| \frac{\Delta\alpha}{\Delta s} \right|$ by

$$\left| \frac{\Delta\alpha}{\Delta s} \right| = \left| \frac{\widehat{NN^*}}{\Delta s} \right| = \left| \frac{\widehat{NN^*}}{\Delta s} \right| \left| \frac{\widehat{NN^*}}{\widehat{NN^*}} \right| = \left| \frac{\tau(s + \Delta s) - \tau(s)}{\Delta s} \right| \left| \frac{\widehat{NN^*}}{\widehat{NN^*}} \right| \quad (10.3.12)$$

The limit of this ratio as $\Delta s \rightarrow 0$ is as follows:

$$\left| \frac{d\alpha}{ds} \right| = \lim_{\Delta s \rightarrow 0} \left| \frac{\Delta\alpha}{\Delta s} \right| = \lim_{\Delta s \rightarrow 0} \left| \frac{\tau(s + \Delta s) - \tau(s)}{\Delta s} \right| \lim_{\Delta s \rightarrow 0} \left| \frac{\widehat{NN^*}}{\widehat{NN^*}} \right| \quad (10.3.13)$$

Vector

$$\frac{\tau(s + \Delta s) - \tau(s)}{\Delta s}$$

as $\Delta s \rightarrow 0$ approaches the derivative is

$$\tau_s = \frac{d}{ds}(\tau_s) = \mathbf{r}_{ss}$$

and

$$\lim_{\Delta s \rightarrow 0} \left| \frac{\tau(s + \Delta s) - \tau(s)}{\Delta s} \right| = |\mathbf{r}_{ss}| \quad (10.3.14)$$

Taking into account that $\widehat{NN^*}$ and $\overline{NN^*}$ represent an arc and its chord, we get

$$\lim_{\Delta s \rightarrow 0} \left| \frac{\widehat{NN^*}}{\overline{NN^*}} \right| = 1 \quad (10.3.15)$$

Equations (10.3.13) to (10.3.15) yield

$$\lim_{\Delta s \rightarrow 0} \left| \frac{\Delta \alpha}{\Delta s} \right| = \mathbf{r}_{ss} = \boldsymbol{\tau}_s \quad (10.3.16)$$

Equation (10.3.5) is proven.

According to the definition of the curvature of a spatial curve, we get

$$\kappa = |\mathbf{r}_{ss}| = |\boldsymbol{\tau}_s| \quad (10.3.17)$$

(See eq. (10.3.2).)

We may represent the curvature of the curve in terms of the acceleration and the velocity of a point which moves with constant velocity along the curve. We consider that the curve is represented by the vector function $\mathbf{r}(s(t))$, where $s(t)$ is a linear function and t is the time. Thus,

$$\mathbf{v}_r = \mathbf{r}_s \frac{ds}{dt} = v \boldsymbol{\tau} \quad \mathbf{a}_r^m = \mathbf{r}_{ss} \left(\frac{ds}{dt} \right)^2 = v_r^2 \mathbf{r}_{ss} \quad (10.3.18)$$

Equations (10.3.17) and (10.3.18) yield

$$\kappa = \frac{|\mathbf{a}_r^m|}{v_r^2} \quad (10.3.19)$$

The curvature of a spatial curve is always positive. The radius of the curvature has the same direction as the vector \mathbf{r}_{ss} or the vector of acceleration \mathbf{a}_r determined with the velocity $|\mathbf{v}_r| = \text{constant}$. The radius of curvature lies in the osculating plane.

10.4 The Meusnier Theorem

Consider that on a surface a set of curves pass through the given point M and have a common unit tangent $\boldsymbol{\tau}$ (fig. 10.2.1). We pick out from this set the curve L_O , which represents the normal section of the surface, and a spatial curve L (fig. 10.2.3). The Meusnier theorem states the relation between the curvatures of curves L and L_O . We assume that the normal curvature of the surface, κ_n , the curvature of curve L_O , is not equal to zero. Plane P is the osculating plane for the spatial curve L , and δ is the angle formed between the surface unit normal \mathbf{n} and the binormal \mathbf{m} to the spatial curve L at point M .

The Meusnier theorem states that the curvatures κ_n and κ are related by the equation $\kappa_n = \kappa \cos \delta$. Here κ_n is the curvature of the curve L_O (which represents the normal section of the surface), κ is the curvature of the curve L , and δ is formed between vectors \mathbf{n} and \mathbf{m} . The product $\kappa \cos \delta$ is of the same magnitude for all spatial curves which pass through the same surface point M and have the common unit tangent $\boldsymbol{\tau}$.

Proof: We employ the following considerations to prove the Meusnier theorem:

(1) The product $\kappa \cos \delta$ may be represented by the equation

$$\kappa \cos \delta = \frac{\text{II}}{\text{I}} = \frac{L du^2 + 2M du d\theta + N d\theta^2}{E du^2 + 2F du d\theta + G d\theta^2} \quad (10.4.1)$$

(2) The ratio $du/d\theta$ determines the direction of the unit tangent to a spatial curve. Assume that a set of spatial curves passes through the given point M and they have a common tangent. Thus, we get

$$\kappa \cos \delta = \text{constant} \quad (10.4.2)$$

(3) The curvature κ_n of the curve L_O (the normal curvature) is represented by

$$\kappa_n = \kappa \cos \delta \quad (10.4.3)$$

(1) Let us begin with the proof of equations (10.4.1). According to equation (10.3.19), the curvature of a spatial curve on the surface may be represented by

$$\kappa = \frac{|\mathbf{a}_r^m|}{v_r^2}$$

Taking into account that the acceleration \mathbf{a}_r^m and the main normal \mathbf{m} (fig. 10.2.3) have the same direction, we get

$$\kappa \mathbf{m} = \frac{\mathbf{a}_r^m}{v_r^2} \quad (10.4.4)$$

We multiply both sides of equation (10.4.4) by the surface unit normal \mathbf{n} . Thus,

$$\kappa \mathbf{m} \cdot \mathbf{n} = \frac{\mathbf{a}_r^m \cdot \mathbf{n}}{v_r^2} = \frac{\mathbf{a}_r \cdot \mathbf{n}}{v_r^2} \quad (10.4.5)$$

Here

$$\mathbf{a}_r \cdot \mathbf{n} = (\mathbf{a}_r^m + \mathbf{a}_r^t) \cdot \mathbf{n} = \mathbf{a}_r^m \cdot \mathbf{n} \quad (10.4.6)$$

because the component \mathbf{a}_r^t is collinear with the unit tangent $\boldsymbol{\tau}$ and is perpendicular to the unit normal \mathbf{n} .

The dot product (fig. 10.2.3)

$$\mathbf{m} \cdot \mathbf{n} = \cos \delta \quad (10.4.7)$$

Applying equations (10.4.5) to (10.4.7), (10.1.28), and (10.1.41), we get

$$\kappa \cos \delta = \frac{\text{II}}{\text{I}} = \frac{L du^2 + 2M du d\theta + N d\theta^2}{E du^2 + 2F du d\theta + G d\theta^2} \quad (10.4.8)$$

Equation (10.4.1) is proven.

(2) Equation (10.4.2) is based on the following considerations: (a) Coefficients L , M , N , E , F , and G are taken at the given point M which is the same for the considered set of spatial curves. (b) The ratio $du/d\theta$ is the same for all the curves above because they have the common tangent $\boldsymbol{\tau}$ at point M (fig. 10.2.1). Thus, the right side of equation (10.4.1) is constant for the given point M and tangent $\boldsymbol{\tau}$. Equation (10.4.2) is proven.

(3) It results from equations (10.4.1) and (10.4.2) that the curvature κ of the spatial curve of the considered set of curves depends on the angle δ which determines the direction of the osculating plane with respect to the surface unit normal. The angle δ is equal to zero for the curve L_O (fig.

10.2.3). Thus the normal curvature, the curvature of the normal section of the surface, is represented by

$$\kappa_n = \frac{\text{II}}{\text{I}} \quad (10.4.9)$$

Equations (10.4.9) and (10.4.8) yield

$$\kappa_n = \kappa \cos \delta \quad (10.4.10)$$

Equation (10.4.3) is proven, and, with this, the proof of the Meusnier theorem is completed.

Example 10.4.1 Consider that a spherical surface is represented by equations (8.4.9).

$$x = \rho \cos \theta \cos \psi \quad y = \rho \cos \theta \sin \psi \quad z = \rho \sin \theta$$

where

$$0 \leq \theta \leq 2\pi \quad 0 \leq \psi \leq 2\pi$$

The surface normal vector is represented by

$$\mathbf{N} = \frac{\partial \mathbf{r}}{\partial \theta} \times \frac{\partial \mathbf{r}}{\partial \psi} = -\rho^2 \cos \theta (\cos \theta \cos \psi \mathbf{i} + \cos \theta \sin \psi \mathbf{j} + \sin \theta \mathbf{k})$$

The surface unit normal (provided by $\cos \theta \neq 0$) is

$$\mathbf{n} = -(\cos \theta \cos \psi \mathbf{i} + \cos \theta \sin \psi \mathbf{j} + \sin \theta \mathbf{k}) \quad (10.4.11)$$

Let the surface be cut by the plane (fig. 10.4.1)

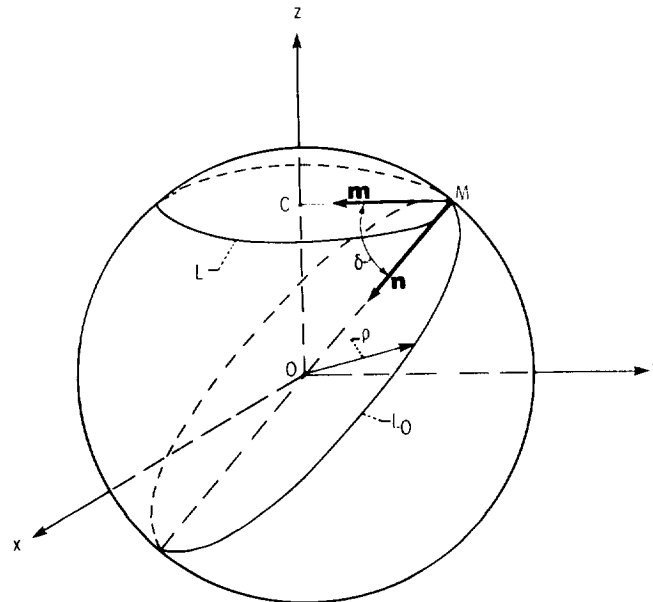


Figure 10.4.1.

$$z = a \quad (a = \text{constant}) \quad (10.4.12)$$

and let L be the curve by which plane (10.4.12) intersects the spherical surface (8.4.7). We may represent the curve L by the equations

$$x = \rho \cos \theta \cos \psi \quad y = \rho \cos \theta \sin \psi \quad z = \rho \sin \theta = a \quad (10.4.13)$$

It is necessary to determine the curvature κ of the curve L at a point with $\psi = \psi_0$ and $\theta = \theta_0$ by using equation (10.3.19).

Considering that $\psi(t)$ is a linear function and θ is constant, we get

$$\mathbf{v}_r = \frac{dx}{dt} \mathbf{i} + \frac{dy}{dt} \mathbf{j} = -\rho \cos \theta \frac{d\psi}{dt} (\sin \psi \mathbf{i} - \cos \psi \mathbf{j}) \quad (10.4.14)$$

$$\mathbf{a}_r^m = \frac{d^2x}{dt^2} \mathbf{i} + \frac{d^2y}{dt^2} \mathbf{j} = -\rho \cos \theta \left(\frac{d\psi}{dt} \right)^2 (\cos \psi \mathbf{i} + \sin \psi \mathbf{j}) \quad (10.4.15)$$

Here \mathbf{v}_r and \mathbf{a}_r^m are the velocity and the normal component of the acceleration of a point in its motion along the curve L .

Equations (10.3.18), (10.4.14), and (10.4.15) yield

$$\kappa = \frac{|\mathbf{a}_r^m|}{v_r^2} = \frac{1}{\rho |\cos \theta|} \quad (10.4.16)$$

It results from equations (10.4.15) and (10.4.11) that vectors \mathbf{n} and \mathbf{a}_r^m form the angle δ (fig. 10.4.1) determined by the equation

$$\cos \delta = \frac{\mathbf{n} \cdot \mathbf{a}_r^m}{|\mathbf{a}_r^m|} = |\cos \theta| \quad (10.4.17)$$

The curvature of the curve L may be determined very easily if we employ the Meusnier theorem. According to equation (10.4.3), we get

$$\kappa = \frac{\kappa_n}{\cos \delta} \quad (10.4.18)$$

Here $\kappa_n = 1/\rho$ is the normal curvature of the spherical surface (the curvature of the curve L_0 , fig. 10.4.1), κ is the curvature of the curve L , and δ is the angle formed by vectors \mathbf{m} and \mathbf{n} . We may interpret equation (10.4.18) geometrically. Curves L and L_0 have a common tangent at point M . It is evident from the drawings of figure 10.4.1 that

$$MC = OM \cos \delta = \rho \cos \delta$$

where MC is the curvature radius of curve L .

10.5 Normal Curvature

Consider that a surface Σ is given and the surface unit normal \mathbf{n} at a regular point M of the surface is determined (fig. 10.5.1). Unit vectors $\boldsymbol{\tau}^{(1)}, \boldsymbol{\tau}^{(2)}, \dots, \boldsymbol{\tau}^{(n)}$ belong to the plane that

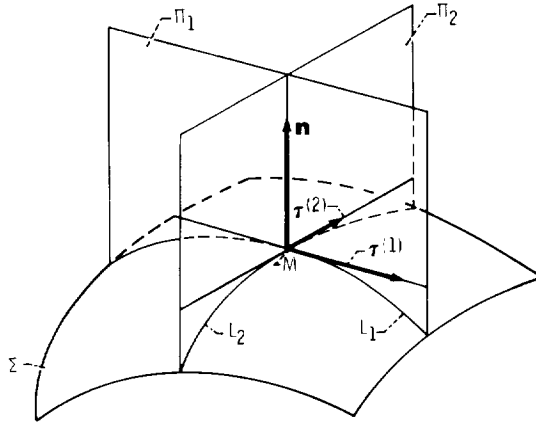


Figure 10.5.1.

is tangent to the surface at point M and represent different directions on the surface. A plane Π_i , drawn through the vectors \mathbf{n} and $\boldsymbol{\tau}^{(i)}$, cuts the surface by a planar line L_i . The normal curvature κ_n of the surface at point M , is the curvature of the planar curve L_i at M_2 ($i = 1, 2$).

Let a regular surface be given by

$$\mathbf{r}(u, \theta) \in C^2 \quad \mathbf{r}_u \times \mathbf{r}_\theta \neq 0 \quad (u, \theta) \in A \quad (10.5.1)$$

Equations (10.4.10) and (10.4.8) yield that the normal curvature may be represented by

$$\kappa_n = \frac{\text{II}}{\text{I}} = \frac{L du^2 + 2M du d\theta + N d\theta^2}{E du^2 + 2F du d\theta + G d\theta^2} \quad (10.5.2)$$

where $L, M, N, E, F,$ and G are functions taken at point M . Expressions for the first and second fundamental forms I and II are given by equations (10.1.3) and (10.1.11), respectively.

Using the kinematic interpretations of forms I and II (eqs. (10.1.28) and (10.1.41)), we get

$$\kappa_n = \frac{\mathbf{a}_r \cdot \mathbf{n}}{v_r^2} \quad (10.5.3)$$

Here \mathbf{a}_r is the acceleration of a point in its motion over the surface in the direction of $\boldsymbol{\tau}$ represented by

$$\mathbf{a}_r = \mathbf{r}_{uu} \left(\frac{du}{dt} \right)^2 + 2\mathbf{r}_{u\theta} \frac{du}{dt} \frac{d\theta}{dt} + \mathbf{r}_{\theta\theta} \left(\frac{d\theta}{dt} \right)^2 \quad (10.5.4)$$

(In deriving eq. (10.5.4), we assumed that $u(t)$ and $\theta(t)$ are linear functions and that du/dt and $d\theta/dt$ are constant.) The velocity \mathbf{v}_r of the point is

$$\mathbf{v}_r = \mathbf{r}_u \frac{du}{dt} + \mathbf{r}_\theta \frac{d\theta}{dt} \quad (10.5.5)$$

The surface unit normal is

$$\mathbf{n} = \frac{\mathbf{N}}{|\mathbf{N}|} = \mathbf{n}(u, \theta) \quad (10.5.6)$$

The surface normal \mathbf{N} is given by

$$\mathbf{N} = \mathbf{r}_u \times \mathbf{r}_\theta \quad (10.5.7)$$

or by

$$\mathbf{N}^* = \mathbf{r}_\theta \times \mathbf{r}_u \quad (10.5.8)$$

Another equation for the surface normal curvature κ_n is based on the following expression:

$$d\mathbf{r} \cdot \mathbf{n} = 0 \quad (10.5.9)$$

The differentiation of equation (10.5.9) results in

$$(d^2\mathbf{r} \cdot \mathbf{n}) + (d\mathbf{r} \cdot d\mathbf{n}) = 0 \quad (10.5.10)$$

which yields

$$\mathbf{a}_r \cdot \mathbf{n} = -\mathbf{v}_r \cdot \dot{\mathbf{n}}_r \quad (10.5.11)$$

Here

$$\dot{\mathbf{n}}_r = \frac{d\mathbf{n}}{dt} = \mathbf{n}_u \frac{du}{dt} + \mathbf{n}_\theta \frac{d\theta}{dt} \quad (10.5.12)$$

is the velocity of the tip of the surface unit normal \mathbf{n} which changes its direction while the point moves over the surface. Equations (10.5.11) and (10.5.3) yield

$$\kappa_n = -\frac{\dot{\mathbf{n}}_r \cdot \mathbf{v}_r}{v_r^2} \quad (10.5.13)$$

A positive sign for the normal curvature determined by equations (10.5.3) and (10.5.13) indicates that the center of curvature is located on the positive normal.

Example problem 10.5.1 Consider a cone surface given by equations (10.1.42). The surface unit normal is represented by equations (10.1.43).

Derive the equation for the normal curvature.

Solution. Velocity vector \mathbf{v}_r is

$$\begin{aligned} \mathbf{v}_r &= \mathbf{r}_u \frac{du}{dt} + \mathbf{r}_\theta \frac{d\theta}{dt} \\ &= \cos \psi_c \frac{du}{dt} \mathbf{i} + \left(\sin \psi_c \sin \theta \frac{du}{dt} + u \sin \psi_c \cos \theta \frac{d\theta}{dt} \right) \mathbf{j} \\ &\quad + \left(\sin \psi_c \cos \theta \frac{du}{dt} - u \sin \psi_c \sin \theta \frac{d\theta}{dt} \right) \mathbf{k} \end{aligned} \quad (10.5.14)$$

$$v_r^2 = \left(\frac{du}{dt} \right)^2 + u^2 \sin^2 \psi_c \left(\frac{d\theta}{dt} \right)^2 \quad (10.5.15)$$

Vector $\dot{\mathbf{n}}_r$ is

$$\dot{\mathbf{n}}_r = \mathbf{n}_u \frac{du}{dt} + \mathbf{n}_\theta \frac{d\theta}{dt} = (\cos \psi_c \cos \theta \mathbf{j} - \cos \psi_c \sin \theta \mathbf{k}) \frac{d\theta}{dt} \quad (10.5.16)$$

The normal curvature is represented by the equation

$$\kappa_n = -\frac{\dot{\mathbf{n}}_r \cdot \mathbf{v}_r}{v_r^2} = -\frac{u \sin \psi_c \cos \psi_c \left(\frac{d\theta}{dt}\right)^2}{\left(\frac{du}{dt}\right)^2 + u^2 \sin^2 \psi_c \left(\frac{d\theta}{dt}\right)^2} \quad (10.5.17)$$

We may get the same result by using equation (10.5.3) for the normal curvature.

The normal curvature depends on the direction of vector $\boldsymbol{\tau}$, on the ratio $du/d\theta$. We consider three particular cases as follows:

(1) The point moves along the u -line (θ is constant). Taking $d\theta/dt = 0$ in equation (10.5.17), we get

$$\kappa_n = 0 \quad (10.5.18)$$

(2) The point moves over the θ -line (u is constant). Taking $du/dt = 0$, we get

$$\kappa_n = -\frac{1}{u \tan \psi_c} \quad (10.5.19)$$

The normal curvature $\kappa_n < 0$ and the curvature center C is located in the negative direction of the surface normal.

(3) The direction of motion of the point over the surface is such that

$$\frac{\boldsymbol{\tau} \cdot \mathbf{r}_u}{|\mathbf{r}_u|} = \cos q \quad (10.5.20)$$

Here

$$\boldsymbol{\tau} = \frac{\mathbf{v}_r}{|\mathbf{v}_r|} \quad (10.5.21)$$

$$\frac{\mathbf{r}_u}{|\mathbf{r}_u|} = \cos \psi_c \mathbf{i} + \sin \psi_c \sin \theta \mathbf{j} + \sin \psi_c \cos \theta \mathbf{k} \quad (10.5.22)$$

Equations (10.5.20) to (10.5.22) and (10.5.14) yield

$$\frac{\frac{du}{dt}}{\sqrt{\left(\frac{du}{dt}\right)^2 + u^2 \sin^2 \psi_c \left(\frac{d\theta}{dt}\right)^2}} = \cos q \quad (10.5.23)$$

The ratio $du/d\theta$ may be determined from equation (10.5.23) by considering q and $u \sin \psi_c$ as given. Then the surface normal curvature may be determined by using equation (10.5.17).

10.6 Principal Directions and Curvatures, Indicatrix of Dupin, and Working Equations

Consider that a regular point M is taken on the given surface and the normal curvatures which correspond to different unit tangents $\tau^{(1)}, \tau^{(2)}, \dots, \tau^{(n)}$ are determined (fig. 10.5.1). As we can see, the normal curvature of the surface depends on the direction of τ . The extreme values of the normal curvature taken at a certain point of the surface are called the principal curvatures. The directions of the normal sections of the surface with the extreme normal curvatures are called the principal directions. We may determine the principal directions as directions for which vectors \mathbf{v}_r and $\dot{\mathbf{n}}_r$ are collinear. (See app. C.) Here

$$\mathbf{v}_r = \mathbf{r}_u \frac{du}{dt} + \mathbf{r}_\theta \frac{d\theta}{dt} \quad (10.6.1)$$

and

$$\dot{\mathbf{n}}_r = \mathbf{n}_u \frac{du}{dt} + \mathbf{n}_\theta \frac{d\theta}{dt} \quad (10.6.2)$$

We assume that the surface unit normal is represented by the equation

$$\mathbf{n} = \mathbf{n}(u, \theta) \quad (10.6.3)$$

Due to the collinearity of vectors \mathbf{v}_r and $\dot{\mathbf{n}}_r$ for the principal directions, we get

$$\frac{x_u \frac{du}{dt} + x_\theta \frac{d\theta}{dt}}{n_{xu} \frac{du}{dt} + n_{x\theta} \frac{d\theta}{dt}} = \frac{y_u \frac{du}{dt} + y_\theta \frac{d\theta}{dt}}{n_{yu} \frac{du}{dt} + n_{y\theta} \frac{d\theta}{dt}} = \frac{z_u \frac{du}{dt} + z_\theta \frac{d\theta}{dt}}{n_{zu} \frac{du}{dt} + n_{z\theta} \frac{d\theta}{dt}} \quad (10.6.4)$$

Here $x_u, y_u, z_u, x_\theta, y_\theta, z_\theta, n_{xu}, n_{yu}, n_{zu}, n_{x\theta}, n_{y\theta},$ and $n_{z\theta}$ are taken at the considered point M of the surface.

According to the results of appendix C, section 3 (eq. (C.3.21)), the principal curvatures are represented by the equation

$$\kappa_{I,II} \mathbf{v}_r = -\dot{\mathbf{n}}_r \quad (10.6.5)$$

that yields

$$\frac{n_{xu} \frac{du}{dt} + n_{x\theta} \frac{d\theta}{dt}}{x_u \frac{du}{dt} + x_\theta \frac{d\theta}{dt}} = \frac{n_{yu} \frac{du}{dt} + n_{y\theta} \frac{d\theta}{dt}}{y_u \frac{du}{dt} + y_\theta \frac{d\theta}{dt}} = \frac{n_{zu} \frac{du}{dt} + n_{z\theta} \frac{d\theta}{dt}}{z_u \frac{du}{dt} + z_\theta \frac{d\theta}{dt}} = -\kappa_{I,II} \quad (10.6.6)$$

The system of three equations (10.6.6) contains three unknowns, the ratio $du/d\theta$, and the principal curvatures κ_I and κ_{II} . The procedure for the solution of these unknowns is as follows:

Using one of the equations from (10.6.4), we may develop a quadratic equation

$$A\left(\frac{du}{d\theta}\right)^2 + 2B\frac{du}{d\theta} + C = 0 \quad (10.6.7)$$

The two roots of this equation correspond to two principal directions on the surface. By putting both roots into equation (10.6.6), we may determine the principal curvatures κ_I and κ_{II} . We emphasize that, in general, two orthogonal principal directions exist at each point of the surface with different values of principal curvatures. A spherical surface is an exception; each direction on the surface may be considered as the principal direction and the normal curvature is the same for all normal sections of the surface.

Another exception is the case when the normal curvature of the surface is equal to zero for all directions. This is true for a plane or for a surface which turns into a plane at a certain point (called a flat point).

The product of the principal curvatures at the considered point M is designated by

$$K = \kappa_I \kappa_{II} \quad (10.6.8)$$

and called the Gaussian curvature of the surface at point M .

Indicatrix of Dupin; Three Types of Surface Points

Consider that the tangent plane T is drawn to a surface at its regular point M (fig. 10.6.1(a)). The coordinate system (η, ξ) , whose axes coincide with the principal directions of the surface at point M , is rigidly connected to plane T . We know that, according to the theorem of Euler, the normal and principal curvatures are related by the equation

$$\kappa_n = \kappa_I \cos^2 q + \kappa_{II} \sin^2 q \quad (10.6.9)$$

(See app. C, sec. 3.)

Function $\kappa_n(q)$ relates the normal curvature κ_n and the angle q . We consider that the principal curvatures κ_I and κ_{II} are given.

We express the normal curvature κ_n by

$$\kappa_n = \pm \frac{1}{|R_n|} \quad (10.6.10)$$

where $|R_n|$ is the magnitude of the curvature radius in the normal curvature. We then represent the position vector ρ (fig. 10.6.1(b)) by

$$\rho(q) = \sqrt{|R_n|} \quad (10.6.11)$$

Equations (10.6.9) to (10.6.11) yield

$$\begin{aligned} \kappa_I |R_n| \cos^2 q + \kappa_{II} |R_n| \sin^2 q &= \kappa_I (\rho \cos q)^2 + \kappa_{II} (\rho \sin q)^2 = \pm 1 \\ \rho \cos q &= \eta \quad \rho \sin q = \xi \end{aligned} \quad (10.6.12)$$

and

$$f(\eta, \xi) = \kappa_I \eta^2 + \kappa_{II} \xi^2 \mp 1 = 0 \quad |f_\eta| + |f_\xi| \neq 0 \quad (10.6.13)$$

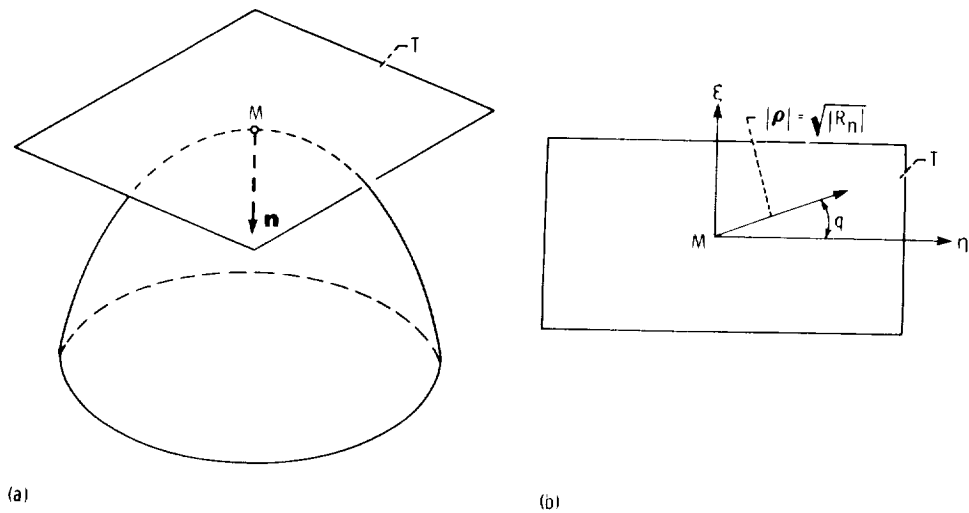


Figure 10.6.1.

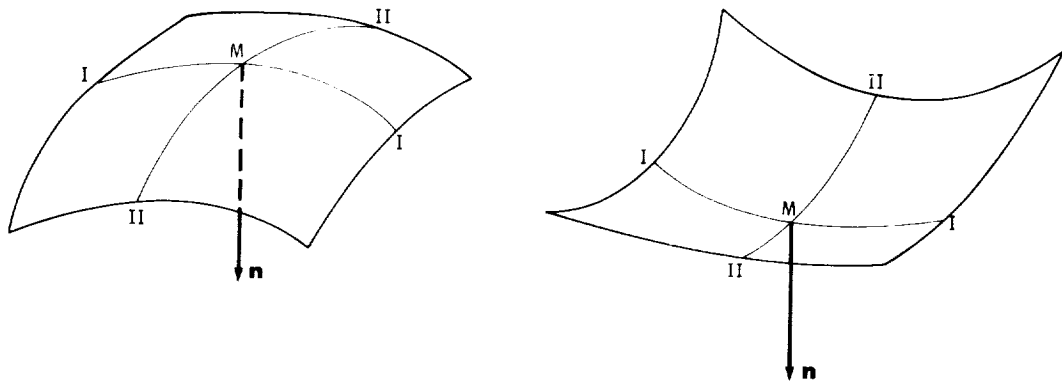


Figure 10.6.2.

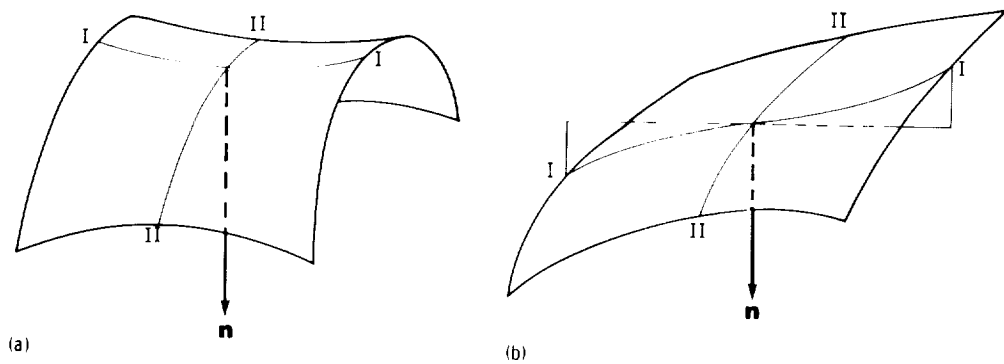


Figure 10.6.3.

Equation (10.6.13) represents a plane curve—the so-called Dupin's indicatrix. The magnitude of the position vector ρ of such a curve is represented by equation (10.6.11).

There are three types of surface points as follows:

(1) The elliptic point—when the principal curvatures are of the same sign and the Gaussian curvature $K > 0$ (fig. 10.6.2). (See eq. (10.6.8).)

(2) The hyperbolic point—when the principal curvatures are of different signs (fig. 10.6.3(a)) and the Gaussian curvature $K < 0$. The surface has the form of a saddle near the considered point M . There are two such directions in the neighborhood of M where the normal curvature is equal to zero. The above directions are called asymptotic.

(3) The parabolic point—when one of the principal curvatures is zero (direction II in fig. 10.6.3(b)) and the Gaussian curvature $K = 0$.

Example problem 10.6.1 Consider a cone surface given by equations (10.1.42). The surface unit normal is represented by equations (10.1.43). Determine the principal directions and curvatures at a point (u, θ) .

Solution. Along principal directions, vectors \mathbf{v}_r and $\dot{\mathbf{n}}_r$ are collinear. (See app. C.) The differentiation of equations (10.1.42) and (10.1.43) yields the expressions for \mathbf{v}_r and $\dot{\mathbf{n}}_r$ represented by (10.5.14) and (10.5.16), respectively. Due to the collinearity of \mathbf{v}_r and $\dot{\mathbf{n}}_r$, we get

$$\frac{\dot{n}_{xr}}{v_{xr}} = \frac{\dot{n}_{yr}}{v_{yr}} = \frac{\dot{n}_{zr}}{v_{zr}} \quad (10.6.14)$$

Thus,

$$\begin{aligned} 0 &= \frac{\cos \psi_c \cos \theta \frac{d\theta}{dt}}{\cos \psi_c \frac{du}{dt}} = \frac{\cos \psi_c \cos \theta \frac{d\theta}{dt}}{\sin \psi_c \sin \theta \frac{du}{dt} + u \sin \psi_c \cos \theta \frac{d\theta}{dt}} \\ &= - \frac{\cos \psi_c \sin \theta \frac{d\theta}{dt}}{\sin \psi_c \cos \theta \frac{du}{dt} - u \sin \psi_c \sin \theta \frac{d\theta}{dt}} \end{aligned} \quad (10.6.15)$$

Equations (10.6.15) are satisfied if

$$\frac{du}{dt} \frac{d\theta}{dt} = 0 \quad (10.6.16)$$

One of the principal directions corresponds to $\frac{du}{dt} = 0$; the other one to $\frac{d\theta}{dt} = 0$. These directions are tangents to the surface coordinate lines as follows: (1) to the θ -line $\left(\frac{du}{dt} = 0\right)$ and (2) to the u -line $\left(\frac{d\theta}{dt} = 0\right)$ that is the generatrix of the cone, OM (fig. 10.1.4).

We determine the principal curvatures by using equations (C.3.16) and (C.3.19), which yield

$$\kappa_{I,II} = - \frac{\dot{n}_{xr}}{v_{xr}} = - \frac{\dot{n}_{yr}}{v_{yr}} = - \frac{\dot{n}_{zr}}{v_{zr}} \quad (10.6.17)$$

(See app. C.) One of the principal curvatures corresponds to $\frac{du}{dt} = 0$, the other one to $\frac{d\theta}{dt} = 0$. Equations (10.6.17), (10.6.15), and (10.6.16) result in

$$\kappa_I = - \frac{1}{u \tan \psi_c} \quad \left(\frac{du}{dt} = 0\right) \quad (10.6.18)$$

$$\kappa_{II} = 0 \quad \left(\frac{d\theta}{dt} = 0 \right) \quad (10.6.19)$$

The center of the curvature κ_I lies on the cone axis, and the curvature radius is perpendicular to the generatrix $OM = u$ (fig. 10.1.4). The negative sign for the curvature κ_I indicates that the curvature radius is directed opposite to the surface unit normal.

Problem 10.6.2 Consider a surface of revolution represented by equations (8.4.3)

$$\begin{aligned} x &= f(\theta) \cos \psi & y &= f(\theta) \sin \psi & z &= g(\theta) \\ \theta_2 &< \theta < \theta_1 & 0 &\leq \psi < 2\pi \end{aligned}$$

The surface unit normal is represented by equations (8.4.7)

$$n_x = -\frac{g_\theta \cos \psi}{A} \quad n_y = -\frac{g_\theta \sin \psi}{A} \quad n_z = \frac{f_\theta}{A}$$

where

$$A^2 = f_\theta^2 + g_\theta^2 \quad f_\theta = \frac{d}{d\theta}[f(\theta)] \quad g_\theta = \frac{d}{d\theta}[g(\theta)]$$

Determine the principal directions and principal curvatures of the surface at a point (θ, ψ) .

Answer. Principal directions I and II correspond to $\frac{d\psi}{dt} = 0$ and $\frac{d\theta}{dt} = 0$, respectively. They may be determined as tangents to the θ -line and ψ -line of the surface.

The principal curvatures are

$$\kappa_I = -\frac{f_{\theta\theta}A - f_\theta A_\theta}{A^2 g_\theta} = \frac{g_{\theta\theta}A - g_\theta A_\theta}{A^2 f_\theta} \quad \left(\frac{d\psi}{dt} = 0 \right)$$

and

$$\kappa_{II} = \frac{g_\theta}{Af(\theta)} \quad \left(\frac{d\theta}{dt} = 0 \right)$$

Here

$$A_\theta = \frac{d}{d\theta}[A(\theta)] \quad f_{\theta\theta} = \frac{d^2}{d\theta^2}[f(\theta)] \quad g_{\theta\theta} = \frac{d^2}{d\theta^2}[g(\theta)]$$

Problem 10.6.3 With the conditions of problem 10.6.2, prove that the principal curvature κ_I may be represented as the curvature of the generating plane curve given by equations (8.4.1) such that $x = f(\theta)$, $y = 0$, and $z = g(\theta)$.

Directions for solution. The curvature of a plane curve may be determined as follows:

$$\kappa = -\frac{dm_x}{d\tau_x} = -\frac{dm_z}{d\tau_z}$$

(See ch. 3.3.) Here

$$\boldsymbol{\tau} = \frac{dx \mathbf{i} + dz \mathbf{k}}{(dx^2 + dz^2)^{1/2}}$$

is the unit tangent to the generating curve;

$$\mathbf{m} = \frac{\mathbf{j} \times \boldsymbol{\tau}}{|\mathbf{j} \times \boldsymbol{\tau}|}$$

is the unit normal to the generating curve.

Problem 10.6.4 An involute screw surface is represented by equations (8.4.30)

$$\mathbf{r} = (\rho \cos \theta - u \cos \lambda_\rho \sin \theta) \mathbf{i} + (\rho \sin \theta + u \cos \lambda_\rho \cos \theta) \mathbf{j} + (h\theta + u \sin \lambda_\rho) \mathbf{k}$$

The surface unit normal is represented by equations (8.4.34) (provided $u \cos \lambda_\rho \neq 0$):

$$\mathbf{n} = \sin \lambda_\rho (\sin \theta \mathbf{i} - \cos \theta \mathbf{j}) + \cos \lambda_\rho \mathbf{k}$$

Determine the principal directions and principal curvatures at a point (u, θ) .

Answer. The derivatives $\frac{d\theta}{dt}$ and $\frac{du}{dt}$, which correspond to the principal directions I and II, are determined as follows:

$$(a) \frac{d\theta}{dt} = 0 \quad \frac{du}{dt} \neq 0 \quad (\text{principal direction I})$$

$$(b) \rho \frac{d\theta}{dt} + \cos \lambda_\rho \frac{du}{dt} = 0 \quad (\text{principal direction II})$$

The principal curvatures are: $\kappa_I = 0$ and $\kappa_{II} = \tan \lambda_\rho / u$.

The radius r of a circle in the cross section, and the parameters $u = MN$ and ρ (fig. 8.4.9) are related by $r^2 = x^2 + y^2 = \rho^2 + u^2 \cos^2 \lambda_\rho$.

10.7 Geodesic Curvature

Consider a spatial curve L on surface Σ (fig. 10.7.1). Vectors $\boldsymbol{\tau}$, \mathbf{n} , and \mathbf{m} , taken at point M , represent the unit tangent to the curve L , the surface unit normal and the main normal \mathbf{m} to the curve, respectively; vector \mathbf{m} lies in the osculating plane.

The radius of the curvature for curve L has the same direction as vector \mathbf{m} and belongs to the osculating plane. The curvature of L is determined by equation (10.3.19).

Now, consider that the spatial curve L is projected on the tangent plane T and on the normal plane N , respectively. Projections of L on planes T and N are designated by L_T and L_N (fig. 10.7.1). Vectors $\boldsymbol{\tau}$, \mathbf{n} , and \mathbf{b} , where $\mathbf{b} = \boldsymbol{\tau} \times \mathbf{n}$, form a right-hand trihedron (fig. 10.7.2). We may express the unit vector \mathbf{m} of the principal normal to curve L as follows:

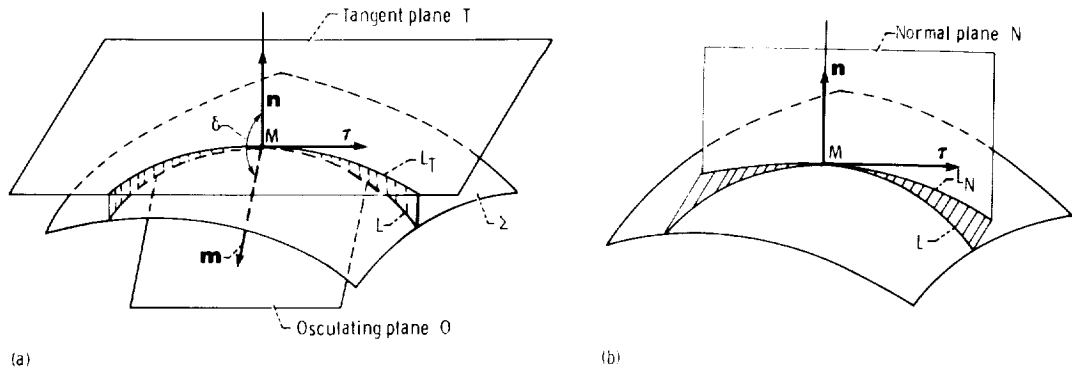


Figure 10.7.1.

$$\mathbf{m} = (\mathbf{m} \cdot \mathbf{n})\mathbf{n} + (\mathbf{m} \cdot \mathbf{b})\mathbf{b} \quad (10.7.1)$$

Multiplying both sides of equation (10.7.1) by the curvature of curve L , (κ), we get

$$\kappa \mathbf{m} = \kappa(\mathbf{m} \cdot \mathbf{n})\mathbf{n} + \kappa(\mathbf{m} \cdot \mathbf{b})\mathbf{b} \quad (10.7.2)$$

We have seen that the normal curvature is represented by the equation

$$\kappa_n = \kappa \cos \delta = \kappa(\mathbf{m} \cdot \mathbf{n}) \quad (10.7.3)$$

(See section 4 of this chapter.) Equation

$$\kappa_g = \kappa(\mathbf{m} \cdot \mathbf{b}) = \kappa[\mathbf{m} \cdot (\boldsymbol{\tau} \times \mathbf{n})] = \kappa[\mathbf{m} \boldsymbol{\tau} \mathbf{n}] \quad (10.7.4)$$

represents the geodesic curvature. The curvatures of curves L_N and L_T at point M (fig. 10.7.1) are designated by κ_n and κ_g , respectively. Here, L_N and L_T are projections of curve L on the normal and tangent planes. It results from equations (10.7.2) to (10.7.4) that

$$\kappa \mathbf{m} = \kappa_n \mathbf{n} + \kappa_g \mathbf{b} \quad (10.7.5)$$

Let us now derive equations of the geodesic curvature. Consider that curve L is represented by

$$\mathbf{R}(s) = \mathbf{r}(u(s), \theta(s)) \in C^2 \quad s_1 < s < s_2 \quad (10.7.6)$$

where s is the arc length. With equations derived in section 10.2, we obtain

$$\kappa \mathbf{m} = \mathbf{R}_{ss} \quad \boldsymbol{\tau} = \mathbf{R}_s \quad (10.7.7)$$

Equations (10.7.4) and (10.7.7) yield

$$\kappa_g = \mathbf{R}_{ss} \cdot \mathbf{b} = [\mathbf{R}_{ss} \mathbf{R}_s \mathbf{n}] \quad (10.7.8)$$

Instead of equation (10.7.8) we may determine the geodesic curvature as follows:

$$\kappa_g = \frac{[\mathbf{a}_r \mathbf{v}_r \mathbf{n}]}{|\mathbf{v}_r|^3} \quad (10.7.9)$$

Here

$$\mathbf{v}_r = \mathbf{R}_s \frac{ds}{dt} = \mathbf{R}_s v_r \quad (10.7.10)$$

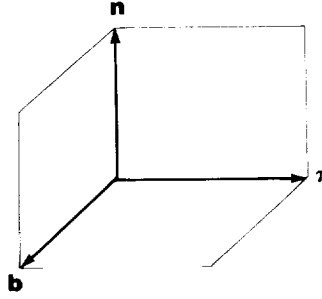


Figure 10.7.2.

where \mathbf{v}_r is the velocity and \mathbf{a}_r is the acceleration of the point which moves along the curve L . The acceleration \mathbf{a}_r may be represented by its two components, \mathbf{a}_r^m and \mathbf{a}_r^l . Here, \mathbf{a}_r^m is directed along the principal normal to the curve (\mathbf{m}) and \mathbf{a}_r^l is collinear to τ . (See sec. 10.3.) Hence, we have

$$\kappa_g = \frac{[\mathbf{a}_r \mathbf{v}_r \mathbf{n}]}{|\mathbf{v}_r|^3} = \frac{[\mathbf{a}_r^m \mathbf{v}_r \mathbf{n}] + [\mathbf{a}_r^l \mathbf{v}_r \mathbf{n}]}{|\mathbf{v}_r|^3} = \frac{[\mathbf{a}_r^m \mathbf{v}_r \mathbf{n}]}{|\mathbf{v}_r|^3} \quad (10.7.11)$$

since $[\mathbf{a}_r^l \mathbf{v}_r \mathbf{n}] = 0$ because of the collinearity of vectors \mathbf{a}_r^l and \mathbf{v}_r .

The positive sense of the geodesic curvature indicates that the curvature center of the curve L_T (fig. 10.7.1(a)) is located on the positive direction of vector \mathbf{b} (fig. 10.7.2); this vector is the normal to curve L_T at point M .

A geodesic line (a geodesic) of the surface is a curve whose geodesic curvature is zero at each curve point. It is proven in differential geometry (Hohn, 1973 and Lipschutz, 1969) that only one geodesic line may be drawn through a regular point of a surface of class C^3 in each direction. A small arc of a geodesic line on the surface is the shortest distance between two surface points. It results from equation (10.7.11) that a regular curve on a surface is a geodesic line if and only if vectors \mathbf{a}_r^m and \mathbf{n} are collinear or if \mathbf{a}_r^m is zero. Vectors \mathbf{a}_r^m and \mathbf{n} are collinear if the osculating plane coincides with the normal plane (fig. 10.7.1). Vector $\mathbf{a}_r^m = 0$ if the curve on the surface is a straight line. A great circle on a spherical surface is a geodesic line since the principal normal to such a curve coincides with the surface normal.

We say that a curve is a geodesic line locally if $\kappa_g = 0$ at the given point M . We must observe the requirement $\kappa_g = 0$ for local synthesis of approximate gearings to obtain a small piece of the contact point path on the gear-tooth surface as a local geodesic line. Such a line does not deviate from the desired direction in the neighborhood of the given contact point.

Consider that a surface is represented in parametric form by

$$\mathbf{r}(u, \theta) \in C^2 \quad \mathbf{r}_u \times \mathbf{r}_\theta \neq 0 \quad (u, \theta) \in A_m \quad (10.7.12)$$

We may represent vectors \mathbf{v}_r and \mathbf{a}_r^m as follows:

$$\mathbf{v}_r = \mathbf{r}_u \frac{du}{dt} + \mathbf{r}_\theta \frac{d\theta}{dt} \quad (10.7.13)$$

$$\mathbf{a}_r^m = \mathbf{r}_{uu} \left(\frac{du}{dt} \right)^2 + 2\mathbf{r}_{u\theta} \frac{du}{dt} \frac{d\theta}{dt} + \mathbf{r}_{\theta\theta} \left(\frac{d\theta}{dt} \right)^2 \quad (10.7.14)$$

The derivatives du/dt and $d\theta/dt$ are related since the ratio $du/d\theta$ depends on the given direction of point motion over the surface.

Example problem 10.7.1 A cylinder surface is represented by

$$x = \rho \cos \theta \quad y = \rho \sin \theta \quad z = u \quad (10.7.15)$$

Consider a helix on the cylinder surface given by the equation

$$u = h\theta \quad (10.7.16)$$

where

$$h = \rho \tan \lambda \quad (10.7.17)$$

λ is the lead angle of the helix. Determine the geodesic curvature of the helix.

Solution.

$$\mathbf{n} = \frac{\mathbf{r}_u \times \mathbf{r}_\theta}{|\mathbf{r}_u \times \mathbf{r}_\theta|} = \cos \theta \mathbf{i} + \sin \theta \mathbf{j} \quad (10.7.18)$$

$$\mathbf{v}_r = \rho \frac{d\theta}{dt} (-\sin \theta \mathbf{i} + \cos \theta \mathbf{j} + \tan \lambda \mathbf{k}) \quad (10.7.19)$$

$$\mathbf{a}_r^m = -\rho \left(\frac{d\theta}{dt} \right)^2 (\cos \theta \mathbf{i} + \sin \theta \mathbf{j}) \quad (10.7.20)$$

The geodesic curvature of the helix κ_g is zero because of the collinearity of vectors \mathbf{a}_r^m and \mathbf{n} .

Chapter 11

Spatial Gearing Analysis

The problem of spatial gearing analysis may be formulated as follows: Given are equations of gear-tooth surfaces, the crossing angle, and the shortest distance between the axes of rotation. The gear-tooth surfaces are in point contact. It is necessary to determine (1) the law of motion (the relation between the angles of gear rotation), (2) the line of action, and (3) the paths of contact on the gear-tooth surfaces.

The method of gearing analysis (Litvin, 1968) may be used for the investigation of approximate gearings (with nonconjugate surfaces), the determination of kinematical errors induced by errors of manufacturing and assembly, and the investigation of the optimal synthesis of gears. The optimal synthesis of spatial gearings is usually an iterative computational procedure, which needs intermediate analysis between iterations. Such analysis provides information about the results obtained and is the basis for the next iteration.

11.1 Tangency of Gear-Tooth Surfaces

We set up three coordinate systems S_1 , S_2 , and S_f , rigidly connected with gears 1 and 2 and the frame, respectively. The tooth surfaces Σ_1 and Σ_2 are represented in coordinate systems S_1 and S_2 , respectively, by the following functions:

$$\mathbf{r}_i(u_i, \theta_i) \in C^2 \quad \frac{\partial \mathbf{r}_i}{\partial u_i} \times \frac{\partial \mathbf{r}_i}{\partial \theta_i} \neq 0 \quad (u_i, \theta_i) \in E_i \quad i = 1, 2 \quad (11.1.1)$$

The surface unit normals are represented as follows:

$$\mathbf{n}_i = \frac{\frac{\partial \mathbf{r}_i}{\partial u_i} \times \frac{\partial \mathbf{r}_i}{\partial \theta_i}}{\left| \frac{\partial \mathbf{r}_i}{\partial u_i} \times \frac{\partial \mathbf{r}_i}{\partial \theta_i} \right|} \quad (11.1.2)$$

Consider that gear i , with the tooth surface Σ_i , rotates about a fixed axis located in the frame. Thus, a locus of gear-tooth surfaces is generated in the coordinate system S_f . The locus of these surfaces may be determined by the matrix equation

$$\left[r_f^{(i)} \right] = [M_{fi}] [r_i] \quad (i = 1, 2) \quad (11.1.3)$$

Here, the column matrix

$$[r_i] = \begin{bmatrix} x_i(u_i, \theta_i) \\ y_i(u_i, \theta_i) \\ z_i(u_i, \theta_i) \\ 1 \end{bmatrix} \quad (11.1.4)$$

represents the homogeneous coordinates of a surface point. The square 4×4 matrix $[M_{fi}]$ describes the coordinate transformation in transition from S_i to S_f . Elements of this matrix are expressed in terms of the parameter of motion ϕ_i . The column matrix

$$[r_f^{(i)}] = \begin{bmatrix} x_i(u_i, \theta_i, \phi_i) \\ y_i(u_i, \theta_i, \phi_i) \\ z_i(u_i, \theta_i, \phi_i) \\ 1 \end{bmatrix} \quad (11.1.5)$$

represents the homogeneous coordinates of a point of the locus of gear tooth surfaces in the coordinate system S_f . This matrix with the fixed parameter of motion ϕ_i represents a point of surface Σ_i in coordinate system S_f .

Similarly, we may also determine the surface unit normals by using the matrix equations

$$[n_f^{(i)}] = [L_{fi}][n_i] \quad (i = 1, 2) \quad (11.1.6)$$

Matrices given by equation (11.1.6) are 3×3 matrices. Matrix $[L_{fi}]$ may be determined from matrix $[M_{fi}]$ by crossing the last row and column in $[M_{fi}]$. (See app. A.)

The point of tangency of gear-tooth surfaces in the coordinate system S_f is a point at which the position vectors and the surface unit normals coincide. Thus,

$$\mathbf{r}_f^{(1)}(u_1, \theta_1, \phi_1) = \mathbf{r}_f^{(2)}(u_2, \theta_2, \phi_2) \quad (11.1.7)$$

$$\mathbf{n}_f^{(1)}(u_1, \theta_1, \phi_1) = \mathbf{n}_f^{(2)}(u_2, \theta_2, \phi_2) \quad (11.1.8)$$

Vector equation (11.1.7) yields three scalar equations, but equation (11.1.8) yields only two independent scalar equations since

$$|\mathbf{n}_f^{(1)}| = |\mathbf{n}_f^{(2)}| = 1 \quad (11.1.9)$$

We may require the collinearity of surface normals with the equation

$$\mathbf{N}^{(1)}(u_1, \theta_1, \phi_1) = \lambda \mathbf{N}^{(2)}(u_2, \theta_2, \phi_2) \quad (11.1.10)$$

instead of equation (11.1.8). However, equation (11.1.8) is preferable since it can be applied as a basis for important kinematic relations.

It is important to emphasize that the directions of unit normals $\mathbf{n}_f^{(1)}$ and $\mathbf{n}_f^{(2)}$ may either coincide or be opposite each other and still insure the tangency of surfaces Σ_1 and Σ_2 . We prefer to apply equation (11.1.8) for the tangency of surfaces, since we can get the desired direction of the surface unit normals by changing the order of factors in one of the cross products. For instance, vectors

$$\mathbf{N}_1^* = \frac{\partial \mathbf{r}_1}{\partial \theta_1} \times \frac{\partial \mathbf{r}_1}{\partial u_1} \quad \text{and} \quad \mathbf{n}_1^* = \frac{\mathbf{N}_1^*}{|\mathbf{N}_1^*|} \quad (11.1.11)$$

are opposite to vectors

$$\mathbf{N}_1 = \frac{\partial \mathbf{r}_1}{\partial u_1} \times \frac{\partial \mathbf{r}_1}{\partial \theta_1} \quad \text{and} \quad \mathbf{n}_1 = \frac{\mathbf{N}_1}{|\mathbf{N}_1|} \quad (11.1.12)$$

11.2 Analysis of Meshing of Spatial Gearings

Equations (11.1.7) and (11.1.8) may be represented as

$$\mathbf{r}_f^{(1)}(u_1, \theta_1, \phi_1) - \mathbf{r}_f^{(2)}(u_2, \theta_2, \phi_2) = 0 \quad (11.2.1)$$

$$\mathbf{n}_f^{(1)}(u_1, \theta_1, \phi_1) - \mathbf{n}_f^{(2)}(u_2, \theta_2, \phi_2) = 0 \quad (11.2.2)$$

Vector equations (11.2.1) and (11.2.2) yield five independent scalar equations in six unknowns, $u_1, \theta_1, \phi_1, u_2, \theta_2$, and ϕ_2 . Here

$$f_i(u_1, \theta_1, \phi_1, u_2, \theta_2, \phi_2) = 0 \quad f_i \in C^1 \quad (i = 1, 2, 3, 4, 5) \quad (11.2.3)$$

The aim of gearing analysis is to obtain from equations (11.2.3) the functions

$$\{u_1(\phi_1), \theta_1(\phi_1), u_2(\phi_1), \theta_2(\phi_1), \phi_2(\phi_1)\} \in C^1 \quad (11.2.4)$$

According to the Theorem of Implicit Function Systems Existence (see app. B), we may state that functions (11.2.4) exist in the neighborhood of a point

$$\mathbf{P}^0 = (u_1^0, \theta_1^0, \phi_1^0, u_2^0, \theta_2^0, \phi_1^0) \quad (11.2.5)$$

if the following are true:

- (1) functions $\{f_1, f_2, f_3, f_4, f_5\} \in C^1$
- (2) equations (11.2.3) are satisfied at point \mathbf{P}^0
- (3) the following Jacobian differs from zero; that is if

$$\frac{D(f_1, f_2, f_3, f_4, f_5)}{D(u_1, \theta_1, u_2, \theta_2, \phi_2)} = \begin{vmatrix} \frac{\partial f_1}{\partial u_1} & \frac{\partial f_1}{\partial \theta_1} & \frac{\partial f_1}{\partial u_2} & \frac{\partial f_1}{\partial \theta_2} & \frac{\partial f_1}{\partial \phi_2} \\ \cdot & \cdot & \cdot & \cdot & \cdot \\ \cdot & \cdot & \cdot & \cdot & \cdot \\ \cdot & \cdot & \cdot & \cdot & \cdot \\ \frac{\partial f_5}{\partial u_1} & \frac{\partial f_5}{\partial \theta_1} & \frac{\partial f_5}{\partial u_2} & \frac{\partial f_5}{\partial \theta_2} & \frac{\partial f_5}{\partial \phi_2} \end{vmatrix} \neq 0 \quad (11.2.6)$$

Functions (11.2.4) provide complete information about the conditions of the meshing of gears which are in point contact. Function $\phi_2(\phi_1)$ represents the relation between angles of gear rotation (the law of motion). Functions

$$\mathbf{r}_1(u_1, \theta_1) \quad u_1(\phi_1) \quad \theta_1(\phi_1) \quad (11.2.7)$$

determine the locus of contact points on surface Σ_1 . Similarly, functions

$$\mathbf{r}_2(u_2, \theta_2) \quad u_2(\phi_2) \quad \theta_2(\phi_2) \quad (11.2.8)$$

determine the locus of contact points on surface Σ_2 . The locus of contact points on surface Σ_i ($i = 1, 2$) is the working line of the gear-tooth surface. The gear-tooth surface contacts the mating surface at points of the working line only. The line of action of gear-tooth surfaces is represented by functions

$$\mathbf{r}_f^{(1)}(u_1, \theta_1, \phi_1) \quad u_1(\phi_1) \quad \theta_1(\phi_1) \quad (11.2.9)$$

or by functions

$$\mathbf{r}_f^{(2)}(u_2, \theta_2, \phi_2) \quad u_2(\phi_2) \quad \phi_2(\phi_1) \quad \theta_2(\phi_1) \quad (11.2.10)$$

In some cases, a variable parameter other than ϕ_1 , for instance u_1 , may be chosen when solving equations (11.2.3). We may solve these equations in the neighborhood of point \mathbf{P}^0 , which is given by equation (11.2.5), if the respective Jacobian differs from zero, that is if

$$\frac{D(f_1, f_2, f_3, f_4, f_5)}{D(\theta_1, \phi_1, u_2, \theta_2, \phi_2)} \neq 0$$

The solution of equations (11.2.3) will be obtained by functions

$$\{\phi_1(u_1), \theta_1(u_1), u_2(u_1), \theta_2(u_1), \phi_2(u_1)\} \in C^1 \quad (11.2.11)$$

11.3 Process of Computation

The determination of functions (11.2.4) (or functions (11.2.11)) requires an iterative numerical procedure, which is based on the computer-aided solution of the system of five nonlinear equations (11.2.3). Litvin and Gutman proposed a simpler method of solution (Litvin and Gutman, 1981a) based on the separate solution of two subsystems which contain two and three equations of system (11.2.3).

Consider a spatial gear mechanism with crossed axes (fig. 11.3.1) where C is the shortest distance between axes of rotation, and H and Q are the axial displacements of pinion 1 and gear 2. We may represent the equations of system (11.2.3) as follows:

$$f_1(u_1, \theta_1, \phi_1, u_2, \theta_2, \phi_2, C, Q, H) = 0 \quad (11.3.1)$$

$$f_2(u_1, \theta_1, \phi_1, u_2, \theta_2, \phi_2, C, Q, H) = 0 \quad (11.3.2)$$

$$f_3(u_1, \theta_1, \phi_1, u_2, \theta_2, \phi_2, C, Q, H) = 0 \quad (11.3.3)$$

$$f_4(u_1, \theta_1, \phi_1, u_2, \theta_2, \phi_2) = 0 \quad (11.3.4)$$

$$f_5(u_1, \theta_1, \phi_1, u_2, \theta_2, \phi_2) = 0 \quad (11.3.5)$$

Equations (11.3.4) and (11.3.5) do not contain parameters C , Q , and H , since projections of the surface unit normal do not depend on the displacement of the surface.

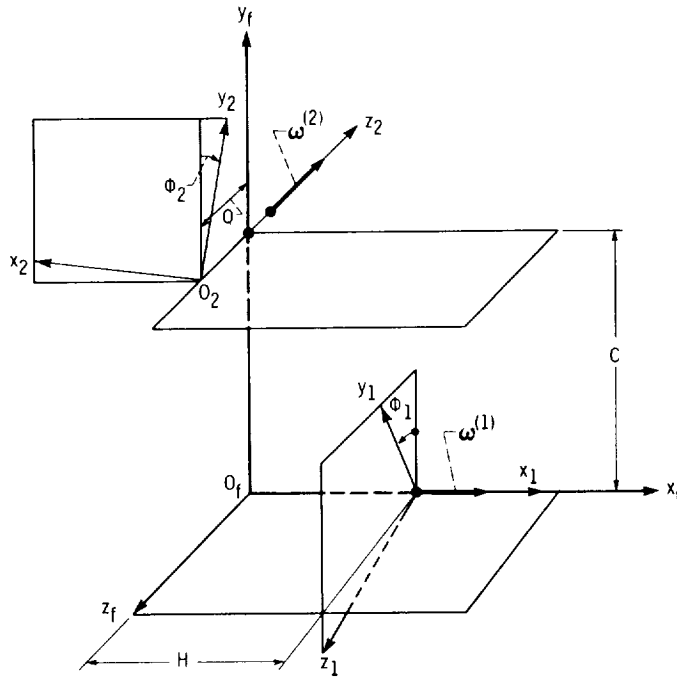


Figure 11.3.1.

The iterative process of computations for the determination of numerical functions (11.2.4) is based on the following procedure:

Step 1.—Choose points $P_1(u_1, \theta_1)$ and $P_2(u_2, \theta_2)$ on surfaces Σ_1 and Σ_2 , respectively, and start computations with the set of parameters $(u_1, \theta_1, u_2, \theta_2)$ as given.

Step 2.—Determine parameters ϕ_1 and ϕ_2 from equations (11.3.4) and (11.3.5).

Step 3.—Rearrange equations (11.3.1) to (11.3.3) as follows:

$$C = F_1(u_1, \theta_1, u_2, \theta_2, \phi_1, \phi_2) \quad (11.3.6)$$

$$Q = F_2(u_1, \theta_1, u_2, \theta_2, \phi_1, \phi_2) \quad (11.3.7)$$

$$H = F_3(u_1, \theta_1, u_2, \theta_2, \phi_1, \phi_2) \quad (11.3.8)$$

and determine C , Q , and H . If the values of C , Q , and H differ from the given ones, change parameters $(u_1, \theta_1, u_2, \theta_2)$ and start the second iteration.

As we can see, the iterative process of computations requires separate solutions of two subsystems; (1) of two equations (eqs. (11.3.4) and (11.3.5)) and (2) of three equations (eqs. (11.3.6) to (11.3.8)).

It is important to notice that at every iteration only three parameters are to be changed. For instance, one of the above parameters u_1 , may have the same value. We say that the system of equations (11.3.1) to (11.3.5) is solved if equations (11.3.4), (11.3.5), and (11.3.6) to (11.3.8) are satisfied by the set of related parameters $(u_1, \theta_1, u_2, \theta_2, \phi_1, \phi_2)$.

Step 4.—Start the computations for the determination of another set of parameters $(u_1, \theta_1, u_2, \theta_2, \phi_1, \phi_2)$ which satisfy equations (11.3.1) to (11.3.5). Choose a new set of four parameters $(u_1, \theta_1, u_2, \theta_2)$ and repeat all operations mentioned in steps 1, 2, and 3.

Using the above procedure, we can determine functions (11.2.4), the law of motion (function $\phi_2(\phi_1)$), the line of action, and the working lines on the surfaces Σ_1 and Σ_2 . (See sec. 11.2.)

Function

$$m_{12}(\phi_1) = \frac{\omega^{(1)}}{\omega^{(2)}} \quad (11.3.9)$$

which represents the angular velocity ratio, may be determined by direct differentiation of function $\phi_2(\phi_1)$ or by using the equation

$$\mathbf{n}_f^{(12)} \cdot \mathbf{v}_f^{(12)} = \mathbf{n}_f \cdot \left\{ \left[(\boldsymbol{\omega}_f^{(1)} - \boldsymbol{\omega}_f^{(2)}) \times \mathbf{r}_f^{(1)} \right] - \mathbf{R}_f \times \boldsymbol{\omega}_f^{(2)} \right\} \quad (11.3.10)$$

Here $\mathbf{v}_f^{(12)}$ is the relative velocity (the velocity of sliding) and $\mathbf{r}_f^{(1)}(x_f, y_f, z_f)$ is the position vector of the contact point. Vectors $\boldsymbol{\omega}_f^{(1)}$ and $\boldsymbol{\omega}_f^{(2)}$ are angular velocities of the gears (it is assumed that the line of action of $\boldsymbol{\omega}_f^{(1)}$ passes through the origin O_f of the coordinate system S_f), and \mathbf{R}_f is a position vector drawn from O_f to any point on the line of action of $\boldsymbol{\omega}_f^{(2)}$, for instance (fig. 11.3.1)

$$\mathbf{R}_f = C\mathbf{j}_f \quad (11.3.11)$$

For the case where $\gamma = 90^\circ$, equation (11.3.10) yields

$$-\omega^{(2)}(y_f - C)n_x + (x_f\omega^{(2)} - z_f\omega^{(1)})n_y + y_f\omega^{(1)}n_z = 0 \quad (11.3.12)$$

Thus,

$$m_{21} = \frac{\omega^{(2)}}{\omega^{(1)}} = \frac{-z_f n_y + y_f n_z}{(y_f - C)n_x - x_f n_y} \quad (11.3.13)$$

By using function $\phi_2(\phi_1)$, we may determine the function of kinematical errors

$$\Delta\phi_2(\phi_1) = \phi_2(\phi_1) - \frac{N_1}{N_2} \phi_1 \quad (11.3.14)$$

where N_1 and N_2 represent the number of gear teeth and the linear function $\phi_1 N_1/N_2$ represents the ideal relation between angles of gear rotation.

As previously mentioned, the locus of contact points on the gear-tooth surface represents the working line of the surface. Because of the elasticity of surfaces, the gears contact each other over an elliptical area whose center coincides with the theoretical contact point. The locus of the contacting ellipses represents the so-called bearing contact. The analysis of bearing contact is considered in section 13.4.

Analysis of conditions of meshing and bearing contact is called tooth contact analysis (TCA). Computer programs for TCA have been worked out by (Gleason Works, 1960) and by (Litvin and Gutman, 1981a). In general, the application of the discussed method for spatial gearing analysis is based upon a computer program from which we obtain numerical results. The following example is a case in which the result may be represented as an analytical solution.

Example 11.3.1 Consider a direct contact mechanism with two movable links (fig. 11.3.2). Links 1 and 2 are interconnected by a highly kinematic pair of surfaces whose elements can be (1) two cylinders as shown in figure 11.3.2, (2) a cylinder and a straight line, (3) a ball and a plane, or (4) two straight lines, etc. We will limit the discussion to the case where links 1 and 2 are interconnected by two cylindrical surfaces.

Links 1 and 2 are connected with the frame by revolute pairs and rotate about crossed axes. We designate the cylinder axes by O_a and O_b . The angle which is made by the cylinder axes and the perpendicular to the axis of rotation is designated by γ_i ($i = 1, 2$). Two planes which are drawn through the axes of link rotation are designated by Π and K , respectively; ρ_1 and ρ_2 are cylinder radii, and A is the shortest distance between the axes of rotation. Design parameters a , b , c , and d determine the location of the link cylinders.

Consider the following coordinate systems: (1) S_1 and S_a , which are rigidly connected to link 1; (2) S_2 and S_b , which are rigidly connected to link 2; and (3) S_f which is rigidly connected to the frame.

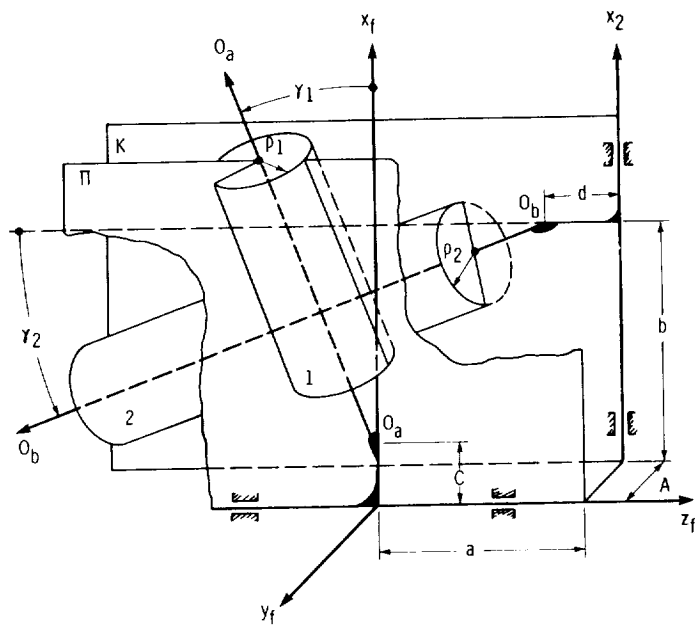


Figure 11.3.2.

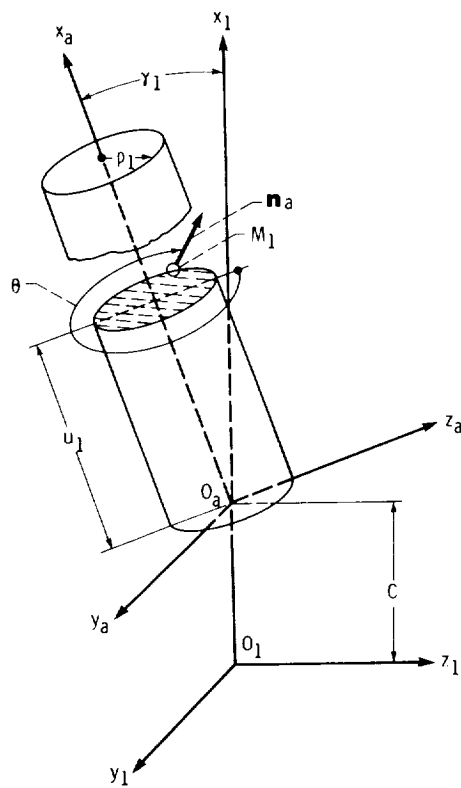


Figure 11.3.3.

The surface Σ_1 of link 1 is represented in the auxiliary coordinate system S_a as follows (fig. 11.3.3):

$$x_a = u_1 \quad y_a = \rho_1 \sin \theta_1 \quad z_a = \rho_1 \cos \theta_1 \quad (11.3.15)$$

The surface unit normal is given by

$$n_{xa} = 0 \quad n_{ya} = \sin \theta_1 \quad n_{za} = \cos \theta_1 \quad (11.3.16)$$

Similarly, surface Σ_2 of link 2 and the surface unit normal are represented in coordinate system S_b by the following equations (fig. 11.3.4):

$$x_b = \rho_2 \cos \theta_2 \quad y_b = \rho_2 \sin \theta_2 \quad z_b = -u_2 \quad (11.3.17)$$

$$n_{xb} = -\cos \theta_2 \quad n_{yb} = -\sin \theta_2 \quad n_{zb} = 0 \quad (11.3.18)$$

We obtain equations of surfaces Σ_1 and Σ_2 and their unit normals in coordinate system S_f (fig. 11.3.5) by using the following matrix equations:

$$[r_f^{(1)}] = [M_{f1}][M_{1a}][r_a] = [M_{fa}][r_a] \quad (11.3.19)$$

$$[n_f^{(1)}] = [L_{f1}][L_{1a}][n_a] = [L_{fa}][n_a] \quad (11.3.20)$$

$$[r_f^{(2)}] = [M_{f2}][M_{2b}][r_b] = [M_{fb}][r_b] \quad (11.3.21)$$

$$[n_f^{(2)}] = [L_{f2}][L_{2b}][n_b] = [L_{fb}][n_b] \quad (11.3.22)$$

Here (see figs. 11.3.3 to 11.3.5)

$$[M_{1a}] = \begin{bmatrix} \cos \gamma_1 & 0 & \sin \gamma_1 & c \\ 0 & 1 & 0 & 0 \\ -\sin \gamma_1 & 0 & \cos \gamma_1 & 0 \\ 0 & 0 & 0 & 1 \end{bmatrix} \quad (11.3.23)$$

$$[M_{f1}] = \begin{bmatrix} \cos \phi_1 & \sin \phi_1 & 0 & 0 \\ -\sin \phi_1 & \cos \phi_1 & 0 & 0 \\ 0 & 0 & 1 & 0 \\ 0 & 0 & 0 & 1 \end{bmatrix} \quad (11.3.24)$$

$$[M_{2b}] = \begin{bmatrix} \cos \gamma_2 & 0 & \sin \gamma_2 & 0 \\ 0 & 1 & 0 & 0 \\ -\sin \gamma_2 & 0 & \cos \gamma_2 & -d \\ 0 & 0 & 0 & 1 \end{bmatrix} \quad (11.3.25)$$

$$[M_{f2}] = \begin{bmatrix} 1 & 0 & 0 & b \\ 0 & \cos \phi_2 & \sin \phi_2 & -A \\ 0 & -\sin \phi_2 & \cos \phi_2 & a \\ 0 & 0 & 0 & 1 \end{bmatrix} \quad (11.3.26)$$

The matrix products are represented as follows:

$$[M_{fa}] = \begin{bmatrix} \cos \phi_1 \cos \gamma_1 & \sin \phi_1 & \cos \phi_1 \sin \gamma_1 & c \cos \phi_1 \\ -\sin \phi_1 \cos \gamma_1 & \cos \phi_1 & -\sin \phi_1 \sin \gamma_1 & -c \sin \phi_1 \\ -\sin \gamma_1 & 0 & \cos \gamma_1 & 0 \\ 0 & 0 & 0 & 1 \end{bmatrix} \quad (11.3.27)$$

$$[M_{fb}] = \begin{bmatrix} \cos \gamma_2 & 0 & \sin \gamma_2 & b \\ -\sin \phi_2 \sin \gamma_2 & \cos \phi_2 & \sin \phi_2 \cos \gamma_2 & -(A + d \sin \phi_2) \\ -\cos \phi_2 \sin \gamma_2 & -\sin \phi_2 & \cos \phi_2 \cos \gamma_2 & a - d \cos \phi_2 \\ 0 & 0 & 0 & 1 \end{bmatrix} \quad (11.3.28)$$

We develop matrices $[L_{fa}]$ and $[L_{fb}]$ from matrices $[M_{fa}]$ and $[M_{fb}]$ by deleting the fourth column and row in the latter two matrices.

Equations (11.3.15) to (11.3.28) yield

$$\begin{aligned} x_f^{(1)} &= u_1 \cos \phi_1 \cos \gamma_1 + \rho_1 \sin \theta_1 \sin \phi_1 \\ &\quad + \rho_1 \cos \theta_1 \cos \phi_1 \sin \gamma_1 + c \cos \phi_1 \\ y_f^{(1)} &= -u_1 \sin \phi_1 \cos \gamma_1 + \rho_1 \sin \theta_1 \cos \phi_1 \\ &\quad - \rho_1 \cos \theta_1 \sin \phi_1 \sin \gamma_1 - c \sin \phi_1 \end{aligned} \quad (11.3.29)$$

$$\begin{aligned} z_f^{(1)} &= -u_1 \sin \gamma_1 + \rho_1 \cos \theta_1 \cos \gamma_1 \\ n_{x_f}^{(1)} &= \sin \theta_1 \sin \phi_1 + \cos \theta_1 \cos \phi_1 \sin \gamma_1 \\ n_{y_f}^{(1)} &= \sin \theta_1 \cos \phi_1 - \cos \theta_1 \sin \phi_1 \sin \gamma_1 \\ n_{z_f}^{(1)} &= \cos \theta_1 \cos \gamma_1 \end{aligned} \quad (11.3.30)$$

$$\begin{aligned} x_f^{(2)} &= \rho_2 \cos \theta_2 \cos \gamma_2 - u_2 \sin \gamma_2 + b \\ y_f^{(2)} &= -\rho_2 \cos \theta_2 \sin \phi_2 \sin \gamma_2 + \rho_2 \sin \theta_2 \cos \phi_2 \\ &\quad - u_2 \sin \phi_2 \cos \gamma_2 - (A + d \sin \phi_2) \end{aligned} \quad (11.3.31)$$

$$\begin{aligned} z_f^{(2)} &= -\rho_2 \cos \theta_2 \cos \phi_2 \sin \gamma_2 - \rho_2 \sin \theta_2 \sin \phi_2 \\ &\quad - u_2 \cos \phi_2 \cos \gamma_2 + (a - d \cos \phi_2) \\ n_{x_f}^{(2)} &= -\cos \theta_2 \cos \gamma_2 \end{aligned}$$

$$\begin{aligned} n_{y_f}^{(2)} &= \cos \theta_2 \sin \phi_2 \sin \gamma_2 - \sin \theta_2 \cos \phi_2 \\ n_{z_f}^{(2)} &= \cos \theta_2 \cos \phi_2 \sin \gamma_2 + \sin \theta_2 \sin \phi_2 \end{aligned} \quad (11.3.32)$$

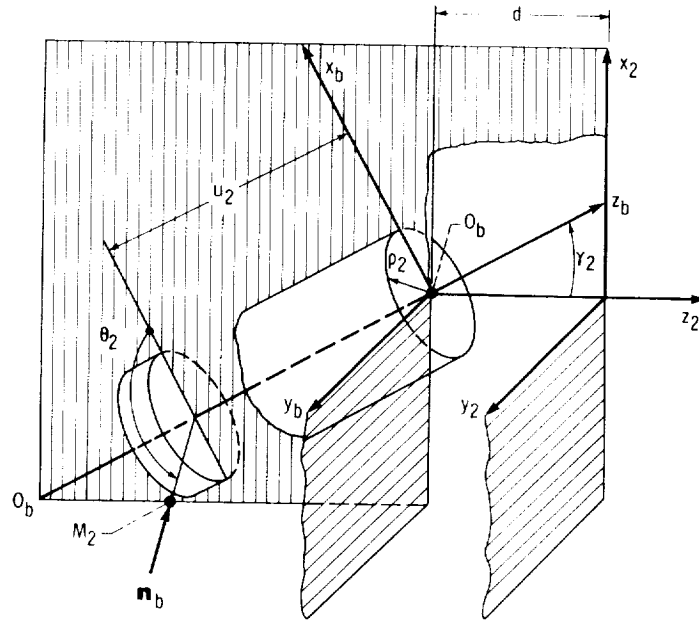


Figure 11.3.4.

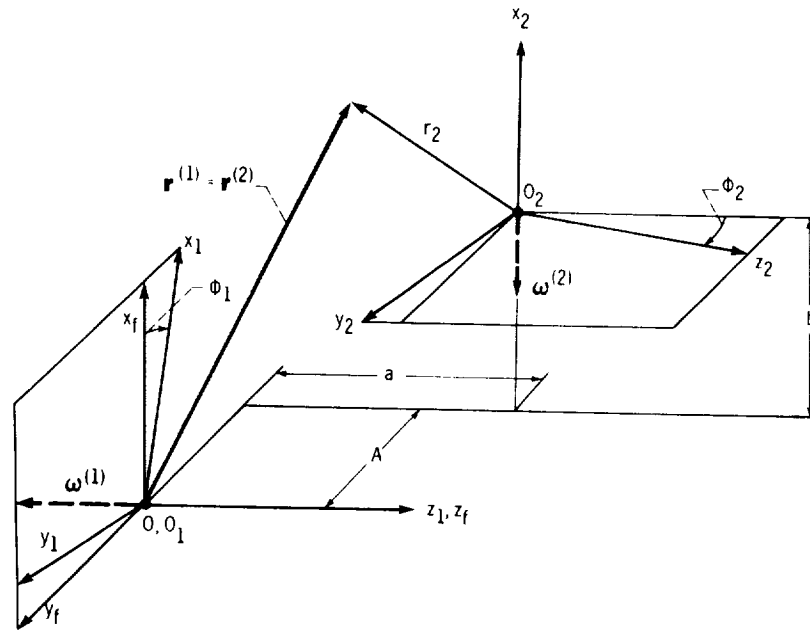


Figure 11.3.5.

At the point of tangency between surfaces Σ_1 and Σ_2 , the following conditions must be observed:

$$\mathbf{r}_f^{(1)}(u_1, \theta_1, \phi_1) = \mathbf{r}_f^{(2)}(u_2, \theta_2, \phi_2) \quad (11.2.33)$$

$$\mathbf{n}_f^{(1)}(\theta_1, \phi_1) = \mathbf{n}_f^{(2)}(\theta_2, \phi_2) \quad (11.2.34)$$

Vector equation (11.3.34) is equivalent to two independent scalar equations only since $|\mathbf{n}^{(1)}| = |\mathbf{n}^{(2)}| = 1$. Equations (11.2.33) and (11.2.34) result in five independent scalar equations in six unknowns, $u_1, \theta_1, u_2, \theta_2, \phi_1$, and ϕ_2 , as follows:

$$f_i(u_1, \theta_1, u_2, \theta_2, \phi_1, \phi_2) = 0 \quad f_i \in C^1 \quad (i = 1, 2, 3, 4, 5) \quad (11.3.35)$$

Remarks: The last two equations of system (11.3.35) do not contain u_1 and u_2 , since the surface unit normals do not depend on these surface coordinates.

Eliminating unknowns u_1 , θ_2 , and u_2 from equations (11.3.35), we get a system of two equations in three unknowns

$$F_1(\theta_1, \phi_1, \phi_2) = \tan \theta_1 - \frac{\sin \phi_1 \sin \phi_2 \sin \gamma_1 - \cos \phi_2 \cos \gamma_1 - \cos \phi_1 \sin \gamma_1 \tan \gamma_2}{\cos \phi_1 \sin \phi_2 + \sin \phi_1 \tan \gamma_2} = 0 \quad (11.3.36)$$

$$\begin{aligned} F_2(\theta_1, \phi_1, \phi_2) &= \left[\frac{b \sin \phi_1 - A \cos \phi_1 - (\rho_1 + \rho_2) \sin \theta_1 - d \cos \phi_1 \sin \phi_2}{\sin \gamma_2 \sin \phi_1 + \cos \phi_1 \sin \phi_2 \cos \gamma_2} \right] \\ &= k[b \sin \gamma_1 - (\rho_1 + \rho_2)(\sin \theta_1 \sin \phi_1 \sin \gamma_1 + \cos \theta_1 \cos \phi_1) \\ &\quad + a \cos \phi_1 \cos \gamma_1 - c \cos \phi_1 \sin \gamma_1 - d \cos \phi_1 \cos \phi_2 \cos \gamma_1] = 0 \end{aligned} \quad (11.3.37)$$

where

$$k = \frac{1}{\sin \gamma_2 \sin \gamma_1 + \cos \phi_1 \cos \phi_2 \cos \gamma_2 \cos \gamma_1}$$

Usually, $A = \rho_1 + \rho_2$, and when $\phi_1 = 0$, we get that $\theta_1 = 3\pi/2$ and $\phi_2 = 0$. The corresponding value of θ_2 is $\pi/2$, which we may get from equations (11.3.35). Assuming that $\{F_1, F_2\} \in C^1$ and

$$\frac{D(F_1, F_2)}{D(\theta_1, \phi_1)} \neq 0$$

we may determine functions $\phi_2(\phi_1)$ and $\theta_1(\phi_1)$.

The remaining unknowns, u_2 , θ_2 , and u_1 , may be determined from the following equations:

$$u_2 = \frac{b \sin \phi_1 - A \cos \phi_1 - (\rho_1 + \rho_2) \sin \theta_1 - d \cos \phi_1 \sin \phi_2}{\sin \phi_1 \sin \gamma_2 + \cos \phi_1 \sin \phi_2 \cos \gamma_2} \quad (11.3.38)$$

$$\cos \theta_2 = - \frac{\sin \theta_1 \sin \phi_1 + \cos \theta_1 \cos \phi_1 \sin \gamma_1}{\cos \gamma_2} \quad (11.3.39)$$

$$u_1 = \frac{(\rho_1 + \rho_2) \cos \theta_1 \cos \gamma_1 - a + (u_2 \cos \gamma_2 + d) \cos \phi_2}{\sin \gamma_1} \quad (11.3.40)$$

The angular velocity ratio may be determined by using equation (11.3.13).

Particular case 1.—The cylinder axes are perpendicular to the axes of rotation. By setting $\gamma_1 = \gamma_2 = 0$ in equations (11.3.26) and (11.3.37), we obtain

$$\cot \theta_1 = -\cos \phi_1 \tan \phi_2 \quad (11.3.41)$$

and

$$\begin{aligned} & \tan^2 \phi_2 [(\rho_1 + \rho_2)^2 - a^2] \cos^2 \phi_1 \\ & - 2a(A \cos \phi_1 - b \sin \phi_1) \cos \phi_1 \tan \phi_2 \\ & + (\rho_1 + \rho_2)^2 - (A \cos \phi_1 - b \sin \phi_1)^2 = 0 \end{aligned} \quad (11.3.42)$$

Equation (11.3.42) represents, in implicit form, the position function of the discussed mechanism. Neglecting radii ρ_1 and ρ_2 of the cylinders, we get

$$\tan \phi_2 = \frac{b \tan \phi_1 - A}{a} \quad (11.3.43)$$

The differentiation of this equation yields

$$m_{21} = \frac{\omega_2}{\omega_1} = \frac{\frac{d\phi_2}{dt}}{\frac{d\phi_1}{dt}} = \frac{b \cos^2 \phi_2}{a \cos^2 \phi_1} \quad (11.3.44)$$

Particular case 2.—The cylinder axes are parallel to the axes of rotation. By setting $\gamma_1 = -\pi/2$ and $\gamma_2 = \pi/2$ in equations (11.3.36) and (11.3.37), we get

$$\theta_1 = \frac{3\pi}{2} - \phi_1 \quad (11.3.45)$$

$$\sin \phi_2 = \frac{c \sin \phi_1 - \ell}{d} \quad (11.3.46)$$

where $\ell = A - (\rho_1 + \rho_2)$.

Equations $n_{zf}^{(2)} = n_{zf}^{(1)}$ (use eqs. (11.3.30) and (11.3.32)) and (11.3.45) yield

$$\theta_2 = \frac{\pi}{2} + \phi_2 \quad (11.3.47)$$

The angular velocity ratio is

$$m_{21} = \frac{c \cos \phi_1}{d \cos \phi_2} = \frac{c \cos \phi_1}{\sqrt{d^2 - (c \sin \phi_1 - \ell)^2}} \quad (11.3.48)$$

The discussed mechanism is applied in gauges. The optimal synthesis of such mechanisms is worked out by (Litvin and Gutman, 1984).

Chapter 12

Basic Kinematic Relations of Spatial Gearings

Kinematic relations of spatial gearings are the relations between velocities and accelerations of the points of contact of gear-tooth surfaces being in mesh, and the relations between velocities and accelerations of the tips of the surface unit normals. These relations may be applied as the basis for effective methods of determination of

- (1) conditions of tooth nonundercutting (ch. 9.5)
- (2) relations between principal curvatures and directions for two surfaces being in mesh (ch. 13)
- (3) kinematical errors of gear trains

Basic kinematic relations and their applications have been proposed (Litvin, 1968 and 1969).

12.1 Relations of Contact Point Velocity and Surface Unit Normal Velocity

Consider two gears being in mesh. Because of the continuous tangency of gear-tooth surfaces, the position vectors and unit normals of both surfaces at their instantaneous contact point must be equal at every instant. These conditions were represented by equations (11.2.1) and (11.2.2). Since these equations are to be observed continuously at every instant, we may differentiate them. This yields

$$\dot{\mathbf{r}}^{(1)}(u_1, \theta_1, \phi_1) = \dot{\mathbf{r}}^{(2)}(u_2, \theta_2, \phi_2) \quad (12.1.1)$$

$$\dot{\mathbf{n}}^{(1)}(u_1, \theta_1, \phi_1) = \dot{\mathbf{n}}^{(2)}(u_2, \theta_2, \phi_2) \quad (12.1.2)$$

Here $\dot{\mathbf{r}}^{(i)}$ ($i = 1, 2$) is the velocity of the contact point in absolute motion (motion relative to the frame), and $\dot{\mathbf{n}}^{(i)}$ is the linear velocity of the tip of the unit normal vector in absolute motion.

Equations (12.1.1) and (12.1.2) may be represented as follows:

$$\begin{aligned} \mathbf{v}_{abs} = \dot{\mathbf{r}}^{(1)}(u_1, \theta_1, \phi_1) &= \frac{\partial \mathbf{r}^{(1)}}{\partial \phi_1} \frac{d\phi_1}{dt} + \frac{\partial \mathbf{r}^{(1)}}{\partial u_1} \frac{du_1}{dt} + \frac{\partial \mathbf{r}^{(1)}}{\partial \theta_1} \frac{d\theta_1}{dt} \\ &= \dot{\mathbf{r}}^{(2)}(u_2, \theta_2, \phi_2) = \frac{\partial \mathbf{r}^{(2)}}{\partial \phi_2} \frac{d\phi_2}{dt} + \frac{\partial \mathbf{r}^{(2)}}{\partial u_2} \frac{du_2}{dt} + \frac{\partial \mathbf{r}^{(2)}}{\partial \theta_2} \frac{d\theta_2}{dt} \end{aligned} \quad (12.1.3)$$

$$\begin{aligned}
\dot{\mathbf{n}}_{abs} &= \dot{\mathbf{n}}^{(1)}(u_1, \theta_1, \phi_1) = \frac{\partial \mathbf{n}^{(1)}}{\partial \phi_1} \frac{d\phi_1}{dt} + \frac{\partial \mathbf{n}^{(1)}}{\partial u_1} \frac{du_1}{dt} + \frac{\partial \mathbf{n}^{(1)}}{\partial \theta_1} \frac{d\theta_1}{dt} \\
&= \dot{\mathbf{n}}^{(2)}(u_2, \theta_2, \phi_2) = \frac{\partial \mathbf{n}^{(2)}}{\partial \phi_2} \frac{d\phi_2}{dt} + \frac{\partial \mathbf{n}^{(2)}}{\partial u_2} \frac{du_2}{dt} + \frac{\partial \mathbf{n}^{(2)}}{\partial \theta_2} \frac{d\theta_2}{dt}
\end{aligned} \tag{12.1.4}$$

Here t represents time.

Let us interpret equations (12.1.3) and (12.1.4) kinematically. The velocity of the contact point observed in the coordinate system S_f is the velocity in absolute motion $\mathbf{v}_{abs}^{(i)}$. This velocity may be represented as the sum of two components

$$\mathbf{v}_{abs}^{(i)} = \mathbf{v}_{ir}^{(i)} + \mathbf{v}_r^{(i)} \quad (i = 1, 2) \tag{12.1.5}$$

Here $\mathbf{v}_r^{(i)}$ is the velocity of the contact point in its motion over the gear-tooth surface (in relative motion with respect to the surface), and $\mathbf{v}_{ir}^{(i)}$ is the velocity of the contact point in its motion with the surface (in transfer motion of the point which is considered as rigidly connected to the surface). The relative motion of the contact point may be observed in a coordinate system rigidly connected to the surface. Here

$$\mathbf{v}_{ir}^{(i)} = \frac{\partial \mathbf{r}^{(i)}}{\partial \phi_i} \frac{d\phi_i}{dt} \tag{12.1.6}$$

$$\mathbf{v}_r^{(i)} = \frac{\partial \mathbf{r}^{(i)}}{\partial u_i} \frac{du_i}{dt} + \frac{\partial \mathbf{r}^{(i)}}{\partial \theta_i} \frac{d\theta_i}{dt} \tag{12.1.7}$$

Equations (12.1.3) and (12.1.5) to (12.1.7) yield

$$\mathbf{v}_{ir}^{(1)} - \mathbf{v}_{ir}^{(2)} = \mathbf{v}_r^{(2)} - \mathbf{v}_r^{(1)} \tag{12.1.8}$$

By using the notation

$$\mathbf{v}^{(12)} = \mathbf{v}_{ir}^{(1)} - \mathbf{v}_{ir}^{(2)} \tag{12.1.9}$$

we obtain

$$\mathbf{v}_r^{(2)} = \mathbf{v}^{(12)} + \mathbf{v}_r^{(1)} \tag{12.1.10}$$

Here $\mathbf{v}^{(12)}$ is the sliding velocity which is the velocity of point M_1 of surface Σ_1 with respect to point M_2 of surface Σ_2 . (Points M_1 and M_2 coincide forming a mutual point which is the point of tangency of the surfaces.)

In addition to the analytical determination of transfer velocity by equation (12.1.6), this velocity may also be determined kinematically as was explained in section 2.3. Equation (12.1.10) is the basic equation which relates the velocities of contact points of mating surfaces.

The advantage of equation (12.1.10) is that we can express the velocity $\mathbf{v}_r^{(2)}$ in terms of $\mathbf{v}_r^{(1)}$ and $\mathbf{v}^{(12)}$. Thus, we may determine the velocity $\mathbf{v}_r^{(2)}$, although the equations of surface Σ_2 are not known.

When using equation (12.1.10) we have to differentiate between the cases of line contact and point contact of mating surfaces. In the case of point contact, only a line of the surface is under the action (fig. 12.1.1(a)). At every instant, surface Σ_i contacts the mating surface at a point, and the working line of the surface is the locus of instantaneous contact points. The velocity $\mathbf{v}_r^{(i)}$ of the contact point in the motion over the gear-tooth surface is the tangent to the working line. In

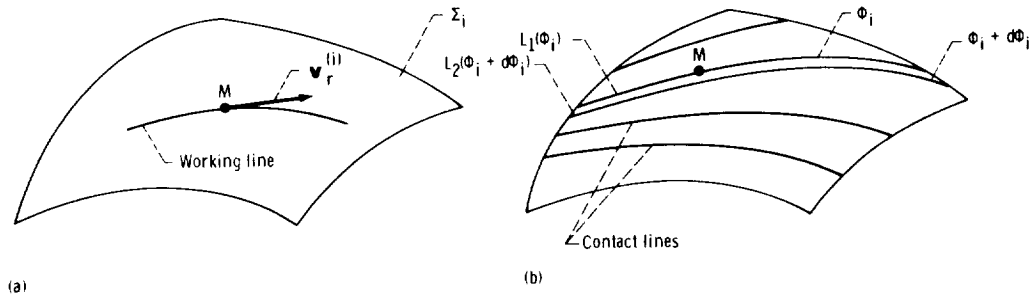


Figure 12.1.1.

the case of line contact surface Σ_i at every instant contacts the mating surface along a line. Thus, the surface is covered with contact lines (fig. 12.1.1(b)). Consider two infinitesimally close contact lines which correspond to the parameters of motion ϕ and $(\phi + d\phi)$, respectively. Let us designate a point of the contact line $L_1(\phi_i)$ by M . To be a point of the new contact line $L_2(\phi_i + d\phi_i)$, point M can be moved over the surface in an arbitrary direction but different from the tangent to the contact line L_1 .

Taking into account that vector $\mathbf{v}^{(12)}$ may be determined for any point of contact of the surfaces, we may state the following results:

(1) In the case of the point contact vector, $\mathbf{v}_r^{(1)}$ has a definite direction. Knowing the magnitude of $\mathbf{v}_r^{(1)}$, we may determine the magnitude and direction of vector $\mathbf{v}_r^{(2)}$ from equation (12.1.10).

(2) In the case of line contact, the direction of $\mathbf{v}_r^{(1)}$ is indefinite. We may determine vector $\mathbf{v}_r^{(2)}$ from equation (12.1.10), if not only the magnitude but also the direction of $\mathbf{v}_r^{(1)}$ is given. Similarly we may kinematically interpret equations (12.1.4)

$$\dot{\mathbf{n}}_{abs} = \dot{\mathbf{n}}_{tr}^{(1)} + \dot{\mathbf{n}}_r^{(1)} = \dot{\mathbf{n}}_{tr}^{(2)} + \dot{\mathbf{n}}_r^{(2)} \quad (12.1.11)$$

Here vector

$$\dot{\mathbf{n}}_{tr}^{(i)} = \frac{\partial \mathbf{n}^{(i)}}{\partial \phi_i} \frac{d\phi_i}{dt} \quad (i = 1, 2) \quad (12.1.12)$$

represents the transfer velocity which is the velocity of the tip of the surface unit normal in its motion with the surface. Vector

$$\dot{\mathbf{n}}_r^{(i)} = \frac{\partial \mathbf{n}^{(i)}}{\partial u_i} \frac{du_i}{dt} + \frac{\partial \mathbf{n}^{(i)}}{\partial \theta_i} \frac{d\theta_i}{dt} \quad (12.1.13)$$

represents the relative velocity of the tip of the surface unit normal which corresponds to the motion of the contact point over the surface.

Equations (12.1.11) to (12.1.13) yield

$$\dot{\mathbf{n}}_r^{(2)} = \dot{\mathbf{n}}_r^{(1)} + \dot{\mathbf{n}}_{tr}^{(1)} - \dot{\mathbf{n}}_{tr}^{(2)} \quad (12.1.14)$$

Thus, we can express vector $\dot{\mathbf{n}}_r^{(2)}$ in terms of $\dot{\mathbf{n}}_r^{(1)}$, $\dot{\mathbf{n}}_{tr}^{(1)}$, and $\dot{\mathbf{n}}_{tr}^{(2)}$. This is a great advantage since we are able to determine $\dot{\mathbf{n}}_r^{(2)}$, although the equations of surface Σ_2 are not defined.

It is known from mechanics that if the transfer motion is rotational about a fixed axis, vector $\dot{\mathbf{n}}_{tr}^{(i)}$ may be represented by

$$\dot{\mathbf{n}}_{tr}^{(i)} = \boldsymbol{\omega}_f^{(i)} \times \mathbf{n}_f^{(i)} \quad (12.1.15)$$

This result may be interpreted kinematically. Consider that \mathbf{n}_f is the surface unit normal vector at point M (fig. 12.1.2), and T is the tangent plane to the surface at point M . (Superscript i 's are

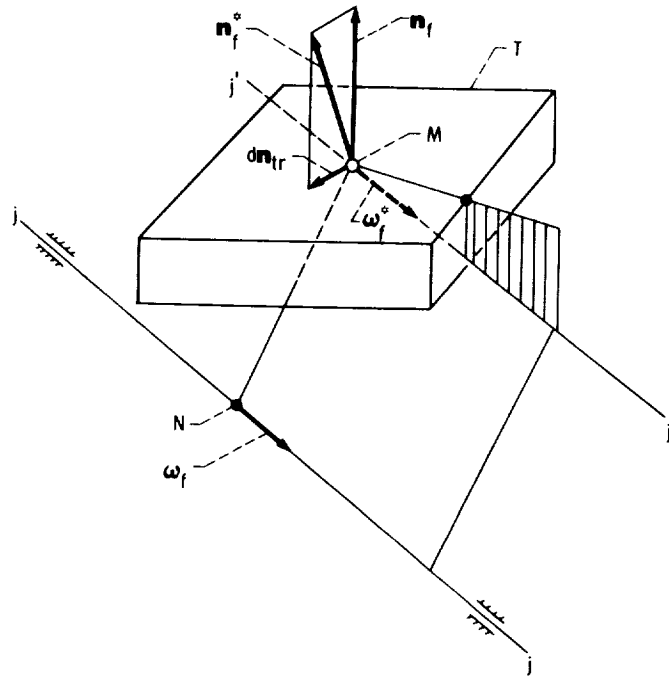


Figure 12.1.2.

dropped.) The surface rotates about axis $j-j'$ with angular velocity ω_f . We may replace the sliding vector ω_f by the equivalent vector ω_f^* passing through point M , and the moment

$$\mathbf{m}_f = \mathbf{R}_f \times \omega_f \quad (12.1.16)$$

Here \mathbf{R}_f is a position vector drawn from point M to an arbitrary point N on the $j-j'$ axis; thus $\mathbf{R}_f = \overline{MN}$. The moment \mathbf{m}_f represents the velocity of point M in translational motion which is perpendicular to the plane formed by vectors ω_f and \overline{MN} . The transfer motion of surface Σ , with unit normal \mathbf{n}_f , may be represented as a resulting motion of the following two components: (1) of translation with velocity \mathbf{m}_f and (2) of rotation about axis $j'-j''$ with angular velocity $\omega_f^* = \omega_f$. Axis $j'-j''$ is drawn through point M parallel to $j-j'$. By translation, the unit normal \mathbf{n}_f will be moved parallel to its original direction being translated with the surface and the surface point M . Thus, while surface Σ with point M and surface unit normal \mathbf{n}_f are translated with velocity

$$\mathbf{m}_f = \mathbf{R}_f \times \omega_f \quad (12.1.17)$$

vector \mathbf{n}_f does not change its original direction. The direction of \mathbf{n}_f , however, will be changed because of the rotation about axis $j'-j''$.

Figure 12.1.2 shows two positions of the unit vector, \mathbf{n}_f is the initial position, and \mathbf{n}_f^* is the changed position after rotation about axis $j'-j''$ through an angle

$$d\phi_f = \omega_f dt \quad (12.1.18)$$

The difference

$$\mathbf{n}_f^* - \mathbf{n}_f = d\mathbf{n}_{tr} \quad (12.1.19)$$

represents the displacement of the surface unit normal by rotation about axis $j'-j''$. Vector $d\mathbf{n}_{tr}$ is represented by the equation

$$d\mathbf{n}_{tr} = d\phi_f \times \mathbf{n}_f = (\omega_f \times \mathbf{n}_f) dt \quad (12.1.20)$$

and

$$\dot{\mathbf{n}}_r = \frac{d\mathbf{n}_r}{dt} = \boldsymbol{\omega}_f \times \mathbf{n}_f \quad (12.1.21)$$

Equations (12.1.14) and (12.1.21) yield

$$\dot{\mathbf{n}}_r^{(2)} = \dot{\mathbf{n}}_r^{(1)} + \left(\boldsymbol{\omega}_f^{(12)} \times \mathbf{n}_f \right) \quad (12.1.22)$$

where $\boldsymbol{\omega}_f^{(12)} = \boldsymbol{\omega}_f^{(1)} - \boldsymbol{\omega}_f^{(2)}$. Equation (12.1.22) is the basic equation which relates the velocities of the surface unit normals for mating surfaces.

12.2 Relations of Contact Point Acceleration and Surface Unit Normal Acceleration

To determine relations between the accelerations of contact points, we may differentiate vector equation (12.1.10). By using expression (2.3.7) for $\mathbf{v}^{(2)}$, we represent equation (12.1.10) as follows:

$$\mathbf{v}_r^{(2)} = \left(\boldsymbol{\omega}_f^{(1)} - \boldsymbol{\omega}_f^{(2)} \right) \times \mathbf{r}_f - \left(\mathbf{R}_f \times \boldsymbol{\omega}_f^{(2)} \right) + \mathbf{v}_r^{(1)} \quad (12.2.1)$$

After differentiation we obtain

$$\begin{aligned} \frac{d}{dt} \left(\mathbf{v}_r^{(2)} \right) &= \mathbf{a}_r^{(2)} + \boldsymbol{\omega}_f^{(2)} \times \mathbf{v}_r^{(2)} = \frac{d}{dt} \left[\left(\boldsymbol{\omega}_f^{(1)} - \boldsymbol{\omega}_f^{(2)} \right) \times \mathbf{r}_f - \left(\mathbf{R}_f \times \boldsymbol{\omega}_f^{(2)} \right) + \mathbf{v}_r^{(1)} \right] \\ &= \left(\dot{\boldsymbol{\omega}}_f^{(1)} - \dot{\boldsymbol{\omega}}_f^{(2)} \right) \times \mathbf{r}_f + \left(\boldsymbol{\omega}_f^{(1)} - \boldsymbol{\omega}_f^{(2)} \right) \times \dot{\mathbf{r}}_f - \left(\mathbf{R}_f \times \dot{\boldsymbol{\omega}}_f^{(2)} \right) + \mathbf{a}_r^{(1)} \\ &\quad + \boldsymbol{\omega}_f^{(1)} \times \mathbf{v}_r^{(1)} \end{aligned}$$

The differentiation of equation (12.2.1) was based on the following considerations:

(1) Vector $\mathbf{v}_r^{(i)}$ ($i = 1, 2$) is represented in a movable coordinate system and therefore

$$\begin{aligned} \mathbf{a}_r^{(2)} &= \mathbf{a}_r^{(1)} + \left(\boldsymbol{\omega}_f^{(12)} \times \dot{\mathbf{r}}_f \right) + \left(\boldsymbol{\omega}_f^{(1)} \times \mathbf{v}_r^{(1)} \right) - \left(\boldsymbol{\omega}_f^{(2)} \times \mathbf{v}_r^{(2)} \right) \\ &\quad + \left(\dot{\boldsymbol{\omega}}_f^{(1)} \times \mathbf{r}_f \right) - \left[\dot{\boldsymbol{\omega}}_f^{(2)} \times \left(\mathbf{r}_f - \mathbf{R}_f \right) \right] \end{aligned} \quad (12.2.2)$$

where

$$\boldsymbol{\omega}_f^{(12)} = \boldsymbol{\omega}_f^{(1)} - \boldsymbol{\omega}_f^{(2)}$$

$$\frac{d}{dt} \left(\mathbf{v}_r^{(i)} \right) = \left(\boldsymbol{\omega}_f^{(i)} \times \mathbf{v}_r^{(i)} \right) + \mathbf{a}_r^{(i)} \quad (12.2.3)$$

The cross product $\boldsymbol{\omega}_f^{(i)} \times \mathbf{v}_r^{(i)}$ may be interpreted kinematically which is similar to the interpretation of the cross product $\boldsymbol{\omega}_f \times \mathbf{n}_f$. (See eq. (12.1.21) and explanations related with fig. 12.1.2.)

(2) Since \mathbf{R}_f is a vector of constant direction and magnitude, its derivative $d/dt (\mathbf{R}_f)$ is equal to zero.

Let us now derive the expression for $\dot{\mathbf{r}}_f$.

Vector \mathbf{r}_f is the position vector of a contact point at which two single points of two surfaces coincide. Thus,

$$\mathbf{r}_f = \mathbf{r}_f^{(1)} = \mathbf{r}_f^{(2)} \quad (12.2.4)$$

The differentiation of equation (12.2.4) yields

$$\dot{\mathbf{r}}_f = \dot{\mathbf{r}}_f^{(1)} = \dot{\mathbf{r}}_f^{(2)} = \mathbf{v}_{abs} \quad (12.2.5)$$

By using equation (12.1.5), we may represent $\dot{\mathbf{r}}_f$ in terms of vectors $\mathbf{v}_r^{(1)}$ and $\mathbf{v}_{ir}^{(1)}$ and obtain

$$\dot{\mathbf{r}}_f = \mathbf{v}_r^{(1)} + \mathbf{v}_{ir}^{(1)} = \mathbf{v}_r^{(1)} + \left(\boldsymbol{\omega}_f^{(1)} \times \mathbf{r}_f^{(1)} \right) \quad (12.2.6)$$

Equations (12.2.2) and (12.2.6) yield

$$\begin{aligned} \mathbf{a}_r^{(2)} = \mathbf{a}_r^{(1)} + \left(\boldsymbol{\omega}_f^{(12)} \times \mathbf{v}_{ir}^{(1)} \right) + \left[\left(\boldsymbol{\omega}_f^{(12)} + \boldsymbol{\omega}_f^{(1)} \right) \times \mathbf{v}_r^{(1)} \right] - \left(\boldsymbol{\omega}_f^{(2)} \times \mathbf{v}_r^{(2)} \right) \\ + \left(\dot{\boldsymbol{\omega}}_f^{(1)} \times \mathbf{r}_f^{(1)} \right) - \left[\dot{\boldsymbol{\omega}}_f^{(2)} \times (\mathbf{r}_f - \mathbf{R}_f) \right] \end{aligned} \quad (12.2.7)$$

Substituting for $\mathbf{v}_r^{(2)}$ in (12.2.7) by

$$\mathbf{v}_r^{(2)} = \mathbf{v}_r^{(1)} + \mathbf{v}_f^{(12)}$$

we get

$$\begin{aligned} \mathbf{a}_r^{(2)} = \mathbf{a}_r^{(1)} + 2 \left(\boldsymbol{\omega}_f^{(12)} \times \mathbf{v}_r^{(1)} \right) + \left(\boldsymbol{\omega}_f^{(12)} \times \mathbf{v}_{ir}^{(1)} \right) - \left(\boldsymbol{\omega}_f^{(2)} \times \mathbf{v}^{(12)} \right) \\ + \left(\dot{\boldsymbol{\omega}}_f^{(1)} \times \mathbf{r}_f^{(1)} \right) - \left[\dot{\boldsymbol{\omega}}_f^{(2)} \times (\mathbf{r}_f - \mathbf{R}_f) \right] \end{aligned} \quad (12.2.8)$$

Equation (12.2.8) is the basic equation which relates the accelerations of contact points of two mating surfaces.

Let us now get the relation between $\ddot{\mathbf{n}}_r^{(2)}$ and $\ddot{\mathbf{n}}_r^{(1)}$. The differentiation of equation (12.1.22) yields

$$\frac{d}{dt} \left(\dot{\mathbf{n}}_r^{(2)} \right) = \boldsymbol{\omega}_f^{(2)} \times \dot{\mathbf{n}}_r^{(2)} + \ddot{\mathbf{n}}_r^{(2)} = \boldsymbol{\omega}_f^{(2)} \times \left[\dot{\mathbf{n}}_r^{(1)} + \left(\boldsymbol{\omega}_f^{(12)} \times \mathbf{n}_f \right) \right] + \ddot{\mathbf{n}}_r^{(2)} \quad (12.2.9)$$

$$\begin{aligned} \frac{d}{dt} \left[\dot{\mathbf{n}}_r^{(1)} + \left(\boldsymbol{\omega}_f^{(12)} \times \mathbf{n}_f \right) \right] &= \left(\boldsymbol{\omega}_f^{(1)} \times \dot{\mathbf{n}}_r^{(1)} \right) + \ddot{\mathbf{n}}_r^{(1)} + \left(\boldsymbol{\omega}_f^{(12)} \times \dot{\mathbf{n}}_f \right) + \left[\left(\dot{\boldsymbol{\omega}}_f^{(1)} - \dot{\boldsymbol{\omega}}_f^{(2)} \right) \times \mathbf{n}_f \right] \\ &= \left(\boldsymbol{\omega}_f^{(1)} \times \dot{\mathbf{n}}_r^{(1)} \right) + \ddot{\mathbf{n}}_r^{(1)} + \left\{ \boldsymbol{\omega}_f^{(12)} \times \left[\left(\boldsymbol{\omega}_f^{(1)} \times \mathbf{n}_f \right) + \dot{\mathbf{n}}_r^{(1)} \right] \right\} \\ &+ \left[\left(\dot{\boldsymbol{\omega}}_f^{(1)} - \dot{\boldsymbol{\omega}}_f^{(2)} \right) \times \mathbf{n}_f \right] \end{aligned} \quad (12.2.10)$$

Equations (12.2.9) and (12.2.10) yield

$$\begin{aligned} \ddot{\mathbf{n}}_r^{(2)} = \ddot{\mathbf{n}}_r^{(1)} + 2\left(\boldsymbol{\omega}_f^{(12)} \times \dot{\mathbf{n}}_r^{(1)}\right) + \boldsymbol{\omega}_f^{(1)}\left(\boldsymbol{\omega}_f^{(12)} \cdot \mathbf{n}_f\right) - \boldsymbol{\omega}_f^{(12)}\left(\boldsymbol{\omega}_f^{(2)} \cdot \mathbf{n}_f\right) \\ - \mathbf{n}_f\left(\boldsymbol{\omega}_f^{(12)}\right)^2 + \left[\left(\dot{\boldsymbol{\omega}}_f^{(1)} - \dot{\boldsymbol{\omega}}_f^{(2)}\right) \times \mathbf{n}_f\right] \end{aligned} \quad (12.2.11)$$

Equation (12.2.11) is the basic equation which relates the accelerations of the surface unit normals of two mating surfaces.

The set of equations (12.1.10), (12.1.22), (12.2.2), and (12.2.11) represent the basic kinematic relations for two mating surfaces of spatial gears.

Chapter 13

Relations Between Curvatures of Mating Surfaces

13.1 Relations Between Principal Curvatures and Directions for Mating Surfaces

Basic equations

Consider two gear-tooth surfaces Σ_1 and Σ_2 that are represented in the coordinate system S_f rigidly connected to the frame. The parameters of motion of both gears are given, and P is the point of tangency of the surfaces. There are two cases of tangency of gear-tooth surfaces: (1) the surfaces are in point contact, and P is the single point of tangency at the considered instant; and (2) surfaces Σ_1 and Σ_2 are in line contact, and P is just a point of the instantaneous line of contact. We assume that at point P the principal curvatures and directions for one of the surfaces, for instance surface Σ_2 , are given. The problem is to determine the principal curvatures and directions of the second surface Σ_1 at the point of tangency P , without knowing the equations of Σ_1 . The key to the solution of this problem is the relationship between the principal curvatures and directions of mating gear-tooth surfaces. (First proposed by Litvin, 1969 and then developed by Litvin and Gutman, 1981.)

Consider that a set of parameters

$$Q = (u_1^0, \theta_1^0, \phi_1^0, u_2^0, \theta_2^0, \phi_2^0) \quad (13.1.1)$$

satisfies the following vector equations (subscript f is dropped):

$$\mathbf{r}^{(1)}(u_1, \theta_1, \phi_1) = \mathbf{r}^{(2)}(u_2, \theta_2, \phi_2) \quad \{\mathbf{r}^{(1)}, \mathbf{r}^{(2)}\} \in C^2 \quad (13.1.2)$$

$$\mathbf{n}^{(1)}(u_1, \theta_1, \phi_1) = \mathbf{n}^{(2)}(u_2, \theta_2, \phi_2) \quad (13.1.3)$$

Here $\mathbf{r}^{(i)}$ is the position vector of the point of contact drawn from the origin of the coordinate system S_f , and $\mathbf{n}^{(i)}$ is the surface unit normal, represented by

$$\mathbf{n}^{(i)} = \frac{\mathbf{N}^{(i)}}{|\mathbf{N}^{(i)}|} \quad \mathbf{N}^{(i)} = \frac{\partial \mathbf{r}^{(i)}}{\partial u_i} \times \frac{\partial \mathbf{r}^{(i)}}{\partial \theta_i} \neq 0 \quad (i = 1, 2) \quad (13.1.4)$$

Parameters u_i and θ_i are the surface coordinates, and ϕ_i is the parameter of motion. It is assumed that the function $\phi_2(\phi_1) \in C^2$ is given. Usually, $\phi_2(\phi_1)$ is a linear function. Surfaces Σ_1 and Σ_2 are in tangency at point P since equations (13.1.2) and (13.1.3) are observed.

In the neighborhood of point P the following equations are observed:

$$\dot{\mathbf{r}}^{(1)}(u_1, \theta_1, \phi_1) = \dot{\mathbf{r}}^{(2)}(u_2, \theta_2, \phi_2) \quad (13.1.5)$$

$$\dot{\mathbf{n}}^{(1)}(u_1, \theta_1, \phi_1) = \dot{\mathbf{n}}^{(2)}(u_2, \theta_2, \phi_2) \quad (13.1.6)$$

$$\frac{d}{dt}(\mathbf{n}^{(i)} \cdot \mathbf{v}^{(12)}) = 0 \quad (i = 1, 2) \quad (13.1.7)$$

Let us note that

$$\mathbf{n}^{(i)} \cdot \mathbf{v}^{(12)} = \mathbf{n}^{(i)} \cdot \left\{ \left[(\boldsymbol{\omega}^{(1)} - \boldsymbol{\omega}^{(2)}) \times \mathbf{r}^{(1)} \right] - (\mathbf{R} \times \boldsymbol{\omega}^{(2)}) \right\} = 0 \quad (13.1.8)$$

is the equation of meshing. (See ch. 9.8.)

It has been proven in chapter 12.1 that equations (13.1.5) and (13.1.6) yield the following relations:

$$\mathbf{v}_r^{(2)} = \mathbf{v}_r^{(1)} + \mathbf{v}^{(12)} \quad (13.1.9)$$

$$\dot{\mathbf{n}}_r^{(2)} = \dot{\mathbf{n}}_r^{(1)} + (\boldsymbol{\omega}^{(12)} \times \mathbf{n}) \quad (13.1.10)$$

To derive equation (13.1.7), we differentiate equation (13.1.8) considering that $\boldsymbol{\omega}^{(1)} = \text{constant}$. This yields

$$\begin{aligned} (\dot{\mathbf{n}}^{(i)} \cdot \mathbf{v}^{(12)}) + \mathbf{n}^{(i)} \cdot \left\{ \left(-\dot{\boldsymbol{\omega}}^{(2)} \times \mathbf{r}^{(1)} \right) \right. \\ \left. + \left[(\boldsymbol{\omega}^{(1)} - \boldsymbol{\omega}^{(2)}) \times \dot{\mathbf{r}}^{(1)} \right] - (\mathbf{R} \times \dot{\boldsymbol{\omega}}^{(2)}) \right\} = 0 \end{aligned} \quad (13.1.11)$$

We may transform equation (13.1.11) by using the following relations:

$$\dot{\mathbf{n}}^{(i)} = \dot{\mathbf{n}}_r^{(i)} + (\boldsymbol{\omega}^{(i)} \times \mathbf{n}) \quad (13.1.12)$$

$$\dot{\mathbf{r}}^{(i)} = \mathbf{v}_r^{(i)} + \mathbf{v}_{ir}^{(i)} \quad (13.1.13)$$

$$\boldsymbol{\omega}^{(2)} = \omega^{(2)} \mathbf{k}_2 = \omega^{(1)} m_{21} \mathbf{k}_2 \quad (13.1.14)$$

where

$$m_{21}(\phi_1) = \frac{\omega^{(2)}}{\omega^{(1)}}$$

Here ϕ_1 is the rotation angle of gear 1, and \mathbf{k}_2 is the unit vector of the axis of rotation of gear 2. The differentiation of equation (13.1.14) gives

$$\frac{d}{dt}(\boldsymbol{\omega}^{(2)}) = \omega^{(1)} \frac{d}{dt} [m_{21}(\phi_1)] \mathbf{k}_2 = \omega^{(1)} \frac{d}{d\phi_1} [m_{21}(\phi_1)] \frac{d\phi_1}{dt} \mathbf{k}_2 = (\omega^{(1)})^2 m'_{21} \mathbf{k}_2 \quad (13.1.15)$$

Here

$$m'_{21} = \frac{d}{d\phi_1} [m_{21}(\phi_1)]$$

Equations (13.1.11) to (13.1.15) yield

$$\begin{aligned} (\dot{\mathbf{n}}_r^{(i)} \cdot \mathbf{v}^{(12)}) + \left[(\boldsymbol{\omega}^{(i)} \times \mathbf{n}) \cdot \mathbf{v}^{(12)} \right] - \left\{ (\omega^{(1)})^2 m'_{21} \mathbf{n}^{(i)} \cdot \left[\mathbf{k}_2 \times (\mathbf{r}^{(1)} - \mathbf{R}) \right] \right\} \\ + \mathbf{n}^{(i)} \cdot \left[\boldsymbol{\omega}^{(12)} \times (\mathbf{v}_r^{(i)} + \mathbf{v}_{ir}^{(i)}) \right] = 0 \quad (i = 1, 2) \end{aligned} \quad (13.1.16)$$

The triple product in equation (13.1.16) is transformed as follows:

$$(\boldsymbol{\omega}^{(i)} \times \mathbf{n}) \cdot \mathbf{v}^{(12)} = (\boldsymbol{\omega}^{(i)} \times \mathbf{n}) \cdot (\mathbf{v}_{ir}^{(1)} - \mathbf{v}_{ir}^{(2)}) \quad (13.1.17)$$

Taking into account that

$$\begin{aligned} (\boldsymbol{\omega}^{(i)} \times \mathbf{n}) \cdot (\mathbf{v}_{ir}^{(1)} - \mathbf{v}_{ir}^{(2)}) + \left\{ \mathbf{n} \cdot \left[\boldsymbol{\omega}^{(12)} \times (\mathbf{v}_r^{(i)} + \mathbf{v}_{ir}^{(i)}) \right] \right\} = \mathbf{n} \cdot \left[(\boldsymbol{\omega}^{(1)} \times \mathbf{v}_{ir}^{(2)}) \right. \\ \left. - (\boldsymbol{\omega}^{(2)} \times \mathbf{v}_{ir}^{(1)}) \right] - \mathbf{v}_r^{(i)} \cdot (\boldsymbol{\omega}^{(12)} \times \mathbf{n}) \quad (i = 1, 2) \end{aligned} \quad (13.1.18)$$

the final expression for equation (13.1.16) is given by

$$\begin{aligned} (\dot{\mathbf{n}}_r^{(i)} \cdot \mathbf{v}^{(12)}) - (\mathbf{v}_r^{(i)} \cdot (\boldsymbol{\omega}^{(12)} \times \mathbf{n})) + \mathbf{n} \cdot \left[(\boldsymbol{\omega}^{(1)} \times \mathbf{v}_{ir}^{(2)}) - (\boldsymbol{\omega}^{(2)} \times \mathbf{v}_{ir}^{(1)}) \right] \\ - (\omega^{(1)})^2 m'_{21} \mathbf{n} \cdot \left[\mathbf{k}_2 \times (\mathbf{r}^{(1)} - \mathbf{R}) \right] = 0 \quad (i = 1, 2) \end{aligned} \quad (13.1.19)$$

Equations (13.1.9), (13.1.10), and (13.1.19) are the basic equations which we will use to derive the desired relations between the principal curvatures and directions of mating surfaces.

Basic Linear Equations

We may transform the system of equations (13.1.9), (13.1.10), and (13.1.19) into a system of linear equations by using a linear vector function that relates vectors $\mathbf{v}_r^{(i)}$ and $\dot{\mathbf{n}}_r^{(i)}$. (See app. C.)

Consider two right-handed trihedrons $S_a(\mathbf{e}_f, \mathbf{e}_h, \mathbf{n})$ and $S_b(\mathbf{e}_s, \mathbf{e}_q, \mathbf{n})$ (fig. 13.1.1). The common origin of the trihedrons coincides with the contact point M , the \mathbf{n} -axis represents the direction of the surface unit normal, \mathbf{e}_f and \mathbf{e}_h are the unit vectors of the principal directions of surface Σ_1 , \mathbf{e}_s and \mathbf{e}_q represent the principal directions of surface Σ_2 , and σ is the angle formed between \mathbf{e}_f and \mathbf{e}_s (measured clockwise from \mathbf{e}_s to \mathbf{e}_f and counterclockwise from \mathbf{e}_f to \mathbf{e}_s). Henceforth, we shall drop the subscript r in notations such as $\mathbf{v}_r^{(i)}$ and $\dot{\mathbf{n}}_r^{(i)}$ and designate these vectors by $\mathbf{v}^{(i)}$ and $\dot{\mathbf{n}}^{(i)}$, respectively. Expressing $\mathbf{v}^{(i)}$ and $\dot{\mathbf{n}}^{(i)}$ by their projections on the trihedron axes, we obtain

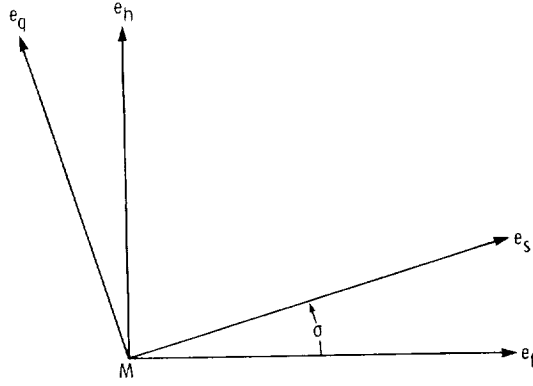


Figure 13.1.1.

$$\mathbf{v}^{(i)} = v_f^{(i)}\mathbf{e}_f + v_h^{(i)}\mathbf{e}_h = v_s^{(i)}\mathbf{e}_s + v_q^{(i)}\mathbf{e}_q \quad (13.1.20)$$

$$\dot{\mathbf{n}}^{(i)} = \dot{n}_f^{(i)}\mathbf{e}_f + \dot{n}_h^{(i)}\mathbf{e}_h = \dot{n}_s^{(i)}\mathbf{i}_s + \dot{n}_q^{(i)}\mathbf{e}_q \quad (13.1.21)$$

The third projection of vectors $\mathbf{v}^{(i)}$ and $\dot{\mathbf{n}}^{(i)}$ is equal to zero because these vectors lie in the plane that is tangent to the surfaces. Projections of vectors $\mathbf{v}^{(i)}$ and $\dot{\mathbf{n}}^{(i)}$ are related by the Rodrigues formula. (See app. C.) Thus

$$\begin{bmatrix} \dot{n}_f^{(1)} \\ \dot{n}_h^{(1)} \end{bmatrix} = \begin{bmatrix} -\kappa_f & 0 \\ 0 & -\kappa_h \end{bmatrix} \begin{bmatrix} v_f^{(1)} \\ v_h^{(1)} \end{bmatrix} \quad (13.1.22)$$

$$\begin{bmatrix} \dot{n}_s^{(2)} \\ \dot{n}_q^{(2)} \end{bmatrix} = \begin{bmatrix} -\kappa_s & 0 \\ 0 & -\kappa_q \end{bmatrix} \begin{bmatrix} v_s^{(2)} \\ v_q^{(2)} \end{bmatrix} \quad (13.1.23)$$

Here κ_f and κ_h are the principal curvatures of surface Σ_1 , and κ_s and κ_q are the principal curvatures of surface Σ_2 . We designate the curvature matrices by

$$[K_1] = \begin{bmatrix} -\kappa_f & 0 \\ 0 & -\kappa_h \end{bmatrix} \quad [K_2] = \begin{bmatrix} -\kappa_s & 0 \\ 0 & -\kappa_q \end{bmatrix} \quad (13.1.24)$$

Matrices

$$[L_{ba}] = \begin{bmatrix} \cos \sigma & \sin \sigma \\ -\sin \sigma & \cos \sigma \end{bmatrix} \quad (13.1.25)$$

and

$$[L_{ab}] = \begin{bmatrix} \cos \sigma & -\sin \sigma \\ \sin \sigma & \cos \sigma \end{bmatrix} \quad (13.1.26)$$

represent the transformation from $S_a(\mathbf{e}_f, \mathbf{e}_h)$ to $S_b(\mathbf{e}_s, \mathbf{e}_q)$ and from $S_b(\mathbf{e}_s, \mathbf{e}_q)$ to $S_a(\mathbf{e}_f, \mathbf{e}_h)$, respectively (fig. 13.1.1).

Equations (13.1.9), (13.1.10), (13.1.19), (13.1.22), (13.1.23), (13.1.25), and (13.1.26) yield a system of three linear equations

$$a_{i1} v_s^{(1)} + a_{i2} v_q^{(1)} = a_{i3} \quad (i = 1, 2, 3) \quad (13.1.27)$$

in two unknowns $v_s^{(1)}$ and $v_q^{(1)}$.

Since equations (13.1.27) are represented in unknowns $v_s^{(1)}$ and $v_q^{(1)}$ instead of unknowns $v_f^{(1)}$ and $v_h^{(1)}$, we are able to obtain a symmetric augmented matrix $[A]$ such as

$$[A] = \begin{bmatrix} a_{11} & a_{12} & a_{13} \\ a_{12} & a_{22} & a_{23} \\ a_{13} & a_{23} & a_{33} \end{bmatrix} \quad (13.1.28)$$

This is the particular advantage of such a presentation.

Let us derive matrix (13.1.28). The matrix representations of equations (13.1.9) and (13.1.10) are given by

$$\begin{bmatrix} v_s^{(2)} \\ v_q^{(2)} \end{bmatrix} = \begin{bmatrix} v_s^{(1)} \\ v_q^{(1)} \end{bmatrix} + \begin{bmatrix} v_s^{(12)} \\ v_q^{(12)} \end{bmatrix} \quad (13.1.29)$$

$$\begin{bmatrix} \dot{n}_s^{(2)} \\ \dot{n}_q^{(2)} \end{bmatrix} = \begin{bmatrix} \dot{n}_s^{(1)} \\ \dot{n}_q^{(1)} \end{bmatrix} + \begin{bmatrix} (\boldsymbol{\omega}^{(12)} \times \mathbf{n}) \cdot \mathbf{e}_s \\ (\boldsymbol{\omega}^{(12)} \times \mathbf{n}) \cdot \mathbf{e}_q \end{bmatrix} \quad (13.1.30)$$

Vectors of equations (13.1.9) and (13.1.10) are expressed in terms of their projections on the axes of the coordinate system $\mathcal{S}_b(\mathbf{e}_s, \mathbf{e}_q)$.

Equations (13.1.23), (13.1.24), and (13.1.30) result in

$$[K_2] \begin{bmatrix} v_s^{(2)} \\ v_q^{(2)} \end{bmatrix} = \begin{bmatrix} \dot{n}_s^{(1)} \\ \dot{n}_q^{(1)} \end{bmatrix} + \begin{bmatrix} (\boldsymbol{\omega}^{(12)} \times \mathbf{n}) \cdot \mathbf{e}_s \\ (\boldsymbol{\omega}^{(12)} \times \mathbf{n}) \cdot \mathbf{e}_q \end{bmatrix} \quad (13.1.31)$$

Take into account that

$$\begin{bmatrix} \dot{n}_s^{(1)} \\ \dot{n}_q^{(1)} \end{bmatrix} = [L_{ba}] \begin{bmatrix} \dot{n}_f^{(1)} \\ \dot{n}_h^{(1)} \end{bmatrix} = [L_{ba}][K_1] \begin{bmatrix} v_f^{(1)} \\ v_h^{(1)} \end{bmatrix} = [L_{ba}][K_1][L_{ab}] \begin{bmatrix} v_s^{(1)} \\ v_q^{(1)} \end{bmatrix} \quad (13.1.32)$$

Equations (13.1.31), (13.1.32), and (13.1.29) yield

$$[K_2] \begin{bmatrix} v_s^{(1)} \\ v_q^{(1)} \end{bmatrix} + [K_2] \begin{bmatrix} v_s^{(12)} \\ v_q^{(12)} \end{bmatrix} = [L_{ba}][K_1][L_{ab}] \begin{bmatrix} v_s^{(1)} \\ v_q^{(1)} \end{bmatrix} + \begin{bmatrix} (\boldsymbol{\omega}^{(12)} \times \mathbf{n}) \cdot \mathbf{e}_s \\ (\boldsymbol{\omega}^{(12)} \times \mathbf{n}) \cdot \mathbf{e}_q \end{bmatrix} \quad (13.1.33)$$

The following equation results from equation (12.3.33):

$$\{[L_{ba}][K_1][L_{ab}] - [K_2]\} \begin{bmatrix} v_s^{(1)} \\ v_q^{(1)} \end{bmatrix} = [K_2] \begin{bmatrix} v_s^{(12)} \\ v_q^{(12)} \end{bmatrix} - \begin{bmatrix} (\boldsymbol{\omega}^{(12)} \times \mathbf{n}) \cdot \mathbf{e}_s \\ (\boldsymbol{\omega}^{(12)} \times \mathbf{n}) \cdot \mathbf{e}_q \end{bmatrix} \quad (13.1.34(a))$$

We may represent equation (13.1.34(a)) as follows:

$$\begin{bmatrix} a_{11} & a_{12} \\ a_{21} & a_{22} \end{bmatrix} \begin{bmatrix} v_s^{(1)} \\ v_q^{(1)} \end{bmatrix} = \begin{bmatrix} a_{13} \\ a_{23} \end{bmatrix} \quad (13.1.34(b))$$

Matrix equation (13.1.34(b)) is the matrix representation of a system of two linear equations in two unknowns. Here

$$\begin{aligned} \begin{bmatrix} a_{11} & a_{12} \\ a_{21} & a_{22} \end{bmatrix} &= [L_{ba}][K_1][L_{ab}] - [K_2] \\ &= \begin{bmatrix} \cos \sigma & \sin \sigma \\ -\sin \sigma & \cos \sigma \end{bmatrix} \begin{bmatrix} -\kappa_f & 0 \\ 0 & -\kappa_h \end{bmatrix} \begin{bmatrix} \cos \sigma & -\sin \sigma \\ \sin \sigma & \cos \sigma \end{bmatrix} - \begin{bmatrix} -\kappa_s & 0 \\ 0 & -\kappa_q \end{bmatrix} \end{aligned} \quad (13.1.35)$$

$$\begin{bmatrix} a_{13} \\ a_{23} \end{bmatrix} = [K_2] \begin{bmatrix} v_s^{(12)} \\ v_q^{(12)} \end{bmatrix} - \begin{bmatrix} (\boldsymbol{\omega}^{(12)} \times \mathbf{n}) \cdot \mathbf{e}_s \\ (\boldsymbol{\omega}^{(12)} \times \mathbf{n}) \cdot \mathbf{e}_q \end{bmatrix} \quad (13.1.36)$$

Let us now transform equation (13.1.19). Taking the superscript index $i = 2$, we represent the scalar products in this equation as follows:

$$\dot{\mathbf{n}}_r^{(2)} \cdot \mathbf{v}^{(12)} = \begin{bmatrix} v_s^{(12)} \\ v_q^{(12)} \end{bmatrix}^T \begin{bmatrix} \dot{n}_s^{(2)} \\ \dot{n}_q^{(2)} \end{bmatrix} \quad (13.1.37)$$

$$-\mathbf{v}_r^{(2)} \cdot (\boldsymbol{\omega}^{(12)} \times \mathbf{n}) = \mathbf{v}_r^{(2)} (\mathbf{n} \times \boldsymbol{\omega}^{(12)}) = \begin{bmatrix} (\mathbf{n} \times \boldsymbol{\omega}^{(12)}) \cdot \mathbf{e}_s \\ (\mathbf{n} \times \boldsymbol{\omega}^{(12)}) \cdot \mathbf{e}_q \end{bmatrix}^T \begin{bmatrix} v_s^{(2)} \\ v_q^{(2)} \end{bmatrix} \quad (13.1.38)$$

The superscript T indicates a transposed matrix. (See app. A.)

Equations (13.1.37) and (13.1.23) yield

$$\dot{\mathbf{n}}_r^{(2)} \cdot \mathbf{v}^{(12)} = \begin{bmatrix} v_s^{(12)} \\ v_q^{(12)} \end{bmatrix}^T [K_2] \begin{bmatrix} v_s^{(2)} \\ v_q^{(2)} \end{bmatrix} \quad (13.1.39)$$

Transform equations (13.1.38) and (13.1.39) by substituting matrix

$$\begin{bmatrix} v_s^{(2)} \\ v_q^{(2)} \end{bmatrix}$$

by its expression (13.1.29). Then we obtain

$$\dot{\mathbf{n}}_r^{(2)} \cdot \mathbf{v}^{(12)} = \begin{bmatrix} v_s^{(12)} \\ v_q^{(12)} \end{bmatrix}^T [K_2] \begin{bmatrix} v_s^{(1)} \\ v_q^{(1)} \end{bmatrix} + \begin{bmatrix} v_s^{(12)} \\ v_q^{(12)} \end{bmatrix}^T [K_2] \begin{bmatrix} v_s^{(12)} \\ v_q^{(12)} \end{bmatrix} \quad (13.1.40)$$

$$\begin{aligned} -\mathbf{v}_r^{(2)} \cdot (\boldsymbol{\omega}^{(12)} \times \mathbf{n}) &= \begin{bmatrix} (\mathbf{n} \times \boldsymbol{\omega}^{(12)}) \cdot \mathbf{e}_s \\ (\mathbf{n} \times \boldsymbol{\omega}^{(12)}) \cdot \mathbf{e}_q \end{bmatrix}^T \begin{bmatrix} v_s^{(1)} \\ v_q^{(1)} \end{bmatrix} + \begin{bmatrix} (\mathbf{n} \times \boldsymbol{\omega}^{(12)}) \cdot \mathbf{e}_s \\ (\mathbf{n} \times \boldsymbol{\omega}^{(12)}) \cdot \mathbf{e}_q \end{bmatrix}^T \begin{bmatrix} v_s^{(12)} \\ v_q^{(12)} \end{bmatrix} \\ &= \begin{bmatrix} (\mathbf{n} \times \boldsymbol{\omega}^{(12)}) \cdot \mathbf{e}_s \\ (\mathbf{n} \times \boldsymbol{\omega}^{(12)}) \cdot \mathbf{e}_q \end{bmatrix}^T \begin{bmatrix} v_s^{(1)} \\ v_q^{(1)} \end{bmatrix} + [\mathbf{n} \boldsymbol{\omega}^{(12)} \mathbf{v}^{(12)}] \end{aligned} \quad (13.1.41)$$

Equations (13.1.19), (13.1.40), and (13.1.41) yield

$$\begin{aligned} \left\{ \begin{bmatrix} v_s^{(12)} \\ v_q^{(12)} \end{bmatrix}^T [K_2] + \begin{bmatrix} (\mathbf{n} \times \boldsymbol{\omega}^{(12)}) \cdot \mathbf{e}_s \\ (\mathbf{n} \times \boldsymbol{\omega}^{(12)}) \cdot \mathbf{e}_q \end{bmatrix}^T \right\} \begin{bmatrix} v_s^{(1)} \\ v_q^{(1)} \end{bmatrix} &= - \begin{bmatrix} v_s^{(12)} \\ v_q^{(12)} \end{bmatrix}^T [K_2] \begin{bmatrix} v_s^{(12)} \\ v_q^{(12)} \end{bmatrix} \\ &\quad - [\mathbf{n} \boldsymbol{\omega}^{(12)} \mathbf{v}^{(12)}] - \mathbf{n} \cdot [(\boldsymbol{\omega}^{(1)} \times \mathbf{v}_{tr}^{(2)}) - (\boldsymbol{\omega}^{(2)} \times \mathbf{v}_{tr}^{(1)})] \\ &\quad + \left\{ [(\boldsymbol{\omega}^{(1)})^2 m'_{21} (\mathbf{n} \times \mathbf{k}_2)] \cdot (\mathbf{r} - \mathbf{R}) \right\} \end{aligned} \quad (13.1.42)$$

This equation may be represented by

$$\begin{bmatrix} a_{31} \\ a_{32} \end{bmatrix}^T \begin{bmatrix} v_s^{(1)} \\ v_q^{(1)} \end{bmatrix} = a_{33} \quad (13.1.43)$$

Here

$$\begin{bmatrix} a_{31} \\ a_{32} \end{bmatrix}^T = \begin{bmatrix} v_s^{(12)} \\ v_q^{(12)} \end{bmatrix}^T [K_2] + \begin{bmatrix} (\mathbf{n} \times \boldsymbol{\omega}^{(12)}) \cdot \mathbf{e}_s \\ (\mathbf{n} \times \boldsymbol{\omega}^{(12)}) \cdot \mathbf{e}_q \end{bmatrix}^T$$

The coefficient a_{33} is represented by the right side of equation (13.1.42).

The final expressions for the coefficients a_{i1} , a_{i2} , and a_{i3} ($i = 1, 2, 3$) of equations (13.1.27) (for the elements of the augmented matrix (13.1.28)) are as follows:

$$\begin{aligned}
a_{11} &= \kappa_s - \kappa_f \cos^2 \sigma - \kappa_h \sin^2 \sigma = \kappa_s - \frac{\kappa_f + \kappa_h}{2} - \frac{\kappa_f - \kappa_h}{2} \cos 2\sigma \\
a_{12} &= a_{21} = \frac{\kappa_f - \kappa_h}{2} \sin 2\sigma \\
a_{13} &= a_{31} = -\kappa_s v_s^{(12)} - \left[\boldsymbol{\omega}^{(12)} \mathbf{n} \mathbf{e}_s \right] \\
a_{22} &= \kappa_q - \kappa_f \sin^2 \sigma - \kappa_h \cos^2 \sigma = \kappa_q - \frac{\kappa_f + \kappa_h}{2} + \frac{\kappa_f - \kappa_h}{2} \cos 2\sigma \quad (13.1.44) \\
a_{23} &= a_{32} = -\kappa_q v_q^{(12)} - \left[\boldsymbol{\omega}^{(12)} \mathbf{n} \mathbf{e}_q \right] \\
a_{33} &= \kappa_s \left(v_s^{(12)} \right)^2 + \kappa_q \left(v_q^{(12)} \right)^2 - \left[\mathbf{n} \boldsymbol{\omega}^{(12)} \mathbf{v}^{(12)} \right] \\
&\quad - \mathbf{n} \cdot \left[\left(\boldsymbol{\omega}^{(1)} \times \mathbf{v}_{ir}^{(2)} \right) - \left(\boldsymbol{\omega}^{(2)} \times \mathbf{v}_{ir}^{(1)} \right) \right] + \left\{ \left[\left(\boldsymbol{\omega}^{(1)} \right)^2 m'_{21} (\mathbf{n} \times \boldsymbol{\kappa}_2) \right] \cdot (\mathbf{r} - \mathbf{R}) \right\}
\end{aligned}$$

Relations Between the Surface Curvatures

Equations (13.1.27) represent a system of three linear equations in two unknowns. Since the number of equations is not equal to the number of unknowns, the system of equations (13.1.27) may possess a solution if certain conditions are observed (see below). We will discuss these conditions for two cases of surface contact, the mating surfaces contacting each other at a line and a single point, respectively.

Consider that the velocity of the contact point in its motion over surface Σ_1 is represented by

$$\mathbf{v}_r^{(1)} = v_s^{(1)} \mathbf{e}_s + v_q^{(1)} \mathbf{e}_q$$

In the case of the line contact of mating surfaces, the direction of $\mathbf{v}_r^{(1)}$ is indefinite (fig. 12.1.1(b)). This yields that equation system (13.1.27) must have an infinite number of solutions for $v_s^{(1)}$ and $v_q^{(1)}$.

It is known from linear algebra that a system of linear equations in two unknowns possesses an infinite number of solutions if the rank of the augmented matrix and the system matrix is equal to one. The augmented matrix $[A]$ is represented by expression (13.1.28). The rank of $[A]$ is equal to one if all determinants of the second order that are formed from the elements of $[A]$ are zero. This yields

$$\frac{a_{11}}{a_{12}} = \frac{a_{12}}{a_{22}} = \frac{a_{13}}{a_{23}} \quad \frac{a_{11}}{a_{13}} = \frac{a_{12}}{a_{23}} = \frac{a_{13}}{a_{33}} \quad \frac{a_{12}}{a_{13}} = \frac{a_{22}}{a_{23}} = \frac{a_{23}}{a_{33}} \quad (13.1.45)$$

Equations (13.1.45) provide relations that may be represented as an equality of the following symmetric matrices:

$$\begin{bmatrix} a_{11} & a_{12} \\ a_{12} & a_{22} \end{bmatrix} = \frac{1}{a_{33}} \begin{bmatrix} a_{13}^2 & a_{13}a_{23} \\ a_{13}a_{23} & a_{23}^2 \end{bmatrix} \quad (13.1.46)$$

Determinants of these matrices are equal to zero.

From equation (13.1.46) we get

$$a_{11} = \frac{a_{13}^2}{a_{33}} \quad a_{12} = \frac{a_{13}a_{23}}{a_{33}} \quad a_{22} = \frac{a_{23}^2}{a_{33}} \quad (13.1.47)$$

Equations (13.1.44) and (13.1.47) yield

$$\tan 2\sigma = \frac{2a_{12}}{a_{22} - a_{11} + \kappa_s - \kappa_q} \quad (13.1.48)$$

$$\kappa_f - \kappa_h = \frac{2a_{12}}{\sin 2\sigma} = \frac{a_{22} - a_{11} + \kappa_s - \kappa_q}{\cos 2\sigma} \quad (13.1.49)$$

$$\kappa_f + \kappa_h = \kappa_s + \kappa_q - a_{11} - a_{22} \quad (13.1.50)$$

Substituting in equations (13.1.48) to (13.1.50) coefficients a_{11} , a_{12} , and a_{22} , which are given by expressions (13.1.47), we determine the desired relations between the principal curvatures and directions of the two mating surfaces. This yields

$$\tan 2\sigma = \frac{2a_{13}a_{23}}{a_{23}^2 - a_{13}^2 + (\kappa_s - \kappa_q)a_{33}} \quad (13.1.51)$$

$$\kappa_f - \kappa_h = \frac{2a_{13}a_{23}}{a_{33} \sin 2\sigma} = \frac{a_{23}^2 - a_{13}^2 + (\kappa_s - \kappa_q)a_{33}}{a_{33} \cos 2\sigma} \quad (13.1.52)$$

$$\kappa_f + \kappa_h = (\kappa_s + \kappa_q) - \frac{a_{13}^2 + a_{23}^2}{a_{33}} \quad (13.1.53)$$

Equations (13.1.51) to (13.1.53) express the principal curvatures κ_f , κ_h , and σ in terms of the known principal curvatures κ_s and κ_q and coefficients a_{13} , a_{23} , and a_{33} , that depend on the given principal curvatures (κ_s and κ_q) and the parameters of motion. (See eq. (13.1.44).) With these equations we may determine the principal curvatures and directions of surface Σ_1 , although equations of this surface are not yet developed.

Let us now consider the case of surfaces that are in point contact. This case is typical for bevel and hypoid gears with localized contact of tooth surfaces. The velocity of the point of contact in its motion over the surface has a definite direction (fig. 12.1.1(a)). Thus the system of linear equations (13.1.27) must possess a unique solution. Since the rank of matrix $[A]$, represented by equation (13.1.28), must be equal to two, we get

$$\begin{vmatrix} a_{11} & a_{12} & a_{13} \\ a_{12} & a_{22} & a_{23} \\ a_{13} & a_{23} & a_{33} \end{vmatrix} = 0 \quad (13.1.54)$$

Thus, there is only one equation

$$F(\kappa_s, \kappa_q, \kappa_f, \kappa_h, \sigma) = 0 \quad (13.1.55)$$

that relates the five parameters. Considering κ_s and κ_q as given, we cannot determine κ_f , κ_h , and σ uniquely. This means that we can synthesize an infinitely large number of the mating surfaces that are in point contact if one of the surfaces is given.

Modified Linear Equations

Consider that principal curvatures κ_f and κ_h of surface Σ_1 are given and κ_s , κ_q , and σ must be determined. In this case it is preferable to use equations

$$b_{i1} v_f^{(2)} + b_{i2} v_h^{(2)} = b_{i3} \quad (i = 1, 2, 3) \quad (13.1.56)$$

instead of system (13.1.27). The coefficients b_{i1} , b_{i2} , and b_{i3} are elements of the symmetric matrix $[B]$ represented by

$$[B] = \begin{bmatrix} b_{11} & b_{12} & b_{13} \\ b_{12} & b_{22} & b_{23} \\ b_{13} & b_{23} & b_{33} \end{bmatrix} \quad (13.1.57)$$

The system of equations (13.1.56), representing equations (13.1.9), (13.1.10), and (13.1.19), are derived as follows:

$$\begin{bmatrix} v_f^{(1)} \\ v_h^{(1)} \end{bmatrix} = \begin{bmatrix} v_f^{(2)} \\ v_h^{(2)} \end{bmatrix} - \begin{bmatrix} v_f^{(12)} \\ v_h^{(12)} \end{bmatrix} \quad (13.1.58)$$

$$[K_1] \begin{bmatrix} v_f^{(1)} \\ v_h^{(1)} \end{bmatrix} = [L_{ab}][K_2][L_{ba}] \begin{bmatrix} v_f^{(2)} \\ v_h^{(2)} \end{bmatrix} - \begin{bmatrix} (\boldsymbol{\omega}^{(12)} \times \mathbf{n}) \cdot \mathbf{e}_f \\ (\boldsymbol{\omega}^{(12)} \times \mathbf{n}) \cdot \mathbf{e}_h \end{bmatrix} \quad (13.1.59)$$

$$\begin{aligned} \begin{bmatrix} v_f^{(12)} \\ v_h^{(12)} \end{bmatrix}^T [K_1] \left\{ \begin{bmatrix} v_f^{(2)} \\ v_h^{(2)} \end{bmatrix} - \begin{bmatrix} v_f^{(12)} \\ v_h^{(12)} \end{bmatrix} \right\} + \begin{bmatrix} (\mathbf{n} \times \boldsymbol{\omega}^{(12)}) \cdot \mathbf{e}_f \\ (\mathbf{n} \times \boldsymbol{\omega}^{(12)}) \cdot \mathbf{e}_h \end{bmatrix}^T \begin{bmatrix} v_f^{(2)} \\ v_h^{(2)} \end{bmatrix} \\ - \left[\mathbf{n} \boldsymbol{\omega}^{(12)} \mathbf{v}^{(12)} \right] + \mathbf{n} \cdot \left[(\boldsymbol{\omega}^{(1)} \times \mathbf{v}_{ir}^{(2)}) - (\boldsymbol{\omega}^{(2)} \times \mathbf{v}_{ir}^{(1)}) \right] \\ + (\boldsymbol{\omega}^{(1)})^2 m_2' \mathbf{n} \cdot \left[\mathbf{k}_2 \times (\mathbf{r}^{(1)} - \mathbf{R}) \right] = 0 \end{aligned} \quad (13.1.60)$$

Equation (13.1.60) was derived from equation (13.1.19) by taking $i = 1$ in the expressions for $\dot{\mathbf{n}}_r^{(i)}$ and $\mathbf{v}_r^{(i)}$.

Equations (13.1.58) and (13.1.59), after elimination of $v_f^{(1)}$ and $v_h^{(1)}$, yield the following two linear equations in unknowns $v_f^{(2)}$ and $v_h^{(2)}$:

$$\begin{bmatrix} b_{11} & b_{12} \\ b_{12} & b_{22} \end{bmatrix} \begin{bmatrix} v_f^{(2)} \\ v_h^{(2)} \end{bmatrix} = \begin{bmatrix} b_{13} \\ b_{23} \end{bmatrix} \quad (13.1.61)$$

Here

$$\begin{bmatrix} b_{11} & b_{12} \\ b_{12} & b_{22} \end{bmatrix} = [K_1] - [L_{ab}][K_2][L_{ba}] \quad (13.1.62)$$

$$\begin{bmatrix} b_{13} \\ b_{23} \end{bmatrix} = \begin{bmatrix} (\mathbf{n} \times \boldsymbol{\omega}^{(12)}) \cdot \mathbf{e}_f \\ (\mathbf{n} \times \boldsymbol{\omega}^{(12)}) \cdot \mathbf{e}_h \end{bmatrix} + [K_1] \begin{bmatrix} v_f^{(12)} \\ v_h^{(12)} \end{bmatrix} \quad (13.1.63)$$

Equation (13.1.60) yields the third linear equation

$$b_{13}v_f^{(2)} + b_{23}v_h^{(2)} = b_{33} \quad (13.1.64)$$

Here

$$\begin{aligned} b_{33} = & -\mathbf{n} \cdot \left[(\boldsymbol{\omega}^{(1)} \times \mathbf{v}_{ir}^{(2)}) - (\boldsymbol{\omega}^{(2)} \times \mathbf{v}_{ir}^{(1)}) \right] + (\omega^{(1)})^2 m'_{21} (\mathbf{n} \times \mathbf{k}_2) \cdot (\mathbf{r}^{(1)} - \mathbf{R}) \\ & + \left[\mathbf{n} \boldsymbol{\omega}^{(12)} \mathbf{v}^{(12)} \right] + \begin{bmatrix} v_f^{(12)} \\ v_h^{(12)} \end{bmatrix}^T [K_1] \begin{bmatrix} v_f^{(12)} \\ v_h^{(12)} \end{bmatrix} \end{aligned} \quad (13.1.65)$$

In the case of line contact of surfaces, the elements of matrix (13.1.57) are related by equations which are similar to equations (13.1.45) and (13.1.46). These relations may be represented by the following matrix equation:

$$\begin{bmatrix} b_{11} & b_{12} \\ b_{12} & b_{22} \end{bmatrix} = \frac{1}{b_{33}} \begin{bmatrix} b_{13}^2 & b_{13}b_{23} \\ b_{13}b_{23} & b_{23}^2 \end{bmatrix} \quad (13.1.66)$$

Matrices (13.1.66) are symmetric and their determinants are equal to zero.

Derivations similar to those discussed above yield the following relations between the principal curvatures and directions of the two mating surfaces:

$$\tan 2\sigma = \frac{2b_{13}b_{23}}{b_{23}^2 - b_{13}^2 - (\kappa_f - \kappa_h)b_{33}} \quad (13.1.67)$$

$$\kappa_q - \kappa_s = \frac{2b_{13}b_{23}}{b_{33} \sin 2\sigma} = \frac{b_{23}^2 - b_{13}^2 - (\kappa_f - \kappa_h)b_{33}}{b_{33} \cos 2\sigma} \quad (13.1.68)$$

$$\kappa_q + \kappa_s = \kappa_f + \kappa_h + \frac{b_{13}^2 + b_{23}^2}{b_{33}} \quad (13.1.69)$$

Equations (13.1.67) to (13.1.69) determine the principal curvatures κ_s and κ_q and the principal directions of surface Σ_2 in terms of the principal curvatures κ_f , κ_h of surface Σ_1 and the parameters of motion.

In the case of point contact, there is only one relation represented by the equation

$$\psi(\kappa_s, \kappa_q, \kappa_f, \kappa_h, \sigma) = 0 \quad (13.1.70)$$

which is provided by the requirement

$$\begin{vmatrix} b_{11} & b_{12} & b_{13} \\ b_{12} & b_{22} & b_{23} \\ b_{13} & b_{23} & b_{33} \end{vmatrix} = 0 \quad (13.1.71)$$

Example Problem 13.1.1. Consider that a rack generates a helical gear (examples 9.8.1 and 9.3.1). Derive equations of the principal curvatures κ_s and κ_q and principal directions of surface Σ_2 of the helical gear. For the solution, use equations (13.1.67) to (13.1.69) and consider the following as given: (1) the principal curvatures and directions of surface Σ_1 , (2) the surface of action, (3) the unit normal to surface Σ_1 , (4) the location of a contact point on the surface of action, and (5) parameters of motion $\mathbf{v}^{(12)}$, $\mathbf{v}_{ir}^{(1)}$, $\mathbf{v}_{ir}^{(2)}$, $\boldsymbol{\omega}^{(1)}$, and $\boldsymbol{\omega}^{(2)}$.

Solution. The surface of action was represented by equations (9.8.61) as follows (the subscript f is dropped):

$$\left. \begin{aligned} x &= u \cos \psi_t & y &= u \sin \psi_t + \ell \sin \beta + r\phi & z &= \ell \cos \beta \\ \cos \beta [\sin \psi_t (r\phi + \ell \sin \beta) + u] &= 0 \end{aligned} \right\} \quad (13.1.72)$$

Consider that the family of surfaces Σ_1 is represented in the coordinate system S_f by the equation

$$\mathbf{r}(u, \ell, \phi) \in C^2 \quad (u, \ell) \in E \quad a < \phi < b \quad \mathbf{r}_u \times \mathbf{r}_\ell \neq 0$$

Here u and ℓ are the surface coordinates and ϕ is the parameter of motion. The unit normal to Σ_1 may be determined by

$$\mathbf{n} = \frac{\mathbf{N}}{|\mathbf{N}|} \quad \mathbf{N} = \mathbf{r}_u \times \mathbf{r}_\ell \quad (13.1.73)$$

After certain transformations, we get

$$N_x = \sin \psi_t \cos \beta \quad N_y = -\cos \psi_t \cos \beta \quad N_z = \cos \psi_t \sin \beta \quad (13.1.74)$$

We use the following relations between the gearing parameters (example 9.3.1):

$$\tan \psi_t = \frac{\tan \psi_n}{\cos \beta} \quad (13.1.75)$$

$$\cos \psi_t = \cos \psi_n \frac{\cos \beta}{\cos \beta_0} = \frac{\tan \beta_0}{\tan \beta} \quad (13.1.76)$$

$$\sin \psi_t = \frac{\sin \psi_n}{\cos \beta_0} \quad (13.1.77)$$

Here ψ_t is the pressure angle in the cross section, ψ_n is the pressure angle in the normal section (fig. 9.3.3), β is the angle formed between the gear axis and the tangent to the helix on the pitch cylinder, and β_0 is the angle formed between the gear axis and the tangent to the helix on the base cylinder.

The derivation of equations (13.1.76) to (13.1.77) is based on the following considerations:
Step 1.—Let

$$\frac{H}{2\pi r} = \cot \beta \quad \frac{H}{2\pi r_0} = \cot \beta_0 \quad r_0 = r \cos \psi_t$$

where r and r_0 are the radii of the pitch and base cylinders and H is the lead of the helices. These equations yield

$$\cos \psi_t = \frac{\tan \beta_0}{\tan \beta} \quad (i)$$

Thus, one of equations (13.1.76) is confirmed.

Step 2.—Using equations (13.1.75) and (i), we get

$$\frac{1}{\cos^2 \psi_t} = 1 + \tan^2 \psi_t = 1 + \frac{\tan^2 \psi_n}{\cos^2 \beta} = \frac{1 + \tan^2 \psi_n - \sin^2 \beta}{\cos^2 \beta} \quad \frac{1}{\cos^2 \psi_t} = \frac{\tan^2 \beta}{\tan^2 \beta_0}$$

The equation

$$\frac{\tan^2 \beta}{\tan^2 \beta_0} = \frac{1 + \tan^2 \psi_n - \sin^2 \beta}{\cos^2 \beta}$$

yields

$$\cos \psi_n = \frac{\sin \beta_0}{\sin \beta} \quad (ii)$$

Then using equations (ii), (13.1.75), and (13.1.76), we obtain

$$\sin \psi_n = \cos \psi_n \tan \psi_n = \frac{\sin \beta_0 \tan \psi_t}{\tan \beta} \quad \frac{\sin \beta_0 \sin \psi_t}{\tan \beta \cos \psi_t} = \sin \psi_t \cos \beta_0$$

Thus

$$\sin \psi_t = \frac{\sin \psi_n}{\cos \beta_0} \quad (iii)$$

and equation (13.1.77) is confirmed.

(3) Equations (iii), and (13.1.75) yield

$$\cos \psi_t = \frac{\sin \psi_t}{\tan \psi_t} = \frac{\cos \beta_0 \sin \psi_t}{\cos \beta_0 \tan \psi_t} = \frac{\sin \psi_n \cos \beta}{\cos \beta_0 \tan \psi_n} = \cos \psi_n \frac{\cos \beta}{\cos \beta_0} \quad (iv)$$

Thus the second one of equations (13.1.76) is confirmed.

We may now derive equations of the surface unit normal by using equations (13.1.74) to (13.1.77) as follows:

$$n_x = \sin \psi_t \cos \beta_0 \quad n_y = -\cos \psi_t \cos \beta_0 \quad n_z = \sin \beta_0 \quad (13.1.78)$$

We will also need the equations for $\mathbf{v}_{ir}^{(1)}$, $\mathbf{v}_{ir}^{(2)}$, $\mathbf{v}^{(12)}$, and $\boldsymbol{\omega}^{(12)}$, which are represented in the coordinate system \mathcal{S}_f (fig. 9.3.2). Since $\boldsymbol{\omega}^{(1)} = 0$, we have

$$\boldsymbol{\omega}^{(12)} = \boldsymbol{\omega}^{(1)} - \boldsymbol{\omega}^{(2)} = -\boldsymbol{\omega} \mathbf{k}_f \quad (13.1.79)$$

where $\boldsymbol{\omega} \equiv \boldsymbol{\omega}^{(2)}$. (The motion of the rack is translation.) The rack translates parallel to the y_f -axis (fig. 9.3.2), and

$$\mathbf{v}_{ir}^{(1)} = \omega r \mathbf{j}_f \quad (13.1.80)$$

The gear rotates about O_2 and

$$\begin{aligned} \mathbf{v}_{ir}^{(2)} &= \boldsymbol{\omega} \times \mathbf{r}^{(1)} + \overline{O_f O_2} \times \boldsymbol{\omega} \\ &= \begin{vmatrix} \mathbf{i}_f & \mathbf{j}_f & \mathbf{k}_f \\ 0 & 0 & \omega \\ x & y & z \end{vmatrix} + \begin{vmatrix} \mathbf{i}_f & \mathbf{j}_f & \mathbf{k}_f \\ -r & 0 & 0 \\ 0 & 0 & \omega \end{vmatrix} = \omega[-y\mathbf{i}_f + (x+r)\mathbf{j}_f] \end{aligned} \quad (13.1.81)$$

The velocity of sliding is given by

$$\mathbf{v}^{(12)} = \mathbf{v}_{ir}^{(1)} - \mathbf{v}_{ir}^{(2)} = \omega(y\mathbf{i}_f - x\mathbf{j}_f) \quad (13.1.82)$$

Here x , y , and z are the coordinates of the contact point represented by equations (13.1.2).

Now, let the trihedron $\mathcal{S}_a(\mathbf{e}_f, \mathbf{e}_h, \mathbf{n})$ be set up such that \mathbf{e}_f and \mathbf{e}_h (fig. 13.1.1) represent the principal directions of surface Σ_1 . Since Σ_1 is a plane, its principal directions κ_f and κ_h are zero, and any pair of two perpendicular lines on the plane Σ_1 may be chosen as principal directions. It is preferable to choose, for the principal direction of the rack, the line of contact of surface Σ_1 and Σ_2 . The line of contact on surface $\Sigma_1(T)$ may be determined by equations (13.1.72) with $\phi = \text{constant}$. Differentiating the fourth equation of equation system (13.1.72), we derive the following relation between the derivatives du/dt and $d\ell/dt$

$$\sin \psi_t \sin \beta d\ell + du = 0 \quad (13.1.83)$$

The tangent to the contact line is given by

$$\mathbf{T} = \left(\cos \psi_t \mathbf{i}_f - \frac{\cos^2 \psi_t}{\sin \psi_t} \mathbf{j}_f - \frac{\cot \beta}{\sin \psi_t} \mathbf{k}_f \right) du \quad (13.1.84)$$

The unit vector \mathbf{e}_f is given by

$$\mathbf{e}_f = \frac{\mathbf{T}}{|\mathbf{T}|} = \frac{1}{\sqrt{\cos^2 \psi_t + \cot^2 \beta}} \left(\cos \psi_t \mathbf{i}_f - \cos^2 \psi_t \mathbf{j}_f - \cot \beta \mathbf{k}_f \right) \quad (13.1.85)$$

Equations (13.1.85) and (13.1.76) yield

$$\mathbf{e}_f = \sin \psi_t \sin \beta_0 \mathbf{i}_f - \cos \psi_t \sin \beta_0 \mathbf{j}_f - \cos \beta_0 \mathbf{k}_f \quad (13.1.86)$$

The unit vector \mathbf{e}_h is determined by the equation

$$\mathbf{e}_h = \mathbf{n} \times \mathbf{e}_f = \begin{vmatrix} \mathbf{i}_f & \mathbf{j}_f & \mathbf{k}_f \\ \sin \psi_t \cos \beta_0 & -\cos \psi_t \cos \beta_0 & \sin \beta_0 \\ \sin \psi_t \sin \beta_0 & -\cos \psi_t \sin \beta_0 & -\cos \beta_0 \end{vmatrix} = \cos \psi_t \mathbf{i}_f + \sin \psi_t \mathbf{j}_f \quad (13.1.87)$$

The sought for principal curvatures and directions of surface Σ_2 are determined by equations (13.1.67) to (13.1.69), for which coefficients b_{13} , b_{23} , and b_{33} are represented by equations (13.1.63) and (13.1.65). Considering that $[K_1] = 0$ (Σ_1 is a plane) and $m'_{21} = 0$, because m_{21} is constant, we get

$$b_{13} = [\mathbf{n}\boldsymbol{\omega}^{(12)}\mathbf{e}_f] = 0 \quad (13.1.88)$$

$$b_{23} = [\mathbf{n}\boldsymbol{\omega}^{(12)}\mathbf{e}_h] = \omega \cos \beta_0 \quad (13.1.89)$$

$$\begin{aligned} b_{33} &= -\mathbf{n} \cdot \left[\left(\boldsymbol{\omega}^{(1)} \times \mathbf{v}_{ir}^{(2)} \right) - \left(\boldsymbol{\omega}^{(2)} \times \mathbf{v}_{ir}^{(1)} \right) \right] + \mathbf{n} \cdot \left(\boldsymbol{\omega}^{(12)} \times \mathbf{v}^{(12)} \right) \\ &= \mathbf{n} \cdot \left[\left(\boldsymbol{\omega}^{(2)} \times \mathbf{v}_{ir}^{(1)} \right) - \left(\boldsymbol{\omega}^{(2)} \times \mathbf{v}^{(12)} \right) \right] = \mathbf{n} \cdot \left(\boldsymbol{\omega}^{(2)} \times \mathbf{v}_{ir}^{(2)} \right) \\ &= -\omega^2 \cos \beta_0 \left[(x+r) \sin \psi_t - y \cos \psi_t \right] \end{aligned} \quad (13.1.90)$$

Substituting in equation (13.1.90) the expressions (13.1.72) for x and y we get

$$b_{33} = -\omega^2 \cos \beta_0 \left(r \sin \psi_t + \frac{u}{\tan \psi_t} \right) \quad (13.1.91)$$

Equations (13.1.67) to (13.1.69), (13.1.88), (13.1.89), and (13.1.91) yield

$$\sigma = 0 \quad \kappa_s = 0 \quad \kappa_q = -\frac{\cos \beta_0}{r \sin \psi_t + u \cot \psi_t} \quad (13.1.92)$$

From equations (13.1.92), we find that one of the principal directions of a helical gear coincides with the line of contact, and the principal curvature along this direction is equal to zero. The negative sign of κ_q indicates that the radius of curvature is directed opposite to that of the normal to the rack.

An alternative way for the determination of the principal curvatures and directions of a helical gear is based on the application of equations of the gear-tooth surface (it is a screw involute surface). The reason the method discussed in chapter 13.1 is applied in this example is to illustrate the power of this method. The advantage of the method is the fact that it is especially effective for the cases when the surface of the generated gear is described by complicated equations (with three surface coordinates related by the equation of meshing). This is typical for surfaces of bevel gears, hypoid gears, and worm gears.

13.2 Contact Point Path as a Local Geodetic Curve

Introduction

Consider two gear-tooth surfaces that are in point contact. The contact point path—the working line of the surface—must be along a definite direction. Figure 13.2.1(a) shows a contact-point path that has the prescribed direction at the main contact point P (at the pitch point), but deviates from this direction at other contact points. We may avoid such deviations, or at least reduce their occurrence if the contact point path is a locally geodetic curve at P (fig. 13.2.1(b)). This means that the projection of the contact point path on the tangent plane is locally a straight line. The above condition may be observed by definite relations between the principal curvatures and directions of mating surfaces (proposed by Litvin and Gutman, 1981). We may determine such relations from conditions that the geodetic curvature of the contact-point path is equal to zero at P .

The geodetic curvature of a curve on surface Σ_i is equal to zero (ch. 10.7) if

$$\kappa_g^{(i)} = \left[\mathbf{a}_r^{(i)} \mathbf{v}_r^{(i)} \mathbf{n}^{(i)} \right] = 0 \quad (i = 1, 2) \quad (13.2.1)$$

where $\mathbf{v}_r^{(i)}$ and $\mathbf{a}_r^{(i)}$ are the velocity and acceleration, respectively, of a point that moves along the curve, and $\mathbf{n}^{(i)}$ is the unit surface normal.

Basic Equations

Consider the contact-point path on surface Σ_2 ($i = 2$). We apply the kinematic relations given by the following equations (ch. 12)

$$\mathbf{v}_r^{(2)} = \mathbf{v}_r^{(1)} + \mathbf{v}^{(12)} \quad (13.2.2)$$

$$\dot{\mathbf{n}}_r^{(2)} = \dot{\mathbf{n}}_r^{(1)} + \boldsymbol{\omega}^{(12)} \times \mathbf{n}^{(1)} \quad (13.2.3)$$

$$\mathbf{a}_r^{(2)} = \mathbf{a}_r^{(1)} + \mathbf{c} \quad (13.2.4)$$

For $\boldsymbol{\omega}^{(1)} = \text{constant}$, \mathbf{c} is represented by (eq. (12.2.8))

$$\mathbf{c} = \left(2\boldsymbol{\omega}^{(12)} \times \mathbf{v}_r^{(1)} \right) + \left(\boldsymbol{\omega}^{(12)} \times \mathbf{v}_{rr}^{(1)} \right) - \left(\boldsymbol{\omega}^{(2)} \times \mathbf{v}^{(12)} \right) - \left[\dot{\boldsymbol{\omega}}^{(2)} \times (\mathbf{r}^{(1)} - \mathbf{R}) \right] \quad (13.2.5)$$

$$\ddot{\mathbf{n}}_r^{(2)} = \ddot{\mathbf{n}}_r^{(1)} + \mathbf{d} \quad (13.2.6)$$

where $\boldsymbol{\omega}^{(1)} = \text{constant}$ and \mathbf{d} is represented as follows:

$$\mathbf{d} = \left(2\boldsymbol{\omega}^{(12)} \times \dot{\mathbf{n}}_r^{(1)} \right) + \boldsymbol{\omega}^{(1)} \left(\boldsymbol{\omega}^{(12)} \cdot \mathbf{n} \right) - \boldsymbol{\omega}^{(12)} \left(\boldsymbol{\omega}^{(2)} \cdot \mathbf{n} \right) - \mathbf{n} \left(\boldsymbol{\omega}^{(12)} \right)^2 - \left(\dot{\boldsymbol{\omega}}^{(2)} \times \mathbf{n} \right) \quad (13.2.7)$$

(See eq. (12.2.11).) The subscript f in the above equations is dropped. To simplify the following expressions, we apply the notations:

$$\mathbf{v}_r^{(i)} = \mathbf{v}^{(i)} \quad \dot{\mathbf{n}}_r^{(i)} = \dot{\mathbf{n}}^{(i)} \quad \mathbf{a}_r^{(i)} = \mathbf{a}^{(i)}$$

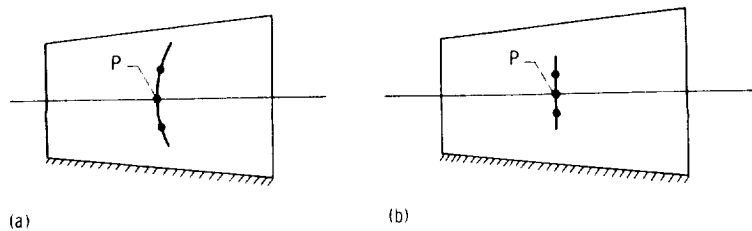


Figure 13.2.1.

Differentiating equations (13.1.22) and (13.1.23), we get

$$\begin{bmatrix} \ddot{n}_f^{(1)} \\ \ddot{n}_h^{(1)} \end{bmatrix} = [K_1] \begin{bmatrix} a_f^{(1)} \\ a_h^{(1)} \end{bmatrix} + [\dot{K}_1] \begin{bmatrix} v_f^{(1)} \\ v_h^{(1)} \end{bmatrix} \quad (13.2.8)$$

$$\begin{bmatrix} \ddot{n}_s^{(2)} \\ \ddot{n}_q^{(2)} \end{bmatrix} = [K_2] \begin{bmatrix} a_s^{(2)} \\ a_q^{(2)} \end{bmatrix} + [\dot{K}_2] \begin{bmatrix} v_s^{(2)} \\ v_q^{(2)} \end{bmatrix} \quad (13.2.9)$$

We substitute the contacting surfaces by two paraboloids. This substitution is equivalent to the representation of surfaces with elements up to the third order. With such limitations we take $[\dot{K}_i] = 0$ where $i = 1, 2$.

Existence of a Locally Geodetic Curve on Surface Σ_2

The contact-point path on surface Σ_2 is a local geodetic curve at the pitch point P , if at point P the following equation is observed

$$[\mathbf{v}_r^{(2)} \mathbf{n}_a^{(2)}] = 0 \quad (13.2.10)$$

It will be proven that this equation provides a linear equation in unknowns $v_f^{(2)}$ and $v_h^{(2)}$ given by

$$b_{41}v_f^{(2)} + b_{42}v_h^{(2)} = b_{43} \quad (13.2.11)$$

where

$$\mathbf{v}_r^{(2)} = v_f^{(2)}\mathbf{i}_f + v_h^{(2)}\mathbf{i}_h \quad (13.2.12)$$

Equation (13.2.11) and the system of equations (13.1.56) represent relations between the principal curvatures and directions of two mating surfaces.

The procedure for the derivation of equation (13.2.11) is as follows:

Step 1.—We derive linear equations in unknowns $a_f^{(2)}$ and $a_h^{(2)}$. To do this we first represent equations (13.2.4) and (13.2.6) as follows:

$$\begin{bmatrix} a_f^{(1)} \\ a_h^{(1)} \end{bmatrix} = \begin{bmatrix} a_f^{(2)} \\ a_h^{(2)} \end{bmatrix} - \begin{bmatrix} c_f \\ c_h \end{bmatrix} \quad (13.2.13)$$

$$\begin{bmatrix} \ddot{n}_f^{(1)} \\ \ddot{n}_h^{(1)} \end{bmatrix} = \begin{bmatrix} \ddot{n}_f^{(2)} \\ \ddot{n}_h^{(2)} \end{bmatrix} - \begin{bmatrix} d_f \\ d_h \end{bmatrix} \quad (13.2.14)$$

From equations (13.2.8), (13.2.9), and (13.2.14), we get

$$\begin{aligned} [K_1] \begin{bmatrix} a_f^{(1)} \\ a_h^{(1)} \end{bmatrix} &= [L_{ab}] \begin{bmatrix} \ddot{n}_s^{(2)} \\ \ddot{n}_q^{(2)} \end{bmatrix} - \begin{bmatrix} d_f \\ d_h \end{bmatrix} = [L_{ab}][K_2] \begin{bmatrix} a_s^{(2)} \\ a_q^{(2)} \end{bmatrix} - \begin{bmatrix} d_f \\ d_h \end{bmatrix} \\ &= [L_{ab}][K_2][L_{ba}] \begin{bmatrix} a_f^{(2)} \\ a_h^{(2)} \end{bmatrix} - \begin{bmatrix} d_f \\ d_h \end{bmatrix} \end{aligned} \quad (13.2.15)$$

Substituting expressions (13.2.13) for $a_f^{(1)}$ and $a_h^{(1)}$ in expression (13.2.15), we obtain the desired system of two linear equations in two unknowns, $a_f^{(2)}$ and $a_h^{(2)}$

$$[Q_2] \begin{bmatrix} a_f^{(2)} \\ a_h^{(2)} \end{bmatrix} = - \begin{bmatrix} d_f \\ d_h \end{bmatrix} + [K_1] \begin{bmatrix} c_f \\ c_h \end{bmatrix} = \begin{bmatrix} u_f \\ u_h \end{bmatrix} \quad (13.2.16)$$

Here

$$[Q_2] = [K_1] - [L_{ab}][K_2][L_{ba}] \quad (13.2.17)$$

is a symmetrical matrix;

$$\begin{bmatrix} u_f \\ u_h \end{bmatrix} = - \begin{bmatrix} d_f \\ d_h \end{bmatrix} + [K_1] \begin{bmatrix} c_f \\ c_h \end{bmatrix} = - \begin{bmatrix} d_f + \kappa_f c_f \\ d_h + \kappa_h c_h \end{bmatrix} \quad (13.2.18)$$

Step 2.—We transform equation system (13.1.61), consisting of two equations in the unknowns $v_f^{(2)}$ and $v_h^{(2)}$, as follows:

$$[Q_2] \begin{bmatrix} v_f^{(2)} \\ v_h^{(2)} \end{bmatrix} = \begin{bmatrix} (\mathbf{n} \times \boldsymbol{\omega}^{(12)}) \cdot \mathbf{e}_f \\ (\mathbf{n} \times \boldsymbol{\omega}^{(12)}) \cdot \mathbf{e}_h \end{bmatrix} + [K_1] \begin{bmatrix} v_f^{(12)} \\ v_h^{(12)} \end{bmatrix} = \begin{bmatrix} b_{13} \\ b_{23} \end{bmatrix} = \begin{bmatrix} m_f \\ m_h \end{bmatrix} \quad (13.2.19)$$

Here, m is the notation of a vector represented by

$$\mathbf{m} = m_f \mathbf{e}_f + m_h \mathbf{e}_h = b_{13} \mathbf{e}_f + b_{23} \mathbf{e}_h$$

Step 3.—Let us prove that equation (13.2.10) yields

$$\begin{bmatrix} v_f^{(2)} \\ v_h^{(2)} \end{bmatrix}^T \begin{bmatrix} 0 & -1 \\ 1 & 0 \end{bmatrix} \begin{bmatrix} a_f^{(2)} \\ a_h^{(2)} \end{bmatrix} = 0 \quad (13.2.20)$$

The proof is based on the following considerations:

(1) Equation (13.2.10) may be represented in matrix form as

$$\begin{bmatrix} \mathbf{v}_r^{(2)} \mathbf{n} a_r^{(2)} \end{bmatrix} = \begin{bmatrix} v_r^{(2)} \end{bmatrix}^T [n]^s \begin{bmatrix} a_r^{(2)} \end{bmatrix} = 0$$

Here superscripts T and s designate a transposed and skew-symmetric matrix, respectively (app. A). Equation (13.2.10) is satisfied because vectors \mathbf{n} and $\mathbf{a}_r^{(2)}$ are collinear, that is, $\mathbf{a}_r^{(2)} = \lambda \mathbf{n}$.

(2) We may represent vectors $\mathbf{v}_r^{(2)}$, \mathbf{n} , and $\mathbf{a}_r^{(2)}$ by the following column matrices.

$$\mathbf{v}_r^{(2)} = \begin{bmatrix} v_f^{(2)} \\ v_h^{(2)} \\ 0 \end{bmatrix} \quad \mathbf{n} = \begin{bmatrix} n_f \\ n_h \\ n_n \end{bmatrix} \quad \mathbf{a}_r^{(2)} = \begin{bmatrix} a_f^{(2)} \\ a_h^{(2)} \\ a_n^{(2)} \end{bmatrix}$$

Here \mathbf{e}_f , \mathbf{e}_h , and \mathbf{e}_n are the unit vectors of the trihedron S_a (fig. 13.1.1), and vector $\mathbf{v}_r^{(2)}$ lies in the tangent plane formed by \mathbf{e}_f and \mathbf{e}_h .

The skew-symmetric matrix $[n]^s$ is given by

$$[n]^s = \begin{bmatrix} 0 & -n_n & n_h \\ n_n & 0 & -n_f \\ -n_h & n_f & 0 \end{bmatrix}$$

We then obtain

$$\begin{bmatrix} v_f^{(2)} \\ v_h^{(2)} \end{bmatrix}^T [n]^s \begin{bmatrix} a_f^{(2)} \\ a_h^{(2)} \end{bmatrix} = \left(-v_f^{(2)} a_h^{(2)} + v_h^{(2)} a_f^{(2)} \right) n_n + \left(v_f^{(2)} n_h - v_h^{(2)} n_f \right) a_n^{(2)} = 0$$

Taking into account the collinearity of vectors $\mathbf{a}_r^{(2)}$ and \mathbf{n} , we get that equation (13.2.10) is satisfied if

$$-v_f^{(2)} a_h^{(2)} + v_h^{(2)} a_f^{(2)} = 0$$

or if

$$\begin{bmatrix} v_f^{(2)} \\ v_h^{(2)} \end{bmatrix}^T \begin{bmatrix} 0 & -1 \\ 1 & 0 \end{bmatrix} \begin{bmatrix} a_f^{(2)} \\ a_h^{(2)} \end{bmatrix} = 0$$

Step 4.—It is easy to verify that we may use the equation

$$\begin{bmatrix} m_f \\ m_h \end{bmatrix}^T \begin{bmatrix} 0 & -1 \\ 1 & 0 \end{bmatrix} \begin{bmatrix} u_f \\ u_h \end{bmatrix} = 0 \quad (13.2.21)$$

instead of equation (13.2.20).

The evidence is based on the considerations that matrices of vectors \mathbf{u} and \mathbf{m} in equation (13.2.21) may be substituted by their expressions (13.2.16) and (13.2.19) that yield

$$\begin{aligned} & \left\{ [Q_2] \begin{bmatrix} v_f^{(2)} \\ v_h^{(2)} \end{bmatrix} \right\}^T \begin{bmatrix} 0 & -1 \\ 1 & 0 \end{bmatrix} [Q_2] \begin{bmatrix} a_f^{(2)} \\ a_h^{(2)} \end{bmatrix} \\ & = \begin{bmatrix} v_f^{(2)} \\ v_h^{(2)} \end{bmatrix}^T [Q_2]^T \begin{bmatrix} 0 & -1 \\ 1 & 0 \end{bmatrix} [Q_2] \begin{bmatrix} a_f^{(2)} \\ a_h^{(2)} \end{bmatrix} = 0 \end{aligned} \quad (13.2.22)$$

(See app. A.) The product of the matrices

$$[Q_2]^T \begin{bmatrix} 0 & -1 \\ 1 & 0 \end{bmatrix} [Q_2] \quad ([Q_2] \text{ is a symmetric matrix.})$$

may be represented as follows:

$$\begin{bmatrix} q_{11} & q_{12} \\ q_{12} & q_{22} \end{bmatrix} \begin{bmatrix} 0 & -1 \\ 1 & 0 \end{bmatrix} \begin{bmatrix} q_{11} & q_{12} \\ q_{12} & q_{22} \end{bmatrix} = \lambda \begin{bmatrix} 0 & -1 \\ 1 & 0 \end{bmatrix} \quad (13.2.23)$$

where

$$\lambda = q_{11}q_{22} - q_{12}^2$$

From equations (13.2.21), (13.2.22), and (13.2.23) we obtain

$$\begin{bmatrix} m_f \\ m_h \end{bmatrix}^T \begin{bmatrix} 0 & -1 \\ 1 & 0 \end{bmatrix} \begin{bmatrix} u_f \\ u_h \end{bmatrix} = \lambda \begin{bmatrix} v_f^{(2)} \\ v_h^{(2)} \end{bmatrix}^T \begin{bmatrix} 0 & -1 \\ 1 & 0 \end{bmatrix} \begin{bmatrix} a_f^{(2)} \\ a_h^{(2)} \end{bmatrix} \quad (13.2.24)$$

and we may indeed use equation (13.2.21) instead of (13.2.20). Equations (13.2.19) and (13.2.21) yield

$$-u_h m_f + u_f m_h = -u_h b_{13} + u_f b_{23} = 0 \quad (13.2.25)$$

Substituting u_f and u_h into equation (13.2.25) by their expressions in equation (13.2.18), we obtain

$$(d_h + \kappa_h c_h) b_{13} - (d_f + \kappa_f c_f) b_{23} = 0 \quad (13.2.26)$$

Step 5.—We transform equations (13.2.26) to derive the desired linear equation (13.2.11) in unknowns $v_f^{(2)}$ and $v_h^{(2)}$. Rearranging equations (13.2.5) and (13.2.7), we may represent them as follows:

$$\begin{aligned} \mathbf{c} &= (2\boldsymbol{\omega}^{(12)} \times \mathbf{v}_r^{(1)}) + (\boldsymbol{\omega}^{(12)} \times \mathbf{v}_{ir}^{(1)}) - (\boldsymbol{\omega}^{(2)} \times \mathbf{v}^{(12)}) - \left[\dot{\boldsymbol{\omega}}^{(2)} \times (\mathbf{r}^{(1)} - \mathbf{R}) \right] \\ &= \left[2\boldsymbol{\omega}^{(12)} \times (\mathbf{v}_r^{(2)} - \mathbf{v}^{(12)}) \right] + (\boldsymbol{\omega}^{(12)} \times \mathbf{v}_{ir}^{(1)}) - (\boldsymbol{\omega}^{(2)} \times \mathbf{v}^{(12)}) \\ &\quad - \left[\dot{\boldsymbol{\omega}}^{(2)} \times (\mathbf{r}^{(1)} - \mathbf{R}) \right] = (2\boldsymbol{\omega}^{(12)} \times \mathbf{v}_r^{(2)}) - (\boldsymbol{\omega}^{(1)} \times \mathbf{v}^{(12)}) + (\boldsymbol{\omega}^{(12)} \times \mathbf{v}_{ir}^{(2)}) \\ &\quad - \left[\dot{\boldsymbol{\omega}}^{(2)} \times (\mathbf{r}^{(1)} - \mathbf{R}) \right] = (2\boldsymbol{\omega}^{(12)} \times \mathbf{v}_r^{(2)}) + \mathbf{t} \end{aligned} \quad (13.2.27)$$

where

$$\mathbf{t} = (-\boldsymbol{\omega}^{(1)} \times \mathbf{v}^{(12)}) + (\boldsymbol{\omega}^{(12)} \times \mathbf{v}_{ir}^{(2)}) - \dot{\boldsymbol{\omega}}^{(2)} \times (\mathbf{r}^{(1)} - \mathbf{R}) \quad (13.2.28)$$

$$\begin{aligned} \mathbf{d} &= (2\boldsymbol{\omega}^{(12)} \times \dot{\mathbf{n}}_r^{(1)}) + \boldsymbol{\omega}^{(1)} (\boldsymbol{\omega}^{(12)} \cdot \mathbf{n}) - \boldsymbol{\omega}^{(12)} (\boldsymbol{\omega}^{(2)} \cdot \mathbf{n}) - \mathbf{n} (\boldsymbol{\omega}^{(12)})^2 \\ &\quad - (\dot{\boldsymbol{\omega}}^{(2)} \times \mathbf{n}) = 2\boldsymbol{\omega}^{(12)} \times \left[\dot{\mathbf{n}}_r^{(2)} - (\boldsymbol{\omega}^{(12)} \times \mathbf{n}) \right] + \boldsymbol{\omega}^{(1)} (\boldsymbol{\omega}^{(12)} \cdot \mathbf{n}) \\ &\quad - \boldsymbol{\omega}^{(12)} (\boldsymbol{\omega}^{(2)} \cdot \mathbf{n}) - \mathbf{n} (\boldsymbol{\omega}^{(12)})^2 - (\dot{\boldsymbol{\omega}}^{(2)} \times \mathbf{n}) = (2\boldsymbol{\omega}^{(12)} \times \dot{\mathbf{n}}_r^{(2)}) + \mathbf{p} \end{aligned} \quad (13.2.29)$$

Here

$$\mathbf{p} = -\boldsymbol{\omega}^{(12)}(\boldsymbol{\omega}^{(1)} \cdot \mathbf{n}) + \boldsymbol{\omega}^{(2)}(\boldsymbol{\omega}^{(12)} \cdot \mathbf{n}) + \mathbf{n}(\boldsymbol{\omega}^{(12)})^2 - (\dot{\boldsymbol{\omega}}^{(2)} \times \mathbf{n}) \quad (13.2.30)$$

Let us transform equations (13.2.27) and (13.2.29). The matrix representation of equation (13.2.27) is as follows:

$$\begin{aligned} \begin{bmatrix} c_f \\ c_h \\ c_n \end{bmatrix} &= 2 [\boldsymbol{\omega}^{(12)}]^s [\mathbf{v}_r^{(2)}] + \begin{bmatrix} t_f \\ t_h \\ t_n \end{bmatrix} = 2 \begin{bmatrix} \mathbf{0} & -\omega_n^{(12)} & \omega_h^{(12)} \\ \omega_n^{(12)} & \mathbf{0} & -\omega_f^{(12)} \\ -\omega_h^{(12)} & \omega_f^{(12)} & \mathbf{0} \end{bmatrix} \begin{bmatrix} v_f^{(2)} \\ v_h^{(2)} \\ \mathbf{0} \end{bmatrix} + \begin{bmatrix} t_f \\ t_h \\ t_n \end{bmatrix} \\ &= 2 \begin{bmatrix} -(\boldsymbol{\omega}^{(12)} \cdot \mathbf{n}) v_h^{(2)} \\ (\boldsymbol{\omega}^{(12)} \cdot \mathbf{n}) v_f^{(2)} \\ -\omega_h^{(12)} v_f^{(2)} + \omega_f^{(12)} v_h^{(2)} \end{bmatrix} + \begin{bmatrix} t_f \\ t_h \\ t_n \end{bmatrix} \end{aligned} \quad (13.2.31)$$

(See app. A.) Here $[\boldsymbol{\omega}^{(12)}]^s$ is the skew-symmetric matrix,

$$\boldsymbol{\omega}^{(12)} \cdot \mathbf{n} = \omega_n^{(12)}$$

Considering the first two projections of vectors only, we may represent equation (13.2.27) by

$$\begin{bmatrix} c_f \\ c_h \end{bmatrix} = 2\alpha \begin{bmatrix} -v_h^{(2)} \\ v_f^{(2)} \end{bmatrix} + \begin{bmatrix} t_f \\ t_h \end{bmatrix} \quad (13.2.32)$$

where $\alpha = \boldsymbol{\omega}^{(12)} \cdot \mathbf{n}$.

For the matrix representation of equation (13.2.29), we use the following relations:

$$\begin{aligned} \begin{bmatrix} \dot{n}_r^{(2)} \\ \dot{n}_q^{(2)} \end{bmatrix} &= \begin{bmatrix} \dot{n}_s^{(2)} \\ \dot{n}_q^{(2)} \end{bmatrix} = [K_2] \begin{bmatrix} v_s^{(2)} \\ v_q^{(2)} \end{bmatrix} = [K_2][L_{ba}] \begin{bmatrix} v_f^{(2)} \\ v_h^{(2)} \end{bmatrix} \\ \begin{bmatrix} \dot{n}_f^{(2)} \\ \dot{n}_h^{(2)} \end{bmatrix} &= [L_{ab}] \begin{bmatrix} \dot{n}_s^{(2)} \\ \dot{n}_q^{(2)} \end{bmatrix} = [L_{ab}][K_2][L_{ba}] \begin{bmatrix} v_f^{(2)} \\ v_h^{(2)} \end{bmatrix} = \{[K_1] - [Q_2]\} \begin{bmatrix} v_f^{(2)} \\ v_h^{(2)} \end{bmatrix} \end{aligned} \quad (13.2.33)$$

(See matrix equation (13.2.17) for $[Q_2]$.)

Equations (13.2.33) and (13.2.19) yield

$$\begin{bmatrix} \dot{n}_f^{(2)} \\ \dot{n}_h^{(2)} \end{bmatrix} = [K_1] \begin{bmatrix} v_f^{(2)} \\ v_h^{(2)} \end{bmatrix} - \begin{bmatrix} m_f \\ m_h \end{bmatrix} = - \begin{bmatrix} \kappa_f v_f^{(2)} + m_f \\ \kappa_h v_h^{(2)} + m_h \end{bmatrix} \quad (13.2.34)$$

The vector product in equation (13.2.29) is represented by

$$\begin{aligned}
\boldsymbol{\omega}^{(12)} \times \dot{\mathbf{n}}_r^{(2)} &= \begin{bmatrix} 0 & -\omega_n^{(12)} & \omega_h^{(12)} \\ \omega_n^{(12)} & 0 & -\omega_f^{(12)} \\ -\omega_h^{(12)} & \omega_f^{(12)} & 0 \end{bmatrix} \begin{bmatrix} \dot{n}_f^{(2)} \\ \dot{n}_h^{(2)} \\ 0 \end{bmatrix} \\
&= \begin{bmatrix} 0 & -\omega_n^{(12)} & \omega_h^{(12)} \\ \omega_n^{(12)} & 0 & -\omega_f^{(12)} \\ -\omega_h^{(12)} & \omega_f^{(12)} & 0 \end{bmatrix} \begin{bmatrix} -\kappa_f v_f^{(2)} - m_f \\ -\kappa_h v_h^{(2)} - m_h \\ 0 \end{bmatrix} \\
&= \begin{bmatrix} (\boldsymbol{\omega}^{(12)} \cdot \mathbf{n})(\kappa_h v_h^{(2)} + b_{23}) \\ -(\boldsymbol{\omega}^{(12)} \cdot \mathbf{n})(\kappa_f v_f^{(2)} + b_{13}) \\ \omega_h^{(12)}(\kappa_f v_f^{(2)} + b_{13}) - \omega_f^{(12)}(\kappa_h v_h^{(2)} + b_{23}) \end{bmatrix} \quad (13.2.35)
\end{aligned}$$

where $\boldsymbol{\omega}^{(12)} \cdot \mathbf{n} = \omega_n^{(12)}$, $m_f = b_{13}$, and $m_h = b_{23}$. (See eq. (13.2.19).)

Considering the first two projections of vectors only, we represent equation (13.2.29) in matrix form as

$$\begin{bmatrix} d_f \\ d_h \end{bmatrix} = \begin{bmatrix} 2\alpha(\kappa_h v_h^{(2)} + b_{23}) + p_f \\ -2\alpha(\kappa_f v_f^{(2)} + b_{13}) + p_h \end{bmatrix} \quad (13.2.36)$$

Step 6.—We can now derive the desired linear equation (13.2.11) in unknowns $v_f^{(2)}$ and $v_h^{(2)}$. Substituting in equation (13.2.26) the expressions d_f , d_h , c_f , and c_h of (13.2.36) and (13.2.32), we get

$$b_{13}v_f^{(2)} - b_{23}v_h^{(2)} = b_{43} \quad (13.2.37)$$

Here, coefficients b_{13} and b_{23} are represented by equation (13.1.63) and

$$b_{43} = \frac{1}{\kappa_h - \kappa_f} \left(b_{13}^2 + b_{23}^2 + \frac{p_f b_{23} - p_h b_{13} + \kappa_f t_f b_{23} - \kappa_h t_h b_{13}}{2\alpha} \right) \quad (13.2.38)$$

Equation (13.2.37) provides conditions for the existence of a locally geodetic curve on surface Σ_2 . This equation with the system of equations (13.1.56) relate the principle curvatures and directions of two mating surfaces in the case when the contact point path is a locally geodetic curve (a geodetic curve in the neighborhood of the considered contact point). One additional linear equation in unknowns $v_f^{(2)}$ and $v_h^{(2)}$ is represented by

$$b_{51}v_f^{(2)} + b_{52}v_h^{(2)} = 0 \quad (13.2.39)$$

This equation determines the direction of the tangent to the contact point path. Consider that the tangent must form the prescribed angle μ with the unit vector \mathbf{e}_h . This condition yields

$$\frac{v_f^{(2)}}{v_h^{(2)}} = -\frac{b_{52}}{b_{51}} = \tan \mu \quad (13.2.40)$$

Equations (13.1.56), (13.2.37), and (13.2.39) represent the following system of five equations in two unknowns $v_f^{(2)}$ and $v_h^{(2)}$:

$$b_{i1}v_f^{(2)} + b_{i2}v_h^{(2)} = b_{i3} \quad (i = 1,2,3,4,5) \quad (13.2.41)$$

Coefficients b_{j1} ($j = 1,2,3$) have been represented by equations (13.1.62) and (13.1.63); $b_{41} = b_{31}$, $b_{42} = -b_{23}$, and the coefficient b_{43} was given by equation (13.2.38). If we take $b_{51} = 1$, then $b_{52} = -\tan \mu$.

It is known from linear algebra that the system of equations (13.2.41) possesses a unique solution if the system matrix and the augmented matrix represented by

$$\begin{bmatrix} b_{11} & b_{12} \\ b_{12} & b_{22} \\ b_{13} & b_{23} \\ b_{13} & -b_{23} \\ 1 & -\tan \mu \end{bmatrix} \quad \begin{bmatrix} b_{11} & b_{12} & b_{13} \\ b_{12} & b_{22} & b_{23} \\ b_{13} & b_{23} & b_{33} \\ b_{13} & -b_{23} & b_{43} \\ 1 & -\tan \mu & 0 \end{bmatrix} \quad (13.2.42)$$

are of equal rank $r = 2$.

Considering the system matrix, we find that the rank r is indeed equal to two since

$$\Delta = \begin{bmatrix} b_{11} & b_{12} \\ b_{12} & b_{22} \end{bmatrix} \neq 0 \quad (13.2.43)$$

We have to remember that $\Delta = 0$ if the surfaces are in line-contact. (See eq. (13.1.62).) We are considering the case of point contact of surfaces, therefore $\Delta \neq 0$. The augmented matrix is of rank $r = 2$ if all six determinants of the third order are equal to zero. This condition yields the three following independent equations:

$$\begin{bmatrix} b_{11} & b_{12} & b_{13} \\ b_{12} & b_{22} & b_{23} \\ b_{13} & b_{23} & b_{33} \end{bmatrix} = 0 \quad \begin{bmatrix} b_{11} & b_{12} & b_{13} \\ b_{12} & b_{22} & b_{23} \\ b_{13} & -b_{23} & b_{43} \end{bmatrix} = 0 \quad \begin{bmatrix} b_{11} & b_{12} & b_{13} \\ b_{12} & b_{22} & b_{23} \\ 1 & -\tan \mu & 0 \end{bmatrix} = 0 \quad (13.2.44)$$

Three equations (13.2.44) yield three relations between four principal curvatures of mating surfaces and the angle σ , formed between the unit vectors \mathbf{e}_f and \mathbf{e}_s (fig. 13.1.1), as follows:

$$F_i(\kappa_f, \kappa_h, \kappa_s, \kappa_h, \sigma) = 0 \quad (i = 1,2,3) \quad (13.2.45)$$

Existence of a Locally Geodetic Curve on Surface Σ_1

Similarly, we may investigate the existence of a local geodetic curve on surface Σ_1 by using the equation

$$\left[\mathbf{v}_r^{(1)} \mathbf{n}_a^{(1)} \right] = 0 \quad (13.2.46)$$

This equation yields a linear equation in unknowns $v_s^{(1)}$ and $v_q^{(1)}$

$$a_{41}v_s^{(1)} + a_{42}v_q^{(1)} = a_{43} \quad (13.2.47)$$

We develop equation (13.2.47) following a similar procedure as discussed in the previous case.

Step 1.—We derive linear equations in unknowns $a_s^{(1)}$ and $a_q^{(1)}$ by using equations (13.2.4) and (13.2.6) which yield

$$\begin{bmatrix} a_s^{(2)} \\ a_q^{(2)} \end{bmatrix} = \begin{bmatrix} a_s^{(1)} \\ a_q^{(1)} \end{bmatrix} + \begin{bmatrix} c_s \\ c_q \end{bmatrix} \quad (13.2.48)$$

$$\begin{bmatrix} \ddot{n}_s^{(2)} \\ \ddot{n}_q^{(2)} \end{bmatrix} = \begin{bmatrix} \ddot{n}_s^{(1)} \\ \ddot{n}_q^{(1)} \end{bmatrix} + \begin{bmatrix} d_s \\ d_q \end{bmatrix} \quad (13.2.49)$$

Here vectors

$$\mathbf{c} = c_s \mathbf{e}_s + c_q \mathbf{e}_q$$

$$\mathbf{d} = d_s \mathbf{e}_s + d_q \mathbf{e}_q$$

are represented by equations (13.2.5) and (13.2.7), respectively.

From equations (13.2.49), (13.2.8), and (13.2.9) we obtain

$$\begin{aligned} [K_2] \begin{bmatrix} a_s^{(2)} \\ a_q^{(2)} \end{bmatrix} &= [L_{ba}] \begin{bmatrix} \ddot{n}_f^{(1)} \\ \ddot{n}_h^{(1)} \end{bmatrix} + \begin{bmatrix} d_s \\ d_q \end{bmatrix} = [L_{ba}][K_1] \begin{bmatrix} a_f^{(1)} \\ a_q^{(1)} \end{bmatrix} + \begin{bmatrix} d_s \\ d_q \end{bmatrix} \\ &= [L_{ba}][K_1][L_{ab}] \begin{bmatrix} a_s^{(1)} \\ a_q^{(1)} \end{bmatrix} + \begin{bmatrix} d_s \\ d_q \end{bmatrix} \end{aligned} \quad (13.2.50)$$

Equations (13.2.48) and (13.2.50) yield

$$[Q_1] \begin{bmatrix} a_s^{(1)} \\ a_q^{(1)} \end{bmatrix} = - \begin{bmatrix} d_s \\ d_q \end{bmatrix} + [K_2] \begin{bmatrix} c_s \\ c_q \end{bmatrix} = - \begin{bmatrix} d_s + \kappa_s c_s \\ d_q + \kappa_q c_q \end{bmatrix} = \begin{bmatrix} u_s^* \\ u_q^* \end{bmatrix} \quad (13.2.51)$$

Here

$$[Q_1] = [L_{ba}][K_1][L_{ab}] - [K_2] \quad (13.2.52)$$

Step 2.—We represent the system of linear equations (13.1.34(a)) as

$$[Q_1] \begin{bmatrix} v_s^{(1)} \\ v_q^{(1)} \end{bmatrix} = \begin{bmatrix} a_{13} \\ a_{23} \end{bmatrix} = \begin{bmatrix} m_s^* \\ m_q^* \end{bmatrix} \quad (13.2.53)$$

where vector \mathbf{m}^* is

$$\mathbf{m}^* = m_s^* \mathbf{e}_s + m_q^* \mathbf{e}_q = a_{13} \mathbf{e}_s + a_{23} \mathbf{e}_q$$

Step 3.—We prove that equation (13.2.46) is equivalent to the equation

$$[\mathbf{m}^* \mathbf{n}^*] = 0 \quad (13.2.54)$$

which yields

$$-u_q^* a_{13} + u_s^* a_{23} = 0 \quad (13.2.55)$$

(See the similar transformations for eq. (13.2.25).)

Substituting in equation (13.2.55) u_s^* and u_q^* for their expressions (13.2.51), we get

$$(d_q + \kappa_q c_q) a_{13} - (d_s + \kappa_s c_s) a_{23} = 0 \quad (13.2.56)$$

Step 4.—We represent equation (13.2.5) as

$$\begin{aligned} \mathbf{c} &= \left(2\boldsymbol{\omega}^{(12)} \times \mathbf{v}_r^{(1)} \right) + \mathbf{t}^* = 2\alpha \left(-v_q^{(1)} \mathbf{e}_s + v_s^{(1)} \mathbf{e}_q \right) \\ &+ 2 \left(\omega_s^{(12)} v_q^{(1)} - \omega_q^{(12)} v_s^{(1)} \right) \mathbf{n} + t_s^* \mathbf{e}_s + t_q^* \mathbf{e}_q + t_n^* \mathbf{e}_n \end{aligned} \quad (13.2.57)$$

Here \mathbf{e}_s , \mathbf{e}_q , and \mathbf{n} are the unit vectors of the coordinate system S_b (fig. 13.1.1), $\alpha = \boldsymbol{\omega}^{(12)} \cdot \mathbf{n}$, and

$$\mathbf{t}^* = \left(\boldsymbol{\omega}^{(12)} \times \mathbf{v}_{rr}^{(1)} \right) - \left(\boldsymbol{\omega}^{(2)} \times \mathbf{v}^{(12)} \right) - \left[\dot{\boldsymbol{\omega}}^{(2)} \times \left(\mathbf{r}^{(1)} - \mathbf{R} \right) \right] \quad (13.2.58)$$

Equation (13.2.57) yields

$$c_s = -2\alpha v_q^{(1)} + t_s^* \quad c_q = 2\alpha v_s^{(1)} + t_q^* \quad (13.2.59)$$

Step 5.—We transform equation (13.2.7). We begin with the transformation of $\dot{\mathbf{n}}_r^{(1)}$ and use equations (13.2.52) and (13.2.53)

$$\begin{aligned} \dot{\mathbf{n}}_r^{(1)} &= \begin{bmatrix} \dot{n}_s^{(1)} \\ \dot{n}_q^{(1)} \end{bmatrix} = [L_{ba}] \begin{bmatrix} \dot{n}_f^{(1)} \\ \dot{n}_h^{(1)} \end{bmatrix} = [L_{ba}][K_1] \begin{bmatrix} v_f^{(1)} \\ v_h^{(1)} \end{bmatrix} \\ &= [L_{ba}][K_1][L_{ab}] \begin{bmatrix} v_s^{(1)} \\ v_q^{(1)} \end{bmatrix} = \{ [Q_1] + [K_2] \} \begin{bmatrix} v_s^{(1)} \\ v_q^{(1)} \end{bmatrix} \\ &= \begin{bmatrix} a_{13} \\ a_{23} \end{bmatrix} + [K_2] \begin{bmatrix} v_s^{(1)} \\ v_q^{(1)} \end{bmatrix} = \begin{bmatrix} a_{13} - \kappa_s v_s^{(1)} \\ a_{23} - \kappa_q v_q^{(1)} \end{bmatrix} \end{aligned} \quad (13.2.60)$$

Equations (13.2.60) and (13.2.7) yield

$$d_s = 2\alpha \left(-a_{23} + \kappa_q v_q^{(1)} \right) + p_s^* \quad d_q = 2\alpha \left(a_{13} - \kappa_s v_s^{(1)} \right) + p_q^* \quad (13.2.61)$$

Here $\alpha = \boldsymbol{\omega}^{(12)} \cdot \mathbf{n}$,

$$\mathbf{p}^* = p_s^* \mathbf{e}_s + p_q^* \mathbf{e}_q = \boldsymbol{\omega}^{(1)} \left(\boldsymbol{\omega}^{(12)} \cdot \mathbf{n} \right) - \boldsymbol{\omega}^{(12)} \left(\boldsymbol{\omega}^{(2)} \cdot \mathbf{n} \right) - \mathbf{n} \left(\boldsymbol{\omega}^{(12)} \right)^2 - \left(\dot{\boldsymbol{\omega}}^{(2)} \times \mathbf{n} \right) \quad (13.2.62)$$

Step 6.—We may now derive the desired linear equation in unknowns $v_s^{(1)}$ and $v_q^{(1)}$. Substituting c_s , c_q , d_s , and d_q for their expressions (13.2.59) and (13.2.61), respectively, in equation (13.2.56) we get

$$a_{13} v_s^{(1)} - a_{23} v_q^{(1)} = a_{43} \quad (13.2.63)$$

Here

$$a_{43} = \frac{1}{\kappa_s - \kappa_q} \left(a_{13}^2 + a_{23}^2 + \frac{p_q^* a_{13} - p_s^* a_{23} + \kappa_q t_q^* a_{13} - \kappa_s t_s^* a_{23}}{2\alpha} \right) \quad (13.2.64)$$

We may now determine relations between the principal curvatures and directions of two mating surfaces which provide the existence of a locally geodetic curve on surface Σ_1 . We consider the following system of linear equations:

$$\begin{aligned} a_{11} v_s^{(1)} + a_{12} v_q^{(1)} &= a_{13} & a_{12} v_s^{(1)} + a_{22} v_q^{(1)} &= a_{23} \\ a_{13} v_s^{(1)} + a_{23} v_q^{(1)} &= a_{33} & a_{13} v_s^{(1)} - a_{23} v_q^{(1)} &= a_{43} \\ v_s^{(1)} + a_{52} v_q^{(1)} &= 0 \end{aligned} \quad (13.2.65)$$

The fifth equation of system (13.2.65) satisfies the condition that the tangent to the contact-point path forms, with the unit vector \mathbf{e}_q , (fig. (13.1.1)) the prescribed angle μ^* . Here $\tan \mu^* = -a_{52}$ and angles μ and μ^* are related because vectors of tangents $\mathbf{v}_r^{(1)}$ and $\mathbf{v}_r^{(2)}$ are related by equation (13.1.9).

We investigate the simultaneous existence of equations (13.2.65) and the existence of a unique solution of these equations similar to the way it was done for the system (13.2.41). This results in the conditions of existence of the three following independent equations:

$$\begin{vmatrix} a_{11} & a_{12} & a_{13} \\ a_{12} & a_{22} & a_{23} \\ a_{13} & a_{23} & a_{33} \end{vmatrix} = 0 \quad \begin{vmatrix} a_{11} & a_{12} & a_{13} \\ a_{12} & a_{22} & a_{23} \\ a_{13} & -a_{23} & a_{43} \end{vmatrix} = 0 \quad \begin{vmatrix} a_{11} & a_{12} & a_{13} \\ a_{12} & a_{22} & a_{23} \\ 1 & -\tan \mu^* & 0 \end{vmatrix} = 0 \quad (13.2.66)$$

Equations (13.2.66) yield the three following equations:

$$\psi_i(\kappa_f, \kappa_h, \kappa_s, \kappa_q, \sigma) = 0 \quad (i = 1, 2, 3) \quad (13.2.67)$$

Total Number of Relations

Consider that locally geodetic curves are provided on both surfaces Σ_1 and Σ_2 . This is possible if both systems of equations, (13.2.65) and (13.2.67), are satisfied. However, the above systems provide only four independent equations since the coefficients of equations are related. The

requirement of the dimension of the contacting ellipse (sec. 13.4) yields the fifth relation between parameters κ_f , κ_h , κ_s , κ_q , and σ . If additional requirements are to be satisfied, only one locally geodetic curve can be provided by the gear synthesis.

13.3 Relative Normal Curvature

The relative normal curvature of two mating surfaces κ_R at the given point P is defined as the difference of the normal curvatures of both surfaces taken in a common normal section of surfaces and represented as

$$\kappa_R = \kappa_n^{(2)} - \kappa_n^{(1)} \quad (13.3.1)$$

Consider that the tangent to the common normal section forms an angle q with the unit vector \mathbf{e}_s and an angle $(q + \sigma)$ with the unit vector \mathbf{e}_f (fig. 13.1.1). Euler's formula yields

$$\kappa_n^{(2)} = \kappa_s \cos^2 q + \kappa_q \sin^2 q \quad \kappa_n^{(1)} = \kappa_f \cos^2 (q + \sigma) + \kappa_h \sin^2 (q + \sigma) \quad (13.3.2)$$

(See eq. C.3.26.) Here $\kappa_n^{(1)}$ and $\kappa_n^{(2)}$ are the normal curvatures of surfaces Σ_1 and Σ_2 in the common normal section. Thus,

$$\kappa_R = \kappa_s \cos^2 q + \kappa_q \sin^2 q - \kappa_f \cos^2 (q + \sigma) - \kappa_h \sin^2 (q + \sigma) \quad (13.3.3)$$

After simple transformations we get

$$\begin{aligned} \kappa_R = & \left(\kappa_s - \kappa_f \cos^2 \sigma - \kappa_h \sin^2 \sigma \right) \cos^2 q + \left(\kappa_q - \kappa_f \sin^2 \sigma - \kappa_h \cos^2 \sigma \right) \sin^2 q \\ & + \left(\kappa_f - \kappa_h \right) \frac{\sin 2\sigma}{2} \sin 2q \end{aligned} \quad (13.3.4)$$

Equation (13.3.4) and expressions for a_{11} , a_{12} , and a_{22} in equation (13.1.44) yield

$$\kappa_R = 0.5 \left[a_{11} + a_{22} + (a_{11} - a_{22}) \cos 2q \right] + a_{12} \sin 2q \quad (13.3.5)$$

The principal values of the relative normal curvature are the extreme values of function $\kappa_R(q)$. The principal directions of the relative normal curvature are determined with the equation

$$\frac{d}{dq} (\kappa_R) = 0 \quad (13.3.6)$$

Equations (13.3.6) and (13.3.5) yield

$$\tan 2q = 2 \frac{a_{12}}{a_{11} - a_{22}} \quad (13.3.7)$$

Equation (13.3.7) determines two solutions for q , which are $q^{(1)}$ and $q^{(1)} + 90^\circ$. This means that there are two perpendicular directions for the principal directions of the relative normal curvature. The principal values of the relative normal curvature are represented by the equation

$$\kappa_R = 0.5 \left\{ (a_{11} + a_{22}) \pm \left[(a_{11} - a_{22})^2 + 4a_{12}^2 \right]^{1/2} \right\} \quad (13.3.8)$$

Equations (13.3.5), (13.3.7), and (13.3.8) work for both cases of contact of mating surfaces, which are point contact and line contact. In the case of line contact, the coefficients a_{11} , a_{12} , and a_{22} are related by

$$a_{22} = \frac{a_{12}^2}{a_{11}} \quad (13.3.9)$$

(See eqs. (13.1.47).) Equations (13.3.8) and (13.3.9) yield that in the case of line contact, the principal values of the relative normal curvature are determined as follows:

$$\kappa_R = 0 \quad \kappa_R = a_{11} + a_{22} = (\kappa_s + \kappa_q) - (\kappa_f + \kappa_h) \quad (13.3.10)$$

One principal direction with $\kappa_R = 0$ coincides with the tangent \mathbf{T} to the line of contact of mating surfaces, and the other principal direction is perpendicular to \mathbf{T} .

The determination of the principal values and directions of the relative normal curvature may be interpreted as the diagonalization of the symmetric matrix

$$[\Pi] = \begin{bmatrix} a_{11} & a_{12} \\ a_{12} & a_{22} \end{bmatrix} \quad (13.3.11)$$

It is known from the Theory of Matrices (Korn, et al., 1968) that such operation may be represented by the matrix equation

$$\begin{bmatrix} p_{11} & 0 \\ 0 & p_{12} \end{bmatrix} = [C]^T \begin{bmatrix} a_{11} & a_{12} \\ a_{12} & a_{22} \end{bmatrix} [C] \quad (13.3.12)$$

where $[C]^T$ is the matrix transpose to $[C]$. We express matrix $[C]$ by

$$[C] = \begin{bmatrix} \cos q & -\sin q \\ \sin q & \cos q \end{bmatrix} \quad (13.3.13)$$

Equations (13.3.10) and (13.3.11) yield

$$p_{12} = a_{12} \cos 2q - \frac{(a_{11} - a_{22}) \sin 2q}{2} = 0$$

and

$$\tan 2q = \frac{2a_{12}}{a_{11} - a_{22}}$$

$$p_{11} = 0.5 \left[a_{11} + a_{22} + (a_{11} - a_{22}) \cos 2q \right] + a_{12} \sin 2q$$

$$p_{22} = 0.5 \left[a_{11} + a_{22} - (a_{11} - a_{22}) \cos 2q \right] - a_{12} \sin 2q$$

These equations are similar to the equations (13.3.7) and (13.3.8), which were determined previously. Equations discussed in this section were first proposed by Litvin (1969).

3.4 Contact Ellipse

Because of the elasticity of tooth surfaces, the contact of surfaces at a point is spread over an elliptical area. The bearing contact of gear-tooth surfaces is formed as a set of contacting ellipses.

Consider that the following are given for the point of contact: (1) the approach of surfaces under the load, (2) the principal curvatures of contacting surfaces, and the parameters of principal directions. To determine the dimensions and orientation of the contacting ellipse, we use a procedure based on the following considerations:

Figure 13.4.1 shows surfaces Σ_1 and Σ_2 in tangency at point M . The unit surface normal and the tangent plane are designated by \mathbf{n} and Π . The area of the deformed surfaces is shown by dashed lines and designated by $K_1M_1L_1$ and $K_2M_2L_2$ for surfaces Σ_1 and Σ_2 , respectively.

Consider points N and N' of surfaces Σ_1 and Σ_2 , respectively (fig. 13.4.1). The locations of N and N' with respect to point M are determined with the coordinates of N and N' which are given by $N(\rho, \ell^{(1)})$ and $N'(\rho, \ell^{(2)})$, respectively (figs. 13.4.2(a) and (b)). The elastic deformation of surfaces at M is designated by δ_1 and δ_2 , and the elastic approach of surfaces at M is given by δ where $\delta = \delta_1 + \delta_2$. The resulting displacement of a surface point may be represented as a displacement having (fig. 13.4.2) (1) a component with the surface (given by δ_i , $i = 1, 2$) and (2) a component with respect to the surface, because of the elastic deformation at points N and N' , (given by f_i , $i = 1, 2$). The resulting location of point N is designated in figure 13.4.2(a) by N_2 , and thus $\overline{N N_2}$ is the resulting displacement. Let us represent $\overline{N N_2}$ as

$$\overline{N N_2} = \overline{N N_1} + \overline{N_1 N_2} \quad (13.4.1)$$

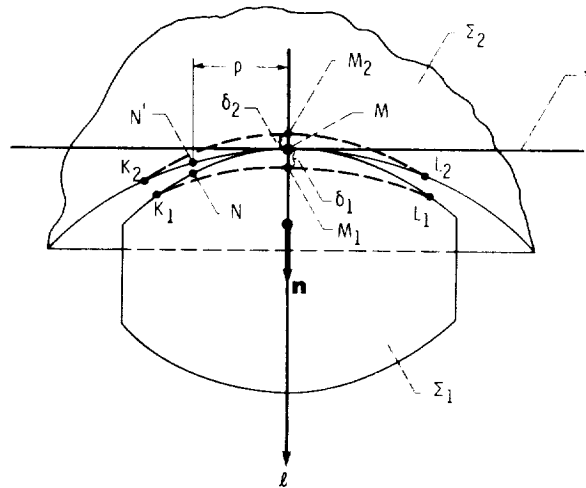


Figure 13.4.1.

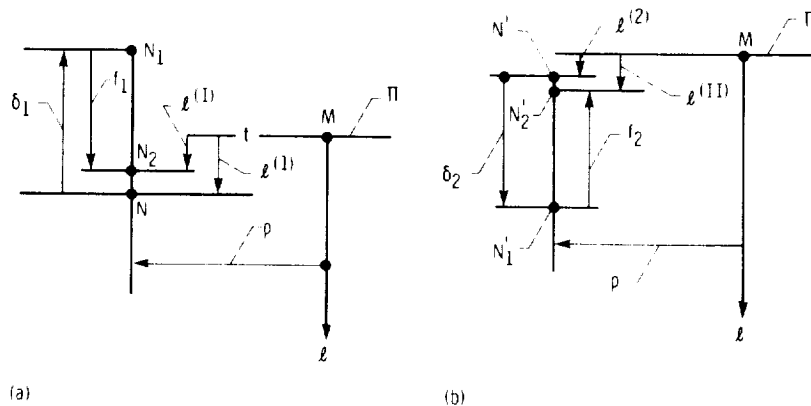


Figure 13.4.2.

Here $|\overline{N N_2}| = \delta_1$ is the displacement with surface Σ_1 and $\overline{N_1 N_2}$ is the displacement with respect to Σ_1 , because of the surface deformation at point N_1 . The location of point N_2 with respect to the tangent plane Π is given by the equation

$$\ell^{(I)} = \ell^{(1)} - \delta_1 + f_1 \quad (13.4.2)$$

Similarly, for point N' , we obtain (fig. 13.4.2(b))

$$\overline{N' N'_2} = \overline{N' N'_1} + \overline{N'_1 N'_2} \quad (13.4.3)$$

which yields

$$\ell^{(II)} = \ell^{(2)} + \delta_2 - f_2 \quad (13.4.4)$$

Here $\ell^{(I)}$ and $\ell^{(II)}$ represent the deviations from the tangent plane for two mating points of contacting surfaces. The notations $\ell^{(1)}$ and $\ell^{(2)}$ represent the initial deviations from the tangent plane Π for points N and N' of surfaces Σ_1 and Σ_2 , respectively. Points N and N' will coincide with each other and form a common point of contact of the deformed surfaces of $\ell^{(I)}$ and $\ell^{(II)}$. This yields

$$\ell^{(1)} - \delta_1 + f_1 = \ell^{(2)} + \delta_2 - f_2 \quad (13.4.5)$$

Equation (13.4.5) yields

$$|\ell^{(1)} - \ell^{(2)}| = \delta_1 + \delta_2 - (f_1 + f_2) \quad (13.4.6)$$

The right-hand side of equation (13.4.6) is always positive since $\delta_1 > f_1$ and $\delta_2 > f_2$. Equation (13.4.6) is satisfied for all mating points of contacting surfaces within the area of deformation and at the edge of this area. However, at the edge of this area $f_1 = 0$ and $f_2 = 0$ and therefore equation (13.4.6) becomes

$$|\ell^{(1)} - \ell^{(2)}| = \delta_1 + \delta_2 = \delta \quad (13.4.7)$$

Outside of the area of deformation

$$|\ell^{(1)} - \ell^{(2)}| > \delta \quad (13.4.8)$$

and within this area

$$|\ell^{(1)} - \ell^{(2)}| < \delta \quad (13.4.9)$$

We may correlate $\ell^{(i)}$ with the surface curvature as follows. Consider that a surface Σ is represented by

$$\mathbf{r}(u, \theta) \in C^2 \quad \mathbf{r}_u \times \mathbf{r}_\theta \neq 0 \quad (u, \theta) \in E \quad (13.4.10)$$

where (u, θ) represent the surface coordinates.

Curve $\overline{M M'}$ on the surface Σ may be represented by the equation

$$\mathbf{r} = \mathbf{r}[u(s), \theta(s)] \quad (13.4.11)$$

where s is the arc length.

Let us designate the length of the arc which connects two neighboring points M and M' of the curve by Δs , where $\Delta s = \overline{M M'}$. The increment of the position vector \mathbf{r} is designated by $\Delta \mathbf{r}$, where $\Delta \mathbf{r} = \overline{M M'}$. Expanding $\Delta \mathbf{r}$ with the Taylor-series expansion, we get

$$\overline{MM'} = \Delta \mathbf{r} = \frac{d\mathbf{r}}{ds} \Delta s + \frac{d^2\mathbf{r}}{ds^2} \frac{(\Delta s)^2}{2!} + \frac{d^3\mathbf{r}}{ds^3} \frac{(\Delta s)^3}{3!} + \dots \quad (13.4.12)$$

Here

$$\frac{d\mathbf{r}}{ds} = \frac{\partial \mathbf{r}}{\partial u} \frac{du}{ds} + \frac{\partial \mathbf{r}}{\partial \theta} \frac{d\theta}{ds}$$

$$\frac{d^2\mathbf{r}}{ds^2} = \frac{\partial^2 \mathbf{r}}{\partial u^2} \left(\frac{du}{ds} \right)^2 + 2 \frac{\partial^2 \mathbf{r}}{\partial u \partial \theta} \frac{du}{ds} \frac{d\theta}{ds} + \frac{\partial^2 \mathbf{r}}{\partial \theta^2} \left(\frac{d\theta}{ds} \right)^2, \dots$$

Plane Π shown in figure 13.4.3 is tangent to the surface at point M . Vector

$$\overline{PM'} = \ell \mathbf{n} \quad (13.4.13(a))$$

is perpendicular to plane Π at point P , and ℓ represents the deviation of the curve point M' from the tangent plane. The deviation ℓ is positive if $\overline{PM'}$ and \mathbf{n} are in the same direction. Equations $\overline{MM'} = \Delta \mathbf{r}$ and $\overline{MM'} = \overline{MP} + \ell \mathbf{n}$ yield

$$\overline{MP} + \ell \mathbf{n} = \frac{d\mathbf{r}}{ds} \Delta s + \frac{d^2\mathbf{r}}{ds^2} \frac{(\Delta s)^2}{2!} + \frac{d^3\mathbf{r}}{ds^3} \frac{(\Delta s)^3}{3!} + \dots \quad (13.4.13(b))$$

Vectors \overline{MP} and \mathbf{n} are mutually perpendicular. Taking the dot product on both sides of equation (13.4.13(b)) with \mathbf{n} , and limiting the expression for ℓ up to terms of the third order, we obtain

$$\ell = \left(\frac{d^2\mathbf{r}}{ds^2} \cdot \mathbf{n} \right) \frac{\Delta s^2}{2} \quad (13.4.14)$$

It was mentioned in chapter 10 that the normal curvature of a surface may be represented by

$$\kappa_n = \frac{d^2\mathbf{r}}{ds^2} \cdot \mathbf{n} \quad (13.4.15)$$

Thus,

$$\ell = \kappa_n \frac{\Delta s^2}{2} \quad (13.4.16)$$

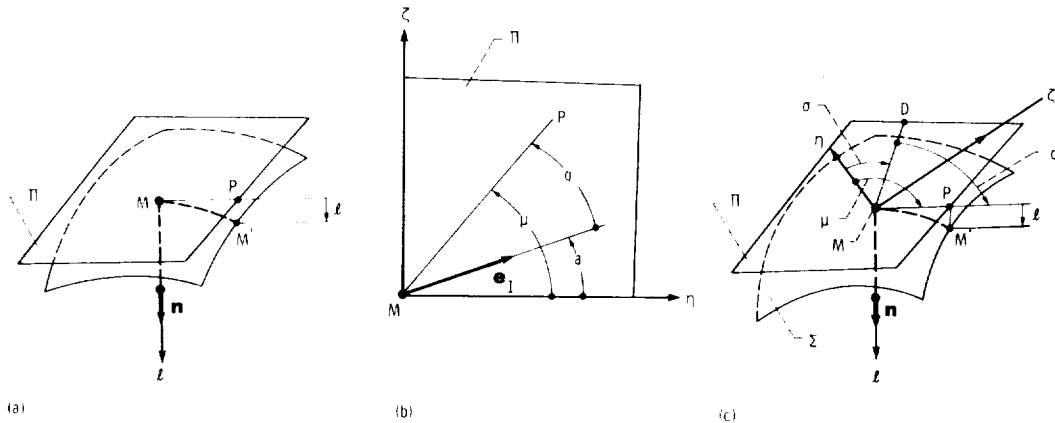


Figure 13.4.3.

Consider the coordinate system with coordinate axes n , η , and ζ (figs. 13.4.3(a) and 13.4.3(b)), whose origin coincides with point M , and axes η and ζ lie in the tangent plane Π . It is easy to verify that

$$\Delta s^2 = \eta^2 + \zeta^2 = \rho^2 \quad (13.4.17)$$

where $\Delta s = \rho = |\overline{MP}|$, and η and ζ are the coordinates of point P .

Equations (13.4.16) and (13.4.17) yield

$$\ell = \frac{1}{2} \kappa_n \rho^2 \quad (13.4.18)$$

The normal curvature and principal curvatures of a surface are related by Euler's equation. (See app. C.) Considering the relations in Euler's equation, the fact that \mathbf{e}_I is the unit vector of the principal direction having principal curvature κ_I , and the fact that vector \overline{MP} makes an angle q with \mathbf{e}_I , we obtain

$$\kappa_n = \kappa_I \cos^2 q + \kappa_{II} \sin^2 q \quad (13.4.19)$$

where κ_I and κ_{II} are the principal curvatures of the surface at point M .

Consider again the coordinate system having coordinate axes n , η , and ζ (fig. 13.4.3), whose origin coincides with point M . The unit vector \mathbf{e}_I makes an angle α with the η -axis, and the orientation of \overline{MP} is determined by angle μ , where $\mu = q + \alpha$. With these designations we obtain

$$\kappa_n = \kappa_I \cos^2 (\mu - \alpha) + \kappa_{II} \sin^2 (\mu - \alpha) \quad (13.4.20)$$

Equations (13.4.17), (13.4.18), and (13.4.20) yield

$$2\ell = \rho^2 \left[\kappa_I \cos^2 (\mu - \alpha) + \kappa_{II} \sin^2 (\mu - \alpha) \right] \quad (13.4.21)$$

Let us now consider the contact of two surfaces, Σ_1 and Σ_2 , whose point of contact is M . The tangent plane is formed by axes η and ζ (fig. 13.4.4); $\mathbf{e}_I^{(1)}$ and $\mathbf{e}_I^{(2)}$ are the unit vectors of the principal directions of surfaces Σ_1 and Σ_2 , respectively; vector \overline{MP} and the surface unit normal \mathbf{n} determine the common normal section of both surfaces. The deviation from the tangent plane for point P ($|\overline{MP}| = \rho$) may be expressed in terms of the curvatures of both surfaces as follows:

$$2\ell^{(1)} = \rho^2 \left[\kappa_I^{(1)} \cos^2 (\mu - \alpha^{(1)}) + \kappa_{II}^{(1)} \sin^2 (\mu - \alpha^{(1)}) \right] \quad (13.4.22)$$

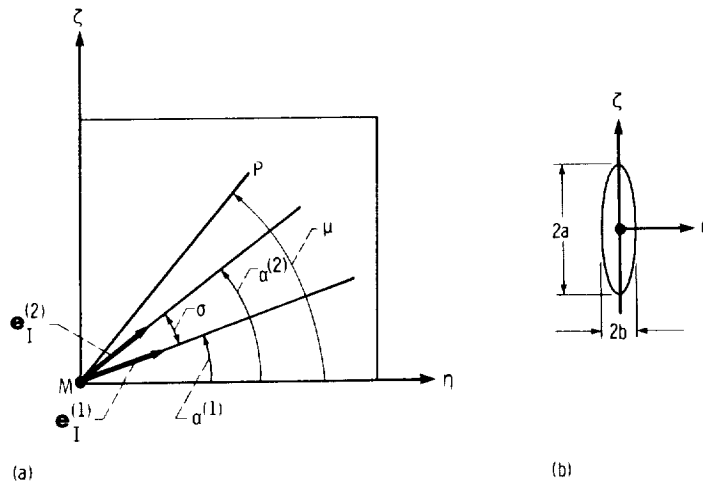


Figure 13.4.4.

$$2\ell^{(II)} = \rho^2 \left[\kappa_I^{(2)} \cos^2 (\mu - \alpha^{(2)}) + \kappa_{II}^{(2)} \sin^2 (\mu - \alpha^{(2)}) \right] \quad (13.4.23)$$

Here $\ell^{(j)}$ ($j = I, II$) is the deviation for point P of surface Σ_i ($i = 1, 2, \dots$).

It was mentioned earlier that at the edge of the area of deformation, the deviations ($\ell^{(I)}, \ell^{(II)}$) and the surface approach at $M(\delta)$ are related by equation (13.4.7). Equations (13.4.7), (13.4.22), and (13.4.23) yield

$$\rho^2 \left[\kappa_I^{(1)} \cos^2 (\mu - \alpha^{(1)}) + \kappa_{II}^{(1)} \sin^2 (\mu - \alpha^{(1)}) - \kappa_I^{(2)} \cos^2 (\mu - \alpha^{(2)}) - \kappa_{II}^{(2)} \sin^2 (\mu - \alpha^{(2)}) \right] = \pm 2\delta \quad (13.4.24)$$

Transforming equation (13.4.24) by using the expressions

$$\rho^2 = \eta^2 + \zeta^2 \quad \cos \mu = \frac{\eta}{\rho} \quad \sin \mu = \frac{\zeta}{\rho} \quad (13.4.25)$$

we obtain

$$\begin{aligned} & \eta^2 \left(\kappa_I^{(1)} \cos^2 \alpha^{(1)} + \kappa_{II}^{(1)} \sin^2 \alpha^{(1)} - \kappa_I^{(2)} \cos^2 \alpha^{(2)} - \kappa_{II}^{(2)} \sin^2 \alpha^{(2)} \right) \\ & + \zeta^2 \left(\kappa_I^{(1)} \sin^2 \alpha^{(1)} + \kappa_{II}^{(1)} \cos^2 \alpha^{(1)} - \kappa_I^{(2)} \sin^2 \alpha^{(2)} - \kappa_{II}^{(2)} \cos^2 \alpha^{(2)} \right) \\ & + \eta\zeta \left(g_1 \sin 2\alpha^{(1)} - g_2 \sin 2\alpha^{(2)} \right) = \pm 2\delta \end{aligned} \quad (13.4.26)$$

where

$$g_1 = \kappa_I^{(1)} - \kappa_{II}^{(1)} \quad g_2 = \kappa_I^{(2)} - \kappa_{II}^{(2)}$$

Angle $\alpha^{(1)}$ that determines the orientation of the coordinate axes η and ζ with respect to $\mathbf{e}_I^{(1)}$, may be chosen arbitrarily. For instance, $\alpha^{(1)}$ may be chosen as satisfying the equation

$$g_1 \sin 2\alpha^{(1)} - g_2 \sin 2\alpha^{(2)} = 0 \quad (13.4.27)$$

where (fig. 13.4.4)

$$\alpha^{(2)} = \alpha^{(1)} + \sigma \quad (13.4.28)$$

Equations (13.3.27) and (13.3.28) yield

$$\tan 2\alpha^{(1)} = \frac{g_2 \sin 2\sigma}{g_1 - g_2 \cos 2\sigma} \quad (13.4.29)$$

Equation (13.3.29) provides two solutions for $2\alpha^{(1)}$. We shall choose the solution represented by equations

$$\cos 2\alpha^{(1)} = \frac{g_1 - g_2 \cos 2\sigma}{\left(g_1^2 - 2g_1g_2 \cos 2\sigma + g_2^2 \right)^{1/2}} \quad (13.4.30)$$

and

$$\sin 2\alpha^{(1)} = \frac{g_2 \sin 2\sigma}{\left(g_1^2 - 2g_1g_2 \cos 2\sigma + g_2^2\right)^{1/2}} \quad (13.4.31)$$

Equations (13.3.30), (13.3.31), and (13.3.28) determine the orientation of axes η and ζ with respect to the principal directions of the contacting surfaces. These equations yield

$$\cos^2 \alpha^{(1)} = 0.5 \left[1 + m(g_1 - g_2 \cos 2\sigma) \right] \quad (13.4.32)$$

$$\sin^2 \alpha^{(1)} = 0.5 \left[1 - m(g_1 - g_2 \cos 2\sigma) \right] \quad (13.4.33)$$

$$\cos^2 \alpha^{(2)} = 0.5 \left[1 + m(g_1 \cos 2\sigma - g_2) \right] \quad (13.4.34)$$

$$\sin^2 \alpha^{(2)} = 0.5 \left[1 - m(g_1 \cos 2\sigma - g_2) \right] \quad (13.4.35)$$

where

$$m = \frac{1}{\left(g_1^2 - 2g_1g_2 \cos 2\sigma + g_2^2\right)^{1/2}} \quad (13.4.36)$$

Equations (13.4.26), (13.4.27), (13.4.32) to (13.4.36) yield

$$B\eta^2 + A\zeta^2 = \pm \delta \quad (13.4.37)$$

Here

$$A = \frac{1}{4} \left[\kappa_{\Sigma}^{(1)} - \kappa_{\Sigma}^{(2)} - \left(g_1^2 - 2g_1g_2 \cos 2\sigma + g_2^2\right)^{1/2} \right] \quad (13.4.38)$$

and

$$B = \frac{1}{4} \left[\kappa_{\Sigma}^{(1)} - \kappa_{\Sigma}^{(2)} + \left(g_1^2 - 2g_1g_2 \cos 2\sigma + g_2^2\right)^{1/2} \right] \quad (13.4.39)$$

Here

$$\kappa_{\Sigma}^{(i)} = \kappa_1^{(i)} + \kappa_{11}^{(i)} \quad g_i = \kappa_1^{(i)} - \kappa_{11}^{(i)}$$

Equation (13.4.37) confirms that the projection of the area of elastic deformations on the tangent plane is an ellipse whose axes coincide with axes η and ζ , respectively (fig. 13.4.4(b)). The axes of the ellipse are

$$2a = 2 \left| \frac{\delta}{A} \right|^{1/2} \quad 2b = 2 \left| \frac{\delta}{B} \right|^{1/2} \quad (13.4.40)$$

Example problem 13.4.1. A cone surface Σ_1 and a spherical surface Σ_2 are in contact at a single point M . Consider as given the approach of surfaces. Determine the dimensions and orientation of the contacting ellipse.

Solution. The cone surface is represented in the coordinate system S_f by equations which are similar to equations (8.4.14):

$$x_f^{(1)} = R \cot \psi_c - u \cos \psi_c \quad y_f^{(1)} = u \sin \psi_c \sin \theta \quad z_f^{(1)} = u \sin \psi_c \cos \theta \quad (13.4.41)$$

The spherical surface is represented in the coordinate system $S_0^{(2)}$ by equations which are similar to equations (8.4.11)

$$x_0^{(2)} = \rho \cos \mu \quad y_0^{(2)} = \rho \sin \mu \cos \phi \quad z_0^{(2)} = \rho \sin \mu \sin \phi \left(\rho < \frac{R}{\cos \psi_c} \right) \quad (13.4.42)$$

The superscripts 1 and 2 in equations (13.4.41) and (13.4.42) indicate surfaces Σ_1 and Σ_2 , respectively.

Point M of surface Σ_1 is represented in the coordinate system S_f by coordinates $x_f^{(1)} = 0$, $y_f^{(1)} = 0$, $z_f^{(1)} = R$. Considering these coordinates and equations (13.4.41) we find that $\theta = 0$ and $\mu = AM = R/\sin \psi_c$ for point M . Point M of Σ_2 is represented in coordinate system S_0 by coordinates $x_0^{(2)} = \rho \sin \psi_c$, $y_0^{(2)} = 0$, $z_0^{(2)} = \rho \cos \psi_c$. With these coordinates and equations (13.4.42), we find that $\mu = 90^\circ - \psi_c$ and $\phi = 90^\circ$ for point M .

Surface Σ_2 may be represented in the coordinate system S_f by the matrix equation

$$\begin{bmatrix} r_f^{(2)} \end{bmatrix} = \begin{bmatrix} M_{f0} \end{bmatrix} \begin{bmatrix} r_0^{(2)} \end{bmatrix} \quad (13.4.43)$$

where

$$\begin{bmatrix} M_{f0} \end{bmatrix} = \begin{bmatrix} 1 & 0 & 0 & -\rho \sin \psi_c \\ 0 & 1 & 0 & 0 \\ 0 & 0 & 1 & R - \rho \cos \psi_c \\ 0 & 0 & 0 & 1 \end{bmatrix} \quad (13.4.44)$$

Equations (13.4.42) to (13.4.44) yield

$$\begin{aligned} x_f^{(2)} &= \rho (\cos \mu - \sin \psi_c) & y_f^{(2)} &= \rho \sin \mu \cos \phi \\ z_f^{(2)} &= \rho (\sin \mu \sin \phi - \cos \psi_c) + R \end{aligned} \quad (13.4.45)$$

It is easy to verify that surfaces Σ_1 and Σ_2 , which are represented by equations (13.4.41) and (13.4.45), are indeed in contact at M , since at this point $\mathbf{r}_f^{(1)} = \mathbf{r}_f^{(2)}$ and the surface normals are collinear. Here $\mathbf{r}_f^{(i)}$ ($i = 1, 2$) is the position vector for the point of contact.

Let us now determine the contacting ellipse with equations (13.4.28) to (13.4.40).

The principal directions of the cone surface at point M may be represented by the unit vectors.

$$\begin{bmatrix} e_I^{(1)} \end{bmatrix} = \begin{bmatrix} 0 \\ -1 \\ 0 \end{bmatrix} \quad \begin{bmatrix} e_{II}^{(1)} \end{bmatrix} = \begin{bmatrix} \cos \psi_c \\ 0 \\ -\sin \psi_c \end{bmatrix}$$

We recall that one of the principal directions of the cone surface coincides with the cone generatrix. (The unit vector $\mathbf{e}_{II}^{(1)}$ of this principal direction is shown in figure 13.4.5.) The principal curvatures of the cone surface (with the chosen direction of the unit vector \mathbf{n}) are given by

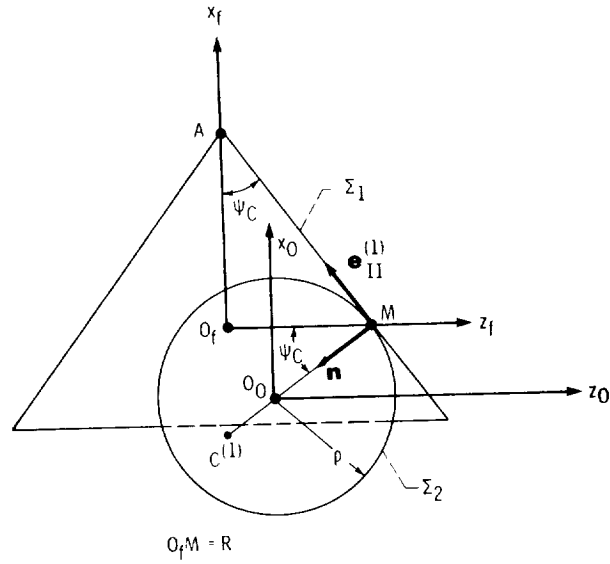


Figure 13.4.5.

$$\kappa_1^{(1)} = \frac{\cos \psi_c}{R} \quad \kappa_{II}^{(1)} = 0$$

The principal directions for a spherical surface may be chosen arbitrarily. Let us choose the same principal directions as that of Σ_1 . Thus $\sigma = 0$ (See fig. 13.4.4.) The principal curvatures of

the spherical surface are given by $\kappa_1^{(2)} = \kappa_{II}^{(2)} = \frac{1}{\rho}$. Thus,

$$\kappa_{\Sigma}^{(1)} = \frac{\cos \psi_c}{R} \quad g_1 = \frac{\cos \psi_c}{R} \quad \kappa_{\Sigma}^{(1)} = \frac{2}{\rho} \quad g_2 = 0.$$

Using equations (13.4.38) to (13.4.40), we obtain

$$A = -\frac{1}{2\rho} \quad B = \frac{1}{2} \left(\frac{\rho \cos \psi_c - R}{\rho R} \right)$$

$$a = (2\rho\delta)^{1/2} \quad b = \left(\frac{2\rho R\delta}{R - \rho \cos \psi_c} \right)^{1/2}$$

The major axis of the contacting ellipse is $2b$ and it is directed along $\mathbf{e}_I^{(1)}$.

Chapter 14

Pitch Surfaces

Limiting Contact Normal

14.1 Introduction

Although the term pitch surfaces (pitch cylinders, pitch cones) may be confusing, we have to apply it since it is widely used in the engineering literature. However, the term pitch surfaces denotes several types of surfaces that differ in a kinematical sense.

Consider a pair of spur or helical gears, both having parallel axes of rotation, in mesh (fig. 14.1.1(a)). The pitch circle is an imaginary circle that rolls without slipping over a pitch circle of a mating gear. The pitch circles are in tangency at the pitch point I . The pitch circles are the centrodes of mating gears, and the pitch point is the instantaneous center of rotation in the relative motion. (See ch. 2.1.) We have to differentiate between the pitch circles of standard and nonstandard gearing.

In the case of standard gearing, the centrodes of mating gears coincide with their pitch circles. The gear pitch circle is a reference circle and, in addition, it is the gear centrode in mesh with a rack (fig. 14.1.1(b)). The centrode of the rack is a straight line that is tangent to the gear centrode and is parallel to the direction of the rack translation.

In the case of nonstandard involute gears, we have to use two different terms, the operating pitch circles and merely pitch circles. The operating pitch circles are the centrodes of the mating gears while the pitch circle of the gear is its centrode in mesh with the rack. The operating gear pitch circles of gears and their pitch circles do not coincide. Figure 14.1.1(c) shows the operating pitch circles and the pitch circles for the case where $C' > C$. We emphasize that only the radius of the pitch circle but not the operating pitch circle may be expressed in terms of the standardized diametral pitch and the number of gear teeth. Thus,

$$r_p = \frac{N}{2P} \quad (14.1.2)$$

The radius of the operating pitch circle is represented by

$$r'_p = \frac{N}{2P'} \quad (14.1.2)$$

where P' is a nonstandardized diametral pitch.

Let us now consider bevel gears. In the case of standard bevel gears the pitch cones are the axodes (ch. 2.3), the loci of the instantaneous axes of rotation in the relative motion (fig. 14.1.2(a)). The line of tangency OI of the pitch cones is the instantaneous axis of rotation in the relative motion

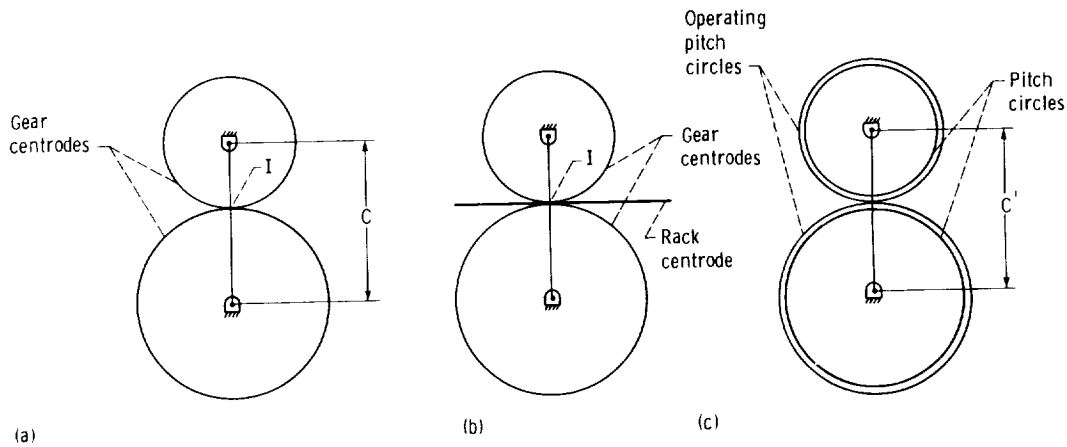


Figure 14.1.1.

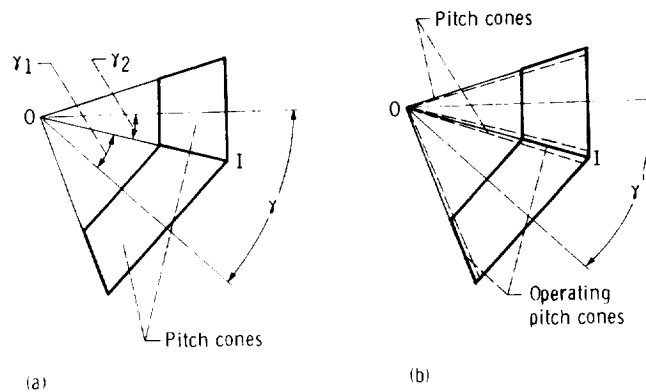


Figure 14.1.2.

and $\gamma = \gamma_1 + \gamma_2$, where γ_1 and γ_2 are the pitch cone angles. In the case of nonstandard bevel gears ($\gamma' \neq \gamma$) the axodes are the operating pitch cones and the pitch cones are not in tangency. The radii of the pitch cones (but not of the operating pitch cones) may be expressed in terms of standardized pitches.

Summarizing, we say that in the case of transformation of rotation between parallel and intersected axes, the operating pitch surfaces are the axodes and they coincide with the pitch surfaces in the case of standard gearing only.

Drives of helical gears with crossed axes, worm-gear drives and hypoid gears transform rotation between crossed axes. The gear axodes are two hyperboloids which roll as well as slide over each other. (See ch. 2.4 and fig. 2.4.) The operating pitch surfaces have nothing in common with the hyperboloids—they are cylinders (cones) with crossed axes in the case of worm-gear drives and helical gears (hypoid gears).

14.2 Operating Pitch Surfaces: Transformation of Rotation Between Crossed Axes

We define the operating pitch surfaces H_1 and H_2 as those surfaces that satisfy the following conditions:

- (1) The axis of rotation of the operating pitch surface coincide with the axis of the gear rotation.
- (2) Surfaces H_1 and H_2 are in tangency at the main contact point P (the pitch point) in the fixed coordinate system S_f .

(3) The relative velocity $\mathbf{v}^{(12)}$ is directed along the common tangent to the helices on the surfaces H_1 and H_2 . (In the case of transformation rotation between parallel and intersected axes the pitch point P belongs to the instantaneous axis of rotation and $\mathbf{v}^{(12)} = 0$).

The last two conditions may be represented by the following equations:

$$\mathbf{n}^{(i)} \bullet \mathbf{v}^{(12)} = 0 \quad (i = 1, 2) \quad (14.2.1)$$

$$[\mathbf{n}^{(i)} \boldsymbol{\omega}^{(i)} \mathbf{r}^{(i)}] = 0 \quad (i = 1, 2) \quad (14.2.2)$$

Here $\mathbf{n}^{(i)}$ is the pitch surface unit normal at P and $\mathbf{r}^{(i)}$ is a position vector drawn to the pitch point P from a point of the line of action of $\boldsymbol{\omega}^{(i)}$. Equation (14.2.1) yields that the operating pitch surfaces H_1 and H_2 have a common tangent plane at P and vector $\mathbf{v}^{(12)}$ lies in this plane.

Equation (14.2.2) is based on the following considerations: (1) the unit normal to H_i at the pitch point P intersects the axis of rotation of H_i (the line of action of $\boldsymbol{\omega}^{(i)}$), since H_i is a surface of revolution. (2) The position vector $\mathbf{r}^{(i)}$ also intersects the axis of rotation. (3) Vectors $\mathbf{n}^{(i)}$, $\mathbf{r}^{(i)}$ and $\boldsymbol{\omega}^{(i)}$ belong to the same plane drawn through the pitch point P and the points of intersection of vectors $\mathbf{n}^{(i)}$ and $\boldsymbol{\omega}^{(i)}$, and $\mathbf{r}^{(i)}$ and $\boldsymbol{\omega}^{(i)}$.

Equations (14.2.1) and (14.2.2) determine the operating pitch surface only locally, within the neighborhood of the pitch point P . This small area of the operating pitch surface may be represented as an area of a cone or a cylinder because of the angle formed by vectors $\mathbf{n}^{(i)}$ and $\boldsymbol{\omega}^{(i)}$. The operating pitch surfaces are usually chosen in the same way as the pitch surfaces of the gears. The operating pitch surfaces of the helical gears (with crossed axes), the worm, and of the worm gear are cylinders; the operating pitch surfaces of hypoid gears are cones.

It was mentioned above that in the case of crossed gear axes the operating pitch surfaces do not coincide with the gear axodes. The gear tooth surface Σ_i and the operating pitch surface H_i intersect each other. The gear tooth surfaces Σ_1 and Σ_2 are to be in tangency at the pitch point P and their common normal $\mathbf{n}^{(\Sigma_i)}$ and the relative velocity $\mathbf{v}^{(12)}$ must be perpendicular to each other; that is

$$\mathbf{n}^{(\Sigma_i)} \bullet \mathbf{v}^{(12)} = 0 \quad (14.2.3)$$

If equation (14.2.3) is satisfied, the gears, with surfaces Σ_1 and Σ_2 , being in contact within the neighborhood of P will transform rotation about the crossed axes with the prescribed angular velocity ratio.

14.3 Helical Gears with Crossed Axes and Worm-Gear Drives: Operating Pitch Surfaces

The operating pitch surfaces are two cylinders of radii $r_p^{(1)}$ and $r_p^{(2)}$ with crossed axes and the pitch point P is located at the line of the shortest distance between the axes of the cylinders (fig. 14.3.1(a)). Point P is the point of tangency of the pitch cylinders. Points P_1 and P_2 of these cylinders coincide with each other forming the common point P .

Let us draw a common tangent plane Π to the cylinders that pass through P . The straight line $t-t$ lies in Π and it is a tangent to the helices on the cylinders (fig. 14.3.1(b) and fig. 14.3.2(a)). Such a helix is the line of intersection of the gear tooth surface with the operating pitch cylinder.

Figure 14.3.2(a),(b) shows two pitch cylinders of helical gears with the crossing angle γ formed by vectors $\boldsymbol{\omega}^{(1)}$ and $\boldsymbol{\omega}^{(2)}$. The gears are provided with left-handed screw surfaces Σ_1 and Σ_2 . Surfaces Σ_1 and Σ_2 are in tangency at P . Vectors $\mathbf{v}^{(1)}$ and $\mathbf{v}^{(2)}$ represent the velocities of points

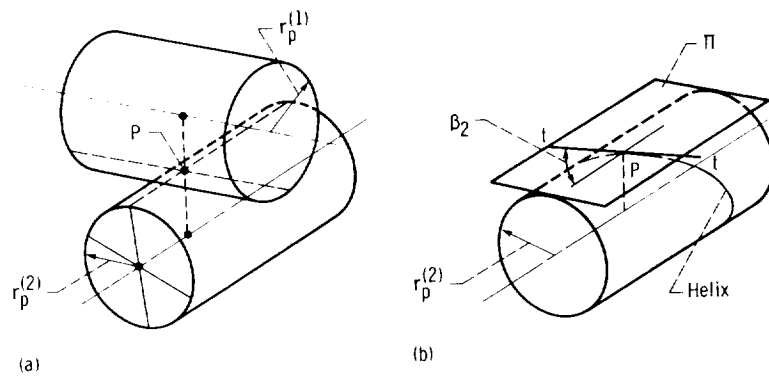


Figure 14.3.1.

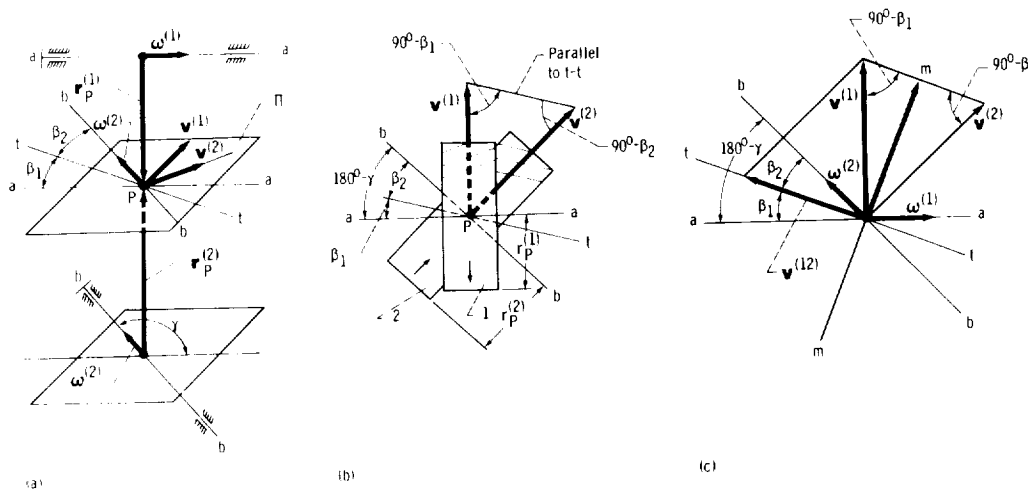


Figure 14.3.2.

P_1 and P_2 , respectively. Because of the continuance of tangency within the neighborhood of P , the velocities $\mathbf{v}^{(1)}$ and $\mathbf{v}^{(2)}$ must be related as follows:

(1) The relative velocity

$$\mathbf{v}^{(12)} = \mathbf{v}^{(1)} - \mathbf{v}^{(2)}$$

is to be directed along $t-t$. Vector $\mathbf{v}^{(12)}$ is the velocity of sliding at P .

(2) Projections of vectors $\mathbf{v}^{(1)}$ and $\mathbf{v}^{(2)}$ on line $m-m$ (fig. 14.3.2(c)) must be of the same direction and have the same magnitude (Line $m-m$ is perpendicular to $t-t$.)

Consider the velocity polygon shown in figure 14.3.2(c). The crossing angle γ which is formed by vectors $\omega^{(1)}$ and $\omega^{(2)}$, is given by (fig. 14.3.2(a))

$$\gamma = 180^\circ - (\beta_1 + \beta_2) \quad (14.3.1)$$

Velocities $\mathbf{v}^{(1)}$ and $\mathbf{v}^{(2)}$ of points P_1 and P_2 are represented by

$$\mathbf{v}^{(1)} = \omega^{(1)} \times \mathbf{r}_p^{(1)} \quad \mathbf{v}^{(2)} = \omega^{(2)} \times \mathbf{r}_p^{(2)} \quad (14.3.2)$$

Here

$$|\mathbf{v}^{(i)}| = \omega^{(i)} r_p^{(i)} \quad (i = 1, 2) \quad (14.3.3)$$

Since projections of $\mathbf{v}^{(1)}$ and $\mathbf{v}^{(2)}$ on $m-m$ must be of the same direction and have the same magnitude, we obtain

$$v^{(1)} \cos \beta_1 = v^{(2)} \cos \beta_2 \quad (14.3.4)$$

Equations (14.3.3) and (14.3.4) yield

$$m_{12} = \frac{\omega^{(1)}}{\omega^{(2)}} = \frac{r_p^{(2)} \cos \beta_2}{r_p^{(1)} \cos \beta_1} \quad (14.3.5)$$

Unlike the case of spur gears or helical gears with parallel axes, the prescribed ratio m_{12} can be satisfied with a various ratio $r_p^{(2)}/r_p^{(1)}$.

The magnitude of sliding velocity is given by (fig. 14.3.2)

$$|\mathbf{v}^{(12)}| = \omega^{(1)} r_p^{(1)} \sin \beta_1 + \omega^{(2)} r_p^{(2)} \sin \beta_2 \quad (14.3.6)$$

Mating helical gears with crossed axes are usually of the same hand as is shown in fig. 14.3.2. Figure 14.3.3 shows helical gears with crossed axes having opposite hands. Considerations similar to the ones discussed above yield that (fig. 14.3.3)

(1) The crossing angle is

$$\gamma = 180^\circ - (\beta_1 - \beta_2) \quad (14.3.7)$$

(2) The projections of vectors $\mathbf{v}^{(1)}$ and $\mathbf{v}^{(2)}$ on line $m-m$ have the same direction and magnitude, (fig. 14.3.3(c)) and the angular velocity ratio is represented by equation (14.3.5) and

(3) The magnitude of the sliding velocity is given by

$$|\mathbf{v}^{(12)}| = |\omega^{(1)} r_p^{(1)} \sin \beta_1 - \omega^{(2)} r_p^{(2)} \sin \beta_2| \quad (14.3.8)$$

Let us differentiate between standard and nonstandard involute helical gears. The pitch cylinders of standard helical gears are the gear axodes in mesh with the rack cutter. The velocity of translation of the rack cutter (v) and the angular velocity of the gear (ω) are related by

$$v = \omega r_p^* \quad (14.3.9)$$

where r_p^* is the radius of the pitch cylinder of a standard helical gear.

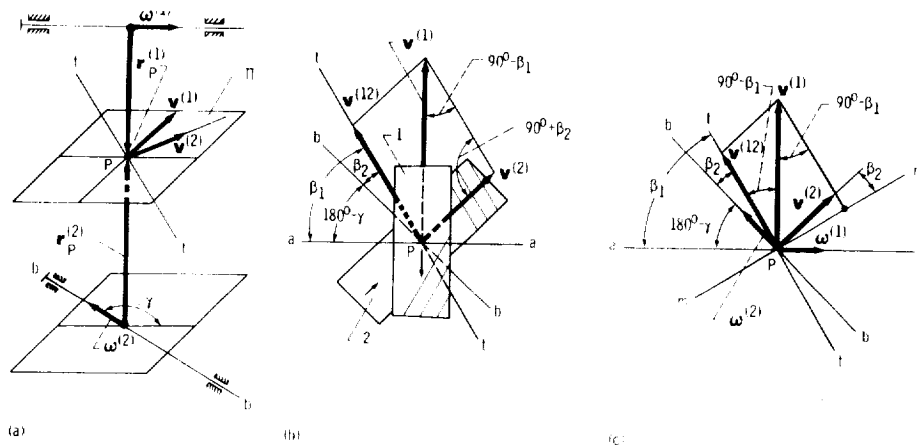


Figure 14.3.3.

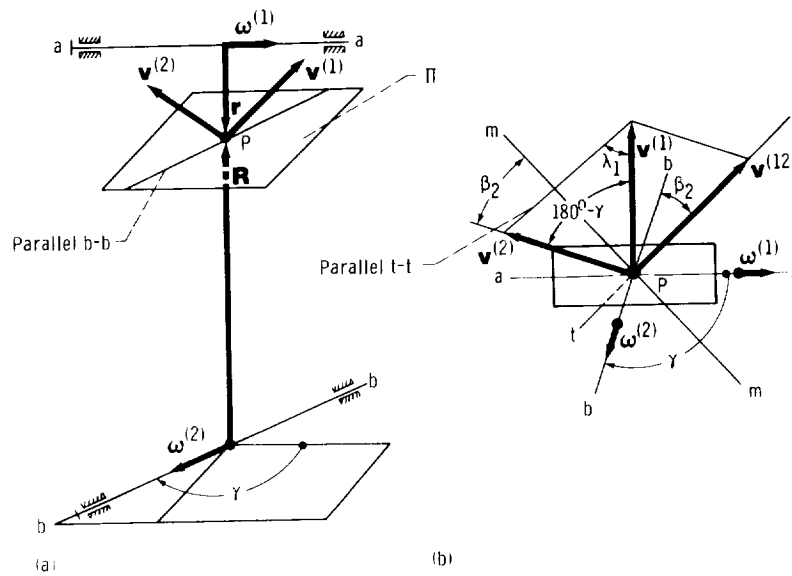


Figure 14.3.4.

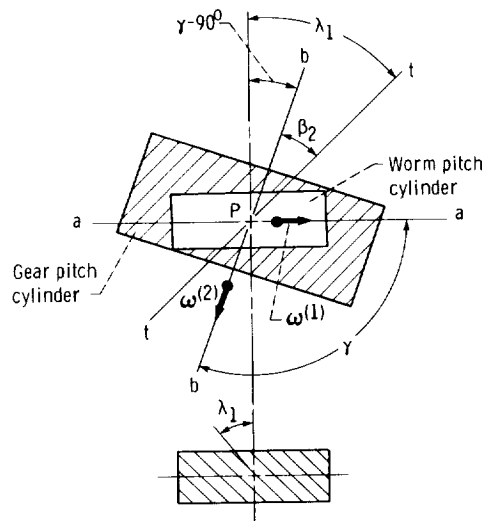


Figure 14.3.5.

The center distance of helical gears is equal to the sum of the radii of the pitch cylinders in the case of standard helical gears. Nonstandard helical gears are generated by special settings of rack cutters and the change of the center distance depends on these settings.

The above derived equations may also be used for the worm-gear drives with cylindrical worms. A worm may be considered as a helical gear for which the number of teeth is equal to the number of worm threads. The pitch point P is located on the line of shortest distance between the crossed axes of the worm and the worm gear. The operating pitch cylinders of the worm and the worm gear are two cylinders that are in tangency at P (fig. 14.3.4 (a); fig. 14.3.5). The radii of pitch cylinders are r and R , respectively.

Plane Π (fig. 14.3.4(a)) is tangent to the pitch cylinders at P . The helices on the pitch cylinders have a common tangent ($t-t$) at P which lies in plane π . Points P_1 and P_2 of both pitch cylinders coincide with each other at the point of tangency P . The worm and the worm gear rotate about

axes $a-a$ and $b-b$ with angular velocities $\omega^{(1)}$ and $\omega^{(2)}$, respectively. The velocity of points P_1 and P_2 are represented by equations

$$\mathbf{v}^{(1)} = \boldsymbol{\omega}^{(1)} \times \mathbf{r} \quad \mathbf{v}^{(2)} = \boldsymbol{\omega}^{(2)} \times \mathbf{R} \quad (14.3.10)$$

Similar to the previous discussions we may state that

- (1) The relative velocity $\mathbf{v}^{(12)}$ (the sliding velocity) must be directed along the tangent $t-t$
- (2) The projections of velocities $\mathbf{v}^{(1)}$ and $\mathbf{v}^{(2)}$ on line $m-m$ (it is perpendicular to $t-t$) must be of the same direction and have the same magnitude.

The velocity polygon (fig. 14.3.4(b)) yields

$$v^{(1)} \sin \lambda_1 = v^{(2)} \cos \beta_2 \quad (14.3.10(a))$$

It is evident from figure 14.3.5 that

$$\beta_2 = \lambda_1 - (\gamma - 90^\circ) = 90^\circ - (\gamma - \lambda_1) \quad (14.3.11)$$

Here λ_1 is the lead angle on the worm pitch cylinder represented by

$$\lambda_1 = \arctan \left(\frac{h}{r} \right) \quad (14.3.12)$$

where h is the screw parameter ($h > 0$ for a right-handed worm)

$$v^{(1)} = \omega^{(1)} r \quad v^{(2)} = \omega^{(2)} R \quad (14.3.13)$$

Equations (14.3.10(a)), (14.3.11), and (14.3.13) yield

$$m_{21} = \frac{\omega^{(2)}}{\omega^{(1)}} = \frac{r \sin \lambda_1}{R \sin (\gamma - \lambda_1)} \quad (14.3.14)$$

We have considered a worm-gear drive with a right-handed worm. Figure 14.3.6 shows the pitch cylinders and the velocity polygon for a worm-gear drive with a left-handed worm. Derivations

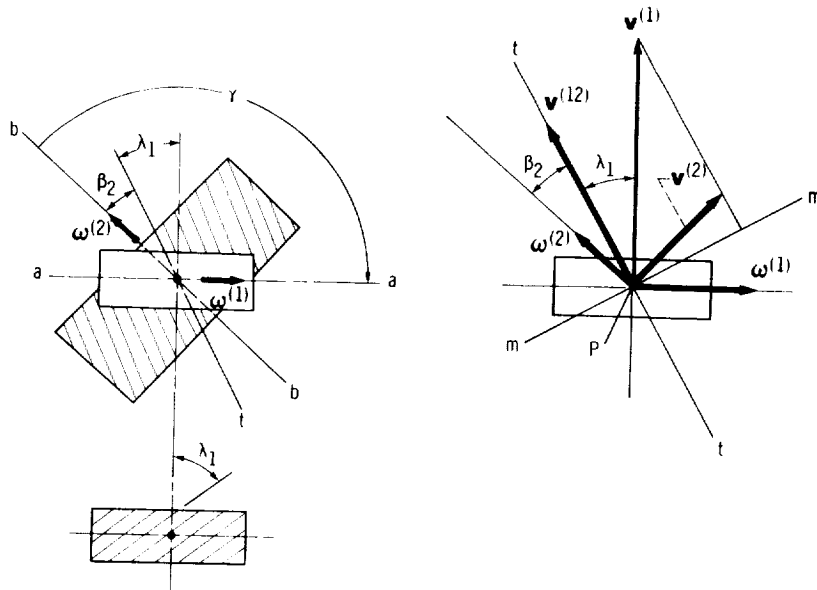


Figure 14.3.6.

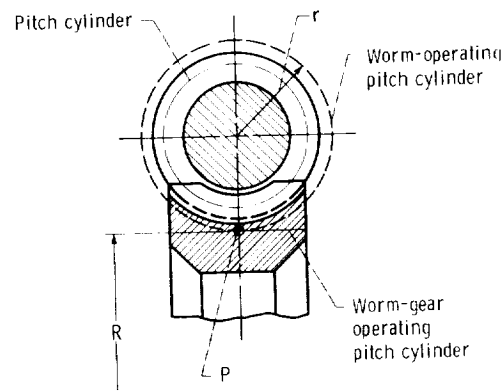


Figure 14.3.7.

based on analysis similar to the one discussed above yield

$$\gamma - 90^\circ = \lambda_1 + \beta_2$$

Thus

$$\beta_2 = (\gamma - \lambda_1) - 90^\circ \quad (14.3.15)$$

and

$$v^{(1)} \sin \lambda_1 = v^{(2)} \cos \beta_2 \quad (14.3.16)$$

Equations (14.3.15) and (14.3.16) yield

$$\omega^{(1)} r \sin \lambda_1 = \omega^{(2)} R \sin (\gamma - \lambda_1) \quad (14.3.17)$$

The lead angle λ_1 , if represented by equation (14.3.12), has a definite sense which depends on the sense of the screw parameter h ($h < 0$ for a left-handed worm). Taking into account that the worm thread is left-handed, and that the screw parameter h and λ_1 are negative, we obtain from equation (14.3.17) that

$$m_{21} = - \frac{r \sin \lambda_1}{R \sin (\gamma + \lambda_1)} \quad (14.3.18)$$

The general expression for the ratio m_{21} may be given by

$$m_{21} = \pm \frac{r \sin \lambda_1}{R \sin (\gamma \mp \lambda_1)} \quad (14.3.19)$$

The upper sign corresponds to a worm-gear drive with a right-handed thread of the worm.

Let us differentiate between standard and nonstandard worm-gear drives. The operating pitch cylinder of the worm of a nonstandard worm-gear drive does not coincide with the pitch cylinder of the worm. The pitch of the worm is given on the pitch cylinder and the addendum and dedendum of the worm are measured from the worm pitch cylinder. The cross section of a nonstandard worm-gear drive is shown in figure 14.3.7. The pitch point P is out of the worm pitch cylinder. However, it is located on the line of the shortest distance between the worm and the worm gear. Nonstandard worm-gear drives are applied to improve the conditions of meshing.

14.4 Hypoid Gears: Operating Pitch Surfaces

Basic Equations

Unlike the helical gears and worm-gear drives, the pitch point P of hypoid gears is located offset of the line of the shortest distance, and the operating pitch surfaces are two cones (fig. 14.4.1).

Let us derive equations which relate parameters of the operating pitch cones with the coordinates of the pitch point. These equations were derived by Baxter (1961), Litvin (1968), and Litvin, Petrov, and Ganshin (1974).

We set up the following three coordinate systems: $S_1(x_1, y_1, z_1)$ and $S_2(x_2, y_2, z_2)$ rigidly connected to gears 1 and 2, respectively, and S_f rigidly connected to the frame (fig. 14.4.2). The origins O_1 and O_2 are the apices of the pitch cones; z_1 and z_2 are the axes of gear rotation (we will limit the discussion to the crossing angle of 90°); d_1 and d_2 determines the location of the cone apices; C is the shortest distance between the gear axes of rotation; and P is the pitch point. The pitch cones are in tangency at point P . The plane drawn through points O_1 , O_2 , and P is the pitch plane; O_1P and O_2P are the lines of tangency of the pitch cones with the pitch plane.

We represent the equations of the pitch cone in the coordinate system S_i as follows (fig. 14.4.3):

$$x_i = u_i \sin \gamma_i \cos \theta_i \quad y_i = u_i \sin \gamma_i \sin \theta_i \quad z_i = u_i \cos \gamma_i \quad (i = 1, 2) \quad (14.4.1)$$

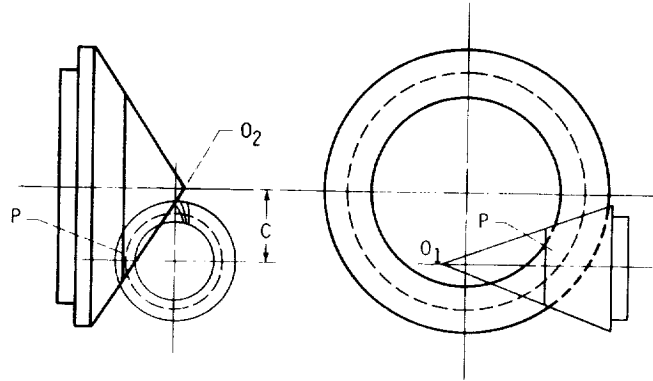


Figure 14.4.1.

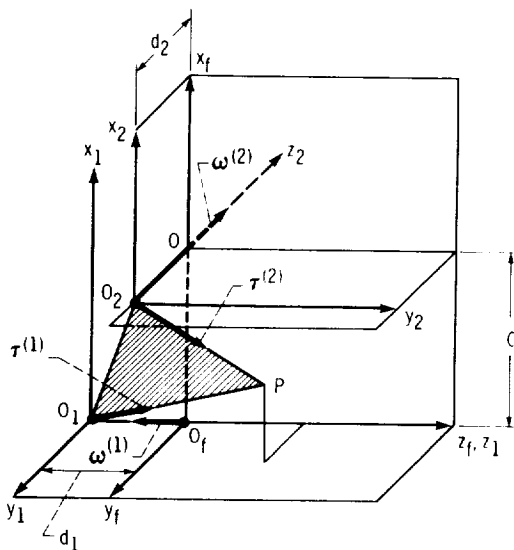


Figure 14.4.2.

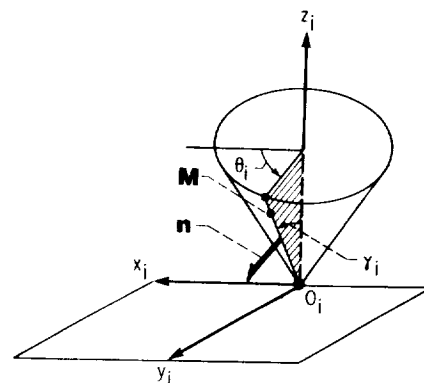


Figure 14.4.3.

Here θ_i and $u_i = |\overline{O_iM}|$ are the surface coordinates, and γ_i is the angle formed by the cone generatrix and the cone axis.

The unit normal to the cone surface is given by

$$\mathbf{n}_i = \frac{\mathbf{N}_i}{|\mathbf{N}_i|} \quad \mathbf{N}_i = \frac{\partial \mathbf{r}_i}{\partial \theta_i} \times \frac{\partial \mathbf{r}_i}{\partial u_i} \quad (14.4.2)$$

Equations (14.4.1) and (14.4.2) yield (provided $u_i \sin \gamma_i \neq 0$)

$$n_{xi} = \cos \theta_i \cos \gamma_i \quad n_{yi} = \sin \theta_i \cos \gamma_i \quad n_{zi} = -\sin \gamma_i \quad (14.4.3)$$

Equations of the pitch cones and the surface unit normals are represented in coordinate system S_f by the following matrix equations

$$\begin{bmatrix} r_f^{(1)} \end{bmatrix} = \begin{bmatrix} M_{f1} \end{bmatrix} \begin{bmatrix} r_1 \end{bmatrix} \quad (14.4.4)$$

$$\begin{bmatrix} n_f^{(1)} \end{bmatrix} = \begin{bmatrix} L_{f1} \end{bmatrix} \begin{bmatrix} n_1 \end{bmatrix} \quad (14.4.5)$$

$$\begin{bmatrix} r_f^{(2)} \end{bmatrix} = \begin{bmatrix} M_{f2} \end{bmatrix} \begin{bmatrix} r_2 \end{bmatrix} \quad (14.4.6)$$

$$\begin{bmatrix} n_f^{(2)} \end{bmatrix} = \begin{bmatrix} L_{f2} \end{bmatrix} \begin{bmatrix} n_2 \end{bmatrix} \quad (14.4.7)$$

Here

$$\begin{bmatrix} M_{f1} \end{bmatrix} = \begin{bmatrix} 1 & 0 & 0 & 0 \\ 0 & 1 & 0 & 0 \\ 0 & 0 & 1 & -d_1 \\ 0 & 0 & 0 & 1 \end{bmatrix} \quad (14.4.8)$$

$$\begin{bmatrix} M_{f2} \end{bmatrix} = \begin{bmatrix} 1 & 0 & 0 & C \\ 0 & 0 & -1 & d_2 \\ 0 & 1 & 0 & 0 \\ 0 & 0 & 0 & 1 \end{bmatrix} \quad (14.4.9)$$

Matrix $[L_{fi}]$ may be derived from matrix $[M_{fi}]$ by deleting the last column and row. Equations (14.4.1) to (14.4.9) yield

$$\begin{bmatrix} r_f^{(1)} \end{bmatrix} = \begin{bmatrix} u_1 \sin \gamma_1 \cos \theta_1 \\ u_1 \sin \gamma_1 \sin \theta_1 \\ u_1 \cos \gamma_1 - d_1 \\ 1 \end{bmatrix} \quad (14.4.10)$$

$$\begin{bmatrix} n_f^{(1)} \end{bmatrix} = \begin{bmatrix} \cos \theta_1 \cos \gamma_1 \\ \sin \theta_1 \cos \gamma_1 \\ -\sin \gamma_1 \end{bmatrix} \quad (14.4.11)$$

$$\begin{bmatrix} r_f^{(2)} \end{bmatrix} = \begin{bmatrix} u_2 \sin \gamma_2 \cos \theta_2 + C \\ -u_2 \cos \gamma_2 + d_2 \\ u_2 \sin \gamma_2 \sin \theta_2 \\ 1 \end{bmatrix} \quad (14.4.12)$$

$$\begin{bmatrix} n_f^{(2)} \end{bmatrix} = \begin{bmatrix} \cos \theta_2 \cos \gamma_2 \\ \sin \gamma_2 \\ \sin \theta_2 \cos \gamma_2 \end{bmatrix} \quad (14.4.13)$$

Since the pitch cones are in tangency at the point P the following equations must be satisfied

$$\begin{bmatrix} r_f^{(1)} \end{bmatrix} = \begin{bmatrix} r_f^{(2)} \end{bmatrix} = \begin{bmatrix} r_f^{(P)} \end{bmatrix} \quad (14.4.14)$$

$$\begin{bmatrix} n_f^{(1)} \end{bmatrix} = - \begin{bmatrix} n_f^{(2)} \end{bmatrix} \quad (14.4.15)$$

(Here $[r_f^{(P)}]$ represents the pitch point P .) We have derived equation (14.4.15) taking into account that the pitch cones are located above and below the pitch plane, and that the surface unit normals are directed opposite to each other.

Equations (14.4.14) and (14.4.15) yield

$$u_1 \sin \gamma_1 \cos \theta_1 = u_2 \sin \gamma_2 \cos \theta_2 + C = x_f^{(P)} \quad (14.4.16)$$

$$u_1 \sin \gamma_1 \sin \theta_1 = -u_2 \cos \gamma_2 + d_2 = y_f^{(P)} \quad (14.4.17)$$

$$u_1 \cos \gamma_1 - d_1 = u_2 \sin \gamma_2 \sin \theta_2 = z_f^{(P)} \quad (14.4.18)$$

$$\cos \theta_1 \cos \gamma_1 = -\cos \theta_2 \cos \gamma_2 \quad (14.4.19)$$

$$\sin \theta_1 \cos \gamma_1 = -\sin \gamma_2 \quad (14.4.20)$$

$$\sin \gamma_1 = \sin \theta_2 \cos \gamma_2 \quad (14.4.21)$$

The system of equations (14.4.19) to (14.4.21) consists of only two independent equations because

$$\left| \mathbf{n}_f^{(1)} \right| = \left| \mathbf{n}_f^{(2)} \right| = 1 \quad (14.4.22)$$

The radius of the cone circle which passes through P may be represented as follows (fig. 14.4.3):

$$u_i \sin \gamma_i = r_i \quad (i = 1, 2)$$

Equations (14.4.16) to (14.4.18) and (14.4.23) yield

$$r_1 \cos \theta_1 = r_2 \cos \theta_2 + C = x_f^{(P)} \quad (14.4.24)$$

$$r_1 \sin \theta_1 = -r_2 \cot \gamma_2 + d_2 = y_f^{(P)} \quad (14.4.25)$$

$$r_1 \cot \gamma_1 - d_1 = r_2 \sin \theta_2 = z_f^{(P)} \quad (14.4.26)$$

Equations (14.4.24) to (14.4.26) and two equations of the system (14.4.19) to (14.4.21) represent the basic system of eight equations, that relate the parameters of the pitch cones, the surface coordinates, and the coordinates of the pitch point. The eleven parameters are the following: r_1 , θ_1 , r_2 , θ_2 , d_1 , d_2 , γ_1 , γ_2 , $x_f^{(P)}$, $y_f^{(P)}$, and $z_f^{(P)}$. Considering three of the parameters from the above set as given, we may determine the remaining eight parameters.

Relations Between Cone Parameters

Let us derive equations that relate the six cone parameters r_1 , r_2 , d_1 , d_2 , γ_1 , and γ_2 . Equations (14.4.25) and (14.4.20) yield

$$-r_2 \cot \gamma_2 + d_2 = r_1 \sin \theta_1 = -r_1 \frac{\sin \gamma_2}{\cos \gamma_1} \quad (14.4.27)$$

Rearranging equations (14.2.27), we get

$$r_2 \cot \gamma_2 \cos \gamma_1 - d_2 \cos \gamma_1 - r_1 \sin \gamma_2 = 0 \quad (14.4.28)$$

From equations (14.4.26) and (14.4.21), we get

$$r_2 \cot \gamma_1 - d_1 = r_2 \sin \theta_2 = r_2 \frac{\sin \gamma_1}{\cos \gamma_2} \quad (14.4.29)$$

Thus

$$r_1 \cot \gamma_1 \cos \gamma_2 - d_1 \cos \gamma_2 - r_2 \sin \gamma_1 = 0 \quad (14.4.30)$$

With equations (14.4.24), (14.4.20), and (14.4.21), we get

$$\begin{aligned} r_1^2(1 - \sin^2 \theta_1) - r_2^2(1 - \sin^2 \theta_2) - 2Cr_2 \cos \theta_2 - C^2 = \\ \frac{r_1^2(\cos^2 \gamma_1 - \sin^2 \gamma_2)}{\cos^2 \gamma_1} - \frac{r_2^2(\cos^2 \gamma_2 - \sin^2 \gamma_1)}{\cos^2 \gamma_2} - C^2 - 2Cr_2 \cos \theta_2 = 0 \end{aligned}$$

Thus

$$\begin{aligned} \left[\frac{r_1^2(\cos^2 \gamma_1 - \sin^2 \gamma_2)}{\cos^2 \gamma_1} - \frac{r_2^2(\cos^2 \gamma_2 - \sin^2 \gamma_1)}{\cos^2 \gamma_2} - C^2 \right]^2 \\ - 4C^2 r_2^2 \left(\frac{\cos^2 \gamma_2 - \sin^2 \gamma_1}{\cos^2 \gamma_2} \right) = 0 \end{aligned} \quad (14.4.31)$$

Three equations (14.4.28), (14.4.30), and (14.4.31) relate six cone parameters. Considering three of these parameters as given, we may determine the remaining three.

It is easy to verify that the cone angles must satisfy the inequality

$$\gamma_1 + \gamma_2 < 90^\circ \quad (14.4.32)$$

if the crossing angle is 90° . From equations (14.4.20) and (14.4.21), we see that since

$$\sin \theta_2 = \frac{\sin \gamma_1}{\cos \gamma_2} \quad \sin \theta_2 \leq 1 \quad (14.4.33)$$

$$\sin \theta_1 = \frac{-\sin \gamma_2}{\cos \gamma_1} \quad |\sin \theta_1| \leq 1 \quad (14.4.34)$$

the following inequalities must be satisfied

$$\frac{\sin \gamma_1}{\cos \gamma_2} \leq 1 \quad \frac{\sin \gamma_2}{\cos \gamma_1} \leq 1 \quad (14.4.35)$$

Inequalities (14.4.35) yield

$$\sin \gamma_1 \leq \sin (90^\circ - \gamma_2) \quad \sin \gamma_2 \leq \sin (90^\circ - \gamma_1) \quad (14.4.36)$$

and

$$\gamma_1 + \gamma_2 \leq 90^\circ \quad (14.4.37)$$

From equation (14.4.31) we obtain that the equality $\gamma_1 + \gamma_2 = 90^\circ$ may be satisfied only if $C = 0$. Since the center distance of hypoid gears $C \neq 0$, the final relation between γ_1 and γ_2 is

$$\gamma_1 + \gamma_2 < 90^\circ \quad (14.4.38)$$

There is an alternative system of equations that relate the pitch cone parameters. Consider that C , γ_2 , r_2 and $\gamma_1 < 90^\circ - \gamma_2$ are given. We may then determine the remaining parameters d_1 , d_2 , and r_1 by using the following procedure for computations:

$$\sin \theta_1 = -\frac{\sin \gamma_2}{\cos \gamma_1} \quad (14.4.39)$$

$$\sin \theta_2 = \frac{\sin \gamma_1}{\cos \gamma_2} \quad \cos \theta_2 = -\cos \theta_1 \frac{\cos \gamma_1}{\cos \gamma_2} \quad (14.4.40)$$

$$r_1 = \frac{C + r_2 \cos \theta_2}{\cos \theta_1} \quad (14.4.41)$$

$$d_2 = r_1 \sin \theta_1 + r_2 \cot \gamma_2 \quad (14.4.42)$$

$$d_1 = r_1 \cot \gamma_1 - r_2 \sin \theta_2 \quad (14.4.43)$$

(See eqs. (14.4.19) to (14.4.26).)

Pitch Point Coordinates

Knowing the pitch cone parameters, we may represent the coordinates of the pitch point as follows: (See eqs. (14.4.24) to (14.4.26).)

$$y_f^{(P)} = -r_2 \cot \gamma_2 + d_2 \quad (14.4.44)$$

$$z_f^{(P)} = r_1 \cot \gamma_1 - d_1 \quad (14.4.45)$$

$$x_f^{(P)} = \pm \sqrt{r_1^2 - (y_f^{(P)})^2} \quad (14.4.46)$$

Pitch Plane Orientation

The pitch plane passes through points O_1 , O_2 , and P (fig. 14.4.2). The pitch cones and the pitch plane have a common normal at point P because they are in tangency at P . Therefore, the unit normal to the pitch plane ($\mathbf{n}_f^{(P)}$) may be determined as the normal to the pitch cone 1 at point P . Equations (14.4.11) and (14.2.24) to (14.4.26) yield

$$\begin{aligned} \mathbf{n}_f^{(P)} &= \cos \theta_1 \cos \gamma_1 \mathbf{i}_f + \sin \theta_1 \cos \gamma_1 \mathbf{j}_f - \sin \gamma_1 \mathbf{k}_f \\ &= \frac{\cos \gamma_1}{r_1} (x_f^{(P)} \mathbf{i}_f + y_f^{(P)} \mathbf{j}_f) - \sin \gamma_1 \mathbf{k}_f \end{aligned} \quad (14.4.47)$$

The Tooth's Longitudinal Shape

We begin with the determination of the unit vectors of the generatrices O_1P and O_2P (fig. 14.4.2). We designate these unit vectors by $\boldsymbol{\tau}^{(1)}$ and $\boldsymbol{\tau}^{(2)}$. Equations (14.4.10) and (14.4.12) yield

$$\boldsymbol{\tau}^{(1)} = \frac{\overline{O_1P}}{|\overline{O_1P}|} = \frac{\frac{\partial \mathbf{r}_f^{(1)}}{\partial u_1}}{\left| \frac{\partial \mathbf{r}_f^{(1)}}{\partial u_1} \right|} = \sin \gamma_1 (\cos \theta_1 \mathbf{i}_f + \sin \theta_1 \mathbf{j}_f) + \cos \gamma_1 \mathbf{k}_f \quad (14.4.48)$$

and

$$\boldsymbol{\tau}^{(2)} = \frac{\overline{O_2P}}{|\overline{O_2P}|} = \frac{\frac{\partial \mathbf{r}_f^{(2)}}{\partial u_2}}{\left| \frac{\partial \mathbf{r}_f^{(2)}}{\partial u_2} \right|} = \sin \gamma_2 \cos \theta_2 \mathbf{i}_f - \cos \gamma_2 \mathbf{j}_f + \sin \gamma_2 \sin \theta_2 \mathbf{k}_f \quad (14.4.49)$$

The unit vectors $\boldsymbol{\tau}^{(1)}$ and $\boldsymbol{\tau}^{(2)}$ form an angle η (figs. 14.4.2 and 14.4.4) given by the equation $\cos \eta = \boldsymbol{\tau}^{(1)} \cdot \boldsymbol{\tau}^{(2)}$.

Equations (14.4.48), (14.4.49), and (14.4.19) to (14.4.21) yield

$$\cos \eta = \tan \gamma_1 \tan \gamma_2 \quad (14.4.50)$$

Let us now determine the relative velocity vector $\mathbf{v}^{(12)}$ at the point P shown in fig. 14.4.2

$$\mathbf{v}^{(12)} = \mathbf{v}^{(1)} - \mathbf{v}^{(2)} = \boldsymbol{\omega}^{(1)} \times \mathbf{r}_f^{(P)} - \left(\boldsymbol{\omega}^{(2)} \times \mathbf{r}_f^{(P)} + \overline{O_fO} \times \boldsymbol{\omega}^{(2)} \right)$$

$$\begin{aligned}
&= \begin{vmatrix} \mathbf{i}_f & \mathbf{j}_f & \mathbf{k}_f \\ 0 & 0 & -\omega^{(1)} \\ x_f^{(P)} & y_f^{(P)} & z_f^{(P)} \end{vmatrix} - \begin{vmatrix} \mathbf{i}_f & \mathbf{j}_f & \mathbf{k}_f \\ 0 & -\omega^{(2)} & 0 \\ x_f^{(P)} & y_f^{(P)} & z_f^{(P)} \end{vmatrix} - \begin{vmatrix} \mathbf{i}_f & \mathbf{j}_f & \mathbf{k}_f \\ C & 0 & 0 \\ 0 & -\omega^{(2)} & 0 \end{vmatrix} \\
&= \left(\omega^{(1)} y_f^{(P)} + \omega^{(2)} z_f^{(P)} \right) \mathbf{i}_f - \omega^{(1)} x_f^{(P)} \mathbf{j}_f - \omega^{(2)} \left(x_f^{(P)} - C \right) \mathbf{k}_f
\end{aligned} \tag{14.4.51}$$

Vector $\mathbf{v}^{(12)}$ is directed along the tangent to the tooth's longitudinal shape.

It is easy to verify that vectors $\mathbf{v}^{(1)}$ and $\mathbf{v}^{(2)}$ lie in the pitch plane and are perpendicular to the unit vectors $\boldsymbol{\tau}^{(1)}$ and $\boldsymbol{\tau}^{(2)}$, respectively. This may be proven with the equations

$$\mathbf{v}^{(i)} \cdot \mathbf{n}_f^{(P)} = 0 \quad \mathbf{v}^{(i)} \cdot \boldsymbol{\tau}^{(i)} = 0 \quad (i = 1, 2) \tag{14.4.52}$$

Since vectors $\mathbf{v}^{(1)}$ and $\mathbf{v}^{(2)}$ lie in the pitch plane, vector $\mathbf{v}^{(12)} = \mathbf{v}^{(1)} - \mathbf{v}^{(2)}$ also lies in this plane.

Let us now determine the angle β_i ($i = 1, 2$) formed between the unit vector $\boldsymbol{\tau}^{(i)}$ and the relative velocity $\mathbf{v}^{(12)}$. Taking into account that

$$\boldsymbol{\tau}^{(1)} \cdot \mathbf{v}^{(1)} = \boldsymbol{\tau}^{(2)} \cdot \mathbf{v}^{(2)} = 0$$

we get

$$\cos \beta_1 = \frac{\boldsymbol{\tau}^{(1)} \cdot \mathbf{v}^{(12)}}{|\mathbf{v}^{(12)}|} = \frac{\boldsymbol{\tau}^{(1)} \cdot (\mathbf{v}^{(1)} - \mathbf{v}^{(2)})}{|\mathbf{v}^{(12)}|} = - \frac{\boldsymbol{\tau}^{(1)} \cdot \mathbf{v}^{(2)}}{|\mathbf{v}^{(12)}|} \tag{14.4.53}$$

and

$$\cos \beta_2 = \frac{\boldsymbol{\tau}^{(2)} \cdot \mathbf{v}^{(12)}}{|\mathbf{v}^{(12)}|} = \frac{\boldsymbol{\tau}^{(2)} \cdot \mathbf{v}^{(1)}}{|\mathbf{v}^{(12)}|} \tag{14.4.54}$$

Here (see eqs. (14.4.51))

$$\mathbf{v}^{(1)} = \boldsymbol{\omega}^{(1)} \times \mathbf{r}_f^{(P)} = \omega^{(1)} \left(y_f^{(P)} \mathbf{i}_f - x_f^{(P)} \mathbf{j}_f \right) \tag{14.4.55}$$

$$\mathbf{v}^{(2)} = \boldsymbol{\omega}^{(2)} \times \mathbf{r}_f^{(P)} + \overline{O_f O} \times \boldsymbol{\omega}^{(2)} = \omega^{(2)} \left[-z_f^{(P)} \mathbf{i}_f + \left(x_f^{(P)} - C \right) \mathbf{k}_f \right] \tag{14.4.56}$$

and

$$\begin{aligned}
|\mathbf{v}^{(12)}| = & \left\{ (\omega^{(1)})^2 \left[\left(y_f^{(P)} \right)^2 + \left(x_f^{(P)} \right)^2 \right] + 2(\omega^{(1)})(\omega^{(2)}) y_f^{(P)} z_f^{(P)} \right. \\
& \left. + (\omega^{(2)})^2 \left[\left(z_f^{(P)} \right)^2 + \left(x_f^{(P)} - C \right)^2 \right] \right\}^{1/2}
\end{aligned} \tag{14.4.57}$$

Equations (14.4.48), (14.4.49), (14.4.55), and (14.4.56) yield that

$$\boldsymbol{\tau}^{(1)} \cdot \mathbf{v}^{(2)} = \omega^{(2)} \left[-z_f^{(P)} \cos \theta_1 \sin \gamma_1 + \left(x_f^{(P)} - C \right) \cos \gamma_1 \right] \tag{14.4.58}$$

and

$$\boldsymbol{\tau}^{(2)} \cdot \mathbf{v}^{(1)} = \omega^{(1)} \left(y_f^{(P)} \cos \theta_2 \sin \gamma_2 + x_f^{(P)} \cos \gamma_2 \right) \tag{14.4.59}$$

We may transform equations (14.4.58), (14.4.59), and (14.4.57) using the following expressions:
(See eqs. (14.4.26), (14.4.21), (14.4.24), (14.4.19), (14.4.25), and (14.4.20).)

$$z_f^{(P)} = r_2 \sin \theta_2 = r_2 \frac{\sin \gamma_1}{\cos \gamma_2} \quad (14.4.60)$$

$$x_f^{(P)} - C = r_2 \cos \theta_2 = -r_2 \frac{\cos \theta_1 \cos \gamma_1}{\cos \gamma_2} \quad (14.4.61)$$

$$y_f^{(P)} = r_1 \sin \theta_1 = -r_1 \frac{\sin \gamma_2}{\cos \gamma_1} \quad (14.4.62)$$

$$x_f^{(P)} = r_1 \cos \theta_1 \quad (14.4.63)$$

$$\left(x_f^{(P)}\right)^2 + \left(y_f^{(P)}\right)^2 = r_1^2 \quad (14.4.64)$$

$$\left(x_f^{(P)} - C\right)^2 + \left(z_f^{(P)}\right)^2 = r_2^2 \quad (14.4.65)$$

We then get

$$\boldsymbol{\tau}^{(1)} \cdot \mathbf{v}^{(2)} = -\omega^{(2)} r_2 \frac{\cos \theta_1}{\cos \gamma_2} = \mp \frac{\omega^{(2)} r_2 \sqrt{\cos^2 \gamma_1 - \sin^2 \gamma_2}}{\cos \gamma_1 \cos \gamma_2} \quad (14.4.66)$$

$$\boldsymbol{\tau}^{(2)} \cdot \mathbf{v}^{(1)} = \omega^{(1)} r_1 \frac{\cos \theta_1}{\cos \gamma_2} = \pm \frac{\omega^{(1)} r_1 \sqrt{\cos^2 \gamma_1 - \sin^2 \gamma_2}}{\cos \gamma_1 \cos \gamma_2} \quad (14.4.67)$$

$$\begin{aligned} |\mathbf{v}^{(12)}| &= \left[\left(\omega^{(1)} r_1\right)^2 - 2\omega^{(1)}\omega^{(2)} r_1 r_2 \tan \gamma_1 \tan \gamma_2 + \left(\omega^{(2)} r_2\right)^2 \right]^{1/2} \\ &= \left[\left(\omega^{(1)} r_1\right)^2 - 2\omega^{(1)}\omega^{(2)} r_1 r_2 \cos \eta + \left(\omega^{(2)} r_2\right)^2 \right]^{1/2} \end{aligned} \quad (14.4.68)$$

Here η is represented by equation (14.4.50). The final expressions for β_1 and β_2 are given by

$$\cos \beta_1 = \pm \frac{\omega^{(2)} r_2 \sqrt{\cos^2 \gamma_1 - \sin^2 \gamma_2}}{|\mathbf{v}^{(12)}| \cos \gamma_1 \cos \gamma_2} \quad (14.4.69)$$

$$\cos \beta_2 = \pm \frac{\omega^{(1)} r_1 \sqrt{\cos^2 \gamma_1 - \sin^2 \gamma_2}}{|\mathbf{v}^{(12)}| \cos \gamma_1 \cos \gamma_2} \quad (14.4.70)$$

Equations (14.4.69) and (14.4.70) determine the direction of the tangent to the tooth's longitudinal shape at P . These equations yield

$$m_{12} = \frac{\omega^{(1)}}{\omega^{(2)}} = \left| \frac{r_2 \cos \beta_2}{r_1 \cos \beta_1} \right| \quad (14.4.71)$$

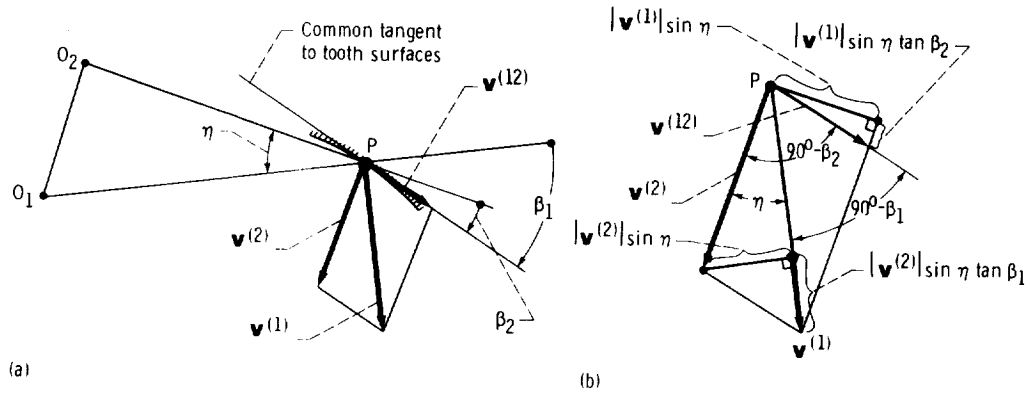


Figure 14.4.4.

We may derive alternative solutions for β_1 and β_2 . It is evident from figure 14.4.4(b) that

$$v^{(1)} = v^{(2)} \cos \eta + v^{(2)} \sin \eta \tan \beta_1 \quad (14.4.72)$$

$$v^{(2)} = v^{(1)} \cos \eta - v^{(1)} \sin \eta \tan \beta_2 \quad (14.4.73)$$

Equations (14.4.72) and (14.4.73) yield

$$\tan \beta_1 = \frac{v^{(1)} - v^{(2)} \cos \eta}{v^{(2)} \sin \eta} \quad (14.4.74)$$

$$\tan \beta_2 = \frac{v^{(1)} \cos \eta - v^{(2)}}{v^{(1)} \sin \eta} \quad (14.4.75)$$

From equations (14.4.55), (14.4.56), and (14.4.24) to (14.4.26), we obtain

$$v^{(1)} = \omega^{(1)} \left[\left(y_f^{(P)} \right)^2 + \left(x_f^{(P)} \right)^2 \right]^{1/2} = \omega^{(1)} r_1 \quad (14.4.76)$$

$$v^{(2)} = \omega^{(2)} \left[\left(z_f^{(P)} \right)^2 + \left(x_f^{(P)} - C \right)^2 \right]^{1/2} = \omega^{(2)} r_2 \quad (14.4.77)$$

Equations (14.4.74) to (14.4.77) yield

$$\tan \beta_1 = \frac{r_1 - m_{21} r_2 \cos \eta}{m_{21} r_2 \sin \eta} \quad (14.4.78)$$

and

$$\tan \beta_2 = \frac{r_1 \cos \eta - m_{21} r_2}{r_1 \sin \eta} \quad (14.4.79)$$

where $m_{21} = \omega^{(2)}/\omega^{(1)}$.

Optimal Synthesis of Pitch Surfaces

Consider that the gear center distance, the crossing angle and the gear ratio are given. To determine the pitch surfaces in contact at the pitch point, we use equations which relate the design parameters. Since the number of equations used is less than the number of varied parameters, the solution is not unique. Thus, the design of pitch surfaces is a problem of optimization with some criteria. For instance, the criteria of force transmission may be used. This problem was solved by Litvin, Petrov, and Ganshin (1974).

14.5 Limiting Contact Normal

Consider that the pitch plane, the pitch point P and the direction of the sliding velocity $\mathbf{v}^{(12)}$ are known (fig. 14.5.1). Let us draw through the pitch point P , the normal plane, which is perpendicular to the pitch plane and to $\mathbf{v}^{(12)}$. The mating surfaces Σ_1 and Σ_2 are in contact at point P and the common unit normal \mathbf{n} to Σ_1 and Σ_2 lies in the normal plane (fig. 14.5.1). The direction of \mathbf{n} is determined by the normal pressure angle ψ_n . Since vector $\mathbf{v}^{(12)}$ is perpendicular to the normal plane, the equation

$$\mathbf{n} \cdot \mathbf{v}^{(12)} = 0 \quad (14.5.1)$$

is satisfied for any pressure angle ψ_n . Equation (14.5.1) is the equation of meshing (sec. 9.8) and the gear tooth surfaces are conjugate at P locally—they transform rotational motion with a prescribed angular velocity ratio.

However, there is a limiting pressure angle ψ_n which determines the direction of the limiting contact normal. The problem of the limiting contact normal was the subject of research done by Wildhaber (1946a), Baxter (1961), and Litvin (1968).

Let surface Σ_1 be covered with lines of contact at which Σ_1 comes into tangency with the mating surface Σ_2 . Consider the particular case when the contact lines on Σ_1 have an envelope at the pitch point P (fig. 14.5.2). As we know, (sec. 12.1) the velocities $\mathbf{v}_r^{(1)}$ and $\mathbf{v}_r^{(2)}$ of the contact point in the motion over surfaces Σ_1 and Σ_2 are related by the equation

$$\mathbf{v}_r^{(2)} = \mathbf{v}_r^{(1)} + \mathbf{v}^{(12)} \quad (14.5.2)$$

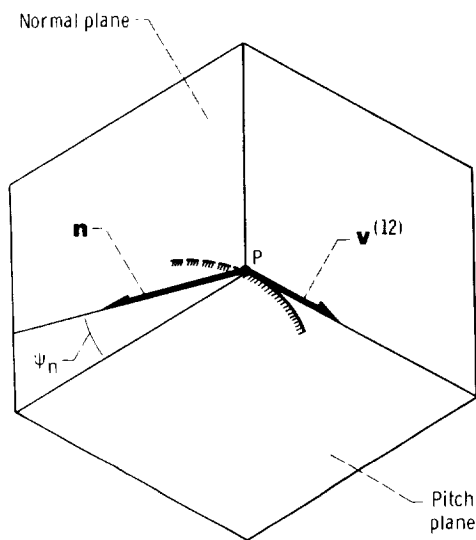


Figure 14.5.1.

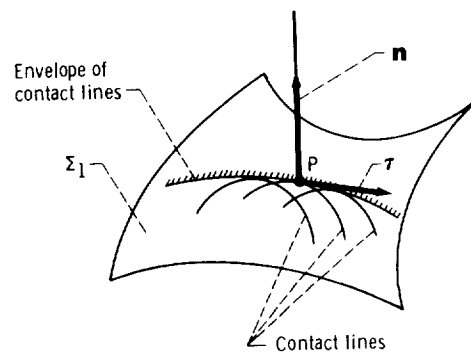


Figure 14.5.2.

This equation is derived with the assumption that vector $\mathbf{v}_r^{(1)}$ can be along any direction but different from the direction of the tangent to the contact line. It is evident that if at P the contact line envelope exists, the velocity $\mathbf{v}_r^{(1)}$ is zero along any direction different from the direction of the tangent T (fig. 15.5.2).

Let us differentiate the equation of meshing given by

$$\mathbf{n}^{(1)} \cdot \mathbf{v}^{(12)} = \mathbf{n}^{(1)} \cdot (\boldsymbol{\omega}^{(12)} \times \mathbf{r}^{(1)} - \mathbf{C} \times \boldsymbol{\omega}^{(2)}) = 0 \quad (14.5.3)$$

taking into account that an envelope of contact lines exists at P and $\mathbf{v}_r^{(1)} = 0$. We assume that the gear ratio and $\boldsymbol{\omega}^{(1)}$ and $\boldsymbol{\omega}^{(2)}$ are constant. Thus

$$\dot{\mathbf{n}}^{(1)} \cdot \mathbf{v}^{(12)} + \mathbf{n}^{(1)} \cdot (\boldsymbol{\omega}^{(12)} \times \dot{\mathbf{r}}^{(1)}) = 0 \quad (14.5.4)$$

Since $\mathbf{v}_r^{(1)} = 0$, we have

$$\dot{\mathbf{n}}^{(1)} = \dot{\mathbf{n}}_{rr}^{(1)} = \boldsymbol{\omega}^{(1)} \times \mathbf{n}^{(1)} \quad \dot{\mathbf{r}}^{(1)} = \mathbf{v}_{rr}^{(1)} \quad (14.5.5)$$

Equations (14.5.4) and (14.5.5) yield

$$\mathbf{n}^{(1)} \cdot \left[-(\boldsymbol{\omega}^{(1)} \times \mathbf{v}^{(12)}) + (\boldsymbol{\omega}^{(12)} \times \mathbf{v}_{rr}^{(1)}) \right] = 0 \quad (14.5.6)$$

With the expressions

$$\mathbf{v}^{(12)} = \mathbf{v}_{rr}^{(1)} - \mathbf{v}_{rr}^{(2)} \quad \boldsymbol{\omega}^{(12)} = \boldsymbol{\omega}^{(1)} - \boldsymbol{\omega}^{(2)} \quad (14.5.7)$$

we may represent equation (14.5.6) as follows:

$$\begin{aligned} & \mathbf{n}^{(1)} \cdot \left[(\boldsymbol{\omega}^{(1)} \times \mathbf{v}_{rr}^{(2)}) - (\boldsymbol{\omega}^{(2)} \times \mathbf{v}_{rr}^{(1)}) \right] = \\ & \mathbf{n}^{(1)} \cdot \left\{ \boldsymbol{\omega}^{(1)} \times \left[\boldsymbol{\omega}^{(2)} \times (\mathbf{r}^{(P)} - \mathbf{C}) \right] - \left[\boldsymbol{\omega}^{(2)} \times (\boldsymbol{\omega}^{(1)} \times \mathbf{r}^{(P)}) \right] \right\} = 0 \end{aligned} \quad (14.5.8)$$

Here $\mathbf{r}^{(P)}$ is the position vector of pitch point, \mathbf{C} is the vector of shortest distance between the axes of rotation. Equation (14.5.8) and equation

$$\mathbf{n}^{(1)} \cdot \mathbf{v}^{(12)} = 0 \quad (14.5.9)$$

determine the direction of the limiting normal at the pitch point P . Synthesizing the gears we have to choose the direction of the surface normal different from the limiting direction. Then the envelope of contact lines at the pitch point will not occur. In the case of gear train with the crossing angle of 90° , we get

$$\boldsymbol{\omega}^{(1)} \cdot \boldsymbol{\omega}^{(2)} = 0 \quad (14.5.10)$$

$$\lambda \mathbf{C} = (\boldsymbol{\omega}^{(1)} \times \boldsymbol{\omega}^{(2)}) \quad (\lambda \neq 0) \quad (14.5.11)$$

(The vector of shortest distance is perpendicular to the axes of rotation.)

$$\boldsymbol{\omega}^{(1)} \times (\boldsymbol{\omega}^{(2)} \times \mathbf{C}) = 0 \quad (14.5.12)$$

(Vectors $\boldsymbol{\omega}^{(1)}$, $\boldsymbol{\omega}^{(2)}$, and \mathbf{C} are mutually perpendicular.) Equations (14.5.10) to (14.5.12) yield that equation (14.5.8) may be represented in the discussed case as follows

$$\mathbf{n} \cdot \left[\mathbf{r}^{(P)} \times (\boldsymbol{\omega}^{(2)} \times \boldsymbol{\omega}^{(1)}) \right] = -\lambda \mathbf{n} \cdot (\mathbf{r}^{(P)} \times \mathbf{C}) = 0 \quad (14.5.13)$$

or (provided $\lambda \neq 0$)

$$[\mathbf{n}\mathbf{r}^{(P)}\mathbf{C}] = (n_y z_f^{(P)} - n_z y_f^{(P)})C = 0 \quad (14.5.14)$$

The derivation of equations (14.5.13) and (14.5.14) from equation (14.5.8) is based on the following considerations:

Step 1.—Considering the triple vector products in equation (14.5.8), we obtain

$$\begin{aligned} \boldsymbol{\omega}^{(1)} \times [\boldsymbol{\omega}^{(2)} \times (\mathbf{r}^{(P)} - \mathbf{C})] - [\boldsymbol{\omega}^{(2)} \times (\boldsymbol{\omega}^{(1)} \times \mathbf{r}^{(P)})] &= \boldsymbol{\omega}^{(2)}(\boldsymbol{\omega}^{(1)} \cdot \mathbf{r}^{(P)}) \\ &- \mathbf{r}^{(P)}(\boldsymbol{\omega}^{(1)} \cdot \boldsymbol{\omega}^{(2)}) - \boldsymbol{\omega}^{(1)} \times (\boldsymbol{\omega}^{(2)} \times \mathbf{C}) - \boldsymbol{\omega}^{(1)}(\boldsymbol{\omega}^{(2)} \cdot \mathbf{r}^{(P)}) \\ &+ \mathbf{r}^{(P)}(\boldsymbol{\omega}^{(1)} \cdot \boldsymbol{\omega}^{(2)}) = \boldsymbol{\omega}^{(2)}(\boldsymbol{\omega}^{(1)} \cdot \mathbf{r}^{(P)}) - \boldsymbol{\omega}^{(1)}(\boldsymbol{\omega}^{(2)} \cdot \mathbf{r}^{(P)}) \end{aligned}$$

because

- (1) $\boldsymbol{\omega}^{(1)} \cdot \boldsymbol{\omega}^{(2)} = 0$ (Because these vectors are perpendicular.)
- (2) $\boldsymbol{\omega}^{(1)} \times (\boldsymbol{\omega}^{(2)} \times \mathbf{C}) = 0$ (See eq. (14.5.12).)

Thus the triple vector product in equation (14.5.8) may be substituted by

$$\boldsymbol{\omega}^{(2)}(\boldsymbol{\omega}^{(1)} \cdot \mathbf{r}^{(P)}) - \boldsymbol{\omega}^{(1)}(\boldsymbol{\omega}^{(2)} \cdot \mathbf{r}^{(P)}) = \mathbf{r}^{(P)} \times (\boldsymbol{\omega}^{(2)} \times \boldsymbol{\omega}^{(1)})$$

Step 2.—With equation (14.5.11), we obtain

$$\boldsymbol{\omega}^{(1)} \times \boldsymbol{\omega}^{(2)} = \lambda \mathbf{C}$$

Thus equation (14.5.13) is confirmed.

Step 3.—We derive equation (14.5.14) as follows:

$$\begin{aligned} [\mathbf{n}\mathbf{r}^{(P)}\mathbf{C}] &= (n_x \mathbf{i}_f + n_y \mathbf{j}_f + n_z \mathbf{k}_f) \cdot \begin{vmatrix} \mathbf{i}_f & \mathbf{j}_f & \mathbf{k}_f \\ x_f^{(P)} & y_f^{(P)} & z_f^{(P)} \\ C & 0 & 0 \end{vmatrix} \\ &= (n_x \mathbf{i}_f + n_y \mathbf{j}_f + n_z \mathbf{k}_f)(z_f^{(P)} \mathbf{j}_f - y_f^{(P)} \mathbf{k}_f)C = (n_y z_f^{(P)} - n_z y_f^{(P)})C = 0 \end{aligned}$$

Thus, equation (14.5.14) is confirmed.

In the case of worm-gear drives, the pitch point P lies on the center distance and vectors $\mathbf{r}^{(P)}$ and \mathbf{C} are collinear. Equation (14.5.14), which only works for orthogonal gear drives, is satisfied with any direction of the surface unit normal \mathbf{n} , since $\mathbf{r}^{(P)} \times \mathbf{C} = 0$. This results in that the existence of the contact line envelope at the pitch point P is inevitable for orthogonal worm-gear drives. This is the reason why nonstandard orthogonal worm-gear drives may result in a better efficiency.

Let us now express equation (14.5.14) in terms of the parameters of a hypoid gear drive with a crossing angle of 90° .

Consider a coordinate system S_e rigidly connected to the pitch plane with the unit vectors of the coordinate axes, \mathbf{e}_1 , \mathbf{e}_2 , and \mathbf{e}_3 (fig. 14.5.3). The unit normal to the pitch plane is given by \mathbf{e}_1 ; \mathbf{e}_3 coincides with $\boldsymbol{\tau}^{(1)}$, the unit tangent to the pitch cone (fig. 14.5.3 and fig. 14.4.2); the unit vector \mathbf{e}_2 is represented by the equation

$$\mathbf{e}_2 = \mathbf{e}_3 \times \mathbf{e}_1 \quad (14.5.15)$$

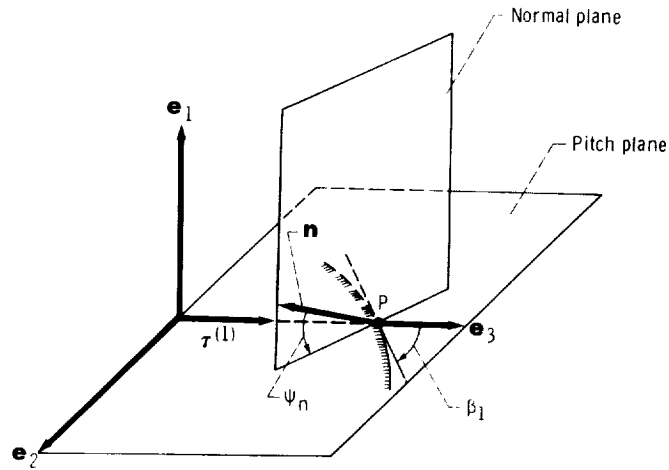


Figure 14.5.3.

The unit vector \mathbf{e}_1 is represented in the coordinate system S_f as follows: (eq. (14.4.47))

$$\mathbf{e}_1 = \begin{bmatrix} \cos \gamma_1 \cos \theta_1 \\ \cos \gamma_1 \sin \theta_1 \\ -\sin \gamma_1 \end{bmatrix} \quad (14.5.16)$$

Vector $\mathbf{e}_3 \equiv \boldsymbol{\tau}^{(1)}$ is represented by (eq. (14.4.48))

$$\mathbf{e}_3 = \begin{bmatrix} \sin \gamma_1 \cos \theta_1 \\ \sin \gamma_1 \sin \theta_1 \\ \cos \gamma_1 \end{bmatrix} \quad (14.5.17)$$

Equations (14.5.15) to (14.5.17) yield

$$\mathbf{e}_2 = \begin{bmatrix} -\sin \theta_1 \\ \cos \theta_1 \\ 0 \end{bmatrix} \quad (14.5.18)$$

Equations (14.5.16) to (14.5.18) result in the following matrix:

$$[L_{fe}] = \begin{bmatrix} \cos \gamma_1 \cos \theta_1 & -\sin \theta_1 & \sin \gamma_1 \cos \theta_1 \\ \cos \gamma_1 \sin \theta_1 & \cos \theta_1 & \sin \gamma_1 \sin \theta_1 \\ -\sin \gamma_1 & 0 & \cos \gamma_1 \end{bmatrix} \quad (14.5.19)$$

Elements of matrix (14.5.19) $a_{k\ell}$ ($k = 1,2,3$; $\ell = 1,2,3$) represent the direction cosines; k is the number of axis of S_f , and ℓ is the number of axis of S_e . (See app. A). For instance,

$$a_{23} = \cos(\mathbf{j}_f \cdot \mathbf{e}_3) = \sin \gamma_1 \sin \theta_1$$

This matrix represents the transformation of a vector in transition from S_e to S_f .
The surface unit normal \mathbf{n} (fig. 14.5.3) is represented in terms of $\mathbf{e}_1, \mathbf{e}_2, \mathbf{e}_3$ by the matrix

$$[n_e] = \begin{bmatrix} \sin \psi_n \\ \cos \psi_n \cos \beta_1 \\ -\cos \psi_n \sin \beta_1 \end{bmatrix} \quad (14.5.20)$$

The surface unit normal is represented in terms of $\mathbf{i}_f, \mathbf{j}_f,$ and \mathbf{k}_f as follows:

$$[n_f] = [L_{fe}][n_e] \quad (14.5.21)$$

Equations (14.5.19) to (14.5.21) yield

$$[n_f] = \begin{bmatrix} \cos \gamma_1 \cos \theta_1 \sin \psi_n - \sin \theta_1 \cos \beta_1 \cos \psi_n - \sin \gamma_1 \cos \theta_1 \sin \beta_1 \cos \psi_n \\ \cos \gamma_1 \sin \theta_1 \sin \psi_n + \cos \theta_1 \cos \beta_1 \cos \psi_n - \sin \gamma_1 \sin \theta_1 \sin \beta_1 \cos \psi_n \\ -\sin \gamma_1 \sin \psi_n - \cos \gamma_1 \sin \beta_1 \cos \psi_n \end{bmatrix} \quad (14.5.22)$$

If the surface unit normal reaches the limiting direction, equation (14.5.14) must be satisfied. Equations (14.5.22) and (14.5.14) yield

$$\begin{aligned} & (\cos \gamma_1 \sin \theta_1 \sin \alpha + \cos \theta_1 \cos \beta_1 \cos \alpha - \sin \gamma_1 \sin \theta_1 \sin \beta_1 \cos \alpha) z_f^{(P)} \\ & + (\sin \gamma_1 \sin \alpha + \cos \gamma_1 \sin \beta_1 \cos \alpha) y_f^{(P)} = 0 \end{aligned} \quad (14.5.23)$$

Here $\alpha = \psi_n$ is the limiting pressure angle, the angle formed by the limiting normal with the pitch plane (fig. 14.5.3); $x^{(P)}, y^{(P)},$ and $z^{(P)}$ are the coordinates of the pitch point.

We may transform equation (14.5.23) by using the following expressions: (see eqs. (14.4.17) to (14.4.21) and (14.4.50))

$$\sin \theta_1 = -\frac{\sin \gamma_2}{\cos \gamma_1} \quad (14.5.24)$$

$$z_f^{(P)} = r_2 \sin \theta_2 = \frac{\sin \gamma_2}{\cos \gamma_1} r_2 \quad (\text{provided } u_2 \sin \gamma_2 = r_2) \quad (14.5.25)$$

$$y_f^{(P)} = r_1 \sin \theta_1 = -\frac{\sin \gamma_2}{\cos \gamma_1} r_1 \quad (\text{provided } u_1 \sin \gamma_1 = r_1) \quad (14.5.26)$$

$$\sin^2 \eta = 1 - \tan^2 \gamma_1 \tan^2 \gamma_2 = \frac{\cos^2 \gamma_1 - \sin^2 \gamma_2}{\cos^2 \gamma_1 \cos^2 \gamma_2} = \frac{1}{\cos^2 \gamma_2} \left(1 - \frac{\sin^2 \gamma_2}{\cos^2 \gamma_1} \right) = \frac{\cos^2 \theta_1}{\cos^2 \gamma_2} \quad (14.5.27)$$

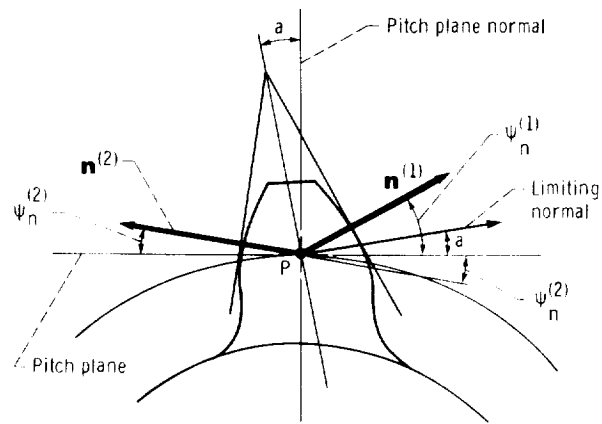


Figure 14.5.4.

$$\cos \theta_1 = -\sin \eta \cos \gamma_2 \quad (\text{provided } \cos \theta_2 > 0) \quad (14.5.28)$$

$$\eta = \beta_1 - \beta_2 \quad (14.5.29)$$

Equations (14.5.23) to (14.5.29) yield that

$$\tan \alpha = \frac{r_2 \sin \beta_2 + y_f^{(P)} \cot \gamma_1 \sin \beta_1}{r_2 \tan \gamma_2 - y_f^{(P)}} \quad (14.5.30)$$

The orientation of the limiting normal (angle α) depends on the location of the pitch point.

Figure 14.5.4 shows tooth shapes of both sides in the normal section which passes through the pitch point P . The surface unit normals $\mathbf{n}^{(1)}$ and $\mathbf{n}^{(2)}$ form angles $\psi_n^{(1)}$ and $\psi_n^{(2)}$ with the pitch plane. These normals make the same angle with the limiting normal, that is, $\psi_n^{(1)} - \alpha = \psi_n^{(2)} + \alpha$. Thus, $\psi_n^{(1)} \neq \psi_n^{(2)}$, $\psi_n^{(1)} - \psi_n^{(2)} = 2\alpha$, and the tooth shapes are asymmetrical.

Chapter 15

Axes of Meshing

We define the axis of meshing as a straight line rigidly connected to the frame through which passes the common normal to the mating surfaces at any point of contact of the surfaces.

In the case of gears having parallel (intersected) axes of gear rotation, there is only one axis of meshing and this axis is the line of contact of pitch cylinders (of pitch cones in the case of intersected axes). It will be proven below that there are two axes of meshing if the axes of gear rotation are crossed. In this case, the relative motion is a screw motion and one of the mating surfaces is a helicoid. (This theorem was first proposed by Litvin, 1955.) The application of the axes of meshing simplifies, in some cases, the gear synthesis and the tool design.

15.1 Crossed Axes of Gear Rotation: Axes of Meshing

Consider that a gear mechanism transforms rotation between crossed axes (fig. 15.1.1). The relative motion is a screw motion, which is represented by rotation about and sliding along an axis called the axis of screw motion. (See ch. 2.4.) Knowing the angular velocities of gear rotation, the shortest distance, and the crossing angle between the axes of gear rotation, we may determine the unique parameters of relative screw motion. The reverse case—the representation of the given screw motion as rotation about two crossed axes—has an infinite number of solutions. However, we may find a unique pair of crossed axes, among all of the pairs of crossed axes, which will serve as a pair of axes of meshing by satisfying the following conditions: (1) The rotations about the axes of meshing may be substituted by the given screw motion. (2) All common normals to the mating surfaces at points of surface contact intersect both axes of meshing.

Consider that such a pair of axes of meshing indeed exists. Since the common normal to the mating surfaces must intersect the axes of meshing, the two following equations must be observed.

$$\frac{X^{(i)} - x}{n_x} = \frac{Y^{(i)} - y}{n_y} = \frac{Z^{(i)} - z}{n_z} \quad (i = I, II) \quad (15.1.1)$$

Here $X^{(i)}$, $Y^{(i)}$, and $Z^{(i)}$ are the coordinates of a point on the axis of meshing; x , y , and z are the coordinates of a point of contact of mating surfaces; and n_x , n_y , and n_z are the projections of

the common unit normal to the mating surfaces. The contact point of surfaces, the common unit normal and the coordinates of the axes of meshing, are considered in the fixed coordinates system $S_f(x_f, y_f, z_f)$ that is connected rigidly to the frame. (The subscript f in equations (15.1.1) is dropped for simplification.)

Considering that the x_f -axis is directed along the shortest distance between the crossed axes (fig. 15.1.1), we may represent equations (15.1.1) as follows:

$$\frac{X^{(i)} - x}{n_x} = \frac{Y^{(i)} - y}{n_y} = \frac{K^{(i)}Y^{(i)} - z}{n_z} \quad (15.1.2)$$

Here $(X^{(i)}, O, O)$ are the coordinates of point O_i ($i = I, II$), the intersection of the axis of meshing with the x_f -axis, and

$$Z^{(i)} = K^{(i)}Y^{(i)} \quad (15.1.3)$$

where $K^{(i)}$ determines the direction of the axis of meshing. Equations (15.1.2) yield

$$X^{(i)} = \frac{K^{(i)}(xn_y - yn_x) - xn_z + zn_x}{K^{(i)}n_y - n_z} \quad (15.1.4)$$

It may be stated that the location and direction of the axis of meshing does not depend on (1) coordinates of the point of surface contact or (2) on the projections of the surface unit normal, if $X^{(i)}$ and $K^{(i)}$ do not depend on the mentioned parameters. Let us prove that the location and direction of the axes of meshing is constant if one of the mating surfaces is a helicoid. We begin with the equation

$$yn_x - xn_y = hn_z \quad (15.1.5)$$

which is satisfied if the gear-tooth surface Σ_1 is a helicoid (sec. 8.4, eq. (8.4.40)); here h is the screw parameter. We then determine the equation of meshing that relates the coordinates of the

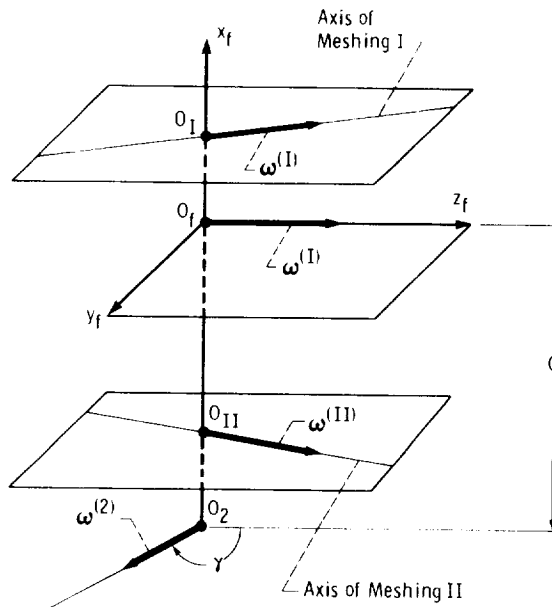


Figure 15.1.1.

point of contact (x, y, z) and the projections of the surface unit normal (n_x, n_y, n_z) . (See ch. 9.8). The derivation is based on the following equation

$$\mathbf{n} \cdot \mathbf{v}^{(12)} = \mathbf{n} \cdot \left[(\boldsymbol{\omega}^{(1)} - \boldsymbol{\omega}^{(2)}) \times \mathbf{r}^{(1)} - (\mathbf{R} \times \boldsymbol{\omega}^{(2)}) \right] = 0 \quad (15.1.6)$$

Here

$$\mathbf{n} = n_x \mathbf{i} + n_y \mathbf{j} + n_z \mathbf{k} \quad (15.1.7)$$

is the surface unit normal;

$$\boldsymbol{\omega}^{(1)} = \omega^{(1)} \mathbf{k} \quad \boldsymbol{\omega}^{(2)} = \omega^{(2)} (\sin \gamma \mathbf{j} + \cos \gamma \mathbf{k}) \quad (15.1.8)$$

are the angular velocities of gears 1 and 2 (fig. 15.1.1); and

$$\mathbf{r}^{(1)} = x \mathbf{i} + y \mathbf{j} + z \mathbf{k} \quad (15.1.9)$$

is the position vector of the point of contact;

$$\mathbf{R} = \overline{O_1 O_2} = -C \mathbf{i} \quad (15.1.10)$$

Equations (15.1.6) to (15.1.10) yield

$$\begin{aligned} -n_x \left[(1 - m_{21} \cos \gamma) y + m_{21} z \sin \gamma \right] + n_y \left[(1 - m_{21} \cos \gamma) x - C m_{21} \cos \gamma \right] \\ + n_z \left[m_{21} \sin \gamma (x + C) \right] = 0 \end{aligned} \quad (15.1.11)$$

Here $m_{21} = \omega^{(2)}/\omega^{(1)}$.

Taking into account that surface Σ_1 is a helicoid and equation (15.1.5) is satisfied, we represent equations (15.1.11) and (15.1.4) as

$$x n_z - z n_x - h \frac{1 - m_{21} \cos \gamma}{m_{21} \sin \gamma} n_z - C (n_y \cot \gamma - n_z) = 0 \quad (15.1.12)$$

$$X^{(i)} = \frac{-K^{(i)} h n_z - x n_z + z n_x}{K^{(i)} n_y - n_z} \quad (15.1.13)$$

Equations (15.1.12) and (15.1.13) yield

$$(X^{(i)} K^{(i)} + C \cot \gamma) n_y + \left(K^{(i)} h - X^{(i)} - C + h \frac{1 - m_{21} \cos \gamma}{m_{21} \sin \gamma} \right) n_z = 0 \quad (15.1.14)$$

To be independent of the parameters of contact point, the coordinates $X^{(i)}$ and $K^{(i)}$ of the axes of meshing must satisfy the following equations:

$$X^{(i)} K^{(i)} + C \cot \gamma = 0 \quad (15.1.14)$$

$$K^{(1)} h - X^{(i)} - C + h \frac{1 - m_{21} \cos \gamma}{m_{21} \sin \gamma} = 0 \quad (15.1.15)$$

Equations (15.1.14) and (15.1.15) yield

$$(K^{(i)})^2 - K^{(i)} \left(\frac{C}{h} - \frac{1 - m_{21} \cos \gamma}{m_{21} \sin \gamma} \right) + \frac{C \cot \gamma}{h} = 0 \quad (15.1.16)$$

$$X^{(i)} = - \frac{C \cot \gamma}{K^{(i)}} \quad (15.1.17)$$

The solutions to these equations for $X^{(i)}$ and $K^{(i)}$ are given by

$$K^{(I)} = \frac{1}{2} \left(\frac{C}{h} - \frac{1 - m_{21} \cos \gamma}{m_{21} \sin \gamma} \right) + \frac{1}{2} \left[\left(\frac{C}{h} - \frac{1 - m_{21} \cos \gamma}{m_{21} \sin \gamma} \right)^2 - \frac{4C \cot \gamma}{h} \right]^{1/2} \quad (15.1.18)$$

$$X^{(I)} = - \frac{C \cot \gamma}{K^{(I)}} \quad (15.1.19)$$

$$K^{(II)} = \frac{1}{2} \left(\frac{C}{h} - \frac{1 - m_{21} \cos \gamma}{m_{21} \sin \gamma} \right) - \frac{1}{2} \left[\left(\frac{C}{h} - \frac{1 - m_{21} \cos \gamma}{m_{21} \sin \gamma} \right)^2 - \frac{4C \cot \gamma}{h} \right]^{1/2} \quad (15.1.20)$$

$$X^{(II)} = - \frac{C \cot \gamma}{K^{(II)}} \quad (15.1.21)$$

For the case when the crossing angle $\gamma = 90^\circ$, we get

$$K^{(I)} = \frac{C}{h} - \frac{1}{m_{21}} \quad (15.1.22)$$

$$X^{(I)} = 0 \quad (15.1.23)$$

$$K^{(II)} = 0 \quad (15.1.24)$$

Using L'Hospital's rule, the fraction in equation (15.1.21) for $\gamma = 90^\circ$ becomes

$$X^{(II)} = \frac{\frac{d}{d\gamma} (-C \cot \gamma)}{\frac{d}{d\gamma} [K^{(II)}(\gamma)]} = -C + \frac{h}{m_{21}} \quad (15.1.25)$$

The angular velocity ratio for the worm-gear drive is (sec. 14.3)

$$m_{21} = \pm \frac{r_p \sin \lambda_p}{R_p \sin (\gamma \pm \lambda_p)} \quad (15.1.26)$$

The upper sign corresponds to worms with the right-handed threads; r_p and R_p are the radii of the pitch cylinders of the worm and the worm-gear; λ_p is the lead angle on the pitch cylinder of the worm. Taking into account that $C = r_p + R_p$, and $h = \pm r_p \tan \lambda_p$ ($h < 0$ for a left-handed thread), we may represent the parameters of the axes of meshing by using table 15.1.1.

TABLE 15.1.1.

| γ | Worm thread | $K^{(I)}$ | $X^{(I)}$ | $K^{(II)}$ | $X^{(II)}$ |
|-----------------------------|----------------|-------------------|---------------------------------|-----------------------------|------------|
| $\gamma \neq \frac{\pi}{2}$ | Right - handed | $\cot \lambda_p$ | $-C \cot \gamma \tan \lambda_p$ | $\frac{C \cot \gamma}{r_p}$ | $-r_p$ |
| | Left - handed | $-\cot \lambda_p$ | $C \cot \gamma \tan \lambda_p$ | $\frac{C \cot \gamma}{r_p}$ | $-r_p$ |
| $\gamma = \frac{\pi}{2}$ | Right - handed | $\cot \lambda_p$ | 0 | 0 | $-r_p$ |
| | Left - handed | $-\cot \lambda_p$ | 0 | 0 | $-r_p$ |

Figures 15.1.2 and 15.1.3 show the location of axes of meshing for a worm-gear drive with the right-handed thread, and with the crossing angles $\gamma = \pi/2$ and $\gamma \neq \pi/2$, respectively. The direction of the thread on the bottom part of the worm is indicated by dashed lines.

Let us now determine the angular velocities of rotation about the axes of meshing. Consider a worm-gear drive. The relative motion of the worm with respect to the gear may be expressed in terms of the angular velocities $\omega^{(1)}$ and $\omega^{(2)}$ of the worm and of the gear (fig. 15.1.1), the crossing angle γ and the shortest distance C . Parameters of the relative motion are represented by the angular velocity

$$\omega^{(12)} = \omega^{(1)} - \omega^{(2)} = -\omega^{(2)} \sin \gamma \mathbf{j} + (\omega^{(1)} - \omega^{(2)} \cos \gamma) \mathbf{k} \quad (15.1.27)$$

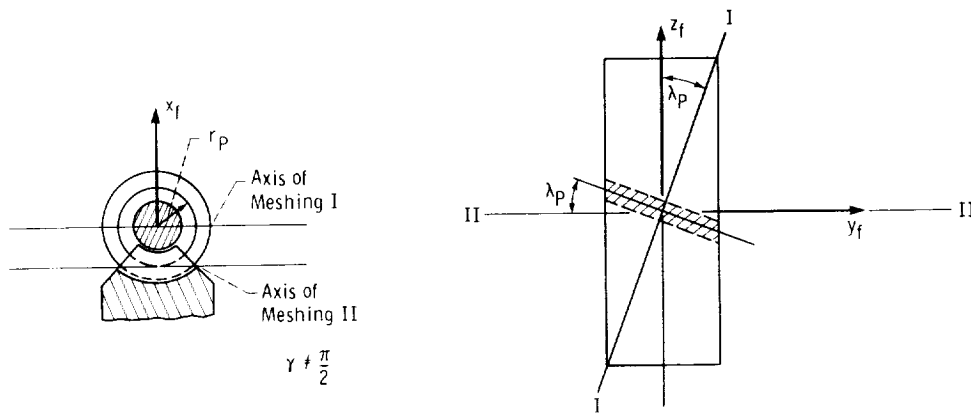


Figure 15.1.2.

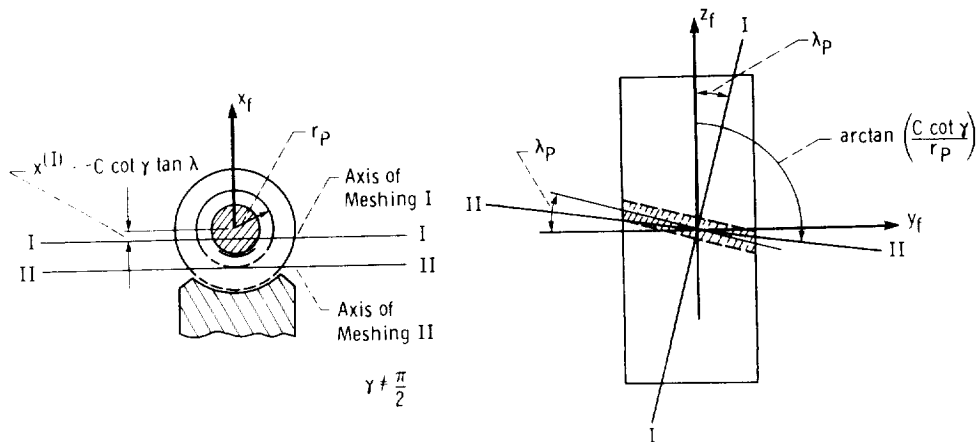


Figure 15.1.3.

and the moment

$$\mathbf{m} = -\mathbf{R} \times \boldsymbol{\omega}^{(2)} = -C\omega^{(2)} \cos \gamma \mathbf{j} + C\omega^{(2)} \sin \gamma \mathbf{k} \quad (15.1.28)$$

We may represent the relative motion as the rotation of the worm about the axes of meshing with angular velocities $\boldsymbol{\omega}^{(I)}$ and $\boldsymbol{\omega}^{(II)}$. We determine $\boldsymbol{\omega}^{(I)}$ and $\boldsymbol{\omega}^{(II)}$ by using the following equations (fig. 15.1.1)

$$\boldsymbol{\omega}^{(I)} + \boldsymbol{\omega}^{(II)} = \boldsymbol{\omega}^{(12)} \quad (15.1.29)$$

$$\overline{O_f O_I} \times \boldsymbol{\omega}^{(I)} + \overline{O_f O_{II}} \times \boldsymbol{\omega}^{(II)} = \mathbf{m} = -\mathbf{R} \times \boldsymbol{\omega}^{(2)} \quad (15.1.30)$$

Equations (15.1.29) and (15.1.30) yield

$$\omega_y^{(I)} + \omega_y^{(II)} = -\omega^{(2)} \sin \gamma \quad (15.1.31)$$

$$\omega_z^{(I)} + \omega_z^{(II)} = K^{(I)}\omega_y^{(I)} + K^{(II)}\omega_y^{(II)} = \omega^{(1)} - \omega^{(2)} \cos \gamma \quad (15.1.32)$$

$$X^{(I)}\omega_z^{(I)} + X^{(II)}\omega_z^{(II)} = X^{(I)}K^{(I)}\omega_y^{(I)} + X^{(II)}K^{(II)}\omega_y^{(II)} = -C\omega^{(2)} \cos \gamma \quad (15.1.33)$$

$$X^{(I)}\omega_y^{(I)} + X^{(II)}\omega_y^{(II)} = C\omega^{(2)} \sin \gamma \quad (15.1.34)$$

Knowing parameters $X^{(i)}$ and $K^{(i)}$ ($i = I, II$), we may determine $\omega_y^{(I)}$ and $\omega_y^{(II)}$ by using only two equations of the equation system (15.1.31) to (15.1.34). This system contains only two independent equations in unknowns $\omega_y^{(I)}$ and $\omega_y^{(II)}$.

15.2 Milling of Worms by Peripheral Milling Cutters: Axes of Meshing

Consider a worm which is generated by a peripheral milling cutter (fig. 15.2.1). Let us set up two fixed coordinate systems $S_c(x_c, y_c, z_c)$ and $S_O(x_O, y_O, z_O)$ (fig. 15.2.2). The surface of the cutter is a surface of revolution. We may imagine that while the cutter is at rest, the worm performs a screw motion which is determined by vectors $\boldsymbol{\omega}$ and $h\boldsymbol{\omega}$, (fig. 15.2.2) where h is the screw parameter. The axis of screw motion is the worm axis z_O . The relative motion of the cutter with respect to the worm is represented by the vectors $(-\boldsymbol{\omega})$ and $(-h\boldsymbol{\omega})$. We do not take into account that the cutter rotates about the z_c -axis, that determines the velocity of cutting only, since this motion is not related with the process of generation of the worm surface.

Let us determine the axes of meshing. We begin with the determination of the equation of meshing of the cutter and the worm that is being generated. We use the equation (ch. 9.8)

$$\mathbf{n}_c \cdot \mathbf{v}_c^{(cw)} = 0 \quad (15.2.1)$$

Here \mathbf{n}_c is the unit normal to the cutter surface, and $\mathbf{v}_c^{(cw)}$ is the relative velocity of the cutter with respect to the worm. We may determine $\mathbf{v}_c^{(cw)}$ by substituting vector $(-\boldsymbol{\omega})$, that is directed along the negative z_O -axis, (fig. 15.2.2) by an equal vector that passes through O_c and the moment given by

$$\mathbf{m} = \overline{O_c O_O} \times (-\boldsymbol{\omega}) \quad (15.2.2)$$

where (fig. 15.2.2) $\overline{O_c O_O} = -C_t \mathbf{i}_c$. Therefore vector $\mathbf{v}_c^{(cw)}$ becomes

$$\mathbf{v}_c^{(cw)} = -\boldsymbol{\omega} \times \mathbf{r}_c - h\boldsymbol{\omega} + \overline{O_c O_O} \times (-\boldsymbol{\omega})$$

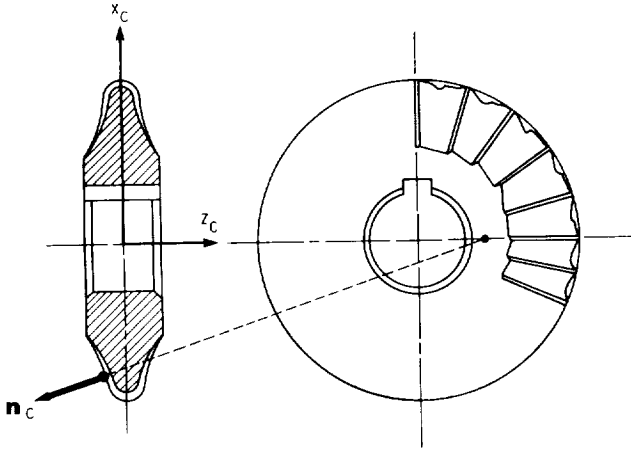


Figure 15.2.1.

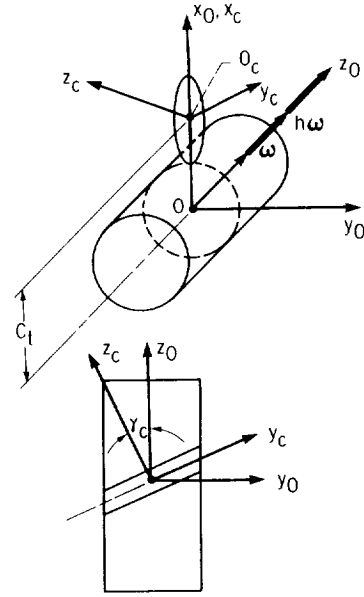


Figure 15.2.2.

$$\begin{aligned}
 &= \begin{vmatrix} \mathbf{i}_c & \mathbf{j}_c & \mathbf{k}_c \\ 0 & -\omega \sin \gamma_c & -\omega \cos \gamma_c \\ x_c & y_c & z_c \end{vmatrix} - \omega h \sin \gamma_c \mathbf{j}_c - \omega h \cos \gamma_c \mathbf{k}_c \\
 &+ \begin{vmatrix} \mathbf{i}_c & \mathbf{j}_c & \mathbf{k}_c \\ -C_t & 0 & 0 \\ 0 & -\omega \sin \gamma_c & -\omega \cos \gamma_c \end{vmatrix} \\
 &= \omega [(-z_c \sin \gamma_c + y_c \cos \gamma_c) \mathbf{i}_c - (x_c \cos \gamma_c + h \sin \gamma_c + C_t \cos \gamma_c) \mathbf{j}_c \\
 &\quad + (x_c \sin \gamma_c - h \cos \gamma_c + C_t \sin \gamma_c) \mathbf{k}_c] \tag{15.2.3}
 \end{aligned}$$

The unit normal to the cutter surface is represented by

$$\mathbf{n}_c = n_{x_c} \mathbf{i}_c + n_{y_c} \mathbf{j}_c + n_{z_c} \mathbf{k}_c \tag{15.2.4}$$

Since the cutter surface is a surface of revolution, a normal to the surface intersects the z_c -axis. The surface coordinates and projections of the unit normal \mathbf{n}_c (fig. 15.2.1) are related as follows:

$$y_c n_{x_c} - x_c n_{y_c} = 0 \tag{15.2.5}$$

(See equations (8.4.7) and (8.4.40).) Equation (15.2.5) is a particular case of equation (15.1.5) because the screw parameter h for a helicoid is zero for a surface of revolution.

Equations (15.2.1), (15.2.3) to (15.2.5) yield the following equation of meshing:

$$x_c n_{z_c} - z_c n_{x_c} - (h + C_t \cot \gamma_c) n_{y_c} - (h \cot \gamma_c - C_t) n_{z_c} = 0 \tag{15.2.6}$$

One of the axes of meshing, axis I-I, coincides with the z_c -axis because the unit normal to the cutter surface intersects the cutter axis (fig. 15.2.1). The other axis of meshing, II-II, may be determined by using the following considerations:

(1) The unit normal at the point of contact must intersect the II-II-axis, and the following equation is to be satisfied:

$$X_c^{(II)}K_c^{(II)}n_{yc} - X_c^{(II)}n_{zc} + x_cn_{zc} - z_cn_{xc} = 0 \quad (15.2.7)$$

Equation (15.2.7) is derived from equation (15.1.4) taking into account that (eq. (15.2.5))

$$x_cn_{yc} - y_cn_{xc} = 0$$

(2) Parameters n_{xc} , n_{yc} , n_{zc} , and x_c, z_c must satisfy the equation of meshing (15.2.6) and parameters $X_c^{(II)}$ and $K_c^{(II)}$ must be independent of the coordinates of the contact point and the projections of the unit normal. Equations (15.2.6) and (15.2.7) yield

$$(X_c^{(II)}K_c^{(II)} + h + C_t \cot \gamma_c)n_{yc} + (-X_c^{(II)} + h \cot \gamma_c - C_t)n_{zc} = 0 \quad (15.2.8)$$

Parameters $X_c^{(II)}$ and $K_c^{(II)}$ do not change in the process of meshing if the following equations are observed:

$$X_c^{(II)} = h \cot \gamma_c - C_t \quad (15.2.9)$$

$$K_c^{(II)} = \frac{h + C_t \cot \gamma_c}{C_t - h \cot \gamma_c} \quad (15.2.10)$$

Equations (15.2.9) and (15.2.10) determine the location and the direction of the second axis of meshing (II-II) in the coordinate system S_c . We may determine the location and the direction of this axis in the coordinate system S_O , by using the matrix equation for the transition from the coordinate system S_c to S_O . Thus

$$\begin{bmatrix} X_O^{(II)} \\ Y_O^{(II)} \\ K_O^{(II)}Y_O^{(II)} \\ 1 \end{bmatrix} = \begin{bmatrix} 1 & 0 & 0 & C_t \\ 0 & \cos \gamma_c & -\sin \gamma_c & 0 \\ 0 & \sin \gamma_c & \cos \gamma_c & 0 \\ 0 & 0 & 0 & 1 \end{bmatrix} \begin{bmatrix} X_c^{(II)} \\ Y_c^{(II)} \\ K_c^{(II)}Y_c^{(II)} \\ 1 \end{bmatrix} \quad (15.2.11)$$

Equations (15.2.9) to (15.2.11) yield

$$X_O^{(II)} = h \cot \gamma_c \quad (15.2.12)$$

$$K_O^{(II)} = -\frac{C_t}{h} \quad (15.2.13)$$

Equations (15.2.12) to (15.2.13) (first proposed by Litvin, 1968) determine the location and the direction of the second axis of meshing (II-II) in the fixed coordinate system S_O . The location of both axes of meshing is shown in figure 15.2.3. The angle δ formed by the axis of meshing II-II and the worm-axis z_O and the parameter a are represented by

$$\delta = \arctan \left(\frac{h}{C_t} \right) \quad (15.2.14)$$

and

$$a = X_O^{(II)} = h \cot \gamma_c \quad (15.2.15)$$

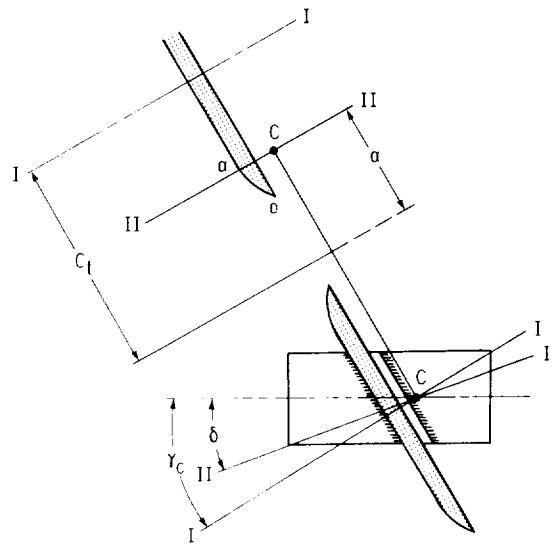


Figure 15.2.3.

15.3 Application of the Theory of Axes of Meshing: Generation of Worm With Concave-Convex Surface

Worm-gear drives with concave-convex surfaces of the worms, proposed by Niemann and Heyer (1953) are produced by the Flender Company. Such worms may be ground with a grinding wheel having a circular arc in the axial section. Generally the line of contact between the grinding-wheel surface and the surface of the worm being generated is a spatial curve.

Litvin (1968) proposed a new type of a concave-convex surface of a worm, that represents a locus of plane curves (circular arcs of the same radius). The proposed surface may be generated by the same grinding wheel, that is applied by the generation of Flender's worms. However, the line of contact between the tool and worm surfaces is not a spatial curve. Rather, it coincides with the axial section of the grinding wheel. This result is provided by special tool settings, that differs from that usually applied.

It was proven in section 15.2 that there are two axes of meshing when a helicoid is generated by a milling cutter with a surface of revolution. One of these axes, I-I, is the z_c -axis of the cutter (grinding wheel) (figs. 15.2.1 and 15.2.3), and the other is the II-II-axis (fig. 15.2.3). Parameters of the II-II-axis of meshing are represented by equations (15.2.14) and (15.2.15).

The line of contact α - α will coincide with the axial section of the grinding wheel if the center C of the circular arc α - α is located at the point of intersection of the II-II-axis with the shortest distance (C_t) between the axes of the cutter and the worm. Parameters a and γ_c of the tool settings are related by the equation (h is given)

$$\gamma_c = \arctan \left(\frac{h}{a} \right) \quad (15.3.1)$$

The above statement is clear if we take into account that the cutter surface is a surface of revolution generated by the circular arc α - α in rotational motion about the cutter axis I-I. Thus the normals to the cutter surface at points of arc α - α indeed intersect the I-I and II-II axes of meshing.

Parameters (a , γ_c) are related by equation (15.3.1) and determine the tool settings; parameter a may be chosen arbitrary. However, the shape of lines of contact of the worm and the worm-gear surfaces depends on parameter a . Litvin (1968) recommended to have

$$a = r_p + h \sin \psi_n \quad (15.3.2)$$

where r_p is the radius of the pitch cylinder of the worm, and ψ_n is the normal pressure angle.

Let us now derive equations of the worm surface. We set up the following coordinate systems:

(1) $S_c(x_c, y_c, z_c)$ rigidly connected to the tool (fig. 15.3.1).

(2) A movable coordinate system S_b (figs. 15.3.1 and 15.3.2), where axis z_b is parallel to the axis z_c , and the origin O_b is located on the circle of radius d , that is drawn in plane $z_c = 0$ and centered at O_c .

(3) The coordinate system $S_1(x_1, y_1, z_1)$ rigidly connected to the worm.

(4) The fixed coordinate system $S_0(x_0, y_0, z_0)$ rigidly connected to the frame (fig. 15.3.3).

The worm being generated performs a screw motion with components ψ and $h\psi$ (fig. 15.3.3(c)) of the angle of rotation about and the translation along the screw axis (z_0), respectively.

The circular arc is represented in the coordinate system S_b by (fig. 15.3.1)

$$x_b = -\rho \sin \theta \quad y_b = 0 \quad z_b = \rho \cos \theta$$

The coordinate transformation in transition from the coordinate system S_b to S_c is represented by the following matrix equation (figs. 15.3.2 and 15.3.1):

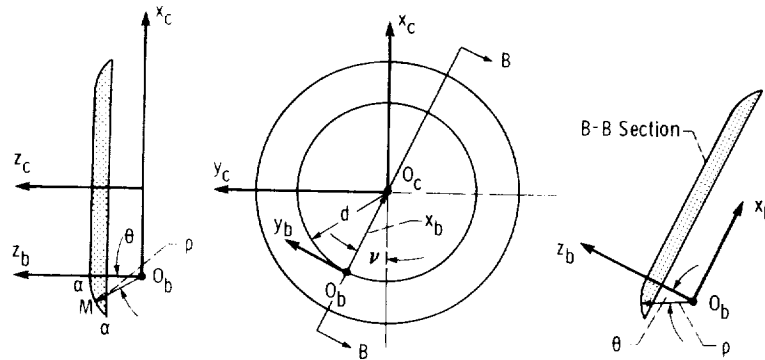


Figure 15.3.1.

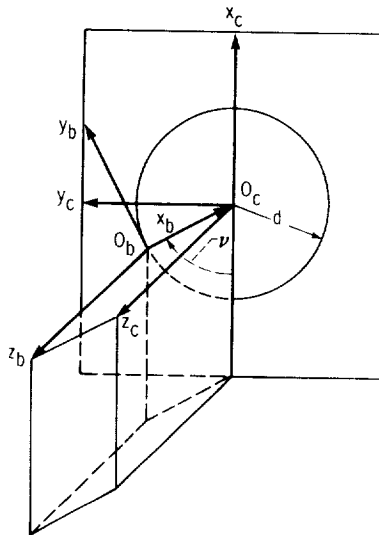


Figure 15.3.2.

$$\begin{bmatrix} x_c \\ y_c \\ z_c \\ 1 \end{bmatrix} = [M_{cb}] \begin{bmatrix} -\rho \sin \theta \\ 0 \\ \rho \cos \theta \\ 1 \end{bmatrix} = \begin{bmatrix} \cos \nu & \sin \nu & 0 & -d \cos \nu \\ -\sin \nu & \cos \nu & 0 & d \sin \nu \\ 0 & 0 & 1 & 0 \\ 0 & 0 & 0 & 1 \end{bmatrix} \begin{bmatrix} -\rho \sin \theta \\ 0 \\ \rho \cos \theta \\ 1 \end{bmatrix} \quad (15.3.3)$$

that yields

$$x_c = -(\rho \sin \theta + d) \cos \nu \quad y_c = (\rho \sin \theta + d) \sin \nu \quad z_c = \rho \cos \theta \quad (15.3.4)$$

Here

$$d = C_t - a \quad (15.3.5)$$

Equations (15.3.4) represent the cutter surface in coordinate system S_c ; ν and θ are the surface coordinates. The surface unit normal is represented by the equations

$$\mathbf{n}_c = \frac{\mathbf{N}_c}{|\mathbf{N}_c|} \quad \text{where} \quad \mathbf{N}_c = \frac{\partial \mathbf{r}_c}{\partial \theta} \times \frac{\partial \mathbf{r}_c}{\partial \nu} \quad (15.3.6)$$

Equations (15.3.4) and (15.3.6) yield that the surface unit normal is represented by (provided $\rho \sin \theta + d \neq 0$)

$$\mathbf{n}_c = \sin \theta (\cos \nu \mathbf{i}_c - \sin \nu \mathbf{j}_c) - \cos \theta \mathbf{k}_c \quad (15.3.7)$$

We represented the equation of meshing in general form by equation (15.2.6) as follows:

$$x_c n_{z_c} - z_c n_{x_c} - (h + C_t \cot \gamma_c) n_{y_c} - (h \cot \gamma_c - C_t) n_{z_c} = 0$$

Substituting in this equation for x_c , z_c , n_{x_c} , n_{y_c} , n_{z_c} , d , $\cot \gamma_c$ the following expressions

$$\begin{aligned} x_c &= -(\rho \sin \theta + d) \cos \nu & z_c &= \rho \cos \theta & n_{x_c} &= \sin \theta \cos \nu \\ n_{y_c} &= -\sin \theta \sin \nu & n_{z_c} &= -\cos \theta & d &= C_t - a \end{aligned}$$

$$\cot \gamma_c = \frac{a}{h}$$

(see equations (15.3.4), (15.3.7), (15.3.5), (15.3.1)), we obtain

$$(C_t - a)(1 - \cos \nu) \cos \theta - (C_t \frac{a}{h} + h) \sin \nu \sin \theta = 0 \quad (15.3.8)$$

There are two solutions of equation (15.3.8) for ν and θ : (1) with $\nu = 0$ and any value of θ , and (2) with values of θ and ν related by the equation

$$\tan \theta = \frac{(C_t - a)h}{C_t a + h^2} \tan \frac{\nu}{2} \quad (15.3.9)$$

These solutions result in the existence of two lines of contact on the surface of the grinding wheel. One of these lines (with $\nu = 0$ and any θ) is the circular arc α - α ; the second line is out of the working space of the worm and we do not take it into account.

With $\nu = 0$ the unit normal of the tool surface is represented by (equations (15.3.7))

$$\mathbf{n}_c = \sin \theta \mathbf{i}_c - \cos \theta \mathbf{k}_c \quad (15.3.10)$$

This means that the normals to the line of contact lie in the same plane ($y_c = 0$). Thus the analytical solution confirms that the line of contact of the surfaces of the tool and the worm being generated is a plane curve, and it is the circular arc α - α (fig. 15.3.1).

In section 15.4 we will need equations of the worm surface. This surface may be determined as a locus of contact lines represented in the coordinate system $S_1(x_1, y_1, z_1)$ (fig. 15.3.3). The coordinate transformation in transition from the coordinate system S_c to the coordinate system S_1 is represented by the following matrix equation (fig. 15.3.3)

$$\begin{bmatrix} x_1 \\ y_1 \\ z_1 \\ 1 \end{bmatrix} = [M_{1c}] \begin{bmatrix} x_c \\ y_c \\ z_c \\ 1 \end{bmatrix} = [M_{1O}][M_{Oc}] \begin{bmatrix} -(\rho \sin \theta + d) \\ 0 \\ \rho \cos \theta \\ 1 \end{bmatrix} \quad (15.3.11)$$

We determined the coordinates x_c, y_c, z_c for the contact line by using equations (15.3.4) and taking into account that $\nu = 0$. Matrices $[M_{1O}]$ and $[M_{Oc}]$ are represented as follows (fig. 15.3.3)

$$[M_{Oc}] = \begin{bmatrix} 1 & 0 & 0 & C_t \\ 0 & \cos \gamma_c & -\sin \gamma_c & 0 \\ 0 & \sin \gamma_c & \cos \gamma_c & 0 \\ 0 & 0 & 0 & 1 \end{bmatrix} \quad (15.3.12)$$

$$[M_{1O}] = \begin{bmatrix} \cos \psi & \sin \psi & 0 & 0 \\ -\sin \psi & \cos \psi & 0 & 0 \\ 0 & 0 & 1 & -h\psi \\ 0 & 0 & 0 & 1 \end{bmatrix} \quad (15.3.13)$$

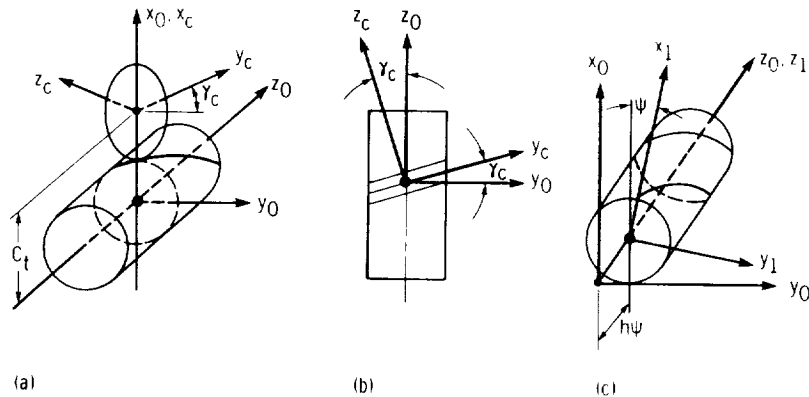


Figure 15.3.3.

where ψ is the angle of rotation of the worm that is in mesh with the tool. Equations (15.3.11) to (15.3.13) and (15.3.5) yield

$$\left. \begin{aligned} x_1 &= -\rho(\sin \theta \cos \psi + \sin \gamma_c \cos \theta \sin \psi) + a \cos \psi \\ y_1 &= \rho(\sin \theta \sin \psi - \sin \gamma_c \cos \theta \cos \psi) - a \sin \psi \\ z_1 &= \rho \cos \gamma_c \cos \theta - h\psi \end{aligned} \right\} \quad (15.3.14)$$

Here θ and ψ are the surface coordinates.
The surface unit normal is given by

$$\mathbf{n}_1 = \frac{\mathbf{N}_1}{|\mathbf{N}_1|} \quad \text{where} \quad \mathbf{N}_1 = \frac{\partial \mathbf{r}_1}{\partial \mathbf{r}} \times \frac{\partial \mathbf{r}_1}{\partial \psi} \quad (15.3.15)$$

Equations (15.3.14), (15.3.15), and (15.3.1) yield

$$\begin{aligned} N_{x1} &= m(\sin \theta \cos \psi + \sin \gamma_c \cos \theta \sin \psi) \\ N_{y1} &= -m(\sin \theta \sin \psi - \sin \gamma_c \cos \theta \cos \psi) \\ N_{z1} &= -m(\cos \gamma_c \cos \theta) \end{aligned} \quad (15.3.16)$$

where $m = \rho^2 \cos \gamma_c \sin \theta - (\rho h / \sin \gamma_c)$. The surface unit normal is represented by the following equations (provided $m \neq 0$)

$$\begin{aligned} n_{x1} &= \sin \theta \cos \psi + \sin \gamma_c \cos \theta \sin \psi \\ n_{y1} &= -\sin \theta \sin \psi + \sin \gamma_c \cos \theta \cos \psi \\ n_{z1} &= -\cos \gamma_c \cos \theta \end{aligned} \quad (15.3.17)$$

We could obtain equations (15.3.17) in a simpler way just by using the matrix equation

$$[n_1] = [L_{1O}][L_{Oc}][n_c] \quad (15.3.18)$$

Matrices $[L_{1O}]$ and $[L_{Oc}]$ may be derived from matrices $[M_{1O}]$ and $[M_{Oc}]$ by deleting the last column and the last row in them. (See appendix A.) Matrix $[n_c]$ is given by (equations (15.3.10))

$$[n_c] = \begin{bmatrix} \sin \theta \\ 0 \\ -\cos \theta \end{bmatrix} \quad (15.3.19)$$

15.4 Knots of Meshing

The surface of action may be represented as a locus of lines of contact of gear-tooth surfaces in the fixed coordinates system rigidly connected to the frame. Generally a section of the surface of action cut by a plane represents a plane curve. There are special cases where a section of the surface of action represents a straight line if the following conditions are satisfied (proven by Litvin, 1968):

- (1) The gears transform rotation between crossed axes with a constant angular velocity ratio.
- (2) The tooth surface of one of the mating gears is a helicoid.
- (3) The surface of action is cut by a plane that is parallel to the shortest distance C between the axes of gear rotation and is located at a definite distance from C . The contact lines of gear tooth surfaces intersect the above mentioned straight lines. These points of intersection are called the knots of meshing, since we may imagine that the lines of contact are attached to the straight lines, that are obtained as sections of the surface of action.

Figures 15.4.1 and 15.4.2 show projections of contact lines of the worm and the worm-gear surfaces on the plane (x_f, y_f) . These contact lines are determined for the worm-gear drives with the concave-convex surfaces of worms generated by methods proposed by Niemann and Heyer (1953) (fig. 15.4.1) and by Litvin (1968) (fig. 15.4.2), respectively. Points $\epsilon, f, \epsilon',$ and f' represent projections of the lines of knots of meshing. Changing the location of the lines of knots, we can improve the shape of contact lines to obtain better conditions of lubrication.

The evidence of the existence of lines of knots is based on the following considerations:

- (1) Since the worm surface is a helicoid, two axes of meshing exist. The normal at any point of contact of the worm and the worm-gear surfaces intersects both axes of meshing. (See sec. 15.1.)
- (2) There can be a limiting case when the common surface normal intersects one of the two axes of meshing and is parallel to the other one. (The normal intersects the other axis of meshing at infinity.)

Figure 15.4.3 shows a cross section of the worm surface at two positions for a worm of a worm-gear drive with a crossing angle of 90° . The normal $n-n$ to the worm surface intersects the I-I-axis of meshing and is parallel to the II-II-axis of meshing. The upper lines of knots of meshing are $f'-f'$ and $\epsilon'-\epsilon'$, respectively.

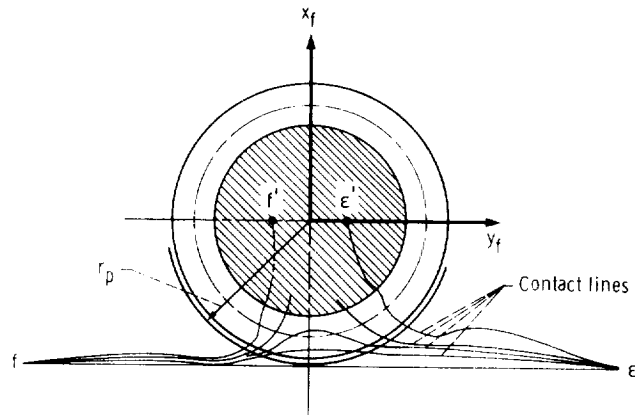


Figure 15.4.1.

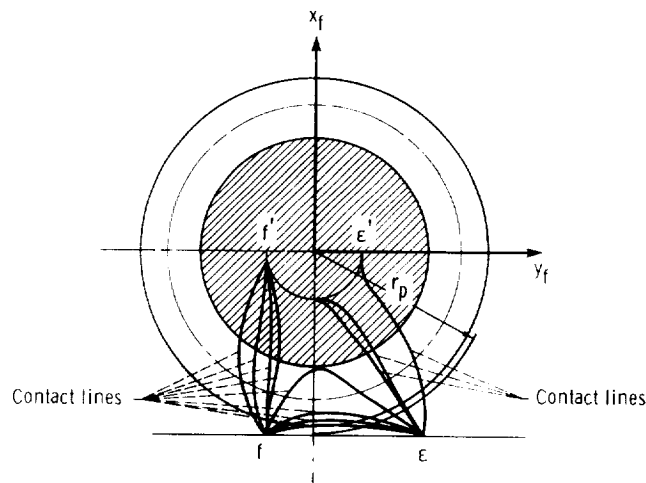


Figure 15.4.2.

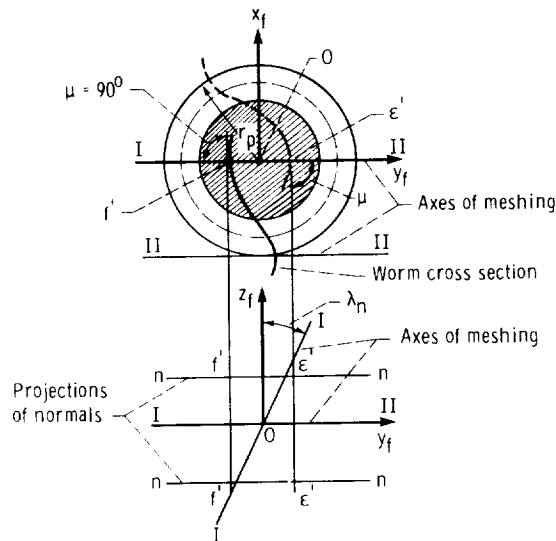


Figure 15.4.3.

Figure 15.4.4 shows a cross section of the worm surface at two other positions. The normal $n-n$ to the worm surface intersects the II-II-axis of meshing. The bottom lines of the knots are $f-f$ and $\epsilon-\epsilon$, respectively.

Considering the general case of the crossing angle $\gamma \neq 90^\circ$, we represent the lines of knots by the following equations. (See table 15.1.1.) (1) The upper lines of knots of meshing are determined by

$$x_f = X_f^{(I)} = \mp C \cot \gamma \tan \lambda_p \quad (15.4.1)$$

$$n_{yf} = 0 \quad (15.4.2)$$

$$\frac{n_{zf}}{n_{yf}} = K^{(II)} = \frac{C \cot \gamma}{r_p} \quad (15.4.3)$$

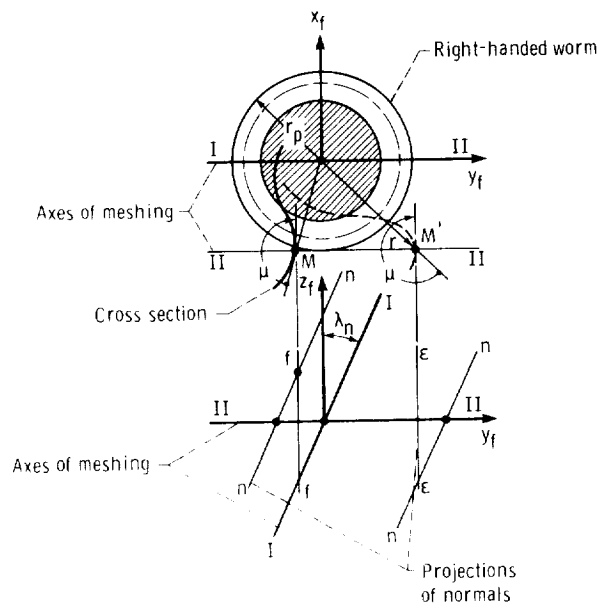


Figure 15.4.4.

Here, (x_f, y_f, z_f) are the coordinates of the point of contact of the worm and the worm-gear surfaces; (n_{xf}, n_{yf}, n_{zf}) are the projections of the common normal to the surfaces; (x_f, y_f, z_f) and (n_{xf}, n_{yf}, n_{zf}) are determined for an angle of the worm rotation when one point of the instantaneous line of contact of mating surfaces is the point of the upper line of knots simultaneously.

Equation (15.4.1) results in that the upper line of knots intersects the I-I-axis of meshing. Equations (15.4.2) and (15.4.3) yield that the common normal to the mating surfaces is parallel to the II-II-axis of meshing.

(2) The bottom lines of knots are represented by

$$x_f = X_f^{(II)} = -r_p \quad (15.4.4)$$

$$n_{xf} = 0 \quad (15.4.5)$$

$$\frac{n_{zf}}{n_{yf}} = K^{(I)} = \pm \cot \lambda_p \quad (15.4.6)$$

Equations (15.4.4) to (15.4.6) are based on the same considerations. The upper and lower signs in equations (15.4.1) and (15.4.6) correspond to the right-handed and left-handed worm thread, respectively.

Example problem 15.4.1 Consider the worm surface and its unit normal that are represented in coordinate system S_1 by equations (15.3.14) and (15.3.17), respectively. The crossing angle $\gamma = 90^\circ$.

Determine the lines of knots of meshing by using equations (15.4.1) to (15.4.3) and (15.4.4) to (15.4.6), respectively.

Solution. We represent the equations of the worm surface and the surface unit normal in coordinate system S_f by using the matrix equations

$$[r_f] = [M_{f1}][r_1] \quad (15.4.7)$$

$$[n_f] = [L_{f1}][n_1] \quad (15.4.8)$$

Here (see equation (1.3.22))

$$[M_{f1}] = \begin{bmatrix} \cos \phi_1 & -\sin \phi_1 & 0 & 0 \\ \sin \phi_1 & \cos \phi_1 & 0 & 0 \\ 0 & 0 & 1 & 0 \\ 0 & 0 & 0 & 1 \end{bmatrix} \quad (15.4.9)$$

$$[L_{f1}] = \begin{bmatrix} \cos \phi_1 & -\sin \phi_1 & 0 \\ \sin \phi_1 & \cos \phi_1 & 0 \\ 0 & 0 & 1 \end{bmatrix} \quad (15.4.10)$$

Equations (15.3.14) and (15.4.9), and (15.3.17) and (15.4.10) yield the equations of the worm surface and the surface unit normal, respectively, as follows:

$$\left. \begin{aligned} x_f &= -\rho[\sin \theta \cos (\psi - \phi_1) + \sin \gamma_c \cos \theta \sin (\psi - \phi_1)] + a \cos (\psi - \phi_1) \\ y_f &= \rho[\sin \theta \sin (\psi - \phi_1) - \sin \gamma_c \cos \theta \cos (\psi - \phi_1)] - a \sin (\psi - \phi_1) \\ z_f &= \rho \cos \gamma_c \cos \theta - h\psi \end{aligned} \right\} \quad (15.4.11)$$

$$\left. \begin{aligned} n_{xf} &= \sin \theta \cos (\psi - \phi_1) + \sin \gamma_c \cos \theta \sin (\psi - \phi_1) \\ n_{yf} &= -\sin \theta \sin (\psi - \phi_1) + \sin \gamma_c \cos \theta \cos (\psi - \phi_1) \\ n_{zf} &= -\cos \gamma_c \cos \theta \end{aligned} \right\} \quad (15.4.12)$$

Here ϕ_1 is the angle of rotation of the worm that is in mesh with the worm gear.

Using equations (15.4.11), (15.4.12), and (15.4.1) to (15.4.4), we obtain for the upper lines of knots that

$$\theta = \frac{\pi}{2} \quad \sin (\psi - \phi_1) = \pm 1 \quad x_f = 0 \quad y_f = \pm (\rho - a) \quad (15.4.13)$$

Similarly, we get for the bottom lines of knots that

$$\tan \theta = -\tan (\psi - \phi_1) \sin \gamma_c \quad \cos (\psi - \phi_1) = -\tan \gamma_c \cot \lambda_p \quad (15.4.14)$$

where ($0 < \theta < 90^\circ$). Equations (15.4.11), (15.3.1) and (15.4.14) yield

$$x_f = -a \tan \gamma_c \cot \lambda_p = -h \cot \lambda_p = -r_p \quad (15.4.15)$$

$$y_f = \rho \frac{\cos \theta \cos \gamma_c}{\cot \lambda_p} - a \sin (\psi - \phi_1) \quad (15.4.16)$$

We may transform equations (15.4.14) taking into account that

$$\cos \theta = \frac{1}{\sqrt{1 + \tan^2 \theta}} = \frac{\cos \lambda_p}{\cos \gamma_c} \quad (15.4.17)$$

$$\tan \lambda_p = \frac{h}{r_p} \quad (15.4.18)$$

$$\sin (\psi - \phi_1) = \pm \sqrt{1 - \tan^2 \gamma_c \cot^2 \lambda_p} = \pm \frac{\sqrt{a^2 - r_p^2}}{a} \quad (15.4.19)$$

From equations (15.4.16) to (15.4.19), we get

$$y_f = \frac{\rho h}{\sqrt{h^2 + r_p^2}} \pm \sqrt{a^2 - r_p^2} \quad (15.4.20)$$

Equations (15.4.15) and (15.4.20) determine the location of the bottom lines of knots.

The upper lines of knots (f' and ϵ') and the bottom lines of knots (f and ϵ) are shown in figure 15.4.3 and figure 15.4.4. The tooth element proportions are nonstandard and r_p is the radius of the operating pitch cylinder of the worm.

Chapter 16

Methods for Generation of Conjugate Gear-Tooth Surfaces

16.1 Introduction to Gear Generation

Gear-tooth surfaces are termed conjugated if the gears, having such surfaces, transform rotation with a prescribed constant angular velocity ratio (the prescribed ratio function for noncircular gears).

The gear-tooth surfaces are usually generated with an auxiliary surface called the generating surface. The methods of generation are applicable in practice if the generating surface (the tool surface) is simple enough and may be manufactured with high precision. We may differentiate between the following methods of generation:

Method 1

The generating surface Σ_g is identical to the tooth surface of one of the mating gears (say Σ_1). In the process of cutting, the meshing of $\Sigma_g \equiv \Sigma_1$ and Σ_2 has to simulate the meshing of Σ_1 and Σ_2 in the designed gear train.

Method 2

The generating surface Σ_g differs from the gear-tooth surfaces, Σ_1 and Σ_2 . The principle of generation is based on the imaginary meshing of three surfaces— Σ_g , Σ_1 , and Σ_2 simultaneously. This method provides conjugate gear tooth surfaces with two types of the instantaneous contact: (1) contact at a point and (2) contact along a line.

Method 3

Two noncoinciding generating surfaces, Σ_F and Σ_P , are used for generation of gears with surfaces Σ_1 and Σ_2 . It is assumed that the generating surfaces contact each other at a line. Generating surface Σ_F generates surface Σ_1 and is in line contact with Σ_1 . Similarly, generating surface Σ_P generates surface Σ_2 of gear 2 and is also in line contact with Σ_2 . However, at every instant, gear surfaces Σ_1 and Σ_2 will contact each other at a point only.

Method 4

The gear-tooth surfaces are generated with one or two auxiliary lines. The shapes of these lines are the shapes of the tool blades.

16.2 Generation Method 1

It was mentioned previously that the generating surface Σ_g is identical to the tooth surface of one of the gears (gear 1). A typical example of this method is the generation of gear-worm drives with cylindrical worms, which is based on the following principles:

(1) The worm gear is generated by a hob, which is identical to the cylindrical worm of the gear-drive.

(2) The meshing of the hob with the worm-gear being generated simulates the meshing of the worm with the worm gear.

To design the generating worm, (the hob), we have to increase its addendums to provide a clearance between the addendums of the worm and the dedendums of the worm gear. We also have to check conditions of nonundercutting of the worm gear by the generating hob. The disadvantages of the method discussed are:

(1) The use of a large number of tools, (the hobs), because for worm-gear drives with different parameters of worms, we have to use different tools.

(2) The sensitivity of the worm-gear drive to misalignment and other errors of assembly and manufacturing as a result of the line contact of surfaces Σ_1 and Σ_2 .

16.3 Generation Method 2

This well-known method is based on the following principles:

(1) Gear-tooth surfaces Σ_1 and Σ_2 are generated by the same generating surface Σ_g .

(2) Surfaces $\Sigma_g - \Sigma_1$ and $\Sigma_g - \Sigma_2$ are in line contact.

(3) The contact of surfaces Σ_1 and Σ_2 are either in (a) line contact or (b) point contact.

General considerations as to the type of contact that surfaces Σ_1 and Σ_2 may have are as follows:

Consider the mesh of surfaces Σ_g and Σ_1 . These surfaces are in line contact at every instant and surface Σ_g may be covered with lines $L_{g1}(\phi)$ (fig. 16.3.1(a)). Here ϕ is the parameter of motion which determines the orientation and location of the generating gear and gear 1 in the fixed coordinate system. Each line of the family $L_{g1}(\phi)$ will be the instantaneous line of contact of surfaces Σ_g and Σ_1 that are in mesh.

Considering the mesh of the generating gear and gear 2, we may also determine the family of instantaneous lines of contact ($L_{g2}(\phi)$) of surfaces Σ_g and Σ_2 . It is evident that gears 1 and 2 will be in line contact if and only if both families of contact lines, $L_{g1}(\phi)$ and $L_{g2}(\phi)$, coincide with each other. Thus, at every instant, surfaces Σ_g , Σ_1 , and Σ_2 will contact each other along the same line; that is, one of the lines of the family $L_{g1}(\phi) \equiv L_{g2}(\phi)$. Gears 1 and 2, with surfaces Σ_1 and Σ_2 , will contact each other at a point only if the families of contact lines, $L_{g1}(\phi)$ and $L_{g2}(\phi)$, do not coincide but have a common point at every instant (fig. 16.3.1(b)).

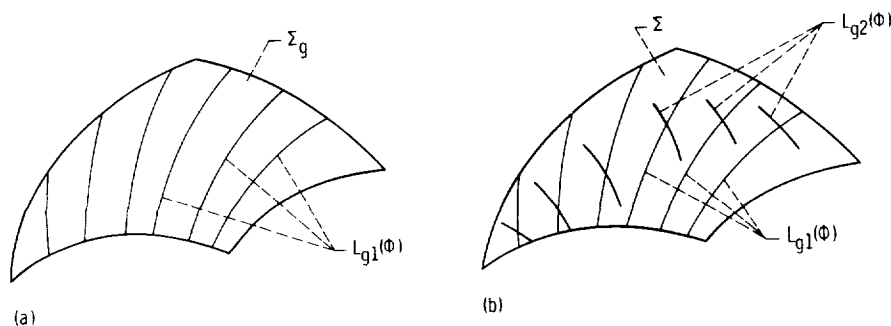


Figure 16.3.1.

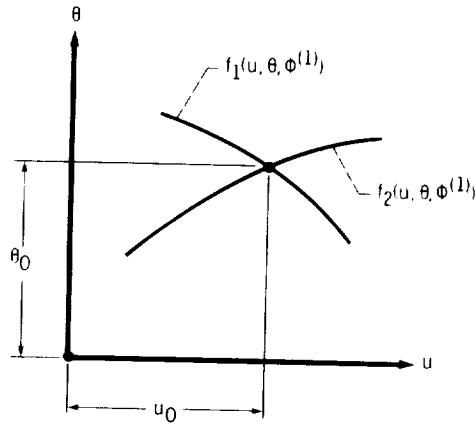


Figure 16.3.2.

The analytical determination of $L_{g1}(\phi)$ and $L_{g2}(\phi)$ is based on the following procedure. Consider that surface Σ_g is represented by the vector function

$$\mathbf{r}(u, \theta) \in C^1 \quad \mathbf{r}_u \times \mathbf{r}_\theta \neq 0 \quad (u, \theta) \in E \quad (16.3.1)$$

where u and θ are the surface coordinates. The surface normal is given by

$$\mathbf{N}(u, \theta) = \mathbf{r}_u \times \mathbf{r}_\theta \quad (16.3.2)$$

Using methods described in section 2.3, we may determine the relative velocity $\mathbf{v}^{(g1)}(\phi)$ and $\mathbf{v}^{(g2)}(\phi)$ of the generating gear with respect to gears 1 and 2.

The family of contacting lines $L_{g1}(\phi)$ on surface Σ_g is represented by the equations

$$\mathbf{r} = \mathbf{r}(u, \theta) \quad \mathbf{N} \cdot \mathbf{v}^{(g1)} = f_1(u, \theta, \phi) = 0 \quad (16.3.3)$$

Similarly, we get that the family of contacting lines $L_{g2}(\phi)$ is represented by the equations

$$\mathbf{r} = \mathbf{r}(u, \theta) \quad \mathbf{N} \cdot \mathbf{v}^{(g2)} = f_2(u, \theta, \phi) = 0 \quad (16.3.4)$$

Surfaces Σ_1 and Σ_2 are in line contact if functions $f_1(u, \theta, \phi)$ and $f_2(u, \theta, \phi)$ are identical. Surfaces Σ_1 and Σ_2 are in point contact if these functions are not identical but the equation

$$f_1(u, \theta, \phi) = f_2(u, \theta, \phi) = 0 \quad (16.3.5)$$

possesses a unique solution for u and θ with a fixed value of ϕ . The graphical solution of equation (16.3.5) with $\phi = \phi^{(1)}$ is (u_0, θ_0) as shown in figure 16.3.2.

An important particular case is when gears 1 and 2 transform rotation between parallel or intersecting axes. In this case, the relative motion of the gears is rotation about the instantaneous axis, that is the line of tangency of pitch cylinders (respectively, pitch cones). The generating gear g will provide an instantaneous contact line for gear surfaces Σ_1 and Σ_2 if the relative motion of g , with respect to gears 1 and 2, is determined with the same instantaneous axis of rotation. This principle of generation is applied to spur gears, (fig. 7.2.1, fig. 7.2.3), to helical gears with parallel axes, and to bevel gears. In the case of generation of bevel gears, the generating gear g , and gears 1 and 2 rotate about axes $O-a_g$, $O-a_1$, and $O-a_2$, respectively (fig. 16.3.3). These axes lie in the same plane and intersect each other at a common point O . Axis $O-I$ will be the instantaneous axis of rotation for any pair of three sets of gears— g and 1, g and 2, and 1 and 2—if the line of action of vectors

$$\boldsymbol{\omega}^{(g1)} = \boldsymbol{\omega}^{(g)} - \boldsymbol{\omega}^{(1)} \quad \boldsymbol{\omega}^{(g2)} = \boldsymbol{\omega}^{(g)} - \boldsymbol{\omega}^{(2)} \quad \boldsymbol{\omega}^{(12)} = \boldsymbol{\omega}^{(1)} - \boldsymbol{\omega}^{(2)}$$

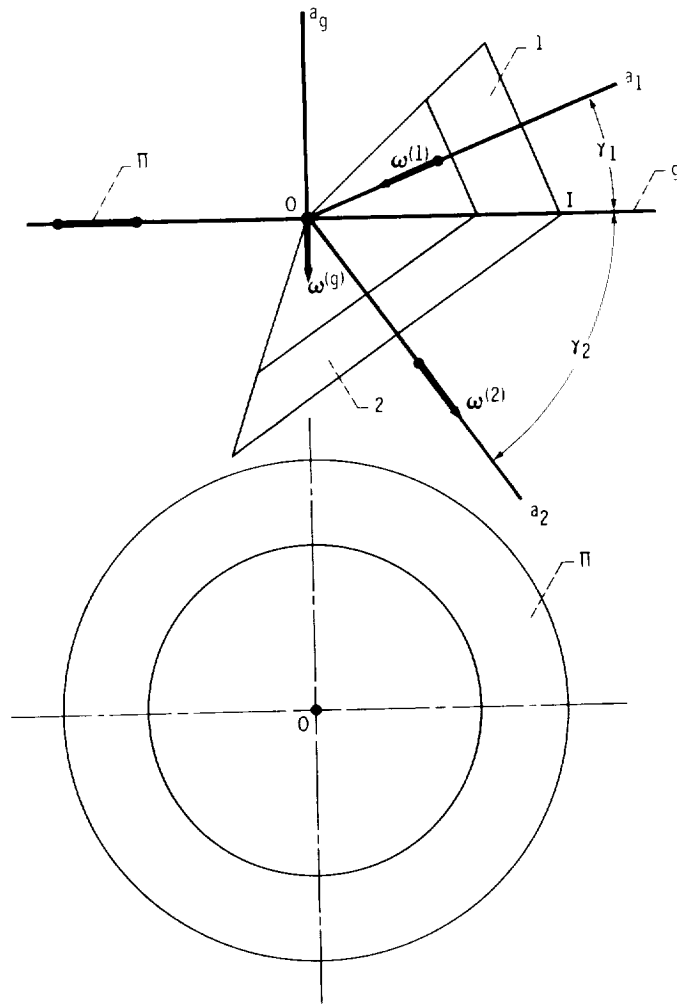


Figure 16.3.3.

coincide with $O-I$. This condition is satisfied with the following relations:

$$\frac{\omega^{(g)}}{\omega^{(1)}} = \sin \gamma_1 \quad \frac{\omega^{(g)}}{\omega^{(2)}} = \sin \gamma_2 \quad \frac{\omega^{(1)}}{\omega^{(2)}} = \frac{\sin \gamma_2}{\sin \gamma_1} \quad (16.3.6)$$

Now consider the generation of gears with crossed axes by the generating surface Σ_g . Gears 1 and 2 rotate about their crossed axes with the prescribed angular velocity ratio $m_{12} = \omega^{(1)}/\omega^{(2)}$. The relative motion of gears 1 and 2 may be represented as a screw motion whose components are: (1) rotation about the axis of screw motion with angular velocity $\omega^{(12)} = \omega^{(1)} - \omega^{(2)}$ and (2) translation along this axis with the velocity $h\omega^{(12)}$. (Here h is the screw parameter.) We can generate gears 1 and 2 having an instantaneous contacting line of their surfaces if and only if the relative motion of the generating gear with respect to gears 1 and 2 is represented by the same screw motion. If this condition is not satisfied, the generating gear g will generate gear-tooth surfaces Σ_1 and Σ_2 , that are in point contact.

Generation of Drives with Beveloid Gearing

The principle of generation discussed is applied, for instance, for the generation of drives with beveloid gearing. Beveloid gearing (Dudley, 1962), proposed by Vinco Corporation of Detroit, is applied for the transformation of rotation between intersecting and crossing axes. Figure 16.3.4

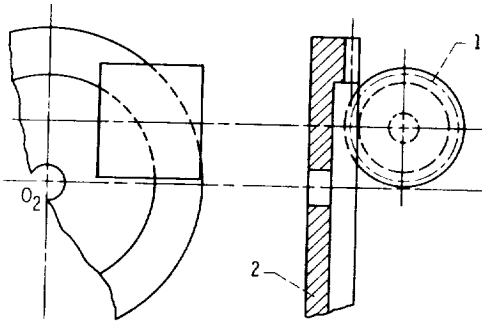


Figure 16.3.4.

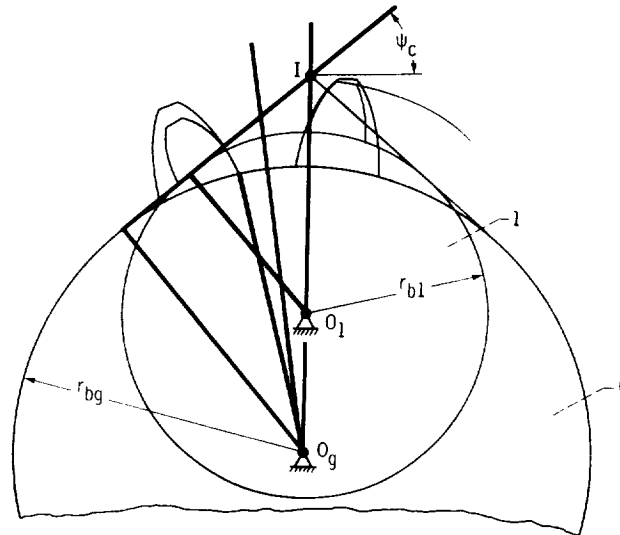


Figure 16.3.5.

shows a beveloid gearing drive with crossed gear axes. One of the gears (gear 1) is a regular involute gear. The other gear (gear 2) is a noninvolute face gear whose generation is based on simulation of the conditions of meshing of the gear train when the generating gear cuts gear 2. This can be done if an involute shaper, identical to gear 1 of the train, would cut the noninvolute gear with the same settings and gear ratio as the ones prescribed for the train. This method provides an instantaneous line contact of gear-tooth surfaces Σ_1 and Σ_2 .

To reduce the sensitivity of the train to gear errors, a point contact of Σ_1 and Σ_2 is to be provided. For this reason, an auxiliary generating surface Σ_g is applied. (A surface of an involute shaper whose number of teeth N_g is larger than the tooth number N_1 of gear 1 is applied.) We may imagine that surface Σ_g , which is in internal tangency with Σ_1 (fig. 16.3.5), is simultaneously in tangency with Σ_2 . The mesh of generating gear g with gear 1 is simply the mesh of two involute gears with base circles of radii r_{b1} and r_{bg} , respectively (fig. 16.3.5). The shapes of gears are in internal tangency and I is the pitch point (the instantaneous center of rotation). However, the mesh of generating gear g with gear 2 is a case of a spatial gearing.

The instantaneous lines of contact $L_{g1}(\phi)$ are straight lines which are parallel to the axes of gear rotation. The instantaneous lines of contact $L_{g2}(\phi)$ are spatial curves and they do not coincide with $L_{g1}(\phi)$. However, lines of contact $L_{g1}(\phi)$ and $L_{g2}(\phi)$ have a common point for a fixed value of ϕ . This point is the instantaneous point of tangency of gears 1 and 2.

It was aforementioned that the disadvantage of gears having line contact of their surfaces is the sensitivity to misalignments and other errors of manufacturing and assembly. For these reasons, it can be expected that the line contact of gears is to be substituted with a point contact, even for the traditional types of gears – spur gears and helical gears with parallel axes.

16.4 Generation Method 3

This method of generation is based on the application of two generating surfaces Σ_F and Σ_P , that separately generate gear 1 and gear 2, respectively. The generating surfaces are so designed that they can contact each other at a line L_{FP} .

Consider that generating surfaces Σ_F and Σ_P , that contact each other at L_{FP} , are rigidly connected to each other. The motion of rigidly connected surfaces Σ_F and Σ_P with respect to gears 1 and 2 may be represented as the motion of a rigid body. However, we assume that in the process of generation surface Σ_1 is in mesh only with surface Σ_F and that Σ_2 is in mesh only with surface Σ_P .

Figure 16.4.1(a) shows the generating surfaces Σ_F and Σ_P , that are in contact at L_{FP} . Surface Σ_F contacts surface Σ_1 at every instant along a line. Figure 16.4.1(b) shows the family of contact lines $L_{F1}(\phi)$ on the generating surface. (Here ϕ is the parameter of generation motion.) Similarly, each line of the set $L_{P2}(\phi)$ is the instantaneous line of contact for surfaces Σ_P and Σ_2 (fig. 16.4.1(c)).

It is evident that the generated surfaces Σ_1 and Σ_2 can have a point contact instead of a line contact only if $L_{F1}(\phi)$ is not identical to $L_{P2}(\phi)$. Such a point lies on line L_{FP} and is the point of intersection of three lines— L_{FP} and two mating lines of families $L_{F1}(\phi)$ and $L_{P2}(\phi)$. (Mating contact lines on surfaces Σ_F and Σ_P are determined for the same fixed value of ϕ .)

The advantage of the method of generation discussed is the localization of the bearing contact, reduced sensitivity of gears to misalignment, and other errors in assembly and manufacturing.

Generation of Bevel Gears

Let us consider the generation process for bevel gears. Two bevel gears transform rotation between intersected axes $O-a_1$ and $O-a_2$ with angular velocities $\omega^{(1)}$ and $\omega^{(2)}$, respectively (fig. 16.3.3). As mentioned above, the pitch surfaces are two cones of angles γ_1 and γ_2 which roll over each other (see ch. 2.2). Axis $O-I$ is the instantaneous axis of rotation which passes through O —the point of intersection of axes $O-a_1$ and $O-a_2$. Axis $O-I$ is the line of action of vector $\omega^{(12)} = \omega^{(1)} - \omega^{(2)}$, that represents the angular velocity in relative motion (rotation about $O-I$).

Plane Π is a tangent plane to the pitch cones. While the pitch cones rotate about $O-a_1$ and $O-a_2$, respectively, plane Π rotates about $O-O_g$ with angular velocity $\omega^{(g)}$ (fig. 16.3.3). Axis $O-I$ represents the line of action of vectors $\omega^{(g1)} = \omega^{(g)} - \omega^{(1)}$ and $\omega^{(g2)} = \omega^{(g)} - \omega^{(2)}$. Thus $O-I$ is the instantaneous axis of rotation of members g and 1, and g and 2. Plane Π is the pitch surface of generating gear g .

We may generate gears 1 and 2 with conjugate surfaces if the following conditions are satisfied: (1) Plane Π is provided with a generating surface Σ_g , (2) surface Σ_g is rotated about $O-a_g$ while members 1 and 2 rotate about $O-a_1$ and $O-a_2$, respectively, and (3) $O-I$ is the instantaneous axis of rotation in the relative motion. With these conditions satisfied, surface Σ_g will generate conjugated surfaces Σ_1 and Σ_2 which are in line contact.

Figure 16.4.2 shows a head cutter that is used for the generation of Gleason's spiral bevel gears. This tool is provided with blades having straight-lined profiles. These profiles being rotated about axis $C-C$ form two cones that cut both sides of the tooth. Thus the generating surface is a cone surface.

In the process of generation the following motions are performed (fig. 16.4.3): (1) a rotational motion of the head cutter about axis $C-C$, that provides the desired velocity of cutting and (2) a

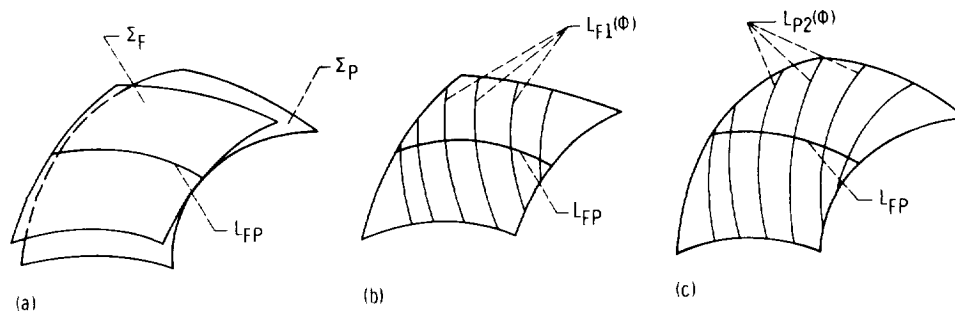


Figure 16.4.1.

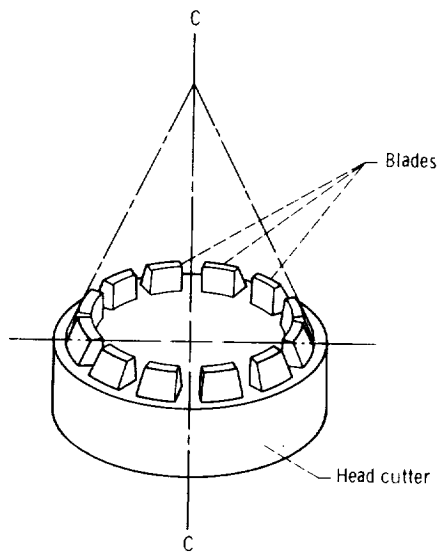


Figure 16.4.2.

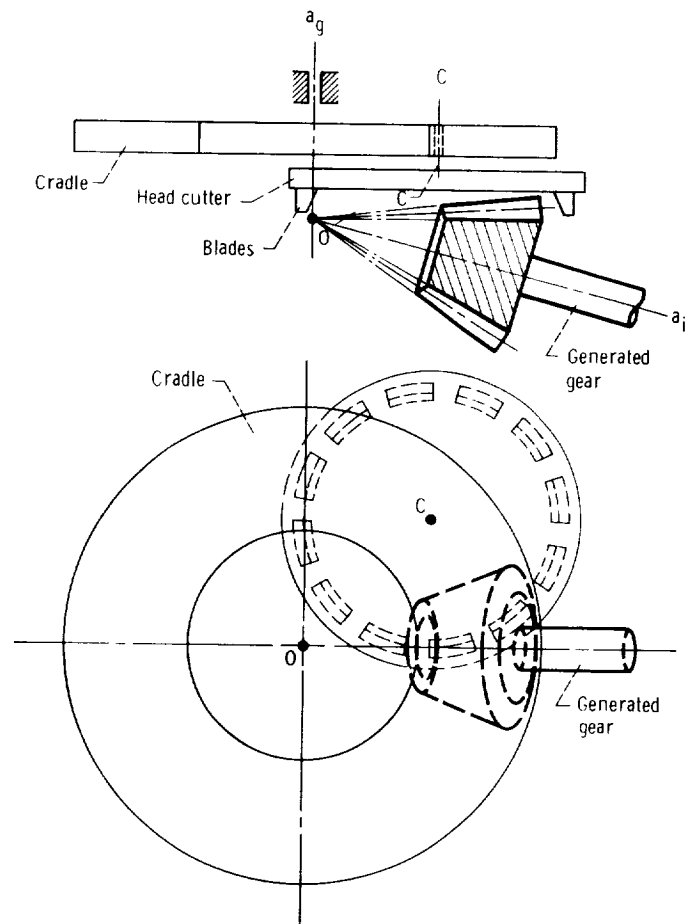


Figure 16.4.3.

rotational motion of the head cutter about axis $O-a_g$ while the gear to be generated rotates about axis $O-a_i$. (The member of the cutting machine, that rotates about $O-a_g$ and carries axis $C-C$, is called the cradle.)

Using the discussed method for generation, we obtain a line contact of gear-tooth surfaces Σ_1 and Σ_2 . To obtain a point contact we have to use two generating surfaces that can contact each other at a line. Two examples of such generating surfaces are shown in figure 16.4.4 and figure 16.4.5, respectively. They are

- (1) Two cone surfaces with the same apex angle ψ_c , that contact each other at a common generatrix (AB).
- (2) A cone surface and a surface of revolution whose contact line is a circle.

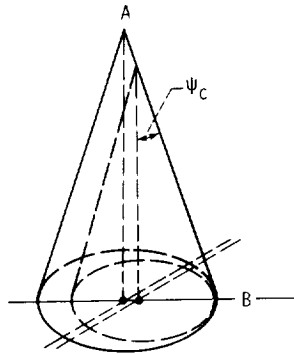


Figure 16.4.4.

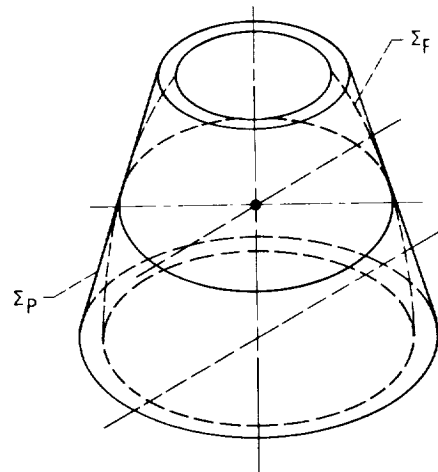
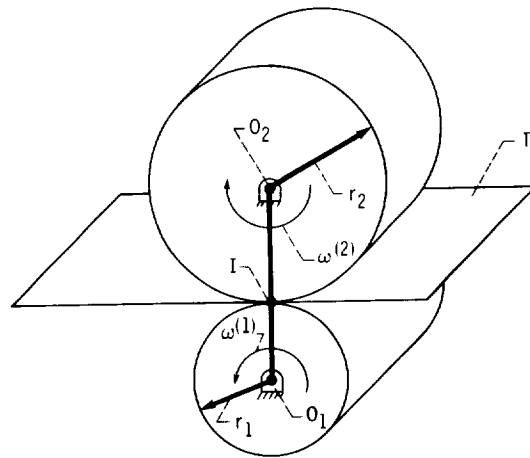
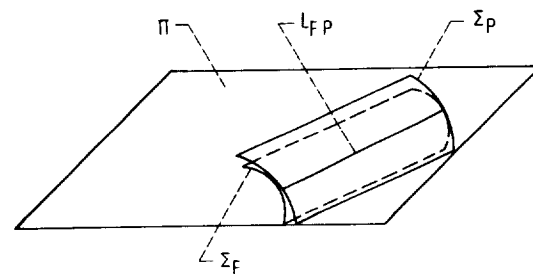


Figure 16.4.5.



(a)



(b)

Figure 16.4.6.

Generation of Helical Gears

Let us now consider the generation process of conjugate surfaces for helical gears with parallel axes. The gears must transform rotation between axes O_1 and O_2 with angular velocities $\omega^{(1)}$ and $\omega^{(2)}$ (fig. 16.4.6(a)). The pitch surfaces of gears 1 and 2 are pitch cylinders of radii r_1 and r_2 , respectively. Plane Π , that is tangent to the pitch cylinders, is the pitch surface of a rack cutter. While the gears are rotating with angular velocities $\omega^{(1)}$ and $\omega^{(2)}$, the rack cutter translates with velocity $v = \omega^{(1)}r_1 = \omega^{(2)}r_2$. To generate gears having a point contact of their surfaces we use two generating surfaces, Σ_F and Σ_P (fig. 16.3.6(b)). Consequently, we use two rack cutters and in this case surfaces Σ_F and Σ_P contact each other along the line L_{FP} . Being rigidly connected, surfaces Σ_F and Σ_P move together with plane Π as one rigid body. They translate with velocity \mathbf{v} while the gears rotate with angular velocities $\omega^{(1)}$ and $\omega^{(2)}$. We may imagine that surface Σ_F generates surface Σ_1 of gear 1 and surface Σ_P generates surface Σ_2 , the tooth surface of gear 2. We assume that lines of contact $L_{F1}(\phi)$ and $L_{P2}(\phi)$ do not coincide, but that they have a common point which lies on L_{FP} —the line of contact of generating surfaces Σ_F and Σ_P . The common point of the three lines (two instantaneous lines $L_{F1}(\phi)$ and $L_{P2}(\phi)$ (ϕ is fixed) and line L_{FP}) is the instantaneous point of contact of gear-tooth surfaces Σ_1 and Σ_2 . The discussed method is used for generation of helical gears with circular arc teeth.

16.5 Generation Method 4

This method is based on the generation of gear tooth surfaces by an auxiliary line L_g , that is the shape of a blade. We set up coordinate systems S_1 , S_2 , and S_g rigidly connected with gears 1, 2, and the generating line L_g , respectively, and the fixed coordinate system S_f . System S_g performs a prescribed motion with respect to S_f , while the coordinate systems S_1 and S_2 perform the prescribed motions with the given gear ratio. Together with these motions, line L_g generates surfaces Σ_1 and Σ_2 in coordinate systems S_1 and S_2 , respectively. Surfaces Σ_1 and Σ_2 have a common line L_g at every instant. However, L_g can just be a line of intersection but not a line of tangency for surfaces Σ_1 and Σ_2 . Surfaces Σ_1 and Σ_2 will be conjugated if line L_g is the line of contact of Σ_1 and Σ_2 at every instant. This condition is satisfied if at any point of L_g the following equations are observed:

$$\mathbf{N}^{(1)} \bullet \mathbf{v}^{(12)} = \mathbf{N}^{(2)} \bullet \mathbf{v}^{(12)} = 0 \quad (16.5.1)$$

Here $\mathbf{N}^{(1)}$ and $\mathbf{N}^{(2)}$ are the surface normals, and $\mathbf{v}^{(12)}$ is the vector of relative velocity. If equations (16.5.1) are satisfied, then line L_g is the instantaneous line of contact of Σ_1 and Σ_2 , vector $\mathbf{v}^{(12)}$, determined for any point of L_g , lies in the tangent plane to Σ_1 and Σ_2 and the surface normals are collinear, that is

$$\mathbf{N}^{(1)} = m\mathbf{N}^{(2)} \quad (16.5.2)$$

We may develop some techniques for the generation of Σ_1 and Σ_2 by L_g based on the following considerations (proposed by Litvin, 1968). The surface normal may be determined by

$$\mathbf{N}^{(i)} = \mathbf{v}^{(ig)} \times \boldsymbol{\tau} \quad (i = 1, 2) \quad (16.5.3)$$

Here $\mathbf{v}^{(ig)}$ is the relative velocity of a point M represented in the coordinate system S_i with respect to the same point represented in the system S_g ; $\boldsymbol{\tau}$ is the tangent vector to L_g at M . Using equation (16.5.3), we consider that the surface coordinate lines on Σ_i are line L_g and the path which is traced out in S_i by a point of L_g .

Equations (16.5.1) and (16.5.3) yield

$$[\mathbf{v}^{(1g)} \boldsymbol{\tau} \mathbf{v}^{(12)}] = 0 \quad (16.5.4)$$

$$[\mathbf{v}^{(2g)} \boldsymbol{\tau} \mathbf{v}^{(12)}] = 0 \quad (16.5.5)$$

We may represent $\mathbf{v}^{(12)}$ in equations (16.5.4) and (16.5.5) by

$$\mathbf{v}^{(12)} = \mathbf{v}^{(1g)} - \mathbf{v}^{(2g)} \quad (16.5.6)$$

and obtain, using equations (16.5.4) to (16.5.6), that

$$[\mathbf{v}^{(1g)} \boldsymbol{\tau} \mathbf{v}^{(2g)}] = 0 \quad (16.5.7)$$

It is easy to verify that equation (16.5.7) if satisfied, provides the collinearity of surface normals $\mathbf{N}^{(1)}$ and $\mathbf{N}^{(2)}$. To prove this we use the equation

$$\begin{aligned} \mathbf{N}^{(1)} \times \mathbf{N}^{(2)} &= (\mathbf{v}^{(1g)} \times \boldsymbol{\tau}) \times (\mathbf{v}^{(2g)} \times \boldsymbol{\tau}) \\ &= \mathbf{v}^{(2g)} [\mathbf{v}^{(1g)} \boldsymbol{\tau} \boldsymbol{\tau}] - \boldsymbol{\tau} [\mathbf{v}^{(1g)} \boldsymbol{\tau} \mathbf{v}^{(2g)}] = -\boldsymbol{\tau} [\mathbf{v}^{(1g)} \boldsymbol{\tau} \mathbf{v}^{(2g)}] \end{aligned} \quad (16.5.8)$$

Equations (16.5.7) and (16.5.8) yield $\mathbf{N}^{(1)} \times \mathbf{N}^{(2)} = 0$, and thus the surface normals are collinear. On the basis of equation (16.5.7), we may propose the following two techniques for the generation of conjugate surfaces Σ_1 and Σ_2 . These techniques are based on the satisfaction of equation (16.5.7) with:

- (1) The collinearity of vectors $\boldsymbol{\tau}$ and $\mathbf{v}^{(12)}$
- (2) The collinearity of vectors $\mathbf{v}^{(1g)}$ and $\mathbf{v}^{(2g)}$ ($i = 1, 2$)

The evidence that equation (16.5.7) is satisfied with the proposed conditions is based on the following considerations:

- (1) Using the equation

$$\boldsymbol{\tau} \times \mathbf{v}^{(12)} = \boldsymbol{\tau} \times (\mathbf{v}^{(1g)} - \mathbf{v}^{(2g)}) = 0$$

we obtain

$$\boldsymbol{\tau} \times \mathbf{v}^{(1g)} = \boldsymbol{\tau} \times \mathbf{v}^{(2g)} \quad (16.5.9)$$

Equations (16.5.9) and (16.5.7) yield

$$[\mathbf{v}^{(1g)} \boldsymbol{\tau} \mathbf{v}^{(2g)}] = [\mathbf{v}^{(1g)} \boldsymbol{\tau} \mathbf{v}^{(1g)}] = 0$$

- (2) Using the equation

$$\mathbf{v}^{(1g)} \times \mathbf{v}^{(12)} = 0$$

we obtain

$$\mathbf{v}^{(1g)} \times (\mathbf{v}^{(1g)} - \mathbf{v}^{(2g)}) = -\mathbf{v}^{(1g)} \times \mathbf{v}^{(2g)} = 0 \quad (16.5.10)$$

Thus, equation (16.5.7) is satisfied due to the collinearity of vectors $\mathbf{v}^{(1g)}$ and $\mathbf{v}^{(2g)}$. A similar result may be obtained by using the equation

$$\mathbf{v}^{(2g)} \times \mathbf{v}^{(12)} = 0$$

Technique 1: Vectors $\boldsymbol{\tau}$ and $\mathbf{v}^{(12)}$ are Collinear

Consider that gears 1 and 2 transform rotation between crossed axes and that the relative motion is represented as a screw motion (fig. 16.5.1). We assume that the conditions of generation are as follows:

- (1) L_g translates along the axis of screw motion A_g with an arbitrary chosen velocity $\mathbf{v}^{(g)}$.
- (2) The shape of L_g is a helix on a cylinder whose axis coincides with the axis of screw motion.
- (3) The screw parameter of the helix is the same as the screw parameter of relative motion for gears 1 and 2.

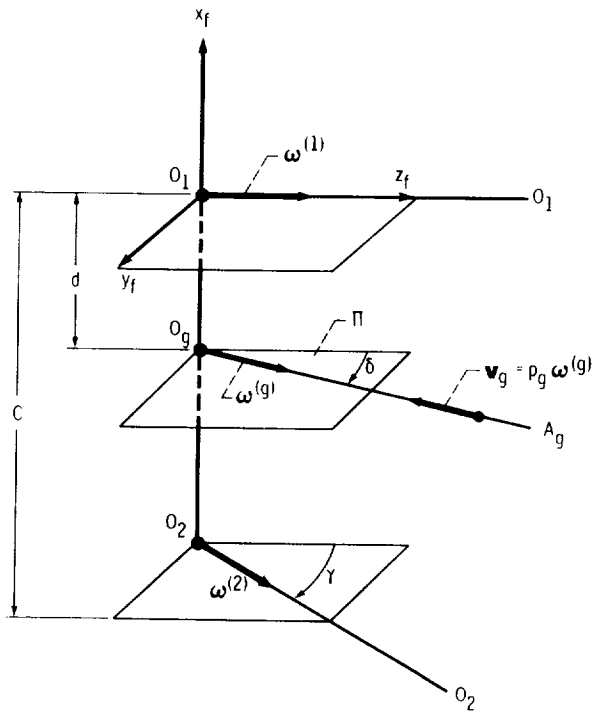


Figure 16.5.1.

Let us prove with the aforementioned conditions, that vectors τ and $v^{(12)}$ are indeed collinear. The velocity of a point in its screw motion is directed along the tangent to the trajectory traced out by such a point. Line L_g is a helix traced out in screw motion. Consequently, the tangent to L_g and vector $v^{(12)}$ are collinear, and equation (16.5.7) is satisfied. Line L_g being translated along the axis of screw motion, while the gears are rotated, generates conjugate surfaces Σ_1 and Σ_2 .

With this method, we may generate, in particular, conjugate surfaces for gears which transform rotation between parallel axes. In such a case the relative motion is rotation about an instantaneous axis I . This axis is a particular case of the screw axis with the screw parameter equal to zero. The generating line L_g becomes an arc of a circle of radius ρ centered at axis I (fig. 16.5.2). Line L_g , being translated along the instantaneous axis of rotation while the gears rotate about axes O_1 and O_2 , generates conjugate surfaces Σ_1 and Σ_2 . Considering that the ratio $v^{(g)}/\omega^{(i)}$ ($i = 1, 2$) is constant, we conclude that surfaces Σ_1 and Σ_2 are two helicodes. Here $v^{(g)}$ is the velocity of L_g in translational motion.

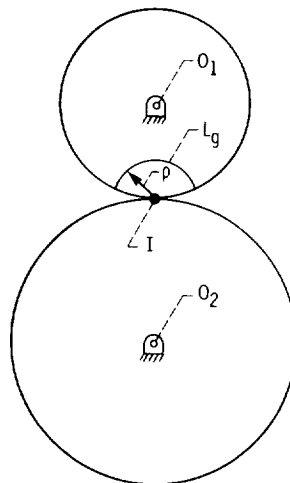


Figure 16.5.2.

Technique 2: Vectors $\mathbf{v}^{(ig)}$ ($i = 1, 2$) and $\mathbf{v}^{(12)}$ are Collinear

Let us prove that vectors $\mathbf{v}^{(ig)}$ and $\mathbf{v}^{(12)}$ become collinear if the generating line L_g performs a screw motion.

Consider that A_g , the axis of screw motion for L_g , intersects the shortest distance between the axes of rotation of gears 1 and 2 and lies in plane Π that is perpendicular to \mathbf{C} (fig. 16.5.1). We may determine the velocity $\mathbf{v}^{(1g)}$ as follows:

$$\mathbf{v}^{(1g)} = \mathbf{v}^{(1)} - \mathbf{v}^{(g)} \quad (16.5.11)$$

Here

$$\mathbf{v}^{(1)} = \boldsymbol{\omega}^{(1)} \times \mathbf{r} \quad (16.5.12)$$

is the velocity in rotational motion of a point for gear 1; \mathbf{r} is a position vector drawn from a point which lies on the axis of rotation of gear 1, O_1 ; and $\boldsymbol{\omega}^{(1)}$ is the angular velocity of rotation about O_1 . Vector

$$\mathbf{v}^{(g)} = (\boldsymbol{\omega}^{(g)} \times \mathbf{r}) + (\mathbf{d} \times \boldsymbol{\omega}^{(g)}) + p_g \boldsymbol{\omega}^{(g)} \quad (16.5.13)$$

is the velocity in screw motion of a point of the generating line L_g . Here $\boldsymbol{\omega}^{(g)}$ and $p_g \boldsymbol{\omega}^{(g)}$ are the angular velocity in rotation about and translation along the screw axis A_g . Here p_g is the screw parameter in screw motion for L_g , and \mathbf{d} is a position vector drawn from O_1 to O_g . We assume that \mathbf{d} is a vector of shortest distance between axis O_1 and O_g .

Equations (16.5.11) to (16.5.13) yield

$$\mathbf{v}^{(1g)} = (\boldsymbol{\omega}^{(1)} - \boldsymbol{\omega}^{(g)}) \times \mathbf{r} - (\mathbf{d} \times \boldsymbol{\omega}^{(g)}) - p_g \boldsymbol{\omega}^{(g)} \quad (16.5.14)$$

Velocity $\mathbf{v}^{(12)}$ in relative motion for gears 1 and 2 is represented by the equation

$$\mathbf{v}^{(12)} = \mathbf{v}^{(1)} - \mathbf{v}^{(2)} = \boldsymbol{\omega}^{(12)} \times \mathbf{r} - \mathbf{C} \times \boldsymbol{\omega}^{(2)} \quad (16.5.15)$$

Here $\boldsymbol{\omega}^{(12)} = \boldsymbol{\omega}^{(1)} - \boldsymbol{\omega}^{(2)}$, and \mathbf{C} is a vector of shortest distance drawn from O_1 to O_2 .

Vectors $\mathbf{v}^{(1g)}$ and $\mathbf{v}^{(12)}$ are collinear, that is,

$$\mathbf{v}^{(1g)} = \lambda \mathbf{v}^{(12)} \quad (16.5.16)$$

Equations (16.5.14) to (16.5.16) yield

$$(\boldsymbol{\omega}^{(1)} - \boldsymbol{\omega}^{(g)}) \times \mathbf{r} - (\mathbf{d} \times \boldsymbol{\omega}^{(g)}) - p_g \boldsymbol{\omega}^{(g)} = \lambda \left[(\boldsymbol{\omega}^{(1)} - \boldsymbol{\omega}^{(2)}) \times \mathbf{r} - (\mathbf{C} \times \boldsymbol{\omega}^{(2)}) \right] \quad (16.5.17)$$

Rearranging equation (16.5.17), we get

$$\left[\boldsymbol{\omega}^{(1)}(1 - \lambda) - \boldsymbol{\omega}^{(g)} + \lambda \boldsymbol{\omega}^{(2)} \right] \times \mathbf{r} + \lambda (\mathbf{C} \times \boldsymbol{\omega}^{(2)}) - (\mathbf{d} \times \boldsymbol{\omega}^{(g)}) - p_g \boldsymbol{\omega}^{(g)} = 0 \quad (16.5.18)$$

Remember that \mathbf{r} is a position vector which is drawn from a point on axis O_1 to a point on line L_g . Equation (16.5.18) will be satisfied for a generating line L_g of any shape if

$$\boldsymbol{\omega}^{(1)}(1 - \lambda) - \boldsymbol{\omega}^{(g)} + \lambda \boldsymbol{\omega}^{(2)} = 0 \quad (16.5.19)$$

$$\lambda (\mathbf{C} \times \boldsymbol{\omega}^{(2)}) - (\mathbf{d} \times \boldsymbol{\omega}^{(g)}) - p_g \boldsymbol{\omega}^{(g)} = 0 \quad (16.5.20)$$

Vector equations (16.5.19) and (16.5.20) are to be used to determine $\boldsymbol{\omega}^{(g)}$, p_g , \mathbf{d} , and λ considering that \mathbf{C} , $\boldsymbol{\omega}^{(1)}$, and $\boldsymbol{\omega}^{(2)}$ are given. The line of action for \mathbf{d} is the same as that for \mathbf{C} , and we may represent \mathbf{d} by

$$\mathbf{d} = \frac{d}{|\mathbf{C}|} \mathbf{C}$$

Vectors of angular and linear velocities represented in equations (16.5.19) to (16.5.20) lie in planes that are perpendicular to \mathbf{C} . Thus vector equations (16.5.19) to (16.5.20) yield only four scalar equations in five unknowns: two projections of ω , d , p_g , and λ . Fixing one of these unknowns, for instance d , we can determine the four remaining unknowns.

Consider that axes O_1-O_1 and O_2-O_2 of gear rotation make an angle γ ; the location and orientation of A_g (the axis of screw motion) is determined with d and δ (fig. 16.5.1). Projections of the vectors of equations (16.5.19) and (16.5.20) on axes x_f , y_f , and z_f are represented as follows:

$$-\omega^{(g)} \sin \delta + \lambda \omega^{(2)} \sin \gamma = 0 \quad (16.5.21)$$

$$(1 - \lambda) \omega^{(1)} - \omega^{(g)} \cos \delta + \lambda \omega^{(2)} \cos \gamma = 0 \quad (16.5.22)$$

$$\lambda \begin{vmatrix} \mathbf{i}_f & \mathbf{j}_f & \mathbf{k}_f \\ -C & 0 & 0 \\ 0 & \omega^{(2)} \sin \gamma & \omega^{(2)} \cos \gamma \end{vmatrix} - \begin{vmatrix} \mathbf{i}_f & \mathbf{j}_f & \mathbf{k}_f \\ -d & 0 & 0 \\ 0 & \omega^{(g)} \sin \delta & \omega^{(g)} \cos \delta \end{vmatrix} - p_g \omega^{(g)} (\sin \delta \mathbf{j}_f + \cos \delta \mathbf{k}_f) = 0 \quad (16.5.23)$$

Equation (16.5.23) yields

$$\lambda C \omega^{(2)} \cos \gamma - d \omega^{(g)} \cos \delta - p_g \omega^{(g)} \sin \delta = 0 \quad (16.5.24)$$

$$-\lambda C \omega^{(2)} \sin \gamma + d \omega^{(g)} \sin \delta - p_g \omega^{(g)} \cos \delta = 0 \quad (16.5.25)$$

Equations (16.5.21) to (16.5.25) give

$$\lambda = \frac{\omega^{(g)} \sin \delta}{\omega^{(2)} \sin \gamma} \quad (16.5.26)$$

$$\omega^{(g)} = \frac{\omega^{(1)} \omega^{(2)} \sin \gamma}{\omega^{(1)} \sin \delta + \omega^{(2)} \sin (\gamma - \delta)} \quad (16.5.27)$$

$$p_g = - \frac{\sin (\gamma - \delta) \sin \delta}{\sin \gamma} C \quad (16.5.28)$$

$$d = - p_g \cot (\gamma - \delta) = \frac{\sin \delta \cos (\gamma - \delta)}{\sin \gamma} C \quad (16.5.29)$$

Equations (16.5.26) to (16.5.29) determine all parameters of the screw motion of generation if δ is chosen.

The discussed method may be used for the generation of conjugated surfaces for gears with crossed axes by a screw motion of a generating line of any shape. The generated surfaces Σ_1 and Σ_2 will contact each other at every instant along the generating line L_g . The discussed technique may also be used for the generation of screws, pumps, and feeders.

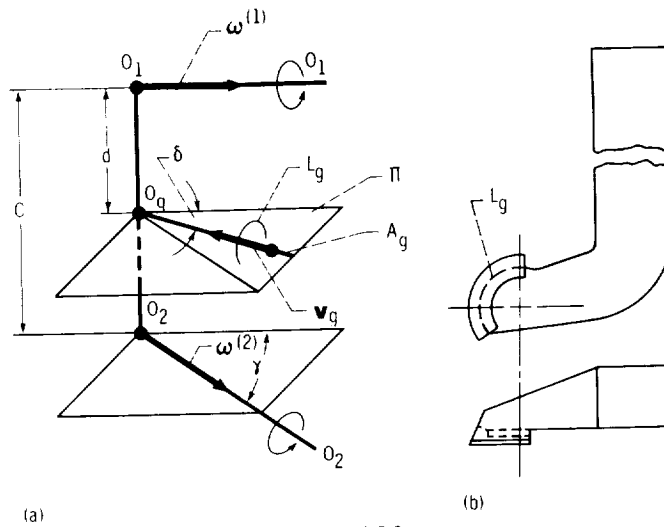


Figure 16.5.3.

There is an important case of screw generation by a circular arc line L_g centered at the axis of screw motion A_g as proposed by Litvin and Polytavkin (Litvin, 1968). Consider that two screws transform rotation between crossed axes O_1-O_1 and O_2-O_2 , that make the angle γ (fig. 16.5.3(a)). Vectors $\omega^{(1)}$ and $\omega^{(2)}$ ($|\omega^{(1)}| = |\omega^{(2)}| = \omega$) are the angular velocities in rotation about these axes, and C is the shortest distance between the axes. Axis A_g of screw motion of generating line is located in plane Π and makes the angle δ with O_1-O_1 . Since L_g is a circular arc centered at A_g , the rotation of L_g about A_g is not necessary. Therefore, the generating motion of L_g can be performed as translation only, instead of screw motion. Thus, while screw i is rotated about axis O_i-O_i with angular velocity ω , the generating line L_g is translated along A_g with velocity $v^{(g)}$. The generating tool can be a blade as shown in figure 16.5.2(b), or as a rotating milling cutter.

As mentioned previously, parameters of generating motion for L_g are determined by equations (16.5.36) to (16.5.29). In the considered case, $\omega^{(1)} = \omega^{(2)} = \omega$, and the angle δ may be chosen as $\delta = 0.5\gamma$. The velocity of L_g in translational motion is given by

$$v^{(g)} = p_g \omega^{(g)} = - \frac{\omega \sin(\gamma - \delta) \sin \delta}{\sin \delta + \sin(\gamma - \delta)} C \quad (16.5.29)$$

The negative sign of p_g and $v^{(g)}$ indicates that the screw parameter p_g is negative and vector $v^{(g)}$ is opposite to $\omega^{(g)}$ (fig. 16.5.3).

Chapter 17

Synthesis of Spiral Bevel Gears

17.1 Introduction to Gear Geometry

There are different types of spiral bevel gears, based on the methods of generation of gear-tooth surfaces. A few notable ones are the Gleason's gearing, the Klingelnberg's Palloid System, and the Klingelnberg's and Oerlikon's Cyclo Palloid System. The design of each type of spiral bevel gear depends on the method of generation used. It is based on specified and detailed directions which have been worked out by the mentioned companies. However, there are some general aspects, such as the concepts of pitch cones, generating gear, and conditions of force transmissions (see ch. 19.2) that are common for all types of spiral bevel gears.

Pitch Cones

Consider that rotation is transformed between two intersected axis, Oa_1 and Oa_2 , which make an angle γ (fig. 17.1.1). (See also sections 2.2 and 14.1.) The angular velocities in rotation about these axes are $\omega^{(1)}$ and $\omega^{(2)}$. The instantaneous axis of rotation (OI) is the line of action of the relative angular velocity

$$\omega^{(12)} = \omega^{(1)} - \omega^{(2)} \quad (17.1.1)$$

or

$$\omega^{(21)} = \omega^{(2)} - \omega^{(1)} \quad (17.1.2)$$

The instantaneous axis of rotation is the line of tangency of the pitch cones that roll over each other without slipping. The apex angles of the pitch cones γ_1 and γ_2 are represented by the following equations:

$$\cot \gamma_1 = \frac{m_{12} + \cos \gamma}{\sin \gamma} \quad (17.1.3)$$

$$\cot \gamma_2 = \frac{m_{21} + \cos \gamma}{\sin \gamma} \quad (17.1.4)$$

Here

$$m_{12} = \frac{\omega^{(1)}}{\omega^{(2)}} = \frac{N_2}{N_1} \text{ and } m_{21} = \frac{\omega^{(2)}}{\omega^{(1)}} = \frac{N_1}{N_2}$$

are the gear ratio; N_1 and N_2 are the number of gear teeth.

For the most common case when $\gamma = 90^\circ$, we obtain

$$\cot \gamma_1 = m_{12} \quad \cot \gamma_2 = m_{21} \quad (17.1.5)$$

Plane Π is a tangent plane to the pitch cones (fig. 17.1.1). We may imagine that plane Π rotates about axis Oa_g with angular velocity $\omega^{(g)}$, while the pitch cones rotate with angular velocities $\omega^{(1)}$ and $\omega^{(2)}$ about axes Oa_1 and Oa_2 , respectively. Plane Π , limited with the circle of radius OI , may be considered as a particular case of a pitch cone surface having an apex angle γ_i , which approaches 90° and has an outer cone distance equal to OI .

Generating Gear: Types of Spiral Bevel Gearing

Consider that a generating surface Σ_g is rigidly connected to the pitch plane Π . Surface Σ_g rotates with the pitch plane Π about Oa_g (fig. 17.1.1) while the gear blanks rotate about Oa_1 and Oa_2 ,

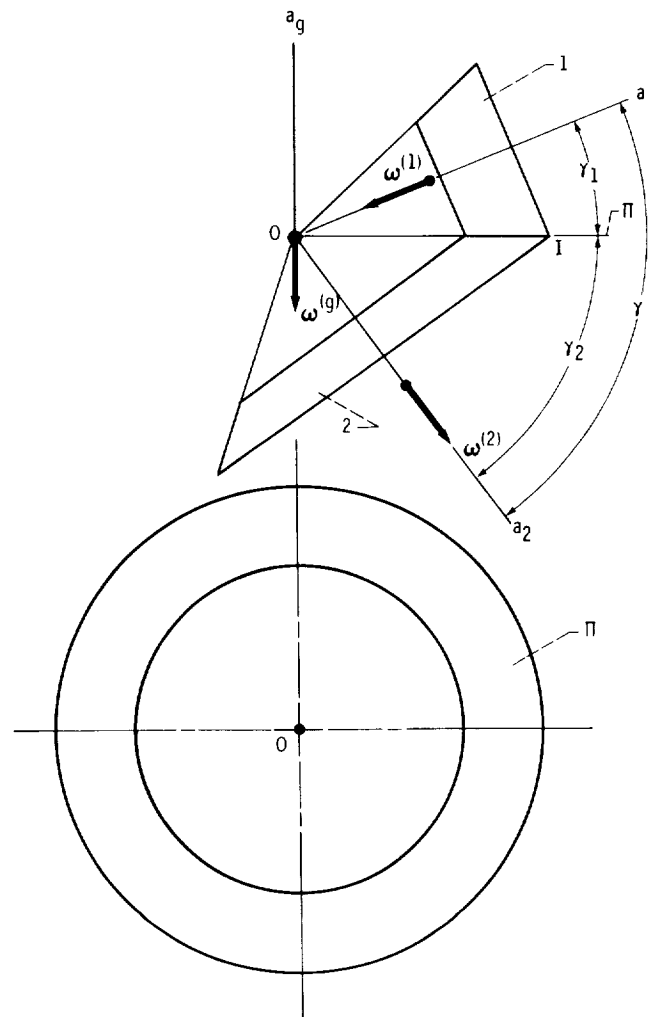


Figure 17.1.1.

respectively. Surface Σ_g generates tooth surfaces Σ_1 and Σ_2 on gears 1 and 2. Such a generating process provides conjugate gear-tooth surfaces Σ_1 and Σ_2 which contact each other along a line at every instant. The instantaneous line of contact moves over surfaces Σ_1 and Σ_2 . Gears 1 and 2, having surfaces Σ_1 and Σ_2 , will transform rotation about axes Oa_1 and Oa_2 with the prescribed gear ratio. The type of spiral bevel gearing depends on the type of generating surface Σ_g .

The generating surface for Gleason's spiral bevel gearing is a cone surface (ch. 16.4). The head cutter (fig. 16.4.2), that cuts the gear, carries blades with straight-lined profiles. Consider a coordinate system S_c that is rigidly connected to the head cutter and rotates with it about the $C-C$ axis. The head-cutter blades, being rotated about $C-C$, generate a cone in the coordinate system S_c . The angular velocity of rotation about $C-C$ does not depend on the generating motions and provides the desired velocity of cutting only.

To generate the gear tooth surface the head cutter has to go through two motions:

- (1) Rotation about Oa_g while the generated gear rotates about Oa_i (fig. 16.4.3)
- (2) Rotation about $C-C$

Rotations of the generating gear and the gear being generated are related since the instantaneous axis of rotation is OI . The rotation of the head cutter about $C-C$ may be ignored by considering that a generating cone surface is rigidly connected to plane Π (with axis $C-C$ of the cone) (fig. 17.1.1) and rotates about axis Oa_g . The motion of the generating gear (rotation about Oa_g) is simulated by the rotation of the cradle of the cutting machine which carries the head cutter.

Consider the line of intersection L of the generating surface with the pitch plane Π . In the case of Gleason's gearing, L is a circular arc of radius R (fig. 17.1.2(a)). Line L generates a spatial curve on the gear pitch cone that is more like a helix rather than a spiral although the gears are called spiral bevel gears.

The type of spiral bevel gears is related to the type of the longitudinal shape of the gear. We differentiate between the following types of spiral bevel gears.

- (1) The Gleason's gearing (fig. 17.1.2(a)): where the longitudinal shape is a circular arc of radius R .
- (2) The Palloid System of Klingelnberg (fig. 17.1.2(b)): where the longitudinal shape is approximately an involute curve for a base circle of radius r_b . The generating surface of the Palloid System of Klingelnberg is generated by a conical worm. The tool is a conical hob which simulates the conical worm.
- (3) The Cyclo-Palloid System of Klingelnberg and Oerlicon System (fig. 17.1.3): where the longitudinal shape is an extended epicycloid, traced out by point P of the finishing blade of the head cutter. The blade and circle of radius ρ are rigidly connected and represent a rigid body. The circle of radius ρ rolls over the gear circle of radius r . Thus these circles are centres of the head-cutter and of the generating gear. The head cutter rotates about O_c and the generating gear rotates about O_g . Unlike the generation of Gleason's gearing, the rotations of the head-cutter and the generating gear in the case of the Cyclo-Palloid System are related: point I is the instantaneous center of rotation in the relative motion of the head cutter with respect to the generating gear.

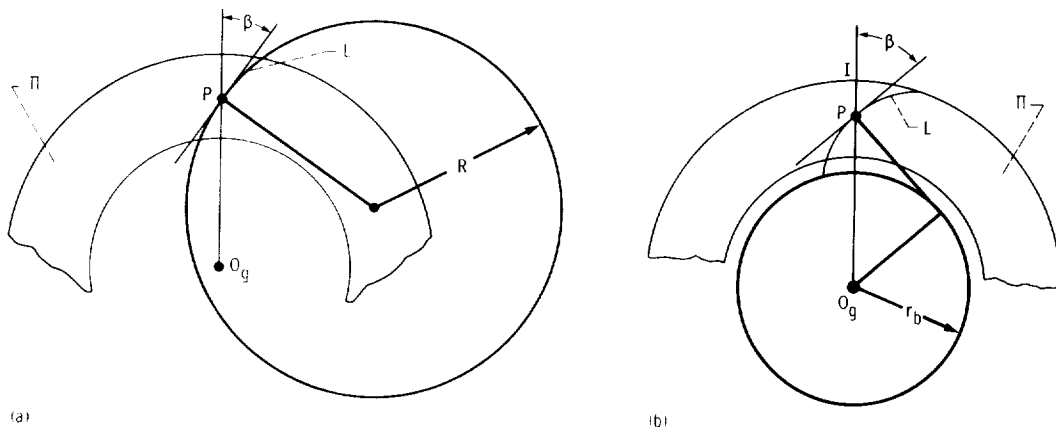


Figure 17.1.2.

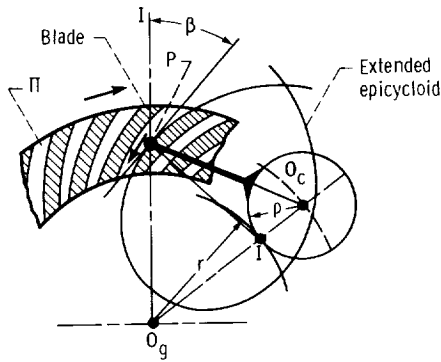


Figure 17.1.3.

In reality the methods of generation discussed are more complicated because they have to provide a localized contact of gear-tooth surfaces. It is for this reason that two generating surfaces are used instead of one. (See ch. 16.4.)

Henceforth, we will designate the direction of the tangent to the longitudinal shape at point P by β . Point P is the point of intersection of the instantaneous axis of rotation $O_g I$ and the shape (figs. 17.1.2 and 17.1.3). The longitudinal shape (the spiral) can be right-handed or left-handed, similar to the right-handed and left-handed helical gears. Figure 17.1.3 shows right-handed spirals.

Tooth Element Proportions

The axial section of the Palloid gearing and the Cyclo Palloid gearing is shown in figure 17.1.4(a). This gearing has a constant height of the teeth.

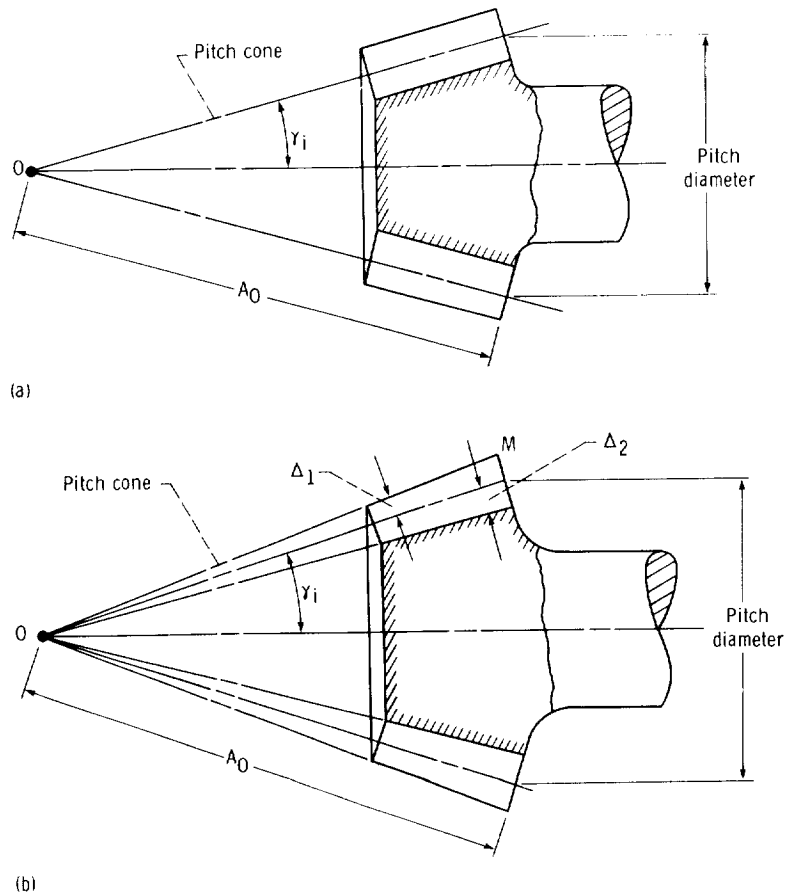


Figure 17.1.4.

The axial section of the Gleason's gearing is shown in figure 17.1.4(b). Tooth height changes proportionally to the distance from the apex and the three cones – the pitch cone, dedendum cone, and addendum cones – have the same apex. In some cases, the gears are designed with different apices for the mentioned cones to provide a constant backlash between the dedendums and addendums of mating gears.

The transverse diametral pitch is given for the back cone. The pitch diameter for the gear is determined by

$$d_i = \frac{N_i}{P} \quad (i = 1,2) \quad (17.1.6)$$

where P is the diametral pitch and N_i is the tooth number.

The outer cone distance A_O is determined by

$$A_O = \frac{d_i}{2 \sin \gamma_i} \quad (17.1.7)$$

The addendum and dedendum angles are represented by (fig. 17.1.4(b))

$$\Delta_1 = \tan^{-1} \frac{a}{A_O} \quad (17.1.8)$$

$$\Delta_2 = \tan^{-1} \frac{b}{A_O} \quad (17.1.9)$$

Here a and b are the dimensions of the addendum and dedendum for the back cone expressed in terms of the diametral pitch.

17.2 Introduction to Synthesis

Gleason's gearing has obvious technological advantages: (1) The velocity of cutting does not depend on the generating velocities. (2) It is easy to grind. (3) The axial shape of teeth (fig. 17.1.4(b)) provides favorable conditions for bending stresses and resistance to elastic deformations. (4) The contact of surfaces is localized. However, the gear-tooth surfaces can be generated as conjugated surfaces if special machine-tool settings are used only. This may be explained with figure 17.2.1. Consider two pitch cones having angles γ_1 and γ_2 . The instantaneous axis of rotation of the pitch cones is OI . Gears 1 and 2 are generated by generating surfaces Σ_F and Σ_P , respectively. The axis of rotation of the generating surface must be perpendicular to the generatrix of the root cone. Thus, the axes of rotation of the generating gears, $Oz^{(F)}$ and $Oz^{(P)}$, do not coincide, but rather make an angle of $\Delta_1 + \Delta_2$, where Δ_i ($i = 1,2$) is the dedendum angle of the gear. Since axes $Oz^{(F)}$ and $Oz^{(P)}$ do not coincide, we cannot use a method of generation that provides the gears with conjugate surfaces. For this reason some compensating machine-tool settings must be used and the determination of such settings is the subject of optimal synthesis. The methods for the synthesis of spiral bevel gears and hypoid gears with Gleason's gearing are based on the application of tooth contact analysis. These methods have been worked out: (1) by Gleason's engineers (1970), (2) by Litvin (1968), and Litvin and Gutman (1980). The approach, proposed by Litvin (1968), and Litvin and Gutman (1980), is based on application in two stages; the local synthesis and the global synthesis.

The purposes of local synthesis are to provide: (1) contact of gear-tooth surfaces at the mean contact point, and (2) improved conditions of meshing within the neighborhood of the mean contact point. The purpose of the global synthesis is to provide optimal conditions of meshing for the whole

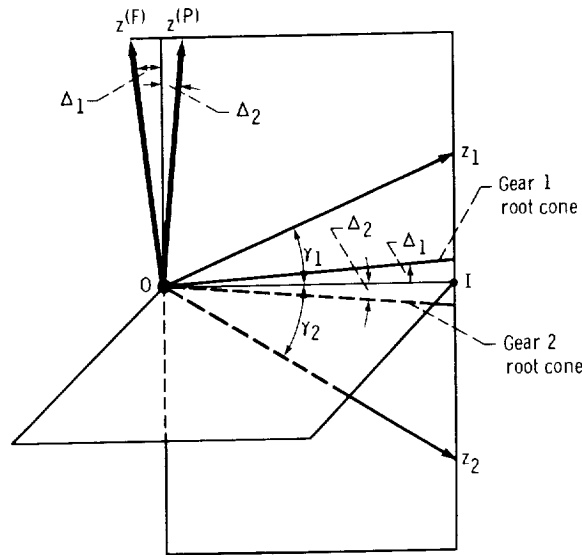


Figure 17.2.1.

area of meshing. The criteria of conditions of meshing are the kinematical errors and the bearing contact.

Synthesis of spiral bevel gears discussed in this chapter is based on the research performed by Litvin, Hayasaka, Rahman, and Wei-Jiung Tsung. A new method for generation of Gleason's spiral bevel gears with conjugate tooth surfaces has been recently developed by Litvin, Tsung, Coy, and Heine (Litvin et al, 1986).

17.3 Generating Surfaces and Coordinate Systems

Here the generating surface is a cone surface (fig. 17.3.1). This surface is generated in the coordinate system $S_c^{(j)}$, while the blades of the head cutter rotate about axis $C-C$ (fig. 16.4.2). The generation of gear-tooth surfaces is based on application of two tool surfaces, Σ_F and Σ_P , which generate gears 1 and 2, respectively. The generating surfaces (generating cones) do not coincide; they have different cone angles, $\psi_c^{(F)}$ and $\psi_c^{(P)}$, and different mean radii, $r_c^{(F)}$ and $r_c^{(P)}$ (fig. 17.3.1(a)). Special machine-tool settings, ΔE_1 and ΔL_1 (fig. 17.3.3(b)), must be used for the generation of the pinion.

Considering the generation of the gear 2 tooth surface we use the following coordinate systems:

- (1) $S_c^{(P)}$, which is rigidly connected to the generating surface Σ_P (fig. 17.3.1(b))
- (2) The fixed coordinate system $S_m^{(2)}$, that is rigidly connected to the frame of the cutting machine
- (3) The coordinate system S_2 , which is rigidly connected to gear 2 (fig. 17.3.2)

In the process of generation, the generating surface rotates about the $x_m^{(2)}$ -axis with angular velocity $\Omega^{(P)}$, while the gear blank rotates about the z_2 -axis with the angular velocity $\Omega^{(2)}$. Axes $x_m^{(2)}$ and z_2 intersect each other and form the angle $90^\circ + \gamma_2 - \Delta_2$, where Δ_2 is the dedendum angle for gear 2. Axis $x_m^{(2)}$ is perpendicular to the generatrix of the root cone of gear 2. The coordinate system S_f shown in figure 17.3.2 is rigidly connected to the housing of the gears and will be used for the analysis of conditions of meshing of the gears.

Considering the generation of the pinion, we use the following coordinate systems:

- (1) $S_c^{(F)}$, that is rigidly connected to the generating surface Σ_F
- (2) $S_m^{(1)}$, that is rigidly connected to the frame of the cutting machine
- (3) S_1 , that is rigidly connected to the pinion (gear 1) (fig. 17.3.3)

Axes $x_m^{(1)}$ and z_1 do not intersect but cross each other; ΔE_1 and ΔL_1 are the corrections of machine-tool settings that are used for the improvement of meshing of the gears. In the process of generation,

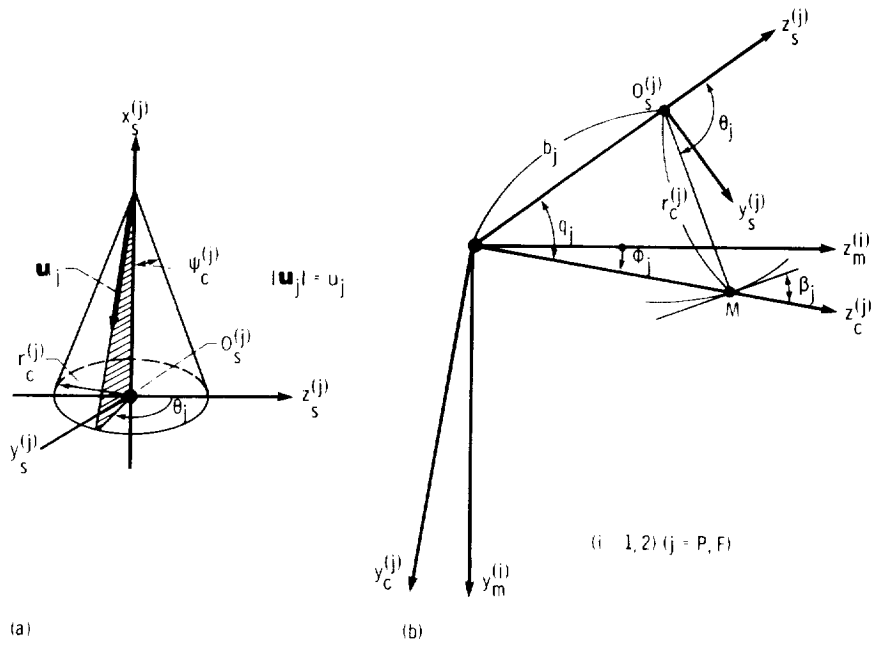


Figure 17.3.1.

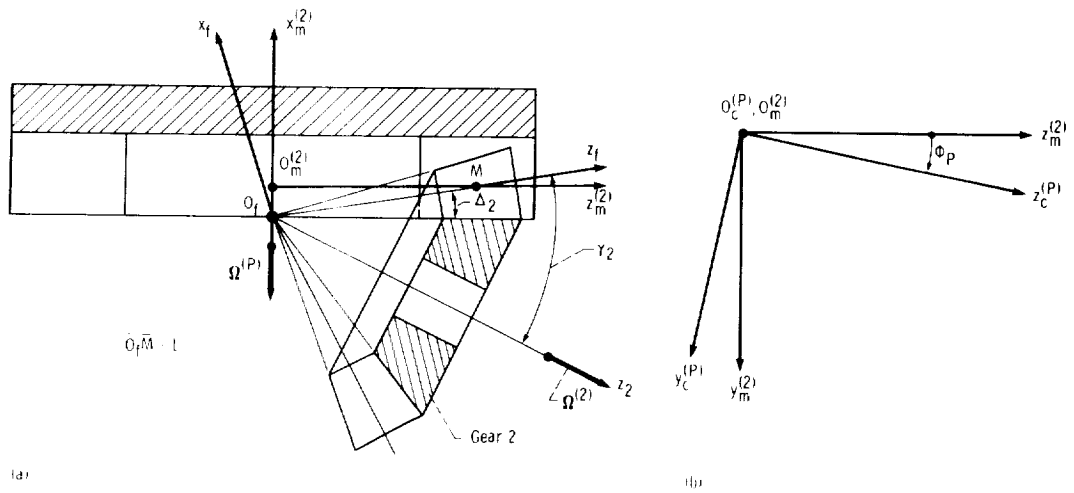


Figure 17.3.2.

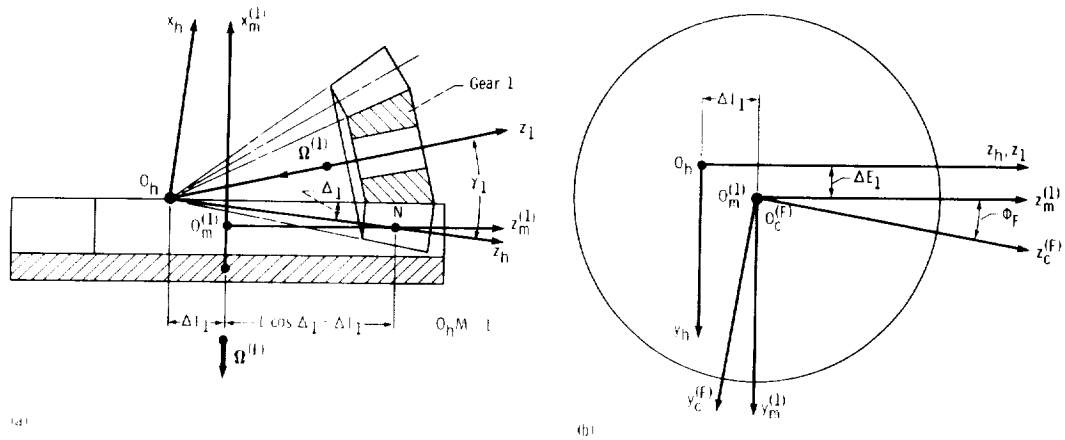


Figure 17.3.3.

the generating surface rotates about the the $x_m^{(1)}$ -axis with angular velocity $\Omega^{(F)}$, while the gear 1 blank rotates about the z_1 -axis with angular velocity $\Omega^{(1)}$. Axes $x_m^{(1)}$ and z_1 form the angle $90^\circ - \gamma_1 + \Delta_1$, where Δ_1 is the dedendum angle of gear 1 and axis $x_m^{(1)}$ is perpendicular to the generatrix of the root cone of gear 1.

17.4 Generating Tool Surfaces

The tool surface is a cone and is represented in the coordinate system $S_s^{(j)}$ as follows (fig. 17.3.1(a))

$$\begin{bmatrix} x_s^{(j)} \\ y_s^{(j)} \\ z_s^{(j)} \\ 1 \end{bmatrix} = \begin{bmatrix} r_c^{(j)} \cot \psi_c^{(j)} - u_j \cos \psi_c^{(j)} \\ u_j \sin \psi_c^{(j)} \sin \theta_j \\ u_j \sin \psi_c^{(j)} \cos \theta_j \\ 1 \end{bmatrix} \quad (j = F, P) \quad (17.4.1)$$

where u_j and θ_j are the surface coordinates.

The coordinate system $S_c^{(j)}$ ($j = F, P$) is an auxiliary coordinate system that is also rigidly connected to the tool (fig. 17.3.1(b)). To represent the generating surface Σ_F and Σ_P in coordinate system $S_c^{(j)}$ we use the following matrix equation (a left-hand generating gear is considered)

$$\begin{bmatrix} x_c^{(j)} \\ y_c^{(j)} \\ z_c^{(j)} \\ 1 \end{bmatrix} = [M_{cs}^{(j)}] \begin{bmatrix} x_s^{(j)} \\ y_s^{(j)} \\ z_s^{(j)} \\ 1 \end{bmatrix} = \begin{bmatrix} 1 & 0 & 0 & 0 \\ 0 & \cos q_j & -\sin q_j & -b_j \sin q_j \\ 0 & \sin q_j & \cos q_j & b_j \cos q_j \\ 0 & 0 & 0 & 1 \end{bmatrix} \begin{bmatrix} x_s^{(j)} \\ y_s^{(j)} \\ z_s^{(j)} \\ 1 \end{bmatrix} \quad (17.4.2)$$

Here b_j and q_j are parameters that determine the location of the tool in coordinate system $S_c^{(j)}$.

Equations (17.4.1) and (17.4.2) yield

$$\begin{aligned} x_c^{(j)} &= r_c^{(j)} \cot \psi_c^{(j)} - u_j \cos \psi_c^{(j)} \\ y_c^{(j)} &= u_j \sin \psi_c^{(j)} \sin (\theta_j - q_j) - b_j \sin q_j \\ z_c^{(j)} &= u_j \sin \psi_c^{(j)} \cos (\theta_j - q_j) + b_j \cos q_j \end{aligned} \quad (17.4.3)$$

where $j = (F, P)$.

The unit normal to the generating surface Σ_j ($j = F, P$) is represented by

$$\mathbf{n}_c^{(j)} = \frac{\mathbf{N}_c^{(j)}}{|\mathbf{N}_c^{(j)}|} \quad \mathbf{N}_c^{(j)} = \frac{\partial \mathbf{r}_c^{(j)}}{\partial \theta_j} \times \frac{\partial \mathbf{r}_c^{(j)}}{\partial u_j} \quad (17.4.4)$$

Using equations (17.4.3) and (17.4.4) (provided $u_j \sin \psi_c^{(j)} \neq 0$), we obtain

$$\mathbf{n}_c^{(j)} = \sin \psi_c^{(j)} \mathbf{i}_c^{(j)} + \cos \psi_c^{(j)} \left[\sin (\theta_j - q_j) \mathbf{j}_c^{(j)} + \cos (\theta_j - q_j) \mathbf{k}_c^{(j)} \right] \quad (17.4.5)$$

17.5 Equations of Meshing by Cutting

Generation of Σ_1

We derive the equation of meshing of the generating surface Σ_F and the gear-tooth surface Σ_1 by using the following procedure:

Step 1.—First, we derive the family of surfaces Σ_F which are represented in the coordinate system $S_m^{(1)}$. Such a family is generated while the coordinate system $S_c^{(F)}$ is rotated about the $x_m^{(1)}$ -axis (fig. 17.3.3). We recall that the generating surface Σ_F is rigidly connected to $S_c^{(F)}$. We use the matrix equation

$$\begin{bmatrix} x_m^{(1)} \\ y_m^{(1)} \\ z_m^{(1)} \\ 1 \end{bmatrix} = \begin{bmatrix} M_m^{(1)c(F)} \end{bmatrix} \begin{bmatrix} x_c^{(F)} \\ y_c^{(F)} \\ z_c^{(F)} \\ 1 \end{bmatrix} \quad (17.5.1)$$

for the coordinate transformation.

Here (fig. 17.3.3)

$$\begin{bmatrix} M_m^{(1)c(F)} \end{bmatrix} = \begin{bmatrix} 1 & 0 & 0 & 0 \\ 0 & \cos \varphi_F & \sin \varphi_F & 0 \\ 0 & -\sin \varphi_F & \cos \varphi_F & 0 \\ 0 & 0 & 0 & 1 \end{bmatrix} \quad (17.5.2)$$

where φ_F is the angle of rotation about the $x_m^{(1)}$ -axis.

Using equations (17.5.1), (17.5.2), and (17.4.3), we obtain

$$\begin{bmatrix} r_m^{(1)} \end{bmatrix} = \begin{bmatrix} x_m^{(1)} \\ y_m^{(1)} \\ z_m^{(1)} \\ 1 \end{bmatrix} = \begin{bmatrix} r_c^{(F)} \cot \psi_c^{(F)} - u_F \cos \psi_c^{(F)} \\ u_F \sin \psi_c^{(F)} \sin \tau_F - b_F \sin (q_F - \varphi_F) \\ u_F \sin \psi_c^{(F)} \cos \tau_F + b_F \cos (q_F - \varphi_F) \\ 1 \end{bmatrix} \quad (17.5.3)$$

where $\tau_F = \theta_F - q_F + \varphi_F$. Equations (17.5.3), with the parameter φ_F fixed, represent a single surface of the family of generating surfaces.

Step 2.—The unit normal to the generating surface Σ_F may be represented in coordinate system $S_m^{(1)}$ as follows:

$$\mathbf{n}_m^{(1)} = \frac{\mathbf{N}_m^{(1)}}{|\mathbf{N}_m^{(1)}|} \quad \mathbf{N}_m^{(1)} = \frac{\partial \mathbf{r}_m^{(1)}}{\partial \theta_F} \times \frac{\partial \mathbf{r}_m^{(1)}}{\partial u_F} \quad (17.5.4)$$

We may also use an alternative method for the derivation of the unit normal. This method is based on the matrix equation

$$\begin{bmatrix} n_m^{(1)} \end{bmatrix} = \begin{bmatrix} L_m^{(1)(F)} \end{bmatrix} \begin{bmatrix} n_c^{(F)} \end{bmatrix} \quad (17.5.5)$$

Matrix $\begin{bmatrix} L_m^{(1)(F)} \end{bmatrix}$ may be determined by deleting the 4th column and row in matrix (17.5.2). The column matrix $\begin{bmatrix} n_c^{(F)} \end{bmatrix}$ is given by vector equation (17.4.4). After transformation, we obtain

$$\begin{bmatrix} n_m^{(F)} \end{bmatrix} = \begin{bmatrix} \sin \psi_c^{(F)} \\ \cos \psi_c^{(F)} \sin \tau_F \\ \cos \psi_c^{(F)} \cos \tau_F \end{bmatrix} \quad (17.5.6)$$

Step 3.—We derive the equations of the relative velocity as follows:

$$\mathbf{v}_m^{(F1)} = \mathbf{v}_m^{(F)} - \mathbf{v}_m^{(1)} \quad (17.5.7)$$

where $\mathbf{v}_m^{(F)}$ is the velocity of a point M on surface Σ_F and $\mathbf{v}_m^{(1)}$ is the velocity of the same point M on surface Σ_1 .

Vector $\mathbf{v}_m^{(F)}$ is represented by the equation

$$\mathbf{v}_m^{(F)} = \mathbf{\Omega}_m^{(F)} \times \mathbf{r}_m^{(1)} \quad (17.5.8)$$

Here (fig. 17.3.3):

$$\begin{bmatrix} \mathbf{\Omega}_m^{(F)} \end{bmatrix} = \begin{bmatrix} -\Omega^{(F)} \\ 0 \\ 0 \end{bmatrix} \quad (17.5.9)$$

Vector $\mathbf{r}_m^{(1)}$ is represented by equation (17.5.3).

Equations (17.5.8) and (17.5.9) yield

$$\begin{bmatrix} \mathbf{v}_m^{(F)} \end{bmatrix} = \Omega^{(F)} \begin{bmatrix} 0 \\ z_m^{(1)} \\ -y_m^{(1)} \end{bmatrix} \quad (17.5.10)$$

Gear 1 rotates about the z_1 -axis with the angular velocity $\mathbf{\Omega}^{(1)}$ (fig. 17.3.3). Since $\mathbf{\Omega}^{(1)}$ does not pass through the origin $O_m^{(1)}$, of the coordinate system $S_m^{(1)}$, we substitute $\mathbf{\Omega}^{(1)}$ by an equal vector which passes through $O_m^{(1)}$ and the vector moment represented by

$$\overline{O_m^{(1)} O_h} \times \mathbf{\Omega}_m^{(1)}$$

Then, we represent $\mathbf{v}_m^{(1)}$ as follows:

$$\mathbf{v}_m^{(1)} = \mathbf{\Omega}_m^{(1)} \times \mathbf{r}_m^{(1)} + \overline{O_m^{(1)} O_h} \times \mathbf{\Omega}_m^{(1)} \quad (17.5.11)$$

Here

$$\overline{O_m^{(1)} O_h} = \begin{bmatrix} L \sin \Delta_1 \\ -\Delta E_1 \\ -\Delta L_1 \end{bmatrix} \quad \left[\Omega_m^{(1)} \right] = -\Omega^{(1)} \begin{bmatrix} \sin (\gamma_1 - \Delta_1) \\ 0 \\ \cos (\gamma_1 - \Delta_1) \end{bmatrix} \quad (17.5.12)$$

where $L = O_h N$. Equations (17.5.11) to (17.5.12) yield

$$\begin{aligned} \left[v_m^{(1)} \right] &= -\Omega^{(1)} \begin{vmatrix} \mathbf{i}_m^{(1)} & \mathbf{j}_m^{(1)} & \mathbf{k}_m^{(1)} \\ \sin (\gamma_1 - \Delta_1) & 0 & \cos (\gamma_1 - \Delta_1) \\ x_m^{(1)} & y_m^{(1)} & z_m^{(1)} \end{vmatrix} \\ &= -\Omega^{(1)} \begin{vmatrix} \mathbf{i}_m^{(1)} & \mathbf{j}_m^{(1)} & \mathbf{k}_m^{(1)} \\ L \sin \Delta_1 & -\Delta E_1 & -\Delta L_1 \\ \sin (\gamma_1 - \Delta_1) & 0 & \cos (\gamma_1 - \Delta_1) \end{vmatrix} \\ &= -\Omega^{(1)} \begin{bmatrix} -\left(y_m^{(1)} + \Delta E_1 \right) \cos (\gamma_1 - \Delta_1) \\ \left(x_m^{(1)} - L \sin \Delta_1 \right) \cos (\gamma_1 - \Delta_1) - \left(z_m^{(1)} + \Delta L_1 \right) \sin (\gamma_1 - \Delta_1) \\ \left(y_m^{(1)} + \Delta E_1 \right) \sin (\gamma_1 - \Delta_1) \end{bmatrix} \end{aligned} \quad (17.5.13)$$

The final expression for $\mathbf{v}_m^{(F1)}$ is

$$\begin{aligned} \left[v_m^{(F1)} \right] &= \\ &= \begin{bmatrix} -\Omega^{(1)} \left(y_m^{(1)} + \Delta E_1 \right) \cos (\gamma_1 - \Delta_1) \\ \Omega^{(F)} z_m^{(1)} + \Omega^{(1)} \left\{ \left(x_m^{(1)} - L \sin \Delta_1 \right) \cos (\gamma_1 - \Delta_1) - \left(z_m^{(1)} + \Delta L_1 \right) \sin (\gamma_1 - \Delta_1) \right\} \\ -\Omega^{(F)} y_m^{(1)} + \Omega^{(1)} \left(y_m^{(1)} + \Delta E_1 \right) \sin (\gamma_1 - \Delta_1) \end{bmatrix} \end{aligned} \quad (7.5.14)$$

Step 4.—The equation of meshing by cutting is represented by

$$\mathbf{n}_m^{(1)} \bullet \mathbf{v}_m^{(F1)} = 0 \quad (17.5.15)$$

Using equations (17.5.15), (17.5.14), (17.5.6), and (17.5.3), we obtain

$$\begin{aligned}
& \left\{ -u_F + \left[r_c^{(F)} \cot \psi_c^{(F)} - L \sin \Delta_1 - \Delta L_1 \tan (\gamma_1 - \Delta_1) \right] \cos \psi_c^{(F)} \right\} \sin \tau_F \\
& + b_F \left[\sin \psi_c^{(F)} \sin (q_F - \varphi_F) + \cos \psi_c^{(F)} \sin \theta_F \frac{m_{F1} - \sin (\gamma_1 - \Delta_1)}{\cos (\gamma_1 - \Delta_1)} \right] \\
& - \Delta E_1 \left[\sin \psi_c^{(F)} - \cos \psi_c^{(F)} \tan (\gamma_1 - \Delta_1) \cos \tau_F \right] \\
& = f_1(u_F, \theta_F, \varphi_F) = 0
\end{aligned} \tag{17.5.16}$$

where $m_{F1} = \Omega^{(F)}/\Omega^{(1)}$. Equation (17.5.6) relates the generating surface coordinates (u_F, θ_F) with the angle of rotation (φ_F) .

Generation of Σ_2

Using a similar procedure, we may obtain the equation of meshing for surface Σ_P by using the following steps.

Step 1.—Equations of the family of generating surfaces Σ_P represented in the coordinate system $S_m^{(2)}$ are

$$\begin{bmatrix} x_m^{(2)} \\ y_m^{(2)} \\ z_m^{(2)} \end{bmatrix} = \begin{bmatrix} r_c^{(P)} \cot \psi_c^{(P)} - u_P \cos \psi_c^{(P)} \\ u_P \sin \psi_c^{(P)} \sin \tau_P - b_P \sin (q_P - \varphi_P) \\ u_P \sin \psi_c^{(P)} \cos \tau_P + b_P \cos (q_P - \varphi_P) \end{bmatrix} \tag{17.5.17}$$

Step 2.—The unit normal to Σ_P is represented in $S_m^{(2)}$ by the column matrix

$$\begin{bmatrix} n_m^{(2)} \end{bmatrix} = \begin{bmatrix} \sin \psi_c^{(P)} \\ \cos \psi_c^{(P)} \sin \tau_P \\ \cos \psi_c^{(P)} \cos \tau_P \end{bmatrix} \tag{17.5.18}$$

where $\tau_P = \theta_P - q_P + \varphi_P$.

Step 3.—The velocities $\mathbf{v}_m^{(P)}$, $\mathbf{v}_m^{(2)}$, and $\mathbf{v}_m^{(P2)}$ are represented in $S_m^{(2)}$ as follows:

$$\begin{bmatrix} v_m^{(P)} \end{bmatrix} = \Omega^{(P)} \begin{bmatrix} 0 \\ z_m^{(2)} \\ -y_m^{(2)} \end{bmatrix} \tag{17.5.19}$$

$$\begin{bmatrix} v_m^{(2)} \end{bmatrix} = -\Omega^{(2)} \begin{bmatrix} y_m^{(2)} \cos (\gamma_2 - \Delta_2) \\ -\left(x_m^{(2)} + L \sin \Delta_2 \right) \cos (\gamma_2 - \Delta_2) - \left(z_m^{(2)} \sin (\gamma_2 - \Delta_2) \right) \\ y_m^{(2)} \sin (\gamma_2 - \Delta_2) \end{bmatrix} \tag{17.5.20}$$

$$\left[v_m^{(P2)} \right] = \left[v_m^{(P)} \right] - \left[v_m^{(2)} \right] \quad (17.5.21)$$

Step 4. –The equation of meshing

$$\mathbf{n}_m^{(2)} \bullet \mathbf{v}_m^{(P2)} = 0$$

yields the following equation:

$$\begin{aligned} f_2(u_P, \theta_P, \varphi_P) = \\ \left[u_P - \left(r_c^{(P)} \cot \psi_c^{(P)} + L \sin \Delta_2 \right) \cos \psi_c^{(P)} \right] \sin \tau_P - b_P \sin (q_P - \varphi_P) \sin \psi_c^{(P)} \\ + b_P \cos \psi_c^{(P)} \sin \theta_P \frac{m_{P2} - \sin (\gamma_2 - \Delta_2)}{\cos (\gamma_2 - \Delta_2)} = 0 \end{aligned} \quad (17.5.22)$$

Here $m_{P2} = \Omega^{(P)} / \Omega^{(2)}$.

17.6 Local Synthesis: Conditions of Tangency

The purpose of local synthesis is to provide (1) tangency of gear-tooth surfaces at the main point of contact, (2) transformation of rotation with an instantaneous gear ratio equal to the given ratio, and (3) determination of the range of machine-tool settings which correspond to the motion of contact point along and across the gear-tooth surfaces, respectively. The solution of the first two problems is discussed in this section.

Tangency of Surfaces Σ_P and Σ_2

We consider that the main contact point M lies on the instantaneous axis of rotation of gears 1 and 2 (fig. 17.3.2). This axis is the pitch line—the line of tangency of gears 1 and 2. The generating surface Σ_P and the gear-tooth surface being cut will be in tangency at M if the following conditions are satisfied: (1) the generating surface Σ_P passes through M and (2) the instantaneous axis of rotation by cutting coincides with the instantaneous axis of rotation for gears 1 and 2.

It is easily verified that the second condition is satisfied with

$$m_{P2} = \frac{\sin \gamma_2}{\cos \Delta_2} \quad (17.6.1)$$

To prove this we consider the collinearity of vectors $\Omega^{(P2)}$ and $\overline{O_f M}$. Here (fig. 17.3.2):

$$\Omega^{(P2)} = \Omega^{(P)} - \Omega^{(2)} = \begin{bmatrix} -\Omega^{(P)} + \Omega^{(2)} \sin (\gamma_2 - \Delta_2) \\ 0 \\ -\Omega^{(2)} \cos (\gamma_2 - \Delta_2) \end{bmatrix} \quad (17.6.2)$$

where $\Omega^{(P2)}$ is the angular velocity of the generating gear P with respect to gear 2 and

$$\overline{O_f M} = L \begin{bmatrix} \sin \Delta_2 \\ 0 \\ \cos \Delta_2 \end{bmatrix} \quad (17.6.3)$$

The conditions of collinearity yield

$$\frac{-\Omega^{(P)} + \Omega^{(2)} \sin (\gamma_2 - \Delta_2)}{\sin \Delta_2} = \frac{-\Omega^{(2)} \cos (\gamma_2 - \Delta_2)}{\cos \Delta_2} \quad (17.6.4)$$

Thus $m_{P2} = \Omega^{(P)}/\Omega^{(2)} = \sin \gamma_2 / \cos \Delta_2$ and equation (17.6.1) is confirmed. Equation (17.6.1) determines the angular velocity ratio for the generation of gear 2.

We may determine the machine-tool settings by taking in equation (17.5.17)

$$x_m^{(2)} = 0 \quad y_m^{(2)} = 0 \quad z_m^{(2)} = L \cos \Delta_2 \quad (17.6.5)$$

where $x_m^{(2)}$, $y_m^{(2)}$, and $z_m^{(2)}$ are the coordinates of point M (fig. 17.3.2). Equations (17.5.17) and (17.6.5) yield

$$u_P = \frac{r_c^{(P)}}{\sin \psi_c^{(P)}} \quad (17.6.6)$$

$$r_c^{(P)} \sin \tau_P - b_P \sin (q_P - \varphi_P) = 0 \quad (17.6.7)$$

$$r_c^{(P)} \cos \tau_P + b_P \cos (q_P - \varphi_P) = L \cos \Delta_2 \quad (17.6.8)$$

where $\tau_P = \theta_P - q_P + \varphi_P$. Using equations (17.6.1), (17.6.6), (17.6.7), and the equation of meshing (17.5.22), we obtain:

$$\sin \theta_P = \frac{L \cos \Delta_2 \sin \tau_P}{b_P} \quad (17.6.9)$$

Equations (17.6.7) to (17.6.9) relate parameters of machine-tool settings: b_P , q_P , and θ_P . These equations may be satisfied for any value of φ_P . For example, with $\varphi_P = 0$ and from drawings of figure 17.3.1, we obtain

$$\beta_P = 90^\circ - (\theta_P - q_P) = 90^\circ - \tau_P \quad (17.6.10)$$

The final expressions for equations (17.6.7) to (17.6.10) therefore become

$$r_c^{(P)} \cos \beta_P - b_P \sin q_P = 0 \quad (17.6.11)$$

$$r_c^{(P)} \sin \beta_P + b_P \cos q_P = L \cos \Delta_2 \quad (17.6.12)$$

$$\sin \theta_P = \frac{L \cos \Delta_2 \cos \beta_P}{b_P} \quad (17.6.13)$$

An alternative solution is based on the equation for θ_P where

$$\theta_P = \tau_P + q_P = 90^\circ - \beta_P + q_P$$

Considering β_P , $r_c^{(P)}$, L , and Δ_2 as given, we may determine the parameters of the machine-tool settings for gear 2 from equations (17.6.11) to (17.6.13).

The common unit normal for surfaces Σ_P and Σ_2 at their contact point M is represented by

$$\begin{bmatrix} n_m^{(2)} \end{bmatrix} = \begin{bmatrix} \sin \psi_c^{(P)} \\ \cos \psi_c^{(P)} \cos \beta_P \\ \cos \psi_c^{(P)} \sin \beta_P \end{bmatrix} \quad (17.6.14)$$

(See eq. (17.5.18).)

Tangency of Surfaces Σ_P , Σ_F , and Σ_2

We set up the following coordinate systems rigidly connected to the frame of the cutting machine: S_h , $S_m^{(1)}$, (fig. 17.3.3), and S_a (fig. 17.6.1(a)). Axis $z_m^{(1)}$ and z_h intersect each other at point N whose location is determined by $O_h N = L$; Δ_1 is the dedendum angle of gear 1; and axis z_a coincides with the rotation axis of gear 1.

We consider also coordinate systems S_f and S_k (fig. 17.6.1(b)) which are rigidly connected to the coordinate system $S_m^{(2)}$ (fig. 17.3.2). Point M which is located on the z_f -axis is the point of tangency of surfaces Σ_P and Σ_2 . In the simplest case, point M may coincide with N and coordinate systems S_f and S_k may coincide with coordinate systems S_h and S_a , respectively. The three surfaces Σ_P , Σ_2 , and Σ_F will then pass through the same point. However, Σ_F will be in tangency with Σ_P and Σ_2 if the normal to Σ_f coincides with the normal to Σ_P . This condition can be satisfied with a special relation between the blade angles $\psi_c^{(F)}$ and $\psi_c^{(P)}$ and special machine-tool settings. For practical reasons it is important to make $\psi_c^{(F)} = \psi_c^{(P)}$ and use blades with the same angle. This becomes possible by choosing a new point of contact A for surfaces Σ_F , Σ_P , and Σ_2 .

Consider that the generating surface Σ_F is set up in the coordinate system S_h , but the settings of Σ_F are not yet determined. The generating surface Σ_P is set up in the coordinate system Σ_f and its settings are known: Σ_P passes through point M and the surface unit normal at M is represented in the coordinate system $S_m^{(2)}$ by equation (17.6.14). Surfaces Σ_P and Σ_2 are in tangency at M . Initially, the coordinate system S_f coincides with S_h , and S_k coincides with S_a . We may consider that coordinate systems S_f , S_k , $S_m^{(2)}$, and surfaces Σ_P and Σ_2 form a rigid body B . Now, consider that B is rotated about the z_a -axis through an angle δ (fig. 17.6.2) which is just a setting angle. Axis z_f being rotated about the z_a -axis will move over the surface of the pitch cone with the apex angle γ_1 . Consequently, point M , which is the point of tangency of surfaces Σ_P and Σ_2 , will come

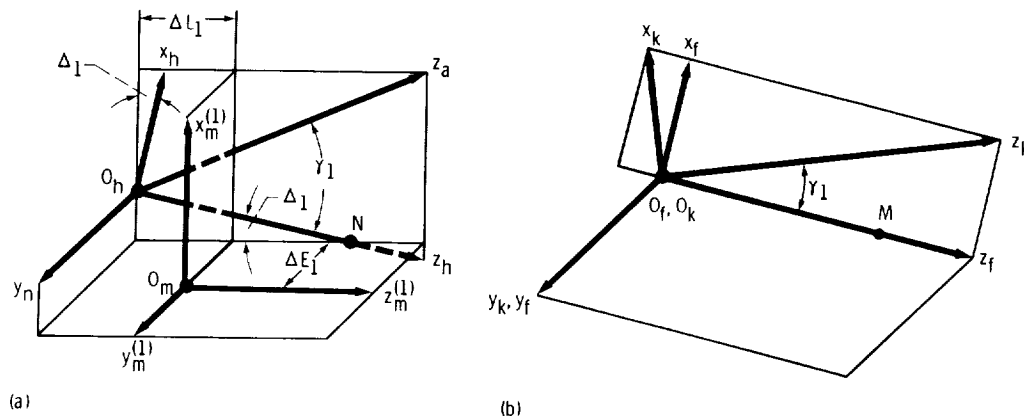


Figure 17.6.1.

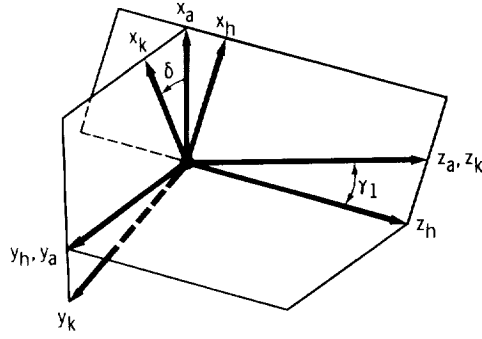


Figure 17.6.2.

to a new position which we designate by N . However, point N lies on the pitch cone of gear 1. Surfaces Σ_F and Σ_P (consequently, Σ_F , Σ_P , and Σ_2) will be in tangency at N , if the following equations are observed:

$$\begin{bmatrix} r_h^{(F)} \end{bmatrix} = \begin{bmatrix} M_{hf} \end{bmatrix} \begin{bmatrix} r_f^{(M)} \end{bmatrix} \quad (17.6.15)$$

$$\begin{bmatrix} n_h^{(F)} \end{bmatrix} = \begin{bmatrix} L_{hf} \end{bmatrix} \begin{bmatrix} n_f^{(M)} \end{bmatrix} \quad (17.6.16)$$

Here

$$\begin{bmatrix} r_f^{(M)} \end{bmatrix} = \begin{bmatrix} 0 \\ 0 \\ L \\ 1 \end{bmatrix} \quad (17.6.17)$$

is the column matrix of point M .

Matrix $\begin{bmatrix} n_f^{(M)} \end{bmatrix}$ is the column matrix of the unit normal to surface Σ_P at point M . Matrix $\begin{bmatrix} M_{hf} \end{bmatrix}$ represents the coordinate transformation in transition from S_f to S_h and is determined as follows (figs. 17.6.1(b) and 17.6.2):

$$\begin{bmatrix} M_{hf} \end{bmatrix} = \begin{bmatrix} M_{ha} \end{bmatrix} \begin{bmatrix} M_{ak} \end{bmatrix} \begin{bmatrix} M_{kf} \end{bmatrix} =$$

$$\begin{bmatrix} \cos \gamma_1 & 0 & \sin \gamma_1 & 0 \\ 0 & 1 & 0 & 0 \\ -\sin \gamma_1 & 0 & \cos \gamma_1 & 0 \\ 0 & 0 & 0 & 1 \end{bmatrix} \begin{bmatrix} \cos \delta & -\sin \delta & 0 & 0 \\ \sin \delta & \cos \delta & 0 & 0 \\ 0 & 0 & 1 & 0 \\ 0 & 0 & 0 & 1 \end{bmatrix} \begin{bmatrix} \cos \gamma_1 & 0 & -\sin \gamma_1 & 0 \\ 0 & 1 & 0 & 0 \\ \sin \gamma_1 & 0 & \cos \gamma_1 & 0 \\ 0 & 0 & 0 & 1 \end{bmatrix}$$

$$\begin{bmatrix} \cos \delta \cos^2 \gamma_1 + \sin^2 \gamma_1 & -\sin \delta \cos \gamma_1 & (1 - \cos \delta) \cos \gamma_1 \sin \gamma_1 & 0 \\ \sin \delta \cos \gamma_1 & \cos \delta & -\sin \delta \sin \gamma_1 & 0 \\ (1 - \cos \delta) \cos \gamma_1 \sin \gamma_1 & \sin \delta \sin \gamma_1 & \cos \delta \sin^2 \gamma_1 + \cos^2 \gamma_1 & 0 \\ 0 & 0 & 0 & 1 \end{bmatrix} \quad (17.6.18)$$

Matrix $[L_{hf}]$ may be derived from $[M_{hf}]$ by deleting the fourth column and row.

The column matrices $[r_h^{(F)}]$ and $[n_h^{(F)}]$, represent in coordinate system S_h , surface Σ_F and the surface unit normal.

Matrix equations (17.6.15) and (17.6.16) provide six equations which determine the machine-tool settings for the generating surface Σ_F . The derivation of these equations is based on the following procedure:

Step 1. Determination of the matrix product $[M_{hf}][r_f^{(M)}]$ in equation (17.6.15).—Using equations (17.6.17) and (17.6.18), we obtain

$$[M_{hf}][r_f^{(M)}] = L \begin{bmatrix} (1 - \cos \delta) \cos \gamma_1 \sin \gamma_1 \\ -\sin \delta \sin \gamma_1 \\ \cos \delta \sin^2 \gamma_1 + \cos^2 \gamma_1 \\ 1 \end{bmatrix} \quad (17.6.19)$$

Step 2. Representation of surface Σ_F in coordinate system S_h .—Surface Σ_F is represented in the coordinate system $S_m^{(1)}$ by equations (17.5.3). We may represent Σ_F in S_h by using the following matrix equation:

$$[r_h^{(F)}] = [M_{hm}^{(1)}][r_m^{(1)}] \quad (17.6.20)$$

where (figs. 17.3.3 and (17.6.1)

$$[M_{hm}^{(1)}] = \begin{bmatrix} \cos \Delta_1 & 0 & \sin \Delta_1 & -(L \cos \Delta_1 - \Delta L_1) \sin \Delta_1 \\ 0 & 1 & 0 & \Delta E_1 \\ -\sin \Delta_1 & 0 & \cos \Delta_1 & L \sin^2 \Delta_1 + \Delta L_1 \cos \Delta_1 \\ 0 & 0 & 0 & 1 \end{bmatrix} \quad (17.6.21)$$

Equations (17.5.3) and (17.6.21) yield

$$\begin{aligned} x_h^{(F)} &= \left(r_c^{(F)} \cot \psi_c^{(F)} - u_F \cos \psi_c^{(F)} \right) \cos \Delta_1 \\ &+ \left[u_F \sin \psi_c^{(F)} \cos \tau_F + b_F \cos (q_F - \varphi_F) \right] \sin \Delta_1 - (L \cos \Delta_1 - \Delta L_1) \sin \Delta_1 \end{aligned} \quad (17.6.22)$$

$$y_h^{(F)} = u_F \sin \psi_c^{(F)} \sin \tau_F - b_F \sin (q_F - \varphi_F) + \Delta E_1 \quad (17.6.23)$$

$$\begin{aligned} z_h^{(F)} &= - \left(r_c^{(F)} \cot \psi_c^{(F)} - u_F \cos \psi_c^{(F)} \right) \sin \Delta_1 \\ &+ \left[u_F \sin \psi_c^{(F)} \cos \tau_F + b_F \cos (q_F - \varphi_F) \right] \cos \Delta_1 + L \sin^2 \Delta_1 + \Delta L_1 \cos \Delta_1 \end{aligned} \quad (17.6.24)$$

Step 3. Determination of basic equations provided by matrix equation (17.6.15). – Using equations (17.6.15), (17.6.19), and (17.6.22) to (17.6.24), we get

$$\begin{aligned} & \left(r_c^{(F)} \cot \psi_c^{(F)} - u_F \cos \psi_c^{(F)} \right) \cos \Delta_1 + \left[u_F \sin \psi_c^{(F)} \cos \tau_F + b_F \cos (q_F - \varphi_F) \right] \sin \Delta_1 \\ & - (L \cos \Delta_1 - \Delta L_1) \sin \Delta_1 = L(1 - \cos \delta) \cos \gamma_1 \sin \gamma_1 \end{aligned} \quad (17.6.25)$$

$$u_F \sin \psi_c^{(F)} \sin \tau_F - b_F \sin (q_F - \varphi_F) + \Delta E_1 = -L \sin \delta \sin \gamma_1 \quad (17.6.26)$$

$$\begin{aligned} & - \left(r_c^{(F)} \cot \psi_c^{(F)} - u_F \cos \psi_c^{(F)} \right) \sin \Delta_1 + \left[u_F \sin \psi_c^{(F)} \cos \tau_F + b_F \cos (q_F - \varphi_F) \right] \cos \Delta_1 \\ & + L \sin^2 \Delta_1 + \Delta L_1 \cos \Delta_1 = L(\cos \delta \sin \gamma_1 + \cos^2 \gamma_1) \end{aligned} \quad (17.6.27)$$

The three basic equations (17.6.25) to (17.6.27) provide that surfaces Σ_F , Σ_P , and Σ_2 have a common point P .

Step 4. Representation in coordinate system S_h of the unit normal to surface Σ_P . – The surface unit normal at point P is represented in coordinate system $S_m^{(2)}$ by equation (17.5.18). Parameter $\tau_P = 90^\circ - \beta_P$ at point M (fig. 17.3.1). The unit normal is represented in the coordinate system S_h by the matrix product $\left[L_{hm}^{(2)} \right] \left[n_m^{(2)} \right]$.
Here (figs. 17.3.2) and (17.6.1)

$$\begin{aligned} & \left[L_{hm}^{(2)} \right] = [L_{hf}] \left[L_{fm}^{(2)} \right] = \\ & \begin{bmatrix} \cos \delta \cos^2 \gamma_1 + \sin^2 \gamma_1 & -\sin \delta \cos \gamma_1 & (1 - \cos \delta) \cos \gamma_1 \sin \gamma_1 \\ \sin \delta \cos \gamma_1 & \cos \delta & -\sin \delta \sin \gamma_1 \\ (1 - \cos \delta) \cos \gamma_1 \sin \gamma_1 & \sin \delta \sin \gamma_1 & \cos \delta \sin^2 \gamma_1 + \cos^2 \gamma_1 \end{bmatrix} \\ & \begin{bmatrix} \cos \Delta_2 & 0 & -\sin \Delta_2 \\ 0 & 1 & 0 \\ \sin \Delta_2 & 0 & \cos \Delta_2 \end{bmatrix} \end{aligned} \quad (17.6.28)$$

Using equations (17.6.28) and (17.5.18), we obtain

$$\begin{aligned} n_{sh}^{(P)} &= \cos \delta \cos \gamma_1 \left[\sin \psi_c^{(P)} \cos (\gamma_1 + \Delta_2) - \cos \psi_c^{(P)} \sin (\gamma_2 + \Delta_2) \sin \beta_P \right] \\ &+ \sin \gamma_1 \left[\sin \psi_c^{(P)} \sin (\gamma_1 + \Delta_2) + \cos \psi_c^{(P)} \cos (\gamma_1 + \Delta_2) \sin \beta_P \right] \\ &- \sin \delta \cos \psi_c^{(P)} \cos \gamma_1 \cos \beta_P \end{aligned} \quad (17.6.29)$$

$$n_{yh}^{(P)} = \sin \delta \left[\sin \psi_c^{(P)} \cos (\gamma_1 + \Delta_2) - \cos \psi_c^{(P)} \sin \beta_P \sin (\gamma_1 + \Delta_2) \right] + \cos \delta \cos \psi_c^{(P)} \cos \beta_P \quad (17.6.30)$$

$$n_{zh}^{(P)} = -\cos \delta \sin \gamma_1 \left[\sin \psi_c^{(P)} \cos (\gamma_1 + \Delta_2) - \cos \psi_c^{(P)} \sin \beta_P \sin (\gamma_1 + \Delta_2) \right] + \cos \gamma_1 \left[\sin \psi_c^{(P)} \sin (\gamma_1 + \Delta_2) + \cos \psi_c^{(P)} \sin \beta_P \cos (\gamma_1 + \Delta_2) \right] + \sin \delta \cos \psi_c^{(P)} \cos \beta_P \sin \gamma_1 \quad (17.6.31)$$

Step 5. Representation in coordinate system S_h of the unit normal to surface Σ_F .—The unit normal to surface Σ_F is represented in coordinate system $S_m^{(1)}$ by equations (17.5.6). We may represent this unit normal in coordinate system S_h by using the following matrix equation:

$$\left[n_h^{(F)} \right] = \left[L_{hm}^{(1)} \right] \left[n_m^{(F)} \right] \quad (17.6.32)$$

Here (see matrix (17.6.21)):

$$\left[L_{hm}^{(1)} \right] = \begin{bmatrix} \cos \Delta_1 & 0 & \sin \Delta_1 \\ 0 & 1 & 0 \\ -\sin \Delta_1 & 0 & \cos \Delta_1 \end{bmatrix} \quad (17.6.33)$$

Using equations (17.6.32), (17.6.33), and (17.5.6), we obtain

$$n_{xh}^{(F)} = \sin \psi_c^{(F)} \cos \Delta_1 + \cos \psi_c^{(F)} \cos \tau_F \sin \Delta_1 \quad (17.6.34)$$

$$n_{yh}^{(F)} = \cos \psi_c^{(F)} \sin \tau_F \quad (17.6.35)$$

$$n_{zh}^{(F)} = -\sin \psi_c^{(F)} \sin \Delta_1 + \cos \psi_c^{(F)} \cos \tau_F \cos \Delta_1 \quad (17.6.36)$$

Step 6. Determination of basic equations provided by matrix equations (17.6.16).—Using equations (17.6.16), (17.6.29) to (17.6.31) and (17.6.34) to (17.6.36), we obtain

$$\begin{aligned} & \sin \psi_c^{(F)} \cos \Delta_1 + \cos \psi_c^{(F)} \cos \tau_F \sin \Delta_1 \\ &= \cos \delta \cos \gamma_1 \left[\sin \psi_c^{(P)} \cos (\gamma_1 + \Delta_2) - \cos \psi_c^{(P)} \sin (\gamma_1 + \Delta_2) \sin \beta_P \right] \\ &+ \sin \gamma_1 \left[\sin \psi_c^{(P)} \sin (\gamma_1 + \Delta_2) + \cos \psi_c^{(P)} \cos (\gamma_1 + \Delta_2) \sin \beta_P \right] \\ &- \sin \delta \cos \psi_c^{(P)} \cos \gamma_1 \cos \beta_P \end{aligned} \quad (17.6.37)$$

$$\begin{aligned} \cos \psi_c^{(F)} \sin \tau_F &= \sin \delta \left[\sin \psi_c^{(P)} \cos (\gamma_1 + \Delta_1) - \cos \psi_c^{(P)} \sin \beta_P \sin (\gamma_1 + \Delta_2) \right] \\ &+ \cos \delta \cos \psi_c^{(P)} \cos \beta_P \end{aligned} \quad (17.6.38)$$

$$\begin{aligned}
& -\sin \psi_c^{(F)} \sin \Delta_1 + \cos \psi_c^{(F)} \cos \tau_F \cos \Delta_1 \\
& = -\cos \delta \sin \gamma_1 \left[\sin \psi_c^{(P)} \cos (\gamma_1 + \Delta_2) - \cos \psi_c^{(P)} \sin \beta_P \sin (\gamma_1 + \Delta_2) \right] \\
& + \sin \delta \cos \psi_c^{(P)} \cos \beta_P \sin \gamma_1 + \cos \gamma_1 \left[\sin \psi_c^{(P)} \sin (\gamma_1 + \Delta_2) \right. \\
& \left. + \cos \psi_c^{(P)} \sin \beta_P \cos (\gamma_1 + \Delta_2) \right] \tag{17.6.39}
\end{aligned}$$

The three basic equations (17.6.37) to (17.6.39) provide that surfaces Σ_F , Σ_P , and Σ_2 have a common normal at point P and are in tangency at this point. Only two equations of (17.6.37) to (17.6.39) are independent since $|\mathbf{n}_h^{(F)}| = |\mathbf{n}_h^{(P)}| = 1$.

The satisfaction of equations (17.6.25) to (17.6.27) and (17.6.37) to (17.6.39) yields that the three surfaces Σ_F , Σ_P , and Σ_2 have a common point N and are in tangency at this point. All four surfaces Σ_1 , Σ_F , Σ_P , and Σ_2 will be in tangency at N if at this point the equation of meshing of Σ_F and Σ_1 is also satisfied. This condition can be fulfilled with the appropriate value of the ratio for cutting $m_{F1} = \Omega^{(F)}/\Omega^{(1)}$. (See sec. 17.7.)

17.7 Basic Machine-Tool Settings

The basic equations (17.6.25) to (17.6.27) and (17.6.37) to (17.6.39) determine the relations between the machine-tool settings for the generating surfaces Σ_P and Σ_F . We may determine these settings by using the following procedure.

Determination of Settings

Step 1. Determination of τ_F .—Consider equations (17.6.37) and (17.6.39). Multiplying these equations by $\sin \gamma_1$ and $\cos \gamma_1$, respectively, we get, after simplifications, that

$$\begin{aligned}
\cos \tau_F = & \\
& \frac{\sin \psi_c^{(P)} \sin (\gamma_1 + \Delta_2) + \cos \psi_c^{(P)} \cos (\gamma_1 + \Delta_2) \sin \beta_P - \sin \psi_c^{(P)} \sin (\gamma_1 - \Delta_1)}{\cos \psi_c^{(F)} \cos (\gamma_1 - \Delta_1)} \tag{17.7.1}
\end{aligned}$$

Using this equation, we make $\psi_c^{(F)} = \psi_c^{(P)} = \psi_c$, where ψ_c is the standard angle of the blades of the head-cutter.

Equation (17.6.40) provides two solutions for τ_F . We have to choose the solution which gives τ_F close to $(90^\circ - \beta_P)$.

Step 2. Determination of δ .—Represent equations (17.6.37) and (17.6.38) as follows:

$$A \sin \delta + B \cos \delta + C = 0 \tag{17.7.2}$$

$$D \sin \delta + E \cos \delta + F = 0 \tag{17.7.3}$$

These equations provide one solution for δ

$$\tan \frac{\delta}{2} = \frac{A(E + F) - D(C + B)}{BF - CE} \tag{17.7.4}$$

Step 3. Determination of u_F .—Consider equations (17.6.25) and (17.6.27) simultaneously. Multiplying these equations by $\cos \Delta_1$ and $\sin \Delta_1$ respectively, we get, after simplifications,

$$u_F = \frac{r_c^{(F)} \cot \psi_c^{(F)} - L \sin \gamma_1 \cos (\gamma_1 - \Delta_1)(1 - \cos \delta)}{\cos \psi_c^{(F)}} \quad (17.7.5)$$

Step 4. Determination of $(q_F - \varphi_F)$ and b_F .—Consider equations (17.6.25) and (17.6.27) simultaneously. Multiplying these equations by $\sin \Delta_1$ and $\cos \Delta_1$, we get, after transformations,

$$b_F \cos (q_F - \varphi_F) = L \left[\cos \gamma_1 \cos (\gamma_1 - \Delta_1) + \cos \delta \sin \gamma_1 \sin (\gamma_1 - \Delta_1) \right] - \Delta L_1 - u_F \sin \psi_c^{(F)} \cos \tau_F \quad (17.7.6)$$

Equations (17.7.6) and (17.6.26) yield

$$\tan (q_F - \varphi_F) = \frac{Q}{G} \quad (17.7.7)$$

$$Q = u_F \sin \psi_c^{(F)} \sin \tau_F + \Delta E_1 + L \sin \delta \sin \gamma_1 \quad (17.7.8)$$

$$G = L \left[\cos \gamma_1 \cos (\gamma_1 - \Delta_1) + \cos \delta \sin \gamma_1 \sin (\gamma_1 - \Delta_1) \right] - \Delta L_1 - u_F \sin \psi_c^{(F)} \cos \tau_F \quad (17.7.9)$$

Equations (17.6.26) and (17.7.9) yield

$$b_F = \frac{Q}{\sin (q_F - \varphi_F)} \quad (17.7.10)$$

Alternative Solutions for $(q_F - \varphi_F)$

We may represent equations (17.6.25) and (17.6.26) as follows:

$$b_F \cos (q_F - \varphi_F) = A \quad (17.7.11)$$

$$b_F \sin (q_F - \varphi_F) = B \quad (17.7.12)$$

Equations (17.7.11) and (17.7.12) yield

$$b_F = \sqrt{A^2 + B^2} \quad (17.7.13)$$

$$\tan \frac{q_F - \varphi_F}{2} = \frac{\sqrt{A^2 + B^2} - A}{B} \quad (17.7.14)$$

Step 5. Determination of θ_F .—Consider that τ_F and $(q_F - \varphi_F)$ are known. Then we may determine θ_F using the equation

$$\theta_F = \tau_F + q_F - \varphi_F \quad (17.7.15)$$

Step 6. Determination of m_{F1} .—Surfaces Σ_F and Σ_1 will be in tangency at point A if the equation of meshing (17.5.16) is satisfied for this point.

We transform equation (17.5.16) by using expressions (17.7.5), (17.7.6), (17.7.10), and (17.7.16) for u_F , $b_F \cos (q_F - \varphi_F)$, $b_F \sin (q_F - \varphi_F)$, and θ_F , respectively. After transformations we get the following equation for m_{F1} :

$$m_{F1} = \frac{T}{E} \quad (17.7.16)$$

Here

$$m_{F1} = \frac{\Omega^{(F)}}{\Omega^{(1)}}$$

is the angular velocity ratio for cutting of gear 1.

$$T = L \sin \gamma_1 \left\{ \cos \delta \sin \tau_F - \sin \delta \left[\cos (\gamma_1 - \Delta_1) \tan \psi_c^{(F)} - \sin (\gamma_1 - \Delta_1) \cos \tau_F \right] \right\} \quad (17.7.17)$$

$$E = L \sin \gamma_1 \left[\cot \gamma_1 \cos (\gamma_1 - \Delta_1) \sin \tau_F + \cos \delta \sin (\gamma_1 - \Delta_1) \sin \tau_F + \sin \delta \cos \tau_F \right] - \Delta L_1 \sin \tau_F + \Delta E_1 \cos \tau_F \quad (17.7.18)$$

Generally, the ratio m_{F1} depends on the corrections of machine-tool settings, ΔL_1 and ΔE_1 . There is a particular case when the corrections ΔE_1 and ΔL_1 are related with the equation

$$\Delta E_1 \cos \tau_F = \Delta L_1 \sin \tau_F \quad (17.7.19)$$

For this particular case the ratio m_{F1} does not depend on the corrections of machine-tool settings.

17.8 Local Synthesis: Determination of Corrections of Machine-Tool Settings

Basic Equations

The purpose of the corrections of machine-tool settings is to make the first derivative of the gear ratio $d/d\varphi_1 (m_{12}(\varphi_1))$, equal to zero at the main contact point A . The determination of the corrections ΔE_1 and ΔL_1 is based on the use of the following equations:

$$\mathbf{v}_r^{(2)} - \mathbf{v}_r^{(1)} = \mathbf{v}^{(12)} \quad (17.8.1)$$

$$\dot{\mathbf{n}}_r^{(2)} - \dot{\mathbf{n}}_r^{(1)} = \boldsymbol{\omega}^{(12)} \times \mathbf{n} \quad (17.8.2)$$

$$\frac{d}{dt} (\mathbf{n}^{(1)} \cdot \mathbf{v}^{(12)}) = 0 \quad (17.8.3)$$

$$\frac{d}{dt} (\mathbf{n}^{(P)} \cdot \mathbf{v}^{(P2)}) = 0 \quad (17.8.4)$$

$$\frac{d}{dt} (\mathbf{n}^{(F)} \cdot \mathbf{v}^{(F1)}) = 0 \quad (17.8.5)$$

(See eqs. (6.1.12) and (6.1.13).)

Equations (17.8.3) to (17.8.5) are the differentiated equations of meshing for gears 1 and 2, the generating gear P and gear 2, and the generating gear F and gear 1, respectively.

Here $\mathbf{v}_r^{(i)}$ ($i = 1, 2$) is the velocity of the contacting point in motion over the surface; $\dot{\mathbf{n}}_r^{(i)}$ is the velocity of the tip of the surface unit normal in motion over the surface; $\mathbf{v}^{(12)}$ is the sliding velocity; \mathbf{n} is the common surface unit normal; and $\boldsymbol{\omega}^{(12)} = \boldsymbol{\omega}^{(1)} - \boldsymbol{\omega}^{(2)}$ where $\boldsymbol{\omega}^{(i)}$ is the gear angular velocity.

Let us transform equation (17.8.1) by using the following relations:

$$\mathbf{v}_r^{(2)} = \mathbf{v}_r^{(P)} + \mathbf{v}^{(P2)} = \mathbf{v}_r^{(P)} \quad (17.8.6)$$

Here $\mathbf{v}^{(P2)} = \mathbf{0}$ since point M of tangency of surfaces Σ_P and Σ_2 lies on the instantaneous axis of rotation (fig. 17.3.2)

$$\mathbf{v}_r^{(1)} = \mathbf{v}_r^{(F)} + \mathbf{v}^{(F1)} \quad (17.8.7)$$

$$\mathbf{v}_r^{(1)} = \mathbf{v}_r^{(2)} \quad (17.8.8)$$

because point N of tangency of surfaces Σ_1 and Σ_2 lies on the pitch line and $\mathbf{v}^{(12)} = \mathbf{0}$.

Equations (17.8.1), (17.8.2), and (17.8.6) to (17.8.8) yield

$$\mathbf{v}_r^{(p)} = \mathbf{v}_r^{(F)} + \mathbf{v}^{(F1)} \quad (17.8.9)$$

Using similar transformations for equation (17.8.2), we get

$$\dot{\mathbf{n}}_r^{(2)} = \dot{\mathbf{n}}_r^{(P)} + \mathbf{\Omega}^{(P2)} \times \mathbf{n}^{(P)} \quad (17.8.10)$$

$$\dot{\mathbf{n}}_r^{(1)} = \dot{\mathbf{n}}_r^{(F)} + \mathbf{\Omega}^{(F1)} \times \mathbf{n}^{(F)} \quad (17.8.11)$$

Here $\mathbf{\Omega}^{(P2)} = \mathbf{\Omega}^{(P)} - \mathbf{\Omega}^{(2)}$ and $\mathbf{\Omega}^{(F1)} = \mathbf{\Omega}^{(F)} - \mathbf{\Omega}^{(1)}$, where $\mathbf{\Omega}$ is the angular velocity in the generating process; $\mathbf{n}^{(1)} = \mathbf{n}^{(2)} = \mathbf{n}^{(F)} = \mathbf{n}^{(P)}$ at the point of contact.

Equations (17.8.2) and (17.8.10) to (17.8.11) yield

$$\dot{\mathbf{n}}_r^{(P)} + \mathbf{\Omega}^{(P2)} \times \mathbf{n}^{(P)} - \omega^{(12)} \times \mathbf{n}^{(P)} = \dot{\mathbf{n}}_r^{(F)} + \mathbf{\Omega}^{(F1)} \times \mathbf{n}^{(F)} \quad (17.8.12)$$

Let us now differentiate the equations of meshing (17.8.3) to (17.8.5) by taking into account that the main contact point $\mathbf{v}^{(12)} = \mathbf{0}$ and $\mathbf{v}^{(P2)} = \mathbf{0}$. Let us also assume that $\omega^{(1)} = \text{constant}$, $\omega^{(2)} = \text{constant}$, and $m_{12}(\varphi_1) = 0$. Thus we obtain

$$\frac{d}{dt} (\dot{\mathbf{n}}^{(1)} \cdot \mathbf{v}^{(12)}) = \dot{\mathbf{n}}^{(1)} \cdot \mathbf{v}^{(12)} + \mathbf{n}^{(1)} \cdot \frac{d}{dt} [\omega^{(12)} \times \mathbf{r}^{(1)}] = [\mathbf{n}^{(1)} \omega^{(12)} \dot{\mathbf{r}}^{(1)}] = 0 \quad (17.8.13)$$

$$\frac{d}{dt} (\mathbf{n}^{(P)} \cdot \mathbf{v}^{(P2)}) = [\mathbf{n}^{(P)} \mathbf{\Omega}^{(P2)} \dot{\mathbf{r}}^{(P)}] = 0 \quad (17.8.14)$$

$$\dot{\mathbf{n}}^{(F)} \mathbf{v}^{(F1)} + [\mathbf{n}^{(F)} \mathbf{\Omega}^{(F1)} \dot{\mathbf{r}}^{(F)}] = 0 \quad (17.8.15)$$

Litvin (1968) proved that the basic equations mentioned provide two sets of the corrections with which the motion of contact point is directed across and along the tooth surface. Of the two motions, the more favorable case is the motion of the contracting point along the tooth surface, because it provides reduced kinematical errors and better conditions of lubrication. For these reasons, we limit the discussion to the mentioned case.

Kinematic Considerations

Consider four surfaces Σ_P , Σ_2 , Σ_F , and Σ_1 which are in tangency at point A . Point A lies on the pitch line of gears 1 and 2. Gear 1, having surface Σ_1 , rotates with angular velocity $\omega^{(1)}$ and is in mesh with surfaces Σ_F and Σ_2 . Thus $\omega^{(1)} \equiv \mathbf{\Omega}^{(1)}$ and $\mathbf{\Omega}^{(F)} \equiv \omega^{(F)}$, where $\omega^{(F)} = \omega^{(1)} m_{F1}$. Similarly, we may state that gear 2, having surface Σ_2 , rotates with angular velocity $\omega^{(2)}$ and is in mesh with surfaces Σ_P and Σ_1 . Here $\omega^{(2)} \equiv \mathbf{\Omega}^{(2)}$, and $\mathbf{\Omega}^{(P)} \equiv \omega^{(P)}$, where $\omega^{(P)} = \omega^{(2)} m_{P2}$. All four surfaces will be in contact within the neighborhood of point A if they have a common point and common normal.

Equations (17.6.37) to (17.6.39) provide that surfaces Σ_P and Σ_F are indeed in tangency at point A . Considering that surfaces Σ_P and Σ_F are in tangency within the neighborhood of A , we have to change β_P for the variable τ_P . Then, equations (17.6.37) to (17.6.39) become equations with

variables $\tau_P = \theta_P - q_P + \varphi_P$ and $\tau_F = \theta_F - q_F + \varphi_F$. These equations can be satisfied in the process of meshing with certain relations between τ_P and τ_F . There is a particular case when equations (17.6.37) to (17.6.39) are satisfied within the neighborhood of A , because τ_P and τ_F are constant. We remind that τ_F and τ_P , for point A , are not equal but related with equation (17.7.1); where $\tau_P = 90^\circ - \beta_P$ for point A . Thus the contacting normal to surfaces Σ_P keeps its original direction within the neighborhood of A .

Figure 17.8.1 shows two longitudinal shapes of surfaces Σ_P and Σ_F at two positions when they contact each other at A and A^* , respectively. The contacting normals have the same direction at A and A^* , and intersect the instantaneous axis of rotation at A and B , respectively.

Considering that τ_P and τ_F are constant within the neighborhood of A , we get

$$\frac{d\tau_P}{dt} = 0 \quad \frac{d\varphi_P}{dt} = -\frac{d\theta_P}{dt} \quad (17.8.15)$$

$$\frac{d\tau_F}{dt} = 0 \quad \frac{d\varphi_F}{dt} = -\frac{d\theta_F}{dt} \quad (17.8.16)$$

Determination of ΔE_1 : Basic Equations

The determination of ΔE_1 is based on the following equations:

$$\frac{\partial f_2}{\partial u_P} \frac{du_P}{dt} + \frac{\partial f_2}{\partial \theta_P} \frac{d\theta_P}{dt} + \frac{\partial f_2}{\partial \varphi_P} \frac{d\varphi_P}{dt} = \frac{\partial f_2}{\partial u_P} \frac{du_P}{dt} + \left(\frac{\partial f_2}{\partial \varphi_P} - \frac{\partial f_2}{\partial \theta_P} \right) \frac{d\varphi_P}{dt} = 0 \quad (17.8.17)$$

$$\frac{\partial f_1}{\partial u_F} \frac{du_F}{dt} + \frac{\partial f_1}{\partial \theta_F} \frac{d\theta_F}{dt} + \frac{\partial f_1}{\partial \varphi_F} \frac{d\varphi_F}{dt} = \frac{\partial f_1}{\partial u_F} \frac{du_F}{dt} + \left(\frac{\partial f_1}{\partial \varphi_F} - \frac{\partial f_1}{\partial \theta_F} \right) \frac{d\varphi_F}{dt} = 0 \quad (17.8.18)$$

$$\mathbf{v}_r^{(P)} \cdot \mathbf{i}_m^{(1)} = \mathbf{v}_r^{(F)} \cdot \mathbf{i}_m^{(1)} + \mathbf{v}^{(F1)} \cdot \mathbf{i}_m^{(1)} \quad (17.8.19)$$

Here

$$f_2(u_P, \theta_P, \varphi_P) = 0 \quad (17.8.20)$$

is the equation of meshing of surfaces Σ_P and Σ_2 , represented by equations (17.5.22), and $f_1(u_F, \theta_F, \varphi_F) = 0$ is the equation of meshing of Σ_F and Σ_1 , represented by equation (17.5.16). Let us differentiate the equations of meshing, considering that τ_P and τ_F are constant. (See eq. (17.8.15) and (17.8.16).) Equations (17.8.17), (17.5.22), and (17.8.15) yield

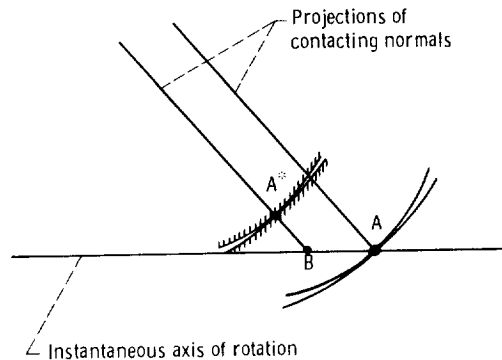


Figure 17.8.1.

$$\begin{aligned}
\frac{du_P}{dt} &= b_P \left[\cos \theta_P \cos \psi_c^{(P)} \tan \Delta_2 - \cos q_P \sin \psi_c^{(P)} \right] \frac{1}{\cos \beta_P} \frac{\partial \varphi_P}{dt} \\
&= \left[L(\sin \Delta_2 \cos \psi_c^{(P)} \sin \beta_P - \cos \Delta_2 \sin \psi_c^{(P)}) \right. \\
&\quad \left. + r_c^{(P)} (\sin \psi_c^{(P)} \sin \beta_P - \cos \psi_c^{(P)} \tan \Delta_2) \right] \frac{1}{\cos \beta_P} \frac{d\varphi_P}{dt} \tag{17.8.21}
\end{aligned}$$

The derivative $d\varphi_P/dt$ may be represented as follows:

$$\frac{\omega^{(P)}}{\omega^{(2)}} = m_{P2} = \frac{\sin \gamma_2}{\cos \Delta_2} \quad \frac{\omega^{(2)}}{\omega^{(1)}} = m_{21} = \frac{\sin \gamma_1}{\sin \gamma_2}$$

Thus

$$\omega^{(P)} = \frac{d\varphi_P}{dt} = m_{P2} m_{21} \omega^{(1)} = \frac{\sin \gamma_2}{\cos \Delta_2} \quad (\text{for } \omega^{(1)} = 1 \text{ rad/sec}) \tag{17.8.22}$$

The final expression for du_P/dt is

$$\begin{aligned}
\frac{du_P}{dt} &= \left[L(\cos \psi_c^{(P)} \sin \beta_P \sin \Delta_2 - \sin \psi_c^{(P)} \cos \Delta_2) \right. \\
&\quad \left. + r_c^{(P)} (\sin \psi_c^{(P)} \sin \beta_P - \cos \psi_c^{(P)} \tan \Delta_2) \right] \frac{\sin \gamma_1}{\cos \beta_P \cos \Delta_2} \tag{17.8.23}
\end{aligned}$$

Equations (17.8.18), (17.5.16), and (17.8.16) yield

$$\frac{\Delta E_1}{L} = - \frac{u_F \sin \psi_c^{(F)} \sin \tau_F}{L} + \frac{K_1 K_2 - K_3}{K_4} + \frac{\sin \tau_F \cos (\gamma_1 - \Delta_1) m_{1F}}{K_4 L} \frac{du_F}{dt} \tag{17.8.24}$$

Here

$$K_1 = - \left[\sin (\gamma_1 - \Delta_1) - m_{F1} \right] \cos \psi_c^{(F)} \cos \tau_F + \sin \psi_c^{(F)} \cos (\gamma_1 - \Delta_1) \tag{17.8.25}$$

$$K_2 = \cos \gamma_1 \cos (\gamma_1 - \Delta_1) + \cos \delta \sin \gamma_1 \sin (\gamma_1 - \Delta_1) \tag{17.8.26}$$

$$K_3 = \sin \delta \sin \gamma_1 \sin \tau_F \cos \psi_c^{(F)} \left[m_{F1} - \sin (\gamma_1 - \Delta_1) \right] \tag{17.8.27}$$

$$K_4 = \frac{- \cos \psi_c^{(F)} \left[\sin (\gamma_1 - \Delta_1) - m_{F1} \right] + \cos \tau_F \sin \psi_c^{(F)} \cos (\gamma_1 - \Delta_1)}{\sin \tau_F} \tag{17.8.28}$$

We may determine $\Delta E_1/L$ by expressing du_F/dt in terms of du_P/dt . The relation between du_F/dt and du_P/dt may be determined by using equation (17.8.19). We obtain vector $\mathbf{v}_{rm}^{(F)}$ by differentiating equations (17.5.3). Then we get

$$\mathbf{v}_{rm}^{(F)} \cdot \mathbf{i}_m^{(1)} = - \cos \psi_c^{(F)} \frac{du_F}{dt} \tag{17.8.29}$$

Vector $\mathbf{v}_m^{(F1)}$ was represented by equations (17.5.14), and for $\Omega^{(1)} \equiv \omega^{(1)} \equiv 1$ rad/sec it yields

$$\mathbf{v}_m^{(F1)} \cdot \mathbf{i}_m^{(1)} = - \left(y_m^{(1)} + \Delta E_1 \right) \cos (\gamma_1 - \Delta_1) \quad (17.8.30)$$

We may express $y_m^{(1)}$ in terms of the coordinates of the contacting point of surfaces Σ_p and Σ_f by using the following coordinate transformation:

$$\begin{bmatrix} x_m^{(1)} \\ y_m^{(1)} \\ z_m^{(1)} \\ 1 \end{bmatrix} = \begin{bmatrix} M_{mh}^{(1)} \end{bmatrix} \begin{bmatrix} M_{hf} \end{bmatrix} \begin{bmatrix} 0 \\ 0 \\ L \\ 1 \end{bmatrix} \quad (17.8.31)$$

Here $(0, 0, L, 1)$ are the homogeneous coordinates of the contacting point M (fig. 17.3.2), which are represented in the coordinate system S_f . Matrix $[M_{hf}]$ was represented by equation (17.6.18) and matrix $[M_{mh}^{(1)}]$ is as follows (fig. 17.3.3):

$$\begin{bmatrix} M_{mh}^{(1)} \end{bmatrix} = \begin{bmatrix} \cos \Delta_1 & 0 & -\sin \Delta_1 & L \sin \Delta_1 \\ 0 & 1 & 0 & -\Delta E_1 \\ \sin \Delta_1 & 0 & \cos \Delta_1 & -\Delta L_1 \\ 0 & 0 & 0 & 1 \end{bmatrix} \quad (17.8.32)$$

Equations (17.8.30) to (17.8.32) yield

$$\mathbf{v}_m^{(F1)} \cdot \mathbf{i}_m^{(1)} = L \sin \delta \sin \gamma_1 \cos (\gamma_1 - \Delta_1) \quad (17.8.33)$$

To determine vector $\mathbf{v}_r^{(P)}$ and represent it in the coordinate system S_m , we differentiate equations (17.5.17). Then we obtain

$$\begin{bmatrix} \mathbf{v}_r^{(P)} \end{bmatrix} = \begin{bmatrix} -\cos \psi_c^{(P)} \frac{du_p}{dt} \\ \sin \psi_c^{(P)} \sin \tau_P \frac{du_p}{dt} + u_p \sin \psi_c^{(P)} \cos \tau_P \frac{d\theta_P}{dt} \\ \sin \psi_c^{(P)} \cos \tau_P \frac{du_p}{dt} - u_p \sin \psi_c^{(P)} \sin \tau_P \frac{d\theta_P}{dt} \end{bmatrix} \quad (17.8.34)$$

We transform equation (17.8.34) as follows:

$$\frac{d\theta_P}{dt} = -\frac{d\varphi_P}{dt} \quad \frac{d\varphi_P}{dt} = \omega^{(P)} = \omega^{(2)} m_{P2} = m_{21} m_{P2} \omega^{(1)} = \frac{\sin \gamma_1}{\cos \Delta_2} \quad (17.8.35)$$

(for $\omega^{(1)} = 1$ rad/sec)

For the main contacting point we have

$$\tau_P = 90^\circ - \beta_P \quad \text{and} \quad u_P \sin \psi_c^{(P)} = r_c^{(P)} \quad (17.8.36)$$

Equations (17.8.34) to (18.8.36) yield

$$\left[v_r^{(P)} \right] = \begin{bmatrix} -\cos \psi_c^{(P)} \frac{du_P}{dt} \\ \sin \psi_c^{(P)} \cos \beta_P \frac{du_P}{dt} - r_c^{(P)} \sin \beta_P \frac{\sin \gamma_1}{\cos \Delta_2} \\ \sin \psi_c^{(P)} \sin \beta_P \frac{du_P}{dt} + r_c^{(P)} \cos \beta_P \frac{\sin \gamma_1}{\cos \Delta_2} \end{bmatrix} \quad (17.8.37)$$

To represent vector $v_r^{(P)}$ in coordinate system $S_m^{(1)}$, we use the matrix product

$$\left[L_m^{(1)} m^{(2)} \right] = \left[L_m^{(1)h} \right] \left[L_{hf} \right] \left[L_{fm}^{(2)} \right] \quad (17.8.38)$$

Here (fig. 17.3.2)

$$\left[L_{fm}^{(2)} \right] = \begin{bmatrix} \cos \Delta_2 & 0 & -\sin \Delta_2 \\ 0 & 1 & 0 \\ \sin \Delta_2 & 0 & \cos \Delta_2 \end{bmatrix} \quad (17.8.39)$$

Using equations (17.8.19), (17.8.29), (17.8.30), and (17.8.37) to (17.8.39), we obtain the following equation which relates du_F/dt and du_P/dt :

$$\frac{du_F}{dt} = a_{11} \frac{du_P}{dt} + b_1 \quad (17.8.40)$$

Here

$$\begin{aligned} a_{11} = & \left[\cos (\gamma_1 + \Delta_2) + \tan \psi_c^{(P)} \sin \beta_P \sin (\gamma_1 + \Delta_2) \right] \cos \delta \cos (\gamma_1 - \Delta_1) \\ & + \left[\sin (\gamma_1 + \Delta_2) - \tan \psi_c^{(P)} \sin \beta_P \cos (\gamma_1 + \Delta_2) \right] \sin (\gamma_1 - \Delta_1) \\ & + \sin \delta \tan \psi_c^{(P)} \cos \beta_P \cos (\gamma_1 - \Delta_1) \end{aligned} \quad (17.8.41)$$

and

$$\begin{aligned} b_1 = & \left\{ L \sin \delta \sin \gamma_1 \cos (\gamma_1 - \Delta_1) + \frac{r_c^{(P)} \cos \beta_P \sin \gamma_1}{\cos \Delta_2} \right. \\ & \left. \left[\cos \delta \cos (\gamma_1 - \Delta_1) \sin (\gamma_1 + \Delta_2) - \sin (\gamma_1 - \Delta_1) \cos (\gamma_1 + \Delta_2) \right] \right. \\ & \left. - \frac{r_c^{(P)} \sin \delta \sin \beta_P \sin \gamma_1}{\cos \Delta_2} \cos (\gamma_1 - \Delta_1) \right\} \frac{1}{\cos \psi_c^{(P)}} \end{aligned} \quad (17.8.42)$$

Equations (17.8.24) to (17.8.28) and (17.8.40) to (17.8.42) determine the required correction $\Delta E_1/L$.

17.9 Bearing Contact at the Main Contact Point

The bearing contact of surfaces Σ_1 and Σ_2 at the main point of contact A may be represented by the contacting ellipse. The dimensions and orientation of the contacting ellipse depend on the principle curvatures of Σ_1 and Σ_2 and the angle which is formed between the principal directions of these surfaces. (See ch. 13.4.)

Principle Curvatures and Directions of Σ_2

Consider that the principal curvatures of Σ_P are known. The principal curvatures and directions of Σ_2 may be determined by using the following equations (ch. 13.1):

$$\tan 2\sigma^{(P2)} = \frac{2F^{(2)}}{\kappa_1^{(P)} - \kappa_{II}^{(P)} + G^{(2)}} \quad (17.9.1)$$

$$\kappa_1^{(2)} + \kappa_{II}^{(2)} = \kappa_1^{(P)} + \kappa_{II}^{(P)} + S^{(2)} \quad (17.9.2)$$

$$\kappa_1^{(2)} - \kappa_{II}^{(2)} = \frac{\kappa_1^{(P)} - \kappa_{II}^{(P)} + G^{(2)}}{\cos 2\sigma^{(P2)}} \quad (17.9.3)$$

$$F^{(2)} = \frac{a_{31}^{(2)} a_{32}^{(2)}}{b_3^{(2)} + (\mathbf{v}^{(P2)} \cdot \mathbf{i}_1^{(P)}) a_{31}^{(2)} + (\mathbf{v}^{(P2)} \cdot \mathbf{i}_{II}^{(P)}) a_{32}^{(2)}} \quad (17.9.4)$$

$$G^{(2)} = \frac{(a_{31}^{(2)})^2 - (a_{32}^{(2)})^2}{b_3^{(2)} + (\mathbf{v}^{(P2)} \cdot \mathbf{i}_1^{(P)}) a_{31}^{(2)} + (\mathbf{v}^{(P2)} \cdot \mathbf{i}_{II}^{(P)}) a_{32}^{(2)}} \quad (17.9.5)$$

$$S^{(2)} = \frac{(a_{31}^{(2)})^2 + (a_{32}^{(2)})^2}{b_3^{(2)} + (\mathbf{v}^{(P2)} \cdot \mathbf{i}_1^{(P)}) a_{31}^{(2)} + (\mathbf{v}^{(P2)} \cdot \mathbf{i}_{II}^{(P)}) a_{32}^{(2)}} \quad (17.9.6)$$

$$a_{31}^{(2)} = [\mathbf{n}^{(P)} \boldsymbol{\omega}^{(P2)} \mathbf{i}_1^{(P)}] \quad \text{with } \mathbf{v}^{(P2)} = \mathbf{0} \quad (17.9.7)$$

$$a_{32}^{(2)} = [\mathbf{n}^{(P)} \boldsymbol{\omega}^{(P2)} \mathbf{i}_{II}^{(P)}] \quad \text{with } \mathbf{v}^{(P2)} = \mathbf{0} \quad (17.9.8)$$

$$b_3^{(2)} = [\mathbf{n}^{(P)} \boldsymbol{\omega}^{(2)} \mathbf{v}_{ir}^{(P)}] - [\mathbf{n}^{(P)} \boldsymbol{\omega}^{(P)} \mathbf{v}_{ir}^{(2)}] \quad (17.9.9)$$

Here (fig. 17.9.1) $\mathbf{i}_1^{(P)}$ and $\mathbf{i}_{II}^{(P)}$ are the unit vectors of the principal directions of Σ_P ; $\mathbf{i}_1^{(2)}$ and $\mathbf{i}_{II}^{(2)}$ are the unit vectors of the principal directions of Σ_2 . Angle $\sigma^{(P2)}$ is formed between the unit vectors $\mathbf{i}_1^{(P)}$ and $\mathbf{i}_1^{(2)}$, and is measured counter-clockwise from $\mathbf{i}_1^{(P)}$ to $\mathbf{i}_1^{(2)}$ (fig. 17.9.1). The principal curvatures of Σ_P and Σ_2 are $\kappa_1^{(2)}$ and $\kappa_{II}^{(2)}$, respectively. Vector $\mathbf{n}^{(P)}$ is the unit normal to surface Σ_P ; $\boldsymbol{\omega}^{(P2)} = \boldsymbol{\omega}^{(P)} - \boldsymbol{\omega}^{(2)}$, where $\boldsymbol{\omega}^{(P)}$ and $\boldsymbol{\omega}^{(2)}$ are the angular velocities of the generating gear P and generated gear 2, respectively.

Vectors $\mathbf{v}_{ir}^{(P)}$ and $\mathbf{v}_{ir}^{(2)}$ represent the transfer velocities of the contact point M in the rotational motion with Σ_P and Σ_2 , respectively (fig. 17.3.2). These vectors are determined as follows:

$$\mathbf{v}_{ir}^{(P)} = \boldsymbol{\omega}^{(P)} \times \mathbf{r}^{(M)} \quad (17.9.10)$$

$$\mathbf{v}_{ir}^{(2)} = \boldsymbol{\omega}^{(2)} \times \mathbf{r}^{(M)} \quad (17.9.11)$$

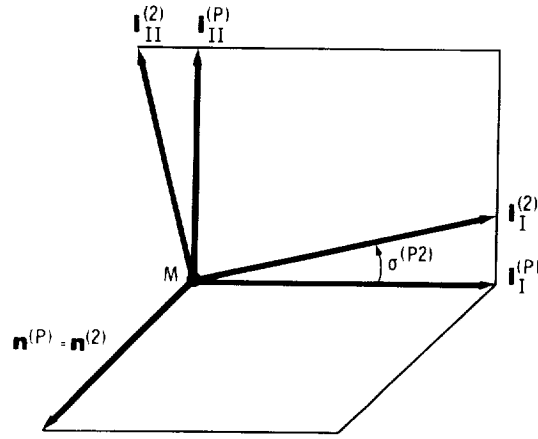


Figure 17.9.1.

$\mathbf{v}_{ir}^{(P)} = \mathbf{v}_{ir}^{(2)}$ because the contact point lies on the instantaneous axis of rotation, z_f (fig. 17.3.2).

The generating surface Σ_P is a cone surface and its principal directions are directed along and perpendicular to the cone generatrix. The unit vectors $\mathbf{i}_{II}^{(P)}$ and $\mathbf{i}_I^{(P)}$ are represented in $S_m^{(2)}$ as follows (see equations (17.5.17)):

$$\mathbf{i}_I^{(P)} = \frac{\frac{\partial \mathbf{r}_m^{(2)}}{\partial \theta_P}}{\left| \frac{\partial \mathbf{r}_m^{(2)}}{\partial \theta_P} \right|} = \begin{bmatrix} 0 \\ \cos \tau_P \\ -\sin \tau_P \end{bmatrix} = \begin{bmatrix} 0 \\ \sin \beta_P \\ -\cos \beta_P \end{bmatrix} \quad (17.9.12)$$

$$\mathbf{i}_{II}^{(P)} = \frac{\frac{\partial \mathbf{r}_m^{(2)}}{\partial u_P}}{\left| \frac{\partial \mathbf{r}_m^{(2)}}{\partial u_P} \right|} = \begin{bmatrix} -\cos \psi_c^{(P)} \\ \sin \psi_c^{(P)} \sin \tau_P \\ \sin \psi_c^{(P)} \cos \tau_P \end{bmatrix} = \begin{bmatrix} -\cos \psi_c^{(P)} \\ \sin \psi_c^{(P)} \cos \beta_P \\ \sin \psi_c^{(P)} \sin \beta_P \end{bmatrix} \quad (17.9.13)$$

Here $\tau_P = 90^\circ - \beta_P$.

The principal curvatures of the cone surface are

$$\kappa_I^{(P)} = -\frac{1}{u_P \tan \psi_c^{(P)}} = -\frac{\cos \psi_c^{(P)}}{r_c^{(P)}} \quad (17.9.14)$$

$$\kappa_{II}^{(P)} = 0 \quad (17.9.15)$$

The unit normal vector $\mathbf{n}^{(P)}$ is given by (eq. (17.5.18))

$$[n^{(P)}] = \begin{bmatrix} \sin \psi_c^{(P)} \\ \cos \psi_c^{(P)} \cos \beta_P \\ \cos \psi_c^{(P)} \sin \beta_P \end{bmatrix} \quad (17.9.16)$$

We represent vectors $\mathbf{r}^{(M)}$, $\boldsymbol{\omega}^{(P)}$, and $\boldsymbol{\omega}^{(2)}$ in the coordinate system $S_m^{(2)}$ as follows (fig. 17.3.2):

$$[r^{(M)}] = \begin{bmatrix} 0 \\ 0 \\ L \cos \Delta_2 \\ 1 \end{bmatrix} \quad (17.9.17)$$

$$[\omega^{(P)}] = \begin{bmatrix} -\omega^{(P)} \\ 0 \\ 0 \end{bmatrix} \quad [\omega^{(2)}] = \omega^{(2)} \begin{bmatrix} -\sin(\gamma_2 - \Delta_2) \\ 0 \\ \cos(\gamma_2 - \Delta_2) \end{bmatrix}$$

$$\omega^{(2)} = \frac{\cos \Delta_2}{\sin \gamma_2} \omega^{(P)}$$

$$[\omega^{(P2)}] = [\omega^{(P)}] - [\omega^{(2)}] = -\frac{\cos(\gamma_2 - \Delta_2)}{\sin \gamma_2} \omega^{(P)} \begin{bmatrix} \sin \Delta_2 \\ 0 \\ \cos \Delta_2 \end{bmatrix} \quad (17.9.18)$$

Using equations (17.9.7) to (17.9.11) and (17.9.16) to (17.9.18), we obtain

$$a_{31} = \frac{\omega^{(P)} \cos(\gamma_2 - \Delta_2)}{\sin \gamma_2} \left(\sin \psi_c^{(P)} \sin \beta_P \cos \Delta_2 - \cos \psi_c^{(P)} \sin \Delta_2 \right) \quad (17.9.19)$$

$$a_{32} = \frac{\omega^{(P)} \cos(\gamma_2 - \Delta_2) \cos \beta_P \cos \Delta_2}{\sin \gamma_2} \quad (17.9.20)$$

$$b_3 = \frac{(\omega^{(P)})^2 L \cos \Delta_2 \cos(\gamma_2 - \Delta_2)}{\sin \gamma_2} \left[\cos \psi_c^{(P)} \sin \beta_P \sin \Delta_2 - \sin \psi_c^{(P)} \cos \Delta_2 \right] \quad (17.9.21)$$

Equations (17.9.1) to (17.9.6) and (17.9.19) to (17.9.21), with $\mathbf{v}^{(P2)} = 0$, determine the principal curvatures $\kappa_1^{(2)}$ and $\kappa_2^{(2)}$ for Σ_2 and the angle $\sigma^{(P2)}$.

Let the principal directions of Σ_2 be represented in the coordinate system S_f . Consider two trihedrons $S_a(\mathbf{i}_1^{(P)}, \mathbf{i}_2^{(P)}, \mathbf{n}_P)$ and $S_b(\mathbf{i}_1^{(2)}, \mathbf{i}_2^{(2)}, \mathbf{n}^{(2)})$ (fig. 17.9.1) which are located in the tangent plane (it is tangent to surfaces Σ_P and Σ_2 at point M). Transformation of vector components in transition from S_b to S_f is represented by the matrix equation

$$[L_{fb}] = [L_{fm}^{(2)}] [L_{ma}^{(2)}] [L_{ab}] \quad (17.9.22)$$

Here

$$[L_{ab}] = \begin{bmatrix} \cos \sigma^{(P2)} & -\sin \sigma^{(P2)} & 0 \\ \sin \sigma^{(P2)} & \cos \sigma^{(P2)} & 0 \\ 0 & 0 & 1 \end{bmatrix} \quad (17.9.23)$$

$$\begin{bmatrix} L_m^{(2)} a \end{bmatrix} = \begin{bmatrix} 0 & -\cos \psi_c^{(P)} & \sin \psi_c^{(P)} \\ \sin \beta_P & \sin \psi_c^{(P)} \cos \beta_P & \cos \psi_c^{(P)} \cos \beta_P \\ -\cos \beta_P & \sin \psi_c^{(P)} \sin \beta_P & \cos \psi_c^{(P)} \sin \beta_P \end{bmatrix} \quad (17.9.24)$$

$$\begin{bmatrix} L_{fm}^{(2)} \end{bmatrix} = \begin{bmatrix} \cos \Delta_2 & 0 & -\sin \Delta_2 \\ 0 & 1 & 0 \\ \sin \Delta_2 & 0 & \cos \Delta_2 \end{bmatrix} \quad (17.9.25)$$

Matrices (17.9.23) and (17.9.25) are based on figure 17.9.1 and figure 17.3.2, respectively. The derivation of matrix (17.9.24) is based on equations (17.9.12), (17.9.13), and (17.9.16). Elements of this matrix represent the direction cosines of angles formed by the unit vectors $\mathbf{i}_1^{(P)}$, $\mathbf{i}_n^{(P)}$, and $\mathbf{n}^{(P)}$ with the unit vectors of the coordinate axes of $S_m^{(2)}$.

We may now represent the unit vectors $\mathbf{i}_1^{(2)}$ and $\mathbf{i}_n^{(2)}$ in the coordinate system S_f as follows:

$$\begin{bmatrix} i_1^{(2)} \end{bmatrix} = [L_{fb}] \begin{bmatrix} 1 \\ 0 \\ 0 \end{bmatrix} =$$

$$\begin{bmatrix} -\cos \psi_c^{(P)} \sin \sigma^{(P2)} \cos \Delta_2 + (\cos \beta_P \cos \sigma^{(P2)} - \sin \psi_c^{(P)} \sin \beta_P \sin \sigma^{(P2)}) \sin \Delta_2 \\ \sin \beta_P \cos \sigma^{(P2)} + \sin \psi_c^{(P)} \cos \beta_P \sin \sigma^{(P2)} \\ -\cos \psi_c^{(P)} \sin \sigma^{(P2)} \sin \Delta_2 - (\cos \beta_P \cos \sigma^{(P2)} - \sin \psi_c^{(P)} \sin \beta_P \sin \sigma^{(P2)}) \cos \Delta_2 \end{bmatrix} \quad (17.9.26)$$

$$\begin{bmatrix} i_n^{(2)} \end{bmatrix} = [L_{fb}] \begin{bmatrix} 0 \\ 1 \\ 0 \end{bmatrix} =$$

$$\begin{bmatrix} -\cos \psi_c^{(P)} \cos \sigma^{(P2)} \cos \Delta_2 - (\cos \beta_P \sin \sigma^{(P2)} + \sin \psi_c^{(P)} \sin \beta_P \cos \sigma^{(P2)}) \sin \Delta_2 \\ -\sin \beta_P \sin \sigma^{(P2)} + \sin \psi_c^{(P)} \cos \beta_P \cos \sigma^{(P2)} \\ -\cos \psi_c^{(P)} \cos \sigma^{(P2)} \sin \Delta_2 + (\cos \beta_P \sin \sigma^{(P2)} + \sin \psi_c^{(P)} \sin \beta_P \cos \sigma^{(P2)}) \cos \Delta_2 \end{bmatrix} \quad (17.9.27)$$

Principal Curvatures and Directions of Σ_1

Consider that the principal curvatures and directions of the generating surface Σ_F are known.

We may determine the principal curvatures and the directions of Σ_1 by using equations similar to equations (17.9.1) to (17.9.27)

$$\tan 2\sigma^{(F1)} = \frac{2F^{(1)}}{\kappa_1^{(F)} - \kappa_{II}^{(F)} + G^{(1)}} \quad (17.9.28)$$

$$\kappa_1^{(1)} + \kappa_{II}^{(1)} = \kappa_1^{(F)} + \kappa_{II}^{(F)} + S^{(1)} \quad (17.9.29)$$

$$\kappa_1^{(1)} - \kappa_{II}^{(1)} = \frac{\kappa_1^{(F)} - \kappa_{II}^{(F)} + G^{(1)}}{\cos 2\sigma^{(F1)}} \quad (17.9.30)$$

$$F^{(1)} = \frac{a_{31}^{(1)}a_{32}^{(1)}}{b_3^{(1)} + (\mathbf{v}^{(F1)} \cdot \mathbf{i}_1^{(F)})a_{31}^{(1)} + (\mathbf{v}^{(F1)} \cdot \mathbf{i}_{II}^{(F)})a_{32}^{(1)}} \quad (17.9.31)$$

$$G^{(1)} = \frac{(a_{31}^{(1)})^2 - (a_{32}^{(1)})^2}{b_3^{(1)} + (\mathbf{v}^{(F1)} \cdot \mathbf{i}_1^{(F)})a_{31}^{(1)} + (\mathbf{v}^{(F1)} \cdot \mathbf{i}_{II}^{(F)})a_{32}^{(1)}} \quad (17.9.32)$$

$$S^{(1)} = \frac{(a_{31}^{(1)})^2 + (a_{32}^{(1)})^2}{b_3^{(1)} + (\mathbf{v}^{(F1)} \cdot \mathbf{i}_1^{(F)})a_{31}^{(1)} + (\mathbf{v}^{(F1)} \cdot \mathbf{i}_{II}^{(F)})a_{32}^{(1)}} \quad (17.9.33)$$

$$a_{31}^{(1)} = [\mathbf{n}^{(F)} \boldsymbol{\omega}^{(F1)} \mathbf{i}_1^{(F)}] - \kappa_1^{(F)} (\mathbf{v}^{(F1)} \cdot \mathbf{i}_1^{(F)}) \quad (17.9.34)$$

$$a_{32}^{(1)} = [\mathbf{n}^{(F)} \boldsymbol{\omega}^{(F1)} \mathbf{i}_{II}^{(F)}] - \kappa_{II}^{(F)} (\mathbf{v}^{(F1)} \cdot \mathbf{i}_{II}^{(F)}) \quad (17.9.35)$$

$$b_3^{(1)} = [\mathbf{n}^{(F)} \boldsymbol{\omega}^{(1)} \mathbf{v}_{rr}^{(F)}] - [\mathbf{n}^{(F)} \boldsymbol{\omega}^{(F)} \mathbf{v}_{rr}^{(1)}] \quad (17.9.36)$$

Here $\mathbf{i}_1^{(F)}$ and $\mathbf{i}_{II}^{(F)}$ are the unit vectors, which are directed along the principal directions of the generating surface Σ_F ; $\kappa_1^{(F)}$ and $\kappa_{II}^{(F)}$ are the principal curvatures of Σ_F ; $\mathbf{i}_1^{(1)}$ and $\mathbf{i}_{II}^{(1)}$ are the unit vectors of the principal directions of Σ_1 ; $\sigma^{(F1)}$ is the angle between the unit vectors $\mathbf{i}_1^{(F)}$ and $\mathbf{i}_1^{(1)}$ measured counter-clockwise from $\mathbf{i}_1^{(F)}$ to $\mathbf{i}_1^{(1)}$.

The generating surface Σ_F is a cone surface and its principal directions are directed along and perpendicular to the cone generatrix. We may represent $\mathbf{i}_1^{(F)}$ and $\mathbf{i}_{II}^{(F)}$ as follows:

$$\mathbf{i}_1^{(F)} = \frac{\partial \mathbf{r}_m^{(1)}}{\partial \theta_F} \div \left| \frac{\partial \mathbf{r}_m^{(1)}}{\partial \theta_F} \right| = \begin{bmatrix} 0 \\ \cos \tau_F \\ -\sin \tau_F \end{bmatrix} \quad (\text{provided } u_F \sin \psi_c^{(F)} \neq 0) \quad (17.9.37)$$

$$\mathbf{i}_{II}^{(F)} = \frac{\partial \mathbf{r}_m^{(1)}}{\partial u_F} \div \left| \frac{\partial \mathbf{r}_m^{(1)}}{\partial u_F} \right| = \begin{bmatrix} -\cos \psi_c^{(F)} \\ \sin \psi_c^{(F)} \sin \tau_F \\ \sin \psi_c^{(F)} \cos \tau_F \end{bmatrix} \quad (17.9.38)$$

Here $\psi_c^{(F)} = \psi_c^{(P)}$ and τ_F is determined by equation (17.7.1).

The principal curvatures of the generating surface Σ_F are represented by the following equations:

$$\kappa_1^{(F)} = -\frac{\cos \psi_c^{(F)}}{r_c^{(F)}} \quad (17.9.39)$$

$$\kappa_{11}^{(F)} = 0 \quad (17.9.40)$$

We may represent vectors $\mathbf{v}_{ir}^{(F)}$, $\mathbf{v}_{ir}^{(1)}$, and $\mathbf{v}^{(F)}$ in the coordinate system $S_m^{(1)}$ by using equations (17.5.10), (17.5.13), and (17.5.14), respectively. The coordinates $x_m^{(1)}$, $y_m^{(1)}$, and $z_m^{(1)}$ of the contact point A may be obtained by using equation (17.8.31). Assuming that $\Omega^{(1)} = 1$ rad/sec, we obtain

$$[v^{(F)}] = m_{F1}L \begin{bmatrix} 0 \\ \cos \delta \sin \gamma_1 \sin (\gamma_1 - \Delta_1) + \cos \gamma_1 \cos (\gamma_1 - \Delta_1) - \frac{\Delta L_1}{L} \\ \sin \delta \sin \gamma_1 + \frac{\Delta E_1}{L} \end{bmatrix} \quad (17.9.41)$$

$$[v^{(1)}] = -L \begin{bmatrix} \sin \delta \sin \gamma_1 \cos (\gamma_1 - \Delta_1) \\ -\cos \delta \sin \gamma_1 \\ -\sin \delta \sin \gamma_1 \sin (\gamma_1 - \Delta_1) \end{bmatrix} \quad (17.9.42)$$

$$[v^{(F)}] = [v^{(F)}] - [v^{(1)}] =$$

$$L \begin{bmatrix} \sin \delta \sin \gamma_1 \cos (\gamma_1 - \Delta_1) \\ m_{F1} \left[\cos \delta \sin \gamma_1 \sin (\gamma_1 - \Delta_1) + \cos \gamma_1 \cos (\gamma_1 - \Delta_1) - \frac{\Delta L_1}{L} \right] - \cos \delta \sin \gamma_1 \\ m_{F1} \left[\sin \delta \sin \gamma_1 + \frac{\Delta E_1}{\Delta L} \right] - \sin \delta \sin \gamma_1 (\gamma_1 - \Delta_1) \end{bmatrix} \quad (17.9.43)$$

Using equations (17.9.28) to (17.9.43) and (17.5.6), we may determine the principal curvatures $\kappa_1^{(1)}$ and $\kappa_{11}^{(1)}$ for Σ_1 and the angle $\sigma^{(F)}$.

Let us represent the principal directions of Σ_1 in the coordinate system S_f . Consider two trihedrons $S_d(\mathbf{i}_1^{(F)}, \mathbf{i}_{11}^{(F)}, \mathbf{n}^{(F)})$ and $S_e(\mathbf{i}_1^{(1)}, \mathbf{i}_{11}^{(1)}, \mathbf{n}^{(1)})$ which are located in the tangent plane. The origin A of these two trihedrons coincides with the point of contact, A , of surfaces Σ_F and Σ_1 . The transformation of vector components in the transition from the coordinate system S_e to S_h is represented by the following matrix equation:

$$[L_{he}] = [L_{hm}^{(1)}] [L_{md}^{(1)}] [L_{de}] \quad (17.9.44)$$

Here

$$[L_{de}] = \begin{bmatrix} \cos \sigma^{(F1)} & -\sin \sigma^{(F1)} & 0 \\ \sin \sigma^{(F1)} & \cos \sigma^{(F1)} & 0 \\ 0 & 0 & 1 \end{bmatrix} \quad (17.9.45)$$

$$\begin{bmatrix} L_{md}^{(1)} \end{bmatrix} = \begin{bmatrix} 0 & -\cos \psi_c^{(F)} & \sin \psi_c^{(F)} \\ \cos \tau_F & \sin \psi_c^{(F)} \sin \tau_F & \cos \psi_c^{(F)} \sin \tau_F \\ -\sin \tau_F & \sin \psi_c^{(F)} \cos \tau_F & \cos \psi_c^{(F)} \cos \tau_F \end{bmatrix} \quad (17.9.46)$$

$$\begin{bmatrix} L_{hm}^{(1)} \end{bmatrix} = \begin{bmatrix} \cos \Delta_1 & 0 & \sin \Delta_1 \\ 0 & 1 & 0 \\ -\sin \Delta_1 & 0 & \cos \Delta_1 \end{bmatrix} \quad (17.9.47)$$

Matrix equations (17.9.45) and (17.9.47) are based on figures 17.9.2 and 17.3.3, respectively. Elements of matrix (17.9.46) represent the direction cosines of angles which are formed by the unit vectors $\mathbf{i}_1^{(F)}$, $\mathbf{i}_{11}^{(F)}$, and $\mathbf{n}^{(F)}$ with the unit vectors of coordinate axes of the coordinate system $S_m^{(1)}$. (See eqs. (17.9.37), (17.9.38), and (17.5.6).)

The final transformation of vector components in transition from S_e to S_f is based on the following matrix equation:

$$[L_{fe}] = [L_{fh}] [L_{hm}^{(1)}] [L_{md}^{(1)}] [L_{de}] \quad (17.9.48)$$

Equation (17.6.18) yields

$$[L_{fh}] = \begin{bmatrix} \cos \delta \cos^2 \gamma_1 + \sin^2 \gamma_1 & \sin \delta \cos \gamma_1 & (1 - \cos \delta) \cos \gamma_1 \sin \gamma_1 \\ -\sin \delta \cos \gamma_1 & \cos \delta & \sin \delta \sin \gamma_1 \\ (1 - \cos \delta) \cos \gamma_1 \sin \gamma_1 & -\sin \delta \sin \gamma_1 & \cos \delta \sin^2 \gamma_1 + \cos^2 \gamma_1 \end{bmatrix} \quad (17.9.49)$$

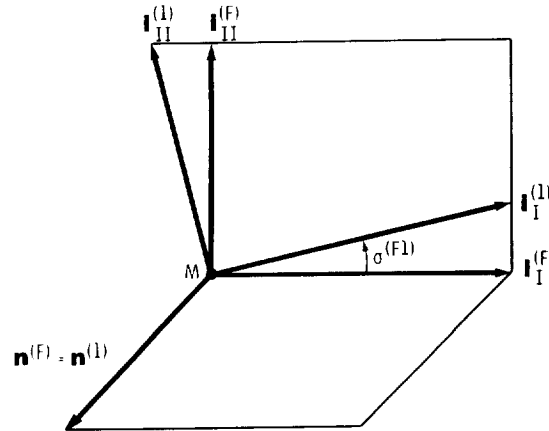


Figure 17.9.2.

We may represent the unit vectors $\mathbf{i}_I^{(1)}$ and $\mathbf{i}_{II}^{(1)}$ in the coordinate system S_f by using the following equations:

$$\begin{bmatrix} i_I^{(1)} \\ i_{II}^{(1)} \end{bmatrix} = [L_{fe}] \begin{bmatrix} 1 \\ 0 \\ 0 \end{bmatrix} \quad (17.9.50)$$

$$\begin{bmatrix} i_I^{(1)} \\ i_{II}^{(1)} \end{bmatrix} = [L_{fe}] \begin{bmatrix} 1 \\ 0 \\ 0 \end{bmatrix} \quad (17.9.51)$$

17.10 Contact Ellipse

Consider that surfaces Σ_2 and Σ_1 are in contact at point A . The principal curvatures $\kappa_I^{(2)}$, $\kappa_{II}^{(2)}$, and $\kappa_I^{(1)}$, $\kappa_{II}^{(1)}$ of both surfaces are known. The unit vectors $\mathbf{i}_I^{(2)}$ and $\mathbf{i}_I^{(1)}$ of the principal directions make an angle $\sigma^{(21)}$, measured counterclockwise from $\mathbf{i}_I^{(2)}$ to $\mathbf{i}_I^{(1)}$ (fig. 17.10.1). The elastic approach of the surfaces is given by δ . The discussion is limited to the case of a left-hand generating gear (fig. 17.3.1). The angle $\sigma^{(21)}$ is determined as follows:

$$\cos \sigma^{(21)} = \mathbf{i}_I^{(2)} \cdot \mathbf{i}_I^{(1)} \quad (17.10.1)$$

$$\sin \sigma^{(21)} = \pm \mathbf{n} \cdot (\mathbf{i}_I^{(2)} \times \mathbf{i}_I^{(1)}) \quad (17.10.2)$$

The upper and lower signs are given for the convex- and concave-gear-tooth side respectively. The axes $2a$ and $2b$ of the contracting ellipse and angle α may be determined as follows:

$$A = \frac{1}{4} \left[\kappa_I^{(1)} - \kappa_I^{(2)} - \left(g_1^2 - 2g_1g_2 \cos 2\sigma^{(21)} + g_2^2 \right)^{1/2} \right] \quad (17.10.3)$$

$$B = \frac{1}{4} \left[\kappa_I^{(1)} - \kappa_I^{(2)} + \left(g_1^2 - 2g_1g_2 \cos 2\sigma^{(21)} + g_2^2 \right)^{1/2} \right] \quad (17.10.4)$$

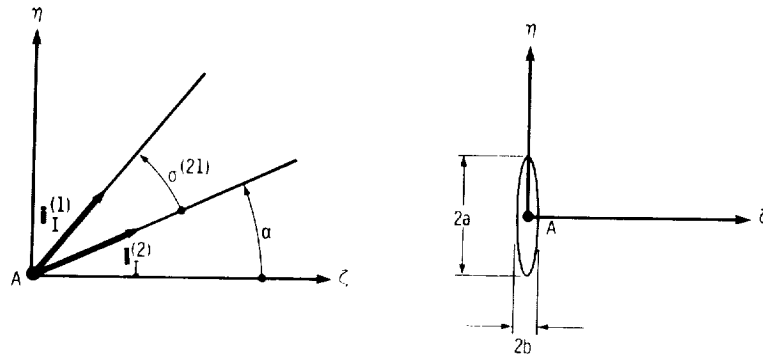


Figure 17.10.1.

$$a = \left(\left| \frac{\delta}{A} \right| \right)^{1/2} \quad b = \left(\left| \frac{\delta}{B} \right| \right)^{1/2} \quad (17.10.5)$$

$$\tan 2\alpha = \frac{g_1 \sin 2\sigma^{(21)}}{g_2 - g_1 \cos \sigma^{(21)}} \quad (17.10.6)$$

(See ch. 13.4.) Here

$$K_\zeta^{(i)} = \kappa_1^{(i)} + \kappa_{11}^{(i)} \quad \text{and} \quad g_i = \kappa_1^{(i)} - \kappa_{11}^{(i)} \quad (i = 1, 2)$$

Angle α is measured counterclockwise from the ζ axis to $\mathbf{i}_1^{(2)}$. The major axis of the ellipse is directed along the η -axis (fig. 17.10.1).

17.11 Tooth-Contact Analysis

The tooth-contact analysis is based on the following equations

$$\mathbf{r}_f^{(1)}(\theta_f, \varphi_f, \varphi_1^1) = \mathbf{r}_f^{(2)}(\theta_P, \varphi_P, \varphi_2^1) \quad (17.11.1)$$

$$\mathbf{n}_f^{(1)}(\theta_F, \varphi_F, \varphi_1^1) = \mathbf{n}_f^{(2)}(\theta_P, \varphi_P, \varphi_2^1) \quad (17.11.2)$$

(See ch. 11.1.)

These equations represent the tangency of surfaces Σ_1 and Σ_2 in the fixed coordinate system S_f , which is rigidly connected to the frame (fig. 17.3.2); φ_1^1 and φ_2^1 represent the angles of rotation of the gears; $\mathbf{r}_f^{(1)}$ and $\mathbf{r}_f^{(2)}$, $\mathbf{n}_f^{(1)}$ and $\mathbf{n}_f^{(2)}$ with fixed values of φ_1^1 and φ_2^1 represent the position vectors and the surface unit normals of Σ_1 and Σ_2 , respectively.

Derivation of $\mathbf{r}_f^{(1)}$ and $\mathbf{n}_f^{(1)}$

Equations (17.5.3) and (17.5.16) represent the family of lines of contact between surfaces Σ_F and Σ_1 . Using these equations, we may eliminate u_F and represent the family of contacting lines by the equation

$$\mathbf{r}_m^{(1)} = \mathbf{r}_m^{(1)}(\theta_F, \varphi_F) \quad (17.11.3)$$

Surface Σ_1 may be determined with the family of contacting lines represented in the coordinate system S_1 rigidly connected to gear 1. The coordinate transformation from $S_m^{(1)}$ to S_1 is based on the following matrix equation:

$$[M_{lm}^{(1)}] = [M_{lr}][M_{rh}][M_{hm}^{(1)}] \quad (17.11.4)$$

Here (fig. 17.11.1)

$$[M_{hm}^{(1)}] = \begin{bmatrix} \cos \Delta_1 & 0 & \sin \Delta_1 & -L \sin \Delta_1 \cos \Delta_1 + \Delta L_1 \sin \Delta_1 \\ 0 & 1 & 0 & \Delta E_1 \\ -\sin \Delta_1 & 0 & \cos \Delta_1 & L \sin^2 \Delta_1 + \Delta L_1 \cos \Delta_1 \\ 0 & 0 & 0 & 1 \end{bmatrix} \quad (17.11.5)$$

Matrix $[M_{hm}^{(1)}]$ is the inverse for matrix $[M_{mh}^{(1)}]$ represented by equation (17.8.32)

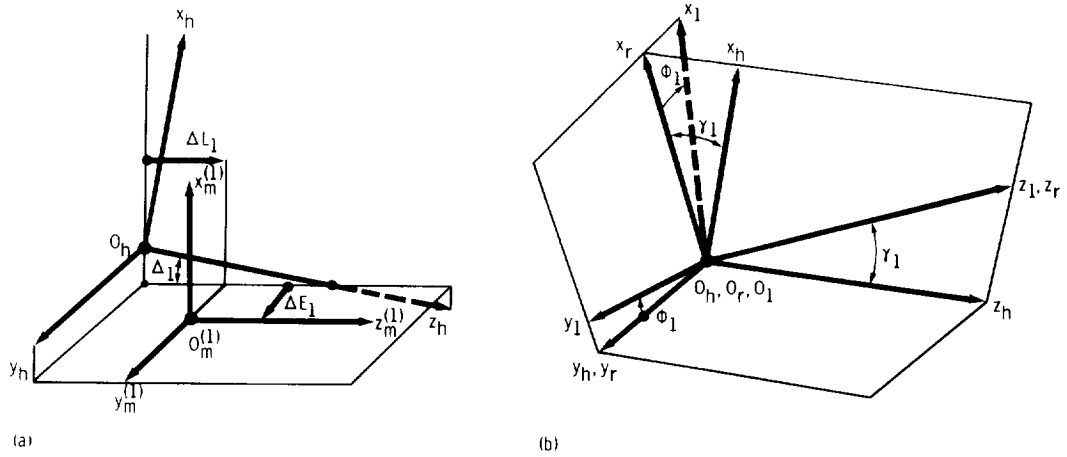


Figure 17.11.1.

$$[M_{rh}] = \begin{bmatrix} \cos \gamma_1 & 0 & -\sin \gamma_1 & 0 \\ 0 & 1 & 0 & 0 \\ \sin \gamma_1 & 0 & \cos \gamma_1 & 0 \\ 0 & 0 & 0 & 1 \end{bmatrix} \quad (17.11.6)$$

$$[M_{lr}] = \begin{bmatrix} \cos \varphi_1 & -\sin \varphi_1 & 0 & 0 \\ \sin \varphi_1 & \cos \varphi_1 & 0 & 0 \\ 0 & 0 & 1 & 0 \\ 0 & 0 & 0 & 1 \end{bmatrix} \quad (17.11.7)$$

Then surface Σ_1 will be represented as follows:

$$[r_1] = [M_{lm}^{(1)}][r_m^{(1)}] \quad (17.11.8)$$

We determine $r_f^{(1)}$ by using the following matrix equation:

$$[r_f^{(1)}] = [M_{fh}][M_{hr}][M_{rl}][r_1] \quad (17.11.9)$$

Here

$$[M_{rl}] = \begin{bmatrix} \cos \varphi'_1 & \sin \varphi'_1 & 0 & 0 \\ -\sin \varphi'_1 & \cos \varphi'_1 & 0 & 0 \\ 0 & 0 & 1 & 0 \\ 0 & 0 & 0 & 1 \end{bmatrix} \quad (17.11.10)$$

where φ'_1 is the angle of rotation of gear 1, which is in mesh with gear 2. We must differentiate between φ_1 and φ'_1 : φ_1 is the angle of rotation of gear 1 which is in mesh with the generating gear provided with the surface Σ_f .

Matrix $[M_{hr}]$ is the inverse matrix of $[M_{rh}]$ which is represented by equation (17.11.6). Matrix $[M_{fh}]$ is the inverse matrix of $[M_{hf}]$ which is represented by equation (17.6.18).

The final expression for $[r_f^{(1)}]$ is as follows:

$$[r_f^{(1)}] = [M_{fh}][M_{hr}][M_{rl}][M_{lr}][M_{rh}][M_{hm}^{(1)}][r_m^{(1)}] \quad (17.11.11)$$

It is important to note that the product of matrices $[M_{rl}][M_{lr}]$ does not yield a unitary matrix since the elements of these matrices depend on different parameters, φ_1' and φ_1 , respectively. However, elements of the matrix $[M_{rr}] = [M_{rl}][M_{lr}]$ may be expressed in terms of $(\varphi_1 - \varphi_1')$.

Similarly, we may derive $[n_f^{(1)}]$ by using the matrix equation

$$[n_f^{(1)}] = [L_{fh}][L_{hr}][L_{rl}][L_{lr}][L_{rh}][L_{hm}^{(1)}][n_m^{(1)}] \quad (17.11.12)$$

where $[n_m^{(1)}]$ is represented by equation (17.5.6).

Derivation of $r_f^{(2)}$ and $n_f^{(2)}$

Equations (17.5.17) and (17.5.22) represent in the coordinate system $S_m^{(2)}$ the family of lines of contact between surfaces Σ_p and Σ_2 . Eliminating u_p , we may represent the family of contacting lines as follows:

$$r_m^{(2)} = r_m^{(2)}(\theta_p, \varphi_p) \quad (17.11.13)$$

Surface Σ_2 is determined by the family of contacting lines represented in the coordinate system S_2 . The coordinate transformation is based on the following matrix equation:

$$[r_2] = [M_{2l}][M_{lf}][M_{fm}^{(2)}][r_m^{(2)}] \quad (17.11.14)$$

Matrix $[M_{fm}^{(2)}]$ is represented as follows (fig. 17.3.2)

$$[M_{fm}^{(2)}] = \begin{bmatrix} \cos \Delta_2 & 0 & -\sin \Delta_2 & L \sin \Delta_2 \cos \Delta_2 \\ 0 & 1 & 0 & 0 \\ \sin \Delta_2 & 0 & \cos \Delta_2 & L \sin^2 \Delta_2 \\ 0 & 0 & 0 & 1 \end{bmatrix} \quad (17.11.15)$$

It is evident from the drawings of figure 17.11.2 that

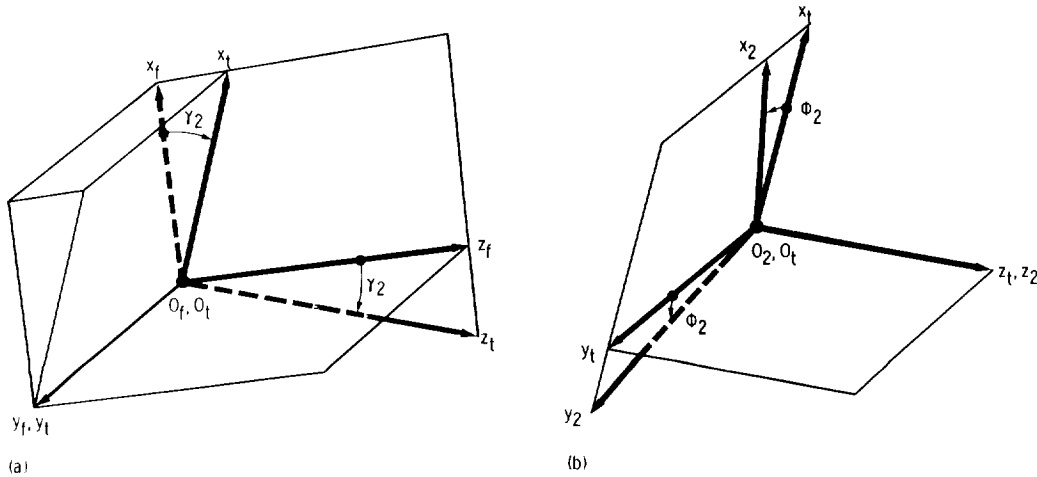


Figure 17.11.2.

$$[M_{if}] = \begin{bmatrix} \cos \gamma_2 & 0 & \sin \gamma_2 & 0 \\ 0 & 1 & 0 & 0 \\ -\sin \gamma_2 & 0 & \cos \gamma_2 & 0 \\ 0 & 0 & 0 & 1 \end{bmatrix} \quad (17.11.16)$$

$$[M_{2i}] = \begin{bmatrix} \cos \varphi_2 & \sin \varphi_2 & 0 & 0 \\ -\sin \varphi_2 & \cos \varphi_2 & 0 & 0 \\ 0 & 0 & 1 & 0 \\ 0 & 0 & 0 & 1 \end{bmatrix} \quad (17.11.17)$$

Equations (17.11.13) to (17.11.17) represent surface Σ_2 in the coordinate system S_2 . A family of surfaces Σ_2 is generated in the coordinate system S_f while gear 2 rotates about the z_2 -axis. Using the matrix equation

$$\begin{bmatrix} r_f^{(2)} \end{bmatrix} = [M_{fi}][M_{i2}][r_2] \quad (17.11.18)$$

we obtain the column matrix $[r_f^{(2)}]$. Equations (17.11.14) and (17.11.18) yield

$$\begin{bmatrix} r_f^{(2)} \end{bmatrix} = [M_{fi}][M_{i2}][M_{2i}][M_{if}][M_{fm}^{(2)}] \begin{bmatrix} r_m^{(2)} \end{bmatrix} \quad (17.11.19)$$

Here $[M_{fi}]$ is the inverse for matrix $[M_{if}]$; elements of matrix $[M_{i2}]$ are expressed in terms of φ_2' where φ_2' is the angle of rotation of gear 2 in mesh with gear 1; but elements of matrix $[M_{2i}]$ are expressed in terms of φ_2 where φ_2 is the angle of rotation of gear 2 in mesh with the generating gear provided with surface Σ_p . Elements of matrix

$$[M_{ii}] = [M_{i2}][M_{2i}] \quad (17.11.20)$$

are expressed in terms of $(\varphi_2 - \varphi_2')$.

Using a similar procedure we may derive $[n_f^{(2)}]$ as follows:

$$\begin{bmatrix} n_f^{(2)} \end{bmatrix} = [L_{fi}][L_{i2}][L_{2i}][L_{if}][L_{fm}^{(2)}] \begin{bmatrix} n_m^{(2)} \end{bmatrix} \quad (17.11.21)$$

where $[n_m^{(2)}]$ is represented by (17.5.18).

Analysis of Contact of Surfaces Σ_1 and Σ_2

Equations (17.11.1) to (17.11.2) yield a system of five independent equations in six unknowns as follows:

$$f_i(\varphi_F, \theta_F, \tau_F, \mu_1, \varphi_P, \theta_P, \tau_P, \mu_2) = 0 \quad (i = 1, 2, 3) \quad (17.11.22)$$

$$f_j(\tau_F, \mu_1, \tau_P, \mu_2) = 0 \quad (j = 4, 5, 6) \quad (17.11.23)$$

Here

$$\begin{aligned} \tau_F &= \theta_F + \varphi_F - q_F & \tau_P &= \theta_P + \varphi_P - q_P & \mu_1 &= \varphi_1 - \varphi_1' \\ \mu_2 &= \varphi_2 - \varphi_2' & \varphi_1 &= \frac{\varphi_F}{m_{F1}} & \varphi_2 &= \frac{\varphi_P}{m_{P2}} \end{aligned} \quad (17.11.24)$$

Vector equation (17.11.1) yields three equations (17.11.22) and vector equation (17.11.2) yield three equations (17.11.23). However, only two equations of (17.11.23) are independent since $|\mathbf{n}_f^{(1)}| = |\mathbf{n}_f^{(2)}| = 1$.

To solve the above system, we adopt the following computational procedure: Fix μ_1 and consider the system of five equations ((17.11.22) to (17.11.12)) in five unknowns (use two of three equations (17.11.23) only). The solution of these equations is based on an iterative process with the following considerations: (1) With the chosen parameter μ_2 , equation system (17.11.23) is a system of two equations in two unknowns, τ_F and τ_P . (2) Then two of the three equations (17.11.22) will represent a system of two equations, θ_F and θ_P , since φ_F and φ_P can be expressed in terms of τ_F , θ_F , and θ_P , respectively. The solution of these two equations will provide θ_F and θ_P . (3) The remaining equation of (17.11.23) is used as a checking equation. (4) The iteration will give the correct solution for all the unknowns with the fixed value of μ_1 if all the unknowns μ_2 , τ_P , τ_F , θ_P , and θ_F satisfy the checking equation. If the checking equation is not satisfied, then we have to try a second iteration. Such an iterative process is a computer method of solution of a system of nonlinear equations which is based on the use of a subroutine. The mentioned subroutine is a part of the computer library.

The solution obtained for the unknowns provides information about (1) the line of action of surfaces Σ_1 and Σ_2 and (2) the kinematical errors of the gear train.

The line of action is the set of points of contact of surfaces Σ_1 and Σ_2 , which is represented in the coordinate system S_f . We may obtain the line of action as a set of points with coordinates $x_f^{(i)}$, $y_f^{(i)}$, and $z_f^{(i)}$, where $i = 1, 2$. The location of each point of contact depends on μ_1 .

To determine the kinematical errors of the gear train, we have to obtain the function $\varphi_2'(\varphi_1')$. The solution of equations (17.11.22) and (17.11.23) provides μ_2 , φ_F , φ_P as numerical functions of μ_1 . Since φ_F and φ_P are known, we may determine φ_1 and φ_2 (eq. (17.11.24)). We may then determine φ_1' and φ_2' by using the following equations:

$$\varphi_1' = \varphi_1 - \mu_1 \quad \varphi_2' = \varphi_2 - \mu_2$$

The kinematical errors may be determined by a function of ϕ_1' as follows:

$$\Delta\varphi_2'(\varphi_1') = \varphi_2' - \varphi_1' \frac{N_1}{N_2}$$

where N_1 and N_2 are the number of gear teeth.

To reduce the kinematical errors we have to use the appropriate values of ΔE_1 for the chosen $|r_c^{(F)} - r_c^{(P)}|$. (It is assumed that the correction of machine tool settings ΔE_1 and ΔL_1 are related by eq. (17.7.19)).

Chapter 18

Kinematic Precision of Gear Trains

18.1 Introduction

Kinematic precision is affected by errors which are the result of either intentional adjustments or accidental defects in the manufacturing and assembly of gear trains. The criteria of kinematic precision of a gear train may be represented by the function

$$\Delta\phi_2(\phi_1, \Delta\mathbf{Q}) \quad (18.1.1)$$

Here ϕ_1 is the angle of rotation of the driving gear 1,

$$\Delta\mathbf{Q} = (\Delta q_1, \Delta q_2, \dots) \quad (18.1.2)$$

is the vector of gear errors, and

$$\Delta\phi_2 = \phi_2^0 - \phi_2 \quad (18.1.3)$$

is the kinematic error of the gear drive, represented as the difference between the theoretical and actual angles of rotation of the driven gear 2. The theoretical function ϕ_2^0 is represented by

$$\phi_2^0 = \phi_1 \frac{N_1}{N_2} \quad (18.1.4)$$

where N_1 and N_2 are the numbers of gear teeth.

Until now, we considered a gear drive consisting of only two gears. Methods for the determination of error functions (18.1.1) is also easy to use for a gear train which is composed of a set of gears. In this case the kinematical error is represented by the function

$$\Delta\phi_n = \phi_n^0 - \phi_n = \phi_1 m_{n1}^0 - \phi_n \quad (18.1.5)$$

where

$$m_{n_1}^0 = m_{n(n-1)}^0 m_{(n-1)(n-2)}^0 \dots m_{21}^0$$

is the angular velocity ratio for an ideal gear train which can be represented by the ratio of the number of teeth of the gears. For instance, the ratio m_{21}^0 is represented by

$$m_{21}^0 = \frac{\omega^{(2)}}{\omega^{(1)}} = \frac{N_1}{N_2} \quad (18.1.6)$$

where $\omega^{(2)}$ and $\omega^{(1)}$ are the angular velocities of the ideal gears 2 and 1. Henceforth, we will differentiate between the ideal gear ratio which is constant and the instantaneous gear ratio which is not constant, if errors of gears exist. Consider gears 2 and 1 which are in mesh. Because of the gear errors, the angles of rotation of the gears are related by a nonlinear function $f(\phi_1)$; that is,

$$\phi_2 = f(\phi_1) \quad (18.1.7)$$

The instantaneous angular velocity ratio is given by

$$m_{21} = \frac{d\phi_2}{d\phi_1} = \frac{\frac{d\phi_2}{dt}}{\frac{d\phi_1}{dt}} = \frac{\omega^{(2)}}{\omega^{(1)}} = f_\phi \quad (18.1.8)$$

where $f_\phi = \frac{d}{d\phi_1} (f(\phi_1))$.

We may also consider the ratio of gear revolutions. This ratio may be represented for both cases, for gears with and without errors, as follows:

$$\frac{n_2}{n_1} = \frac{N_1}{N_2}$$

where n_1 and n_2 are the revolutions of the gears.

The precision of gears was investigated by Litvin (1968), Litvin, Goldrich, Coy and Zaretsky (1983b), Michalec (1966), and other authors.

In this chapter two methods to determine function (18.1.1) worked out by Litvin and his coauthors are presented: (1) a numerical method for computer solution and (2) an appropriate solution which leads to simple results in analytical form.

18.2 Theory and Exact Solution Method for Kinematic Precision

In the process of motion the tooth surfaces of two gears, Σ_1 and Σ_2 (fig. 18.2.1), are in tangency if the following equations are satisfied (see ch. 11):

$$\mathbf{r}_f^{(1)}(u_1, \theta_1, \phi_1) = \mathbf{r}_f^{(2)}(u_2, \theta_2, \phi_2) \quad (18.2.1)$$

$$\mathbf{n}_f^{(1)}(u_1, \theta_1, \phi_1) = \mathbf{n}_f^{(2)}(u_2, \theta_2, \phi_2) \quad (18.2.2)$$

Here $\mathbf{r}_f^{(i)}$ is the position vector of the contact point on gear i ; $\mathbf{n}_f^{(i)}$ is the surface unit normal vector at the contact point M ; u_i , and θ_i are the surface coordinates of the gear surfaces; and ϕ_i is the

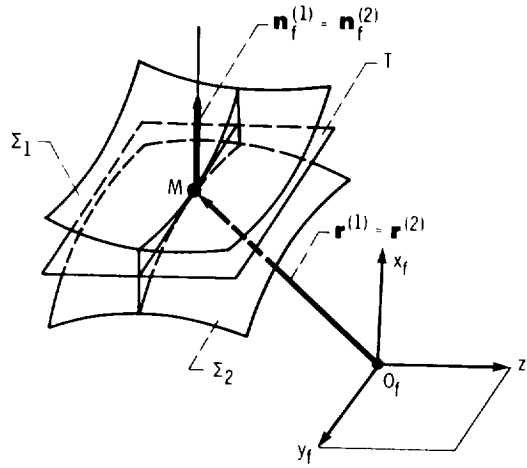


Figure 18.2.1.

angle of rotation of gear i ($i = 1, 2$). Subscript f denotes a coordinate system which is rigidly connected to the frame.

For a gear set with kinematic errors, represented by ΔQ_1 and ΔQ_2 , conditions for tangency may be expressed as

$$\mathbf{r}_f^{(1)}(u_1, \theta_1, \phi_1, \Delta Q_1) = \mathbf{r}_f^{(2)}(u_2, \theta_2, \phi_2, \Delta Q_2) \quad (18.2.3)$$

$$\mathbf{n}_f^{(1)}(u_1, \theta_1, \phi_1, \Delta Q_1) = \mathbf{n}_f^{(2)}(u_2, \theta_2, \phi_2, \Delta Q_2) \quad (18.2.4)$$

Equations (18.2.3) and (18.2.4) yield the functions

$$\phi_2(\phi_1, \Delta Q_1, \Delta Q_2) = \phi_2^0(\phi_1) + \Delta \phi_2(\phi_1, \Delta Q_1, \Delta Q_2) \quad (18.2.5)$$

$$u_i(\phi_1, \Delta Q_1, \Delta Q_2) \quad \theta_i(\phi_1, \Delta Q_1, \Delta Q_2) \quad (i = 1, 2) \quad (18.2.6)$$

The functions

$$\mathbf{r}_f^{(i)}(u_i, \theta_i) \quad u_i(\phi_1, \Delta Q_1, \Delta Q_2) \quad \theta_i(\phi_1, \Delta Q_1, \Delta Q_2) \quad (i = 1, 2) \quad (18.2.7)$$

represent the path of the contact point on gear surface Σ_i corresponding to the meshing of gears with errors of manufacturing and assembly. Functions

$$\mathbf{r}_f^{(i)}(u_i^0(\phi_1), \theta_i^0(\phi_1)) \quad u_i^0(\phi_1), \theta_i^0(\phi_1) \quad (i = 1, 2) \quad (18.2.8)$$

represent the path of the contact point on gear surface Σ_i corresponding to meshing without errors. Comparison of functions (18.2.7) and (18.2.8) yields the change of the contact point path induced by errors.

Consider the solution of equations (18.2.1) to (18.2.2) and (18.2.3) and (18.2.4). Vector equations (18.2.1) to (18.2.2) yield only five independent scalar equations, since $|\mathbf{n}^{(1)}| = |\mathbf{n}^{(2)}| = 1$. These equations may be represented as

$$f_j(u_1, \theta_1, \phi_1, u_2, \theta_2, \phi_2) = 0 \quad (j = 1, 2, \dots, 5) \quad (18.2.9)$$

It is assumed that $\{f_1, f_2, f_3, f_4, f_5\} \in C^1$. Let us mention once again that the symbol C^1 indicates that functions f_j have continuous partial derivatives at least of the first order for all its arguments.

It is assumed that equation system (18.2.9) is satisfied by a set of parameters

$$P^{(1)} = (u_1^{(1)}, \theta_1^{(1)}, \phi_1^{(1)}, u_2^{(1)}, \theta_2^{(1)}, \phi_2^{(1)}) \quad (18.2.10)$$

and that surfaces Σ_1 and Σ_2 are in tangency at point M_0 . Surfaces Σ_1 and Σ_2 will be in point contact in the neighborhood of M_0 if for the set of parameters $P^{(1)}$ the following Jacobian is not equal to zero (see app. B)

$$\frac{D(f_1, f_2, f_3, f_4, f_5)}{D(u_1, \theta_1, u_2, \theta_2, \phi_2)} = \begin{vmatrix} \frac{\partial f_1}{\partial u_1} & \frac{\partial f_1}{\partial \theta_1} & \frac{\partial f_1}{\partial u_2} & \frac{\partial f_1}{\partial \theta_2} & \frac{\partial f_1}{\partial \phi_2} \\ \cdot & \cdot & \cdot & \cdot & \cdot \\ \cdot & \cdot & \cdot & \cdot & \cdot \\ \cdot & \cdot & \cdot & \cdot & \cdot \\ \frac{\partial f_5}{\partial u_1} & \frac{\partial f_5}{\partial \theta_1} & \frac{\partial f_5}{\partial u_2} & \frac{\partial f_5}{\partial \theta_2} & \frac{\partial f_5}{\partial \phi_2} \end{vmatrix} \neq 0 \quad (18.2.11)$$

If inequality (18.2.11) is satisfied, equation system (18.2.9) may be solved in the neighborhood of $P^{(1)}$ with the functions

$$\{u_1(\phi_1), \theta_1(\phi_1), u_2(\phi_1), \theta_2(\phi_1), \phi_2^0(\phi_1)\} \in C^1 \quad (18.2.12)$$

The function $\phi_2^0(\phi_1)$ represents the ideal law of motion. In most cases (for conjugate tooth action) function $\phi_2^0(\phi_1)$ is linear.

Equations (18.2.3) to (18.2.4) also yield a system of five independent equations in six unknowns ($u_1, \theta_1, \phi_1, u_2, \theta_2, \phi_2$)

$$g_j(u_1, \theta_1, \phi_1, u_2, \theta_2, \phi_2, \Delta Q) = 0 \quad (j = 1, 2, \dots, 5) \quad (18.2.13)$$

It is assumed that this system is satisfied by a set of parameters

$$P^{(2)} = (u_1^{(2)}, \theta_1^{(2)}, \phi_1^{(1)}, u_2^{(2)}, \theta_2^{(2)}, \phi_2^{(2)}) \quad (18.2.14)$$

with the same value of $\phi_1^{(1)}$ as in the set $P^{(1)}$. If in the neighborhood of $P^{(2)}$ the Jacobian

$$\frac{D(g_1, g_2, g_3, g_4, g_5)}{D(u_1, \theta_1, u_2, \theta_2, \phi_2)} \neq 0 \quad (18.2.15)$$

then system (18.2.13) may be solved with the functions

$$\{u_1(\phi_1, \Delta Q), \theta_1(\phi_1, \Delta Q), u_2(\phi_1, \Delta Q), \theta_2(\phi_1, \Delta Q), \phi_2(\phi_1, \Delta Q)\} \in C^1 \quad (18.2.16)$$

Function $\phi_2(\phi_1, \Delta Q)$ represents the actual law of motion transformation—the law of transformation of motion which corresponds to errors of manufacturing and assembly. Kinematic errors of the gear drive are represented by the function

$$\Delta \phi_2 = \phi_2(\phi_1, \Delta Q) - \phi_2^0(\phi_1) \quad (18.2.17)$$

This method of solution can provide, not only the kinematic errors of a gearset, but also the new path of the contact point. (See functions (18.2.7).)

In general, the numerical solution of a system of five nonlinear equations is a difficult problem which requires many iterations. To save computer time an effective method of solution was proposed by Litvin and Gutman (1981a). The principle of this method is as follows:

The system of equation (18.2.13) may be represented as

$$f_1(u_1, \theta_1, \phi_1, u_2, \theta_2, \phi_2, A, H_1, H_2, \Delta Q) = 0 \quad (18.2.18)$$

$$f_2(u_1, \theta_1, \phi_1, u_2, \theta_2, \phi_2, A, H_1, H_2, \Delta Q) = 0 \quad (18.2.19)$$

$$f_3(u_1, \theta_1, \phi_1, u_2, \theta_2, \phi_2, A, H_1, H_2, \Delta Q) = 0 \quad (18.2.20)$$

$$f_4(u_1, \theta_1, u_2, \theta_2, \phi_2, \Delta Q) = 0 \quad (18.2.21)$$

$$f_5(u_1, \theta_1, u_2, \theta_2, \phi_2, \Delta Q) = 0 \quad (18.2.22)$$

Equations (18.2.18) to (18.2.20) are determined from vector equation (18.2.3), and equations (18.2.21) to (18.2.22) from vector equation (18.2.4). Here, A represents the shortest distance between the axes of rotation of the two gears and H_1 and H_2 represent the axial settings of the gears (fig. 18.2.2). Systems $S_1(x_1, y_1, z_1)$ and $S_2(x_2, y_2, z_2)$ shown in figure 18.2.2 are rigidly connected to the driving and driven gears, respectively. Let us now suppose that two arbitrary points $M_1(u_1, \theta_1)$ and $M_2(u_2, \theta_2)$ on surfaces Σ_1 and Σ_2 are chosen. With a set of known parameters $(u_1, \theta_1, u_2, \theta_2)$, equations (18.2.21) and (18.2.22) become a system of two equations in two unknowns which may be expressed as

$$F_1(\phi_1, \phi_2) = 0 \quad (18.2.23)$$

$$F_2(\phi_1, \phi_2) = 0 \quad (18.2.24)$$

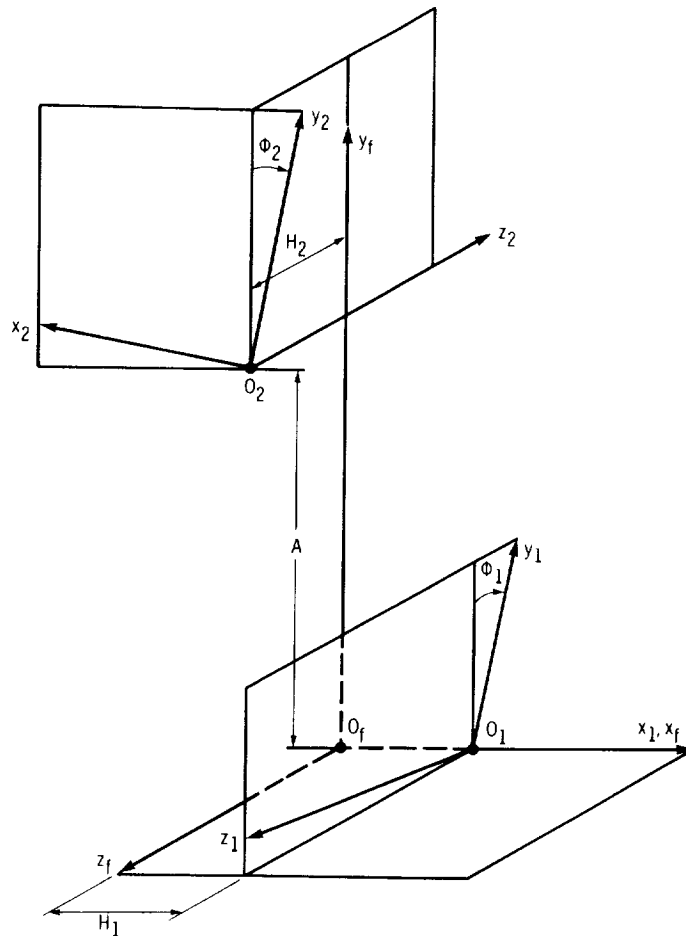


Figure 18.2.2.

Upon solving for ϕ_1 and ϕ_2 , one can check that the following equations are satisfied:

$$A - K_1(u_1, \theta_1, \phi_1, u_2, \theta_2, \phi_2, \Delta Q) = 0 \quad (18.2.25)$$

$$H_1 - K_2(u_1, \theta_1, \phi_1, u_2, \theta_2, \phi_2, \Delta Q) = 0 \quad (18.2.26)$$

$$H_2 - K_3(u_1, \theta_1, \phi_1, u_2, \theta_2, \phi_2, \Delta Q) = 0 \quad (18.2.27)$$

where A , H_1 , H_2 , and ΔQ are given values.

In general, the solution of the above two systems of equations (18.2.23) to (18.2.24) and (18.2.25) to (18.2.27) requires an iterative procedure. In practice, one of the four variable parameters ($u_1, \theta_1, u_2, \theta_2$) is to be fixed, and the other three are changed such that the two-equation system is satisfied.

The advantage of the above method lies in the ability to divide the system of five equations ((18.2.23) to (18.2.27)) into two subsystems of two and three equations, and to solve them separately.

18.3 Application of Theory to Helical Gears with Circular Arc Teeth: Sensitivity to the Change of Center Distance

Generation of Gear-Tooth Surfaces

The generation of gear-tooth surfaces is based on application of two rack cutters (fig. 16.4.6, see ch. 16.4). The surfaces of these rack cutters contact each other along a straight line; the normal section of each rack cutter surface is a circular arc. The generated surfaces of gears are in contact at a point at every instant.

Using the method for an exact solution (see sec. 18.2), we will investigate the influence of change of center distance on the conditions of meshing. It will be proven that the change of center distance may cause an unfavorable bearing contact if some gear parameters are not limited. The solution of the discussed problem is based on the research completed by Litvin (1968) and Litvin and Tsay (1986).

Rack Cutter Surface

The normal section of the rack cutter is a circular arc which is represented in an auxiliary coordinate system $S_a^{(i)}$ as follows (fig. 18.3.1):

$$x_a^{(i)} = \rho_i \sin \theta_i + x_a^{(C_i)} \quad y_a^{(i)} = -(\rho_i \cos \theta_i - y_a^{(C_i)}) \quad z_a^{(i)} = 0 \quad (i = I, II) \quad (18.3.1)$$

Here $x_a^{(C_i)}$ and $y_a^{(C_i)}$ are the coordinates of the circle center, C_i . Equations (18.3.1), with $i = I, II$, represent the normal sections of rack cutters which generate gears 1 and 2, respectively.

The generating surface of the rack cutter is obtained by the translational motion of the coordinate system $S_a^{(i)}$ along a straight line $O_c^{(i)} O_a^{(i)}$ (fig. 18.3.1). The coordinate transformation is represented by the matrix equation

$$\begin{bmatrix} x_c^{(i)} \\ y_c^{(i)} \\ z_c^{(i)} \\ 1 \end{bmatrix} = \begin{bmatrix} 1 & 0 & 0 & 0 \\ 0 & \sin \lambda & \cos \lambda & u_i \cos \lambda \\ 0 & -\cos \lambda & \sin \lambda & u_i \sin \lambda \\ 0 & 0 & 0 & 1 \end{bmatrix} \begin{bmatrix} x_a^{(i)} \\ y_a^{(i)} \\ z_a^{(i)} \\ 1 \end{bmatrix} \quad (18.3.2)$$

Here $u_i = \left| \overline{O_c^{(i)} O_a^{(i)}} \right|$, and λ is the lead angle of the helix on the gear pitch cylinder. Equations (18.3.1) and (18.3.2) yield

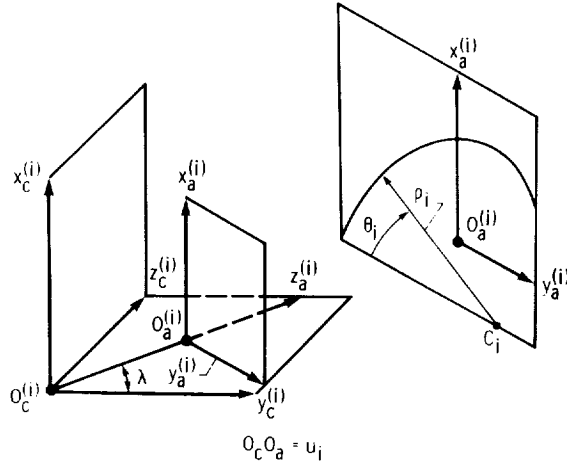


Figure 18.3.1.

$$\begin{aligned}
 x_c^{(i)} &= \rho_i \sin \theta_i + x_a^{(C_i)} \\
 y_c^{(i)} &= -(\rho_i \cos \theta_i - y_a^{(C_i)}) \sin \lambda + u_i \cos \lambda \\
 z_c^{(i)} &= (\rho_i \cos \theta_i - y_a^{(C_i)}) \cos \lambda + u_i \sin \lambda
 \end{aligned} \tag{18.3.3}$$

Equations (18.3.3) represent the generating surface of the rack cutter, $\Sigma_c^{(i)}$, in the coordinate system $S_c^{(i)}$.

The surface unit normal is represented by the equation

$$\mathbf{n}_c^{(i)} = \frac{\mathbf{N}_c^{(i)}}{|\mathbf{N}_c^{(i)}|} \quad \text{where } \mathbf{N}_c^{(i)} = \frac{\partial \mathbf{r}_c^{(i)}}{\partial \theta_1} \times \frac{\partial \mathbf{r}_c^{(i)}}{\partial u_i} \tag{18.3.4}$$

Equations (18.3.3) and (18.3.4) yield

$$[n_c^{(i)}] = \begin{bmatrix} \sin \theta_i \\ -\cos \theta_i \sin \lambda \\ \cos \theta_i \cos \lambda \end{bmatrix} \tag{18.3.5}$$

It was mentioned above that we consider two generating surfaces of rack cutters. These surfaces contact each other along a straight line determined as follows:

$$\begin{aligned}
 x_c^{(I)} &= x_c^{(II)} & y_c^{(I)} &= y_c^{(II)} & z_c^{(I)} &= z_c^{(II)} & n_{x_c}^{(I)} &= n_{x_c}^{(II)} \\
 n_{y_c}^{(I)} &= n_{y_c}^{(II)} & n_{z_c}^{(I)} &= n_{z_c}^{(II)}
 \end{aligned} \tag{18.3.6}$$

Equations (18.3.3) to (18.3.6) yield the following relations:

$$\begin{aligned}
 u_I &= u_{II}, & \rho_I \sin \theta_I + x_a^{(C_I)} &= \rho_{II} \sin \theta_{II} + x_a^{(C_{II})} \\
 -\rho_I \cos \theta_I + y_a^{(C_I)} &= -\rho_{II} \cos \theta_{II} + y_a^{(C_{II})} & \theta_I &= \theta_{II} = \psi_c
 \end{aligned}$$

where ψ_c is the pressure angle at the point of contact of helical gears measured in the normal section of the rack cutter.

Tooth Surface of Gear 1

We set up three coordinate systems considering the mesh of the rack cutter with the gear being generated (fig. 18.3.2). Systems $S_c^{(i)}$ ($i = I, II$) and S_j ($j = 1, 2$) which are rigidly connected to the rack cutter and the gear, respectively, and a fixed coordinate, $S_p^{(i)}$ ($i = I, II$).

While the rack cutter with the coordinate system $S_c^{(I)}$ translates, the gear being generated rotates about axis $z_p^{(I)}$. The instantaneous axis of rotation is $I-I$, and the axodes of the gear and of the rack cutter are the pitch cylinder of radius r_1 and plane Π , respectively. Plane Π is tangent to the pitch cylinder.

The line of contact of the generating surface $\Sigma_c^{(I)}$ with the gear-tooth surface Σ_1 may be determined in the coordinate system $S_c^{(I)}$ as follows (see ch. 9.8):

$$\mathbf{r}_c^{(I)} = \mathbf{r}_c^{(I)}(u_1, \theta_1) \quad \mathbf{N}_c^{(I)} \cdot \mathbf{v}_c^{(I)} = 0 \quad (18.3.7)$$

Here $\mathbf{r}_c^{(I)}(u_1, \theta_1)$ is the vector function which represents in the coordinate system $S_c^{(I)}$ the generating surface $\Sigma_c^{(I)}$; $\mathbf{N}_c^{(I)}$ is the normal to the generating surface; $\mathbf{v}_c^{(I)}$ is the relative velocity; the subscript c indicates that the vector components are represented in the coordinate system $S_c^{(I)}$.

There is an alternative solution for the case of transformation of motions represented in figure 18.3.2(a). Instead of equation $\mathbf{N}_c \cdot \mathbf{v}_c^{(I)} = 0$, we may use the equation

$$\frac{X_c^{(I)} - x_c^{(I)}}{N_{xc}^{(I)}} = \frac{Y_c^{(I)} - y_c^{(I)}}{N_{yc}^{(I)}} = \frac{Z_c^{(I)} - z_c^{(I)}}{N_{zc}^{(I)}} \quad (18.3.8)$$

Equation (18.3.8), if satisfied, provides that the common normal to surfaces $\Sigma_c^{(I)}$ and Σ_1 at their points of contact intersects the instantaneous axis of rotation $I-I$. Here (fig. 18.3.2)

$$X_c^{(I)} = 0 \quad Y_c^{(I)} = r_1 \phi_1 \quad Z_c^{(I)} = \ell \quad (18.3.9)$$

are the coordinates of a point of $I-I$ represented in the coordinate system $S_c^{(I)}$; ϕ_1 is the angle of rotation of gear 1; parameter ℓ determines the location of a point on the axis $I-I$; $x_c^{(I)}$, $y_c^{(I)}$, and $z_c^{(I)}$ are the coordinates of a point on surface $\Sigma_c^{(I)}$ which are represented by equations (18.3.3); $N_{xc}^{(I)}$, $N_{yc}^{(I)}$, and $N_{zc}^{(I)}$ are the projections of the surface normal. (We may also use $n_{xc}^{(I)}$, $n_{yc}^{(I)}$, and $n_{zc}^{(I)}$ instead of $N_{xc}^{(I)}$, $N_{yc}^{(I)}$, and $N_{zc}^{(I)}$.)

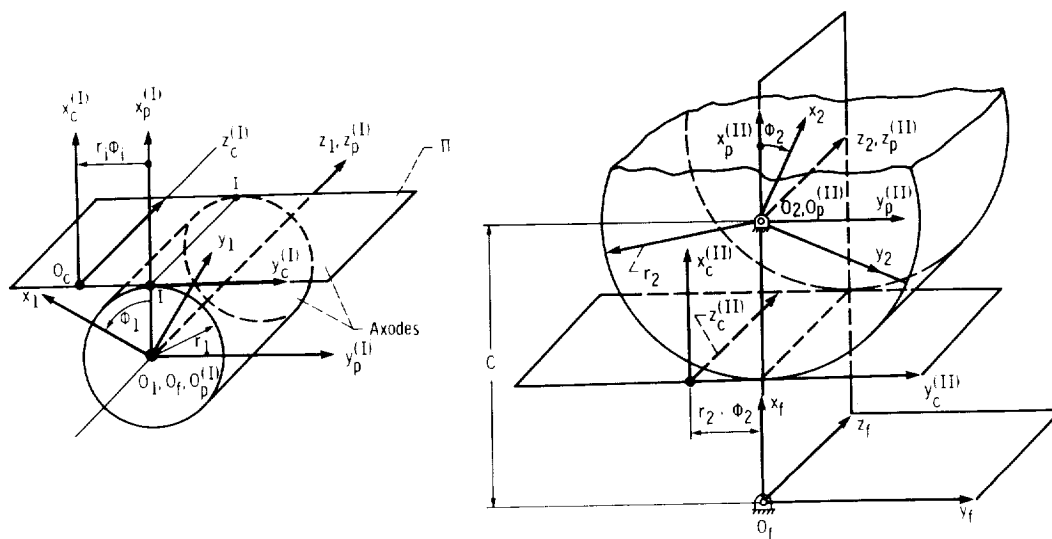


Figure 18.3.2.

Equations (18.3.3), (18.3.5), (18.3.8), and (18.3.9) yield the equation of meshing represented by

$$(r_1 \phi_1 - u_1 \cos \lambda - a_1 \sin \lambda) \sin \theta_1 + b_1 \cos \theta_1 \sin \lambda = f_1(u_1, \theta_1, \phi_1) = 0 \quad (18.3.10)$$

Here $x_a^{(C_1)} = -b_1$, $y_a^{(C_1)} = a_1$ are the coordinates of center C_1 (fig. 16.4.6(a)).

The equation of meshing (18.3.10) and equations (18.3.3) of the generating surface $\Sigma_c^{(1)}$ considered simultaneously represent a line on surface $\Sigma_c^{(1)}$ (line L_1), which is the line of contact of $\Sigma_c^{(1)}$ and Σ_1 . The location of this line on $\Sigma_c^{(1)}$ depends on the parameter of motion ϕ_1 . In the case of $b_1 = 0$, equation (18.3.10) yields that

$$u_1 = \frac{r_1 \phi_1 - a_1 \sin \lambda}{\cos \lambda} \quad (18.3.11)$$

for any θ_1 . Thus the line of contact is a circle of radius ρ_1 (fig. 18.3.3(a)).

Figure 18.3.3(b) shows the contact lines for the case where $b_1 \neq 0$. From equation (18.3.10), we obtain

$$u_1 = b_1 \cot \theta_1 \tan \lambda + \frac{r_1 \phi_1}{\cos \lambda} - a_1 \tan \lambda \quad (18.3.12)$$

Parameter u_1 and the contact lines approach infinity if θ_1 approaches zero.

Surface Σ_1 may be determined with the family of contact lines represented in the coordinate system S_1 . Using the matrix equation

$$[r_1] = [M_{1c}^{(1)}][r_c^{(1)}] = [M_{1p}][M_{pc}^{(1)}][r_c^{(1)}]$$

$$= \begin{bmatrix} \cos \phi_1 & -\sin \phi_1 & 0 & r_1(\cos \phi_1 + \phi_1 \sin \phi_1) \\ \sin \phi_1 & \cos \phi_1 & 0 & r_1(\sin \phi_1 - \phi_1 \cos \phi_1) \\ 0 & 0 & 1 & 0 \\ 0 & 0 & 0 & 1 \end{bmatrix} \begin{bmatrix} x_c^{(1)} \\ y_c^{(1)} \\ z_c^{(1)} \\ 1 \end{bmatrix} \quad (18.3.13)$$

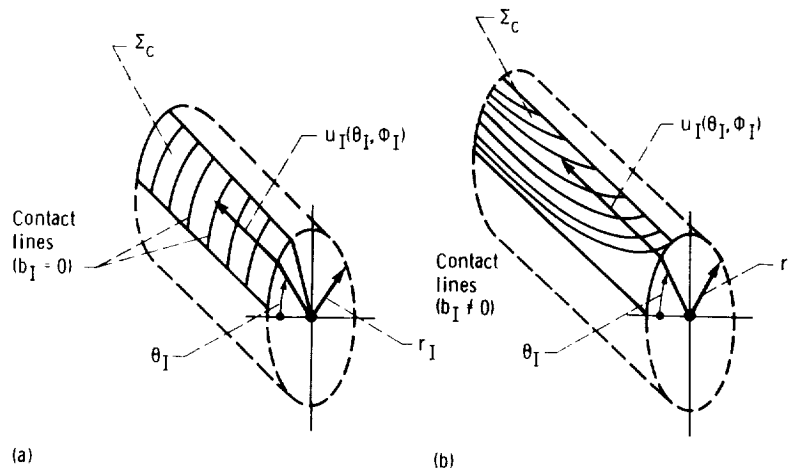


Figure 18.3.3.

and equations (18.3.3) and (18.3.12), we obtain

$$\begin{aligned}
 x_1 &= (\rho_1 \sin \theta_1 - b_1 + r_1) \cos \phi_1 + (\rho_1 \cos \theta_1 - b_1 \cot \theta_1) \sin \phi_1 \sin \lambda \\
 y_1 &= (\rho_1 \sin \theta_1 - b_1 + r_1) \sin \phi_1 - (\rho_1 \cos \theta_1 - b_1 \cot \theta_1) \cos \phi_1 \sin \lambda \\
 z_1 &= \rho_1 \cos \theta_1 \cos \lambda - \frac{a_1}{\cos \lambda} + b_1 \cot \theta_1 \tan \lambda \sin \lambda + r_1 \phi_1 \tan \lambda
 \end{aligned}
 \tag{18.3.14}$$

Equations (18.3.14) represent the tooth surface of gear 1 with surface coordinates θ_1 and ϕ_1 .

To derive the surface unit normal, we may follow the usual procedure and use the following equations

$$\mathbf{n}_1 = \frac{\mathbf{N}_1}{|\mathbf{N}_1|} \quad \text{where } \mathbf{N}_1 = \frac{\partial \mathbf{r}_1}{\partial \phi_1} \times \frac{\partial \mathbf{r}_1}{\partial \theta_1}
 \tag{18.3.15}$$

Here $\mathbf{r}_1(\phi_1, \theta_1)$ is the vector function which represents the surface given by equations (18.3.14).

A simpler way of derivation is based on the consideration that the rack cutter surface $\Sigma_c^{(1)}$ and the gear-tooth surface Σ_1 have a common normal at points of contact. Thus

$$[n_1] = [L_{1c}^{(1)}][n_c^{(1)}]
 \tag{18.3.16}$$

Here $[L_{1c}^{(1)}]$ is the matrix which transforms the direction cosines in transition from $S_c^{(1)}$ to S_1 . Deleting the last column and last row in matrix $[M_{1c}^{(1)}]$, we obtain

$$[L_{1c}^{(1)}] = \begin{bmatrix} \cos \phi_1 & -\sin \phi_1 & 0 \\ \sin \phi_1 & \cos \phi_1 & 0 \\ 0 & 0 & 1 \end{bmatrix}
 \tag{18.3.17}$$

Equations (18.3.16), (18.3.17), and (18.3.5) yield

$$[n_1] = \begin{bmatrix} \sin \theta_1 \cos \phi_1 + \cos \theta_1 \sin \lambda \sin \phi_1 \\ \sin \theta_1 \sin \phi_1 - \cos \theta_1 \sin \lambda \cos \phi_1 \\ \cos \theta_1 \cos \lambda \end{bmatrix}
 \tag{18.3.18}$$

Tooth Surface of Gear 2

Similarly, we may derive equations of the tooth surface of gear 2. The equation of meshing of the rack cutter II and gear 2 is given by

$$(r_2 \phi_2 - u_{II} \cos \lambda - a_{II} \sin \lambda) \sin \theta_{II} + b_{II} \cos \theta_{II} \sin \lambda = f_{II}(u_{II}, \theta_{II}, \phi_2) = 0
 \tag{18.3.19}$$

The line of contact of $\Sigma_c^{(II)}$ and Σ_2 is represented in $S_c^{(II)}$ by equations

$$\begin{aligned}x_c^{(II)} &= \rho_{II} \sin \theta_{II} - b_{II} \\y_c^{(II)} &= -(\rho_{II} \cos \theta_{II} - a_{II}) \sin \lambda + b_{II} \cot \theta_{II} \sin \lambda - a_{II} \sin \lambda + r_2 \phi_2 \\z_c^{(II)} &= \rho_{II} \cos \theta_{II} \cos \lambda - \frac{a_{II}}{\cos \lambda} + b_{II} \cot \theta_{II} \tan \lambda \sin \lambda + r_2 \phi_2 \tan \lambda\end{aligned}\tag{18.3.20}$$

Fixing the parameter of motion ϕ_2 , we may determine coordinates of the contact line on $\Sigma_c^{(II)}$ as functions of θ_{II} .

To derive equations of tooth surface 2, we have to use the coordinate transformations from $S_c^{(II)}$ to S_2 , which is represented as follows (fig. 18.3.2(b)):

$$\begin{aligned}[r_2] &= [M_{2p}][M_{pc}][r_c^{(II)}] \\&= \begin{bmatrix} \cos \phi_2 & \sin \phi_2 & 0 & 0 \\ -\sin \phi_2 & \cos \phi_2 & 0 & 0 \\ 0 & 0 & 1 & 0 \\ 0 & 0 & 0 & 1 \end{bmatrix} \begin{bmatrix} 1 & 0 & 0 & -r_2 \\ 0 & 1 & 0 & -r_2 \phi_2 \\ 0 & 0 & 1 & 0 \\ 0 & 0 & 0 & 1 \end{bmatrix} \begin{bmatrix} x_c^{(II)} \\ y_c^{(II)} \\ z_c^{(II)} \\ 1 \end{bmatrix} \\&= \begin{bmatrix} \cos \phi_2 & \sin \phi_2 & 0 & -r_2(\cos \phi_2 + \phi_2 \sin \phi_2) \\ -\sin \phi_2 & \cos \phi_2 & 0 & r_2(\sin \phi_2 - \phi_2 \cos \phi_2) \\ 0 & 0 & 1 & 0 \\ 0 & 0 & 0 & 1 \end{bmatrix} \begin{bmatrix} x_c^{(II)} \\ y_c^{(II)} \\ z_c^{(II)} \\ 1 \end{bmatrix}\end{aligned}\tag{18.3.21}$$

Equations (18.3.21) and (18.3.20) yield

$$\begin{aligned}x_2 &= (\rho_{II} \sin \theta_{II} - b_{II} - r_2) \cos \phi_2 - (\rho_{II} \cos \theta_{II} - b_{II} \cot \theta_{II}) \sin \phi_2 \sin \lambda \\y_2 &= -(\rho_{II} \sin \theta_{II} - b_{II} - r_2) \sin \phi_2 - (\rho_{II} \cos \theta_{II} - b_{II} \cot \theta_{II}) \cos \phi_2 \sin \lambda \\z_2 &= \rho_{II} \cos \theta_{II} \cos \lambda - \frac{a_{II}}{\cos \lambda} + b_{II} \cot \theta_{II} \sin \lambda \tan \lambda + r_2 \phi_2 \tan \lambda\end{aligned}\tag{18.3.22}$$

The surface unit normal is represented by the following matrix equation:

$$[n_2] = [L_{2c}^{(II)}][n_c^{(II)}]\tag{18.3.23}$$

From the matrix equation (18.3.21), we obtain

$$[L_{2c}^{(II)}] = \begin{bmatrix} \cos \phi_2 & \sin \phi_2 & 0 \\ -\sin \phi_2 & \cos \phi_2 & 0 \\ 0 & 0 & 1 \end{bmatrix} \quad (18.3.24)$$

Equations (18.3.23), (18.3.24), and (18.3.5) yield

$$[n_2] = \begin{bmatrix} \sin \theta_{II} \cos \phi_2 - \cos \theta_{II} \sin \lambda \sin \phi_2 \\ -\sin \theta_{II} \sin \phi_2 - \cos \theta_{II} \sin \lambda \cos \phi_2 \\ \cos \theta_{II} \cos \lambda \end{bmatrix} \quad (18.3.25)$$

Simulation of Conditions of Meshing

The conditions of meshing of gears which have some errors may be simulated by using equations of continuous tangency of gear-tooth surfaces. We set up three coordinate systems S_1 and S_2 , rigidly connected to the gears, and S_f , rigidly connected to the frame. Using these coordinate systems, we may simulate the errors of manufacturing and assembly of the gears, such as the change of center distance, the misalignment of axes of rotation, and so on. We limit the discussion to the case of the change of center distance, C , considering that the operating center distance C (fig. 18.3.4) is not equal to the sum of the radii of pitch cylinders. Thus $C \neq r_1 + r_2$.

Consider that the gear-tooth surfaces, Σ_1 and Σ_2 , and their unit normals, \mathbf{n}_1 and \mathbf{n}_2 , are represented in the coordinate systems S_1 and S_2 , respectively. We represent Σ_i and \mathbf{n}_i , ($i = 1, 2$) in the coordinate system S_f by using the following matrix equations:

$$[r_f^{(i)}] = [M_{fi}][r_i] \quad [n_f^{(i)}] = [L_{fi}][n_i] \quad (i = 1, 2) \quad (18.3.26)$$

Here (fig. 18.3.3)

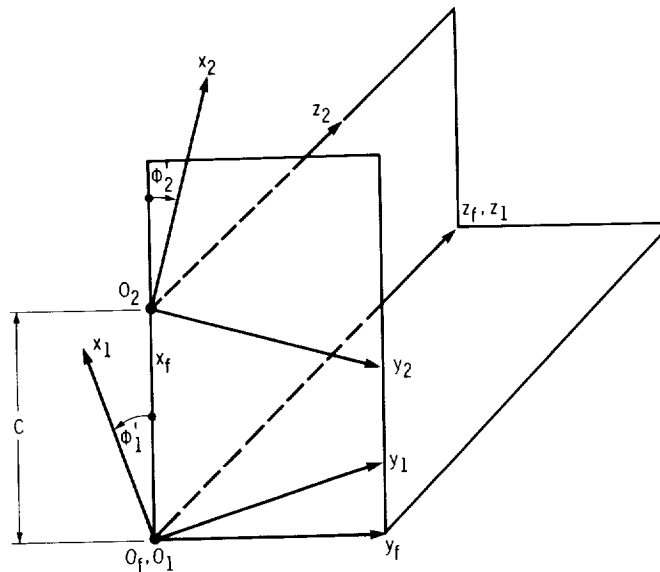


Figure 18.3.4.

$$[M_{f1}] = \begin{bmatrix} \cos \phi'_1 & \sin \phi'_1 & 0 & 0 \\ -\sin \phi'_1 & \cos \phi'_1 & 0 & 0 \\ 0 & 0 & 1 & 0 \\ 0 & 0 & 0 & 1 \end{bmatrix} \quad [L_{f1}] = \begin{bmatrix} \cos \phi'_1 & \sin \phi'_1 & 0 \\ -\sin \phi'_1 & \cos \phi'_1 & 0 \\ 0 & 0 & 1 \end{bmatrix} \quad (18.3.27)$$

$$[M_{f2}] = \begin{bmatrix} \cos \phi'_2 & -\sin \phi'_2 & 0 & C \\ \sin \phi'_2 & \cos \phi'_2 & 0 & 0 \\ 0 & 0 & 1 & 0 \\ 0 & 0 & 0 & 1 \end{bmatrix} \quad [L_{f2}] = \begin{bmatrix} \cos \phi'_2 & -\sin \phi'_2 & 0 \\ \sin \phi'_2 & \cos \phi'_2 & 0 \\ 0 & 0 & 1 \end{bmatrix} \quad (18.3.28)$$

ϕ'_1 and ϕ'_2 are the angles of rotation of the gears in mesh; recall that ϕ_1 and ϕ_2 are the angles of rotation of the gears while they are generated with the rack cutters (fig. 18.3.2).

Using equations (18.3.26) to (18.3.28), (18.3.14), (18.3.18), (18.3.22), and (18.3.25), we obtain

$$\begin{aligned} x_f^{(1)} &= A_1 \cos \mu_1 + B_1 \sin \mu_1 & y_f^{(1)} &= A_1 \sin \mu_1 - B_1 \cos \mu_1 \\ z_f^{(1)} &= \rho_1 \cos \theta_1 \cos \lambda - \frac{a_1}{\cos \lambda} + b_1 \cot \theta_1 \tan \lambda \sin \lambda + r_1 \phi_1 \tan \lambda \end{aligned} \quad (18.3.29)$$

Here

$$\begin{aligned} A_1(\theta_1) &= \rho_1 \sin \theta_1 - b_1 + r_1 & B_1(\theta_1) &= (\rho_1 \cos \theta_1 - b_1 \cot \theta_1) \sin \lambda \\ \mu_1 &= \phi_1 - \phi'_1 \end{aligned}$$

$$[n_f^{(1)}] = \begin{bmatrix} \sin \theta_1 \cos \mu_1 + \cos \theta_1 \sin \lambda \sin \mu_1 \\ \sin \theta_1 \sin \mu_1 - \cos \theta_1 \sin \lambda \cos \mu_1 \\ \cos \theta_1 \cos \lambda \end{bmatrix} \quad (18.3.30)$$

$$\begin{aligned} x_f^{(2)} &= A_2 \cos \mu_2 - B_2 \sin \mu_2 + C \\ y_f^{(2)} &= -A_2 \sin \mu_2 - B_2 \cos \mu_2 \end{aligned} \quad (18.3.31)$$

$$z_f^{(2)} = \rho_{II} \cos \theta_{II} \cos \lambda - \frac{a_{II}}{\cos \lambda} + b_{II} \cot \theta_{II} \sin \lambda \tan \lambda + r_2 \phi_2 \tan \lambda$$

Here

$$\begin{aligned} A_2(\theta_{II}) &= \rho_{II} \sin \theta_{II} - b_{II} - r_2 & B_2(\theta_{II}) &= (\rho_{II} \cos \theta_{II} - b_{II} \cot \theta_{II}) \sin \lambda \\ \mu_2 &= \phi_2 - \phi'_2 \end{aligned}$$

$$[n_f^{(2)}] = \begin{bmatrix} \sin \theta_{II} \cos \mu_2 - \cos \theta_{II} \sin \lambda \sin \mu_2 \\ -\sin \theta_{II} \sin \mu_2 - \cos \theta_{II} \sin \lambda \cos \mu_2 \\ \cos \theta_{II} \cos \lambda \end{bmatrix} \quad (18.3.32)$$

The gear-tooth surfaces are in continuous tangency and therefore the following equations must be satisfied (see ch. 11, eqs. (11.1.17) and (11.1.8))

$$\mathbf{r}_f^{(1)}(\theta_1, \mu_1, \phi_1) = \mathbf{r}_f^{(2)}(\theta_{II}, \mu_2, \phi_2) \quad (18.3.33)$$

$$\mathbf{n}_f^{(1)}(\theta_1, \mu_1) = \mathbf{n}_f^{(2)}(\theta_{II}, \mu_2) \quad (18.3.34)$$

Equation (18.3.33), if satisfied, yields that the position vectors $\mathbf{r}_f^{(1)}$ and $\mathbf{r}_f^{(2)}$ coincide at the point of contact of gear-tooth surfaces, Σ_1 and Σ_2 . Equation (18.3.34) if satisfied yields that the surfaces have a common unit normal at the point of contact.

Equations (18.3.33) to (18.3.34) yield a system of five independent equations only since $|\mathbf{n}^{(1)}| = |\mathbf{n}^{(2)}| = 1$. These five equations relate six unknowns: $\theta_1, \mu_1, \phi_1, \theta_{II}, \mu_2, \phi_2$; thus, one of these parameters may be varied.

The equation system (18.3.22) to (18.3.34) yields the following procedure for computations.

Step 1.—Using equation $n_{z_f}^{(1)} = n_{z_f}^{(2)}$, we obtain

$$\cos \theta_1 \cos \lambda = \cos \theta_{II} \cos \lambda$$

Thus

$$\theta_1 = \theta_{II} = \theta \quad (18.3.35)$$

Step 2.—Using equation $n_{y_f}^{(1)} = n_{y_f}^{(2)}$, $y_f^{(1)} = y_f^{(2)}$, and $x_f^{(1)} = x_f^{(2)}$, we obtain a system of three equations in three unknowns (θ, μ_1 , and μ_2) where

$$\sin \theta \sin \mu_1 - \cos \theta \sin \lambda \cos \mu_1 = -\sin \theta \sin \mu_2 - \cos \theta \sin \lambda \cos \mu_2 \quad (18.3.36)$$

$$\begin{aligned} (\rho_1 \sin \theta - b_1)(\sin \theta \sin \mu_1 - \cos \theta \sin \lambda \cos \mu_1) + r_1 \sin \theta \sin \mu_1 \\ = -(\rho_{II} \sin \theta - b_{II})(\sin \theta \sin \mu_2 + \cos \theta \sin \lambda \cos \mu_2) + r_2 \sin \theta \sin \mu_2 \end{aligned} \quad (18.3.37)$$

$$\begin{aligned} (\rho_1 \sin \theta - b_1)(\sin \theta \cos \mu_1 + \cos \theta \sin \lambda \sin \mu_1) + r_1 \sin \theta \cos \mu_1 \\ = (\rho_{II} \sin \theta - b_{II})(\sin \theta \cos \mu_2 - \cos \theta \sin \lambda \sin \mu_2) - r_2 \sin \theta \cos \mu_2 + C \sin \theta \end{aligned} \quad (18.3.38)$$

We may check the solution for θ, μ_1 , and μ_2 by using equation $n_{x_f}^{(1)} = n_{x_f}^{(2)}$ which yields

$$\sin \theta \cos \mu_1 + \cos \theta \sin \lambda \sin \mu_1 = \sin \theta \cos \mu_2 - \cos \theta \sin \lambda \sin \mu_2 \quad (18.3.39)$$

The solution for θ, μ_1 , and μ_2 provides constant values whose magnitude depends on the operating center distance C . The magnitude of θ determines the new location of the contact point caused by the change of C .

Step 3.—Knowing θ , we may determine the relation between parameters ϕ_1 and ϕ_2 by using equation $z_f^{(1)} = z_f^{(2)}$ which yields

$$\begin{aligned} & \rho_I \cos \theta \cos \lambda - \frac{a_I}{\cos \lambda} + b_I \cot \theta \tan \lambda \sin \lambda + r_1 \phi_1 \tan \lambda \\ & = \rho_{II} \cos \theta \cos \lambda - \frac{a_{II}}{\cos \lambda} + b_{II} \cot \theta \tan \lambda \sin \lambda + r_2 \phi_2 \tan \lambda \end{aligned} \quad (18.3.40)$$

Equation (18.3.40) provides a linear function which relates ϕ_1 and ϕ_2 since θ is constant.

Step 4.—It is easy to prove that since θ , μ_1 , and μ_2 are constant values, the angular velocity ratio for the gears does not depend on the center distance. The proof is based on the following considerations:

- (1) Equation (18.3.40) with $\theta = \text{constant}$ yields that $r_1 d\phi_1 = r_2 d\phi_2$ and $d\phi_1/d\phi_2 = r_2/r_1$.
- (2) Since $\mu_1 = \phi_1 - \phi_1'$ and $\mu_2 = \phi_2 - \phi_2'$ are constant, we obtain $d\phi_1' = d\phi_1$, $d\phi_2' = d\phi_2$ and

$$m_{12} = \frac{\omega^{(1)}}{\omega^{(2)}} = \frac{d\phi_1'}{d\phi_2'} = \frac{d\phi_1}{d\phi_2} = \frac{r_2}{r_1}$$

Thus the gears keep the same angular velocity ratio although the center distance is changed. The disadvantage of the discussed gears is the substantial change of location of contact point caused by the change of center distance.

Step 5.—It is evident that since θ , μ_1 , and μ_2 are constant values, the line of action of the gear-tooth surfaces in the fixed coordinate system represents a straight line, which is parallel to the z_f -axis. We may determine coordinates $x_f^{(i)}$ and $y_f^{(i)}$ of the line of action by using equations (18.3.29) or (18.3.31). The location of the instantaneous point of contact on the line of action may be represented as a function of the angle of rotation ϕ_1' of gear 1. Knowing μ_1 and fixing ϕ_1' , we determine ϕ_1 by using the equation

$$\phi_1 = \mu_1 + \phi_1' \quad (18.3.41)$$

Equation (18.3.41) and the equation for $z_f^{(1)}$ in the system equation (18.3.29) yield

$$z_f^{(1)} = \rho_I \cos \theta \cos \lambda - \frac{a_I}{\cos \lambda} + b_I \cot \theta \tan \lambda \sin \lambda + r_1 \tan \lambda (\mu_1 + \phi_1') \quad (18.3.42)$$

Step 6.—We may also derive an approximate equation which relates θ and the center distance C . Since μ_1 and μ_2 are small values, we make $\cos \mu_i = 1$ and $\sin \mu_i = 0$ ($i = 1, 2$) in equation (18.3.38). Then we get

$$\begin{aligned} \rho_I \sin \theta - b_I + r_1 &= \rho_{II} \sin \theta - b_{II} - r_2 + C \\ &= \rho_{II} \sin \theta - b_{II} - r_2 + (r_1 + r_2 + \Delta C) \end{aligned} \quad (18.3.43)$$

Here $C = r_1 + r_2 + \Delta C$ where ΔC is the change of center distance. Equations (18.3.43) yield

$$\sin \theta = \frac{\Delta C + b_I - b_{II}}{\rho_I - \rho_{II}} \quad (18.3.44)$$

The nominal value of θ which corresponds to the theoretical value of the center distance is given by

$$\sin \theta^0 = \frac{b_I - b_{II}}{\rho_I - \rho_{II}} \quad (18.3.45)$$

Compensation of Location of Bearing Contact

It results from equation (18.3.44) that the location of the bearing contact depends on the error ΔC of the center distance. If the normal pressure angle θ becomes too small, the bearing contact will be located on the bottom of the tooth of one gear and on the top of the tooth of the other gear. Such a bearing is not acceptable and should be avoided.

The sensitivity of the discussed gears to the change of center distance ΔC may be reduced by increasing the difference $|\rho_{II} - \rho_I|$. However, this results in the increase of the contacting stresses. The dislocation of the bearing contact may be compensated by regrinding one of the gears (preferably the pinion) with new tool settings.

Consider that θ^0 is the theoretical value of the normal pressure angle, b_I^0 and b_{II}^0 are the theoretical values of tool settings, and ρ_I^0 and ρ_{II}^0 are the theoretical values of the radii of circular arcs. These parameters are related by equation (18.3.45). Equation (18.3.44) yields that the location of the bearing will not be changed if the pinion will be reground with new tool setting b_I determined as follows:

$$\sin \theta^0 = \frac{\Delta C + b_I - b_{II}^0}{\rho_I^0 - \rho_{II}^0} \quad (18.3.46)$$

Equations (18.3.46) and (18.3.45) yield

$$b_I = b_I^0 - \Delta C \quad (18.3.47)$$

18.4 Approximate Method for Calculation of Gear Drive Kinematic Errors

As a general rule, when using exact methods, the determination of kinematic errors of a gear drive must be obtained numerically by using a computer. This is a disadvantage of the exact method. Therefore, an approximate method with the idea of obtaining accurate results analytically is now presented.

Figure 18.4.1 shows two gear surfaces Σ_1 and Σ_2 which are not in tangency due to errors of manufacturing and assembly. Points $M^{(1)}$ and $M^{(2)}$ and surface unit normal vectors $\mathbf{n}_f^{(1)}$ and $\mathbf{n}_f^{(2)}$ do not coincide, and position vectors $\mathbf{r}_f^{(1)}$ and $\mathbf{r}_f^{(2)}$ are not equal. To bring the two surfaces into contact it is sufficient to hold one gear fixed and rotate the other gear by an additional small angle. Since the gear with surface Σ_1 is the driving gear, it is preferable to fix the position of surface Σ_1 and rotate surface Σ_2 to bring it back into contact with Σ_1 . The additional angle of rotation $\Delta\phi_2$ represents the change of the theoretical angle of rotation ϕ_2^0 , which is brought about by errors of manufacturing and assembly. The angle $\Delta\phi_2$ is as yet an unknown function of the vector of errors $\Delta\mathbf{Q}$ and varies in the process of motion. Thus

$$\Delta\phi_2 = f(\phi_1, \Delta\mathbf{Q}) \quad (18.4.1)$$

The determination of function (18.4.1) is based on kinematic relations between velocities (displacements) for a contact point and a surface unit normal which move over the tooth surfaces of mating gears. (See ch. 12.1.)

The following equations are used for the determination

$$ds_{ir}^{(1)} + ds_r^{(1)} + ds_q^{(1)} = ds_{ir}^{(2)} + ds_r^{(2)} + ds_q^{(2)} \quad (18.4.2)$$

$$d\mathbf{n}_{ir}^{(1)} + d\mathbf{n}_r^{(1)} + d\mathbf{n}_q^{(1)} = d\mathbf{n}_{ir}^{(2)} + d\mathbf{n}_r^{(2)} + d\mathbf{n}_q^{(2)} \quad (18.4.3)$$

Here $ds_{ir}^{(i)}$ is the displacement of the theoretical contact point in transfer motion, with the tooth surface; $ds_r^{(i)}$ is the displacement of the theoretical contact point in the motion over the tooth

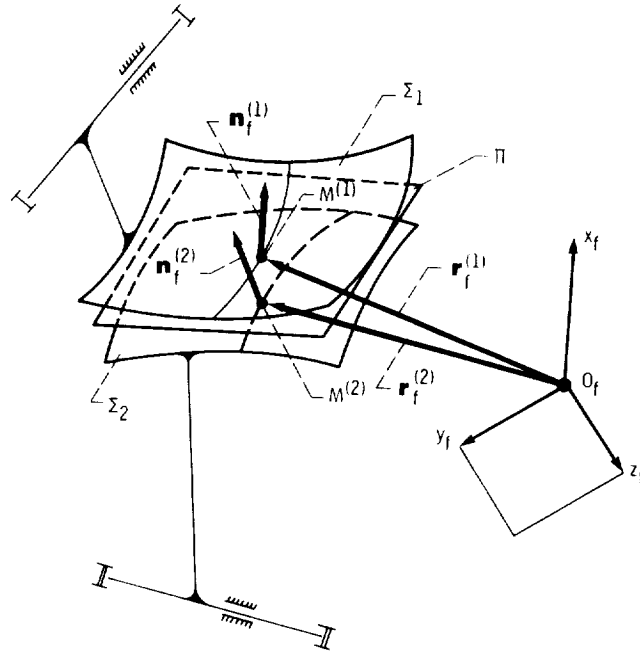


Figure 18.4.1.

surface; $ds_q^{(i)}$ is the displacement of the contact point caused by the gear errors ($i = 1, 2$). Similarly, $dn_{ir}^{(i)}$, $dn_r^{(i)}$, and $dn_q^{(i)}$ ($i = 1, 2$) are the changes in the direction of the surface unit normal in transfer and relative motion and due to the errors. Unlike equations (12.1.9) and (12.1.15), both equations (18.4.2) and (18.4.3) consist of additional members having the subscript q . These members are due to gear errors. To bring surfaces into contact, it is sufficient to rotate only gear 2, holding gear 1 at rest. Therefore, $ds_{ir}^{(1)}$ and $dn_{ir}^{(1)}$ are zero and

$$ds_r^{(1)} + ds_q^{(1)} = ds_{ir}^{(2)} + ds_r^{(2)} + ds_q^{(2)} \quad (18.4.4)$$

$$dn_r^{(1)} + dn_q^{(1)} = dn_{ir}^{(2)} + dn_r^{(2)} + dn_q^{(2)} \quad (18.4.5)$$

To determine relations between $ds_{ir}^{(2)}$, $ds_q^{(1)}$, and $ds_q^{(2)}$, we take the following scalar products:

$$\mathbf{n} \cdot (ds_r^{(1)} + ds_q^{(1)}) = \mathbf{n} \cdot (ds_{ir}^{(2)} + ds_r^{(2)} + ds_q^{(2)}) \quad (18.4.6)$$

Since vectors $ds_r^{(1)}$ and $ds_r^{(2)}$ lie in the common tangent plane Π , equation (18.4.6) is transformed as follows:

$$\mathbf{n} \cdot ds_{ir}^{(2)} = \mathbf{n} \cdot (ds_q^{(1)} - ds_q^{(2)}) \quad (18.4.7)$$

Vector $ds_{ir}^{(2)}$ may be represented by the following cross product:

$$ds_{ir}^{(2)} = d\phi^{(2)} \times \mathbf{r}_2^{(M)} \quad (18.4.8)$$

where $d\phi^{(2)}$ is the vector of the incremental angle of rotation of gear 2 and $\mathbf{r}_2^{(M)}$ is the position vector drawn from an arbitrary point on the axis of rotation to the contact point M . Equations (18.4.7) and (18.4.8) yield

$$\left[d\phi^{(2)} \mathbf{r}_2^{(M)} \mathbf{n} \right] = (ds_q^{(1)} - ds_q^{(2)}) \cdot \mathbf{n} \quad (18.4.9)$$

Equation (18.4.9) is the basic equation for the determination of kinematic errors of gear drives. Its application will be demonstrated in subsequent sections.

Similar scalar products can be derived on the basis of equation (18.4.5). It may be proven that these scalar products are zero because the vectors in equation (18.4.5) all belong to the tangent plane. Henceforth, the following notations will be used:

$$\Sigma \Delta \mathbf{q}_i^{(1)} \equiv \Delta \mathbf{s}_q^{(1)} \quad \Sigma \Delta \mathbf{q}_j^{(2)} \equiv \Delta \mathbf{s}_q^{(2)} \quad (18.4.10)$$

where $\Sigma \Delta \mathbf{q}_i^{(1)}$ and $\Sigma \Delta \mathbf{q}_j^{(2)}$ represent the sum of linear error vectors due to errors of manufacturing and assembly of gears 1 and 2, respectively.

In many cases, however, errors in gear trains do not result from linear displacements, but rather from angular displacements. For instance, kinematic errors may result from the misalignment of gear shafts.

Figure 18.4.2 shows the axis of gear 2 rotation $a-a$ in its ideal position. Consider that, because of an error of assembly, axis $a-a$ is rotated about the crossed axis $B-B$. Such an error of assembly may be represented by vector $\Delta \delta$, which is directed along axis $B-B$, where the direction of $\Delta \delta$ corresponds to the direction of rotation by the right-hand rule. With the given vector $\Delta \delta$, the displacement $\Delta \mathbf{q}^{(2)}$ of contact point M may be determined as follows:

(1) Vector $\Delta \delta$, directed along the axis $B-B$, is substituted by an equal vector $\Delta \delta$, which passes through the origin O_2 , and the vector moment $\mathbf{R} \times \Delta \delta$. Here \mathbf{R} is a position vector drawn from O_2 to an arbitrary point on the line of action of vector $\Delta \delta$ (fig. 18.4.2).

(2) The displacement $\Delta \mathbf{q}^{(2)}$ of the contact point M caused by the angular errors $\Delta \delta$ may be represented by

$$\Delta \mathbf{q}^{(2)} = \Delta \delta \times \mathbf{r}_2^{(M)} + \mathbf{R} \times \Delta \delta = \Delta \delta \times (\mathbf{r}_2^{(M)} - \mathbf{R}) \quad (18.4.11)$$

A similar equation may be derived to determine the displacement of the contact point M brought about by an angular error of assembly of gear 1.

With notations (18.4.10) equation (18.4.9) which determines the kinematic errors may be represented as follows:

$$(\Delta \phi^{(2)} \times \mathbf{r}_2^{(M)} + \Sigma \Delta \mathbf{q}) \cdot \mathbf{n}^{(M)} = 0 \quad (18.4.12)$$

where $\Sigma \Delta \mathbf{q} = \Sigma \Delta \mathbf{q}_j^{(2)} - \Sigma \Delta \mathbf{q}_i^{(1)}$ and $\mathbf{n}^{(M)}$ is the surface unit normal at the contact point M .

The location of the contact point M and the direction of the unit normal $\mathbf{n}^{(M)}$ change in the process of motion. A further simplification of equation (18.4.12) is based on the following considerations: (1) The contacting tooth surfaces have a common normal at all positions and (2) this normal passes through the contact point M and the pitch point P . For planar gears the pitch point P coincides with the point of tangency of the pitch circles (gear centrodes). The pitch point for bevel gears is located on the line of tangency of pitch cones. In both cases the surface unit normal \mathbf{n} is collinear with \overline{PM} and

$$\mathbf{r}_2^{(M)} = \mathbf{r}_2^{(P)} + \overline{PM} = \mathbf{r}_2^{(P)} + \lambda \mathbf{n}^{(M)} \quad (18.4.13)$$

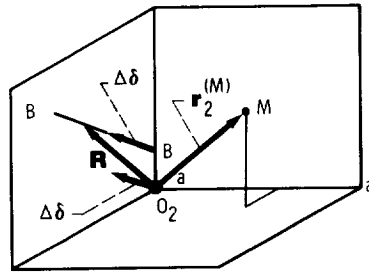


Figure 18.4.2.

Equations (18.4.12) and (18.4.13) yield

$$\left[(\Delta\phi^{(2)} \times \mathbf{r}_2^{(P)}) + \Sigma\Delta\mathbf{q} \right] \cdot \mathbf{n}^{(M)} = 0 \quad (18.4.14)$$

because

$$\begin{aligned} (\Delta\phi^{(2)} \times \mathbf{r}_2^{(M)}) \cdot \mathbf{n}^{(M)} &= \left[\Delta\phi^{(2)} \times (\mathbf{r}_2^{(P)} + \lambda\mathbf{n}^{(M)}) \right] \cdot \mathbf{n}^{(M)} \\ &= (\Delta\phi^{(2)} \times \mathbf{r}_2^{(P)}) \cdot \mathbf{n}^{(M)} + \left[\Delta\phi^{(2)} \lambda \mathbf{n}^{(M)} \cdot \mathbf{n}^{(M)} \right] \\ &= (\Delta\phi^{(2)} \times \mathbf{r}_2^{(P)}) \cdot \mathbf{n}^{(M)} \end{aligned} \quad (18.4.15)$$

The application of equation (18.4.14) instead of equation (18.4.12) has the advantage that the location of the pitch point may be considered as a constant ($\mathbf{r}_2^{(P)} = \text{const}$). However, the direction of the surface unit normal is a function of ϕ_1 . Three types of gears—involute (spur and helical) and Wildhaber-Novikov—are exceptions to this statement. For these gears the unit normal of the gear surfaces, at their contact point, does not change its direction.

Because of kinematic errors, the angular velocity ratio fluctuates in the process of meshing of the gears. Figure 18.4.3 shows functions for two types of kinematic errors. The first is a piecewise, nonlinear, periodic function whose period depends on the ratio

$$m_{12} = \frac{N_2}{N_1} = \frac{b}{a} \quad (18.4.16)$$

Here N_i ($i = 1, 2$) is the number of gear teeth and b and a are the minimum integral numbers with which the ratio m_{12} can be expressed. The angle of rotation of gear 1, which corresponds to the period of function $\Delta\phi^{(2)}(\phi_1)$, is equal to $2\pi a$. Such functions of kinematic errors are caused by (1) the eccentricity of gears or (2) by the noncoincidence of the theoretical axis of the gear and the axis of rotation, and thus making a crossing angle with it.

The second type of function $\Delta\phi^{(2)}(\phi_1)$, shown in figure 18.4.3(b), has a period of $\phi_1 = 2\pi/N_1$ (periodic with tooth mesh cycle). This function of errors is typical for the case when the generating process provides nonconjugated tooth surfaces, but all teeth of a gear have the same surfaces. An example of such a generating process is the generation of Gleason's gearing.

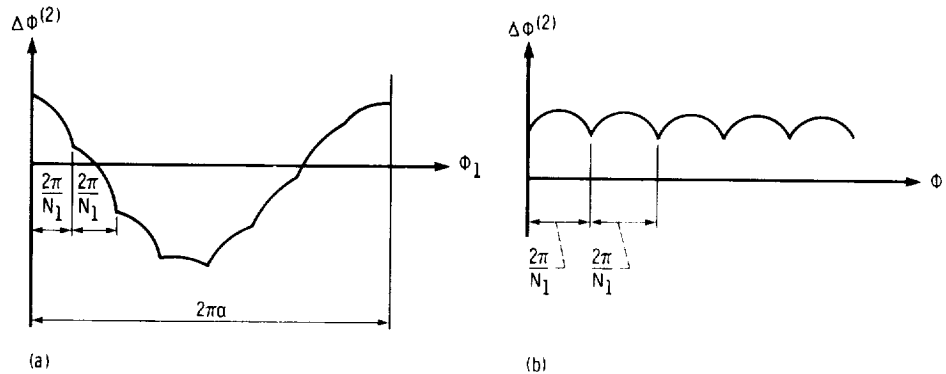


Figure 18.4.3.

18.5 Application of Theory to Eccentricity of Involute Spur Gears

Figure 18.5.1 shows two base circles of radii $r_b^{(1)}$ and $r_b^{(2)}$ for two involute spur gears. The rotation centers of the gears are designated by $O^{(1)}$ and $O^{(2)}$. The involute shapes are in tangency at point M of the line of action KL , if the centers of base circles O_i coincide with centers of rotation $O^{(i)}$ and vectors of gear eccentricity $\Delta \mathbf{e}_i = \overline{O^{(i)} O_i}$ ($i = 1, 2$) are zero.

To model the meshing of gears with eccentricity, we translate the gears from their theoretical positions by a distance $\overline{O^{(i)} O_i} = \Delta \mathbf{e}_i$, where $\Delta \mathbf{e}_i$ is the gear eccentricity. Now, center O_i of the base circle does not coincide with the center of gear rotation. After the displacement, the involute shapes are no more in tangency, rather they intersect each other or lose the contact.

To bring the involute shapes into tangency once again, it is sufficient to rotate gear 2 through a small angle $\Delta \phi^{(2)}$. Using equation (18.4.14), we obtain

$$(\Delta \phi^{(2)} \times \mathbf{r}_2^{(P)}) \cdot \mathbf{n}^{(M)} = (\Delta \mathbf{e}_1 - \Delta \mathbf{e}_2) \cdot \mathbf{n}^{(M)} \quad (18.5.1)$$

The triple product results in (fig. 18.5.1)

$$(\Delta \phi^{(2)} \times \mathbf{r}_2^{(P)}) \cdot \mathbf{n}^{(M)} = \Delta \phi^{(2)} r_2^{(P)} \cos \psi_c \quad (18.5.2)$$

where ψ_c is the pressure angle. Vectors of eccentricity $\Delta \mathbf{e}_1$ and $\Delta \mathbf{e}_2$ form angles β_1 and β_2 with vector $\overline{O^{(1)} O^{(2)}}$; these angles are measured in the direction of gear rotation (fig. 18.5.1). The scalar products yield

$$\Delta \mathbf{e}_1 \cdot \mathbf{n}^{(M)} = \Delta e_1 \sin(\psi_c + \beta_1) \quad (18.5.3)$$

$$\Delta \mathbf{e}_2 \cdot \mathbf{n}^{(M)} = \Delta e_2 \sin(\psi_c + \beta_2)$$

From equations (18.5.1) to (18.5.3), we obtain

$$\Delta \phi^{(2)} = \frac{\Delta e_1 \sin(\beta_1 + \psi_c) + \Delta e_2 \sin(\beta_2 - \psi_c)}{r_b^{(2)}} \quad (18.5.4)$$

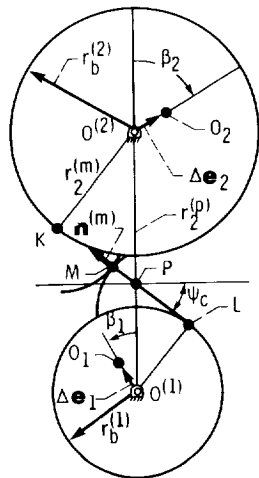


Figure 18.5.1.

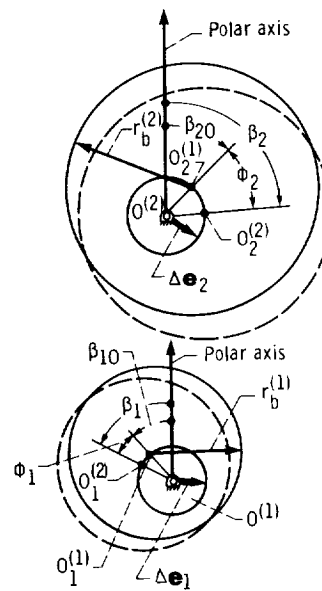


Figure 18.5.2.

where the radius of the base circle of gear 2 is

$$r_b^{(2)} = r_2^{(P)} \cos \psi_c \quad (18.5.5)$$

The center O_i ($i = 1, 2$) of the base circle rotates in the process of meshing; $O_i^{(1)}$ and $O_i^{(2)}$ are two instantaneous positions of this center (fig. 18.5.2). Angles β_1 and β_2 may be represented as follows:

$$\beta_1 = \beta_{1O} + \phi_1 \quad \beta_2 = \beta_{2O} + \phi_2 \quad (18.5.6)$$

where β_{1O} and β_{2O} correspond to the initial positions of centers O_1 and O_2 , with $\phi_1 = \phi_2 = 0$. Equations (18.5.4) and (18.5.6) yield

$$\Delta\theta^{(2)} = \frac{\Delta e_1 \sin(\phi_1 + \gamma_1) + \Delta e_2 \sin(\phi_2 + \gamma_2)}{r_b^{(2)}} \quad (18.5.7)$$

where $\gamma_1 = (\beta_{1O} + \psi_c)$ and $\gamma_2 = (\beta_{2O} - \psi_c)$.

For convenience, consider the kinematic error function to have zero magnitude at $\phi^{(1)} = \phi^{(2)} = 0$. Then, the kinematic error becomes

$$\begin{aligned} \Delta\theta^{(2)} &= \Delta\phi^{(2)}(\phi_1) - \Delta\phi^{(2)}(0) = \\ &= \frac{\Delta e_1 [\sin(\phi_1 + \gamma_1) - \sin \gamma_1]}{r_b^{(1)}} m_{21} + \frac{\Delta e_2 [\sin(\phi_2 + \gamma_2) - \sin \gamma_2]}{r_b^{(2)}} \end{aligned} \quad (18.5.8)$$

where $m_{21} = \omega^{(2)}/\omega^{(1)} = r_b^{(1)}/r_b^{(2)} = N_1/N_2$. Equation (18.5.8) represents the kinematic error of a gear train with two gears as the sum of two harmonics. The periods of these harmonics are equal to the periods of complete revolutions of the gears.

Equation (18.5.8) may be represented symmetrically as follows:

$$\begin{aligned} \Delta\theta^{(2)} &= \frac{\Delta e_1 [\sin(\phi_1 + \gamma_1) - \sin \gamma_1]}{r_b^{(1)}} m_{21} + \frac{\Delta e_2 [\sin(\phi_2 + \gamma_2) - \sin \gamma_2]}{r_b^{(2)}} m_{22} \\ &= \sum_{i=1}^2 \frac{\Delta e_i [\sin(\phi_i + \gamma_i) - \sin \gamma_i]}{r_b^{(i)}} \end{aligned} \quad (18.5.9)$$

Here, $m_{22} = 1$ and $\phi_2 = \phi_1 m_{21}$.

Equation (18.5.9) may be generalized for a train with n gears as follows:

$$\Delta\theta^{(n)} = \sum_{i=1}^n \frac{\Delta e_i [\sin(\phi_i + \gamma_i) - \sin \gamma_i]}{r_b^{(i)}} m_{ni} \quad (18.5.10)$$

where $\Delta\theta^{(n)}$ is the resulting kinematic error of the gear train represented as the angle of rotation of gear n (the output gear).

A complicated gear train is a combination of pairs of gears. The parameter γ_1 may be represented as

$$\gamma_i = \beta_{iO} + \psi_c$$

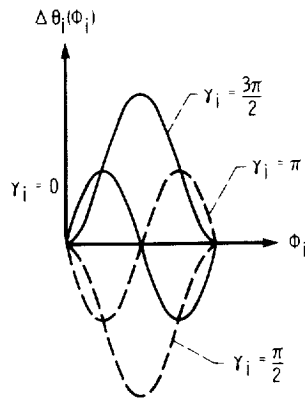


Figure 18.5.3.

for the driving gear of the pair, and as

$$\gamma_i = \beta_{iO} - \psi_c$$

for the driven gear of the pair. For instance, for computational purposes, a train of three gears must be replaced by two pairs of gears. The idler (intermediate gear) is considered as the driven gear in the first pair, and as the driving gear in the second pair.

We designate the kinematic error exerted by the eccentricity Δe_i of gear number i as

$$\Delta\theta_i = \frac{\Delta e_i [\sin(\phi_i + \gamma_i) - \sin \gamma_i]}{r_b^{(i)}} \quad (18.5.11)$$

where $\Delta\theta_i$ is the error of the rotation angle ϕ_i . The maximum possible value of this error is

$$\Delta\theta_{i\max} - \Delta\theta_{i\min} = \frac{2 \Delta e_i}{r_b^{(i)}} \quad (18.5.12)$$

The kinematic error of the train may be represented as

$$\Delta\theta^{(n)} = \sum_{i=1}^n \Delta\theta_i m_{ni} \quad (18.5.13)$$

Gear trains are usually applied for the reduction of angular velocities and thus m_{ni} is less than 1. It results from equation (18.5.13) that the last gears of a train (numbers $n, n-1, n-2$) induce the largest part of the resultant kinematic error $\Delta\theta^{(n)}$. Therefore, the precision of these gears must be higher than the others.

The largest value of the kinematic error function $\Delta\theta^{(n)}$ and its distribution above and below the abscissa depends on the combination of parameters γ_i ($i = 1, 2, \dots, n$). Figure (18.5.3) shows the distribution of a function $\Delta\theta_i(\phi_i)$ exerted by eccentricity of gear i of the train.

The resulting errors of a gear train may be compensated partly by using definite rules of assembly of gears with eccentricity. For instance, for gears with tooth numbers $N_1 = N_2$ and equal eccentricities $\Delta e_1 = \Delta e_2$, the resultant kinematic error will be approximately zero if the eccentricity vectors Δe_1 and Δe_2 (fig. 18.5.1) are directed opposite each other.

18.6 Application of Theory to Eccentricity of Spiral Bevel Gears

For spatial gears the term “eccentricity” is used to describe that the geometrical axis of a gear is parallel to, but does not coincide with, its axis of rotation (fig. 18.6.1). As the eccentric gear rotates, its geometrical axis generates a cylindrical surface of radius Δe . The eccentricity vector Δe is a vector which rotates about the gear axis. The initial position of vector Δe (its position at the beginning of motion) is given by angle α (fig. 18.6.1).

Figure (18.6.2) shows coordinate systems $S_1(x_1, y_1, z_1)$ and $S_f(x_f, y_f, z_f)$ which are rigidly connected to gear 1 and the frame, respectively. System S_h is an auxiliary coordinate system, which is also rigidly connected to the frame. Driving gear 1 rotates about axis z_h . The position of Δe_1 in coordinate system S_1 is given by the angle α_1 , which is made by Δe_1 and axis x_1 . The current position of Δe_1 in coordinate system S_f (or S_h) is determined by the angle $(\phi_1 + \alpha_1)$ and the matrix equation

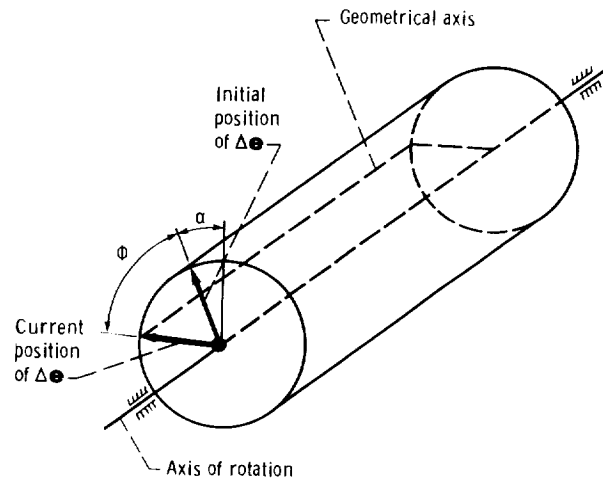


Figure 18.6.1.

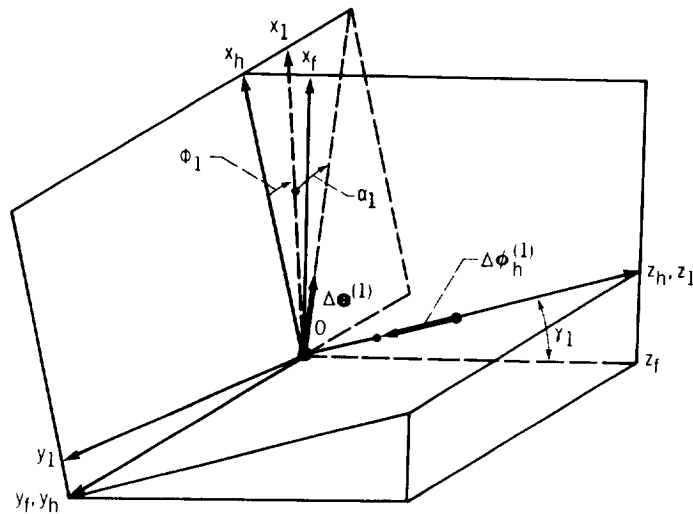


Figure 18.6.2.

$$[\Delta e_f^{(1)}] = [L_{fh}] [\Delta e_h^{(1)}] = \begin{bmatrix} \cos \gamma_1 & 0 & \sin \gamma_1 \\ 0 & 1 & 0 \\ -\sin \gamma_1 & 0 & \cos \gamma_1 \end{bmatrix} \begin{bmatrix} \Delta e_1 \cos (\phi_1 + \alpha_1) \\ -\Delta e_1 \sin (\phi_1 + \alpha_1) \\ 0 \end{bmatrix} \quad (18.6.1)$$

Here $[\Delta e_h^{(1)}]$ is the matrix of vector Δe_1 , which is represented in the coordinate system S_h . The 3×3 matrix $[L_{fh}]$ transforms elements of the column matrix $[\Delta e_h^{(1)}]$ to coordinate system S_f from the coordinate system S_h .

Matrix equation (18.6.1) yields

$$[\Delta e_f^{(1)}] = \begin{bmatrix} \Delta e_1 \cos (\phi_1 + \alpha_1) \cos \gamma_1 \\ -\Delta e_1 \sin (\phi_1 + \alpha_1) \\ -\Delta e_1 \cos (\phi_1 + \alpha_1) \sin \gamma_1 \end{bmatrix} \quad (18.6.2)$$

The vector of eccentricity of the driven gear may be determined similarly. Figure 18.6.3 shows coordinate systems S_2 and S_f rigidly connected to gear 2 and the frame, respectively. The auxiliary coordinate system S_p is also rigidly connected to the frame.

Vector $\Delta e_f^{(2)}$ is represented by matrix equation

$$[\Delta e_f^{(2)}] = [L_{fp}] [\Delta e_p^{(2)}] = \begin{bmatrix} \cos \gamma_2 & 0 & -\sin \gamma_2 \\ 0 & 1 & 0 \\ \sin \gamma_2 & 0 & \cos \gamma_2 \end{bmatrix} \begin{bmatrix} \Delta e_2 \cos (\phi_2 + \alpha_2) \\ \Delta e_2 \sin (\phi_2 + \alpha_2) \\ 0 \end{bmatrix} \quad (18.6.3)$$

which after matrix multiplication gives

$$[\Delta e_f^{(2)}] = \begin{bmatrix} \Delta e_2 \cos (\phi_2 + \alpha_2) \cos \gamma_2 \\ \Delta e_2 \sin (\phi_2 + \alpha_2) \\ \Delta e_2 \cos (\phi_2 + \alpha_2) \sin \gamma_2 \end{bmatrix} \quad (18.6.4)$$

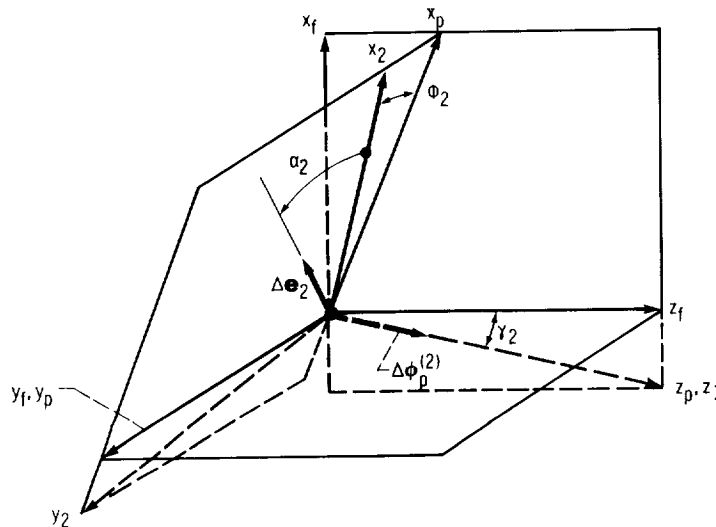


Figure 18.6.3.

Kinematic errors induced by gear eccentricities may now be found by using equation (18.4.9) as follows:

$$\left[\Delta\phi_f^{(2)} \rho_f^{(2)} \mathbf{n}_f^{(2)} \right] = \left(\Delta\mathbf{e}_f^{(1)} - \Delta\mathbf{e}_f^{(2)} \right) \bullet \mathbf{n}_f^{(2)} \quad (18.6.5)$$

Here $\Delta\mathbf{e}_f^{(1)}$ and $\Delta\mathbf{e}_f^{(2)}$ are given by matrices (18.6.2) and (18.6.4), and vector $\Delta\phi_f^{(2)}$ (fig. 18.6.3) is represented by the matrix

$$\left[\Delta\phi_f^{(2)} \right] = \left[L_{fp} \right] \left[\Delta\phi_p^{(2)} \right] = \begin{bmatrix} \cos \gamma_2 & 0 & -\sin \gamma_2 \\ 0 & 1 & 0 \\ \sin \gamma_2 & 0 & \cos \gamma_2 \end{bmatrix} \begin{bmatrix} 0 \\ 0 \\ \Delta\phi_2 \end{bmatrix} = \begin{bmatrix} -\Delta\phi_2 \sin \gamma_2 \\ 0 \\ \Delta\phi_2 \cos \gamma_2 \end{bmatrix} \quad (18.6.6)$$

Vector $\rho_f^{(2)}$ represents the position vector of the contact point which lies on the line of action of the gears and \mathbf{n}_f represents the common unit normal of the gear surfaces at their point of tangency.

Equations (18.6.5) and (18.6.6) yield

$$\Delta\phi_2 = \frac{n_x \Sigma\Delta e_x + n_y \Sigma\Delta e_y + n_z \Sigma\Delta e_z}{-y \cos \gamma_2 n_x + (x \cos \gamma_2 + z \sin \gamma_2) n_y - y \sin \gamma_2 n_z} \quad (18.6.7)$$

where

$$\Sigma\Delta e_x = \Delta e_x^{(1)} - \Delta e_x^{(2)}, \quad \Sigma\Delta e_y = \Delta e_y^{(1)} - \Delta e_y^{(2)}, \quad \text{and} \quad \Sigma\Delta e_z = \Delta e_z^{(1)} - \Delta e_z^{(2)}$$

(the subscript f was dropped).

Projections n_y and n_z of the surface unit normal \mathbf{n} , and coordinates x , y , and z of the contact point change in the process of motion. But since the changes in these variables are relatively small, they may be neglected. The surface unit normal \mathbf{n}_f and the point of contact P may be represented as follows (fig. 18.6.4).

$$\mathbf{n}_f = \sin \psi_c \mathbf{i}_f + \cos \psi_c (\cos \beta \mathbf{j}_f + \sin \beta \mathbf{k}_f) \quad (18.6.8)$$

$$x_f = 0 \quad y_f = 0 \quad z_f = L \quad (18.6.9)$$

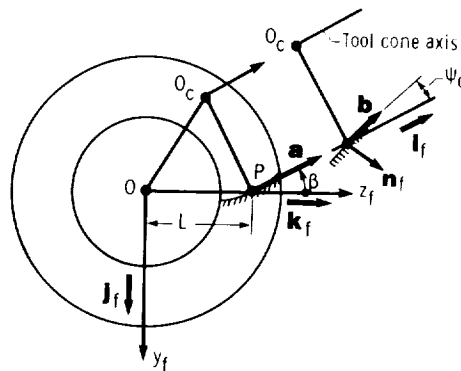


Figure 18.6.4.

The derivation of equations (18.6.8) and (18.6.9) is based on the following considerations:

(1) Axis z_f is the instantaneous axis of rotation of the generating gear and the gear being generated.

(2) Point P is the point of tangency of the gear-tooth surfaces, because it lies on the axis of instantaneous rotation.

(3) The common surface unit normal to gear-tooth surfaces, \mathbf{n}_f , coincides with the unit normal to the generating surface which is the cone surface. Vector \mathbf{n}_f is determined as follows:

$$\mathbf{n}_f = \mathbf{a} \times \mathbf{b}$$

where \mathbf{a} and \mathbf{b} are two unit vectors which are mutually perpendicular (fig. 18.6.4).

Equations (18.6.7) to (18.6.9) yield

$$\Delta\phi_2(\phi_1) = \frac{A(\phi_1)}{L \sin \gamma_2 \cos \psi_c \cos \beta} \quad (18.6.10)$$

where

$$A(\phi_1) = a_1 \sin(\phi_1 + \alpha_1) + b_1 \cos(\phi_1 + \alpha_1)$$

$$+ a_2 \sin(\phi_2 + \alpha_2) + b_2 \cos(\phi_2 + \alpha_2)$$

$$a_1 = -\Delta e_1 \cos \psi_c \cos \beta$$

$$a_2 = -\Delta e_2 \cos \psi_c \cos \beta$$

$$b_1 = \Delta e_1 (\cos \gamma_1 \sin \psi_c - \sin \gamma_1 \cos \psi_c \sin \beta)$$

$$b_2 = -\Delta e_2 (\cos \gamma_2 \sin \psi_c + \sin \gamma_2 \cos \psi_c \sin \beta)$$

$$\phi_2 = \phi_1 \frac{N_1}{N_2}$$

Equation (18.6.10) yields that the kinematic errors caused by the eccentricity of spiral-bevel gears may be represented as the sum of four harmonics: the period of two harmonics coincides with the period of revolution of gear 1; and the period of the other two coincides with the period of revolution of gear 2.

Function $\Delta\phi_2(\phi_1)$, represented by equation (18.6.10), is a smooth function with continuous derivatives which serves as a first approximation. In reality, the derivative of function $\phi_2(\phi_1)$ breaks as different sets of teeth come into mesh. (See fig. 18.4.3(a).) This break can be discovered if $\Delta\phi_2(\phi_1)$ is determined by equation (18.6.7).

18.7 Backlash of Spur Gears

The driving gear 1, if reversed, puts into motion the driven gear not right away, but only after the driving gear is rotated through a small angle. The contact of gear-tooth surfaces stops temporarily if the gear motion is reversed for the following reasons: (1) There is a backlash between the teeth on the other side; and (2) because of the change of direction of the elastic torsion of the gear shafts. The backlash between the surfaces depends on the errors of the center distance, errors of the distance between the teeth, shape errors, and gears eccentricity. The magnitude of the backlash is changed in the process of meshing due to the gears eccentricity.

Consider two mating gears without errors. The direction of rotation of the driving gear (gear 1) is indicated by k (fig. 18.7.1) and M is the point of contact for the indicated direction of rotation.

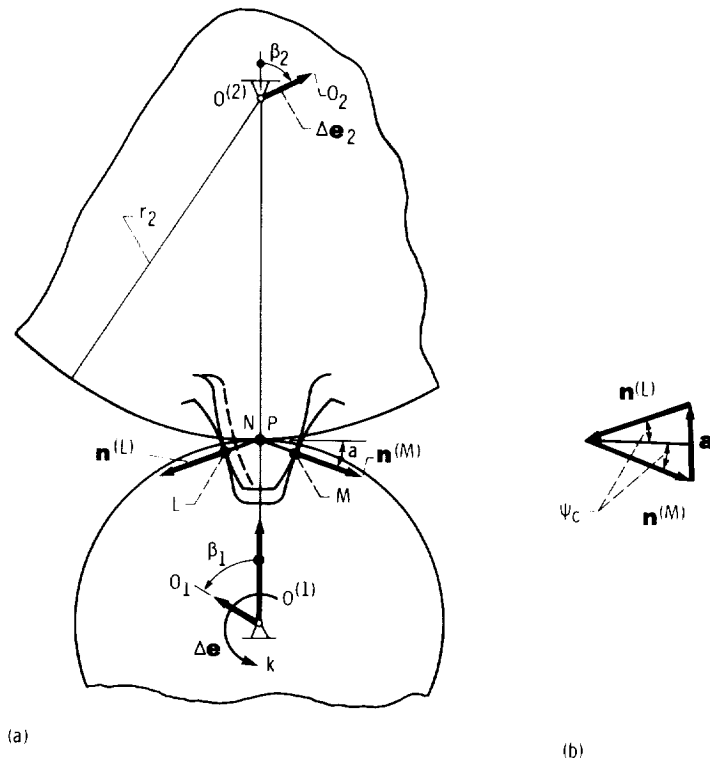


Figure 18.7.1.

Assuming that the backlash is zero, we say that the nonworking shapes (shapes on the other side of teeth) are in tangency at point L . Because of gear errors, the shapes will be jammed if the backlash is zero. To avoid this, we have to foresee a backlash magnitude. We designate the vector of initial backlash at point L by \overline{NL} . This vector is directed along $\mathbf{n}^{(L)}$ —the unit normal to the nonworking shapes at L .

We have to differentiate between two types of backlash which may be exerted at point M and point N , respectively. Consider first that the mating gears do not have errors and the gear-tooth surfaces contact each other at point M . We then consider new conditions—the contact of tooth surfaces of gears 1 and 2 having some errors $\Sigma\Delta q_i^{(1)}$ and $\Sigma\Delta q_j^{(2)}$, respectively. Because of these errors gear-tooth surfaces cannot contact each other at M until gear 2 will be turned through a small angle $\Delta\theta_2^{(M)}$. We may determine this angle ($\Delta\theta_2^{(M)}$) by using the following equation (it is similar to equation (18.4.14)):

$$\left[(\Delta\theta_2^{(M)} \times \mathbf{r}_2^{(P)}) + \Sigma\Delta q_j^{(2)} - \Sigma\Delta q_i^{(1)} \right] \cdot \mathbf{n}^{(M)} = 0 \quad (18.7.1)$$

The superscript M in $\Delta\theta_2^{(M)}$ indicates that we consider the angle of turn of gear 2 with which the contact of working shapes at M can be reestablished again. However, the turn of gear 2 changes the initial backlash at N between the nonworking shapes.

Consider then that we try to put the nonworking shapes into contact at N . We can obtain this contact by turning of gear 2 through an angle $\Delta\theta_2^{(N)}$ (the superscript N in $\Delta r_2^{(N)}$ indicates that contact at N is provided). We determine $\Delta\theta_2^{(N)}$ by using the following equation

$$\left[(\Delta\theta_2^{(N)} \times \mathbf{r}_2^{(M)}) + \Sigma\Delta\mathbf{Q}^{(2)} \right] \cdot \mathbf{n}^{(N)} = 0 \quad (18.7.2)$$

Here vector $\Sigma\Delta\mathbf{Q}^{(2)}$ represents all of the “errors” which induce a backlash N ; this vector is represented by

$$\Sigma\Delta\mathbf{Q}^{(2)} = (\Delta\theta_2^{(M)} \times \mathbf{r}_2^{(P)}) + \Sigma\Delta q_j^{(2)} - \Sigma\Delta q_i^{(1)} + \overline{NL} \quad (18.7.3)$$

Equations (18.7.2) and (18.7.3) yield

$$\left[\left(\Delta\theta_2^{(N)} \times \mathbf{r}_2^{(N)} \right) + \left(\Delta\theta_2^{(M)} \times \mathbf{r}_2^{(P)} \right) + \Sigma\Delta\mathbf{q}_j^{(2)} - \Sigma\Delta\mathbf{q}_i^{(1)} + \overline{LN} \right] \bullet \mathbf{n}^{(N)} = 0 \quad (18.7.4)$$

The further transformation of equation (18.7.4) is based on the following considerations:

(1) The unit vectors $\mathbf{n}^{(M)}$ and $\mathbf{n}^{(N)}$ make an angle $2\psi_c$, where ψ_c is the pressure angle.

Thus

$$\mathbf{n}^{(N)} + \mathbf{n}^{(M)} + \mathbf{a} = 0 \quad (18.7.5)$$

Here $|\mathbf{a}| = 2 \sin \psi_c$ and vector \mathbf{a} has the same direction as vector $\overline{O^{(1)}O^{(2)}}$ of the shortest center distance.

Equation (18.7.5) yields

$$\mathbf{n}^{(N)} = -(\mathbf{n}^{(M)} + \mathbf{a}) \quad (18.7.6)$$

(2) Using equations (18.7.4), (18.7.6), and (18.7.1), we get

$$\begin{aligned} & - \left[\left(\Delta\theta_2^{(N)} \times \mathbf{r}_2^{(N)} \right) + \left(\Delta\theta_2^{(M)} \times \mathbf{r}_2^{(P)} \right) + \Sigma\Delta\mathbf{q}_j^{(2)} - \Sigma\Delta\mathbf{q}_i^{(1)} + \overline{LN} \right] \bullet (\mathbf{n}^{(M)} + \mathbf{a}) \\ & = \left[\left(\Delta\theta_2^{(N)} \times \mathbf{r}_2^{(N)} \right) + \overline{LN} \right] \bullet \mathbf{n}^{(N)} - \left[\left(\Delta\theta_2^{(M)} \times \mathbf{r}_2^{(P)} \right) + \Sigma\Delta\mathbf{q}_j^{(2)} - \Sigma\Delta\mathbf{q}_i^{(1)} \right] \bullet (\mathbf{n}^{(M)} + \mathbf{a}) \\ & = \left[\left(\Delta\theta_2^{(N)} \times \mathbf{r}_2^{(N)} \right) + \overline{LN} \right] \bullet \mathbf{n}^{(N)} - \left[\left(\Delta\theta_2^{(M)} \times \mathbf{r}_2^{(P)} \right) + \Sigma\Delta\mathbf{q}_j^{(2)} - \Sigma\Delta\mathbf{q}_i^{(1)} \right] \bullet \mathbf{a} = 0 \end{aligned} \quad (18.7.7)$$

Then, we have that

$$\left[\Delta\theta_2^{(M)} \mathbf{r}_2^{(P)} \mathbf{a} \right] = 0 \quad (18.7.8)$$

because of the collinearity of vectors $\mathbf{r}_2^{(P)}$ and \mathbf{a} .

Equations (18.7.8) and (18.7.7) yield

$$\left(\Delta\theta_2^{(N)} \times \mathbf{r}_2^{(N)} \right) \bullet \mathbf{n}^{(N)} = \left(\Sigma\Delta\mathbf{q}_j^{(2)} - \Sigma\Delta\mathbf{q}_i^{(1)} \right) \bullet \mathbf{a} + \Delta b_n \quad (18.7.9)$$

Here

$$\Delta b_n = -(\overline{LN} \bullet \mathbf{n}^{(L)}) = \overline{NL} \bullet \mathbf{n}^{(L)} \quad (18.7.10)$$

is the initial backlash NL measured from N to L along the unit normal $\mathbf{n}^{(L)}$.

(3) A further simplification of equation (18.7.9) is based on the following:

$$\mathbf{r}_2^{(N)} = \mathbf{r}^{(P)} + \overline{PN} \quad \left[\Delta\theta_2^{(N)} \mathbf{r}_2^{(N)} \mathbf{n}^{(N)} \right] = \left[\Delta\theta_2^{(N)} \mathbf{r}_2^{(P)} \mathbf{n}^{(N)} \right] \quad (18.7.11)$$

because $\left[\Delta\theta_2^{(N)} \overline{PN} \mathbf{n}^{(L)} \right] = 0$, due to the collinearity of vectors \overline{PN} and $\mathbf{n}^{(L)}$.

Equations (18.7.9) and (18.7.11) yield

$$\left(\Delta\theta_2^{(N)} \times \mathbf{r}_2^{(P)} \right) \bullet \mathbf{n}^{(L)} = \left(\Sigma\Delta\mathbf{q}_j^{(2)} - \Sigma\Delta\mathbf{q}_i^{(1)} \right) \bullet \mathbf{a} + \Delta b_n \quad (18.7.12)$$

It is easy to verify that

$$\left[\Delta\theta_2^{(N)} \mathbf{r}_2^{(P)} \mathbf{n}^{(L)} \right] = \Delta\theta_2^{(N)} r_2^{(P)} \cos \psi_c = \Delta\theta_2^{(N)} r_{b2} \quad (18.7.13)$$

where r_{b2} is the radius of the base circle of gear 2; $\Delta\theta_2^{(N)}$ is positive if gear 2 is rotated counterclockwise.

The final equation is

$$\Delta\theta_2^{(N)} = \frac{(\Sigma\Delta\mathbf{q}_j^{(2)} - \Sigma\Delta\mathbf{q}_i^{(1)}) \cdot \mathbf{a} + \Delta b_n}{r_{b2}} \quad (18.7.14)$$

Using this equation, we can determine the backlash $\Delta\theta_2^{(N)}$ in radians induced by errors of gears.

Example problem 18.7.1 Consider that the acting error is the increment ΔC of the center distance due to the displacement of the rotation center of gear 2. Determine the angular backlash $\Delta\theta_2^{(N)}$ (take $\Delta b_n = 0$).

Solution. Using equation (18.7.14), we get

$$\Delta\theta_2^{(N)} = \frac{\Delta C \cdot \mathbf{a}}{r_{b2}} = \frac{2 \Delta C \sin \psi_c}{r_{b2}} = \frac{2 \Delta C}{r_2} \tan \psi_c \quad (18.7.15)$$

where r_2 is the pitch radius of gear 2.

Example problem 18.7.2 Given the eccentricity vectors $\Delta\mathbf{e}_1 = \Delta\mathbf{q}_1^{(1)}$ and $\Delta\mathbf{e}_2 = \Delta\mathbf{q}_1^{(2)}$ of gears 1 and 2, respectively (fig. 18.7.1(a)). Determine the angular backlash induced by the eccentricity of gears.

Solution. Using equation (18.7.14), we obtain

$$\Delta\theta_2^{(N)} = \frac{(\Delta\mathbf{e}_2 - \Delta\mathbf{e}_1) \cdot \mathbf{a} + \Delta b_n}{r_{b2}} = \frac{2 \sin \psi_c (\Delta e_2 \cos \beta_2 - \Delta e_1 \cos \beta_1) + \Delta b_n}{r_{b2}} \quad (18.7.16)$$

Here $|\mathbf{a}| = 2 \sin \psi_c$ and vectors $\Delta\mathbf{e}_2$ and $\Delta\mathbf{e}_1$ make angles β_2 and β_1 , respectively with vector \mathbf{a} which is directed along $O^{(1)}O^{(2)}$. We represent angles β_2 and β_1 as follows

$$\beta_2 = \beta_{20} - \phi_2, \text{ and } \beta_1 = \beta_{10} + \phi_1 \quad (18.7.17)$$

where β_{10} and β_{20} determine the initial positions of eccentricity vectors, and ϕ_2 and ϕ_1 are the angles of rotation of the gears.

Equations (18.7.16) and (18.7.17) yield

$$\Delta\theta_2^{(N)} = \frac{2 \sin \psi_c [\Delta e_2 \cos (\beta_{20} - \phi_2) - \Delta e_1 \cos (\beta_{10} + \phi_1)] + \Delta b_n}{r_{b2}} \quad (18.7.18)$$

Here Δb_n is the constant part of the linear backlash represented in inches; $\Delta\theta_2^{(N)}(\phi_1)$ is the variable part of the angular backlash represented in radians.

The gear teeth will not be jammed if

$$\Delta\theta_2^{(N)}(\phi_1) > 0 \quad 0 \leq \phi_1 \leq 2\pi n_1 \quad \phi_2 = \phi_1 \frac{N_2}{N_1} \quad (18.7.19)$$

where n_1 is the number of revolutions of gear 1, which determines the period of function $\Delta\theta_2^{(N)}(\phi_1)$, and N_2 and N_1 are the numbers of gear teeth. Using equation (18.7.18) and expression (18.7.19), we may determine the initial backlash Δb_n with which we can avoid the tooth jam.

18.8 Application of Theory to Transformation of Rotation With a Varied Ratio by Eccentric Gears

Noncircular gears are applied for transformation of rotation with a nonlinear relation between the angles of gear rotation. For some cases, eccentric gears can be used instead of noncircular gears. However, the application of eccentric gears is limited due to the jamming of gear teeth which have great magnitudes of eccentricities. The danger of the jamming of teeth is substantially decreased if identical eccentric gears are applied. Equation (18.7.18) yields that

$$\Delta\theta^{(N)} = \frac{\Delta b_n}{r_{b2}} \quad (18.8.1)$$

if $\Delta e_1 = \Delta e_2$, $N_1 = N_2$, and $\beta_{1O} = \beta_{2O}$.

Thus $\Delta\theta_2^{(N)}$ is constant (it does not change in the process of meshing). The position function of such eccentric gears may be determined with equation (18.5.4). Taking in this equation $\Delta e_1 = \Delta e_2 = \Delta e$, $\phi_1 = \phi_2 = \phi$, and $\beta_{1O} = \beta_{2O} = \beta_O$, we get

$$\Delta\phi^{(2)} = \frac{2 \Delta e [\sin(\phi + \beta_O) \cos \psi_c]}{r_b^{(2)}} \quad (18.8.2)$$

Equation (18.8.2) represents the varied part of the angle of rotation of gear 2, ϕ_2 . The total angle of rotation of gear 2, $\phi^{(2)}$, is represented as follows:

$$\phi^{(2)} = \phi + \frac{2 \Delta e [\sin(\phi + \beta_O) \cos \psi_c]}{r_b^{(2)}} \quad (18.8.3)$$

where ϕ is the angle of rotation of gear 1, and $r_b^{(2)}$ is the radius of base circles of the gears.

18.9 Measurement of Rotation Angles With Eccentric Disks

The theory of eccentric gears may be also applied for the measurement of angles of rotation with eccentric disks. Such disks, provided with scores, are the basic part of optical, electro-optical, and electromagnetic instruments designed for the measurement of angles of rotation. Because of the eccentricity of disks, the angle of rotation registered by the instrument differs from the real angle of rotation. This error may be compensated if the angle of rotation is registered by taking signals (or reading the rotation angles) from the opposite scores that are located on the same diameter of the disk. Figure 18.9.1(a) shows a disk whose center of rotation is O and the geometric center is O_1 ; $\overline{OO_1} = \Delta e_1$ is the eccentricity vector; a is the fixed index; and M_O is the point of the disk which is under the index at the initial position. The eccentricity vector forms with OM_O at the initial position the angle β_O , which is measured from OM_O to OO_1 in the direction of disk rotation. While the disk is being rotated, the geometric center O_1 of the disk and the eccentricity vector rotate about O .

Consider that the disk was rotated about O through the angle ϕ and the position vector \overline{OM} coincides with \overline{Oa} . If the disk would be rotated about O_1 instead of O , point M would be under the index a after rotation through the angle $\phi_1 = M_O O_1 M$. The error of measurement of the angle of rotation is represented by

$$\Delta\phi = \phi_1 - \phi \quad (18.9.1)$$

It is evident from the drawings of figure 18.9.1(a) that

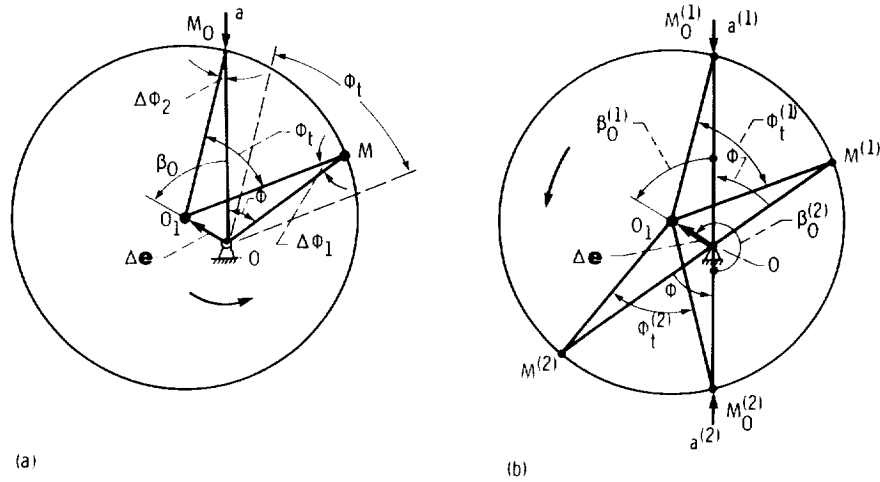


Figure 18.9.1.

$$\phi_t = \phi - \Delta\phi_2 + \Delta\phi_1 \quad (18.9.2)$$

where

$$\Delta\phi_1 = \widehat{O_1MO}, \text{ and } \Delta\phi_2 = \widehat{O_1M_0O} \quad (18.9.3)$$

Thus

$$\Delta\phi = \Delta\phi_1 - \Delta\phi_2 \quad (18.9.4)$$

Considering the triangles O_1MO and O_1M_0O , we get

$$\sin \Delta\phi_1 = \frac{\Delta e}{r} (\phi + \beta_0) \quad \sin \Delta\phi_2 = \frac{\Delta e}{r} \sin \beta_0 \quad (18.9.5)$$

Since $\Delta\phi_1$ and $\Delta\phi_2$ are small angles, we may represent equation (18.9.5) as follows:

$$\Delta\phi_1 = \frac{\Delta e}{r} \sin (\phi + \beta_0) \quad \Delta\phi_2 = \frac{\Delta e}{r} \sin \beta_0 \quad (18.9.6)$$

where r is the disk radius.

Equations (18.9.4) and (18.9.6) yield

$$\Delta\phi = \frac{\Delta e}{r} [\sin (\phi + \beta_0) - \sin \beta_0] \quad (18.9.7)$$

Equation (18.9.7) represents $\Delta\phi(\phi)$, the error of measurement of the angle of rotation caused by disk eccentricity.

The error $\Delta\phi(\phi)$ can be compensated for if the angle of rotation is registered with the aid of two indices which are located opposite each other at the line $a^{(1)}Oa^{(2)}$ (fig. 18.9.1(b)). Consider that point $M^{(1)}$ and $M^{(2)}$ are under the indices $a^{(1)}$ and $a^{(2)}$ at the initial position. The eccentricity vector $(\overline{OO_1})$ makes angles $\beta_0^{(1)}$ and $\beta_0^{(2)}$ with $\overline{Oa^{(1)}}$ and $\overline{Oa^{(2)}}$, respectively. Disk points $M^{(1)}$ and $M^{(2)}$ will be under $a^{(1)}$ and $a^{(2)}$, respectively, after the disk rotation through the angle ϕ .

However, the instrument will register angles $\phi_i^{(1)}$ and $\phi_i^{(2)}$ with the aid of indices $a^{(1)}$ and $a^{(2)}$, respectively. Here

$$\phi_i^{(1)} = \widehat{M_O^{(1)}O_1M^{(1)}}, \text{ and } \phi_i^{(2)} = \widehat{M_O^{(2)}O_1M^{(2)}} \quad (18.9.8)$$

Using equation (18.9.7), we may determine the errors of measurement as follows

$$\Delta\phi^{(1)} = \frac{\Delta e}{r} [\sin(\phi + \beta_O^{(1)}) - \sin\beta_O^{(1)}] \quad (18.9.9)$$

$$\Delta\phi^{(2)} = \frac{\Delta e}{r} [\sin(\phi + \beta_O^{(2)}) - \sin\beta_O^{(2)}] \quad (18.9.10)$$

where $\beta_O^{(2)} = \beta_O^{(1)} + \pi$ (fig. 18.9.1(b)). The superscripts 1 and 2 correspond to $a^{(1)}$ and $a^{(2)}$, respectively.

It is easy to verify that the true angle of rotation ϕ may be determined with the equation

$$\phi = \frac{\phi_i^{(1)} + \phi_i^{(2)}}{2} \quad (18.9.11)$$

where $\phi_i^{(1)}$ and $\phi_i^{(2)}$ are the angles which were registered by indices $a^{(1)}$ and $a^{(2)}$, respectively. Thus, using two indices, we may compensate the error of measurement exerted by the eccentricity of the disk.

The derivation of equation (18.9.11) is based on the following considerations:

(1) Equation (18.9.1) yields that

$$\phi^{(1)} = \phi + \Delta\phi^{(1)} \quad (18.9.12)$$

$$\phi^{(2)} = \phi + \Delta\phi^{(2)} \quad (18.9.13)$$

where $\Delta\phi^{(i)}$ ($i = 1, 2$) is the measurement error.

(2) Equations (18.9.9) and (18.9.10) yield that

$$\Delta\phi^{(1)} + \Delta\phi^{(2)} = 0 \text{ because } \beta_O^{(2)} = \beta_O^{(1)} + \pi$$

Thus $\phi_i^{(1)} + \phi_i^{(2)} = 2\phi + \Delta\phi^{(1)} + \Delta\phi^{(2)} = 2\phi$ and equation (18.9.11) is confirmed.

Chapter 19

Force Transmission

The problem of force transmission by spatial gears is related to the type of gear geometry. However, a general solution of this problem may be proposed. This solution is based on the use of geometric parameters of gear surfaces which are common for all types of gears. The proposed solution is applied in this book for helical and spur gears, worm-gear drives, and bevel gears.

19.1 Force Transmission of Gears With Crossed Axes

Force Transmission

Consider a gear mechanism with crossed axes of rotation—a worm-gear drive or a mechanism formed by two crossing helical gears (fig. 19.1.1(a)). We set up two fixed coordinate systems rigidly connected to the frame, $S_f(x_f, y_f, z_f)$ and $S_p(x_p, y_p, z_p)$. Gears 1 and 2 rotate about axes z_f and z_p , respectively, which form the crossing angle γ . This angle is measured counterclockwise from $\omega^{(1)}$ to $\omega^{(2)}$. Gear 1 is the driving gear and gear 2 is the driven gear. Gears 1 and 2 are loaded with the driving moment \mathbf{M}_d and the resisting moment \mathbf{M}_r . Here P is the pitch point and $O_fP = r_1$ and $O_pP = r_2$ are the radii of pitch cylinders; C is the shortest distance between the axes of rotation. Figure 19.1.1(b) shows the velocity polygon at point P . (See ch. 14.3.) The common tangent to the helices on the pitch cylinders is $t-t$; β_1 and β_2 are the angles formed between $t-t$ and the gear axes. Projections of vectors $\mathbf{v}^{(1)}$ and $\mathbf{v}^{(2)}$ on line Pm must be of the same magnitude and direction. (Line Pm is perpendicular to $t-t$.)

Considering as given the driving and resisting moments, \mathbf{M}_d and \mathbf{M}_r , we have to derive equations for the normal reaction $\mathbf{F}^{(12)}$ transmitted from gear 1 to gear 2. We assume that the gear-tooth surfaces contact each other at the pitch point, and $\mathbf{F}^{(12)}$ is directed along the common normal to the gear-tooth surfaces.

We recall that the normal to a surface Σ may be represented by (see ch. 8.3)

$$\mathbf{N} = \mathbf{a} \times \mathbf{b} \quad (19.1.1)$$

where \mathbf{a} and \mathbf{b} are the tangents to lines L_2 and L_1 on the surface (fig. 19.1.2(a)). Line L_2 is the line of intersection of gear-tooth surface Σ_2 with the pitch cylinder of radius r_2 (fig. 19.1.2(b)). The unit tangent to line L_2 , \mathbf{a} , makes an angle β_2 with the z_p -axis. Line L_1 on surface Σ_2 is the line of intersection of Σ_2 with plane $d-d$, which passes through point P and axis x_p , and is perpendicular to vector \mathbf{a} . The section of pitch cylinder represented by plane $d-d$ is the ellipse with axes $2r_2$ and $2r_2/\cos \beta_2$, respectively. The section of Σ_2 represented by plane $d-d$ defines the normal section of the surface. The unit tangent \mathbf{b} to the tooth shape in the normal section forms an angle

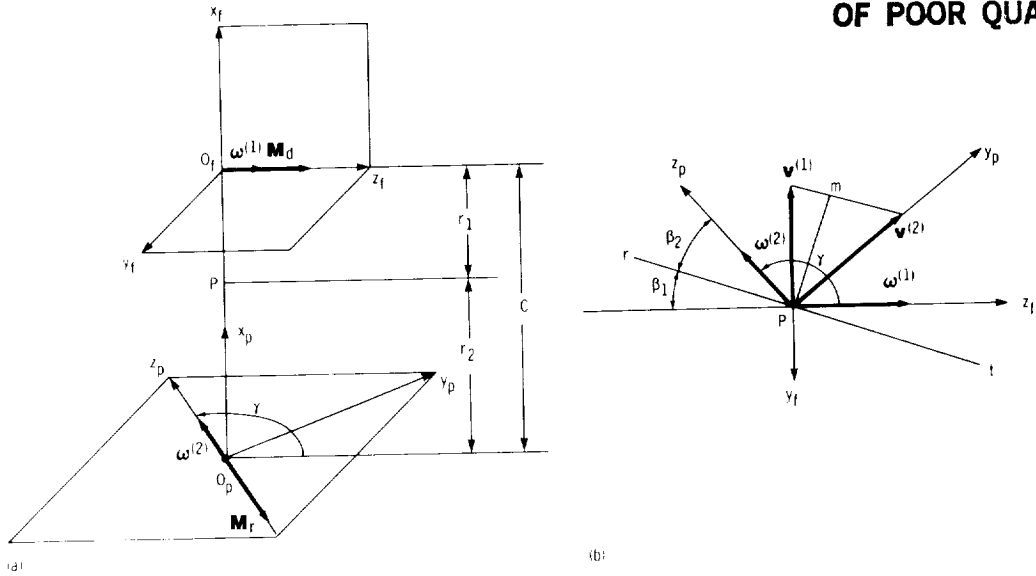


Figure 19.1.1.

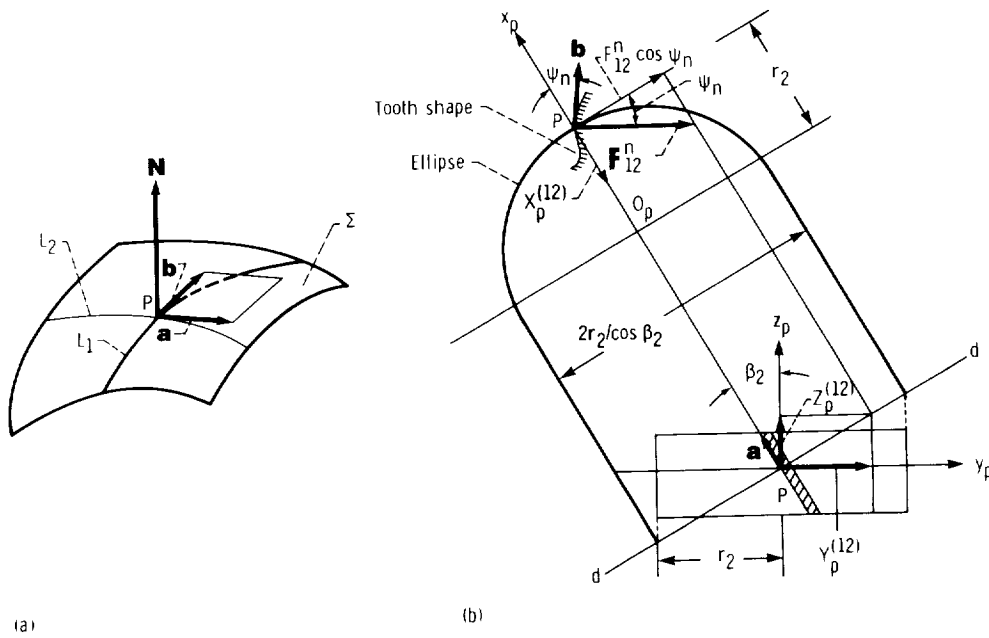


Figure 19.1.2.

ψ_n with the x_p -axis (ψ_n is the normal pressure angle). We represent vectors \mathbf{a} and \mathbf{b} in the coordinate system S_p as follows:

$$\mathbf{a} = -\sin \beta_2 \mathbf{j}_p + \cos \beta_2 \mathbf{k}_p \quad (19.1.2)$$

$$\mathbf{b} = \cos \psi_n \mathbf{i}_p + \sin \psi_n \cos \beta_2 \mathbf{j}_p + \sin \psi_n \sin \beta_2 \mathbf{k}_p \quad (19.1.2a)$$

where \mathbf{i}_p , \mathbf{j}_p , and \mathbf{k}_p are the unit vectors of the coordinate axes x_p , y_p , and z_p , respectively. The surface normal is represented by

$$\mathbf{N} = \mathbf{a} \times \mathbf{b} = \begin{vmatrix} \mathbf{i}_p & \mathbf{j}_p & \mathbf{k}_p \\ 0 & -\sin \beta_2 & \cos \beta_2 \\ \cos \psi_n \sin \psi_n \cos \beta_2 & \sin \psi_n \sin \beta_2 & \end{vmatrix}$$

$$= -\sin \psi_n \mathbf{i}_p + \cos \beta_2 \cos \psi_n \mathbf{j}_p + \sin \beta_2 \cos \psi_n \mathbf{k}_p \quad (19.1.3)$$

Since $|\mathbf{N}| = (N_{xp}^2 + N_{yp}^2 + N_{zp}^2)^{1/2} = 1$, we get that the surface unit normal is as follows:

$$n_{xp} = -\sin \psi_n \quad n_{yp} = \cos \psi_n \cos \beta_2 \quad n_{zp} = \cos \psi_n \sin \beta_2 \quad (19.1.4)$$

Equations (19.1.4) may be used for all types of worm-gear drives and helical gears.

We may now determine the contacting force $\mathbf{F}^{(12)}$ which is directed along the unit normal to the gear-tooth surfaces.

$$\mathbf{F}^{(12)} = F^{(12)} \mathbf{n}_p \quad (19.1.5)$$

Representing $\mathbf{F}^{(12)}$ in terms of $X_p^{(12)}$, $Y_p^{(12)}$, and $Z_p^{(12)}$, we obtain

$$X_p^{(12)} = -F^{(12)} \sin \psi_n \quad Y_p^{(12)} = F^{(12)} \cos \psi_n \cos \beta_2$$

$$Z_p^{(12)} = F^{(12)} \cos \psi_n \sin \beta_2 \quad (19.1.6)$$

Consider conditions of static equilibrium of gear 2. The gear is loaded with $\mathbf{F}^{(12)}$, \mathbf{M}_r , and reactions $\mathbf{F}^{(OA)}$ and $\mathbf{F}^{(OB)}$ (fig. 19.1.3) transmitted from bearings *A* and *B* (we neglect the forces of friction). The conditions of static equilibrium provide six equations. We may express the components of $\mathbf{F}^{(12)}$ in terms of the resisting moment \mathbf{M}_r and the geometric parameters β_2 and ψ_n by using one of the six equations, that is

$$[\mathbf{M}_r + (\overline{O_p P} \times \mathbf{F}^{(12)})] \cdot \mathbf{k}_p = 0 \quad (19.1.7)$$

Here (fig. 19.1.1(a))

$$\mathbf{M}_r = -M_r \cdot \mathbf{k}_p \quad (19.1.8)$$

and

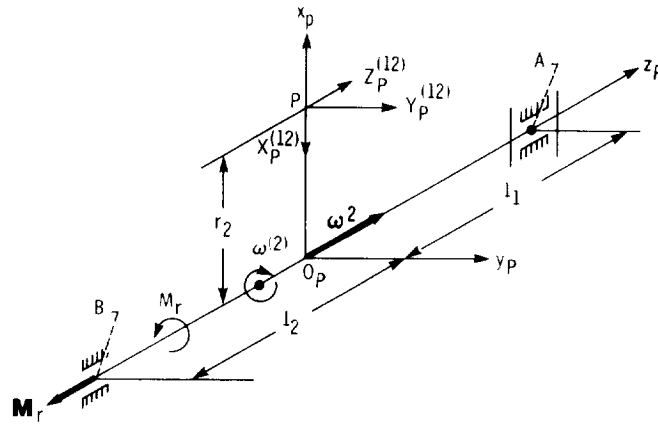


Figure 19.1.3.

$$\overline{O_p P} \times \mathbf{F}^{(12)} = \begin{vmatrix} \mathbf{i}_p & \mathbf{j}_p & \mathbf{k}_p \\ r_2 & 0 & 0 \\ X_p^{(12)} & Y_p^{(12)} & Z_p^{(12)} \end{vmatrix} \quad (19.1.9)$$

Equations from (19.1.7) to (19.1.9) and (19.1.6) yield

$$Y_p^{(12)} = \frac{M_r}{r_2} = F^{(12)} \cos \psi_n \cos \beta_2 \quad (19.1.10)$$

Thus, the contacting force is given by

$$F^{(12)} = \frac{M_r}{r_2 \cos \psi_n \cos \beta_2} \quad (19.1.11)$$

Using equations (19.1.6) and (19.1.11), we get

$$X_p^{(12)} = -\frac{M_r \tan \psi_n}{r_2 \cos \beta_2} \quad (19.1.12)$$

$$Y_p^{(12)} = \frac{M_r}{r_2} \quad (19.1.13)$$

$$Z_p^{(12)} = \frac{M_r}{r_2} \tan \beta_2 \quad (19.1.14)$$

Component $Z_p^{(12)}$ represents the thrust load of contacting force $\mathbf{F}^{(21)}$. The derivation of $\mathbf{F}^{(21)}$, which is transmitted from gear 2 to gear 1, is based on the following considerations:

$$(1) \mathbf{F}^{(21)} = -\mathbf{F}^{(12)} \quad (19.1.15)$$

and

(2) $\mathbf{F}^{(21)}$ is represented in the coordinate system S_f by using the matrix equation

$$[F_f^{(21)}] = -[L_{fp}][F_p^{(12)}] \quad (19.1.16)$$

Matrix $[L_{fp}]$ transforms projections of vectors in transition from the coordinate system S_p to S_f . This matrix is given by (fig. 19.1.1(a)):

$$[L_{fp}] = \begin{bmatrix} 1 & 0 & 0 \\ 0 & \cos \gamma & -\sin \gamma \\ 0 & \sin \gamma & \cos \gamma \end{bmatrix} \quad (19.1.17)$$

It is also known that

$$-[F_p^{(12)}] = [F_p^{(21)}] \quad (19.1.18)$$

where $[F_p^{(12)}]$ is the column matrix represented by equations (19.1.12) to (19.1.14). Equations (19.1.16) to (19.1.18) and (19.1.12) to (19.1.14) yield

$$X_f^{(21)} = \frac{M_r \tan \psi_n}{r_2 \cos \beta_2} \quad (19.1.19)$$

$$Y_f^{(21)} = -\frac{M_r \cos (\gamma + \beta_2)}{r_2 \cos \beta_2} \quad (19.1.20)$$

$$Z_f^{(21)} = -\frac{M_r \sin (\gamma + \beta_2)}{r_2 \cos \beta_2} \quad (19.1.21)$$

We may express components of $F^{(21)}$ in terms of M_d , β_1 , and ψ_n based on the following considerations:

(1) $\gamma = 180^\circ - (\beta_1 + \beta_2)$ (see fig. 19.1.1(b))

and

$$\gamma + \beta_2 = 180^\circ - \beta_1 \quad (19.1.22)$$

(2) The gear ratio is

$$m_{12} = \frac{\omega^{(1)}}{\omega^{(2)}} = \frac{r_2 \cos \beta_2}{r_1 \cos \beta_1}$$

(See sec. 14.3, figs. 14.3.2, 14.3.3, and fig. 19.1.1(b).)

(3) Since the friction forces are neglected, the power of gears 1 and 2 is the same and

$$M_d \omega^{(1)} = M_r \omega^{(2)}$$

Thus

$$M_r = \frac{M_d \omega^{(1)}}{\omega^{(2)}} = \frac{r_2 \cos \beta_2}{r_1 \cos \beta_1} M_d \quad (19.1.23)$$

Equations (19.1.18) to (19.1.22) yield

$$X_f^{(21)} = \frac{M_d \tan \psi_n}{r_1 \cos \beta_1} \quad (19.1.24)$$

$$Y_f^{(21)} = \frac{M_d}{r_1} \quad (19.1.25)$$

$$Z_f^{(21)} = -\frac{M_d}{r_1} \tan \beta_1 \quad (19.1.26)$$

Equations (19.1.12) to (19.1.14) and (19.1.24) to (19.1.26) may be used for all types of worm-gear drives, crossing helical gears and helical gears with parallel axes. However, we have to abide by the following rules: (1) The directions of axes z_f and z_p must coincide with the directions of $\omega^{(1)}$ and $\omega^{(2)}$, respectively, and the coordinate systems S_f and S_p must be right-handed. (2) Both gears must be left-handed. For a right-handed gear we have to change the sign of $\tan \beta_i$ in the derived equations. In the case of helical gears with parallel axes one of the gears is left-handed and the other is right-handed; however $|\beta_1| = |\beta_2|$.

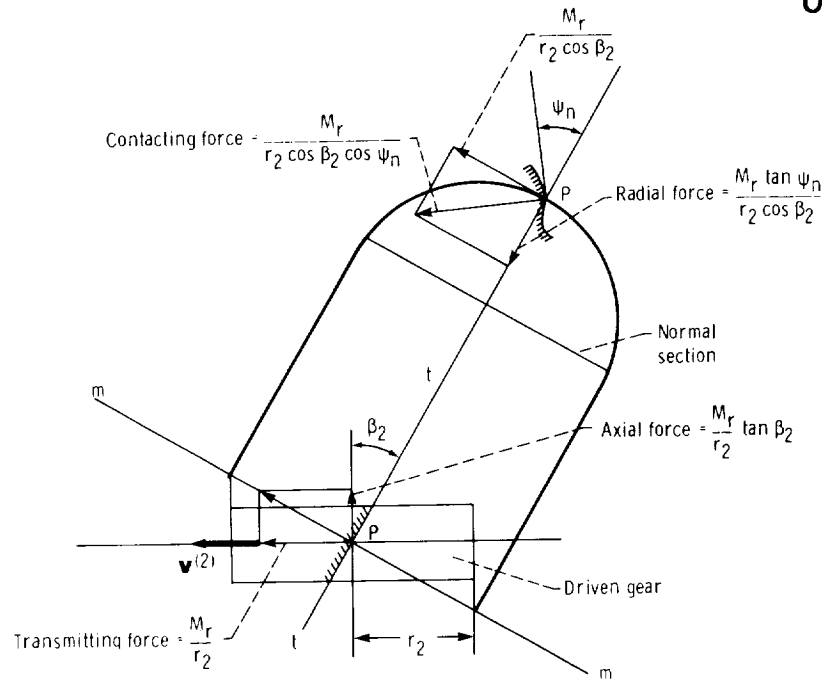


Figure 19.1.4.

In the case of spur gears, we make angles $\beta_1 = \beta_2 = 0$ in equations (19.1.11) to (19.1.14), (19.1.24), and (19.1.26), following the rule of orientation of the coordinate systems S_f and S_p . Axes z_f and z_p make an angle $\gamma = 180^\circ$ and 0° for external and internal spur gears, respectively.

The derivation of equations (19.1.12) to (19.1.14) may also be based upon geometric consideration (fig. 19.1.4). Consider that the driven gear rotates in the direction represented by vector $\mathbf{v}^{(2)}$. The direction of the transmitting force coincides with $\mathbf{v}^{(2)}$ and its magnitude is equal to M_r/r_2 . The direction and magnitude of the axial force are determined from the condition that the geometric sum of the transmitting and axial forces is perpendicular to line $t-t$ (which is the tangent to the helix at the pitch point P). Considering the normal section of the gear, we can determine the contacting force and the radial component.

Bearing Reactions

The determination of bearing reactions is based on equations of static equilibrium of the gear. Considering the driven gear (fig. 19.1.3), we may represent these equations as follows

$$\mathbf{F}^{(12)} + \mathbf{F}^{(OA)} + \mathbf{F}^{(OB)} = 0 \quad (19.1.27)$$

$$\left(\overline{OP} \times \mathbf{F}^{(12)} \right) + \left(\overline{OA} \times \mathbf{F}^{(OA)} \right) + \left(\overline{OB} \times \mathbf{F}^{(OB)} \right) + \mathbf{M}_r = 0 \quad (19.1.28)$$

Here $\mathbf{F}^{(12)}$ is the force transmitted from the driving gear which passes through the pitch point P . Force $\mathbf{F}^{(12)}$ is represented in the coordinate system S_p by equations (19.1.12) to (19.1.14). Reactions $\mathbf{F}^{(OA)}$ and $\mathbf{F}^{(OB)}$ are transmitted from the frame and pass through points A and B . Only one bearing, say A , resists not only the radial load but also the axial load.

We transform equation (19.1.28) as follows:

$$\overline{OP} \times \mathbf{F}^{(12)} = \begin{vmatrix} \mathbf{i}_p & \mathbf{j}_p & \mathbf{k}_p \\ r_2 & 0 & 0 \\ X_p^{(12)} & Y_p^{(12)} & Z_p^{(12)} \end{vmatrix} = \begin{bmatrix} 0 \\ -Z_p^{(12)} r_2 \\ Y_p^{(12)} r_2 \end{bmatrix} \quad (19.1.29)$$

$$\overline{O_p A} \times \mathbf{F}^{(OA)} = \begin{vmatrix} \mathbf{i}_p & \mathbf{j}_p & \mathbf{k}_p \\ 0 & 0 & \ell_1 \\ X_p^{(OA)} & Y_p^{(OA)} & Z_p^{(OA)} \end{vmatrix} = \begin{bmatrix} -Y_p^{(OA)} \ell_1 \\ X_p^{(OA)} \ell_2 \\ 0 \end{bmatrix} \quad (19.1.30)$$

$$\overline{O_p B} \times \mathbf{F}^{(OB)} = \begin{vmatrix} \mathbf{i}_p & \mathbf{j}_p & \mathbf{k}_p \\ 0 & 0 & -\ell_2 \\ X_p^{(OB)} & Y_p^{(OB)} & 0 \end{vmatrix} = \begin{bmatrix} Y_p^{(OB)} \ell_2 \\ -X_p^{(OB)} \ell_2 \\ 0 \end{bmatrix} \quad (19.1.31)$$

Equations (19.1.27) to (19.1.31) and (19.1.12) to (19.1.14) yield

$$X^{(OA)} = M_r \frac{\frac{\ell_2 \tan \psi_n}{r_2 \cos \beta_2} + \tan \beta_2}{\ell_1 + \ell_2} \quad (19.1.32)$$

$$Y^{(OA)} = -M_r \frac{\ell_2}{r_2 (\ell_1 + \ell_2)} \quad (19.1.33)$$

$$Z^{(OA)} = -\frac{M_r}{r_2} \tan \beta_2 \quad (19.1.34)$$

$$X^{(OB)} = M_r \frac{\frac{\ell_1 \tan \psi_n}{r_2 \cos \beta_2} - \tan \beta_2}{\ell_1 + \ell_2} \quad (19.1.35)$$

$$Y^{(OB)} = -M_r \frac{\ell_1}{r_2 (\ell_1 + \ell_2)} \quad (19.1.36)$$

The bearing reaction

$$\mathbf{F}^{(OA)} = X^{(OA)} \mathbf{i} + Y^{(OA)} \mathbf{j} + Z^{(OA)} \mathbf{k}$$

exerts a radial and axial load. The radial load in bearing A is given by

$$|\mathbf{F}_r^{(OA)}| = \sqrt{(X^{(OA)})^2 + (Y^{(OA)})^2} \quad (19.1.37)$$

and the axial load is given by

$$|\mathbf{F}_a^{(OA)}| = Z^{(OA)} \quad (19.1.38)$$

The bearing reaction

$$\mathbf{F}^{(OB)} = X^{(OB)} \mathbf{i} + Y^{(OB)} \mathbf{j}$$

exerts only a radial load represented by

$$|\mathbf{F}_r^{(OB)}| = |\mathbf{F}^{(OB)}| = \sqrt{(X^{(OB)})^2 + (Y^{(OB)})^2} \quad (19.1.39)$$

Similarly, we may determine reactions in the bearings of the driving gear by using equations of equilibrium for this gear.

19.2 Force Transmission for Spiral Bevel Gears

Surface Unit Normal

The mean contact point is represented in the fixed coordinate system S_f (fig. 19.2.1). We consider two lines on the gear-tooth surface and two unit tangents to these lines: (1) vector \mathbf{b}_f is the unit tangent to the longitudinal shape and (2) vector \mathbf{a}_f is the unit tangent to the tooth shapes in the normal section $A-A$. The normal to the tooth surface is represented as follows

$$\mathbf{N}_f = \mathbf{b}_f \times \mathbf{a}_f \quad (19.2.1)$$

Here

$$\mathbf{a}_f = \cos \psi_c \mathbf{i}_f + \sin \psi_c \cos \beta \mathbf{j}_f + \sin \psi_c \sin \beta \mathbf{k}_f \quad (19.2.2)$$

and

$$\mathbf{b}_f = -\sin \beta \mathbf{j}_f + \cos \beta \mathbf{k}_f \quad (19.2.3)$$

where \mathbf{i}_f , \mathbf{j}_f , and \mathbf{k}_f are the unit vectors of axes x_f , y_f , and z_f ; and ψ_c is the pressure angle in the normal section.

Using equation (19.2.1) to (19.2.3), we get

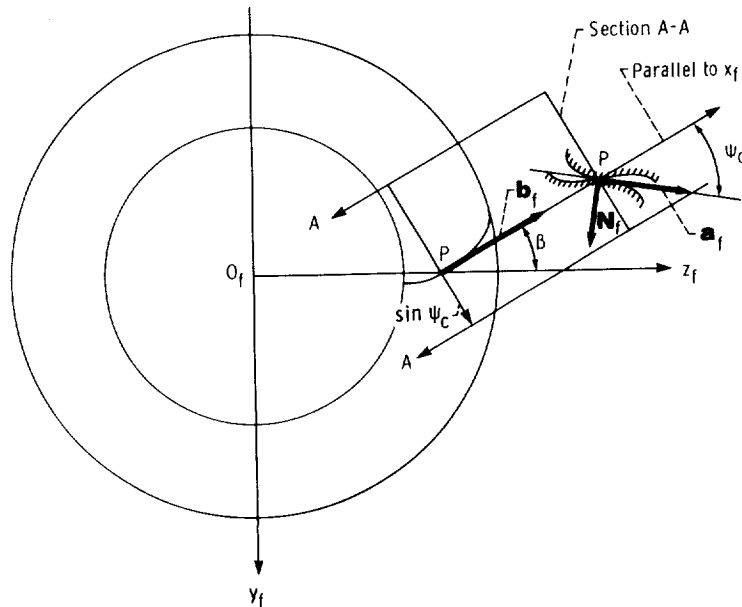


Figure 19.2.1.

$$\mathbf{N}_f = \begin{vmatrix} \mathbf{i}_f & \mathbf{j}_f & \mathbf{k}_f \\ 0 & -\sin \beta & \cos \beta \\ \cos \psi_c & \sin \psi_c \cos \beta & \sin \psi_c \sin \beta \end{vmatrix}$$

$$= -\sin \psi_c \mathbf{i}_f + \cos \psi_c \cos \beta \mathbf{j}_f + \cos \psi_c \sin \beta \mathbf{k}_f \quad (19.2.4)$$

The unit surface normal \mathbf{n}_f is given by the equation

$$\mathbf{n}_f = \frac{\mathbf{N}_f}{|\mathbf{N}_f|}$$

Equation (19.2.4) yields

$$|\mathbf{N}_f| = (N_{x_f}^2 + N_{y_f}^2 + N_{z_f}^2)^{1/2} = 1$$

and

$$[n_f] = \begin{bmatrix} -\sin \psi_c \\ \cos \psi_c \cos \beta \\ \cos \psi_c \sin \beta \end{bmatrix} \quad (19.2.5)$$

Contacting Force $\mathbf{F}^{(12)}$

The driven gear 2 is loaded with: (1) the resisting moment \mathbf{M}_r , (2) the contacting force $\mathbf{F}^{(12)}$, which is transmitted from gear 1, and (3) the bearing reactions. The contacting force is directed along the normal \mathbf{n}_f . To determine the contacting force and its components, we use the following procedure:

Step 1. – We must represent the surface unit normal in coordinate system S_p (fig. 19.2.2) whose axis z_p is the axis of gear rotation. Matrix equation

$$[n_p] = [L_{pf}][n_f] \quad (19.2.6)$$

represents the transformation of vector projections in transition from S_f to S_p . Here (fig. 19.2.2)

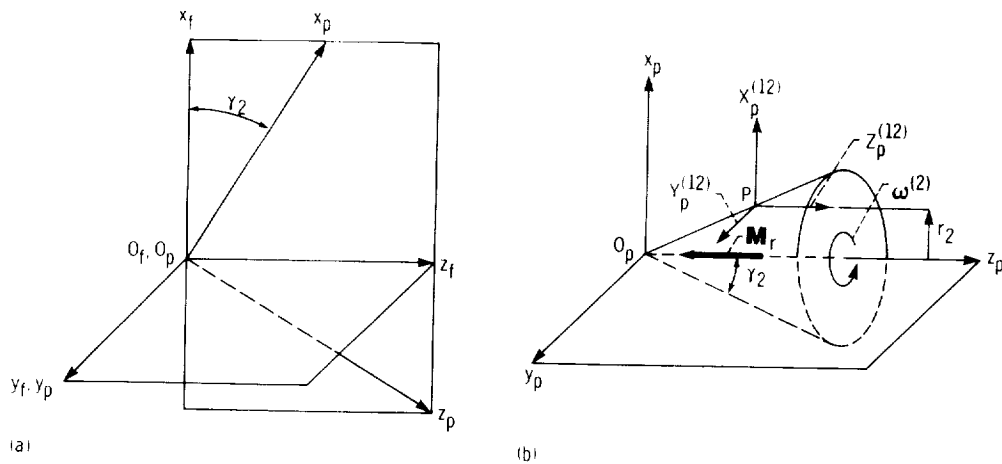


Figure 19.2.2.

$$[L_{pj}] = \begin{bmatrix} \cos \gamma_2 & 0 & \sin \gamma_2 \\ 0 & 1 & 0 \\ -\sin \gamma_2 & 0 & \cos \gamma_2 \end{bmatrix} \quad (19.2.7)$$

where γ_2 is the apex angle of the pitch cone. Equations (19.2.5) to (19.2.7) yield

$$[n_p] = \begin{bmatrix} -\cos \gamma_2 \sin \psi_c + \sin \gamma_2 \cos \psi_c \sin \beta \\ \cos \psi_c \cos \beta \\ \sin \gamma_2 \sin \psi_c + \cos \gamma_2 \cos \psi_c \sin \beta \end{bmatrix} \quad (19.2.8)$$

Step 2.—The contacting force $\mathbf{F}^{(12)}$ may be represented by

$$[\mathbf{F}_p^{(12)}] = \begin{bmatrix} X_p^{(12)} \\ Y_p^{(12)} \\ Z_p^{(12)} \end{bmatrix} = F_p^{(12)} \begin{bmatrix} -\cos \gamma_2 \sin \psi_c + \sin \gamma_2 \cos \psi_c \sin \beta \\ \cos \psi_c \cos \beta \\ \sin \gamma_2 \sin \psi_c + \cos \gamma_2 \cos \psi_c \sin \beta \end{bmatrix} \quad (19.2.9)$$

Step 3.—One of the equations of static equilibrium of gear 2 is based on the consideration that the sum of projections of the torques on the z_p -axis is equal to zero. This condition yields

$$[\mathbf{M}_r + (\overline{O_p P} \times \mathbf{F}^{(12)})] \cdot \mathbf{k}_p = 0 \quad (19.2.10)$$

Here (fig. 19.2.2)

$$\mathbf{M}_r \cdot \mathbf{k}_p = -M_r \quad (19.2.11)$$

and

$$\overline{O_p P} \times \mathbf{F}^{(12)} = \begin{vmatrix} \mathbf{i}_p & \mathbf{j}_p & \mathbf{k}_p \\ r_2 & 0 & r_2 \cot \gamma_2 \\ X_p^{(12)} & Y_p^{(12)} & Z_p^{(12)} \end{vmatrix} = \begin{bmatrix} -Y_p^{(12)} r_2 \cot \gamma_2 \\ X_p^{(12)} r_2 \cot \gamma_2 - Z_p^{(12)} r_2 \\ Y_p^{(12)} r_2 \end{bmatrix} \quad (19.2.12)$$

$$(\overline{O_p P} \times \mathbf{F}^{(12)}) \cdot \mathbf{k}_p = Y_p^{(12)} r_2 \quad (19.2.13)$$

The radial components of bearing reactions are perpendicular to axis z_p and the axial component is directed along this axis. Therefore the projection of the moment of bearing reactions on axis z_p is zero.

Equations (19.2.10) to (19.2.13) yield

$$Y_p^{(12)} = \frac{M_r}{r_2} \quad (19.2.14)$$

Step 4.—Using equation (19.2.14) and (19.2.9), we obtain

$$F^{(12)} = \frac{M_r}{r_2 \cos \psi_c \cos \beta} \quad (19.2.15)$$

$$X_p^{(12)} = \frac{M_r}{r_2 \cos \beta} (-\cos \gamma_2 \tan \psi_c + \sin \gamma_2 \sin \beta) \quad (19.2.16)$$

$$Y_p^{(12)} = \frac{M_r}{r_2}$$

$$Z_p^{(12)} = \frac{M_r}{r_2 \cos \beta} (\sin \gamma_2 \tan \psi_c + \cos \gamma_2 \sin \beta) \quad (19.2.17)$$

Equations (19.2.15) represent the magnitude and components of the contacting force $\mathbf{F}^{(12)}$.

Contacting force $\mathbf{F}^{(21)}$

Gear 1 is loaded with (1) the driving moment \mathbf{M}_d , (2) the contacting force $\mathbf{F}^{(21)}$ which is transmitted from gear 2, and (3) bearing reactions which are transmitted from the frame. The contacting force $\mathbf{F}^{(21)}$ is of the same magnitude as $\mathbf{F}^{(12)}$, but it has an opposite direction. To derive the contacting force $\mathbf{F}^{(21)}$ and its components, we use the following procedure:

Step 1. — We represent the unit normal $[n_f]$ in coordinate system S_h whose location with respect to the coordinate system S_f is shown in figure 19.2.3. Coordinate transformation from S_f to S_h is represented by the matrix (fig. 19.2.3)

$$[L_{hf}] = \begin{bmatrix} \cos \gamma_1 & 0 & -\sin \gamma_1 \\ 0 & 1 & 0 \\ \sin \gamma_1 & 0 & \cos \gamma_1 \end{bmatrix} \quad (19.2.18)$$

Using the matrix equation

$$[n_h] = [L_{hf}][n_f] \quad (19.2.19)$$

where $[n_f]$ is represented by the column matrix (19.2.5), we obtain

$$[n_h] = \begin{bmatrix} -\cos \gamma_1 \sin \psi_c - \sin \gamma_1 \cos \psi_c \sin \beta \\ \cos \psi_c \cos \beta \\ -\sin \gamma_1 \sin \psi_c + \cos \gamma_1 \cos \psi_c \sin \beta \end{bmatrix} \quad (19.2.20)$$

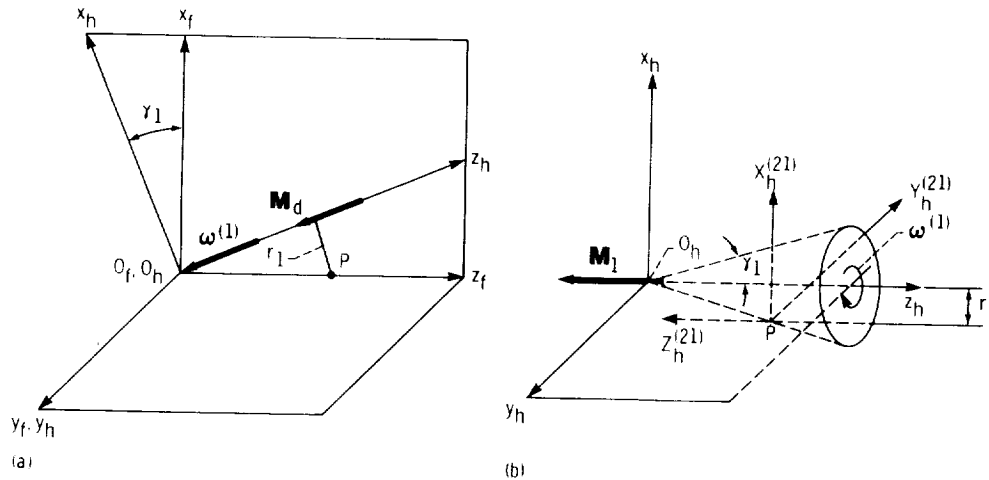


Figure 19.2.3.

Step 2.—We represent the contacting force $\mathbf{F}^{(21)}$ as follows

$$\mathbf{F}^{(21)} = -F^{(21)} \mathbf{n}_h = \begin{bmatrix} X_h^{(12)} \\ Y_h^{(12)} \\ Z_h^{(12)} \end{bmatrix} = -F^{(21)} \begin{bmatrix} -\cos \gamma_1 \sin \psi_c - \sin \gamma_1 \cos \psi_c \sin \beta \\ \cos \psi_c \cos \beta \\ -\sin \gamma_1 \sin \psi_c + \cos \gamma_1 \cos \psi_c \sin \beta \end{bmatrix} \quad (19.2.21)$$

Step 3.—The sum of projections of the torques on the z_h -axis is equal to zero. Thus

$$[\mathbf{M}_d + (\overline{O_h P} \times \mathbf{F}^{(21)})] \cdot \mathbf{k}_h = 0 \quad (19.2.22)$$

Here (fig. 19.2.3)

$$\mathbf{M}_d \cdot \mathbf{k}_h = -M_d \quad (19.2.23)$$

$$\overline{O_h P} = -r_1 \mathbf{i}_h + r_1 \cot \gamma_1 \mathbf{k}_h \quad (19.2.24)$$

and

$$\overline{O_h P} \times \mathbf{F}^{(21)} = \begin{vmatrix} \mathbf{i}_h & \mathbf{j}_h & \mathbf{k}_h \\ -r_1 & 0 & r_1 \cot \gamma_1 \\ X_h^{(21)} & Y_h^{(21)} & Z_h^{(21)} \end{vmatrix} \quad (19.2.25)$$

Equations (19.2.22) to (19.2.25) yield

$$Y_h^{(21)} = -\frac{M_d}{r_1} \quad (19.2.26)$$

The negative sign of $Y_h^{(21)}$ indicates that $Y_h^{(21)}$ is directed parallel to the negative y_h -axis.

Step 4.—Using equations (19.2.21) and (19.2.27), we represent the magnitude of the contacting force $\mathbf{F}^{(21)}$ and its components as follows:

$$F^{(21)} = \frac{M_d}{r_1 \cos \psi_c \cos \beta} \quad (19.2.27)$$

$$X_h^{(21)} = \frac{M_d}{r_1 \cos \beta} (\cos \gamma_1 \tan \psi_c + \sin \gamma_1 \sin \beta) \quad (19.2.28)$$

$$Y_h^{(21)} = -\frac{M_d}{r_1} \quad (19.2.29)$$

$$Z_h^{(21)} = \frac{M_d}{r_1 \cos \beta} (\sin \gamma_1 \tan \psi_c - \cos \gamma_1 \sin \beta) \quad (19.2.30)$$

Appendix A

Matrices: Properties and Operations

A.1 Introduction

A rectangular array of numbers or functions represented in the form

$$[A] = \begin{bmatrix} a_{11} & a_{12} & a_{13} & \dots & a_{1n} \\ a_{21} & a_{22} & a_{23} & \dots & a_{2n} \\ \vdots & & & & \\ a_{m1} & a_{m2} & a_{m3} & \dots & a_{mn} \end{bmatrix} \quad (\text{A.1.1})$$

is called a rectangular matrix with m rows and n columns. A matrix may be denoted with a pair of brackets, [], a pair of double bars, |||, or a pair of parenthesis, ().

Quantities a_{ij} ($i = 1, 2, \dots, m; j = 1, 2, \dots, n$) are known as the elements of matrix A . Here, subscripts i and j correspond, respectively, to the row number and column number where element a_{ij} is located. For instance, element a_{23} is located in the second row and the third column of matrix $[A]$. It is assumed in this book that all matrix elements are either real numbers or real-valued functions.

The order of a matrix, denoted $m \times n$ or (m, n) , indicates that the matrix has m rows and n columns. The so-called row, column, and square matrices are matrices of a particular order $m \times n$.

If a matrix has as many rows as it does columns (i.e., $m = n$) it is known as a square matrix. Elements $a_{11}, a_{22}, a_{33}, \dots, a_{nn}$ of a square matrix are located on its main diagonal, whereas elements $a_{1n}, a_{2(n-1)}, a_{3(n-2)}, \dots, a_{n1}$ form its secondary diagonal. The main and secondary diagonals of a 4×4 square matrix are illustrated as follows:

$$\begin{bmatrix} a_{11} & a_{12} & a_{13} & a_{14} \\ a_{21} & a_{22} & a_{23} & a_{24} \\ a_{31} & a_{32} & a_{33} & a_{34} \\ a_{41} & a_{42} & a_{43} & a_{44} \end{bmatrix}$$

Secondary diagonal
 Main diagonal

A column matrix is a rectangular matrix of order $n \times 1$ (n rows and 1 column). For instance, coordinates of a point M in three-dimensional space (fig. A.1.1) may be represented by a column matrix of order 3×1

$$[R_m] = \begin{bmatrix} a_{11} \\ a_{21} \\ a_{31} \end{bmatrix} = \begin{bmatrix} x_m \\ y_m \\ z_m \end{bmatrix} \quad (\text{A.1.2})$$

Here $[R_m]$ is the matrix of radius-vector

$$\mathbf{R} = x_m \mathbf{i} + y_m \mathbf{j} + z_m \mathbf{k} \quad (\text{A.1.3})$$

where \mathbf{i} , \mathbf{j} , and \mathbf{k} are unit vectors of the coordinate axes.

A matrix of order $1 \times n$ (1 row and n columns) is called a row matrix. It may be represented as

$$[B] = [b_{11} \ b_{12} \ \dots \ b_{1n}] \quad (\text{A.1.4})$$

The identity or unitary matrix is a square matrix such that elements $a_{11}, a_{22}, \dots, a_{nn}$ (located on the main diagonal) are equal to one, and all other elements equal to zero. The unitary matrix is denoted as

$$[I] = \begin{bmatrix} 1 & 0 & 0 & \dots & 0 \\ 0 & 1 & 0 & \dots & 0 \\ \vdots & & & & \\ 0 & 0 & 0 & \dots & 1 \end{bmatrix}$$

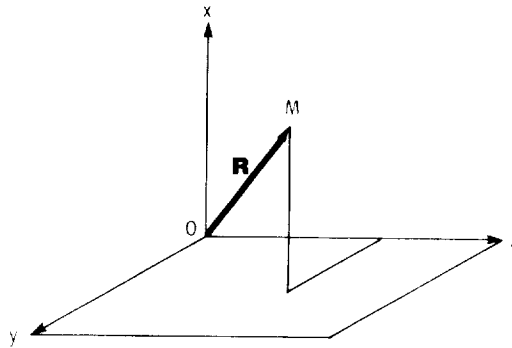


Figure A.1.1.

A symmetric matrix is a square matrix in which all elements are related by the equation

$$a_{ij} = a_{ji} \quad (\text{A.1.6})$$

To determine a symmetric matrix it is sufficient to be given the elements located on its main diagonal, and a definite number of the other elements. For instance, a symmetric matrix of order 4×4 is determined if, from its 16 elements, only a certain 10 elements are given

$$[A] = \begin{bmatrix} a_{11} & a_{12} & a_{13} & a_{14} \\ " & a_{22} & a_{23} & a_{24} \\ " & " & a_{33} & a_{34} \\ " & " & " & a_{44} \end{bmatrix}$$

A skew-symmetric matrix is a square matrix such that all its elements are related by

$$a_{ij} = -a_{ji} \quad (\text{A.1.7})$$

It results from equation (A.1.7) that the elements which lie on the main diagonal of a skew-symmetric matrix are equal to zero. For these elements $i = j$ and the equality

$$a_{ii} = -a_{ii}$$

can be satisfied only if a_{ii} is equal to zero.

A skew-symmetric matrix is determined if a definite number N of its elements a_{ij} ($i \neq j$) is given (N depends on the order of matrix). For a skew-symmetric matrix of order 3×3 $N = 3$:

$$\begin{bmatrix} 0 & a_{12} & a_{13} \\ " & 0 & a_{23} \\ " & " & 0 \end{bmatrix}$$

One application of skew-symmetric matrices is in the determination of a vector product in matrix representation. (See sec. A.8.)

A.2 Equality of Matrices

Two matrices $[A]$ and $[B]$ are equal, that is,

$$[A] = [B] \quad (\text{A.2.1})$$

if they are of the same order and if their respective elements are related as follows:

$$a_{k\ell} = b_{k\ell} \quad (\text{A.2.2})$$

for all k, ℓ .

A.3 Addition and Subtraction of Matrices

To be conformable for addition (subtraction), the considered matrices must be of the same order. Suppose that matrices $[A]$ and $[B]$, both of order $m \times n$, are given

$$[A] = \begin{bmatrix} a_{11} & a_{12} & \dots & a_{1n} \\ a_{21} & a_{22} & \dots & a_{2n} \\ \vdots & & & \\ a_{m1} & a_{m2} & \dots & a_{mn} \end{bmatrix} \quad [B] = \begin{bmatrix} b_{11} & b_{12} & \dots & b_{1n} \\ b_{21} & b_{22} & \dots & b_{2n} \\ \vdots & & & \\ b_{m1} & b_{m2} & \dots & b_{mn} \end{bmatrix}$$

Matrix $[C]$, the sum of matrices $[A]$ and $[B]$, also has the order $m \times n$ and is determined as follows:

$$\begin{aligned} [C] = [A] + [B] &= \begin{bmatrix} c_{11} & c_{12} & \dots & c_{1n} \\ c_{21} & c_{22} & \dots & c_{2n} \\ \vdots & & & \\ c_{m1} & c_{m2} & \dots & c_{mn} \end{bmatrix} \\ &= \begin{bmatrix} a_{11} + b_{11} & a_{12} + b_{12} & \dots & a_{1n} + b_{1n} \\ a_{21} + b_{21} & a_{22} + b_{22} & \dots & a_{2n} + b_{2n} \\ \vdots & & & \\ a_{m1} + b_{m1} & a_{m2} + b_{m2} & \dots & a_{mn} + b_{mn} \end{bmatrix} \end{aligned} \quad (\text{A.3.1})$$

The addition (subtraction) of matrices is commutative

$$[A] + [B] = [B] + [A]$$

and is associative

$$([A] + [B]) + [C] = [A] + ([B] + [C]) \quad (\text{A.3.2})$$

A.4 Multiplication of Matrices

The matrix equation

$$[C] = [A][B] \quad (\text{A.4.1})$$

means that the matrices $[A]$ and $[B]$ are to be multiplied and constitute a product matrix $[C]$. Elements of matrix $[C]$ are expressed in terms of elements of $[A]$ and $[B]$.

To be conformable for matrix product (A.4.1) (with the mentioned order of factors) the number of columns in $[A]$ must be equal to the number of rows in $[B]$. For instance, if the order of $[A]$ is $m \times n$, and the order of $[B]$ is $n \times q$, matrices $[A]$ and $[B]$ are conformable for the product $[A][B]$. This conformity does not depend on m and q , but the same matrices are not conformable for the product $[B][A]$, because by changing the order of factors, the number of columns in $[B]$ is not equal to the number of rows in $[A]$, that is $q \neq m$.

Let $[A]$ be an $m \times n$ matrix, and $[B]$ an $n \times q$ matrix. The element c_{ij} in the i th row and j th column of the product matrix $[C]$ is determined by multiplying corresponding elements of the i th row of $[A]$ and the j th column of $[B]$, and then adding the products. Consequently,

$$c_{ij} = a_{i1}b_{1j} + a_{i2}b_{2j} + \dots + a_{in}b_{nj} = \sum_{k=1}^n a_{ik}b_{kj} \quad (i = 1, \dots, m; j = 1, \dots, q) \quad (\text{A.4.2})$$

Equation (A.4.2) yields that if $[A]$ is an $m \times n$ matrix and $[B]$ is an $n \times q$ matrix, the product $[C]$ is an $m \times q$ matrix.

Sample problem A.4.1 The following matrices are given

$$[A] = \begin{bmatrix} a_{11} & a_{12} & a_{13} & a_{14} \\ a_{21} & a_{22} & a_{23} & a_{24} \\ \boxed{a_{31}} & \boxed{a_{32}} & \boxed{a_{33}} & \boxed{a_{34}} \\ a_{41} & a_{42} & a_{43} & a_{44} \\ a_{51} & a_{52} & a_{53} & a_{54} \end{bmatrix} \quad [B] = \begin{bmatrix} b_{11} & \boxed{b_{12}} & b_{13} \\ b_{21} & \boxed{b_{22}} & b_{23} \\ b_{31} & \boxed{b_{32}} & b_{33} \\ b_{41} & \boxed{b_{42}} & b_{43} \end{bmatrix} \quad (\text{A.4.3})$$

These matrices are conformable for multiplication since the number of columns in $[A]$ is the same as the number of rows in $[B]$. The product $[C]$ is a matrix of order 5×3 and may be represented as

$$[C] = \begin{bmatrix} c_{11} & c_{12} & c_{13} \\ c_{21} & c_{22} & c_{23} \\ c_{31} & \boxed{c_{32}} & c_{33} \\ c_{41} & c_{42} & c_{43} \\ c_{51} & c_{52} & c_{53} \end{bmatrix}$$

Element c_{32} is found by multiplying the corresponding elements of the 3rd row of $[A]$ and the 2nd column of $[B]$, and then by adding these products

$$c_{32} = a_{31}b_{12} + a_{32}b_{22} + a_{33}b_{32} + a_{34}b_{42}$$

The product of an $n \times n$ square matrix $[A]$ and an $n \times n$ identity matrix $[I]$ yields a product

$$[A][I] = [I][A] = [A] \quad (\text{A.4.4})$$

The multiplication of several matrices, for instance, $[A]$, $[B]$, and $[C]$, is conformable if their orders are as follows: $m \times n$, $n \times q$, and $q \times p$.

The multiplication of matrices is associative

$$([A][B])[C] = [A]([B][C]) \quad (\text{A.4.5})$$

Matrix operation

$$[D] = [A]([B] + [C]) \quad (\text{A.4.6})$$

is conformable if $[B]$ and $[C]$ have the same order and the number of columns in $[A]$ is equal to the number of rows in $[B]$ (or $[C]$).

Matrix multiplication is distributive with respect to addition, thus

$$[D] = [A]([B] + [C]) = [A][B] + [A][C] \quad (\text{A.4.7})$$

Problem A.4.2 Find the product $[C] = [A][B]$ where

$$[A] = \begin{bmatrix} 3 & 2 & 2 & 1 \\ 4 & -3 & 0 & 2 \\ 5 & 0 & 5 & 3 \\ 0 & 6 & 7 & 4 \end{bmatrix} \quad [B] = \begin{bmatrix} 1 & 3 & 0 & -1 \\ -1 & 0 & 1 & 2 \\ 2 & 5 & 2 & 3 \\ 3 & 0 & 4 & 1 \end{bmatrix}$$

Answer.

$$[C] = \begin{bmatrix} 8 & 19 & 10 & 8 \\ 13 & 12 & 5 & -8 \\ 24 & 40 & 22 & 13 \\ 20 & 35 & 36 & 37 \end{bmatrix}$$

Problem A.4.3 Find the product $[C] = [A][B]$ where

$$[A] = \begin{bmatrix} 1 & 3 & 0 & 1 \\ -1 & 0 & 1 & 2 \\ 2 & 5 & 2 & 3 \\ 3 & 0 & 4 & 4 \end{bmatrix} \quad [B] = \begin{bmatrix} 4 \\ 6 \\ 7 \\ 8 \end{bmatrix}$$

Answer.

$$[C] = \begin{bmatrix} 30 \\ 19 \\ 76 \\ 72 \end{bmatrix}$$

A.5 Transpose Matrix

Let $[A]$ be an $m \times n$ matrix. The transpose matrix $[A]^T$ of order $n \times m$ may be obtained by interchanging the corresponding rows and columns of matrix $[A]$. For instance, the transpose of

$$[A] = \begin{bmatrix} a_{11} & a_{12} & a_{13} \\ a_{21} & a_{22} & a_{23} \end{bmatrix} \quad (\text{A.5.1})$$

is

$$[A]^T = \begin{bmatrix} a_{11}^T & a_{12}^T \\ a_{21}^T & a_{22}^T \\ a_{31}^T & a_{32}^T \end{bmatrix} = \begin{bmatrix} a_{11} & a_{21} \\ a_{12} & a_{22} \\ a_{31} & a_{23} \end{bmatrix} \quad (\text{A.5.2})$$

Assuming that $[A]$ is an $m \times n$ matrix, we get that

$$a_{ji}^T = a_{ij} \quad (i = 1, 2, \dots, m; j = 1, 2, \dots, n), \quad (\text{A.5.3})$$

where a_{ji}^T and a_{ij} are elements of matrices $[A]^T$ and $[A]$, respectively.

Equations (A.1.6) and (A.5.3) yield that if $[A]$ is a symmetric matrix, the transpose matrix $[A]^T$ is equal to $[A]$. For instance, let $[A]$ be given as a symmetric matrix

$$[A] = \begin{bmatrix} a_{11} & a_{12} & a_{13} \\ a_{21} & a_{22} & a_{23} \\ a_{31} & a_{32} & a_{33} \end{bmatrix} = \begin{bmatrix} a_{11} & a_{12} & a_{13} \\ a_{12} & a_{22} & a_{23} \\ a_{13} & a_{23} & a_{33} \end{bmatrix} \quad (\text{A.5.4})$$

The interchanging of rows and columns in the symmetric matrix

$$[A] = \begin{bmatrix} a_{11} & a_{12} & a_{13} \\ a_{12} & a_{22} & a_{23} \\ a_{13} & a_{23} & a_{33} \end{bmatrix} \quad (\text{A.5.5})$$

does not change the matrix and $[A]^T = [A]$.

In three-dimensional space, a vector \mathbf{R} may be represented by the 3×1 matrix

$$[R] = \begin{bmatrix} R_x \\ R_y \\ R_z \end{bmatrix} \quad (\text{A.5.6})$$

where R_x , R_y , and R_z are the projections of vector \mathbf{R} . The transpose of $[R]$, matrix $[R]^T$, is the 1×3 matrix

$$[R]^T = [R_x R_y R_z] \quad (\text{A.5.7})$$

It can be proven that equation (1.5.3) yields the following relations:

$$([A]^T)^T = [A] \quad (\text{A.5.8})$$

$$(\alpha[A])^T = \alpha[A]^T \quad (\text{A.5.9})$$

$$([A] + [B])^T = [A]^T + [B]^T \quad (\text{A.5.10})$$

$$([A][B])^T = [B]^T[A]^T \quad (\text{A.5.11})$$

$$([A_1][A_2] \dots [A_n])^T = [A_n]^T [A_{n-1}]^T \dots [A_2]^T [A_1]^T \quad (\text{A.5.12})$$

A.6 Inverse Matrix

Inverse matrices (designated by $[A]^{-1}$) find many applications in mathematics and mechanics. In this publication, the problem of determining the inverse of a given matrix occurs by coordinate transformation. (See ch. 1.) A unique inverse matrix $[A]^{-1}$ exists if the given matrix $[A]$ is square and its determinant, $\det A \neq 0$. A matrix $[A]$ such that $\det A \neq 0$ is known as a nonsingular matrix; $[A]$ is singular if $\det A = 0$.

To find the inverse matrix $[A]^{-1}$, it is necessary (1) to determine the cofactors B_{ij} of elements a_{ij} in $\det A$ and (2) to determine the so-called adjoint matrix

$$[B] = [B_{ij}]^T \quad (\text{A.6.1})$$

Once this is done the inverse matrix may be obtained as

$$[A]^{-1} = \frac{[B]}{\det A} \quad (\text{A.6.2})$$

Let $\det A$, of order n , be given as

$$\det A = \begin{vmatrix} a_{11} & a_{12} & a_{13} & \dots & a_{1n} \\ a_{21} & a_{22} & a_{23} & \dots & a_{2n} \\ \vdots & & & & \\ a_{n1} & a_{n2} & a_{n3} & \dots & a_{nn} \end{vmatrix} \quad (\text{A.6.3})$$

According to the definition known from linear algebra, the cofactor B_{ij} of a_{ij} in $\det A$, is $(-1)^{i+j}$ times the determinant of order $n-1$ obtained from $\det A$ upon erasing the i th row and j th column.

For instance, the cofactor B_{23} is obtained from $\det A$ upon erasing the second row and the third column

$$B_{23} = (-1) \begin{vmatrix} a_{11} & a_{12} & a_{13} & \dots & a_{1n} \\ \hline a_{21} & a_{22} & a_{23} & \dots & a_{2n} \\ \vdots & & & & \\ a_{n1} & a_{n2} & a_{n3} & \dots & a_{nn} \end{vmatrix} \quad (\text{A.6.4})$$

The adjoint matrix is

$$[B] = \begin{bmatrix} B_{11} & B_{12} & B_{13} & \dots & B_{1n} \\ B_{21} & B_{22} & B_{23} & \dots & B_{2n} \\ \vdots & & & & \\ B_{n1} & B_{n2} & B_{n3} & \dots & B_{nn} \end{bmatrix}^T = \begin{bmatrix} B_{11} & B_{21} & B_{31} & \dots & B_{n1} \\ B_{12} & B_{22} & B_{32} & \dots & B_{n2} \\ \vdots & & & & \\ B_{1n} & B_{2n} & B_{3n} & \dots & B_{nn} \end{bmatrix} \quad (\text{A.6.5})$$

The inverse matrix $[A]^{-1}$ is represented by equation (A.6.2), where $\det A$ may be represented in terms of the elements and cofactors of any one row or column. For instance, corresponding to elements and cofactors of the 1st row, we get

$$\det A = a_{11}B_{11} + a_{12}B_{12} + \dots + a_{1n}B_{1n} \quad (\text{A.6.6})$$

Sample problem A.6.1

Let $[A]$ be a 3×3 matrix as follows

$$[A] = \begin{bmatrix} a_{11} & a_{12} & a_{13} \\ a_{21} & a_{22} & a_{23} \\ a_{31} & a_{32} & a_{33} \end{bmatrix} = \begin{bmatrix} 1 & 3 & 5 \\ 2 & 4 & 6 \\ 3 & 7 & 8 \end{bmatrix}$$

The cofactors are

$$B_{11} = (-1)^{(1+1)} \begin{vmatrix} a_{22} & a_{23} \\ a_{32} & a_{33} \end{vmatrix} = -10 \quad B_{12} = (-1)^{(1+2)} \begin{vmatrix} a_{21} & a_{23} \\ a_{31} & a_{33} \end{vmatrix} = 2$$

$$B_{13} = (-1)^{(1+3)} \begin{vmatrix} a_{21} & a_{22} \\ a_{31} & a_{32} \end{vmatrix} = 2 \quad B_{21} = (-1)^{(2+1)} \begin{vmatrix} a_{12} & a_{13} \\ a_{32} & a_{33} \end{vmatrix} = 11$$

$$B_{22} = (-1)^{(2+2)} \begin{vmatrix} a_{11} & a_{13} \\ a_{31} & a_{33} \end{vmatrix} = -7 \quad B_{23} = (-1)^{(2+3)} \begin{vmatrix} a_{11} & a_{12} \\ a_{31} & a_{32} \end{vmatrix} = 2$$

$$B_{31} = (-1)^{(3+1)} \begin{vmatrix} a_{12} & a_{13} \\ a_{22} & a_{23} \end{vmatrix} = -2 \quad B_{32} = (-1)^{(3+2)} \begin{vmatrix} a_{11} & a_{13} \\ a_{21} & a_{23} \end{vmatrix} = 4$$

$$B_{33} = (-1)^{(3+3)} \begin{vmatrix} a_{11} & a_{12} \\ a_{21} & a_{22} \end{vmatrix} = -2$$

The adjoint matrix is

$$[B] = \begin{bmatrix} B_{11} & B_{12} & B_{13} \\ B_{21} & B_{22} & B_{23} \\ B_{31} & B_{32} & B_{33} \end{bmatrix}^T = \begin{bmatrix} B_{11} & B_{21} & B_{31} \\ B_{12} & B_{22} & B_{32} \\ B_{13} & B_{23} & B_{33} \end{bmatrix} = \begin{bmatrix} -10 & 11 & -2 \\ 2 & -7 & 4 \\ 2 & 2 & -2 \end{bmatrix}$$

The det A is

$$\det A = a_{11}B_{11} + a_{12}B_{12} + a_{13}B_{13} = 6$$

The inverse matrix is

$$[A]^{-1} = \frac{[B]}{\det A} = \frac{1}{6} \begin{bmatrix} -10 & 11 & -2 \\ 2 & -7 & 4 \\ 2 & 2 & -2 \end{bmatrix}$$

It is easy to verify that

$$[A][A]^{-1} = \begin{bmatrix} 1 & 3 & 5 \\ 2 & 4 & 6 \\ 3 & 7 & 8 \end{bmatrix} \begin{bmatrix} -10 & 11 & -2 \\ 2 & -7 & 4 \\ 2 & 2 & -2 \end{bmatrix} \frac{1}{6} = \begin{bmatrix} 1 & 0 & 0 \\ 0 & 1 & 0 \\ 0 & 0 & 1 \end{bmatrix}$$

There is a class of nonsingular matrices $[A]$ such that the inverse matrix $[A]^{-1}$ coincides with the transpose $[A]^T$. A matrix $[A]$ with this property is known as an orthogonal matrix. Equations

$$[A]^{-1} = [A]^T; [A][A]^T = [A][A]^{-1} = [I] \quad (\text{A.6.7})$$

yield that

$$\det ([A][A]^T) = \det A \cdot \det A^T = (\det A)^2 = \pm \det I = \pm 1 \quad (\text{A.6.8})$$

Orthogonal matrices find an application by coordinate transformations for cartesian coordinate systems with a common origin. (See ch.1.)

An inverse matrix of a product

$$[C] = [A][B] \quad (\text{A.6.9})$$

may be represented by the equation

$$[C]^{-1} = [B]^{-1}[A]^{-1} \quad (\text{A.6.10})$$

This statement can be proven as follows: Multiplying both parts of equation (A.6.9) by the product $[B]^{-1}[A]^{-1}$, we get

$$[B]^{-1}[A]^{-1}[C] = [B]^{-1}[A]^{-1}[A][B] \quad (\text{A.6.11})$$

The product $[A]^{-1}[A][B]$ yields that $([A]^{-1}[A])[B] = [I][B] = [B]$ and

$$[B]^{-1}([A]^{-1}[A][B]) = [B]^{-1}[B] = [I] \quad (\text{A.6.12})$$

Equations (A.6.11) and (A.6.12) yield that

$$[B]^{-1}[A]^{-1}[C] = [I] \quad (\text{A.6.13})$$

and that $[B]^{-1}[A]^{-1} = [C]^{-1}$. Thus, statement (A.6.10) has been proven.

By analogy with equations (A.6.9) and (A.6.10), we get that the inverse matrix $[C]^{-1}$ of a product

$$[C] = [A_1][A_2] \dots [A_n]$$

is

$$[C]^{-1} = [A_n]^{-1}[A_{n-1}]^{-1} \dots [A_2]^{-1}[A_1]^{-1} \quad (\text{A.6.14})$$

A.7 Matrix Differentiation

Matrix elements may be functions of a variable (for example, t). The derivative of an $m \times n$ matrix $[A]$ is

$$\left[\frac{dA}{dt} \right] = \begin{bmatrix} \frac{da_{11}}{dt} & \frac{da_{12}}{dt} & \dots & \frac{da_{1n}}{dt} \\ \frac{da_{m1}}{dt} & \frac{da_{m2}}{dt} & \dots & \frac{da_{mn}}{dt} \end{bmatrix} \quad (\text{A.7.1})$$

The derivative of a matrix product

$$[C] = [A][B] \quad (\text{A.7.2})$$

is determined as follows:

$$\left[\frac{dC}{dt} \right] = [A] \left[\frac{dB}{dt} \right] + [B] \left[\frac{dA}{dt} \right] \quad (\text{A.7.3})$$

A.8 Matrix Representation of Vector Formulas

Henceforth, it will be assumed that a vector \mathbf{A} is represented by its projections a_1, a_2, a_3 on the axes of orthogonal coordinate system as follows:

$$\mathbf{A} = a_1\mathbf{i} + a_2\mathbf{j} + a_3\mathbf{k} \quad (\text{A.8.1})$$

where \mathbf{i} , \mathbf{j} , and \mathbf{k} are the unit vectors of the axes. The matrix representation of vector \mathbf{A} is

$$[A] = \begin{bmatrix} a_1 \\ a_2 \\ a_3 \end{bmatrix} \quad (\text{A.8.2})$$

or

$$[A]^T = [a_1 a_2 a_3] \quad (\text{A.8.3})$$

where $[A]^T$ is the transpose of matrix $[A]$. The matrix representation of vector addition

$$\mathbf{D} = \mathbf{A} + \mathbf{B} + \dots + \mathbf{C} \quad (\text{A.8.4})$$

is

$$\begin{aligned} \begin{bmatrix} d_1 \\ d_2 \\ d_3 \end{bmatrix} &= \begin{bmatrix} a_1 \\ a_2 \\ a_3 \end{bmatrix} + \begin{bmatrix} b_1 \\ b_2 \\ b_3 \end{bmatrix} + \dots + \begin{bmatrix} c_1 \\ c_2 \\ c_3 \end{bmatrix} \\ &= \begin{bmatrix} a_1 + b_1 + \dots + c_1 \\ a_2 + b_2 + \dots + c_2 \\ a_3 + b_3 + \dots + c_3 \end{bmatrix} \end{aligned} \quad (\text{A.8.5})$$

The scalar product of vectors

$$\mathbf{A} \cdot \mathbf{B} = a_1 b_1 + a_2 b_2 + a_3 b_3 = C \quad (\text{A.8.6})$$

may be represented in the matrix form as follows:

$$C = [A]^T [B] = [a_1 a_2 a_3] \begin{bmatrix} b_1 \\ b_2 \\ b_3 \end{bmatrix} = a_1 b_1 + a_2 b_2 + a_3 b_3 \quad (\text{A.8.7})$$

or

$$C = [B]^T [A] = [b_1 b_2 b_3] \begin{bmatrix} a_1 \\ a_2 \\ a_3 \end{bmatrix} = a_1 b_1 + a_2 b_2 + a_3 b_3 \quad (\text{A.8.8})$$

We use the order of factors in the matrix products as follows:

$$C = [A]^T [B] = [B]^T [A] \quad (\text{A.8.9})$$

The 1×3 and 3×1 matrices are conformable for multiplication.

A vector product of two vectors is represented by the equation

$$\mathbf{A} \times \mathbf{B} = \begin{vmatrix} \mathbf{i}_1 & \mathbf{i}_2 & \mathbf{i}_3 \\ a_1 & a_2 & a_3 \\ b_1 & b_2 & b_3 \end{vmatrix} = \begin{vmatrix} a_2 & a_3 \\ b_2 & b_3 \end{vmatrix} \mathbf{i}_1 - \begin{vmatrix} a_1 & a_3 \\ b_1 & b_3 \end{vmatrix} \mathbf{i}_2 + \begin{vmatrix} a_1 & a_2 \\ b_1 & b_2 \end{vmatrix} \mathbf{i}_3 \quad (\text{A.8.10})$$

The matrix representation of vector product $\mathbf{A} \times \mathbf{B}$ is

$$[\mathbf{C}] = [\mathbf{A}]^{sk} [\mathbf{B}] = \begin{bmatrix} 0 & -a_3 & a_2 \\ a_3 & 0 & -a_1 \\ -a_2 & a_1 & 0 \end{bmatrix} \begin{bmatrix} b_1 \\ b_2 \\ b_3 \end{bmatrix} = \begin{bmatrix} -a_3b_2 + a_2b_3 \\ a_3b_1 - a_1b_3 \\ -a_2b_1 + a_1b_2 \end{bmatrix} \quad (\text{A.8.11})$$

The scalar triple product is represented by the equation

$$d = \mathbf{A} \cdot (\mathbf{B} \times \mathbf{C}) = [ABC] = [BCA] = [CAB] = -[BAC] = -[CBA] = -[ACB]$$

$$= \begin{vmatrix} a_1 & a_2 & a_3 \\ b_1 & b_2 & b_3 \\ c_1 & c_2 & c_3 \end{vmatrix} = a_1 \begin{vmatrix} b_2 & b_3 \\ c_2 & c_3 \end{vmatrix} - a_2 \begin{vmatrix} b_1 & b_3 \\ c_1 & c_3 \end{vmatrix} + a_3 \begin{vmatrix} b_1 & b_2 \\ c_1 & c_2 \end{vmatrix} \quad (\text{A.8.12})$$

The matrix representation of the scalar triple product is

$$\begin{aligned} d &= [\mathbf{A}]^T [\mathbf{B}]^{sk} [\mathbf{C}] = [\mathbf{B}]^T [\mathbf{C}]^{sk} [\mathbf{A}] = [\mathbf{C}]^T [\mathbf{A}]^{sk} [\mathbf{B}] \\ &= -[\mathbf{B}]^T [\mathbf{A}]^{sk} [\mathbf{C}] = -[\mathbf{C}]^T [\mathbf{B}]^{sk} [\mathbf{A}] = -[\mathbf{A}]^T [\mathbf{C}]^{sk} [\mathbf{B}] \end{aligned} \quad (\text{A.8.13})$$

The superscript *sk* denotes a skew-symmetric matrix. Each matrix triple product in equation (A.8.13) yields the same scalar d . For instance, the multiplication of matrices in equation (A.8.13) yield

$$\begin{aligned} d &= [\mathbf{A}]^T [\mathbf{B}]^{sk} [\mathbf{C}] \\ &= [a_1 a_2 a_3] \begin{bmatrix} 0 & -b_3 & b_2 \\ b_3 & 0 & -b_1 \\ -b_2 & b_1 & 0 \end{bmatrix} \begin{bmatrix} c_1 \\ c_2 \\ c_3 \end{bmatrix} \\ &= a_1(-b_3c_2 + b_2c_3) + a_2(b_3c_1 - b_1c_3) + a_3(-b_2c_1 + b_1c_2) \end{aligned} \quad (\text{A.8.14})$$

Appendix B

Theorem of Implicit Function System Existence

A system of j equations in n unknowns

$$f_i(x_1, x_2, \dots, x_n) = 0 \quad f_i \in C^1 \quad (x_1, x_2, \dots, x_n) \in G$$

$$(i = 1, 2, \dots, j = n - 1) \tag{B1}$$

is considered. This equation system is satisfied at the point

$$X^0 = (x_1^0, x_2^0, \dots, x_n^0) \tag{B2}$$

The theorem of implicit function system existence states that in the neighborhood of point X^0 the solution of equation system (B1) may be represented by functions

$$\{x_2(x_1), x_3(x_1), \dots, x_n(x_1)\} \in C^1 \tag{B3}$$

if the following Jacobian differs from zero:

$$\frac{D(f_1, f_2, \dots, f_j)}{D(x_2, x_3, \dots, x_n)} = \begin{bmatrix} \frac{\partial f_1}{\partial x_2} & \frac{\partial f_1}{\partial x_3} & \dots & \frac{\partial f_1}{\partial x_n} \\ \dots & \dots & \dots & \dots \\ \frac{\partial f_j}{\partial x_2} & \frac{\partial f_j}{\partial x_3} & \dots & \frac{\partial f_j}{\partial x_n} \end{bmatrix} \neq 0 \tag{B4}$$

Here x_1 is the independent variable of functions (B3).

The solution of equation system (B1) may be represented by functions of another variable, for instance, x_2 , if the following Jacobian differs from zero:

Appendix C

Linear Vector Function. Principal Curvatures and Directions of a Surface

Usually, the determination of the principal curvatures and directions of a surface is based on Dupin's indicatrix. Another approach, proposed by Rashevsky, 1956, is based on the properties of linear vector functions and we employ his proposal in this section.

C.1. Linear Vector Function

Consider two planar vectors \mathbf{a} and \mathbf{b} . We assume that there is a rule which determines vector \mathbf{b} if \mathbf{a} is given. Such a rule may be represented by a function $A(\mathbf{a})$. Thus

$$\mathbf{b} = A(\mathbf{a}) \tag{C.1.1}$$

Such a vector function may be represented by a matrix equation with which we express the components of vector \mathbf{b} in terms of the components of vector \mathbf{a} . The type of such a matrix depends on the type of the vector function $A(\mathbf{a})$. (See the following examples.)

Figure C.1.1 corresponds to the case when vector \mathbf{b} is obtained from \mathbf{a} as follows: vector \mathbf{a} is rotated about point O_n through an angle ϕ and then extended corresponding to the ratio

$$\frac{|\mathbf{b}|}{|\mathbf{a}|} = \lambda \tag{C.1.2}$$

We set up two coordinate systems S_m and S_n rigidly connected to vectors \mathbf{a} and \mathbf{b} , respectively. Figure C.1.1(a) and figure C.1.1(b) show the coordinate systems S_m before and after the rotation through the angle ϕ , respectively. The direction of vector \mathbf{a} will coincide with the direction of \mathbf{b} after the rotation through the angle ϕ (fig. C.1.1(b)). Then by the extension of the length of vector \mathbf{a} , the two vectors will become equal. We describe the correspondence between vectors \mathbf{b} and \mathbf{a} by the following matrix equation:

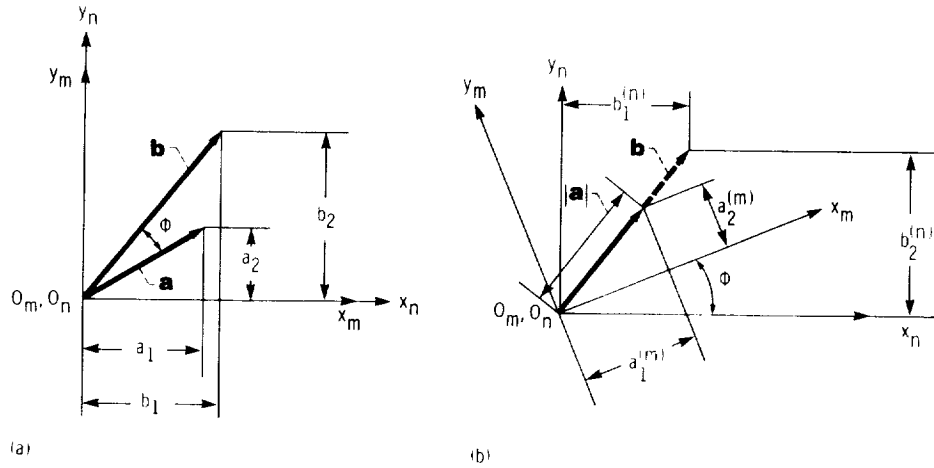


Figure C.1.1.

$$\begin{aligned}
 \begin{bmatrix} b_1^{(n)} \\ b_2^{(n)} \end{bmatrix} &= \lambda [L_1] \begin{bmatrix} a_1^{(m)} \\ a_2^{(m)} \end{bmatrix} = \lambda \begin{bmatrix} \cos \phi & -\sin \phi \\ \sin \phi & \cos \phi \end{bmatrix} \begin{bmatrix} a_1^{(m)} \\ a_2^{(m)} \end{bmatrix} \\
 &= \begin{bmatrix} \lambda \cos \phi & -\lambda \sin \phi \\ \lambda \sin \phi & \lambda \cos \phi \end{bmatrix} \begin{bmatrix} a_1^{(m)} \\ a_2^{(m)} \end{bmatrix} \quad (C.1.3)
 \end{aligned}$$

Taking into account that

$$\begin{bmatrix} a_1^{(m)} \\ a_2^{(m)} \end{bmatrix} = \begin{bmatrix} a_1 \\ a_2 \end{bmatrix} \quad \begin{bmatrix} b_1^{(n)} \\ b_2^{(n)} \end{bmatrix} = \begin{bmatrix} b_1 \\ b_2 \end{bmatrix}$$

we get

$$\begin{bmatrix} b_1 \\ b_2 \end{bmatrix} = \begin{bmatrix} \lambda \cos \phi & -\lambda \sin \phi \\ \lambda \sin \phi & \lambda \cos \phi \end{bmatrix} \begin{bmatrix} a_1 \\ a_2 \end{bmatrix} = [L] \begin{bmatrix} a_1 \\ a_2 \end{bmatrix} \quad (C.1.4)$$

Equation (C.1.4) is an example of matrix representation of vector equation (C.1.1).

Another example of a correspondence between vectors **a** and **b** may be represented as follows. Consider that vector **b** is obtained by extension or compression of components of vector **a**. Thus

$$b_1 = \lambda_1 a_1 \quad b_2 = \lambda_2 a_2 \quad (C.1.5)$$

The matrix representation of (C.1.5) is

$$\begin{bmatrix} b_1 \\ b_2 \end{bmatrix} = \begin{bmatrix} \lambda_1 & 0 \\ 0 & \lambda_2 \end{bmatrix} \begin{bmatrix} a_1 \\ a_2 \end{bmatrix} = [L] \begin{bmatrix} a_1 \\ a_2 \end{bmatrix} \quad (C.1.6)$$

On the basis of the two examples discussed, we could see that vector equation (C.1.1) may be represented in the matrix form by

$$[b] = [L][a] = \begin{bmatrix} a_{11} & a_{12} \\ a_{21} & a_{22} \end{bmatrix} [a] \quad (\text{C.1.7})$$

Here, $[L]$ is the matrix with which we may express the components of vector \mathbf{b} through the components of vector \mathbf{a} (fig. C.1.2(a)). Thus

$$b_1 = a_{11}a_1 + a_{12}a_2 \quad (\text{C.1.8})$$

$$b_2 = a_{21}a_1 + a_{22}a_2$$

Knowing matrix $[L]$ (the matrix representation of function A), we may determine for any given vector \mathbf{c} its corresponding vector \mathbf{d} (fig. C.1.2(b)). Henceforth we will assume that $A(\mathbf{a})$ is a linear function. For such a function the following equations must be observed:

(1) The first equation is

$$\mathbf{m} = A(\mathbf{a} + \mathbf{c}) = A(\mathbf{a}) + A(\mathbf{c}) \quad (\text{C.1.9})$$

This equation expresses that vector \mathbf{m} —the function of the sum of any pair of vectors, \mathbf{a} and \mathbf{c} ,—is equal to the sum of functions of each item. The matrix representation of equation (C.1.9) is

$$\begin{bmatrix} m_1 \\ m_2 \end{bmatrix} = [L] \begin{bmatrix} a_1 + c_1 \\ a_2 + c_2 \end{bmatrix} = [L] \begin{bmatrix} a_1 \\ a_2 \end{bmatrix} + [L] \begin{bmatrix} c_1 \\ c_2 \end{bmatrix} \quad (\text{C.1.10})$$

(2) The second equation is

$$\ell = A(\lambda\mathbf{a}) = \lambda A(\mathbf{a}) \quad (\text{C.1.11})$$

where factor λ is a constant. Vector equations (C.1.11) may be represented in matrix form as follows:

$$\begin{bmatrix} \ell_1 \\ \ell_2 \end{bmatrix} = [L] \begin{bmatrix} \lambda a_1 \\ \lambda a_2 \end{bmatrix} = \lambda [L] \begin{bmatrix} a_1 \\ a_2 \end{bmatrix} \quad (\text{C.1.12})$$

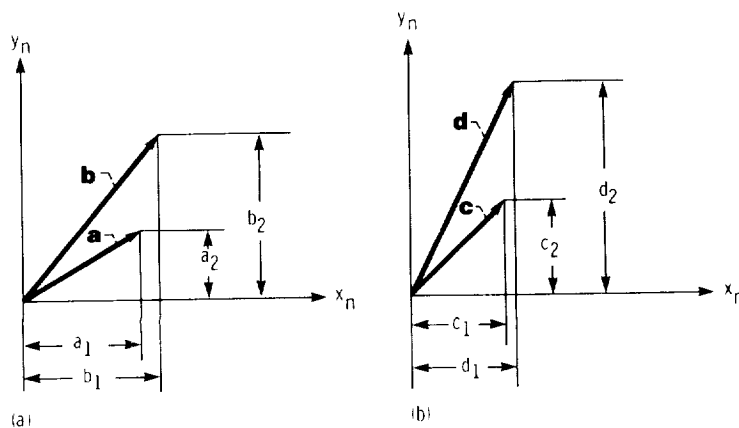


Figure C.1.2.

(3) We also assume that the linear vector function is symmetric. This means that the following equation is to be observed for any pair of vectors:

$$\mathbf{d} \cdot A(\mathbf{a}) = \mathbf{a} \cdot A(\mathbf{d}) \quad (\text{C.1.13})$$

The matrix representation of equation (C.1.13) is

$$[d]^T [L][a] = [a]^T [L][d] \quad (\text{C.1.14})$$

Here, the superscript T designates the transposed matrix. (See app. A.)

Equation (C.1.14) is observed if and only if matrix $[L]$ is symmetric. We may prove this as follows. Using the designation

$$[c] = [L][a] \quad (\text{C.1.15})$$

we represent the scalar product of vectors \mathbf{d} and \mathbf{c} by (see app. A)

$$[d]^T [c] = [c]^T [d] \quad (\text{C.1.16})$$

Equations (C.1.15) and (C.1.16) yield

$$[d]^T [c] = [d]^T [L][a]$$

$$[c]^T = ([L](a))^T = [a]^T [L]^T$$

$$[c]^T [d] = [a]^T [L]^T [d] = [a]^T [L][d]$$

(assuming that $[L]$ is a symmetric matrix and therefore $[L]^T = [L]$).

Thus the matrix equation $[d]^T [c] = [c]^T [d]$ yields $[d]^T [L][a] = [a]^T [L][d]$ and equation (C.1.14) is proven.

Matrix $[L]$ may be determined if a pair of noncollinear vectors \mathbf{c} and \mathbf{b} and their corresponding vectors

$$p = A(\mathbf{c}) \quad q = A(\mathbf{b}) \quad (\text{C.1.17})$$

are given.

Using matrix equations

$$\begin{bmatrix} p_1 \\ p_2 \end{bmatrix} = \begin{bmatrix} a_{11} & a_{12} \\ a_{21} & a_{22} \end{bmatrix} \begin{bmatrix} c_1 \\ c_2 \end{bmatrix} \quad (\text{C.1.18})$$

$$\begin{bmatrix} q_1 \\ q_2 \end{bmatrix} = \begin{bmatrix} a_{11} & a_{12} \\ a_{21} & a_{22} \end{bmatrix} \begin{bmatrix} b_1 \\ b_2 \end{bmatrix}$$

we get a system of four linear equations in four unknowns: a_{11} , a_{12} , a_{21} , a_{22} .

$$\begin{aligned} c_1 a_{11} + c_2 a_{12} &= p_1 \\ c_1 a_{21} + c_2 a_{22} &= p_2 \\ b_1 a_{11} + b_2 a_{12} &= q_1 \\ b_1 a_{21} + b_2 a_{22} &= q_2 \end{aligned} \quad (\text{C.1.19})$$

Here, due to the symmetry of matrix $[L]$, $a_{12} = a_{21}$. Thus equation system (C.1.19) is a system of four equations in three unknowns. Such a system possesses a unique solution if and only if the system matrix and the augmented matrix are of equal rank $r = 3$. The system matrix is

$$\begin{bmatrix} c_1 & c_2 & 0 \\ 0 & c_1 & c_2 \\ b_1 & b_2 & 0 \\ 0 & b_1 & b_2 \end{bmatrix} \quad (\text{C.1.20})$$

and its rank $r = 3$.

The augmented matrix is of rank $r = 3$ if

$$\begin{vmatrix} c_1 & c_2 & 0 & p_1 \\ 0 & c_1 & c_2 & p_2 \\ b_1 & b_2 & 0 & q_1 \\ 0 & b_1 & b_2 & q_2 \end{vmatrix} = (c_2 b_1 - c_1 b_2)(c_1 q_1 + c_2 q_2 - p_1 b_1 - p_2 b_2) = 0 \quad (\text{C.1.21})$$

Equation (C.1.21) relates the four vectors— \mathbf{c} , \mathbf{b} , $\mathbf{p} = A(\mathbf{c})$, and $\mathbf{q} = A(\mathbf{b})$ —which must be given for the determination of the symmetric matrix $[L]$. Equation (C.1.21) may be represented in the following vector form

$$[\mathbf{b} \ \mathbf{c} \ \mathbf{k}] (\mathbf{q} \cdot \mathbf{c} - \mathbf{p} \cdot \mathbf{b}) = 0 \quad (\text{C.1.21(a)})$$

where \mathbf{k} is the unit vector which is perpendicular to the plane in which vectors \mathbf{c} , \mathbf{b} , \mathbf{p} , and \mathbf{q} are located. The scalar triple product $[\mathbf{b} \ \mathbf{c} \ \mathbf{k}]$ cannot be equal to zero because the vectors do not belong to the same plane and no two vectors of \mathbf{b} , \mathbf{c} , and \mathbf{k} are collinear. Thus

$$\mathbf{q} \cdot \mathbf{c} - \mathbf{p} \cdot \mathbf{b} = A(\mathbf{b}) \cdot \mathbf{c} - A(\mathbf{c}) \cdot \mathbf{b} = 0 \quad (\text{C.1.22})$$

Now, considering as given the four vectors— \mathbf{c} , \mathbf{b} , $\mathbf{p} = A(\mathbf{c})$, and $\mathbf{q} = A(\mathbf{b})$ —which are related by the equation (C.1.22), we may determine the symmetric matrix $[L]$. For the solution we have to apply a subsystem of three linear equations which is chosen from equation system (C.1.19). For instance, the following subsystem may be chosen:

$$\begin{aligned} c_1 a_{11} + c_2 a_{12} &= p_1 \\ c_1 a_{12} + c_2 a_{22} &= p_2 \\ b_1 a_{11} + b_2 a_{12} &= q_1 \end{aligned} \quad (\text{C.1.23})$$

The solution for the unknowns a_{11} , a_{12} , and a_{22} is given by

$$a_{11} = \frac{p_1 b_2 - c_2 q_1}{c_1 b_2 - c_2 b_1} \quad a_{12} = a_{21} = \frac{c_1 q_1 - p_1 b_1}{c_1 b_2 - c_2 b_1} \quad a_{22} = \frac{c_1 q_2 - p_2 b_1}{c_1 b_2 - c_2 b_1} \quad (\text{C.1.24})$$

The expression for a_{22} has been simplified with the aid of relation (C.1.22).

Equations (C.1.24) determine the matrix $[L]$ of the vector function A considering vectors \mathbf{c} and \mathbf{b} and their corresponding vectors $\mathbf{p} = A(\mathbf{c})$, $\mathbf{q} = A(\mathbf{b})$ as given. Here, A is the vector function whose matrix representation is given by $[L]$.

We can now obtain more easily the correspondence between any given vector \mathbf{d} represented by

$$\mathbf{d} = \lambda_1 \mathbf{c} + \lambda_2 \mathbf{b} \quad (\text{C.1.25})$$

and the corresponding vector ℓ given by

$$\ell = A(\mathbf{d}) \quad (\text{C.1.26})$$

It is easy to prove that the sought-for vector ℓ may be expressed in terms of vectors \mathbf{p} and \mathbf{q} by the equation

$$\ell = \lambda_1 \mathbf{p} + \lambda_2 \mathbf{q} \quad (\text{C.1.27})$$

The proof is based on the following considerations: Considering matrix $[L]$ as known, we get

$$[p] = [L][c] \quad [q] = [L][b] \quad [\ell] = [L][d] \quad (\text{C.1.28})$$

Equations (C.1.25) and (C.1.28) yield

$$[\ell] = [L]\lambda_1[c] + \lambda_2[b] = \lambda_1[L][c] + \lambda_2[L][b] = \lambda_1[p] + \lambda_2[q] \quad (\text{C.1.29})$$

This equation is the same as equation (C.1.27).

C.2. Characteristic Roots and Vectors

Consider that the linear and symmetric vector function $A(\mathbf{c})$ must determine a corresponding vector

$$\mathbf{p} = A(\mathbf{c}) \quad (\text{C.2.1})$$

which has to be collinear with the given vector \mathbf{c} . Thus

$$A(\mathbf{c}) = \lambda \mathbf{c} \quad (\text{C.2.2})$$

The matrix representation of equation (C.2.1) is

$$[L][c] = \lambda[c] \quad (\text{C.2.3})$$

which yields

$$\begin{bmatrix} a_{11} & a_{12} \\ a_{12} & a_{22} \end{bmatrix} \begin{bmatrix} c_1 \\ c_2 \end{bmatrix} = \lambda \begin{bmatrix} c_1 \\ c_2 \end{bmatrix} \quad (\text{C.2.4})$$

Matrix equation (C.2.4) represents a system of two linear equations

$$\begin{aligned} a_{11}c_1 + a_{12}c_2 &= \lambda c_1 \\ a_{12}c_1 + a_{22}c_2 &= \lambda c_2 \end{aligned} \quad (\text{C.2.5})$$

From equations (C.2.5), we get

$$\begin{aligned}(a_{11} - \lambda)c_1 + a_{12}c_2 &= 0 \\ a_{12}c_1 + (a_{22} - \lambda)c_2 &= 0\end{aligned}\tag{C.2.6}$$

Equation system (C.2.6) contains two homogeneous linear equations in two unknowns c_1 and c_2 . The nontrivial solution for c_1 and c_2 (it differs from $c_1 = 0$ and $c_2 = 0$) exists if and only if

$$\begin{vmatrix} a_{11} - \lambda & a_{12} \\ a_{12} & a_{22} - \lambda \end{vmatrix} = 0\tag{C.2.7}$$

Thus, we may determine two solutions for the ratio c_1/c_2 , which represent two directions of the characteristic vector \mathbf{c} . The characteristic values (roots) and characteristic vectors are also called ‘‘eigen values’’ and ‘‘eigen vectors’’, respectively.

Henceforth, we will assume that $\lambda_1 \neq \lambda_2$. Equation (C.2.7) yields that

$$\begin{aligned}\lambda_1 &= \frac{a_{11} + a_{22}}{2} + \sqrt{\left(\frac{a_{11} + a_{22}}{2}\right)^2 - a_{11}a_{22} + a_{12}^2} \\ \lambda_2 &= \frac{a_{11} + a_{22}}{2} - \sqrt{\left(\frac{a_{11} + a_{22}}{2}\right)^2 - a_{11}a_{22} + a_{12}^2}\end{aligned}\tag{C.2.8}$$

Directions of the characteristic vectors $\mathbf{c}^{(1)}$ and $\mathbf{c}^{(2)}$ are determined by (see eq. (C.2.6))

$$\frac{c_1^{(1)}}{c_2^{(1)}} = -\frac{a_{12}}{a_{11} - \lambda_1} \quad \frac{c_1^{(2)}}{c_2^{(2)}} = -\frac{a_{12}}{a_{11} - \lambda_2}\tag{C.2.9}$$

Equations (C.2.8) and (C.2.9) yield that the characteristic vectors $\mathbf{c}^{(1)}$ and $\mathbf{c}^{(2)}$ are perpendicular. We may prove it as follows:

(1) Using the equation

$$\mathbf{c}^{(1)} \cdot \mathbf{c}^{(2)} = c_1^{(1)}c_1^{(2)} + c_2^{(1)}c_2^{(2)} = 0\tag{C.2.10}$$

we get

$$\frac{c_1^{(1)}}{c_2^{(1)}} + \frac{c_2^{(2)}}{c_1^{(2)}} = -\frac{a_{12}}{a_{11} - \lambda_1} - \frac{a_{11} - \lambda_2}{a_{12}} = 0\tag{C.2.11}$$

Thus

$$a_{11}^2 - a_{11}(\lambda_1 + \lambda_2) + \lambda_1\lambda_2 + a_{12}^2 = 0\tag{C.2.12}$$

(2) Substituting for λ_1 and λ_2 in equation (C.2.12) the expressions (C.2.8), we see that equation (C.2.12) is indeed observed and the characteristic vectors are perpendicular. Knowing the characteristic direction, we may simplify the matrix $[L]$ by using a new coordinate system.

Consider that the initial coordinate system is determined by unit vectors \mathbf{i}_1 and \mathbf{i}_2 (fig. C.2.1). Having the pair of noncollinear vectors \mathbf{c} and \mathbf{b} and the corresponding vectors $\mathbf{p} = A(\mathbf{c})$ and $\mathbf{q} = A(\mathbf{b})$, we may determine the elements of matrix $[L]$. (See eq. (C.1.24).) We may then find

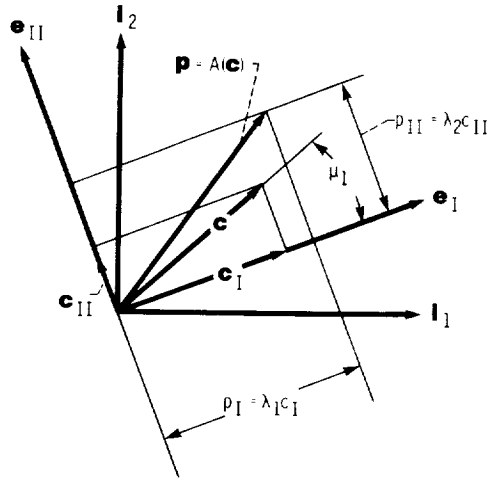


Figure C.2.1.

the characteristic values λ_1 and λ_2 (eq. (C.2.8)) and the directions of the characteristic vectors \mathbf{e}_I and \mathbf{e}_{II} (fig. C.2.1). The angle μ_1 of the characteristic vector \mathbf{e}_I is represented by the equation (see eq. (C.2.9))

$$\tan \mu_1 = \frac{a_{12}}{\lambda_1 - a_{11}} \quad (\text{C.2.13})$$

The positive angle μ_1 is measured from vector \mathbf{e}_I to \mathbf{e}_{II} .

We may now represent the given vector \mathbf{c} (fig. C.2.1) by

$$\mathbf{c} = \mathbf{c}_I + \mathbf{c}_{II} = c_I \mathbf{e}_I + c_{II} \mathbf{e}_{II} \quad (\text{C.2.14})$$

Because vectors \mathbf{c}_I and \mathbf{c}_{II} are characteristic vectors, we may represent the linear vector function as

$$\mathbf{p} = A(\mathbf{c}) = A(\mathbf{c}_I + \mathbf{c}_{II}) = A(\mathbf{c}_I) + A(\mathbf{c}_{II}) = \lambda_1 \mathbf{c}_I + \lambda_2 \mathbf{c}_{II} \quad (\text{C.2.15})$$

The matrix representation of $A(\mathbf{c}_I)$ and $A(\mathbf{c}_{II})$ is:

$$\begin{aligned} \lambda_1 \begin{bmatrix} c_I \\ 0 \end{bmatrix} &= [\Lambda] \begin{bmatrix} c_I \\ 0 \end{bmatrix} = \begin{bmatrix} m_{11} & m_{12} \\ m_{12} & m_{22} \end{bmatrix} \begin{bmatrix} c_I \\ 0 \end{bmatrix} = \begin{bmatrix} m_{11}c_I \\ m_{12}c_I \end{bmatrix} \\ \lambda_2 \begin{bmatrix} 0 \\ c_{II} \end{bmatrix} &= [\Lambda] \begin{bmatrix} 0 \\ c_{II} \end{bmatrix} = \begin{bmatrix} m_{11} & m_{12} \\ m_{12} & m_{22} \end{bmatrix} \begin{bmatrix} 0 \\ c_{II} \end{bmatrix} = \begin{bmatrix} m_{12}c_{II} \\ m_{22}c_{II} \end{bmatrix} \end{aligned} \quad (\text{C.2.16})$$

Here, the symmetric matrix $[\Lambda]$ with elements m_{11} , m_{12} , and m_{22} is the matrix representation of the linear vector function $A(\mathbf{c})$.

Matrix equations (C.2.15) and (C.2.16) yield

$$m_{11} = \lambda_1 \quad m_{12} = 0 \quad m_{22} = \lambda_2$$

and

$$[\Lambda] = \begin{bmatrix} \lambda_1 & 0 \\ 0 & \lambda_2 \end{bmatrix} \quad (\text{C.2.17})$$

We determine the sought-for vector \mathbf{p} by its projections

$$p_I = \lambda_1 c_I \quad p_{II} = \lambda_2 c_{II} \quad (\text{C.2.18})$$

Thus, the vector function $A(\mathbf{c})$ may be interpreted as a corresponding extension (or compression) of projections of the given vector \mathbf{c} in the characteristic directions.

C.3. Surface Principal Directions and Curvatures

Consider a regular surface represented in parametric form by

$$\mathbf{r}(u, \theta) \in C^2 \quad \mathbf{r}_u \times \mathbf{r}_\theta \neq 0 \quad (u, \theta) \in A \quad (\text{C.3.1})$$

The tangent plane, the surface normal \mathbf{N} , and the unit normal \mathbf{n} are determined at the surface point $M(u_0, \theta_0)$. The tangent plane is drawn through vectors \mathbf{r}_u and \mathbf{r}_θ ; the surface normal \mathbf{N} and the unit normal \mathbf{n} are represented as follows:

$$\mathbf{N} = \mathbf{r}_u \times \mathbf{r}_\theta = \mathbf{N}(u, \theta) \quad (\text{C.3.2})$$

$$\mathbf{n} = \frac{\mathbf{N}}{|\mathbf{N}|} = \mathbf{n}(u, \theta) \quad (\text{C.3.3})$$

The partial derivatives

$$\mathbf{r}_u = \frac{\partial \mathbf{r}}{\partial u} \quad \mathbf{r}_\theta = \frac{\partial \mathbf{r}}{\partial \theta} \quad \mathbf{n}_u = \frac{\partial \mathbf{n}}{\partial u} \quad \mathbf{n}_\theta = \frac{\partial \mathbf{n}}{\partial \theta}$$

are taken at the point $M(u_0, \theta_0)$.

The surface normal curvature is determined by the equation (see sec. 10.5)

$$\kappa_n = - \frac{d\mathbf{r} \cdot d\mathbf{n}}{ds^2} = - \frac{\mathbf{v}_r \cdot \dot{\mathbf{n}}_r}{v_r^2} \quad (\text{C.3.4})$$

Here

$$d\mathbf{r} = \mathbf{r}_u du + \mathbf{r}_\theta d\theta \quad (\text{C.3.5})$$

$$d\mathbf{n} = \mathbf{n}_u du + \mathbf{n}_\theta d\theta \quad (\text{C.3.6})$$

$$\mathbf{v}_r = \mathbf{r}_u \frac{du}{dt} + \mathbf{r}_\theta \frac{d\theta}{dt} \quad (\text{C.3.7})$$

$$\dot{\mathbf{n}}_r = \mathbf{n}_u \frac{du}{dt} + \mathbf{n}_\theta \frac{d\theta}{dt} \quad (\text{C.3.8})$$

$$ds^2 = d\mathbf{r}^2 \quad (\text{C.3.9})$$

where t represents time. The subscript “ r ” means that the relative motion of a point (relative with respect to the surface) is considered. In other words, we consider that the above vectors are determined for the motion of a point over the surface.

Vectors $d\mathbf{r}$ and \mathbf{v}_r belong to the tangent plane P . Vectors $d\mathbf{n}$ and $\dot{\mathbf{n}}_r$ belong to the same plane P , which results from the following considerations

$$\mathbf{n} \cdot \mathbf{n} = 1 \quad (\text{C.3.10})$$

Thus

$$2\mathbf{n} \cdot d\mathbf{n} = 0 \quad (\text{C.3.11})$$

This yields that vector $d\mathbf{n}$ (consequently, vector $\dot{\mathbf{n}}_r$) is perpendicular to the surface unit normal \mathbf{n} and belongs to the tangent plane P .

Assume that the surface is given and that we take partial derivatives \mathbf{r}_u , \mathbf{r}_θ , \mathbf{n}_u , and \mathbf{n}_θ at a definite point M . Choosing the ratio

$$\frac{\frac{du}{dt}}{\frac{d\theta}{dt}} \quad (\text{C.3.11})$$

we may determine the direction of vector \mathbf{v}_r and of the corresponding vector $\dot{\mathbf{n}}_r$ (fig. C.3.1). If, in addition to the ratio (C.3.11), one of the derivatives (du/dt , $d\theta/dt$) is chosen, then vector \mathbf{v}_r and the corresponding vector $\dot{\mathbf{n}}_r$ are determined. We can see that by fixing one of the derivatives (du/dt , $d\theta/dt$) and by changing the ratio (C.3.11), new pairs of related planar vectors \mathbf{v}_r and $\dot{\mathbf{n}}_r$ can be determined. In other words, there is a definite linear vector function

$$\dot{\mathbf{n}}_r = A(\mathbf{v}_r) \quad (\text{C.3.12})$$

at any regular point M of the surface which relates vectors $\dot{\mathbf{n}}_r$ and \mathbf{v}_r . The matrix representation of (C.3.12) is given by

$$[\dot{\mathbf{n}}_r] = [L][\mathbf{v}_r] \quad (\text{C.3.13})$$

Using equations (C.3.13), (C.3.7), and (C.3.8), we get

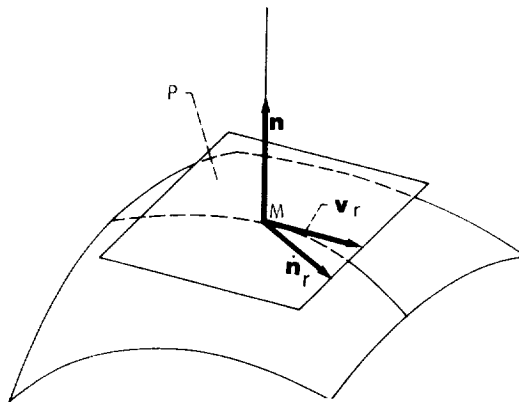


Figure C.3.1.

$$[n_u] \frac{du}{dt} + [n_\theta] \frac{d\theta}{dt} = [L] \left\{ [r_u] \frac{du}{dt} + [r_\theta] \frac{d\theta}{dt} \right\} = [L][r_u] \frac{du}{dt} + [L][r_\theta] \frac{d\theta}{dt} \quad (\text{C.3.14})$$

Thus

$$[n_u] = [L][r_u] \quad [n_\theta] = [L][r_\theta] \quad (\text{C.3.15})$$

We have seen in section C.2, that there is only a single matrix $[L]$ if equations (C.3.15) are to be observed. In addition, this matrix is symmetric if the above four vectors are related by the equation.

$$\mathbf{n}_u \cdot \mathbf{r}_\theta = \mathbf{n}_\theta \cdot \mathbf{r}_u \quad (\text{C.3.16})$$

This equation is indeed observed (see eqs. (10.1.17) and (10.1.18)). Thus, we may determine the single symmetric matrix $[L]$ which transforms $[v_r]$ into $[\dot{n}_r]$, $[r_u]$ into $[n_u]$, and $[r_\theta]$ into $[n_\theta]$.

Because matrix $[L]$ is symmetric, we may determine two perpendicular characteristic directions on the tangent plane with characteristic values of λ_1 and λ_2 ($\lambda_1 \neq \lambda_2$). These two directions may be determined from the collinearity of vectors \mathbf{v}_r and $\dot{\mathbf{n}}_r$ as follows:

$$\frac{\dot{n}_{xr}}{v_{xr}} = \frac{\dot{n}_{yr}}{v_{yr}} = \frac{\dot{n}_{zr}}{v_{zr}} = \alpha \quad (\text{C.3.17})$$

or

$$\begin{aligned} \frac{(\mathbf{n}_u \cdot \mathbf{i}) \frac{du}{dt} + (\mathbf{n}_\theta \cdot \mathbf{i}) \frac{d\theta}{dt}}{(\mathbf{r}_u \cdot \mathbf{i}) \frac{du}{dt} + (\mathbf{r}_\theta \cdot \mathbf{i}) \frac{d\theta}{dt}} &= \frac{(\mathbf{n}_u \cdot \mathbf{j}) \frac{du}{dt} + (\mathbf{n}_\theta \cdot \mathbf{j}) \frac{d\theta}{dt}}{(\mathbf{r}_u \cdot \mathbf{j}) \frac{du}{dt} + (\mathbf{r}_\theta \cdot \mathbf{j}) \frac{d\theta}{dt}} \\ &= \frac{(\mathbf{n}_u \cdot \mathbf{k}) \frac{du}{dt} + (\mathbf{n}_\theta \cdot \mathbf{k}) \frac{d\theta}{dt}}{(\mathbf{r}_u \cdot \mathbf{k}) \frac{du}{dt} + (\mathbf{r}_\theta \cdot \mathbf{k}) \frac{d\theta}{dt}} = \alpha \end{aligned} \quad (\text{C.3.18})$$

where \mathbf{i} , \mathbf{j} , and \mathbf{k} are the unit vectors of the coordinate axes.

Equations (C.3.18) provide a quadratic equation in du/dt and $d\theta/dt$. Two solutions of this equation for du/dt and $d\theta/dt$ correspond to two characteristic directions on the tangent plane. These two characteristic directions are the so-called principal directions of the surface at its point M . Curvatures of the surface determined on the principal directions are called the principal curvatures. We may use equation (C.3.4) to determine the principal curvatures taking into account that

$$\alpha \mathbf{v}_r = \dot{\mathbf{n}}_r \quad (\text{C.3.19})$$

because of the collinearity of these vectors. Equations (C.3.19) and (C.3.4) yield

$$\kappa_{I,II} = -\alpha \quad (\text{C.3.20})$$

where $\kappa_{I,II}$ are the two principal curvatures of the surface in the two principal directions. We may represent the principal curvatures of the surface by the equation

$$\kappa_{I,II} \mathbf{v}_r = -\dot{\mathbf{n}}_r \quad (\text{C.3.21})$$

which is known as the Rodrigues' equation.

Now, consider that a coordinate system with unit vectors \mathbf{e}_I and \mathbf{e}_{II} is rigidly connected to the tangent plane. The origin of the coordinate system coincides with the surface point M , and \mathbf{e}_I and \mathbf{e}_{II} represent the principal directions of the surface at M . Equation (C.3.20) yields

$$\dot{n}_{rI} = -\kappa_I v_{rI} \quad \dot{n}_{rII} = -\kappa_{II} v_{rII} \quad (\text{C.3.22})$$

The linear vector function given by

$$\dot{\mathbf{n}}_r = A(\mathbf{v}_r)$$

may be represented in matrix form as follows:

$$\begin{bmatrix} \dot{n}_{rI} \\ \dot{n}_{rII} \end{bmatrix} = \begin{bmatrix} -\kappa_I & 0 \\ 0 & -\kappa_{II} \end{bmatrix} \begin{bmatrix} v_{rI} \\ v_{rII} \end{bmatrix} \quad (\text{C.3.23})$$

Let us express the normal curvature of the surface κ_n in terms of the principal curvatures κ_I , κ_{II} , and the angle q (fig. C.3.2) which is formed between vectors \mathbf{v}_r and \mathbf{e}_I . Using equations (C.3.4) and (C.3.23), we get

$$\kappa_n = -\frac{\dot{\mathbf{n}}_r \cdot \mathbf{v}_r}{(v_r)^2} = -\frac{\dot{n}_{rI} v_{rI} + \dot{n}_{rII} v_{rII}}{(v_{rI})^2 + (v_{rII})^2} = \frac{\kappa_I (v_{rI})^2 + \kappa_{II} (v_{rII})^2}{(v_{rI})^2 + (v_{rII})^2} \quad (\text{C.3.24})$$

It is evident from figure C.3.2 that

$$\cos q = \frac{v_{rI}}{|\mathbf{v}_r|} = \frac{v_{rI}}{\sqrt{(v_{rI})^2 + (v_{rII})^2}} \quad \sin q = \frac{v_{rII}}{\sqrt{(v_{rI})^2 + (v_{rII})^2}} \quad (\text{C.3.25})$$

Equations (C.3.24) and (C.3.25) yield

$$\kappa_n = \kappa_I \cos^2 q + \kappa_{II} \sin^2 q \quad (\text{C.3.26})$$

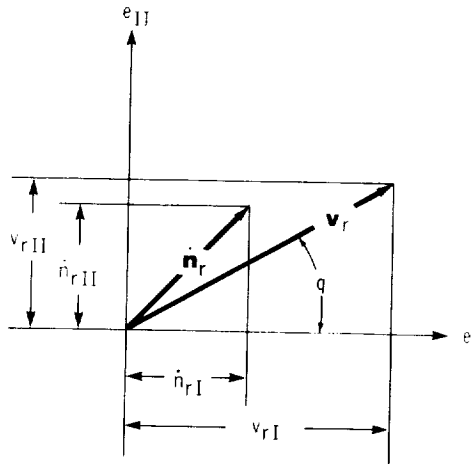


Figure C.3.2.

This equation is known as Euler's equation. From equation (C.3.26), we may obtain two important results:

(1) The principal curvatures are the extreme values of the function

$$\kappa_n(q) \quad 0 \leq q \leq 2\pi \quad (\text{C.3.27})$$

represented by equation (C.3.26). The extreme values of function (C.3.27) occur at those values of q for which

$$\frac{d\kappa_n}{dq} = (\kappa_{II} - \kappa_I) \sin 2q = 0 \quad (\text{C.3.28})$$

Considering the case when $\kappa_I \neq \kappa_{II}$, we can see that the extreme values of the function $\kappa_n(q)$ occur at $q = 0^\circ$ and $q = 90^\circ$. Thus, the extreme values of the normal curvature are simultaneously the principal curvatures.

(2) The sum of two normal curvatures taken for two perpendicular normal sections, $\kappa_n^{(1)}$ and $\kappa_n^{(2)}$, is equal to the sum of principal curvatures κ_I and κ_{II} . We may get this result from equation (C.3.26), taking into account that $|q_2 - q_1| = 90^\circ$. Thus

$$\kappa_n^{(1)} = \kappa_I \cos^2 q_1 + \kappa_{II} \sin^2 q_1 \quad (\text{C.3.29})$$

$$\kappa_n^{(2)} = \kappa_I \cos^2 q_2 + \kappa_{II} \sin^2 q_2 = \kappa_I \sin^2 q_1 + \kappa_{II} \cos^2 q_1 \quad (\text{C.3.30})$$

Thus

$$\kappa_n^{(1)} + \kappa_n^{(2)} = \kappa_I + \kappa_{II} \quad (\text{C.3.31})$$

References

- Baxter, M.L., 1961, "Basic Geometry and Tooth Contact of Hypoid Gears," *Industrial Mathematik*, No. 2.
- Buckingham, E., 1963, *Analytical Mechanics of Gears*, 2nd ed., Dover, New York.
- Denavit, J., and Hartenberg, R.S., 1955, "A Kinematic Notation for Lower Pair Mechanisms based on Matrices," *Journal of Applied Mechanics*, Vol. 22, No. 2, pp. 215-221.
- Dudley, D.W., 1962, *Gear Handbook, The Design, Manufacture, and Application of Gears*, McGraw Hill, New York.
- Favard, J., 1957, *Course of Local Differential Geometry*, Gauthier-Villars, Paris, (in French).
- Gleason Works, 1970, *Understanding Tooth Contact Analysis*, Rochester, NY.
- Goetz, A., 1970, *Introduction to Differential Geometry*, Addison Wesley, Reading.
- Hohn, F.E., 1973, *Elementary Matrix Algebra*, 3rd ed., McMillan Co, New York.
- Korn, G.A., and Corn, T.M., 1968, *Mathematical Handbook for Scientists and Engineers*, 2nd ed., McGraw Hill, New York.
- Lipschutz, M.M., 1969, *Theory and Problems of Differential Geometry*, McGraw Hill, New York.
- Litvin, F.L., 1955, "Application of Matrices and Dual Number Calculations to Analysis of Spatial Gearings," *Proceedings of Leningrad Politekhnik Institute*, No. 182.
- Litvin, F.L., 1968, *Theory of Gearing*, 2nd ed., Nauka, Moscow, (in Russian).
- Litvin, F.L., 1969, "Die Beziehungen zwischen den Krümmungen der Zahnoberflächen bei Räumlichen Verzahnungen," *Zeitschrift für Angewandte Mathematik und Mechanik*, Vol. 49, pp. 685-690.
- Litvin, F.L., Petrov, K.M., and Ganshin, V.A., 1974, "The Effect of Geometrical Parameters of Hypoid and Spiroid Gears on Its Quality Characteristics," *Journal of Engineering for Industry*, Vol. 96, pp. 330-334.
- Litvin, F.L., and Gutman, Y., 1980, "Analysis and Synthesis of a Three-Link Linkage with an Intermediate Higher Kinematic Pair," ASME Paper 80-DET-94.
- Litvin, F.L., Coy, J.J., and Rahman, P., 1981, "Two Mathematical Models of Spiral Bevel Gears Applied to Lubrication and Fatigue Life," *Proceedings of the International Symposium on Gearing and Power Transmissions*, Japan Society of Mechanical Engineers, Tokyo, pp. 281-286.
- Litvin, F.L., and Gutman, Y., 1981a, "Methods of Synthesis and Analysis For Hypoid Gear-Drives of Formate and Helixform," *Journal of Mechanical Design*, Vol. 103, pp. 83-113.
- Part 1. - Calculations for Machine Setting for Member Gear Manufacture of the Formate and Helixform Hypoid Gears, pp. 83-88.
- Part 2. - Machine Setting Calculations for the Pinions of Formate and Helixform Gears, pp. 89-101.
- Part 3. - Analysis and Optimal Synthesis Methods for Mismatched Gearing and Its Application for Hypoid Gears of Formate and Helixform, pp. 102-113.
- Litvin, F.L., and Gutman, Y., 1981b, "A Method of Local Synthesis of Gears Based on the Connection Between the Principal and Geodetic Curvatures of Surfaces," *Journal of Mechanical Design*, Vol. 103, pp. 114-125.
- Litvin, F.L., Rahman, P., and Goldrich, N., 1982, "Mathematical Models for the Synthesis and Optimization of Spiral Bevel Gear Tooth Surfaces," NASA CR-3553.
- Litvin, F.L., Goldrich, R.N., Coy, J.J., and Zaretsky, E.V., 1983a, "Precision of Spiral-Bevel Gears," *Journal of Mechanisms, Transmissions and Automation in Design*, Vol. 105, pp. 310-316.
- Litvin, F.L., Goldrich, R.N., Coy, J.J., and Zaretsky, E.V., 1983b, "Kinematic Precision of Gear Trains," *Journal of Mechanisms, Transmissions, and Automation in Design*, Vol. 105 No. 3, pp. 317-326.
- Litvin, F.L.; and Tsay, C.B., 1985, "Helical Gears With Circular Arc Teeth: Simulation of Conditions of Meshing and Bearing Contact," *Journal of Mechanisms, Transmissions, and Automation in Design*, Vol. 107, No. 4, pp. 556-564.
- Litvin, F.L., W.-J. Tsung, J.J. Coy, and C. Heine, 1987, "Method for Generation of Spiral Bevel Gears with Conjugate Gear Tooth Surfaces," *Journal of Mechanisms, Transmissions and Automation in Design*, Vol. 109, No. 2, pp. 163-170.

- Michalek, G.W., 1966, *Precision Gearing: Theory and Practice*, John Wiley & Sons, New York.
- Niemann, G., and Heyer, E., 1953. "Investigations of Worm Gears," *VDI*, Vol. 95, No. 6, pp. 141-157.
- Rashevsky, P.K., 1956, *Course of Differential Geometry*, 4th ed., State Publishing House of Technical and Theoretical Literature, Moscow, (in Russian).
- Stipelman, B.A., 1978, *Design and Manufacture of Hypoid Gears*, John Wiley & Sons, New York.
- Wildhaber, E., 1946a, "Basic Relationships of Hypoid Gears," *American Machinist*, Vol. 90, No. 4, pp. 108-111.
- Wildhaber, E., 1946b, "Conjugate Pitch Surfaces," *American Machinist*, Vol. 90, No. 13, pp. 150-152.
- Wildhaber, E., 1946c, "Tooth Contact," *American Machinist*, Vol. 90, No. 12, pp. 110-114.
- Wildhaber, E., 1956, "Surface Curvature," *Product Engineering*, Vol. 27, No. 5, pp. 184-191.
- Zalgaller, V.A., 1975, *Theory of Envelopes*, Nauka, Moscow, (in Russian).

INDEX

- Acceleration, of contact points, 257,258
 - relative, 220
 - of surface unit normal, 259
- Angle, crossing, 299
 - lead, 302,303
- Apex angle, of the pitch cone, 431
- Axes, crossed, 35
 - parallel, 35
 - intersecting, 35
 - screw, 36
- Axes of meshing, 319,324
 - crossed axes of gear rotation, 319
 - second, 326
- Axis, of relative rotation, instantaneous, 30
 - of rotation, instantaneous, 21,30,350
- Axodes, 397
- Backlash, of spur gears, 415
- Bearing contact, 377
 - compensation of, location of, 405
 - of gear tooth surfaces, 288
 - reactions, 427
- Bevel gears, generation of, 341
- Beveloid gearing, 339
- Body axode, 31
- Camus' theorem, 132,133
- Center distance, sensitivity to change of, 395
- Center of rotation instantaneous, 21,22,27
- Centroides, 23-28,296
 - link, 22
 - movable, fixed, 14
 - radius of gear, 103
- Centroid and shape curvatures, relations between, 112
- Characteristic roots and vectors, 454
- Compensation, of location of bearing
 - contact, 405
- Computation, process, 90,244
- Cone, parameters, 307,308
 - surface of, 220,230,235
- Conjugate, action, 63
 - gear tooth surfaces, 336
- Conjugate shapes, 63,83
 - generation of, 128
 - principles of generation of, 130
 - relations between curvatures, 97
- Conjugate surfaces, general theorem, 195
 - working equations, 200
- Contact, ellipse, 293,377,384
 - lines, 170,214,395
 - normal limiting, 313
- Contacting force, 430,432
 - stresses, 405
- Coordinates curvilinear, 149,150
 - homogenous, 8,172,194,242
- Coordinate transformation, 1,4,5,8,9,11,12,14,15
- Curvature, cam, 108
 - center of, 56,106
 - equations of, 60
 - Gaussian, 233
 - geodetic, 237,238,275
 - Normal, 227-231
 - Normal, relative, 286
 - of a plane curve, 56
 - principle, 232,233,268,276
 - radius of, 56
 - of a spatial curve, 221,222,225,226
 - of a surface normal, 228-230
- Curvatures, principle, 232,291,379,380
- Curve, elementary arc of, 223
 - generation of, 14
 - parametric form, 42
 - plane, 16, 42

- regular, 43,68,71
- regular point of, 50
- Cycloid, 133
- Cyclo-Palloid gearing, 353
 - system, 350,352
- Cylinder, surface, 240

- Deformation, area of, 292
 - elastic, 288
- Direction, cosine, 4
 - principle, 377
- Dupin's indicatrix, 233,234,449

- Eccentricity, of involute spur gears, 409
 - of spiral bevel gears, 412
- Ellipse, contacting, 288,293-295
- Envelope, concept of, 68
 - of contact lines, 196,202,208,214
 - determination of, 193
 - existence theorem, 69,75
 - of a family of contact lines, 196
 - of a family of surfaces, 168,193
 - necessary conditions of existence, 168,181,197
 - of planar curve locus, 79
 - representation of, 200
 - sufficient conditions of existence, 76,169,182,197,
 - tangent, 137,199
- Epicycloid, 14,54,133
 - extended, 54
 - ordinary, 55,62
- Equations of meshing by cutting, 358,398,399
- Errors of manufacturing, 401,405
- Euler, theorem of, 233
- Euler-Savary equation, 112,115
- Euler's, equation, 291,461
 - formula, 286
- Evolute, 136-144

- Family of surfaces, 167
- Fillet, of the gear, 109
- Flender's worms, 327
- Force, contacting
 - transmission, 422
- Forms, fundamental, 215,217 -220
- Function, explicit, 42
 - gradient of, 153
 - implicit, 42,46

- Gear geometry, introduction to, 350
- Gearing analysis, method of, 241
- Gearing standard, 296
- Gear tooth surface, 208
 - tangency of, 241,242
- Generating gear, spiral bevel, 351
- Generation, of beveloid gearing, 339
 - of helical gears, 344
 - methods, 336,337,341
- Gleason's, gearing, 408
 - spiral bevel gears, 341,352

- Head cutter, 341
- Helical gear, 271
 - with circular arc teeth, 395
 - conjugate surfaces for, 344
 - with crossed axes, 298,300
 - standard and nonstandard, 300
- Helicoid, 16,17,158,207,320,332
 - ruled surface, 160
 - general equations of, 159
- Helix, 180,202,298
- Hob, 128
 - single thread, 128
- Hyperboloid, surfaces of revolution, 40,41
- Hyploid gears, center distance of, 308
 - operating pitch surfaces, 304
- Hypocycloid, 133

- Implicit function system existence, theorem of, 89,148,243,447,
- Interference, 127
- Involute, curve 45,72,175
 - extended, 43
 - locus of curves, 73
 - nonstandard, gears, 296
 - screw surface, 237

- Kinematic, method of envelope
 - determination, 193
 - precision of gear trains, 390
 - relations, 93-95,405
 - representation of curvature, 59
- Kinematical errors, 87,141,389,407
- Kinematic errors, 39,405-407
 - function of, 246,410
 - types of, 408
- Klingelnberg, cyclo-palloid system, 352
- Knots of meshing, 331

- Line, of action, 38,244
 - geodesic, 239
 - working, 244
- Linear vector function, 449
- Locus, of planar curves, 63,68,74
 - of regular curves, 65

- Machine tool settings, basic, 369
 - corrections, 371

- special, 364
- Mapping, 42
- Main contact point, 362
- Matrix, addition and subtraction, 437
 - column, 435
 - differentiation, 444
 - equality of, 436
 - identity, 435
 - inverse, 4,441
 - multiplication, 437
 - nonsingular, 441
 - order of, 434
 - orthogonal, 443
 - representation of vector formulas, 444
 - row, 435
 - skew symmetric, 277,436,446
 - symmetric, 436
 - transpose, 277,439
- Meshing, analysis of, 89
 - equations of, 79,83,174,200,207, 210,261
 - of gears with errors, 392
- Meusnier theorem, 225,227,228
- Moment, 33
 - driving and resisting, 422
- Motion instantaneous relative, 29
 - screw, 16,319,339
 - transformation, 22,26
- Newton algorithm, 91
- Noncircular gears, 419
- Nonundercutting, conditions of tooth, 120,124,126,213
 - of the generated surface, 201
- Normal, to a plane curve, 50
 - to a plane curve, unit, 53
 - surface, 151
 - surface unit, 225,226
 - unit, 151
- Oerlikon's Cyclo-Paloid Systems, 350,352
- Osculating plane, 221,237
- Outer cone distance, 354
- Paraboloids, 276
 - of the generating surface, 201
- Pitch, circles, 296
 - cones, 304,350
 - plane, 309,407
 - point, location of, 83
 - surfaces, 296
 - surfaces, operating, 297,298
- Plane gearing, analysis of, 87
 - general theorem, 82
- Point, flat, 233
 - locus of contact, 244
 - pseudosingular, 156,157
 - regular, 50,151
 - singular, 50,151,152,156
- Point path, 275,281,285
- Point of surface, elliptic, 234
 - hyperbolic, 234
 - parabolic, 235
- Pressure angle, 313,423,429
- Principle curvatures, of mating surfaces, 260,262,367-370
 - of a surface, 449,459
- Rack cutter, 105,109,124,126,128, 143,395
- Rack parameter, 176
- Rack surface, equations of, 172
- Rays, limiting, 150,151
- Regression point, 52
- Regrinding, 405
- Rodriques formula, 263,460
- Roots blower, 86
- Rotation, instantaneous center of, 20, 83,119
 - intersected axes of, 29
- Scalar, product, 79
 - triple product, 70
- Screw, generation, by a circular arc, 349
 - motion, 37
 - parameter, 302,303,324,339
- Shaper, 130
- Simulation of meshing, 401
- Singular points, determination of, 196
 - existence of, 121
 - of generated surface, 187,190
- Spatial gearing, analysis, 241,243
 - analysis of meshing, 243
 - kinematic relations of, 253,259
- Spiral bevel gearing, 352
 - force transmission for, 429
- Surface of action, 171,177,201,208, 211,214
 - Archimedes screw, 162,165
 - cone, 154,157,158
 - coordinate line on, 150
 - curvatures, 267
 - examples of, 154
 - family of generating, 174
 - generating, 202,208,214,355,357,358, 361,362,364
 - generated, 201,212,213
 - point, 151-154,157,158
 - principal directions and curvatures,

457,459
 problem of conjugate, 166
 of revolution, 17,154,324,325
 ruled, 153,154,158,160,161
 screw, 18
 screw involute, 162
 simple, 147
 spherical, 18,155-157
 unit normal, 226,227
 Symmetric augmented matrix, 264
 Synthesis, of gears, 87
 local, 354,362

 Taylor's formula, 219
 Tangency, external and internal, 114
 of gear tooth shapes, 87,88
 of gear tooth surfaces, 242
 point of, 250
 Tangent, of a plane curve, 50,52
 Tooth, contact analysis (TCA), 246,385
 cutting, 128
 element proportions, 353
 longitudinal shape, 309-311
 Transformation, coordinate, 1,4,5,8,9,
 11,12,14,15
 inverse coordinate, 9
 matrix, 4,12,13
 of motion, 22,26,103
 reverse, 4
 of translation to rotation, 103
 of vector components, 11
 Trihedron, 56,57,93
 Frenet's, 56
 right handed, 262

 Undercutting, 124,127,177,192

 Vector, sliding, 33
 unit tangent, 52
 Velocity, angular, 83
 of contact point, 253
 linear, 79,253
 relative, 20,32,80,82,255
 of sliding, 273,300,313
 transfer, 95,254,255

 Worm, cylindrical, 301
 gear, 209
 gear drives, 298,301,302,303,315,322,
 327,422
 generation of, 337
 thread surface, 202
 Worms, milling of, 324
 Worm surface, 332
 equations of, 328,330,332

| | | | | | |
|---|--|--|---|---|------------|
| 1. Report No. NASA RP-1212 AVSCOM TR-88-C-035 | | 2. Government Accession No. | | 3. Recipient's Catalog No. | |
| 4. Title and Subtitle Theory of Gearing | | | | 5. Report Date December 1989 ↙ | |
| | | | | 6. Performing Organization Code | |
| 7. Author(s) Faydor L. Litvin | | | | 8. Performing Organization Report No. None (E-2641) | |
| | | | | 10. Work Unit No. 1L162209AH76 505-42-94 | |
| 9. Performing Organization Name and Address The University of Illinois at Chicago Department of Mechanical Engineering Chicago, Illinois 60680 | | | | 11. Contract or Grant No. NAG3-783 and NAG3-655 | |
| | | | | 13. Type of Report and Period Covered Reference Publication | |
| 12. Sponsoring Agency Name and Address Propulsion Directorate U.S. Army Aviation Research and Technology Activity—AVSCOM Cleveland, Ohio 44135-3127 and NASA Lewis Research Center Cleveland, Ohio 44135-3191 | | | | 14. Sponsoring Agency Code | |
| | | | | 15. Supplementary Notes Project Managers: John J. Coy, Propulsion Systems Division, NASA Lewis Research Center and Robert F. Handschuh, Propulsion Directorate, U.S. Army Aviation Research and Technology Activity—AVSCOM. | |
| 16. Abstract The contents of the monograph covers the following main aspects of the modern theory of gearing: (1) Necessary and sufficient conditions of the existence of the surface that is generated by the tool as an envelope of the family of tool surfaces, (2) Avoidance of surface singularities and conditions of nonundercutting of the generated surface, (3) Avoidance of unfavorable zones of contact where an envelope of lines of contact on the generating surface appears, (4) Relations between principal curvatures and directions for two surfaces being either in line contact or in point contact, (5) Principles of computer-aided methods for simulation of meshing and contact of gear-tooth surfaces, (6) Geometric concepts and analytical representation of curves and surfaces that are applied as tooth profiles and tooth surfaces, and (7) Methods for generation of tooth surfaces. The contents of the book also covers the matrix representation of coordinate transformation, determination of gear centrodes, axodes, and operating pitch surfaces. The monograph is provided with sample problems and problems to be solved by the reader as a tool for the effective study of the contents of the monograph. | | | | | |
| 17. Key Words (Suggested by Author(s)) Gear-tooth surface Surface generation Simulation of meshing and contact | | | 18. Distribution Statement Unclassified—Unlimited Subject Category 37 | | |
| 19. Security Classif. (of this report) Unclassified | | 20. Security Classif. (of this page) Unclassified | | 21. No of pages 481 | 22. Price* |

